



D5.3: Integrated FOWT test report

FIHAC/POLIMI/INNOSEA /UPC/COBRA/ESTEYCO/JDR

January 2023

Disclaimer:



This project has received funding from the European Union's Horizon 2020 Research and Innovation programme under grant agreement No 815083.

Project details:

Duration:
1 Sep 2019 - 28 Feb 2023
Grant agreement:
No: 815083

Document information

Deliverable number	D5.3
Deliverable name	D5.3: Integrated FOWT test report
Reviewed by	UPC, DTU
Date	31-01-2023
Work Package and Task	Task 5.4: Fully coupled experimental tests towards a reference benchmark case for operating and extreme conditions assessment
Lead Beneficiary for this Deliverable	FIHAC
Dissemination Level	PUBLIC

Authors

Name	Organisation	E-mail
Raúl Guanche	FIHAC	guancher@unican.es
Miguel Somoano	FIHAC	somoanom@unican.es
Tommaso Battistella	FIHAC	battistellat@unican.es
Álvaro Rodríguez-Luis	FIHAC	rodriguezluisa@unican.es
Sergio Fernández-Ruano	FIHAC	fernandezruanos@unican.es
Javier Sarmiento	FIHAC	sarmientoj@unican.es
Álvaro Álvarez	FIHAC	alvareza@unican.es
David Blanco	FIHAC	blancod@unican.es
Alan Facchinetti	POLIMI	alan.facchinetti@polimi.it
Alessandro Fontanella	POLIMI	alessandro.fontanella@polimi.it
Simone Di Carlo	POLIMI	simone.dicarlo@polimi.it
Valentin Arramounet	INNOSEA	valentin.arramounet@innosea.fr
Florian Castillo	INNOSEA	florian.castillo@innosea.fr
Climent Molins	UPC	climent.molins@upc.edu
Pau Trubat Casal	UPC	pau.trubat.casal@upc.edu
Sara Muñoz	GRUPO COBRA	sara.munoz@grupocobra.com
Ignacio Romero	GRUPO COBRA	ignacio.romero@grupocobra.com
Francisco Javier Comas	ESTEYCO	francisco.comas@esteyco.com
Diego Sisí	ESTEYCO	diego.sisi@esteyco.com
Siobhan Doole	JDR	siobhan.doole@jdr cables.com

Version control

Version	Date	Author	Description of Changes
[1.0]	[2022-07-27]		Draft version
[2.0]	[2022-11-30]		Version to be reviewed
[3.0]	[2023-01-31]		Final version

EXECUTIVE SUMMARY

Deliverable D5.3 summarizes the fully coupled experimental tests conducted in both POLIMI and FIHAC facilities carried out within the framework of Task 5.4. The test programmed aims to create a benchmarking data base which will be the base of the numerical modelling strategy. This will contribute to set future engineering process towards optimized floating designs.

The physical experiments were focused on the seakeeping of WINDCRETE and ACTIVEFLOAT floating concepts under different environmental conditions, including waves, current and wind actions. The test program has been conducted at the CCOB (Cantabria Coastal and Ocean Basin) a Singular Techno-Scientific Facility (ICTS) from the Ministry of Science and Innovation and managed by FIHAC.

Considering the dimensions of the basin, as well as the wave generator capabilities, the selected test scales are 1:55 for the WINDCRETE platform and 1:40 for the ACTIVEFLOAT one. Hence, physical experiments are conducted at 165 meters of water depth in WINDCRETE case and at 120 m in ACTIVEFLOAT case (3 m at model scale).

During the physical experiments the main properties of the models are scaled down following the Froude scaling laws of similitude. The mock-ups are designed to be able to reproduce the external geometry of the platforms, as well as their mass properties (centre of gravity and inertia moments). The mock-ups are made of steel, except from the lower hemisphere of the WINDCRETE platform which is made of ABS by means of a 3D printer and the tower of the ACTIVEFLOAT which is made of aluminium. The wind loads are generated using the multi-fan system designed by FIHAC, reproducing an IEA-15MW. The mooring systems are designed based on commercial chains and tested springs, which reproduce the weight and the axial stiffness of each mooring system.

An extensive tests programme has been designed to evaluate the dynamic performance of the floating concepts. For each platform an equivalent test plan has been reproduced. The physical experiments are divided into five groups of tests, namely: (1) Dry Characterization tests, (2) Wet Characterization Tests, (3) Installation Tests, (4) Wave Tests, (5) Current Tests, (6) Wind Tests, (7) Coupled Tests: Wave + Current + Wind Tests. A total number of more than 120 tests are conducted. All the tests are carried out according to DNV recommendations.

Table of contents

EXECUTIVE SUMMARY	3
1 BACKGROUND	7
2 INTRODUCTION	8
2.1 Objectives	9
2.2 Report structure	10
3 GENERAL DESCRIPTION OF THE FLOATING WIND CONCEPTS	10
3.1 Definition of the spar-based wind concept: WINDCRETE	10
3.1.1 The floater	12
3.1.2 Mooring system	14
3.1.3 Dynamic power export cable	16
3.2 Definition of the semisub-based wind concept: ACTIVEFLOAT	18
3.2.1 The floater	20
3.2.2 Mooring system	25
3.2.3 Dynamic power export cable	27
3.3 Wind turbine	27
4 PHYSICAL MODELLING: Hydrodynamic tests	30
4.1 The facility: Cantabria Coastal and Ocean Basin (CCOB)	30
4.2 Description of the scaling laws of similitude	32
4.3 WINDCRETE scaled model design and manufacturing	33
4.3.1 Platform target values	33
4.3.2 Mockup design	34
4.3.3 Mockup manufacturing	36
4.3.4 Mooring system	39
4.3.5 Soft-mooring system for installation tests	44
4.3.6 Dynamic cable	47
4.3.7 Aerodynamic generation by the FIHAC's multi-fan system	48
4.4 ACTIVEFLOAT scaled model design and manufacturing	51
4.4.1 Platform target values	51
4.4.2 Mockup Design	54
4.4.3 Mockup manufacturing	56
4.4.4 Mooring system	59
4.4.5 Soft-mooring system for installation tests	64
4.4.6 Dynamic power export cable	67

4.4.7	Aerodynamic generation by the FIHAC’s multi-fan system	68
4.5	Instrumentation	68
4.5.1	Data acquisition system.....	69
4.5.2	Free surfaces gauges.....	70
4.5.3	Acoustic Doppler Velocimetry (ADV-Vectrino)	71
4.5.4	Qualisys Tracking Motion system (QTM)	72
4.5.5	Axial force transducers	72
4.5.6	Multi-axis force-torque transducer	73
4.5.7	Accelerometer	74
4.5.8	Digital image and video recording system.....	74
4.6	Test Programme	75
4.6.1	First round of wave basin tests.....	75
4.6.2	Second round of wave basin tests	76
4.7	Experimental Layouts.....	89
4.7.1	First round of wave basin tests.....	89
4.7.2	Second round of wave basin tests	89
4.8	Data analysis	99
4.8.1	Characterization tests.....	99
4.8.2	Wind tests.....	99
4.8.3	Wave, current and coupled tests.....	99
4.8.4	Statistical analysis	100
5	RESULTS FROM FIRST ROUND OF WAVE BASIN TESTS	101
5.1	WINDCRETE wind turbine	102
5.2	ACTIVEFLOAT wind turbine	103
6	RESULTS FROM SECOND ROUND OF WAVE BASIN TESTS	105
6.1	WINDCRETE spar-based wind concept.....	105
6.1.1	Wave calibration.....	105
6.1.2	Characterization Tests Results.....	106
6.1.3	Seakeeping tests results	111
6.1.4	Installation Tests.....	155
6.2	ACTIVEFLOAT semisub-based wind concept.....	159
6.2.1	Wave calibration.....	160
6.2.2	Characterization Tests Results.....	161
6.2.3	Seakeeping tests results	167
6.2.4	Installation Tests.....	209



7	CONCLUSIONS.....	219
8	ANNEXES.....	223
9	REFERENCES.....	224

1 BACKGROUND

In experimental tests conducted in FIHAC's flume (COCOTSU) and described in Deliverable D5.2, research efforts were focused on two essential components: the mooring line (Task 5.2) and the dynamic cable (Task 5.3) for power extraction [1]. Since the dominant factor in the tension of the lines is the movement imposed by the platform [2], for these experiments the fairlead displacement was forced by a linear actuator. Axial stiffness of the 'all chain' mooring line was achieved by including calibrated spring within the line. Mooring quasistatic and dynamic performances were distinguished as a function of the actual energy dissipated, thanks to the novel tracking images. Bending stiffness of the dynamic cable was replicated by using an equivalent elastic string based on synthetic materials [3].

Previously, the uncertainties of physical models (Task 5.1) were described in both wave basin and wind tunnel testing within Deliverable D5.1 [4]. The best scale factor for a physical model comes from the balance between working at a large scale which minimizes scale effects and complying with the test facility constraints. On one hand, the methodology for truncating the mooring system was explained to limit the scale model within reasonable depth and footprint, considering the dimensions of the ocean basin as well as the wave generator capabilities. Thus, with a truncated version of the physical model that correctly captures the influence of mooring loads on the structure, the size of the tests can be maximized and the potential effects of using small scale factors can be reduced. On the other hand, HIL (Hardware in the Loop) methodologies try to solve the Froude-Reynolds scaling incompatibility, since the floating platform and the mooring system are governed by gravity-influenced forces, whereas the wind turbine is dominated by the aerodynamic forces.

In the POLIMI wind tunnel testing, the wind turbine subsystem is emulated by means of a physical scale model and the wind environment is recreated inside the atmospheric boundary layer test section of the wind tunnel. The rigid-body motion of the floating structure is applied to the wind turbine scale model with an actuation system, controlled by a numerical simulation of the floating platform. Conversely, the HIL method applied to the FIHAC's basin (CCOB) is used to provide the aerodynamic data numerically and the hydrodynamic data physically. The real-time hybrid model considered includes a multi-fan system which consists of coupling a set of small fans at the aero-rotor interface and hence, permits to generate the aerodynamic loads reducing the limitations typically given by scaled problems [5].

In Deliverable D5.1 [4], POLIMI and FIHAC recommended the following procedure (Task 5.1) when performing hybrid scale model experiments with a floating wind turbine in a wind tunnel and a wave basin:

- Accurate analysis of the IEA 15MW wind turbine modelling in POLIMI Wind Tunnel (GVPM): Bottom fixed tests, as well as a set of tests considering prescribed movements based on a realistic range of amplitudes and frequencies for both floating platforms, are planned to validate the turbine control system. This testing campaign in the wind tunnel facility is focused on studying the effects of the turbine controller on the dynamic thrust force and the unsteady aerodynamics because of the turbine motions.
- Calibration of the FIHAC's multi-fan system: An equivalent test campaign covering fixed tests and analogous prescribed movements to the ones performed by POLIMI, are programmed to be conducted. This set of tests aims to be able to reproduce accurately the aerodynamic forces observed in the wind tunnel, including control induced effects and unsteady aerodynamic effects. Thus, the IEA 15MW turbine controller modelling is equivalent at FIHAC and POLIMI.
- Validation of the innovations proposed by previous Tasks by means of fully coupled hybrid modelling in the Cantabria Coastal and Ocean Basin (CCOB): A full set of tests are conducted for both floating concepts: WINDCRETE and ACTIVEFLOAT. This test campaign in FIHAC's basin contributes to improve the knowledge about the applicability and extrapolation criteria of coupled aero-hydro-servo-elastic numerical models for spar and semi-submersible wind turbines.
- Calibration of the actuation system on the tower-base to conduct fully coupled hybrid modelling in the POLIMI Wind Tunnel (GVPM): The hydrodynamic damping terms of both floating concepts from

the tests conducted in the FIHAC's basin are considered for the numerical model that supports the hydrodynamics on the tower-platform interface in the wind tunnel.

2 INTRODUCTION

The current Deliverable D5.3 describes the performance of several physical model test campaigns in POLIMI wind tunnel and FIHAC's basin facilities. Task 5.4 includes fully coupled experimental tests of two novel concrete-based concepts of floating offshore wind platforms towards a reference benchmark case for operating and extreme conditions assessment. The tests campaigns aim to deep into the dynamics understanding of:

- WINDCRETE spar platform designed by UPC.
- ACTIVEFLOAT semi-submersible platform developed by GRUPO COBRA/ESTEYCO.

The site B has been established to serve as the basis for hybrid testing of the optimized concrete-based spar and semi-submersible floating concepts. The site B selected for the COREWIND project is located off the southeast coast of Gran Canaria (GC) island, in the Canary Islands, Spain ($27^{\circ}45'0.00''\text{N}$, $15^{\circ}19'48.00''\text{W}$) shown in Figure 2-1. From Deliverable D1.2 [6]. The design depth of this site is 200 meters.



Figure 2-1. Gran Canaria Site. Location [6]

In order to achieve the targets of the physical experiments, a set of tests were carried specially selected to evaluate the dynamic response of WINDCRETE and ACTIVEFLOAT floating platforms behaviour considering the environmental conditions of site B.

The wave, current and wind basin testing campaigns are conducted in the CCOB (Cantabria Coastal and Ocean Basin), managed by FIHAC. More details of the facility are available in the Section 4.1. Considering the

dimensions of the basin as well as the wave and current generator capabilities, it is concluded that the most suitable test scales to carry out the physical experiments are:

- 1:55 for the WINDCRETE spar-based wind concept. These physical experiments are conducted for a water depth of 165 meters.
- 1:40 for the ACTIVEFLOAT semisub-based wind concept. These physical experiments are conducted for a water depth of 120 meters.

During the physical experiments the main properties of the model are scaled following the Froude scaling laws of similitude, trying to minimise scale effects that significantly perturb the model scale tests results. The basin layout can be seen in Section 4.7.

The mock-up is designed to be able to reproduce the external geometry of the platform, as well as its mass properties (centre of gravity and inertia moments). The mock-ups are made of steel, except from the lower hemisphere of the WINDCRETE platform which is made of ABS by means of a 3D printer and the tower of the ACTIVEFLOAT which is made of aluminium. The wind loads are generated using the multi-fan system designed by FIHAC, reproducing the IEA 15MW. The mooring system is designed based on commercial chains and tested springs able to reproduce the weight and the axial stiffness of the system.

On the other hand, an extensive tests programme is designed to evaluate the dynamic performance of both floating wind concepts. The physical experiments are divided into seven groups of tests depending on their nature, namely: (1) Dry Characterization tests, (2) Wet Characterization Tests, (3) Installation Tests, (4) Wave Tests, (5) Current Tests, (6) Wind Tests, (7) Coupled Tests: Wave + Current + Wind Tests.

Finally, a total of more than 120 tests are conducted. Main results and findings of the physical experiments can be reviewed in Section 5.

2.1 Objectives

The main goal of Task 5.4 is to validate mooring and power cable dynamics through the large-scale experimental testing based on a scaled concept for +15 MW FOWT of the two concrete-based floating substructures designs: WINDCRETE spar and ACTIVEFLOAT semi-submersible.

To aim this, the following specific objectives are contemplated:

- Development of new hybrid testing techniques to evaluate wind-turbine control impact over the mooring system, power cable dynamics and platform performance.
- Platform hydrodynamics, mooring and power cable dynamic analysis considering different environmental conditions, such as waves, current and wind action.
- Experimental validation of the mooring system and power cable optimizations based on two novel concrete-based floating concepts: WINDCRETE spar and ACTIVE-FLOAT semi-submersible.
- To study the general dynamics of both floaters including natural periods and hydrodynamic damping of the system.
- To identify any unexpected behaviour that may be out of the capabilities of state-of-the-art numerical models.
- Generation of an experimental data base to be used as a benchmark of coupled aero-hydro-servo-elastic numerical models for spar and semi-submersible wind turbines.

The following specific tasks were carried out at FIHAC facilities for each floating concept, according to the technical specification provided by previous COREWIND Deliverables:

1. Reduced scale model (mock-up) design and construction of the floating concept.
2. Preliminary works and mock-up set-up: dynamic cable, mooring line and anchoring system layout, and cable routing.

3. Installation of sensors on the model and basin: free surface sensors, ADVs, load cells, accelerometers, and motion capture system.
4. As built mock-up characterization: platform centre of gravity position and inertias.
5. Characterization testing under wet conditions of the floating platform: tilt tests, decay tests (free floating and moored configurations) and static offset tests.
6. Seakeeping testing: wave, current and wind tests to verify the coupled hydrodynamic and aerodynamic behaviour of the floating concept.

2.2 Report structure

The methodology and the results obtained during the execution of the test program is summarized, following the next report structure:

- **Section 1.** Background.
- **Section 2.** Introduction.
- **Section 3.** General description of the floating wind concepts.
- **Section 4.** Physical modelling in the FIHAC's basin: Methodology applied to conduct the physical experiments at reduced scale. Description of the Cantabria Coastal and Ocean Basin (CCOB), Scaling laws of similitude, Description of the WINDCRETE and ACTIVEFLOAT physical models, Tests programme, Basin layout, Description of the instrumentation, Data analysis.
- **Section 5.** Results summary in the FIHAC's basin: Characterization tests results, Seakeeping tests results.
- **Section 6.** Conclusions from the FIHAC's basin testing campaigns.

3 GENERAL DESCRIPTION OF THE FLOATING WIND CONCEPTS

3.1 Definition of the spar-based wind concept: WINDCRETE

WINDCRETE is a spar concrete-based concept designed by UPC to support very large wind turbines (+15 MW) at water depths larger than 165 m. It is composed of platform and rotor-nacelle assembly (RNA), which is equipped with the IEA 15 MW wind turbine. The monolithic concrete spar platform includes both the tower and the floater in a unique concrete member shown in Figure 3-1.



Figure 3-1. WINDCRETE concrete-based concept of spar wind turbine

The platform consists of a floater with large draft which minimizes heave motion, and whose pitch/roll stability is managed by proper combination of ballast and buoyancy achieved thanks to the spar-based shape of the floater.

The mooring system which also helps to stabilize the system, is designed as a three single catenary mooring shape lines composed by one type of chain distributed each 120°, intending to avoid uplifting forces at the anchor. The upper end of each main line splits up into two delta lines by a crow-foot element (delta connection) to provide enough yaw stiffness to the platform, as can be seen in Figure 3-2.

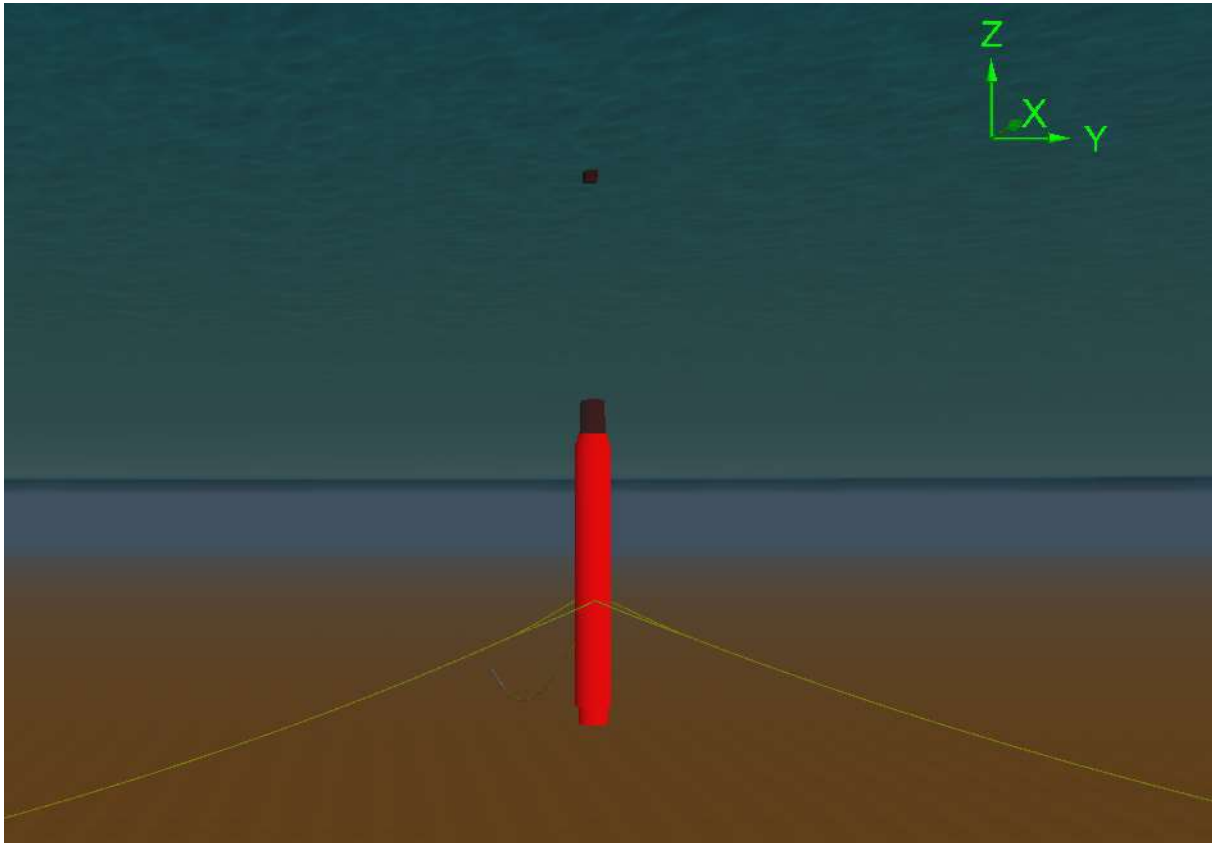


Figure 3-2. WINDCRETE at Gran Canaria site. OrcaFlex 3D view of the substructure [7]

3.1.1 The floater

Although the IEA-15MW initially is set to 150 m, according to the constraints referred to Gran Canaria location based on IEC 61400-3-2 standard [8], the hub height of the platform is adjusted to be located lower at 135 m above sea level as explained in Deliverable D1.3 [9]. The tower height is 129.495 m to have a hub height of 135 m.

The tower in the WINDCRETE design is a tapered cylinder made of concrete with a constant thickness of 0.4 m. The tower base, which is defined at the mean sea level (MSL), has a diameter of 13.2 m, and the top tower diameter of 6.5 m is the same as the IEA design, to ensure the connection with the wind turbine.

The substructure consists of a tapered transition piece of 10m length, which connects the lower part of the platform and the tower, a cylindrical spar of 135.7m length and a hemisphere of 9.3m radius at the bottom of the substructure. Then, the total draft of the platform is 155m [9].

The cylindrical spar has a diameter of 18.6m and the tapered transition piece has a top diameter of 13.2m and a bottom diameter of 18.6m. Figure 3-3 shows a sketch of the WINDCRETE with its main dimensions in meters. The origin of the reference system used in the WINDCRETE description and its mooring system is set at the MSL, in the intersection with the WINDCRETE axis of symmetry, that coincides with the tower base on its undisplaced position.

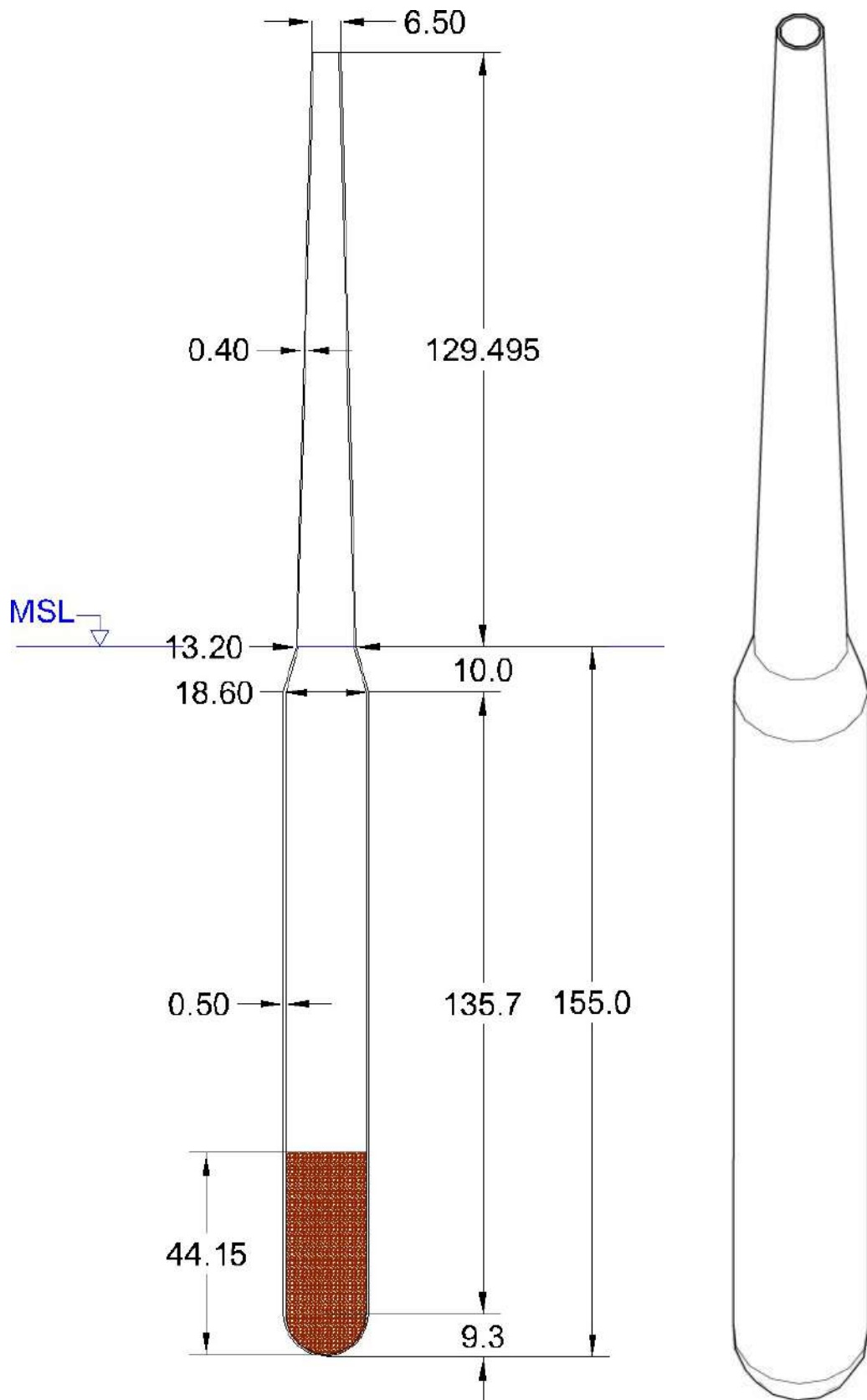


Figure 3-3. WINDCRETE sketch with values in meters [9]. Units are in meters

The required hydrostatic stiffness in the pitch/roll degree of freedom is achieved by adding a solid aggregate ballast at the platform keel with a bulk density of 2500 kg/m³. In Figure 3-3, the aggregate ballast is coloured in brown. The internal height of the ballast is not anymore 44.15 m (based on the preliminary mooring system), but 44.675 m from the keel (based on the optimized mooring system) to fit with the prescribed draft of the platform.

Table 3-1 shows the main characteristics of the WINDCRETE platform.

	Mass [kg]	CoGx [m]	CoGy [m]	CoGz [m]	Ixx [kgm ²]	Iyy [kgm ²]	Izz [kgm ²]
SUBMERGED w/o Ballast	1.148E+07						
Ballast	2.539E+07						
SUBMERGED SPAR	3.687E+07	0	0	-113.058	5.590E+10	5.590E+10	1.828E+09
Tower	3.250E+06	0	0	66.659	9.168E+10	9.168E+10	8.700E+07
SPAR	4.012E+07	0	0	-98.500	1.554E+11	1.554E+11	1.915E+09
Wind Turbine	1.020E+06	-6.857	0	133.013	5.218E+10	5.218E+10	7.700E+07
SPAR w/ WT	4.114E+07	-0.170	0	-92.760	2.089E+11	2.089E+11	1.992E+09

Table 3-1. Mass and inertia properties of WINDCRETE prototype at full scale, in the operational configuration

In the installation configuration, the WINDCRETE platform is in horizontal position un-ballasted and without the wind turbine. However, as in horizontal position a little deviation in CoGx or CoGy results in instability in yaw around its local axes, a part of the ballast is remained to provide some angle respecting the free surface. Table 3-2 shows the main characteristics for this configuration.

	Mass [kg]	CoGx [m]	CoGy [m]	CoGz [m]
SUBMERGED w/o Ballast	1.148E+07			
Ballast	1.469E+07			
SUBMERGED SPAR	2.617E+07	0	0	-113.314
Tower	3.250E+06	0	0	66.659
SPAR	2.942E+07	0	0	-93.432

Table 3-2. Mass properties of WINDCRETE prototype at full scale, un-ballasted and without the wind turbine in the installation configuration

3.1.2 Mooring system

From Deliverable D2.2 [7], the optimized mooring system currently obtained for the WINDCRETE floating offshore wind turbine located in Gran Canaria Island, uses chain lines only. Gentle environmental loads combined with higher water depth makes the use of synthetic rope or clump weights unnecessary on this site. The mooring system is composed of three catenary mooring lines. At the top of the mooring system, the lines are equipped with the crowfoot system (delta connection) as can be seen in Figure 3-4.

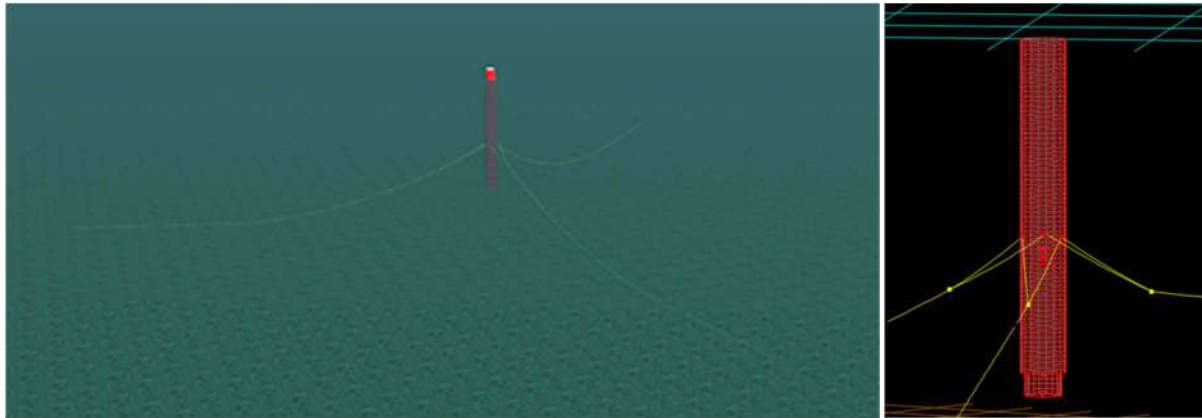


Figure 3-4. 3D view of the OrcaFlex model of the mooring system of WINDCRETE [7]

Three types of chain are used in this system. Table 3-3 summarizes physical properties of chains used.

Line #		Chain bar diameter [mm]	Equivalent diameter [mm]	Line Length [m]	Dry mass per meter length [kg/m]	Axial stiffness [kN]	Steel Grade
1	Main line	111	199.8	700	245.19	10.52e5	R4
	Delta Lines	111	199.8	50	245.19	10.52e5	R3
2	Main Line	100	180	750	199	8.54e5	R3S
	Delta Lines	111	199.8	50	245.19	10.52e5	R3
3	Main Line	100	180	750	199	8.54e5	R3S
	Delta Lines	111	199.8	50	245.19	10.52e5	R3

Table 3-3. Physical properties of the chain lines used for the optimized mooring system [7]

The radius to anchor is 728m. Table 3-4 gives anchors and fairleads coordinates.

Line #	Anchor coordinates [m]			Fairlead coordinates [m]		
	X	Y	Z	X	Y	Z
1	-743.34	0	-200	-4.65	8.05	-90
				-4.65	-8.05	-90
2	396.33	-686.47	-200	-4.65	-8.05	-90
				9.3	0	-90
3	396.33	686.47	-200	-4.65	8.05	-90
				9.3	0	-90

Table 3-4. Mooring system anchors and fairlead location

Static offsets in surge direction have been performed to assess the stiffness of the mooring system. Figure 3-5 reports the relation between the forces in the mooring line 1 and the platform displacements following the direction of this mooring line. The range of offsets expected for WINDCRETE platform at Gran Canaria site under DLCs 6.1 and 6.2, is below 10m. To keep enough chain of mooring line 1 laying on the seabed, maximum allowed offsets are [-9 m, 5 m].

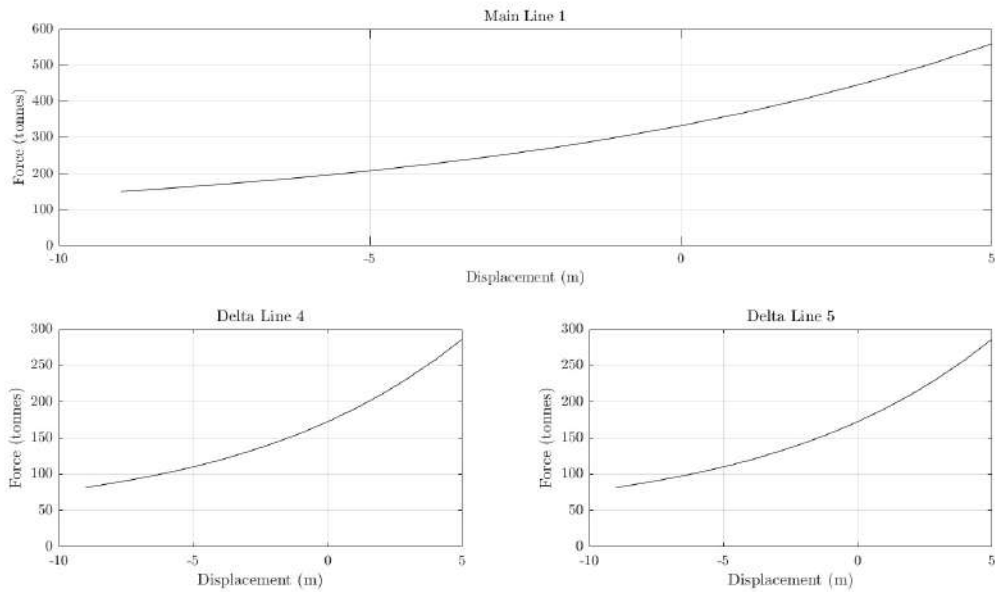


Figure 3-5. Mooring forces of Line 1 vs its delta-connection displacements

Figure 3-6 shows the relation between the forces in the mooring line 2 and the platform displacements following the direction of this mooring line. To keep enough chain of mooring line 2 laying on the seabed, maximum allowed offsets are [-5 m, 9 m].

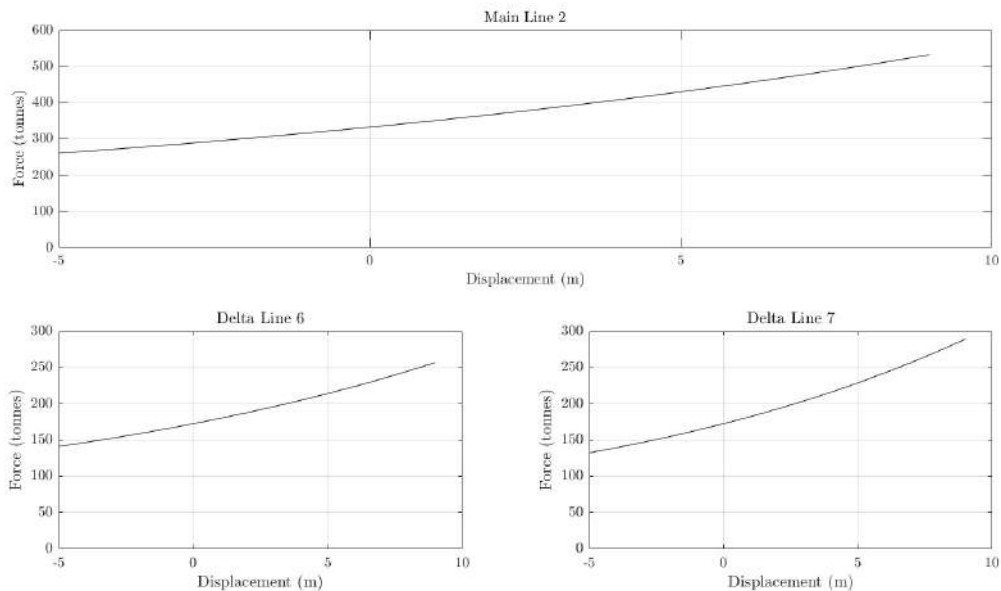


Figure 3-6. Mooring forces of Line 2 vs its delta-connection displacements

3.1.3 [Dynamic power export cable](#)

Copper cores and XLPE insulation has been selected to minimise cable size of the cable and achieve a cost-optimised solution while retaining functional requirements as described in Deliverable D3.1 [10]. Table 3-5 presents JDR high voltage cable with 66 kV rating. Considering mechanical characteristics, the following CW002 size has been selected for modelling cables.

Cable Property	CW002
Cable Voltage Rating [kV]	36 / 66 (72.5)
Core Material	Copper
Core Size [mm ²]	800
Nominal Outer Diameter [mm]	192
Nominal Weight in air [kg/m]	72.3
Nominal Weight in seawater [kg/m]	45.4
Nominal Axial Stiffness [MN]	830
Terminated Axial Working Load Limit (TWWL) [kN]	155
Nominal Bend Stiffness [kN·m ²]	22.2

Table 3-5. JDR 66kV dynamic cable properties [10]

The dynamic cable is designed as a lazy wave configuration, which provides lift to at a midwater cable section by attached buoyancy modules, as shown in Figure 3-8. The Buoyant Section decouples the dynamic motions of the platform from the Touchdown Point fixed on the subsea end. In the Buoyant Section, there are 16 buoyancy modules of 527.5 kg of net buoyancy force each one.

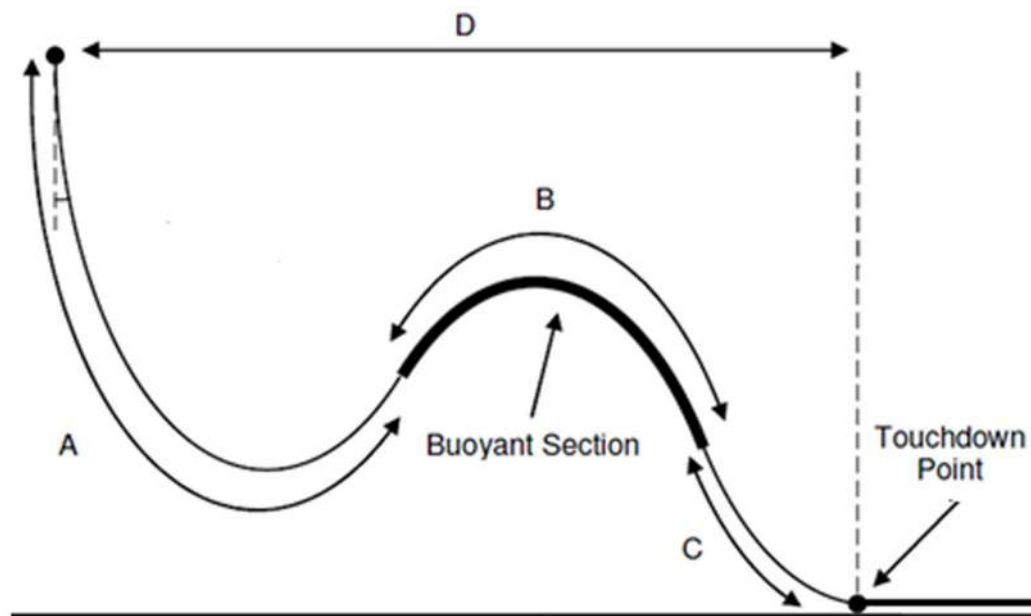


Figure 3-7. Dynamic cable sections [11]

In Deliverable D3.2 [11], to minimize risks of clashing while allowing reasonable horizontal movement due to wind of the dynamic cabling system in the water column, the cabling system is configured equidistant between mooring lines 2 and 3, orientated with x-axis in the leeward side when the platform is located at 0°. The exit angle azimuth of the J-tube presented in Figure 3-8 on the left, is 30° outwards from vertical down to tolerate dynamic loading and prevent clashing in service configuration. However, to minimize excessive dynamic movement and as shown on the right plot, the connection point is below the splash zone beneath the water level, specifically at a depth of 36.5 m below sea level and 2 m away from the edge of the structure.

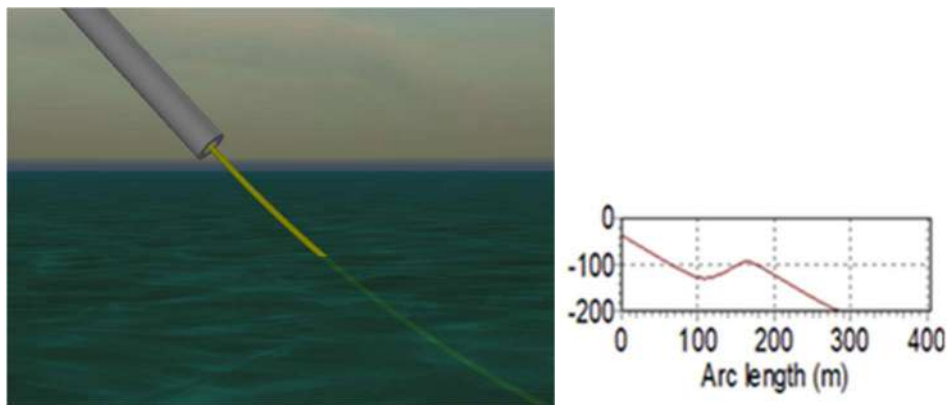


Figure 3-8. Exit angle (left) and static configuration (right) targeted

A polyurethane dynamic Bend Stiffener (BSR) works as a transition piece between the J-Tube and the dynamic cable, optimising the stiffness profile along the length. Table 3-6 presents the BSR details.

BSR characteristics	
Length (m)	Diameter (m)
0	0.7
7	0.215
Strain-Stress curve	
Stress (%)	Strain (kPa)
0	0
3	4000
10	7000

Table 3-6. Physical properties of the BSR used

3.2 Definition of the semisub-based wind concept: ACTIVEFLOAT

ACTIVEFLOAT is a concrete-based semi-submersible floater developed by GRUPO COBRA, and engineered by ESTEYCO to support very large wind turbines (+15 MW) at water depths greater than 40 m. It is composed of platform and rotor-nacelle assembly (RNA), which is equipped with the IEA 15 MW wind turbine. As shown in Figure 3-9, a central shaft that holds the connection with the tower that ends in the turbine, is connected to three external vertical columns placed at 120 degrees through three pontoons.

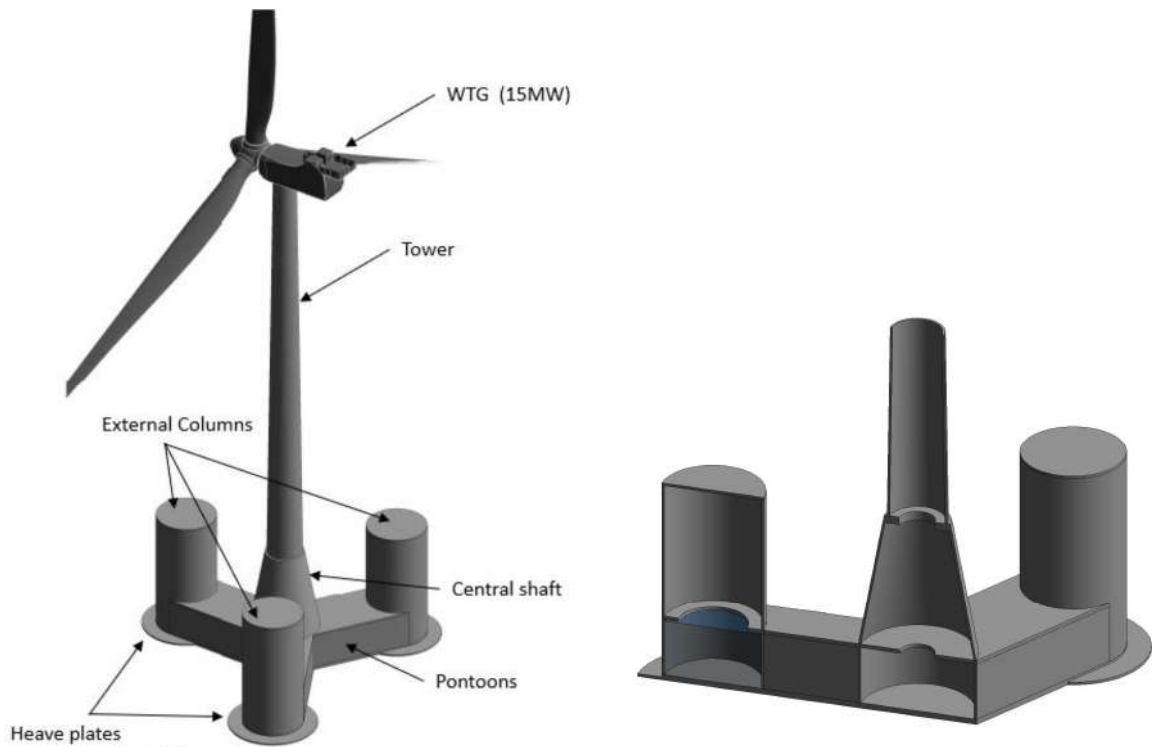


Figure 3-9. ACTIVEFLOAT concrete-based concept of semi-submersible wind turbine (left) and sectional isometric view of the platform along the cut plane XZ (right)

The platform is made of reinforced concrete, except for the tower that is made of structural steel. The vertical columns provide the required buoyancy and stability to the system. The stability in pitch/roll in this case is due to the large inertia of the waterplane area. The mooring system which also helps to stabilize the floating concept consists of three catenaries modelled as chain lines moored to the external columns (Figure 3-10) and intending to avoid vertical forces be applied on the anchor.

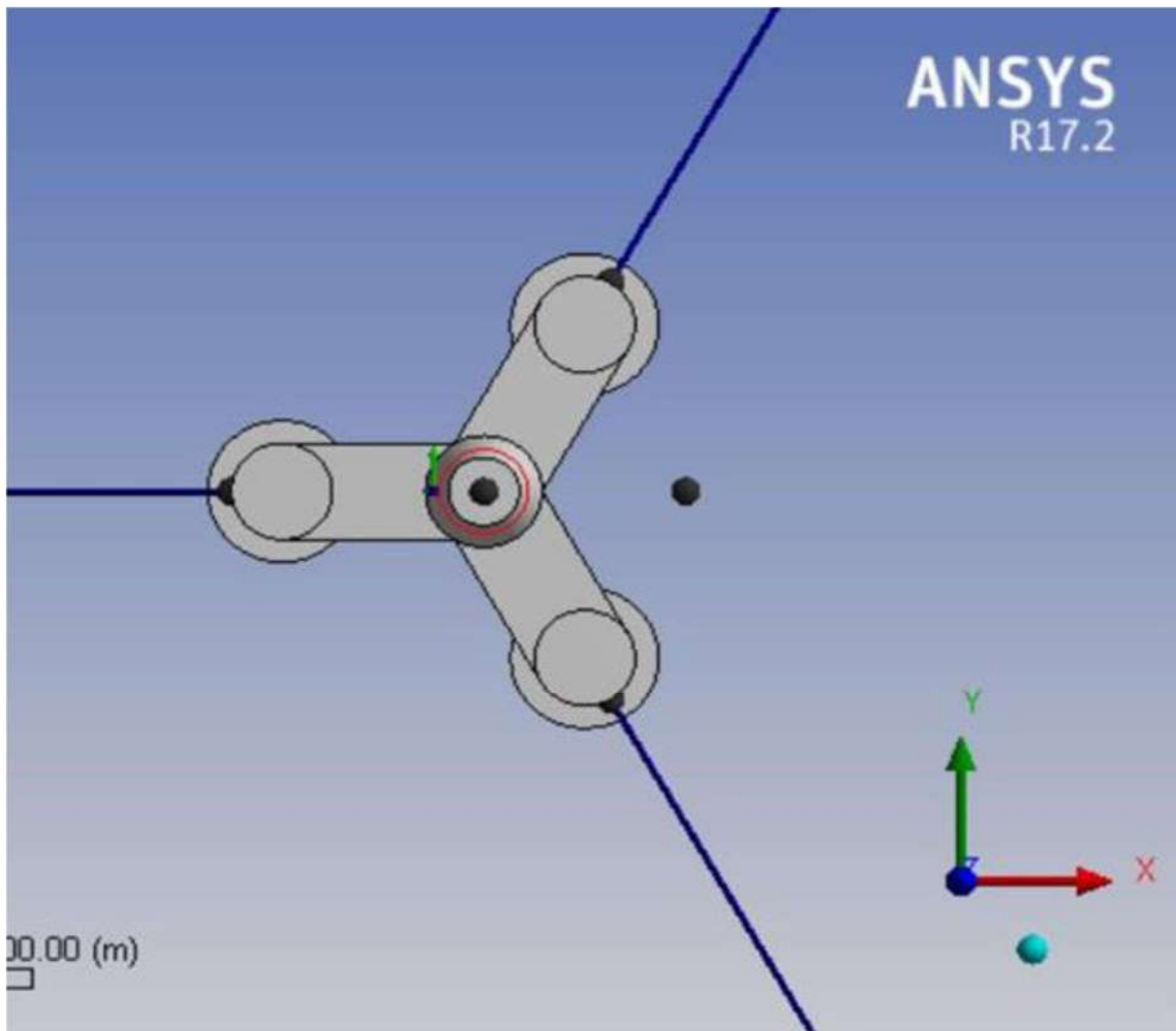


Figure 3-10. Mooring fairlead connection to ACTIVEFLOAT [9]

3.2.1 The floater

The platform external columns have the same height as the central cone, where the access platform is located to avoid waves passing over. One of the external columns is orientated with x-axis in the windward side whereas the other two are axisymmetric in the leeward side. The pontoons are structural members as the central shaft from where the turbine loads are transferred, and also add some heave damping. The column diameter is kept equal to the pontoons beam. The pontoons have a rectangular cross-section member with a central bulkhead that split the span of the pontoon decks. Circular heave plates are provided at the bottom of each external column, in order to increase hydrodynamic damping and added mass.

The main dimensions are indicated in the following Table 3-7.

Hub height (m above sea level)	135.00
Columns Diameter (m)	17.00
Columns separation (centre to tower centre) (m)	34.00
Columns height (m)	35.50

Central cone base diameter (m)	19.60
Central cone top diameter (m)	11.00
Tower base diameter (m)	10.00
Tower top diameter (m)	6.50
Tower length (m)	120.50
Pontoons height (m)	11.50
Heave plate cantilever (m)	4.00
Overall beam (m)	83.90

Table 3-7. Main dimensions of ACTIVEFLOAT platform

The hub height of the floating system is adjusted to be at 135 m above sea level according to the referred to Gran Canaria location based on IEC 61400-3-2 standard [8]. As explained in Deliverable D1.3 [9], the platform is transported un-ballasted in order to reduce draught requirements of navigation channels or shipyards where the fabrication takes place. ACTIVEFLOAT is designed to have an installation draft between 11 and 13 meters whereas the operational draft is 26.50 meters. The tower starts at the top of the central concrete cone of the platform, at 9.0 meters above sea level.

Figure 3-11 summarizes the general arrangement of the design.

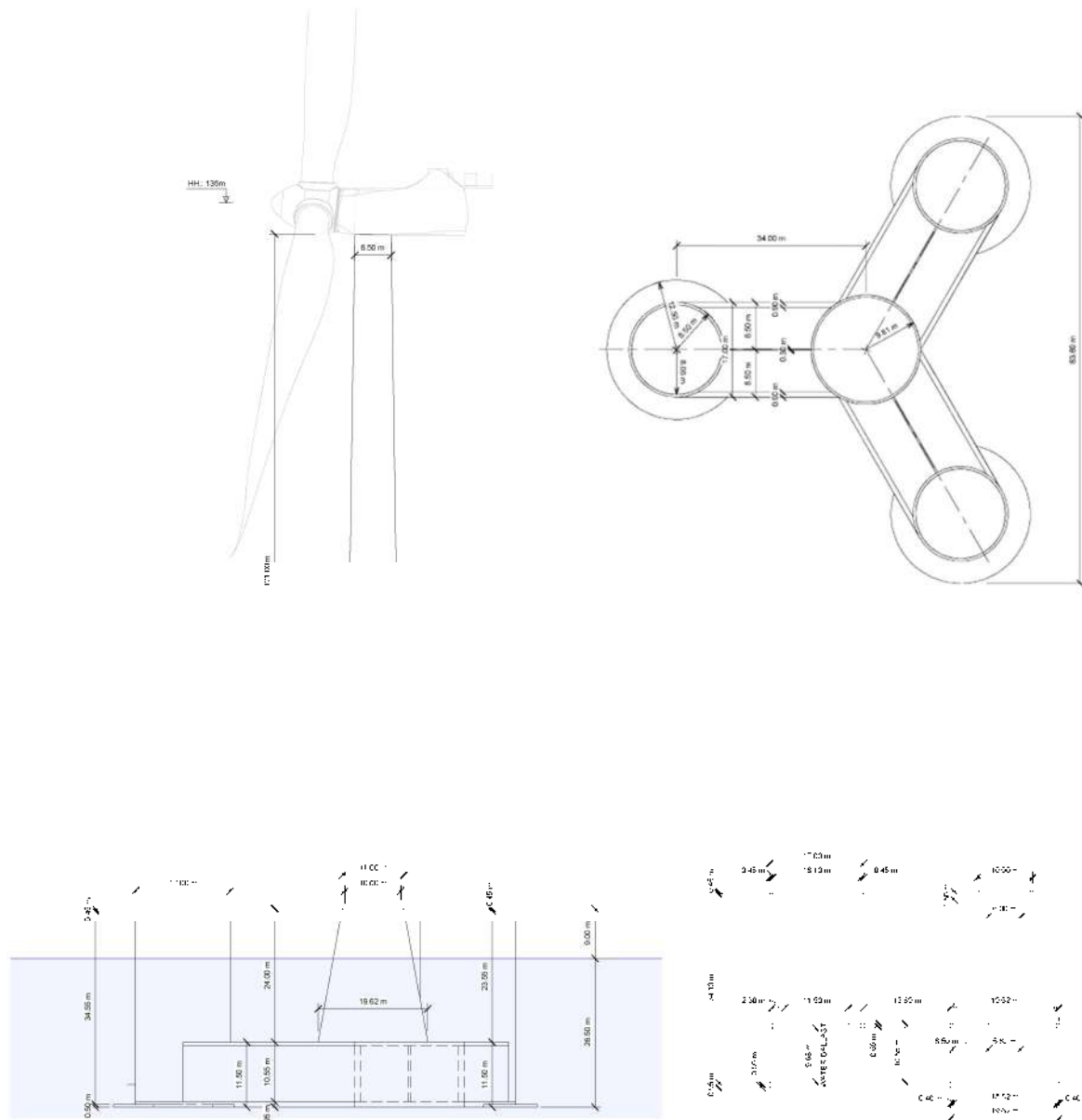


Figure 3-11. Side view (left), plant view (top right) and sectional side view (bottom right) of ACTIVEFLOAT platform. Units are in meters

The central shaft is left empty in order to allocate the corresponding machinery in a dry environment (i.e. the active ballast system). Thus, the lower slab of the central shaft requires a heavy structure since it has to resist permanently a differential pressure (26.5 meters of water column in the operational configuration). The ballast water is divided in two:

- The permanent ballast inside the pontoons that does not change after the installation of the platform. The pontoons fully ballasted are structurally efficient.
- The active ballast in tanks or external columns that may be varied in order to trim the platform as demanded by the external conditions. The active ballast system consists in a pump arrangement that allows to transfer water from column to column, providing a corrective moment that reduces the mean pitch produced by the mean thrust potentially to zero.

Table 3-8 shows the main characteristics of the ACTIVEFLOAT platform in the operational configuration (draft of 26.5 meters) when the pontoons are fully ballasted, and the tanks are evenly ballasted.

EVENLY BALLASTED	Mass [kg]	CoGx [m]	CoGy [m]	CoGz [m]	Ixx [kgm ²]	Iyy [kgm ²]	Izz [kgm ²]
SUBMERGED w/o Ballast	2.125E+07	0	0	-15.730	1.090E+10	1.090E+10	1.587E+10
Permanent Ballast	7.528E+06	0	0	-20.600			
Tank 1 Ballast	1.860E+06	-34.000	0	-21.093			
Tank 2 Ballast	1.860E+06	17.000	-29.445	-21.093			
Tank 3 Ballast	1.860E+06	17.000	29.445	-21.093			
Active Ballast	5.581E+06	0	0	-21.093			
TOTAL BALLAST	1.311E+07	0	0	-20.810	6.046E+09	6.046E+09	9.376E+09
SUBMERGED SEMI-SUBMERSIBLE	3.436E+07	0	0	-17.668	1.695E+10	1.695E+10	2.525E+10
Tower + internals + equipment	1.189E+06	0	0	56.920	7.344E+09	7.344E+09	1.921E+07
SEMI-SUBMERSIBLE	3.555E+07	0	0	-15.174	2.429E+10	2.429E+10	2.527E+10
RNA	1.017E+06	-7.023	0	133.840	2.135E+10	2.136E+10	2.064E+07
SEMI-SUBMERSIBLE w/ WT	3.656E+07	-0.195	0	-11.032	4.564E+10	4.565E+10	2.529E+10

Table 3-8. Mass and inertia properties of ACTIVEFLOAT prototype at full scale, evenly ballasted in the operational configuration

Table 3-9 shows the main characteristics of the ACTIVEFLOAT platform in the operational configuration (draft of 26.5 meters) when there is no wind, and the active ballast compensates the deviation of the CoGx due to the RNA.

BALLASTED Om/s	Mass [kg]	CoGx [m]	CoGy [m]	CoGz [m]
SUBMERGED w/o Ballast	2.125E+07	0	0	-15.730
Permanent Ballast	7.528E+06	0	0	-20.600
Tank 1 Ballast	1.720E+06	-34.000	0	-21.428
Tank 2 Ballast	1.930E+06	17.000	-29.445	-20.925
Tank 3 Ballast	1.930E+06	17.000	29.445	-20.925
Active Ballast	5.581E+06	1.279	0.000	-21.080
TOTAL BALLAST	1.311E+07	0.544	0.000	-20.804
SUBMERGED SEMI-SUBMERSIBLE	3.436E+07	0.208	0.000	-17.666
Tower + internals + equipment	1.189E+06	0	0	56.920

SEMI-SUBMERSIBLE	3.555E+07	0.201	0.000	-15.172
RNA	1.017E+06	-7.023	0	133.840
SEMI-SUBMERSIBLE w/ WT	3.656E+07	0.000	0.000	-11.030

Table 3-9. Mass properties of ACTIVEFLOAT prototype at full scale, ballasted in the operational configuration with no wind

Table 3-10 shows the main characteristics of the ACTIVEFLOAT platform in the operational configuration (draft of 26.5 meters) when there is rated wind at 0° and the active ballast compensates the thrust.

BALLASTED 10.5m/s at 0°	Mass [kg]	CoGx [m]	CoGy [m]	CoGz [m]
SUBMERGED w/o Ballast	2.125E+07	0	0	-15.730
Permanent Ballast	7.528E+06	0	0	-20.600
Tank 1 Ballast	2.285E+06	-34.000	0	-20.074
Tank 2 Ballast	1.648E+06	17.000	-29.445	-21.602
Tank 3 Ballast	1.648E+06	17.000	29.445	-21.602
Active Ballast	5.581E+06	-3.884	0.000	-20.976
TOTAL BALLAST	1.311E+07	-1.653	0.000	-20.760
SUBMERGED SEMI-SUBMERSIBLE	3.436E+07	-0.631	0.000	-17.649
Tower + internals + equipment	1.189E+06	0	0	56.920
SEMI-SUBMERSIBLE	3.555E+07	-0.610	0.000	-15.156
RNA	1.017E+06	-7.023	0	133.840
SEMI-SUBMERSIBLE w/ WT	3.656E+07	-0.788	0.000	-11.014

Table 3-10. Mass properties of ACTIVEFLOAT prototype at full scale, ballasted in the operational configuration with rated wind at 0°

Table 3-11 shows the main characteristics of the ACTIVEFLOAT platform in the installation configuration (draft between 11 and 13 meters) when all the three tanks and pontoons are un-ballasted.

UN-BALLASTED	Mass [kg]	CoGx [m]	CoGy [m]	CoGz [m]	Ixx [kgm2]	Iyy [kgm2]	Izz [kgm2]
SUBMERGED w/o Ballast	2.125E+07	0	0	-15.730	1.263E+10	1.263E+10	1.587E+10
Tower + internals + equipment	1.189E+06	0	0	56.920	6.497E+09	6.497E+09	1.921E+07
SEMI-SUBMERSIBLE	2.244E+07	0	0	-11.882	1.913E+10	1.913E+10	1.589E+10
RNA	1.017E+06	-7.023	0	133.840	1.977E+10	1.978E+10	2.064E+07

SEMI-SUBMERSIBLE w/ WT	2.346E+07	-0.304	0	-5.567	3.889E+10	3.890E+10	1.591E+10
------------------------	-----------	--------	---	--------	-----------	-----------	-----------

Table 3-11. Mass and inertia properties of ACTIVEFLOAT prototype at full scale, un-ballasted in the installation configuration

3.2.2 Mooring system

From Deliverable D2.2 [7], the optimized mooring system for the ACTIVEFLOAT floating offshore wind turbine, in the Gran Canaria Island site is detailed. The mooring system is composed of three catenary mooring lines. The three lines are composed of chain sections. Gentle environmental loads combined with higher water depth makes the use of synthetic rope or clump weights unnecessary on this site. Figure 3-12 shows a 3D view of the optimized mooring system as represented in OrcaFlex, in the static position.

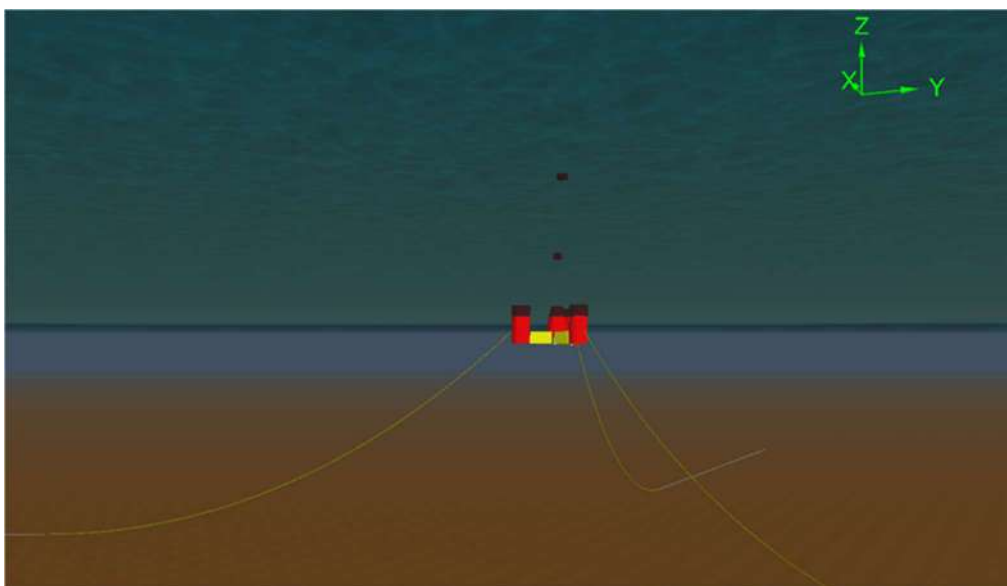


Figure 3-12. 3D view of the OrcaFlex model of the mooring system ACTIVEFLOAT [7]

Two types of chain are used in this system: one for the main line 1 in the windward side and the other one for both main lines 2 and 3 in the leeward side. Physical properties of the two types of chain use are summarized in Table 3-12.

Line #		Chain bar diameter [mm]	Equivalent diameter [mm]	Line Length [m]	Dry mass per meter length [kg/m]	Axial stiffness [kN]	Steel Grade
1	Main line	120	216	832	286.56	12.297e5	R3
2	Main Line	70	126	832	97.51	4.1846e5	R3
3	Main Line	70	126	832	97.51	4.1846e5	R3

Table 3-12. Physical properties of the chain lines used for the optimized mooring system [7]

The radius to anchor is 872 m. Anchors and fairleads coordinates are presented in Table 3-13.

Line #	Anchor coordinates [m]			Fairlead coordinates [m]		
	X	Y	Z	X	Y	Z
1	-799.588	0	-200	-42.5	0	-15
2	465.31	-681.07	-200	21.25	-36.806	-15
3	465.31	681.07	-200	21.25	36.806	-15

Table 3-13. Mooring system anchors and fairlead location

Static offsets in surge direction have been performed to assess the stiffness of the mooring system. Figure 3-13 reports the relation between the forces in the mooring line 1 and its fairlead displacements following the direction of this mooring line. The maximum offsets expected for the line 1 moored to ACTIVEFLOAT platform at Gran Canaria site under DLCs 6.1 and 6.2, are [-43 m, 51 m].

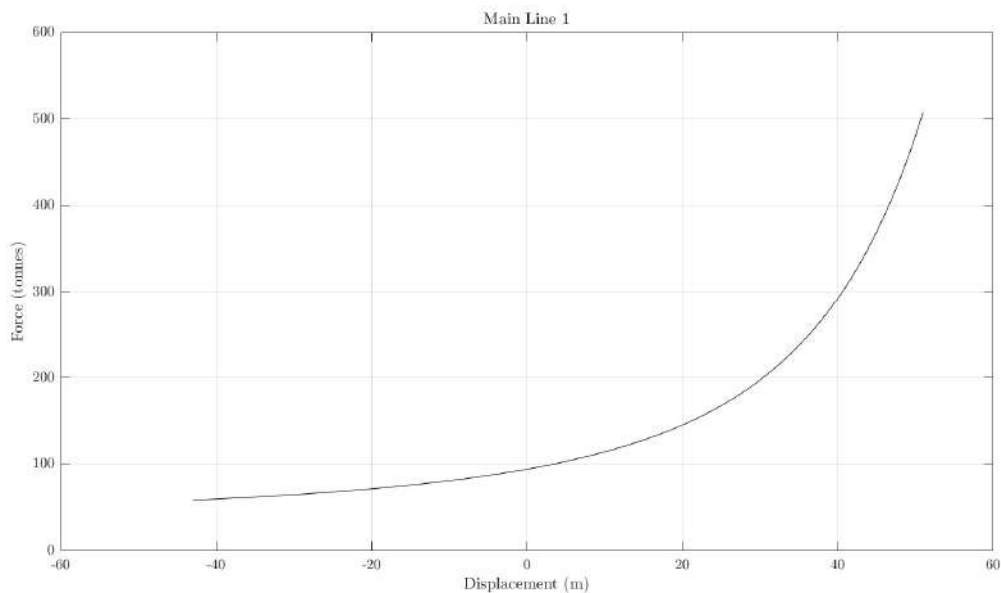


Figure 3-13. Mooring forces of Line 1 vs its fairlead displacements

Figure 3-14 shows the relation between the forces in forces in the mooring line 2 and its fairlead displacements following the direction of this mooring line. The maximum offsets expected for the line 2 moored to ACTIVEFLOAT platform at Gran Canaria site under DLCs 6.1 and 6.2, are [-55 m, 25 m].

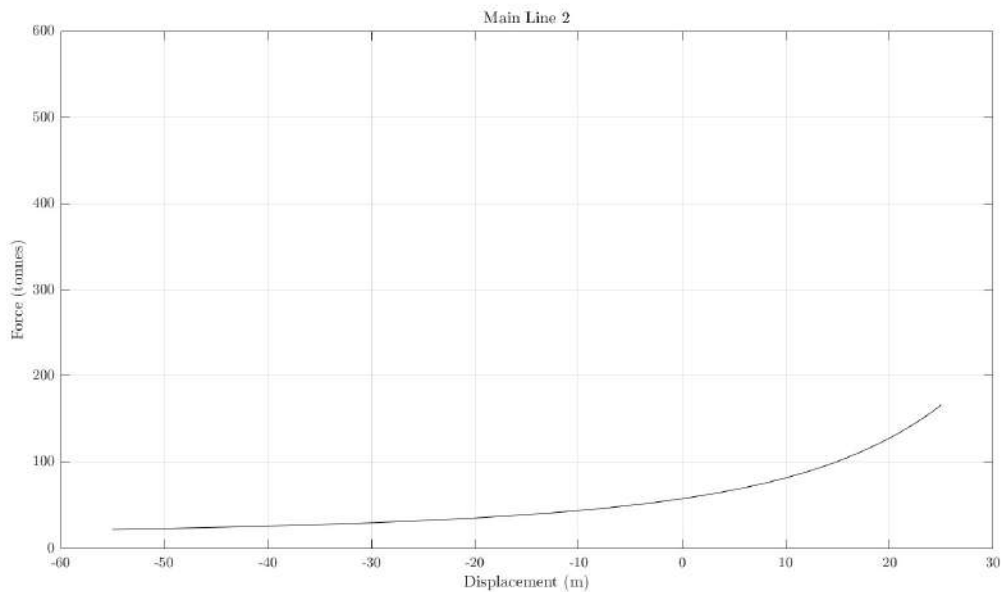


Figure 3-14. Mooring forces of Line 2 vs its fairlead displacements

3.2.3 Dynamic power export cable

The ACTIVEFLOAT platform includes the JDR high voltage cable with 66 kV rating selected is the same CW002 size, whose mechanical characteristics are already presented in Table 3-5.

The dynamic cable is designed as a lazy wave configuration (Figure 3-8) which provides lift to at a midwater buoyant section by attached 16 buoyancy modules, decoupling the dynamic motions of the platform from the Touchdown Point fixed on the subsea end.

The details of the polyurethane dynamic Bend Stiffener (BSR) which works as a transition piece between the J-Tube and the dynamic cable, are already presented in Table 3-6.

In Deliverable D3.2 [11], the cabling system is configured equidistant between mooring lines 2 and 3, orientated with x-axis in the leeward side when the platform is located at 0°. The connection point is between the two pontoon corners of the leeward side at 10 m depth below the bottom of pontoons.

3.3 Wind turbine

The wind turbine selected for both cases is the IEA 15MW. From Deliverable D1.1 [12], the turbine generator is a three-bladed upwind rotor with a diameter of 240 m, located 150 metres above mean sea level. The other key features are: (1) a 10.59 m/s rated wind speed, (2) a direct drive generator and (3) a provisional bend-twist coupled design in the HAWC2 version, intending to reduce the loads around rated wind speed. The overall parameters for the turbine are stated in Table 3-14.

Parameter	IEA 15MW turbine
Turbine Class	IEC Class 1B
Specific rating	332 W/m ²
Rotor orientation	Upwind
Control	Variable speed, collective pitch

Cut-in wind speed	3 m/s
Rated wind speed	10.59 m/s
Cut-out wind speed	25 m/s
Rotor diameter	240 m
Hub height	150 m
Hub diameter	7.94 m
Drive train	Low speed, direct drive
Design tip speed ratio	9.0
Minimum rotor speed	5.0 rpm
Maximum rotor speed	7.56 rpm
Maximum tip speed	95 m/s
Shaft tilt angle	6 deg
Rotor pre-cone angle	-4.0 deg
Blade pre-bend	4 m
Blade mass	65 t
RNA mass	1017 t
Tower mass	860 t
Tower diameter at base	10 m

Table 3-14. Overall parameters for the IEA 15MWturbine [13]

The controller regulation trajectory, the power and thrust curves, as well as the aerodynamic performance coefficients are draw as a function of the wind speed in Figure 3-15.

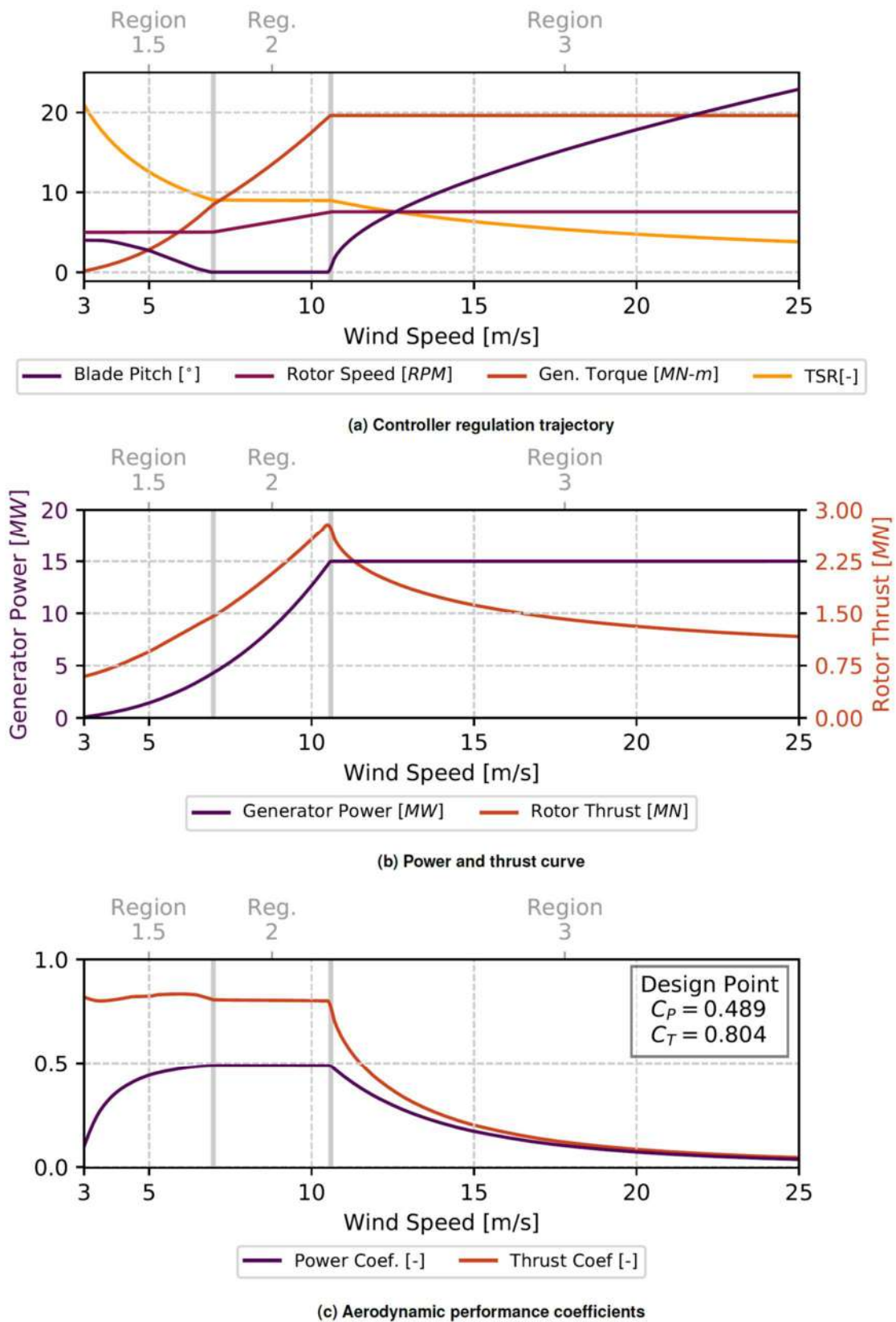


Figure 3-15. OpenFAST blade element momentum performance and operation of the 15-MW rotor with the ROSCO controller [13]

4 PHYSICAL MODELLING: Hydrodynamic tests

4.1 The facility: Cantabria Coastal and Ocean Basin (CCOB)

The CCOB is a combination of three integrated systems to be used in the applied research of coastal and offshore engineering; these being: (1) an experimental management system, (2) a numerical modelling system and (3) a physical modelling system. The main goal of the physical modelling system is to carry out testing to measure hydrodynamic and wave-structure interaction processes which can include the sediment transport effects, the effects of tsunamis and the wave-current and wave-wind interaction. The physical modelling system includes: a) generation of multidirectional waves, wind and currents in a large basin capable of operating at many different water depths, from shallow to deep waters; b) a wave/current flume able to generate waves, including long-waves such as tsunamis, and following or opposing currents; c) a large open-area reserve for physical modelling of undefined boundary studies, such as river meanders, estuaries and ports; and d) a recently refurbished shallow water multidirectional wave basin.

The numerical modelling system includes several numerical bi- and three-dimensional models, representing the channel and the wave basins as mirrors of the physical modelling facilities.

The experimental Management system integrates both the numerical and physical modelling Systems to: 1) optimize the design, construction and measurement process during the laboratory experiments, 2) calibrate and validate the numerical mirrors with the test results, and 3) generate additional numerical cases which assist in the design of alternatives or extend the applicability of the empirical formulations. The numerical mirrors in both the channel and basin are offered to external researchers as part of the services included within the CCOB facilities.

The CCOB is framed within the Singular Techno-Scientific Facilities (ICTS) of the Spanish Ministry for Science and Innovation in which the Government of Cantabria participates financially while being managed by the Environmental Hydraulics Institute Foundation. The construction and set up of this facility have required an investment of over 35 million Euros, provided by the Spanish Ministry for Science and Innovation and the Regional Government of Cantabria.

CCOB applications include marine hydrodynamics, flow-structure interaction, coastal engineering, port engineering, maritime works and coastal protection structures, study of tsunamis and coastal risk, offshore technology, safety and reliability of marine structures, offshore platforms, marine renewable energy, floating structures, marine geotechnics, materials engineering for marine environment, design of submarine vehicles, design of oceanographic instrumentation, analysis of constructive systems in the marine environment, as well as nuclear power plant applications and device testing.

Table 4-1 shows the Multidirectional Wave Basin main characteristics.

Length	30 m
Width	44 m
Minimum dept	0.2 m
Maximum depth	3.7 m
Pit	6 m in diameter, 8 m depth, allows testing in maximum depths of almost 12 m. Includes a floating lid for variable depth testing

Maximum available testing area	760 m ²
Wave generation	Segmented system formed by 64 independent wave paddles (0.5m wide and 4.5 m high). Each one is triggered by two articulated arms and a vertical connecting rod. Full 3D active wave absorption. Passive wave absorbers around the full perimeter. Non-linear wave generation, and second order long-wave generation. Lateral panels for directional wave generation with virtual paddles (corner reflection method, increases the width of the wave machine)
Generation mode	Piston and combined
Actuator systems	Hydraulic pistons, configured in 2 interconnected hydraulic groups which are commutable and with Nitrogen accumulators. Ability to disengage and block individually each wave paddle for special applications.
Generated wave characteristics	$H_{max} = 1.1$ m, $T = 3$ s (regular waves) $H_{m0} = 0.6$ m y $T_p = 3$ s (random waves) ($h=3$ m) $T_p = 0.5$ s – 20 s for $h=0.2$ to 3.7 m Multidirectional long- and short-crested waves ($\pm 45^\circ$, $\pm 60^\circ$ for longer waves)
Current generator	12 thrusters, 900 mm in diameter and 25 kW/thruster
Currents	Nominal design currents 0.2 m/s at a depth of 3 m, which is equivalent to a flow rate of 19.2 m ³ /s perpendicular to the wave generation device
Wind generator	Group of 9 computer controlled wind fans mounted on a closed portable and variable height frame with a wind stabilisation system and funnel
Wind characteristics	Nominal design wind above 10 m/s, 1 m from the fans covering an area which is 2.3 m wide by 2.3 m high
Power	Wave generator device: 950kW Current generator device: 300 kW Wind generator device: 100 kW
Filling and draining system	Fully automated and controlled, with 4 submersible pumps with a total discharge of 400 l/s available for all facilities in the laboratory
Lifting capacities	10 ton bridge crane spanning the full laboratory length and width

Table 4-1. Multidirectional Wave Basin main characteristics

Figure 4-1 shows the Cantabria Coastal and Ocean Basin while tests are being conducted.

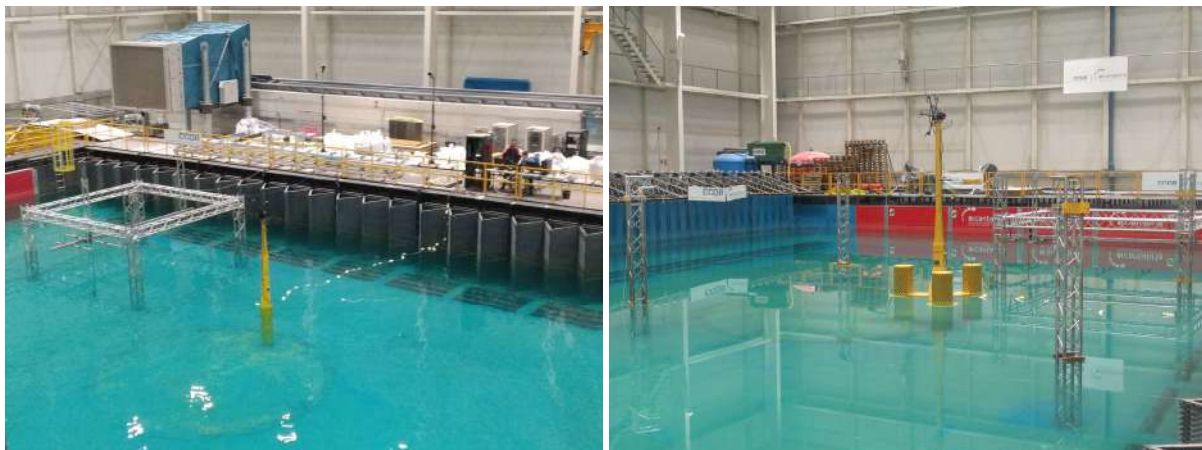


Figure 4-1. Cantabria Coastal and Ocean Basin (CCOB)

4.2 Description of the scaling laws of similitude

Normally, the scaling of hydraulics models is carried out applying the Froude scaling laws of similitude, which keeps constant the inertial and gravity forces at full and laboratory scales (Equation 1, Froude Number). It must be noticed that in waves gravity is the primary restoring force.

$$F_r = \frac{U}{\sqrt{gh}} \quad \text{Equation 1}$$

Where, U is the flow speed, g is the acceleration due to gravity and h is water depth.

However, in some cases the influence of the fluid viscosity may be important. Then, other approaches, such as the Reynolds similitude (Equation 2) should be applied to scale the hydrodynamic processes (viscous and turbulent processes).

$$R_e = \frac{UD}{\nu} \quad \text{Equation 2}$$

Where the D is a suitable length scale (water depth or pile diameter), and ν is the kinematic viscosity of the fluid.

Viscous effects can be considered almost null if the Re number based on the water depth is higher than 10000, in those cases the flow can be considered a turbulent flow. In our physical experiments, Re is always higher than 10000 therefore, the Froude scaling laws of similitude will be applied to carry out the wave basin testing campaign.

Moreover, larger models provide more accurate tests of wave-structure interactions and therefore more reliable results because the larger the scale the reduced the scale effects are. Therefore, the best scale factor for a physical (hydraulic) model study usually comes from the balance between working at a large scale to minimize scale effects and working within the constraints of the test facility such as basin dimensions, wave and current generation limits. Considering the geometry of the structure and the mooring, the target water depth, the environmental conditions, and the size of FIHAC facilities (CCOB), the most suitable scale is:

- 1/55 for the WINDCRETE spar-based wind concept.
- 1/40 for the ACTIVEFLOAT semisub-based wind concept.

All results, statistical values and figures/plots of the model tests are presented here as full-scale values. The full-scale results have been obtained by multiplying the measured value by the corresponding scaling factor E_f for the magnitude "f".

$$\text{Full scale Magnitude} = E_f \cdot \text{Model Magnitude (laboratory data)}$$

The Table 4-2 shows the main Froude scaling laws of similitude obtained for the hydrodynamic variables as a function of the geometric scale ($\lambda = 55$ for the WINDCRETE and $\lambda = 40$ for the ACTIVEFLOAT floating concept), for a sea-water density of 1025 kg/m³ and assuming that the cinematic viscosity of salt water and testing water (fresh water) are the same.

Magnitude	Unit	Dimension	Ratio
Length	M	L	λ
Time	S	T	$\sqrt{\lambda}$

Mass	Kg	M	$1.025 \cdot \lambda^3$
Velocity	m/s	LT^{-1}	$v\lambda$
Acceleration	m/s^2	LT^{-2}	1
Force	N	MLT^{-2}	$1.025 \cdot \lambda^3$
EA/L	N/m	MT^{-2}	$1.025 \cdot \lambda^2$
Pressure	Pa	$ML^{-1}T^{-2}$	$1.025 \cdot \lambda$
Re	-	-	$\lambda^{1.5}$

Table 4-2. Froude scaling laws of similitude

4.3 WINDCRETE scaled model design and manufacturing

4.3.1 Platform target values

Considering the dimensions of the FIHAC wave basin (CCOB) as well as the wave and current generator capabilities, it was concluded that 1:55 was the most suitable test scale to carry out the physical experiments on WINDCRETE platform.

Target mass and inertia properties of the prototype are reported at laboratory scale in Table 4-3.

	Mass [kg]	CoGx [m]	CoGy [m]	CoGz [m]	Ixx [kgm ²]	Iyy [kgm ²]	Izz [kgm ²]
SUBMERGED w/o Ballast	67.318						
Ballast	148.885						
SUBMERGED SPAR	216.203	0	0	-2.056	108.365	108.365	3.544
Tower	19.058	0	0	1.212	177.727	177.727	0.169
SPAR	235.260	0	0	-1.791	301.241	301.241	3.712
Wind Turbine	5.981	-0.125	0	2.418	101.147	101.147	0.149
SPAR w/ WT	241.242	-0.003	0	-1.687	404.950	404.950	3.861

Table 4-3. Theoretical mass and inertia properties of WINDCRETE at laboratory scale (E=1/55), in the operational configuration

Target mass properties of the prototype in the installation configuration, without the wind turbine and un-ballasted but not completely to provide enough stability in yaw around its local axes, are reported at laboratory scale in Table 4-4.

	Mass [kg]	CoGx [m]	CoGy [m]	CoGz [m]
SUBMERGED w/o Ballast	67.318			
Ballast	86.138			
SUBMERGED SPAR	153.456	0	0	-2.060
Tower	19.058	0	0	1.212
SPAR	172.514	0	0	-1.699

Table 4-4. Mass properties of WINDCRETE prototype at laboratory scale (E=1/55), un-ballasted and without the wind turbine in the installation configuration

4.3.2 Mockup design

All the physical model is designed in steel, except from the lower hemisphere of the spar which is made of Acrylonitrile Butadiene Styrene (ABS) by means of a 3D printer (Figure 4-2). The junction of this element with the submerged spar is waterproof.

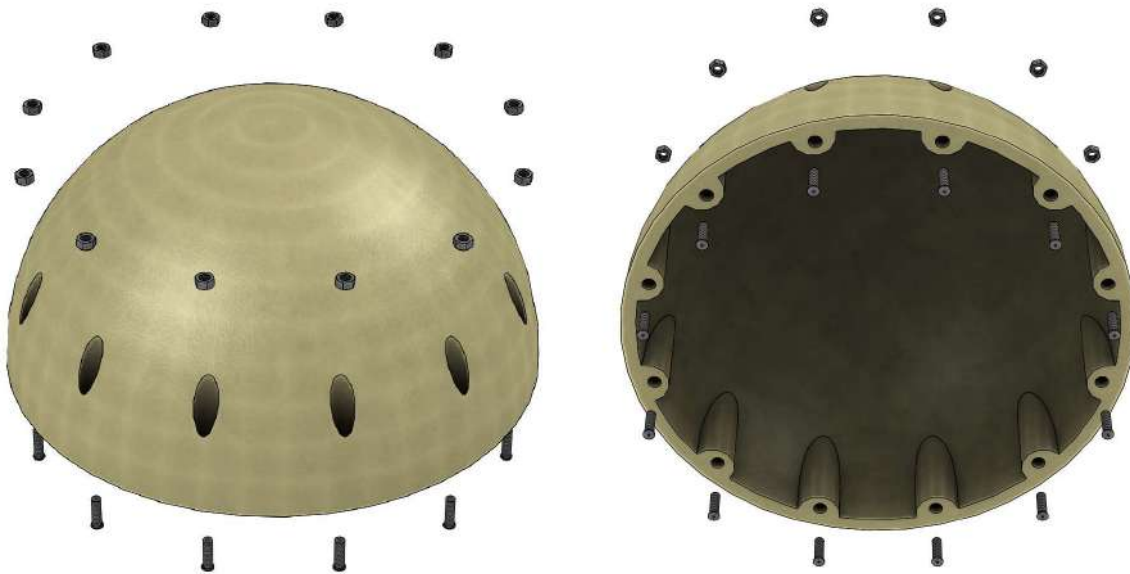


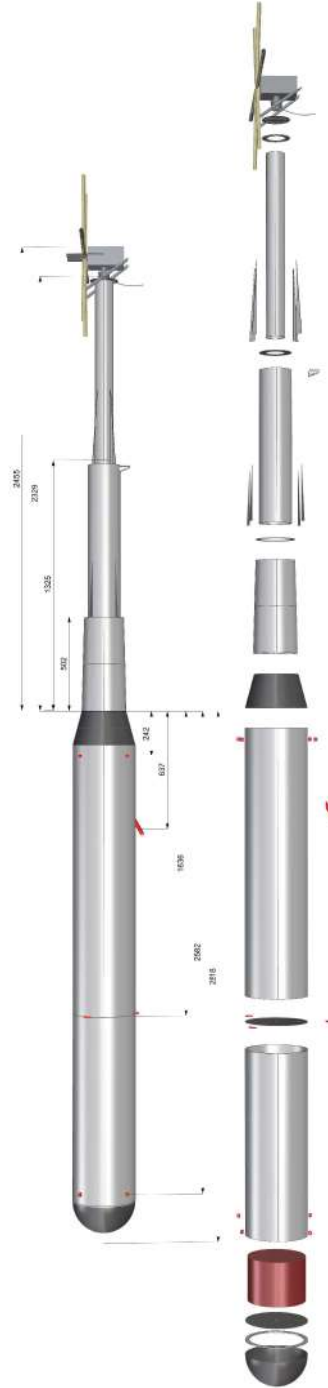
Figure 4-2. Lower hemisphere of the spar printed in ABS

The mass and inertia properties of the designed model, as well as the deviations in comparison to the target values, are presented in Table 4-5.

	Mass [kg]	error [%]	CoGz [m]	error [%]	Ixx [kgm ²]	error [%]	Iyy [kgm ²]	error [%]	Izz [kgm ²]	error [%]
SUBMERGED w/o Ballast	69.752	3.616	-1.400		49.878		49.878		1.860	
Ballast	144.676	-2.827	-2.403		75.842		75.842		1.783	
SUBMERGED SPAR	214.428	-0.821	-2.077	1.022	125.720	16.015	125.720	16.015	3.643	2.798
Tower	19.039	-0.098	0.994	-18.012	145.185	-18.310	145.185	-18.310	0.143	-15.301
SPAR	233.467	-0.762	-1.826	1.973	270.905	-10.070	270.905	-10.070	3.786	1.976
Wind Turbine	7.900	32.081	2.442	0.993	134.762	33.234	134.762	33.234	0.080	-46.403
SPAR w/ WT	241.367	0.052	-1.687	-0.001	405.667	0.177	405.667	0.177	3.866	0.105

Table 4-5. Mass and inertia properties of WINDCRETE designed model at laboratory scale (E=1/55), in the operational configuration

Figure 4-3 includes geometrical and mass properties of the different designed elements that make up the physical model.



	PROTOTYPE			TARGET MODEL			DESIGNED MODEL								
	Mass [kg]	CoG [m]	Ixx [kgm ²]	Iyy [kgm ²]	Izz [kgm ²]	Mass [kg]	CoG [m]	Ixx [kgm ²]	Iyy [kgm ²]	Izz [kgm ²]	error [%]	Ixx [kgm ²]	Iyy [kgm ²]	Izz [kgm ²]	error [%]
SUBMERGED w/o Ballast	1.148E+07					69.232	-3.616					49.878			1.800
Ballast	2.539E+07					144.076	-2.827					75.842			1.783
SUBMERGED SPAR	3.687E+07	-113.058	5.59E+10	5.59E+10	1.83E+09	234.428	-0.827	-2.077	1.022	125.720	16.015	325.720	16.015	16.015	3.643
Tower	3.250E+06	66.659	9.17E+10	9.17E+10	8.70E+07	19.039	-0.098	0.994	-18.012	145.185	-18.310	145.185	-18.310	0.143	-15.301
SPAR	4.012E+07	-98.500	1.554E+11	1.554E+11	1.92E+09	233.467	-0.762	3.712	177.727	301.241	1.973	270.905	-10.070	270.905	3.786
Wind Turbine	1.020E+06	133.013	5.22E+10	5.22E+10	7.70E+07	7.900	32.081	2.442	0.993	101.147	2.442	134.762	33.234	134.762	0.080
SPAR w/ WT	4.114E+07	-92.760	2.089E+11	2.089E+11	1.99E+09	241.242	-1.687	-1.687	0.052	404.950	-1.687	405.667	0.177	405.667	3.866



UNIVERSIDAD DE CANTABRIA

Project Engineer:
Sergio GALÁN FRANCO
Bsc. Ingeniero Marino

Project Manager:
Raúl GUANICHE GARCÍA
PhD. Ingeniero de C. y P.



Project:
Corewind

Title:
WindCres Mass Properties

Scale:
1:1
Dimensions in mm

Sheet:
01
Rev. 0

Figure 4-3 Schematic and breakdown of WINDCRETE designed model with values in millimetres Platform manufacturing

4.3.3 [Mockup manufacturing](#)

Once the mockup is designed, it is built in a metalwork close to FIHAC facilities. Figure 4-4 shows how it is constructed, embedding the ballast.



Figure 4-4. WINDCRETE mockup being manufactured (left) with the ballast embedded (right)

The manufactured model is supplied painted in yellow and with the lugs to be hung (Figure 4-5). Moreover, the lower hemisphere made of ABS is protected with a removable steel strut (painted in red) to avoid any structural damage before entering the wave basin.



Figure 4-5. WINDCRETE manufactured mockup being hung by the lugs at FIHAC facility

A dimensional and weight distribution control are carried out in the dry characterization to ensure the quality of the manufactured mockup, fulfilling the tolerances demanded. The geometric dimensions are checked and the mockup geometry presents a diameter 0.7 mm smaller, what represents a deviation of -0.21%.

The determination of the model weight and CoG position is obtained by hanging the model by a system of chains provided of axial load cells at two chain-model joint points, as shown in Figure 4-6.



Figure 4-6. Weight and CoGz position test (left) and detail of hanging (right)

The inertia is measured by swinging the model with respect to its three main axes. The inertias I_{xx} , I_{yy} and I_{zz} are obtained based on the period of oscillation, the model mass, and with the application of the Huygens–Steiner theorem. Figure 4-7 and Figure 4-8 show some moments of the Inertias characterization.



Figure 4-7. I_{xx} Inertia test (left) I_{yy} Inertia test (centre) and detail of hanging (right)



Figure 4-8. I_{zz} Inertia test (left) and detail of hanging (right)

Table 4-6 reports the values of mass, CoG position and Inertias obtained over the 5 repetitions performed. The theoretical mass is equal to 241.242 kg (target value at laboratory scale). Therefore, there is a negligible

discrepancy between the measured mass and the target value of 0.16%. The target CoGz value is -1.687 m from free surface, thus the deviation with respect to the experimental value is 0.51%. The target Ixx and Iyy values are the same 404.950 kg m², hence the deviations with respect to the experimental values are 1.08% and 0.45%, respectively. The target Izz value is 3.861 kg m², thus the deviation with respect to the experimental value is 3.23%.

	Mass [kg]	CoGx [m]	CoGy [m]	CoGz [m]	Ixx [kg m ²]	Iyy [kg m ²]	Izz [kg m ²]
Measured	241.639	-0.001	0	-1.695	409.312	406.768	3.986
Target	241.242	-0.003	0	-1.687	404.950	404.950	3.861
Deviation	0.397	0.002	0	-0.009	4.362	1.818	0.125
Rel. Deviation [%]	0.16			0.51	1.08	0.45	3.23

Table 4-6. Model weight, CoG position (referred to free surface) and Inertias

Table 4-7 presents the values of mass and CoG position analytically obtained after removing the wind turbine and part of the ballast for the installation configuration. The theoretical mass and CoGz are equal to 172.514 kg and -1.699 m, respectively. Thus, there is no discrepancy between the measured and the target values neither for the mass nor the CoGz.

	Mass [kg]	CoGx [m]	CoGy [m]	CoGz [m]
Measured	172.514	0	0	-1.699
Target	172.514	0	0	-1.699
Deviation	0	0	0	0
Rel. Deviation [%]	0			0

Table 4-7. Model weight and CoG position (referred to free surface), un-ballasted and without the wind turbine in the installation configuration

4.3.4 Mooring system

Target physical properties of chains and calibrated springs to be used at laboratory scale 1:55 are summarized in Table 4-8.

Line #		Chain bar diameter [mm]	Equivalent diameter [mm]	Line Length [m]	Dry mass per meter length [kg/m]	Axial stiffness [kN]
1	Main line	2.02	3.63	12.727	0.079	6.169
	Delta Lines	2.02	3.63	0.909	0.079	6.169
2	Main Line	1.82	3.27	13.636	0.064	5.008
	Delta Lines	2.02	3.63	0.909	0.079	6.169
3	Main Line	1.82	3.27	13.636	0.064	5.008
	Delta Lines	2.02	3.63	0.909	0.079	6.169

Table 4-8. Physical properties of the chain lines used for the optimized mooring system

Table 4-9 reports target anchors and fairleads coordinates at laboratory scale. Because of the limits of the basin dimensions, mooring lines are truncated in both water depth and footprint size. The anchor coordinates after the truncation to perform the experimental tests in the Cantabria Coastal and Ocean Basin (CCOB), are also included.

Line #	Anchor coordinates [m]			Truncated anchor coordinates [m]			Fairlead coordinates [m]		
	X	Y	Z	X	Y	Z	X	Y	Z
1	-13.515	0	-3.636	-8.846	0	-3.000	-0.085	0.146	-1.636
							-0.085	-0.146	-1.636
2	7.206	-12.481	-3.636	4.728	-8.207	-3.000	-0.085	-0.146	-1.636
							0.169	0	-1.636
3	7.206	12.481	-3.636	4.728	8.207	-3.000	-0.085	0.146	-1.636
							0.169	0	-1.636

Table 4-9. Mooring system anchors and fairlead location (truncated)

The truncation cases were very demanding, where in case of the horizontal span 4% has truncated, but in case of the vertical span 35% of it was truncated. The methodology for single mooring lines static truncation based in the catenary equations and evolutionary optimization algorithms has been applied. The truncated mooring system is designed as simple as possible, to reduce uncertainties and simplify numerical models validation. To avoid complex truncated mooring systems, only the main lines are truncated using simple spring. Extra clump weights are added to capture properly the original line pretension. The truncated line may not capture perfectly the dry mass of the real line, in order to compensate the rate at which mass is lifted from the seabed. Figure 4-9 shows the comparison of tension-surge excursion curves between objective and truncated main lines. For the main line 1, the vertical pretension relative error is 0.32 %. The objective angle at fairlead is 19.96° and the truncated one is 20.55°. Respecting the main lines 2-3, the vertical pretension relative error is 0.04 %. The target angle at fairlead is 18.23° and the truncated one is 19.32°.

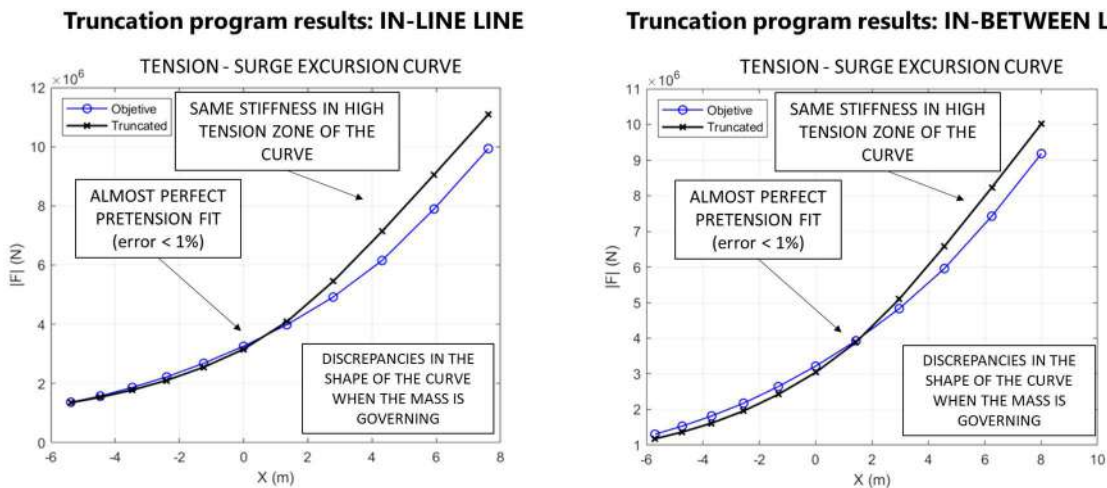


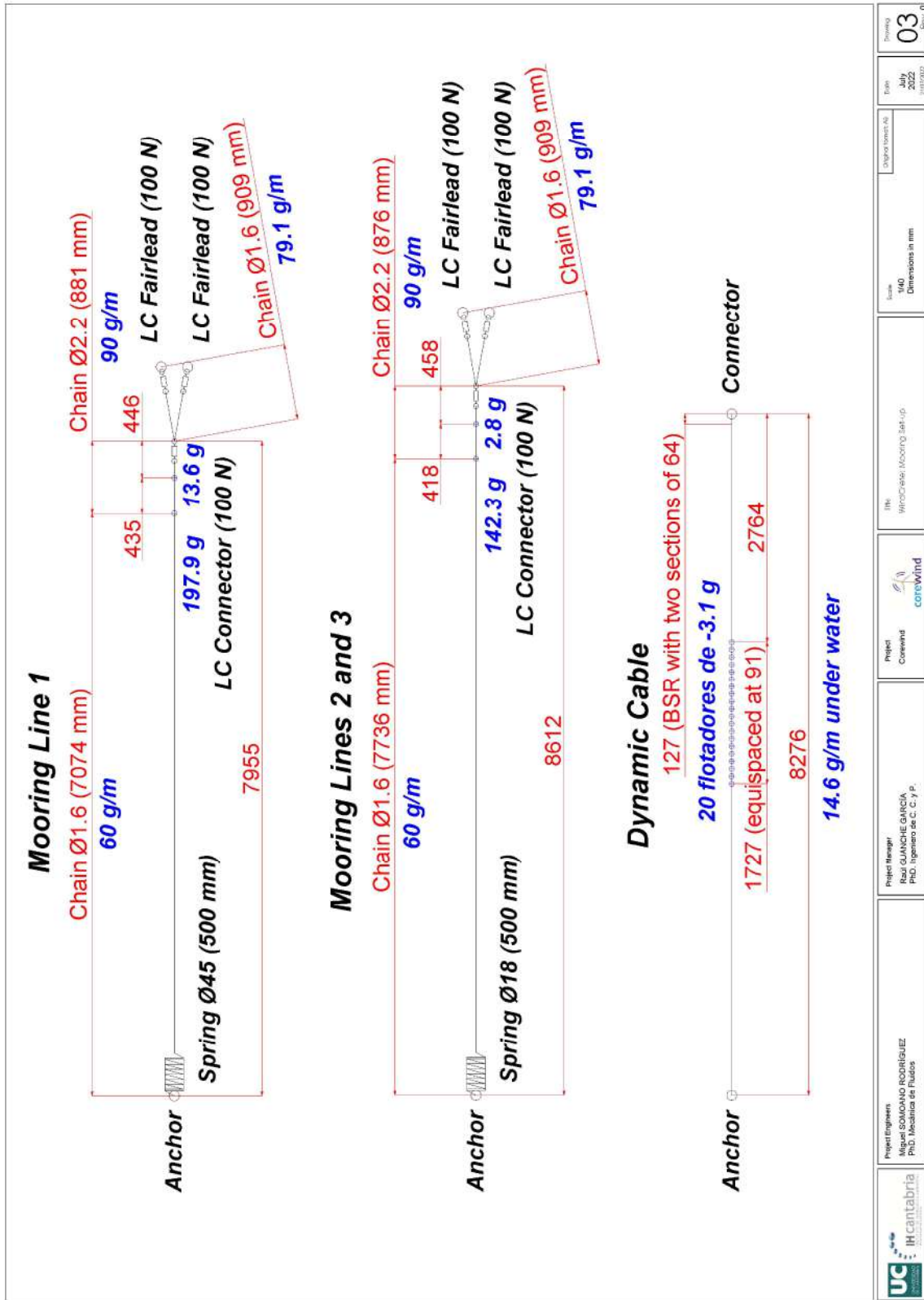
Figure 4-9. Comparison of tension-surge excursion curves between objective and truncated main line 1 (left) and main lines 2-3 (right)

Table 4-10 shows the truncated line details. The 0.881 m of chain in line 1 and the 0.876m in lines 2 and 3 which had to weight 0.090 kg/m, weight actually 0.086 kg/m. And the 0.909 m of delta lines weight 0.080 kg/m, instead of 0.079 kg/m. The relative deviations are below 5%, being -4.44% and 1.27%, respectively. The 7.074 m of chain in line 1 and the 7.736m in lines 2 and 3 are manufactured adding distributed weights to get the target 0.060 kg/m.

Line #		Line Length (including spring, load cells and connectors) [m]			Dry mass per meter length [kg/m]			Intermediate weights [kg]		K spring [N/m]
1	Main line	7.074	0.435	0.446	0.060	0.090 designed 0.086 as-built	0.090 designed 0.086 as-built	0.198	0.014	374
	Delta Lines	0.909			0.079 designed 0.080 as-built			-		-
2	Main Line	7.736	0.418	0.458	0.060	0.090 designed 0.086 as-built	0.090 designed 0.086 as-built	0.142	0.003	323
	Delta Lines	0.909			0.079 designed 0.080 as-built			-		-
3	Main Line	7.736	0.418	0.458	0.060	0.090 designed 0.086 as-built	0.090 designed 0.086 as-built	0.142	0.003	323
	Delta Lines	0.909			0.079 designed 0.080 as-built			-		-

Table 4-10. Line details of the truncated mooring system

Figure 4-10 presents the set-up of each truncated mooring line including spring, load cells and connectors.



Project Manager Rafael GUANACHE GARCIA PhD, Ingeniero de C. y P.	Project Corewind	File WindCable_Mooring Set-Up	Scale 1:10 Dimensions in mm	Date July 2018 18/07/2018	Revisión 03
--	---------------------	----------------------------------	-----------------------------------	---------------------------------	----------------

Figure 4-10. Set-up of mooring lines and dynamic cable

In all sections, the spring, load cells and connectors are provided with floaters to obtain the same wet weight as the chains used. Figure 4-11 shows images of the resulting mooring lines once manufactured.



Figure 4-11. Manufactured mooring line 1 (top) and mooring lines 2-3 (bottom)

The actual springs have axial stiffness of 372 N/m in line 1 and 333 N/m in lines 2 and 3. The relative deviations respect the target ones are also below 5%, being a -0.46% in the main line 1 and a 2.95% in the main lines 2-3. Figure 4-10 shows the validation tests of both springs by means of a set of axial tests.

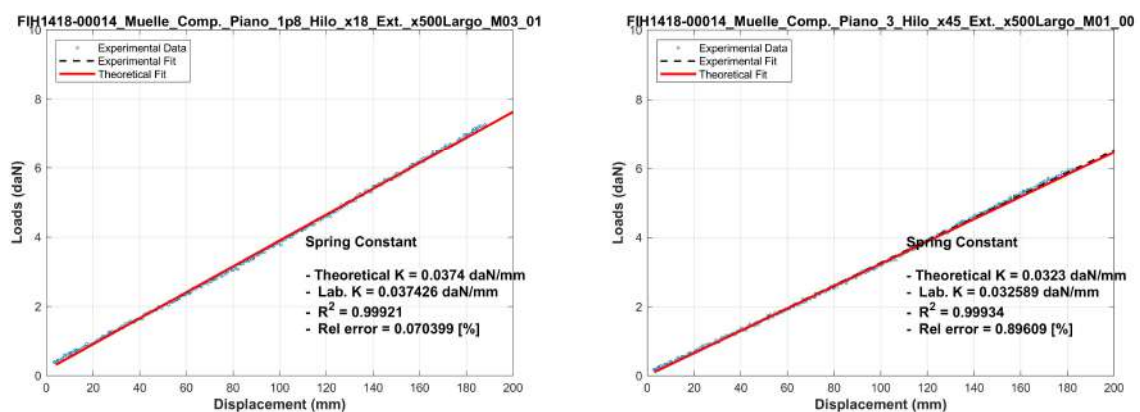


Figure 4-12. Example of axial tests to springs in main line 1 (left) and main lines 2-3 (right)

The layout of all the mooring system inside the Cantabria Coastal and Ocean Basin (CCOB) is shown in Section 4.7.

4.3.5 [Soft-mooring system for installation tests](#)

Table 4-11 and Table 4-12 show the soft-mooring line details for the installation tests of the WINDCRETE un-ballasted and without the wind turbine in horizontal position and the raising-up tests, respectively.

Line #	Line Length (including spring, load cells and connectors) [m]	K spring [N/m]
1	6.039	1.4
2	6.039	1.4
3	7.686	1.4
4	7.686	1.4

Table 4-11. Line details of the soft-mooring system for installation tests

Line #	Line Length (including spring, load cells and connectors) [m]	K spring [N/m]
1	7.686	1.4
2	7.686	1.4

Table 4-12. Line details of the soft-mooring system for raising-up tests

Figure 4-13 and Figure 4-14 present the set-up of each soft-mooring line for the installation tests of the WINDCRETE un-ballasted and without the wind turbine in horizontal position and the raising-up tests, respectively, including spring, load cells and connectors.

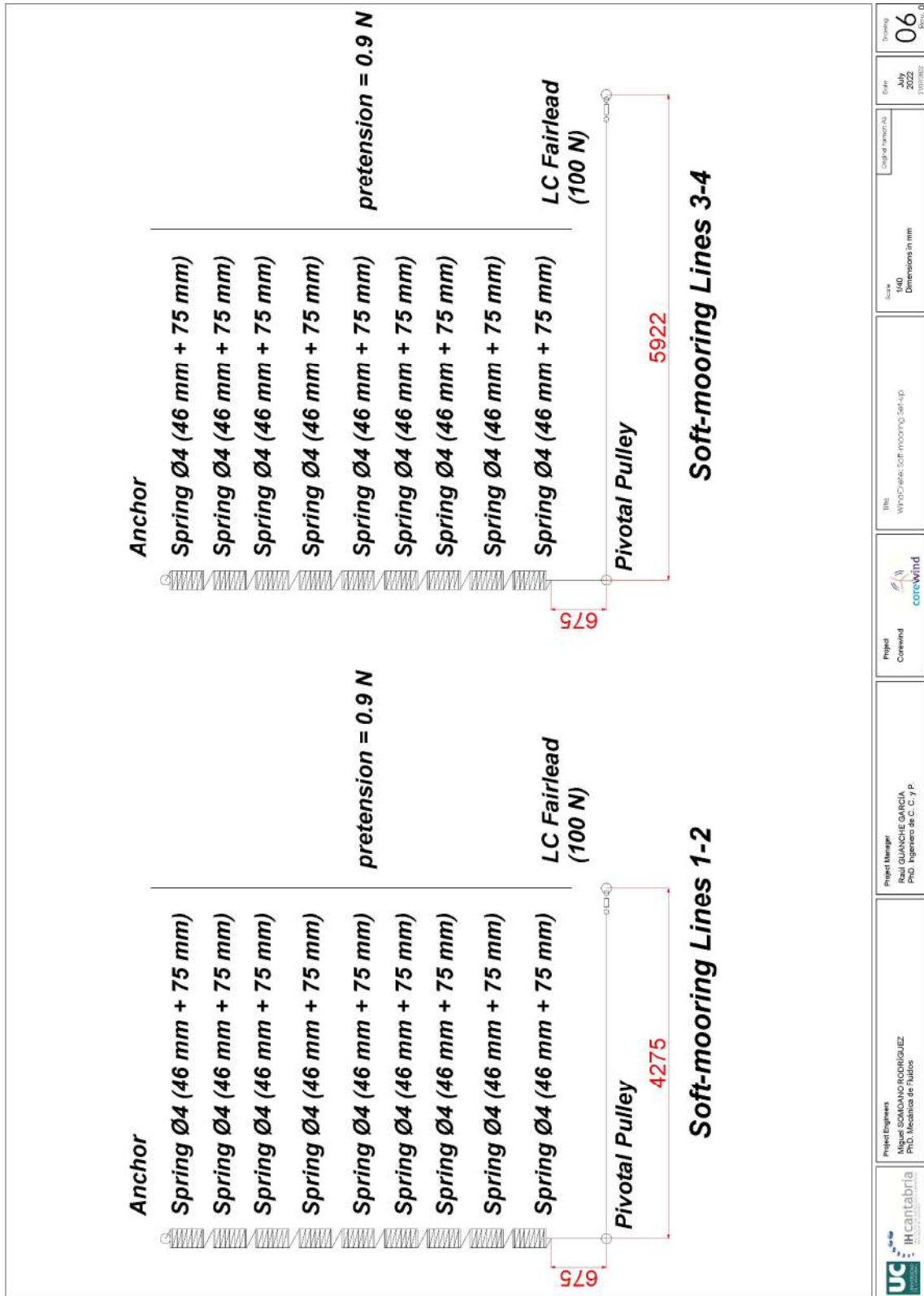


Figure 4-13. Set-up of soft-mooring lines for installation tests

		Project Engineers Algoel SOMOLANO RODRIGUEZ PhD. Mechanical Engineer	Project Manager Real GUANCHÉ GARCÍA PhD. Engineer in C. y P.	Project Corewind		File WTCables_Soft-mooring_Set-up	Scale 1:100 Dimensions in mm	Drawn July 2018 13/07/2018	Revising 06 13/07/2018
---	---	---	---	----------------------------	--	---	---	---	-------------------------------------

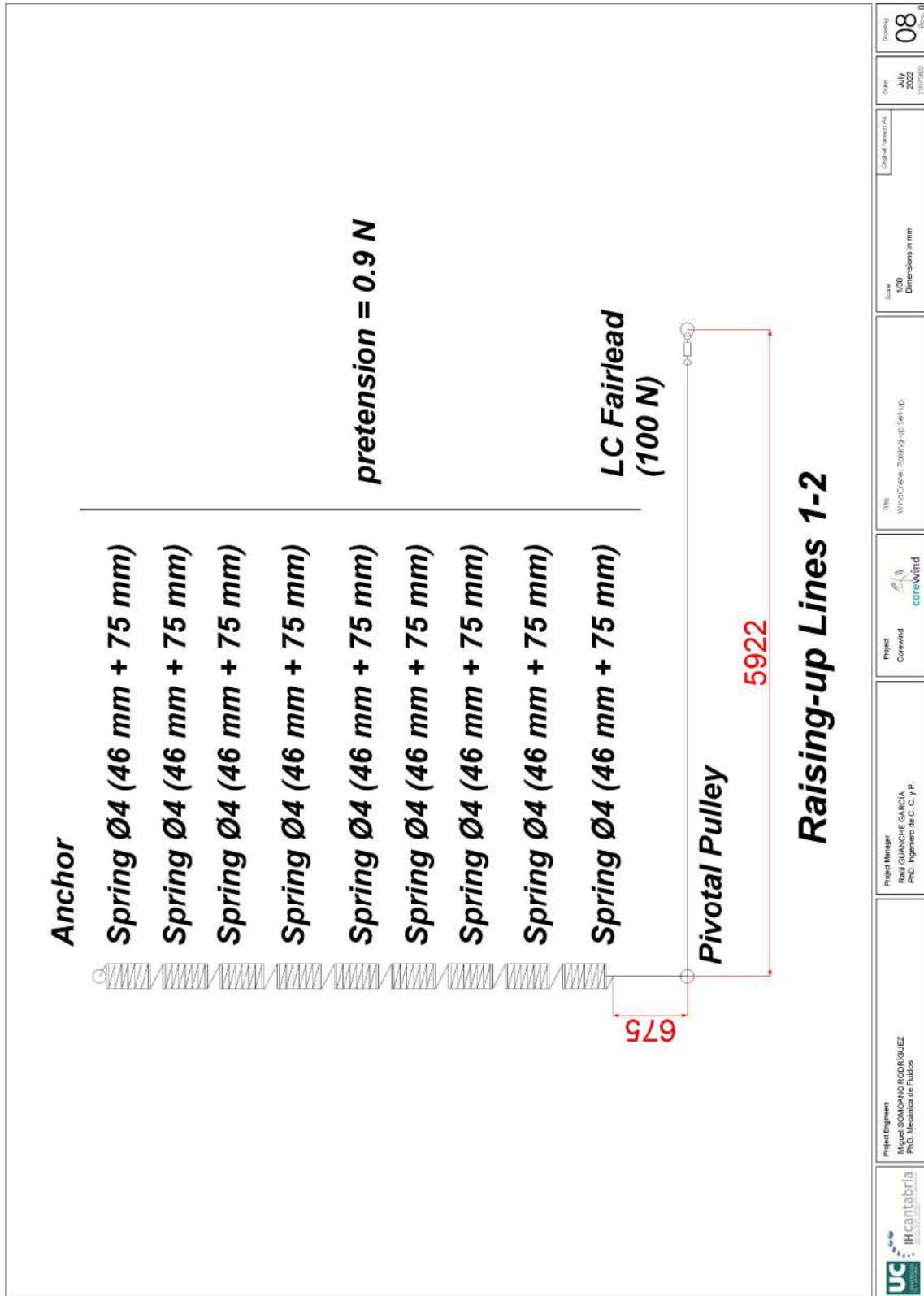


Figure 4-14. Set-up of soft-mooring lines for raising-up tests

Lines used a cable of 2mm diameter in order to be stiff as well as light. The nine actual springs in series provide an axial stiffness of 1.4 N/m in soft-mooring lines, with no deviation respecting the target one. Figure 4-15 shows the validation tests of a spring by means of a set of axial tests.

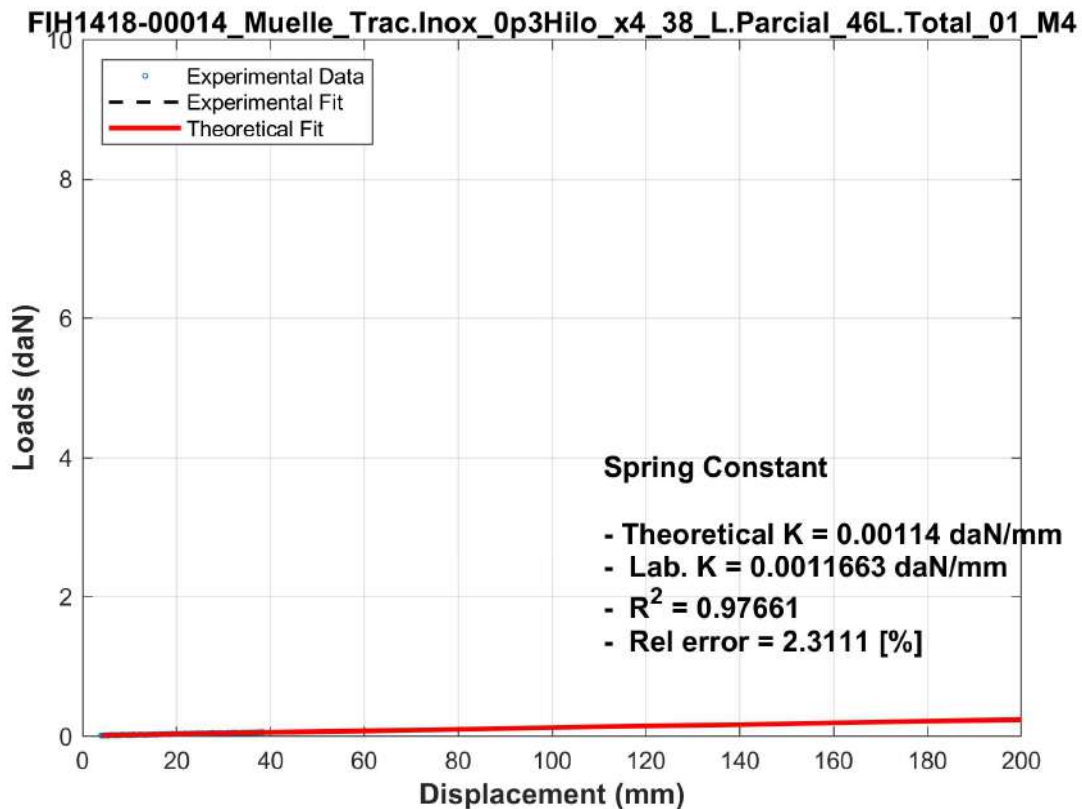


Figure 4-15. Example of axial tests to a spring in soft-mooring lines

The layout of all the soft-mooring system inside the Cantabria Coastal and Ocean Basin (CCOB) is shown in Section 4.7.

4.3.6 [Dynamic cable](#)

The dynamic cable to be used at laboratory scale 1:55 has a target bending stiffness of $4.3 \times 10^{-5} \text{ N m}^2$. To select an appropriate elastic material, we use the catalogue generated for previous Task 5.3 within Deliverable D5.2 [1].

The Bend Stiffener (BSR) works as a transition piece between the J-Tube and the dynamic cable, and to simulate the optimisation of the stiffness profile along its length, its 0.127 m are divided into two sections with higher bending stiffness by adding one (in the section connected to the dynamic cable) and two heat shrink tubing (in the stiffer section connected to the J-Tube).

Because of the limits of the basin dimensions, dynamic cable is truncated in water depth as can be seen in Table 4-13.

Truncated anchor coordinates [m]			Connector coordinates [m]		
X	Y	Z	X	Y	Z
6.966	0	-3.000	0.205	0	-0.664

Table 4-13. Dynamic cable anchor and connector location

Details of truncated cable are presented in Table 4-14.

	Line Length (including connectors) [m]		Wet mass per meter length [kg/m]	Bending Stiffness [kg m ²]	
Dynamic Cable	8.276		0.0146	5.8 x 10 ⁻⁵	
BSR	0.064	0.064	0.0146	2.1 x 10 ⁻⁴	5.3 x 10 ⁻⁴

Table 4-14. Details of the truncated dynamic cable

In the buoyant section, there are 20 buoyancy modules of 3.1 g of net buoyancy force equally spaced at 91 mm, as described in Figure 4-10. When manufactured, the buoyant section is displaced 10 mm towards the anchor, what implies a deviation of 0.36%. An image of the manufactured buoyant section is shown in Figure 4-16.



Figure 4-16. Manufactured buoyant section

4.3.7 Aerodynamic generation by the FIHAC's multi-fan system

The turbine aerodynamic loads are defined and generated by means of a Hardware In the Loop (HIL) layout developed at FIHAC (Pat. ES 2 632 187 B1). The setup involves the FIHAC Multi-fan system, a device that permits to generate with high fidelity the rotor aerodynamics.

Such strategy is intended to simulate the aerodynamic loads acting on the turbine in real time and reproduce them at the same time, avoiding the scale conflicts that notoriously affect this kind of model tests. The loads definition is obtained by means of a numerical module integrated within the HIL layout, which is based on a Blade Element Momentum method (BEM). This setup permits to generate the desired thrust related to constant and turbulent winds in both operational and extreme conditions, as well as reproduce the occurrence of grid and controller failures.

The aforementioned numerical module is fed in real time with the position of the model. This information is expressed by the 6 DoF that define the platform rigid body position and orientation, allowing to link the physical test with its numerical counterpart. The describe procedure is also known as Real Time Hybrid Modelling (ReaTHM) method. This implies that the aerodynamic thrust experienced by the platform is dependent to:

- *Platform movement.* Tracked and passed to the aerodynamic module by Qualisys®, a high accuracy tracking motion system based on visual sensors (described in section 4.5).
- *Rotor aerodynamics.* Defined based on the geometrical and aerodynamic characteristics of the airfoil mounted on the blades. Such information is defined in each point of the rotor discretization.

- *Inflow wind data.* The simulated wind is passed to the aerodynamic module by means of full-field input files. Such data is provided in binary format and is based on the coherence models indicated on the IEC standards. The turbulence model used is the Kaimal model.
- *Controller strategy.* The effects of the controller operations on the thrust forces are considered by the integration of Servodyn in the aerodynamic module. Servodyn is an open-source code developed at NREL (US National Renewable Energy Laboratory) and used to apply different rotor control strategies by operating the blades pitch angle, the generator torque, the nacelle yaw angle and other features. ServoDyn is optionally run by reading a bladed-style external dll.

Physical properties of FIHAC Multi-fan

The reproduction of the aerodynamic forces is assigned to a device constituted by an array of six fans operated independently to minimize the error related to the generated loads. The array is mounted at the tower top of the mockup to maintain the correspondence between the position of the resultant of the forces generated by the Multi-fan itself and the centre of the turbine rotor. Figure 4-17 shows a view of the IHC Multi-fan.



Figure 4-17. FIHAC Multi-fan mounted on the top of the mockup

Hardware-In-the-Loop (HIL)

The HIL method is a RealTime Hybrid Model (ReaTHM) testing procedure that during the last years has gained considerable popularity for its capacity to overcome some critical issues existing in wave basin tests when involve wind turbine models.

A critical barrier present in basin tests campaigns with wind turbines regards the scalability of the aerodynamic forces. In fact, a reliable reproduction of the hydrodynamics forces to scale the model by following the Froude law which respects the ratio between inertia and mass forces, conversely does not permit to obtain a correct correspondence between the prototype and model Reynolds numbers. The latter parameter governs the

aerodynamic behaviour of airfoils, hence the utilization of the Froude scaling law in a wind turbine rotor would result in a deficit in the aerodynamic forces reproduced.

These difficulties are eliminated by assigning the definition of the aerodynamic loads to a numerical code, and the reproduction of the same loads to an actuator acting on the physical model, in this case placed in correspondence with the scaled turbine hub.

The implementation of the HIL method reproduces numerically, in prototype scale, the wind turbine rotor and the incoming wind. The numerical representation of the turbine includes the definition of the geometry of the structure and the aerodynamic characteristics of the rotor, as well as the wind turbine controller. The numerical modules calculate the aerodynamic forces also considering the turbine movements which contribute to the calculation of the relative wind speed seen by the rotor. Such information is provided by an optical tracking system which traces the platform model position in subsequent instants, allowing to derive the translational and rotational speed of the platform. Before being provided to the numerical code, positions and velocities are upscaled to prototype scale. The aerodynamic force definition is carried out by an unsteady BEM model. The solution of the problem in prototype scale allows to avoid the aforementioned scale conflicts.

During the same loop the aerodynamic forces are scaled back to model scale and used to operate the multi-fan system to reproduce the correct scaled force at the hub height of the mockup.

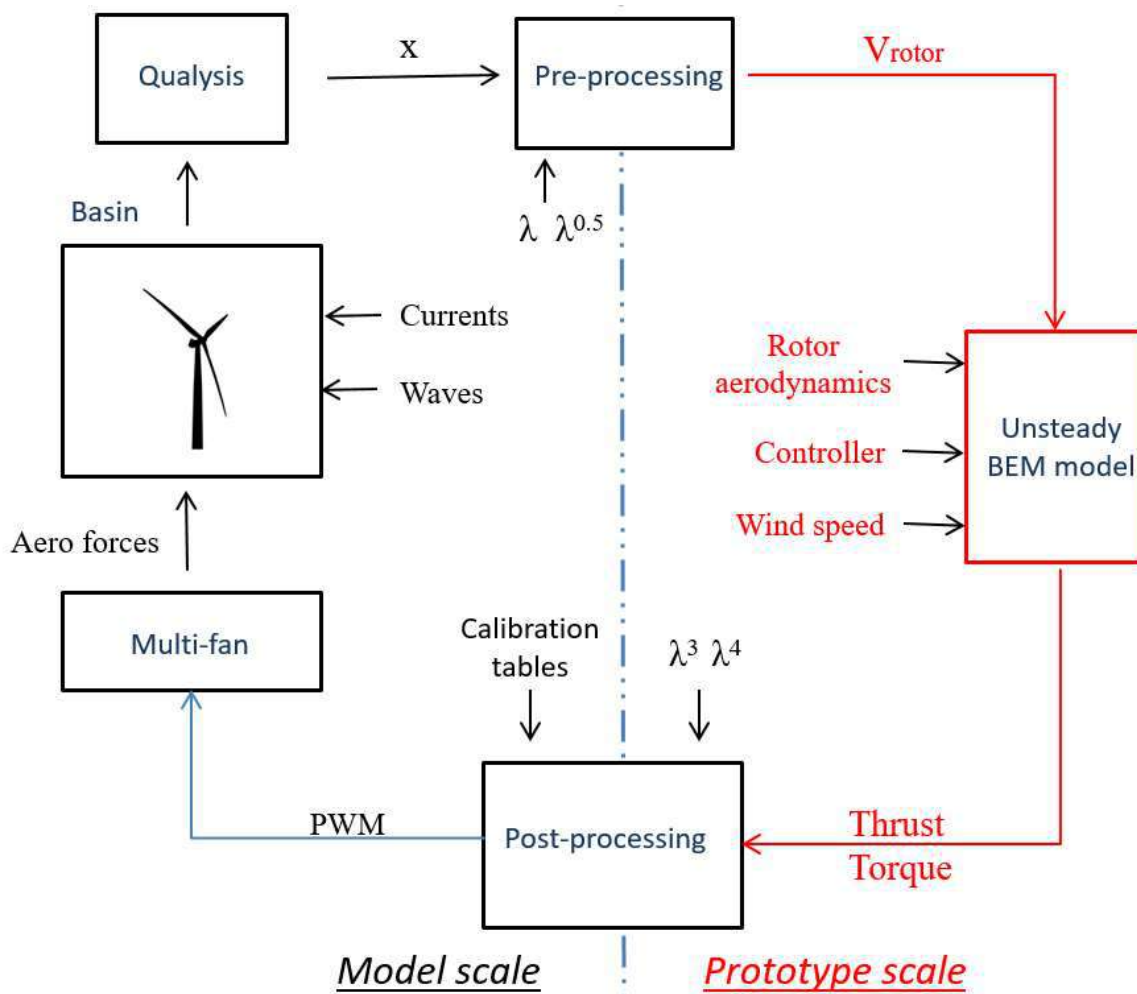


Figure 4-18. Hardware-In-the-Loop diagram included in the basin testing campaign [14]

4.4 ACTIVEFLOAT scaled model design and manufacturing

4.4.1 Platform target values

Considering the dimensions of the FIHAC wave basin (CCOB) as well as the wave and current generator capabilities, it is concluded that 1:40 is the most suitable test scale to carry out the physical experiments on ACTIVEFLOAT platform.

Target mass and inertia properties of the prototype are reported at laboratory scale in Table 4-18 to Table 4-17.

Table 4-15 shows the main characteristics of the ACTIVEFLOAT platform in the operational configuration (draft of 26.5 meters) when the pontoons are fully ballasted, and the tanks are evenly ballasted. Note that SEMI-SUBMERSIBLE is composed of SURMERGED SEMI-SUBMERSIBLE and Tower + internals + equipment.

EVENLY BALLASTED	Mass [kg]	CoGx [m]	CoGy [m]	CoGz [m]	Ixx [kgm ²]	Iyy [kgm ²]	Izz [kgm ²]
SUBMERGED w/o Ballast	323.941	0	0	-0.393	103.883	103.883	151.226
Permanent Ballast	114.755	0	0	-0.515			
Tank 1 Ballast	28.357	-0.850	0	-0.527			
Tank 2 Ballast	28.357	0.425	-0.736	-0.527			
Tank 3 Ballast	28.357	0.425	0.736	-0.527			
Active Ballast	85.072	0	0	-0.527			
TOTAL BALLAST	199.827	0	0	-0.520	57.608	57.608	89.328
SUBMERGED SEMI-SUBMERSIBLE	523.768	0	0	-0.442	161.491	161.491	240.553
Tower + internals + equipment	18.117	0	0	1.423	69.970	69.970	0.183
SEMI-SUBMERSIBLE	541.886	0	0	-0.379	231.461	231.461	240.736
RNA	15.495	-0.176	0	3.346	203.380	203.464	0.197
SEMI-SUBMERSIBLE w/ WT	557.381	-0.005	0	-0.276	434.841	434.925	240.933

Table 4-15. Theoretical mass and inertia properties of ACTIVEFLOAT at laboratory scale (1/40), evenly ballasted in the operational configuration

Table 4-16 shows the main characteristics of the ACTIVEFLOAT platform in the operational configuration when there is no wind, and the active ballast compensates the deviation of the CoGx due to the RNA.

BALLASTED 0m/s	Mass [kg]	CoGx [m]	CoGy [m]	CoGz [m]
SUBMERGED w/o Ballast	323.941	0.000	0.000	-0.393
Permanent Ballast	114.755	0.000	0.000	-0.515
Tank 1 Ballast	26.224	-0.850	0.000	-0.536
Tank 2 Ballast	29.424	0.425	-0.736	-0.523
Tank 3 Ballast	29.424	0.425	0.736	-0.523
Active Ballast	85.072	0.032	0.000	-0.527
TOTAL BALLAST	199.827	0.014	0.000	-0.520
SUBMERGED SEMI- SUBMERSIBLE	523.768	0.005	0.000	-0.442
Tower + internals + equipment	18.117	0.000	0.000	1.423
SEMI- SUBMERSIBLE	541.886	0.005	0.000	-0.379
RNA	15.495	-0.176	0.000	3.346
SEMI- SUBMERSIBLE w/ WT	557.381	0.000	0.000	-0.276

Table 4-16. Theoretical mass properties of ACTIVEFLOAT at laboratory scale (1/40), ballasted in the operational configuration with no wind

Table 4-17 shows the main characteristics of the ACTIVEFLOAT platform in the operational configuration when there is rated wind at 0° and the active ballast compensates the thrust.

BALLASTED 10.5m/s at 0°	Mass [kg]	CoGx [m]	CoGy [m]	CoGz [m]
SUBMERGED w/o Ballast	323.941	0.000	0.000	-0.393
Permanent Ballast	114.755	0.000	0.000	-0.515
Tank 1 Ballast	34.836	-0.850	0.000	-0.502
Tank 2 Ballast	25.118	0.425	-0.736	-0.540
Tank 3 Ballast	25.118	0.425	0.736	-0.540
Active Ballast	85.072	-0.097	0.000	-0.524
TOTAL BALLAST	199.827	-0.041	0.000	-0.519
SUBMERGED SEMI- SUBMERSIBLE	523.768	-0.016	0.000	-0.441
Tower + internals + equipment	18.117	0.000	0.000	1.423
SEMI- SUBMERSIBLE	541.886	-0.015	0.000	-0.379
RNA	15.495	-0.176	0.000	3.346
SEMI- SUBMERSIBLE w/ WT	557.381	-0.0197	0.000	-0.275

Table 4-17. Theoretical mass properties of ACTIVEFLOAT at laboratory scale (1/40), ballasted in the operational configuration with rated wind at 0°

Table 4-18 shows the main characteristics of the ACTIVEFLOAT platform in the installation configuration when all the three tanks and pontoons are un-ballasted.

UN- BALLASTED	Mass [kg]	CoGx [m]	CoGy [m]	CoGz [m]	Ixx [kgm ²]	Iyy [kgm ²]	Izz [kgm ²]
SUBMERGED w/o Ballast	323.941	0	0	-0.393	120.326	120.326	151.226
Tower + internals + equipment	18.117	0	0	1.423	61.899	61.899	0.183
SEMI- SUBMERSIBLE	342.058	0	0	-0.297	182.225	182.225	151.409
RNA	15.495	-0.176	0	3.346	188.335	188.419	0.197
SEMI- SUBMERSIBLE w/ WT	357.554	-0.008	0	-0.139	370.560	370.644	151.605

Table 4-18. Theoretical mass and inertia properties of ACTIVEFLOAT at laboratory scale (1/40), un-ballasted in the installation configuration

4.4.2 Mockup Design

All the physical model is designed in steel, except from the aluminium tower and the waterproof joints on the top covers of the pontoons and the external columns, which need to be accessible for introducing permanent ballast and changing active ballast, respectively.

The mass and inertia properties of the designed model, as well as the deviations in comparison to the target values in the operational configuration when the mock-up is evenly ballasted, are presented in Table 4-19.

EVENLY BALLASTED	Mass [kg]	error [%]	CoGz [m]	error [%]	Ixx [kgm ²]	error [%]	Iyy [kgm ²]	error [%]	Izz [kgm ²]	error [%]
SUBMERGED w/o Ballast	322.756	-0.366	-0.396	0.726	108.112	4.070	108.140	4.097	149.885	-0.887
Permanent Ballast	114.223	-0.464	-0.515	0.000	18.996		18.996		23.806	
Active Ballast	85.015	-0.066	-0.525	-0.439	36.806		36.806		62.081	
TOTAL BALLAST	199.238	-0.295	-0.519	-0.188	55.801	-3.135	55.801	-3.135	85.887	-3.852
SUBMERGED SEMI-SUBMERSIBLE	521.994	-0.339	-0.443	0.320	163.913	1.500	163.941	1.517	235.772	-1.988
Tower + internals + equipment	24.497	35.213	1.774	24.637	127.337	81.988	127.336	81.986	0.196	6.966
SEMI-SUBMERSIBLE	546.491	0.850	-0.344	-9.386	291.250	25.831	291.277	25.843	235.967	-1.981
RNA	10.300	-33.529	3.366	0.589	136.615	-32.828	136.615	-32.856	0.080	-59.310
SEMI-SUBMERSIBLE w/ WT	556.791	-0.106	-0.275	-0.240	427.865	-1.604	427.892	-1.617	236.047	-2.028

Table 4-19. Mass and inertia properties of ACTIVEFLOAT designed model at laboratory scale (1/40), evenly ballasted in the operational configuration

The mass and inertia properties of the designed model, as well as the deviations in comparison to the target values in the installation configuration when the mock-up is un-ballasted, are presented in Table 4-20.

UN-BALLASTED	Mass [kg]	error [%]	CoGz [m]	error [%]	Ixx [kgm ²]	error [%]	Iyy [kgm ²]	error [%]	Izz [kgm ²]	error [%]
SUBMERGED w/o Ballast	322.756	-0.366	-0.396	0.726	124.708	3.642	124.708	3.642	149.885	-0.887
Tower + internals + equipment	24.497	35.213	1.774	24.637	114.136	84.390	114.134	84.388	0.196	6.966
SEMI-SUBMERSIBLE	347.253	1.519	-0.243	-18.181	238.844	31.071	238.843	31.070	150.081	-0.877
RNA	10.300	-33.529	3.366	0.589	126.602	-32.778	126.602	-32.808	0.080	-59.310
SEMI-SUBMERSIBLE w/ WT	357.553	0.000	-0.139	-0.061	365.446	-1.380	365.446	-1.402	150.161	-0.953

Table 4-20. Mass and inertia properties of ACTIVEFLOAT designed model at laboratory scale (1/40), un-ballasted in the installation configuration

Figure 4-19 includes geometrical and mass properties of the different designed elements that make up the physical model.

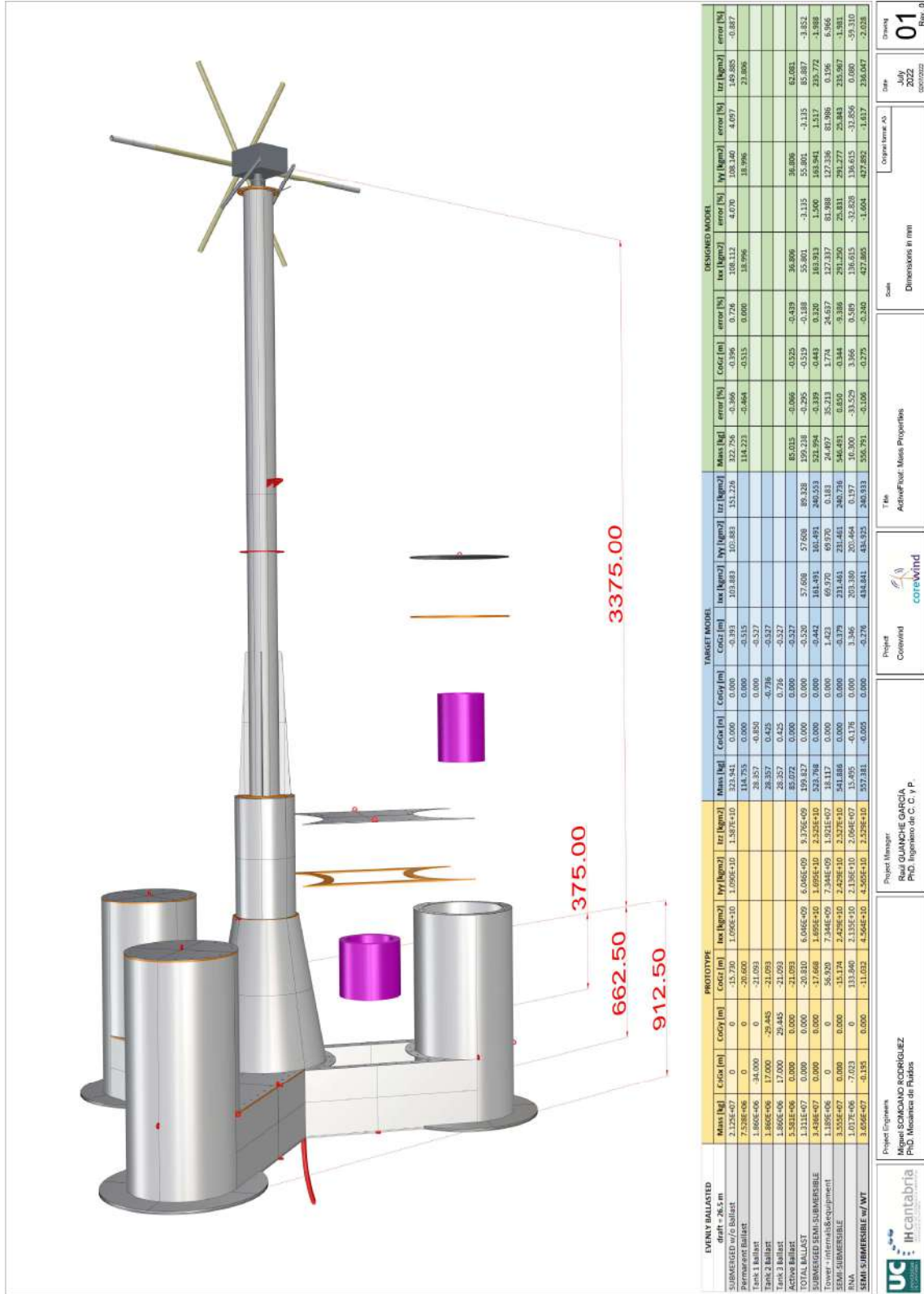


Figure 4-19. Schematic of un-ballasted ACTIVEFLOAT designed model with values in millimetres

4.4.3 [Mockup manufacturing](#)

Once the mock-up is designed, it is built in a metalwork close to FIHAC facilities. Figure 4-20 shows the substructure model painted in yellow and with the lugs manufactured to be hung.



Figure 4-20. ACTIVEFLOAT substructure mock-up hung by the lugs after being painted in yellow

A dimensional and weight distribution control are carried out in the dry characterization to ensure the quality of the manufactured mock-up, fulfilling the tolerances demanded. The geometric dimensions are checked and the mock-up geometry presents no deviations.

The determination of the model weight and CoG position is obtained by hanging the model by a system of chains, containing axial load cells at two chain-model joint points, as shown in Figure 4-21 and Figure 4-22.



Figure 4-21. Weight, CoGx and CoGy position test (left) and detail of hanging (right)



Figure 4-22. Weight and CoGz position test (left) and detail of hanging (right)

The inertia is measured by making swing the model with respect to its three main axes. The inertias I_{xx} , I_{yy} and I_{zz} are obtained based on the period of oscillation, the model mass, and with the application of the Huygens–Steiner theorem. Figure 4-23 and Figure 4-24 show some moments of Inertias characterization.



Figure 4-23. I_{xx} Inertia test (left) I_{yy} Inertia test (centre) and detail of hanging (right)



Figure 4-24. Izz Inertia test (left) and detail of hanging (right)

Table 4-24 reports the values of mass, CoG position and Inertias obtained over the 5 repetitions performed. The theoretical mass is equal to 557.381 kg (target value at laboratory scale). Therefore, there is a negligible discrepancy between the measured mass and the target value. The target CoGz value is -0.276 m from free surface, thus the deviation with respect to the experimental value is -3%. The target Ixx and Iyy values are almost 435 kg.m², hence the deviations with respect to the experimental values are 3.96% and -1.67%, respectively. The target Izz value is almost 241 kg.m² and the deviation with respect to the experimental value is -0.16%.

	Mass [kg]	CoGx [m]	CoGy [m]	CoGz [m]	Ixx [kg m ²]	Iyy [kg m ²]	Izz [kg m ²]
Measured	557.394	0.0009	-0.0007	-0.268	452.074	427.659	240.558
Target	557.381	0	0	-0.276	434.841	434.925	240.933
Deviation	0.013	0.0009	-0.0007	0.008	17.233	-7.266	-0.375
Rel. Deviation [%]	0.00			-3.00	3.96	-1.67	-0.16

Table 4-21. Model weight, CoG position (referred to free surface) and Inertias

Note that the mock-up uses a Multi-fan as the RNA, introducing a negligible CoGx and hence, there is no need to compensate any deviation with the active ballast and the evenly ballasted is the configuration used in absence of wind loads.

Table 4-22 presents the values of mass and CoG position analytically obtained after moving part of the active ballast for the configuration used in the presence of rated wind loads. The discrepancy between the measured mass and the target value remains negligible, and the deviation of the experimental CoGz with respect to the target value is reduced to -2.34%.

	Mass [kg]	CoGx [m]	CoGy [m]	CoGz [m]
Measured	557.394	-0.0186	-0.0007	-0.269
Target	557.381	-0.0197	0	-0.275
Deviation	0.013	0.0011	-0.0007	0.006
Rel. Deviation [%]	0.00			-2.34

Table 4-22. Model weight and CoG position (referred to free surface), un-ballasted and without the wind turbine in the installation configuration

Table 4-23 presents the values of mass, CoG position and Inertias analytically obtained after removing both the active ballast and the permanent ballast for the installation configuration. The discrepancy between the

measured mass and the target value is increased to 2%, while the deviation of the experimental CoGz with respect to the target value is -3.09%. The discrepancies between the measured Inertias and their target values remain also below 5%.

	Mass [kg]	CoGx [m]	CoGy [m]	CoGz [m]	Ixx [kg m ²]	Iyy [kg m ²]	Izz [kg m ²]
Measured	364.720	0.0012	-0.0010	-0.135	379.695	355.280	154.671
Target	357.554	0	0	-0.139	370.560	370.644	151.605
Deviation	7.166	0.0012	-0.0010	0.004	9.135	-15.365	3.066
Rel. Deviation [%]	2.00			-3.09	2.47	-4.15	2.02

Table 4-23. Model weight, CoG position (referred to free surface) and Inertias, un-ballasted in the installation configuration

4.4.4 Mooring system

Target physical properties of chains and calibrated springs to be used at laboratory scale 1:40 are summarized in Table 4-24.

Line #		Chain bar diameter [mm]	Equivalent diameter [mm]	Line Length [m]	Dry mass per meter length [kg/m]	Axial stiffness [kN]
1	Main line	3.00	5.40	20.800	0.175	18.745
2	Main Line	1.75	3.15	20.800	0.060	6.379
3	Main Line	1.75	3.15	20.800	0.060	6.379

Table 4-24. Physical properties of the chain lines used for the optimized mooring system

Table 4-25 reports target anchors and fairleads coordinates at laboratory scale. Because of the limits of the basin dimensions, mooring lines are truncated in both water depth and footprint size. The anchor coordinates after the truncation to perform the experimental tests in the Cantabria Coastal and Ocean Basin (CCOB), are also included.

Line #	Anchor coordinates [m]			Truncated anchor coordinates [m]			Fairlead coordinates [m]		
	X	Y	Z	X	Y	Z	X	Y	Z
1	-19.990	0	-5.000	-13.034	0	-3.000	-1.063	0	-0.375
2	11.633	-17.027	-5.000	6.966	-10.196	-3.000	0.531	-0.920	-0.375
3	11.633	17.027	-5.000	6.966	10.196	-3.000	0.531	0.920	-0.375

Table 4-25. Mooring system anchors and fairlead location

The truncation cases were very demanding, where 35% of the horizontal span and 43% of the vertical span was truncated. The methodology for single mooring lines static truncation based in the catenary equations and evolutionary optimization algorithms has been applied. The truncated mooring system is designed as simple as possible, to reduce uncertainties and simplify numerical models validation. As these mooring lines are simpler, complex springs are used. Extra clump weights are added to capture properly the original line pretension. The truncated line may not capture perfectly the dry mass of the real line, in order to compensate the rate at which mass is lifted from the seabed. Figure 4-29 shows the comparison of tension-surge excursion curves between objective and truncated lines. For the line 1, the vertical pretension relative error is 1.13%. The objective angle at fairlead is 59.2° and the truncated one is 60.5°. Respecting the lines 2-3, the vertical pretension relative error is 1.31%. The target angle at fairlead is 43.1° and the truncated one is 43.9°.

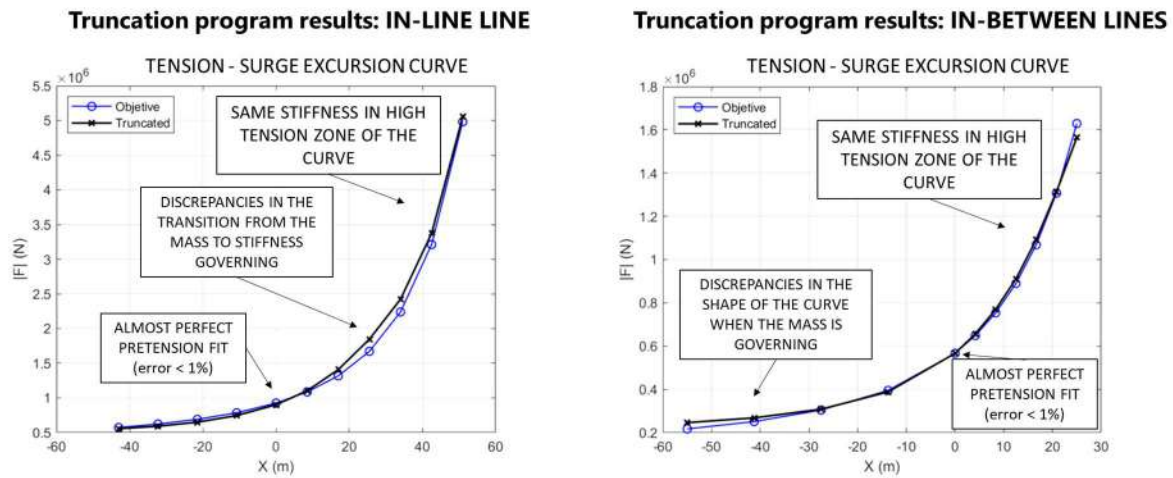


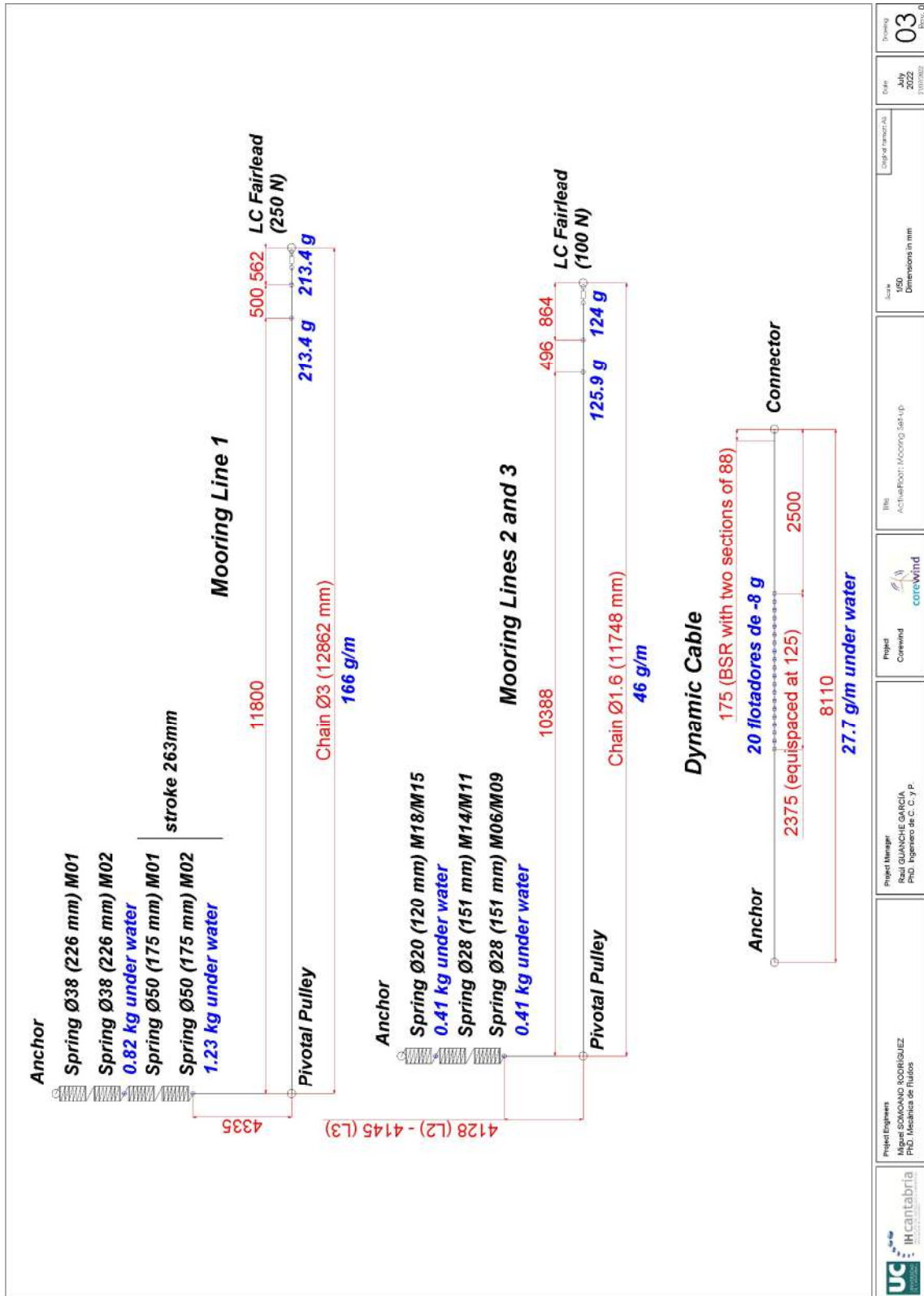
Figure 4-25. Comparison of tension-surge excursion curves between objective and truncated line 1 (left) and lines 2-3 (right)

Table 4-26 shows the truncated line details.

Line #		Line Length (including load cell and connectors) [m]			Dry mass per meter length [kg/m]	K spring [N/m]		First spring stroke [m]
1	Main line	11.800	0.500	0.562	0.166	138	171	0.263
2	Main Line	10.388	0.496	0.864	0.046	45	-	-
3	Main Line	10.388	0.496	0.864	0.046	45	-	-

Table 4-26. Line details of the truncated mooring system

The set-up of each truncated mooring line including spring, load cells and connectors are presented in Figure 4-26.



Project Engineers Iñigo DOMÍNGO RODRÍGUEZ PhD, Inicial de Tutores	Project Manager Raúl GUANICHE GARCÍA PhD, Ingeniero de C. C. y P.	Project Corewind	File ActualPost: Mooring Set-up	Scale ISO Dimensions in mm	Date July 2018 13/07/2018	Revisión 03 03
---	---	---------------------	------------------------------------	----------------------------------	------------------------------------	----------------------

Figure 4-26. Set-up of mooring lines and dynamic cable

The 10.388 m of chain in lines 2 and 3 which had to weight 0.046 kg/m, weight actually 0.045 kg/m. The relative deviation is below 5%, being -2.17%. The 11.800 m of chain in line 1 are manufactured adding distributed weights to get the target 0.166 g/m. In all sections, the spring, load cells and connectors are provided with floaters to obtain the same wet weight as the chains used. Figure 4-27 and Figure 4-28 show images of the resulting mooring lines once manufactured.

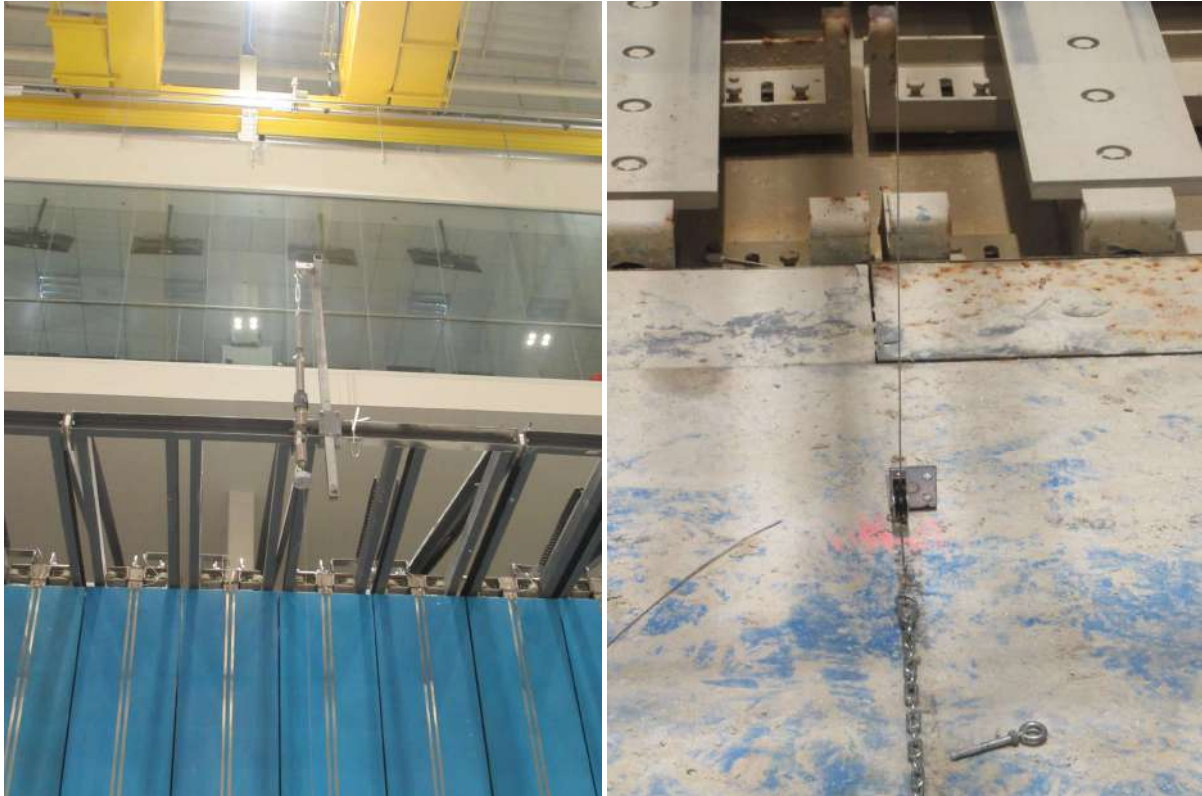


Figure 4-27. Manufactured mooring line 1



Figure 4-28. Manufactured mooring lines 2-3

For mooring line 1, we have a target axial stiffness of 76 N/m at the beginning of the deformation and 171 N/m afterwards. We solve it by using two springs in series with $K = 277$ N/m and a stroke of 0.263 m, and with other two springs in series with $K = 340$ N/m. The relative deviations respect the target ones are below 5%, being 0.30% for the first section and -0.50% for the second one. Figure 4-29 shows the validation tests of both springs by means of a set of axial tests.

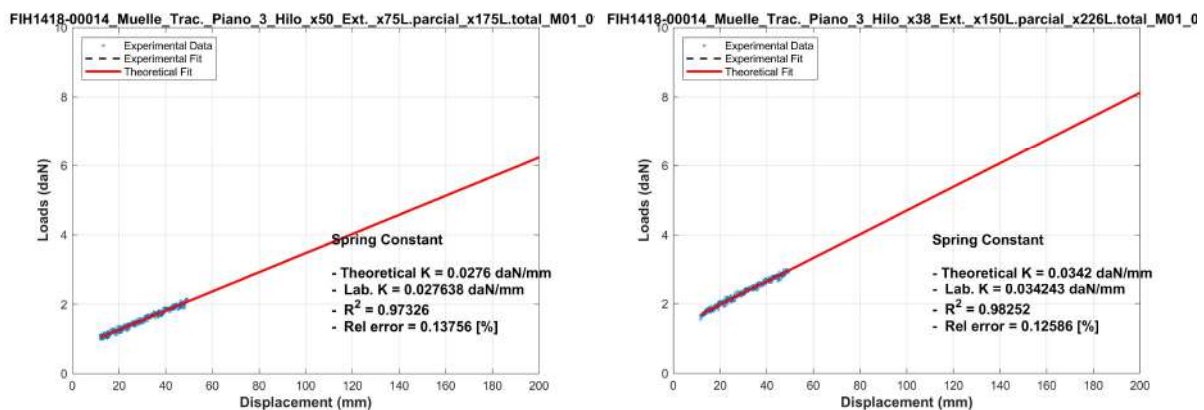


Figure 4-29. Example of axial tests to springs in section 1 (left) and section 2 (right) of main line 1

For mooring lines 2-3, we have a target axial stiffness of 45 N/m. We use three springs in series: two of them with $K = 124$ N/m and the third one with $K = 154$ N/m. The relative deviation with respect to the target one is also below 5%, being -1.57%. Figure 4-30 shows the validation tests of both springs by means of a set of axial tests.

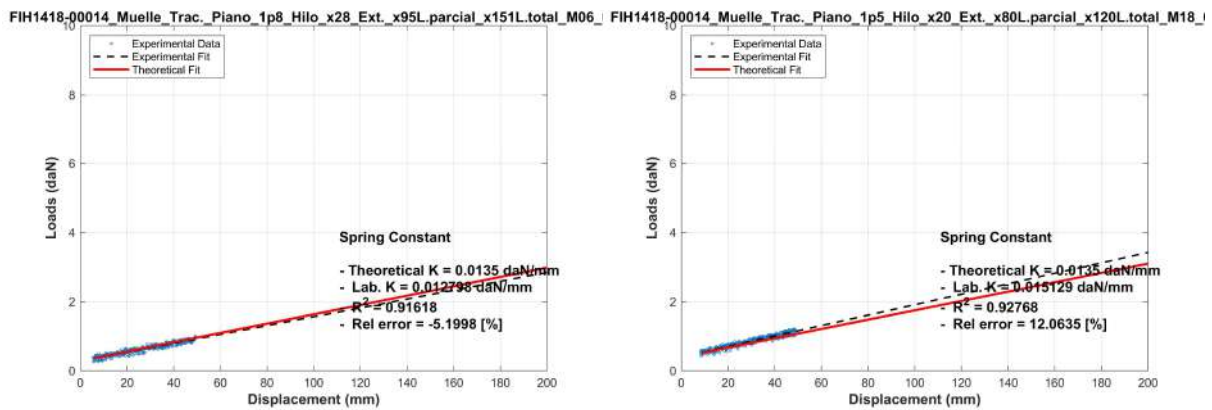


Figure 4-30. Example of axial tests to springs in main lines 2-3

The layout of all the mooring system inside the CCOB is shown in Section 4.7.

4.4.5 [Soft-mooring system for installation tests](#)

Table 4-27 shows the soft-mooring line details for the installation tests of the ACTIVEFLOAT un-ballasted.

Line #	Line Length (including spring, load cells and connectors) [m]	K spring [N/m]
1	7.072	9.1
2	7.072	9.1
3	7.072	9.1
4	7.072	9.1

Table 4-27. Line details of the soft-mooring system for installation tests

Figure 4-31 presents the set-up of each soft-mooring line for the installation tests of the ACTIVEFLOAT un-ballasted, including spring, load cells and connectors.

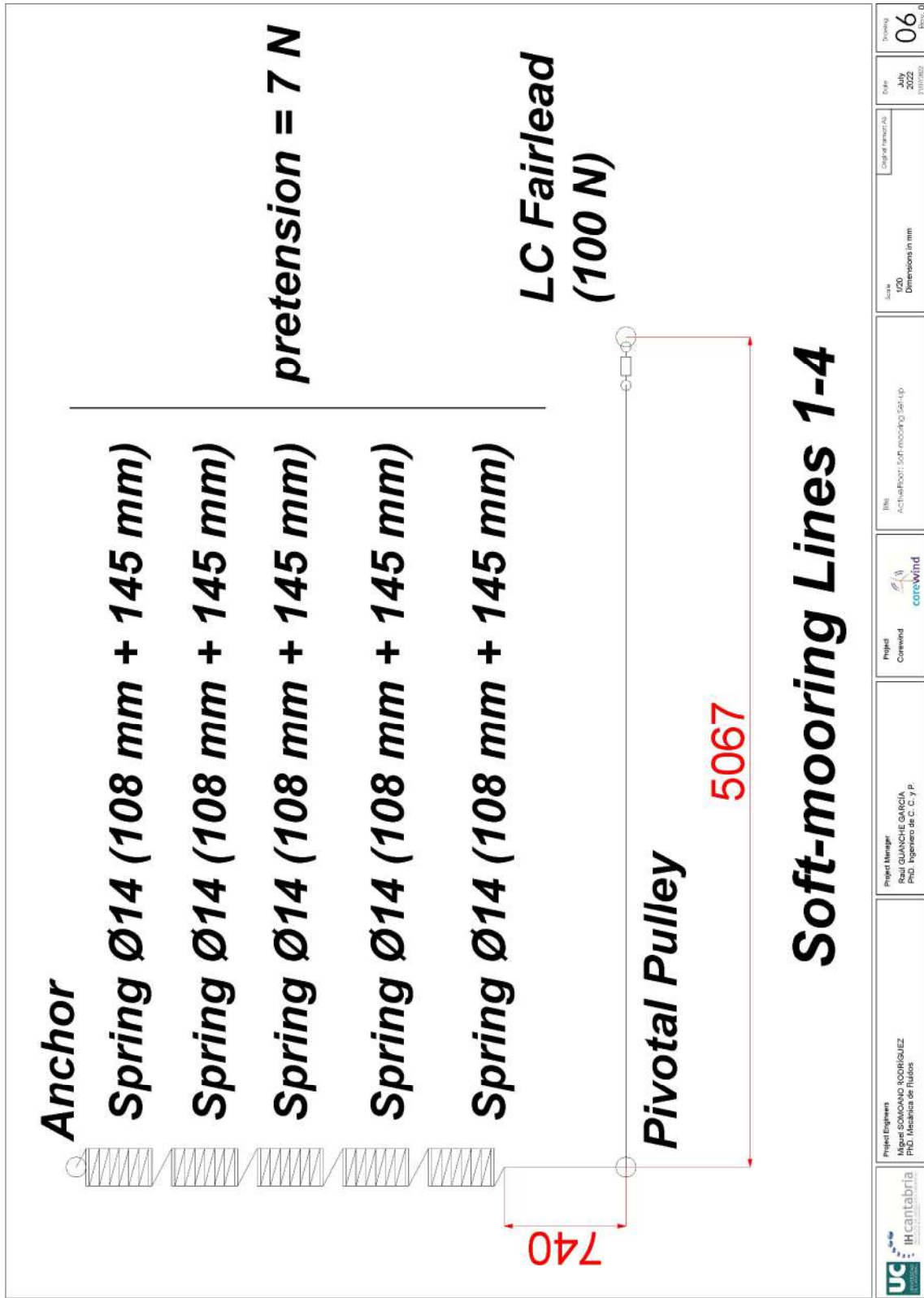


Figure 4-31. Set-up of soft-mooring lines for installation tests

Lines use a cable of 2mm diameter in order to be stiff as well as light. Figure 4-32 shows images of the resulting mooring lines once manufactured.

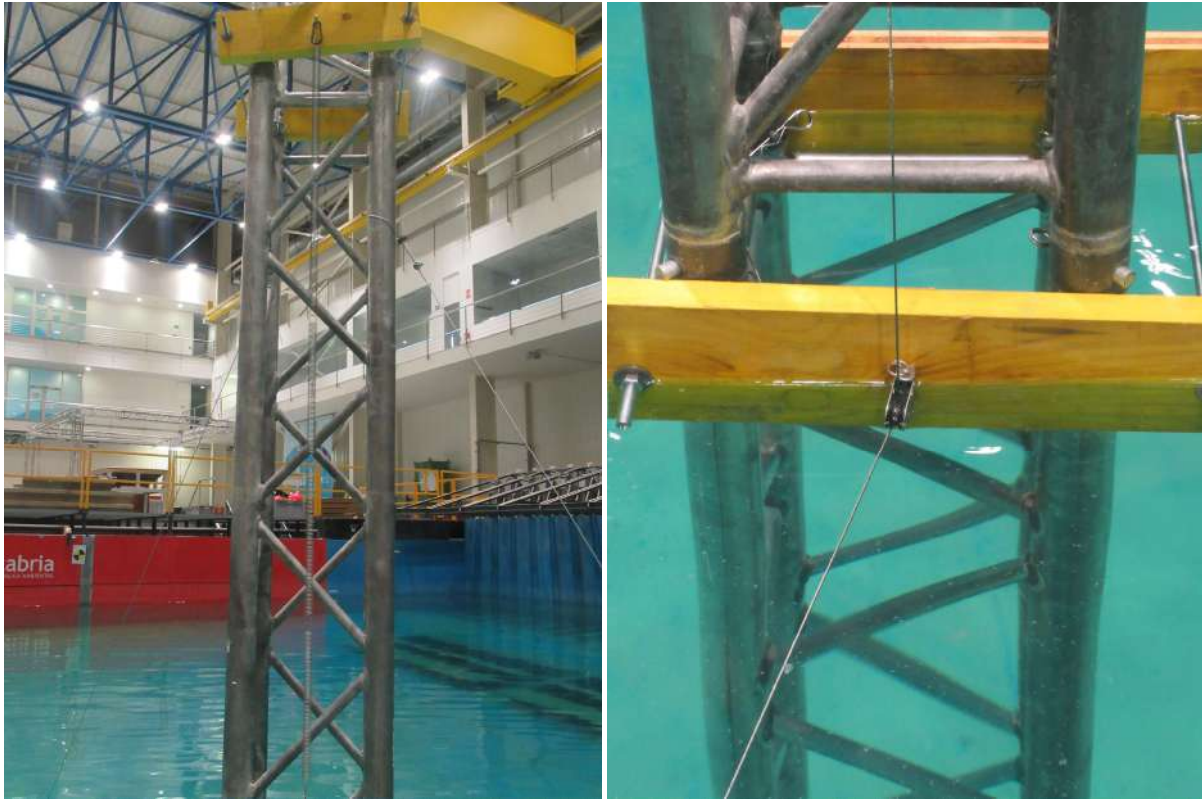


Figure 4-32. Manufactured soft-mooring lines

The five actual springs in series provide an axial stiffness of 9.5 N/m in soft-mooring lines. The relative deviation with respect to the target one is also below 5%, being 4.25%. Figure 4-33 shows the validation tests of a spring by means of a set of axial tests.

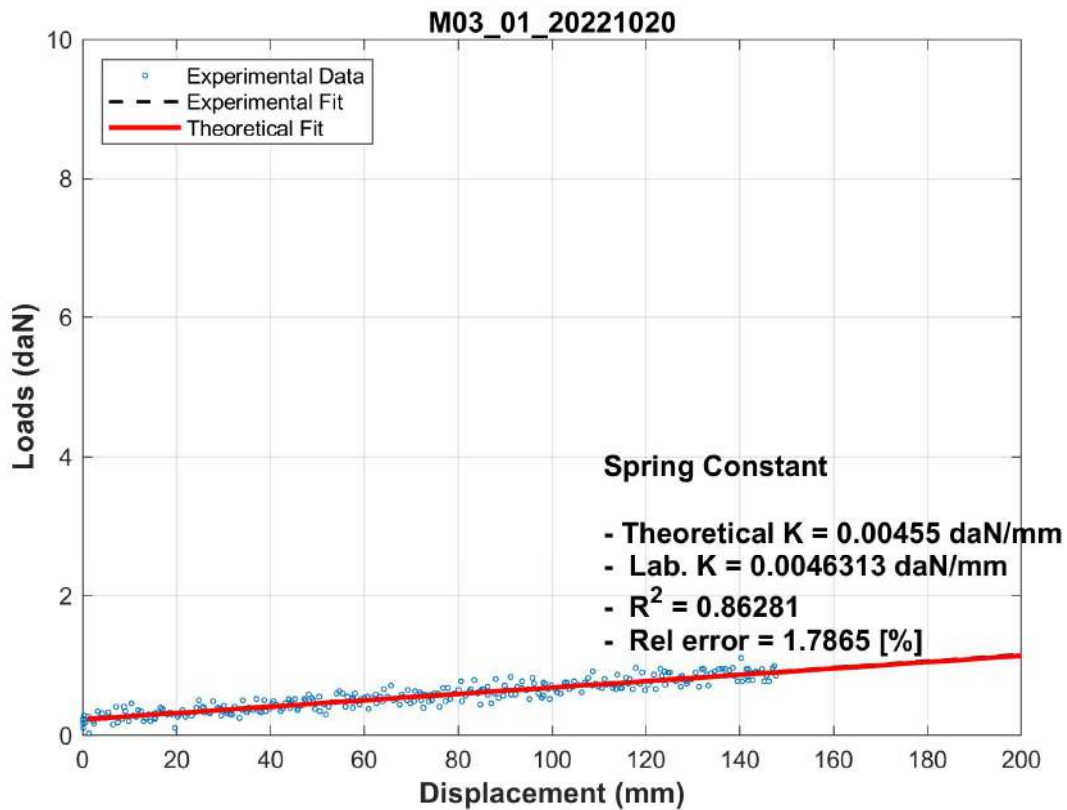


Figure 4-33. Example of axial tests to a spring in soft-mooring lines

The layout of all the soft-mooring system inside the Cantabria Coastal and Ocean Basin (CCOB) is shown in Section 4.7.

4.4.6 [Dynamic power export cable](#)

The dynamic cable to be used at laboratory scale 1:40 has a target bending stiffness of $2.1 \times 10^{-4} \text{ N m}^2$. To select an appropriate elastic material, we use the catalogue generated for previous Task 5.3 within Deliverable D5.2 [1].

The Bend Stiffener (BSR) works as a transition piece between the J-Tube and the dynamic cable, and to simulate the optimisation of the stiffness profile along its length, its 0.175 m are divided into two sections with higher bending stiffness by adding one and two heat shrink tubing, respectively.

Because of the limits of the basin dimensions, dynamic cable is truncated in water depth as can be seen in Table 4-28.

Truncated anchor coordinates [m]			Connector coordinates [m]		
X	Y	Z	X	Y	Z
6.966	0	-3.000	0.292	0	-0.913

Table 4-28. Dynamic cable anchor and connector location

In the buoyant section, there are 20 buoyancy modules of 8 g of net buoyancy force equally spaced at 125 mm, as shown in Figure 4-26. The rest of details of truncated cable are presented in Table 4-29.

	Line Length (including connectors) [m]		Wet mass per meter length [kg/m]	Bending Stiffness [kg m ²]	
	Dynamic Cable				
Dynamic Cable	8.110		0.0277	1.4 x 10 ⁻⁴	
BSR	0.088	0.088	0.0277	1.6 x 10 ⁻³	2.1 x 10 ⁻³

Table 4-29. Details of the truncated dynamic cable

When manufactured, the buoyant section is displaced 10 mm towards the anchor, what implies a deviation of 0.36%. An image of the manufactured buoyant section is shown in Figure 4-34.

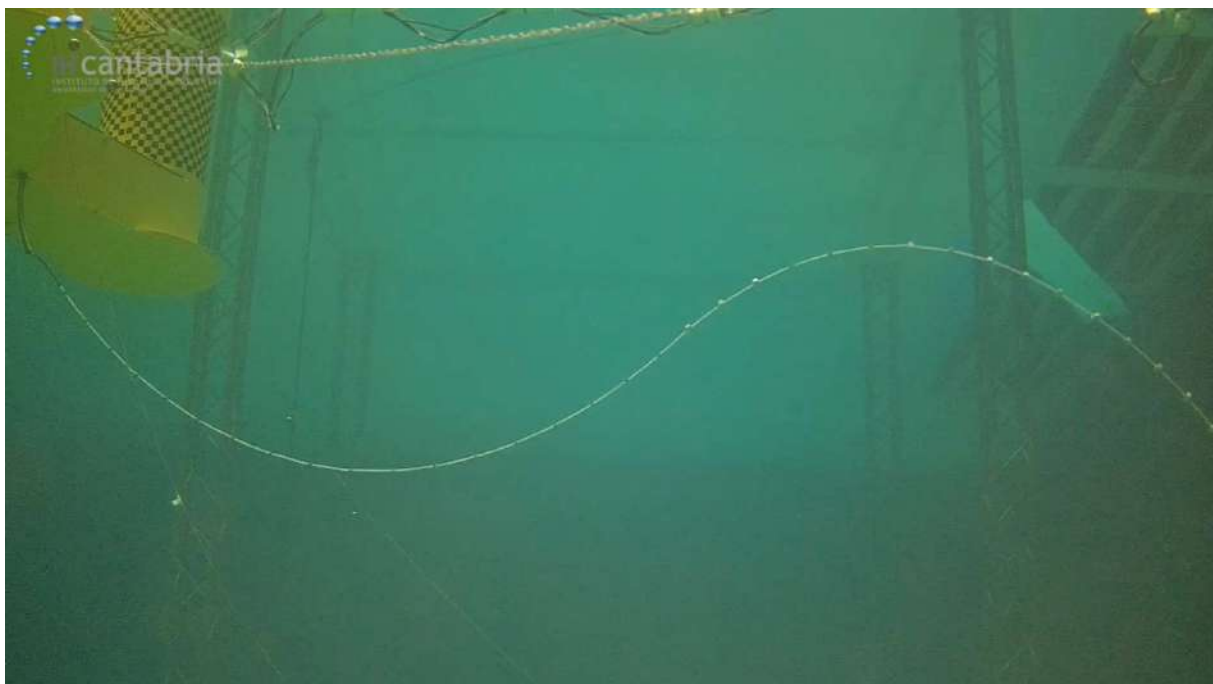


Figure 4-34. Manufactured dynamic cable

4.4.7 [Aerodynamic generation by the FIHAC’s multi-fan system](#)

As previously described in Section 4.3.7, the turbine aerodynamic loads are defined and generated by means of a Hardware In the Loop (HIL) layout developed at FIHAC (Pat. ES 2 632 187 B1). The setup involves the FIHAC Multi-fan system, a device that permits to generate with high fidelity the rotor aerodynamics.

The physical properties of FIHAC Multi-fan are already presented in Figure 4-17. The Hardware-In-the-Loop (HIL) is already described in Figure 4-18.

4.5 Instrumentation

With the aim of recording the expected physical processes, the following set of instruments and sensors have been used during the physical experiments:

- Data acquisition system for data monitoring and collection.
- Free surface transducers for water level measurements (Akamina System).

- Acoustic Doppler Velocimetries (ADV-Vectrino).
- Track motion system (Qualisys) to measure the floating platform motions.
- Axial load cells to measure forces on mooring lines.
- Multi-axis load cell beneath FIHAC Multi-fan to records the generated aerodynamic loads.
- Accelerometers to record accelerations at the nacelle.
- Video cameras, including a subaquatic one to monitor the kinematics of the dynamic cable and mooring system.

The location of the instrumentation during the wave and current calibrations, as well as during the standard tests execution can be found in Section 4.7.

4.5.1 [Data acquisition system](#)

The data acquisition system collects all the data coming from the sensors. It is a system of great importance since it has to sample and store all the signals in a transparent way, without distortion in order to reproduce them with the highest fidelity during their analysis.

The available equipment for this purpose is the PXI acquisition system from National Instruments. Well known for its versatility, reliability and performance, this is the best acquisition system a researcher may have nowadays in the laboratory. It is equipped with a set of analogue and digital cards, hence it can interface and measure a huge variety of sensor types. The PXI is mounted in a rack cabinet where other racks work together to patch all the signals from and to the sensors (sensors power supply, control signals, analogue and digital inputs / outputs). Finally, a rugged computer of NI (RMC-8354) is mounted in the cabinet as the controller for the PXI system.

There are three complete systems like the one described above, one of them shown in Figure 4-35.

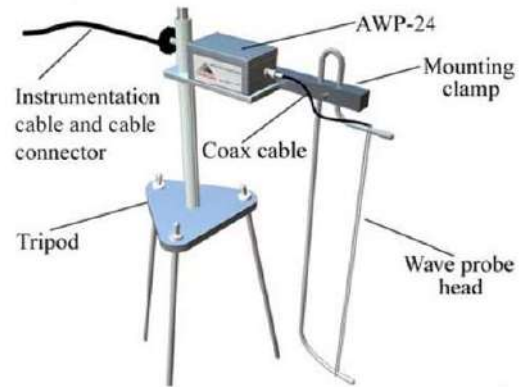


Figure 4-35. Acquisition system cabinet based on NI PXI chassis

4.5.2 [Free surfaces gauges](#)

The measurement and characterization of water level fluctuations is carried out by means of free surface gauges. Two different technologies are feasible and available to be used, resistive and capacitive sensors. The former one is preferred to the latter one and thus, the one specified in this document.

The available gauge type is the AWP-24 from Akamina Technologies depicted in Figure 4-36 on the left. It is a wave height gauge that provides an accurate, highly responsive measure of depth changes from sub-millimeter to meters. At the same time, it shows a very good stability versus temperature and water conductivity variations, which minimize the number of calibrations to be performed during the tests. Its main features are summarized in Figure 4-36 on the right.



Parameter	Value
Linearity:	0.15% Full Scale
Accuracy:	0.15% Full Scale
Air temperature coefficient:	0.03% Full Scale/°C
Water temperature coefficient:	0.03% Full Scale/°C
Operating temperature:	-10°C to 50°C
Response time:	5ms
Output signal:	-5Vdc to +5Vdc
Power Supply:	8Vdc to 20Vdc
Power consumption:	0.21W (21mA @ 10V)
Size:	6.4 x 7.6 x 12.7cm
Wave probe length:	1000mm

Figure 4-36. Akamina AWP-24 free surface gauges (left) and their main features (right)

4.5.3 [Acoustic Doppler Velocimetry \(ADV-Vectrino\)](#)

The basic operation consists in an acoustic transmitter that sends out a short acoustic pulse and one or more receivers receive the echo at a specific distance and find its Doppler shift to compute the speed of the water.

The equipment used is the Vectrino from Nortek depicted in Figure 4-37. The Vectrino is a high-resolution acoustic velocimeter used to measure turbulence and 3D water velocity in a wide variety of applications from the laboratory to the ocean. The basic measurement technology is coherent Doppler processing, which is characterized by accurate data and no appreciable zero offset.



Parameter	Value
Range:	± 0.01, 0.1, 0.3, 1, 2, 4 m/s (selectable)
Accuracy:	± 0.5% of measured value ±1 mm/s
Measurement distance:	0.05 m from probe
Sampling volume:	6 mm Ø; 3-15 mm height (selectable)
Power supply:	12 - 48 VDC
Output signal:	0 - 5 V or Digital (RS-232)
Sampling frequency:	From 1 to 200 Hz (User selectable)
Size:	70 Ø x 39 cm

Figure 4-37. Nortek Vectrino ADV (left) main features (right)

4.5.4 [Qualisys Tracking Motion system \(QTM\)](#)

Qualisys Track Manager (QTM) is a Windows-based data acquisition software with an interface that allows the user to perform 2D and 3D motion capture. Together with the Qualisys line of optical measurement hardware, QTM streamlines the coordination of all features in a sophisticated motion capture system and provide the possibility of rapid production of different and accurate 2D, 3D and 6D data.

During the capture, real time 2D, 3D and 6D (3 translations and 3 rotations) camera information is displayed allowing instant confirmation of accurate data acquisition. The individual 2D camera data is quickly processed and converted into 3D or 6D data by advanced algorithms, which are adaptable to different movement characteristics. The data can then be exported to different analysis software via several external formats.

The cameras are suitable to capture the movement produced at the platform for all possible applications. They are ideal for tracking the movement of a floating object or to know the displacement of the object in the 6 degrees of freedom.

Oqus cameras (Figure 4-38) are designed to capture accurate trackers (mocap) data with very low latency and works with both passive and active markers. The high-quality threaded markers are designed for maximum roundness. In the current test program, the super-spherical markers used have a diameter of 19 mm and a mass of 2.5 g. Data acquired by Qualisys in the test campaign is used for recording the platform behaviour in terms of translations and rotations.

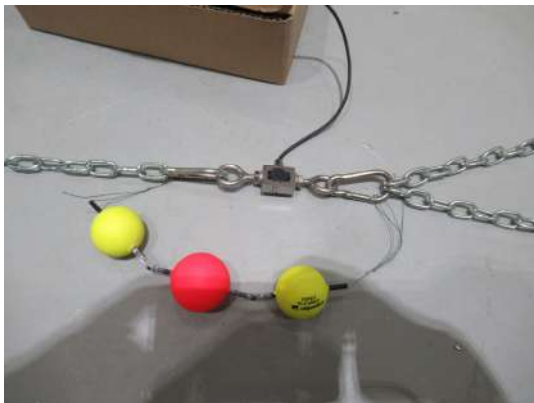


Figure 4-38. DoFs captured (left) and Oqus 3+ camera from Qualisys system (right)

4.5.5 [Axial force transducers](#)

Force transducers are widely used in field and laboratory to measure the forces applied to a device. They are available in a great variety of sizes and shapes, some of them come with integrated electronics, special environmental protection. However, all of them basically consist of strain gauges attached to a metallic body, hence an external force is transformed into an electrical signal variation.

F2808 series from TECSIS are used on the present test program. They are miniature load cells with low profile and ultra-compact build size. They measure both tension and compression and are suitable for underwater use thanks to an additional protection cover. They are intended for space constrain applications or for applications where the transducer's size and weight have a significant impact in the measurements. The axial load cell and its main features are summarized in Figure 4-39.



Parameter	Value			
	20N	100N	250N	500N
Material:	Stainless steel			
Size [mm]:	19X16X6			
Weight [g]:	100			
Thread:	M3	M4		
Capacity [N]:	20	100	250	500
Overload [%]:	150			
Accuracy [%]:	0.1			
Resolution [%]:	≤0.01			
Output signal:	mV (Wheatstone bridge)			
Sensitivity [mV/V]:	2			
Protection degree:	IP68			

Figure 4-39. TECSIS F2808 force transducer with floaters to have the same wet weight as the chain (left) and its main features (right)

4.5.6 Multi-axis force-torque transducer

Multi-axis transducers allow characterization of scale models behaviour in terms of forces and torques in different directions at the same time.

The forces and torque over the wind turbine nacelle are measured using one multi-axis sensor K6D, suitable for the force and torque measurement into three mutually perpendicular axes: the K6D40 from ME-SYSTEME.

The K6D sensors from ME-SYSTEME measure the forces and moments in the three directions of space. These sensors are integrated in a small cylindrical body with symmetrical mounting flanges. Despite their small dimensions, they offer high robustness and accuracy. They are well suited for applications where a small size and low weight transducer is required. The K6D sensors are available in different measurement ranges and sizes, they come with an amplifier module which is calibrated together with the sensor.

Due to the low weight of the multi-axis sensor, 450 g, it is suitable for applications in robotics and in research and development, such as small-scale models for laboratory testing. The multi-axis load cell is used for tracking forces and moments generated by the Multi-fan. Figure 4-40 shows the tri-axial load cell and summarizes its main technical specifications.



Figure 4-40. K6D40 multi-axis force transducer and amplifier (left) technical specifications (right)

4.5.7 [Accelerometer](#)

Accelerometers can be used to measure acceleration directly in a specific part of a moving object, avoiding the distortion introduced by other techniques like velocity or position derivation.

For this project, model 4030 from Measurement Specialties is used to record accelerations at the nacelle. Model 4030 is a triaxial, low noise accelerometer packaged in a light and durable moulded housing. It provides linear acceleration within a ±6g range. Figure 4-41 shows the Model 4030 accelerometer and summarizes its specifications.



Figure 4-41. Model 4030 accelerometer (left) technical specifications (right)

4.5.8 [Digital image and video recording system](#)

Photographs and continuous video recordings are usually required from all physical experiments. The high-resolution quality of present available digital equipment makes this a very helpful tool. It serves primarily as model behaviour visualization purpose (qualitative info).

The main elements are photographed and all the tests are video recorded, using also a subaquatic video camera to monitor the kinematics of the dynamic cable and mooring system.

4.6 Test Programme

To facilitate the understanding of this report and the results included on it, the following sub-sections summarise the structure of the test program, as well as the physical variables studied, and the statistical analysis carried out on each of them.

Two testing rounds are programmed in the FIHAC facilities:

- The first round of tests is focused on calibrating of the FIHAC’s multi-fan system on a bench.
- The second round of tests is devoted to the fully coupled hybrid modelling in the CCOB for both floating concepts: WINDCRETE and ACTIVEFLOAT.

4.6.1 First round of wave basin tests

An equivalent test round to POLIMI first round of tests is conducted at FIHAC, with the main outcome of calibrating the Multi-fan system at the FIHAC wave basin to be able to reproduce accurately the IEA 15MW Wind Turbine control system already proven and validated at POLIMI wind tunnel. Figure 4-42 shows the comparison of the wind turbine modelling in both approaches.

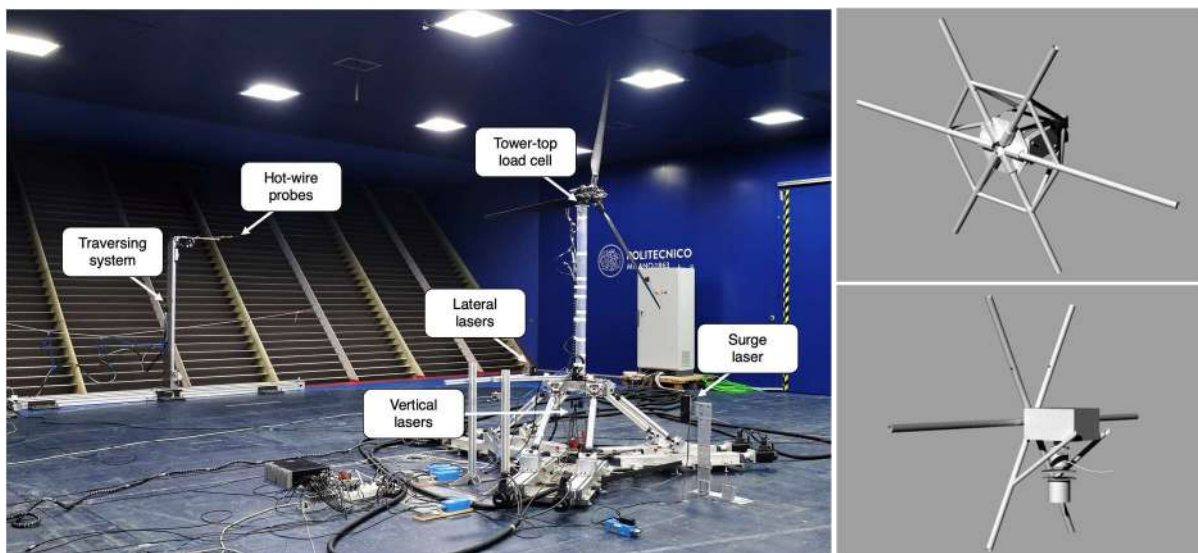


Figure 4-42. IEA 15MW wind turbine modelling in POLIMI Wind Tunnel (left) vs Multi-fan system at the FIHAC wave basin (right)

The test plan proposed covers bottom fixed tests as well as prescribed movements tests, to reproduce accurately the aerodynamic forces observed at the wind tunnel, including control induced effects and unsteady aerodynamic effects.

Table 4-30 presents a comparison of the scaling laws of similitude used at POLIMI wind tunnel and FIHAC wave basin applying Reynolds number and Froude number, respectively.

	Reynolds		Froude	WINDCRETE	ACTIVEFLOAT
Magnitude	Scale factor	Value	Scale factor	Value	Value
Length	λ_L	1/100	λ	1/55	1/40
Velocity	λ_v	1/3	$\sqrt{\lambda}$	1/7.4	1/6.3
Frequency	$\lambda_\omega = \lambda_v/\lambda_L$	33.3	$1/\sqrt{\lambda}$	7.4	6.3

Table 4-30. Reynolds vs Froude scaling laws of similitude

To validate the basic aerodynamics of the 15MW Wind Turbine, the FIHAC Multi-fan is tested in a fixed condition with several different wind speeds, including different below rated, above rated and wind rated cases, as well as under unsteady wind conditions. The load cases carried out simulates the aerodynamic response of the IEA 15 MW in the corresponding wind conditions.

4.6.2 [Second round of wave basin tests](#)

During the physical experiments, different tests are carried out. Variables, such as loads, movements and environmental loads (wave, current or wind/thrust), are recorded to study the coupled hydrodynamic and aerodynamic response of the floating platform.

Based on that, the execution of the tests campaign is developed through four phases where two models are tested in several different configurations.

The test set-ups or configurations tested are the followings:

- **Configuration WC0:** Free floating WINDCRETE without wind turbine and without ballast for installation tests.
- **Configuration WC1:** Free floating WINDCRETE.
- **Configuration WC2:** Moored WINDCRETE with environmental loads aligned at 0°.
- **Configuration AF0:** Free floating ACTIVEFLOAT without ballast for installation tests.
- **Configuration AF1:** Free floating ACTIVEFLOAT.
- **Configuration AF2:** Moored ACTIVEFLOAT with wave loads at 0°.
- **Configuration AF3:** Moored ACTIVEFLOAT with environmental loads aligned at 0°.

Those configurations are distributed along the four campaign phases as follows:

1. **Dry characterization tests**
Weight control, verification of CoG and inertia moments.
2. **Basin calibration tests**
Prior to execute the physical model tests, sea states are previously calibrated in absence of both structures to guarantee that the metocean condition are properly generated.
3. **Installation tests**
 - Configuration WC0
 - Installation tests in horizontal position.
 - Installation tests of raising up (verticalization).
 - Configuration AF0
 - Installation tests.
4. **Hydrodynamic characterization tests**
 - Configuration WC1
 - Free-floating decay tests: linear damping and natural period.
 - Configuration WC2
 - Moored decay tests: linear damping and natural period.
 - Static offset tests: combined stiffness of the mooring system and floating platform.
 - Configuration AF1
 - Inclining Tests (Tilt tests): initial stability and metacentric height (GM).
 - Free-floating decay tests: linear damping and natural period.
 - Configuration AF2
 - Moored decay tests: linear damping and natural period.
 - Static offset tests: combined stiffness of the mooring system and floating platform.

- Configuration AF3
 - Moored decay tests: linear damping and natural period.

5. Seakeeping tests

- Configuration WC2
 - Only wave tests: regular waves, irregular waves, white noise tests.
 - Only wind tests.
 - Only current tests.
 - Coupled tests: wave-wind tests, wave-current-wind tests.
- Configuration AF2
 - Only wave tests: regular waves, irregular waves, white noise tests.
- Configuration AF3
 - Only wind tests.
 - Only current tests.
 - Coupled tests: wave-wind tests, wave-current-wind tests.

All the measurements taken during the test campaign are recorded using a sampling frequency of 100 Hz.

Calibration Tests

The calibration tests are performed in absence of the model in the basin for avoiding disturbances upon the basin free surface measurements. These tests are focused on ensuring the correct reproduction of the target sea-state conditions during the tests. The steps followed during the calibration are the following:

1. Wave calibration (in absence of current).
2. Current calibration (in absence of wave).
3. Combining wave and current calibration.

During the wave calibration stage, the measurement instruments are placed at two locations within the basin. The first set of sensors is referred as control array, the second as calibration array. The layout of all sensors employed during calibration is described in section 4.7.

- Calibration array
 - Position: Sensors placed along the basin x-axis, starting from the X coordinate of the platform CoG in quiet conditions.
 - Installation period: Calibration phase.
 - Sensors array:
 - x12 - Free surface gauges (WG 13-14-15-16-17-18-19-20-21-22-23-24).
 - x2 - ADV current sensors (ADV 3-4).
- Control array
 - Position: Parallel to the Calibration array.
 - Installation period: Whole test campaign.
 - Sensors array:
 - x12 - Free Surfaces Gauges (WG 1-2-3-4-5-6-7-8-9-10-11-12).
 - x2 - ADV current sensors (ADV 1-2)

Table 4-31 shows the distance between the first eight wave gauges (WG) of the same array, respect the first one.

Wave Gauges Array	
Id	Distance [m]

1-2	0.16
1-3	0.23
1-4	0.53
1-5	0.74
1-6	1.00
1-7	1.37
1-8	2.46

Table 4-31. Wave Gauges Placement in an Array

Table 4-32 presents the location of the last four WG of the same array, respect the first one, in a star configuration to characterize the short-crested waves.

Wave Gauges Array		
Id	X distance [m]	Y distance [m]
1-9	-0.534	-0.388
1-10	-0.534	0.388
1-11	0.204	-0.628
1-12	0.204	0.628

Table 4-32. Wave Gauges Placement in a Star configuration. X coordinate is the predominant wave direction

The comparison between measurements recorded by the control array during calibration and seakeeping tests provides a reference to verify the validity of the generated sea state conditions. Figure 4-43 shows the control array during tests in the Cantabria Coastal and Ocean Basin (CCOB). Incident wave is obtained using WaveLab 3 software from Aalborg University.

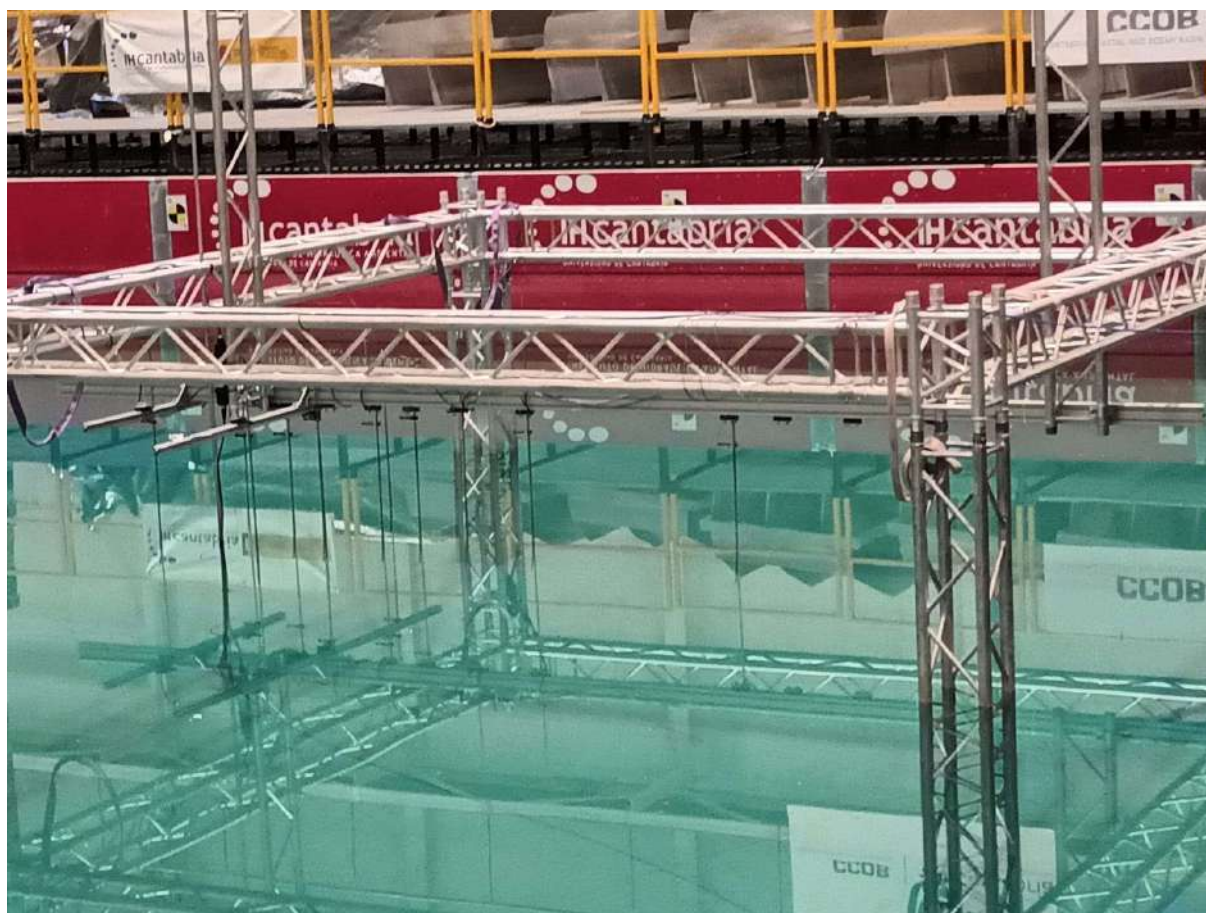


Figure 4-43. Control array in the CCOB

Respecting the ADV depths of the same array, the first one is located close to the free surface. The second ADV is positioned at 60% of the basin depth from free surface to measure the mean current velocity.

WINDCRETE Characterization Tests

The characterisation tests are a set of tests essential to validate that the model behaviour reflects the one of the designed full-scale prototype for both the platform and mooring system. Table 4-33 shows the characterisation tests and the parameters obtained in each of them.

- **Decay tests**

Decay tests are carried out in free floating (Configuration WC1) in heave/roll/pitch and in moored conditions (Configuration WC2) in all system DoFs, as well as in surge/pitch with rated, below rated and above rated wind speed. The purpose of these tests is to evaluate the natural periods and the non-dimensional linear damping coefficients of each of the six degrees of freedom of the platform system.

Each test plans to alter the equilibrium position of a single degree of freedom and let the system reach its equilibrium again. The transient of the process is recorded by the tracking motion system and provides the pursued information.

- **Static offset tests**

The aim of these tests is to validate the stiffness of the mooring system. To do this, the platform is progressively displaced along the DoF of interest, measuring both the force required to apply the displacement and the

displacement itself. The displacement is measured by the tracking position system, while the applied force is measured by an axial load cell installed in the device used to apply the platform displacement.

These tests evaluate the stiffness of the mooring for positive and negative surge displacements in Configuration WC2.

Data analysis of hydrodynamic characterization tests					
Test	Mooring	Configuration	DOF	Results from data	
01	Free floating	WC1	Heave	Natural periods and non-dimensional coefficient of linear damping	
02			Roll		
03			Pitch		
04	Moored	WC2	Surge		
05			Sway		
06			Heave		
07			Roll		
08			Pitch		
09			Yaw		
10			Surge with rated wind		
11			Pitch with rated wind		
12			Surge below rated wind		
13			Pitch below rated wind		
14			Surge above rated wind		
15			Pitch above rated wind		
16	Moored	WC2	Positive Surge	Mooring system stiffness	
17			Negative Surge		

Table 4-33. Summary of hydrodynamic characterization tests

WINDCRETE Seakeeping Tests

WINDCRETE platform has been tested under different metocean conditions: (1) regular wave tests, (2) irregular wave tests, (3) white noise tests, (4) wind tests, (5) regular wave tests with wind, (6) irregular wave tests with wind, (7) current tests, (8) irregular wave tests with wind and with current.

The parameters defining the environmental conditions are the following: water depth (h), draught, regular wave height (H), regular wave period (T), significant wave height (H_s), peak period (T_p), wave spectrum and peakness (γ in this case), wind velocity (U_w) and current velocity (U_c).

The following sections summarise the test matrix executed during the basin testing campaign. All tests have been classified according to the environmental conditions tested and all the environmental parameters are given in prototype scale. Each table includes the test configuration used in each case and the laboratory identification code.

- **Configuration WC2: Wave + Current + Wind direction 0 degrees**

This paragraph resumes the characteristics of the tests executed in Configuration WC2, that is when the environmental conditions are aligned with the platform main axis. Table 4-34 lists the tests executed generating regular waves.

Configuration WC2 [0 degrees]											
Regular Wave											
Test	H [m]		T [s]		h [m]	Current [m/s]		Wind [m/s]	Thrust [tonnes]	Direction [°]	Duration [Waves]
	1/1	1/55	1/1	1/55		1/1	1/55				
18	2.75	0.050	7.5	1.011	165	0	0	0	0	0	200
19	2.75	0.050	9	1.214	165	0	0	0	0	0	200
20	2.75	0.050	11	1.483	165	0	0	0	0	0	200
21	2.75	0.050	14	1.888	165	0	0	0	0	0	200
22	2.75	0.050	17	2.292	165	0	0	0	0	0	200
23	2.75	0.050	20	2.697	165	0	0	0	0	0	200
24	5.11	0.093	7.5	1.011	165	0	0	0	0	0	200
25	5.11	0.093	9	1.214	165	0	0	0	0	0	200
26	5.11	0.093	11	1.483	165	0	0	0	0	0	200
27	5.11	0.093	14	1.888	165	0	0	0	0	0	200
28	5.11	0.093	17	2.292	165	0	0	0	0	0	200
29	5.11	0.093	20	2.697	165	0	0	0	0	0	200

Table 4-34. Configuration WC2: Regular wave tests. All values are presented at full scale, except for the wave heights, wave periods and current velocities which are also presented at model scale

Table 4-35 presents the tests executed with irregular waves. The waves are generated based on Jonswap spectrum.

Configuration WC2 [0 degrees]												
Irregular Wave												
Test	Hs [m]		Tp [s]		Spectrum	h [m]	Current [m/s]		Wind [m/s]	Thrust [tonnes]	Direction [°]	Duration [h]
	1/1	1/55	1/1	1/55			1/1	1/55				
30	2.75	0.050	9	1.214	JS-3.3	165	0	0	0	0	0	3
31	2.75	0.050	11	1.483	JS-3.3	165	0	0	0	0	0	3
32	2.75	0.050	14	1.888	JS-3.3	165	0	0	0	0	0	3
33	5.11	0.093	9	1.214	JS-1.2	165	0	0	0	0	0	3
34	5.11	0.093	11	1.483	JS-1.2	165	0	0	0	0	0	3
35	2.75	0.050	9	1.214	JS-3.3 s = 6	165	0	0	0	0	0	3
36	2.75	0.050	9	1.214	JS-3.3 s = 12	165	0	0	0	0	0	3

37	5.11	0.093	11	1.483	JS-1.2 s = 6	165	0	0	0	0	0	3
38	5.11	0.093	11	1.483	JS-1.2 s = 12	165	0	0	0	0	0	3

Table 4-35. Configuration WC2: Irregular wave tests. All values are presented at full scale, except for the wave significant heights, wave peak periods and current velocities which are also presented at model scale

Table 4-36 provides the details of the white noise tests included in the campaign. These tests are used to build the platform RAOs.

Configuration WC2 [0 degrees]													
White Noise													
Test	Hs [m]		T1 [s]		T2 [s]		h [m]	Current [m/s]		Wind [m/s]	Thrust [tonnes]	Direction [°]	Duration [h]
	1/1	1/55	1/1	1/55	1/1	1/55		1/1	1/55				
39	2.75	0.050	7.5	1.011	22	2.967	165	0	0	0	0	0	3
40	5.11	0.093	7.5	1.011	22	2.967	165	0	0	0	0	0	3

Table 4-36. Configuration WC2: White noise tests. All values are presented at full scale, except for the wave significant heights, wave periods and current velocities which are also presented at model scale

Table 4-37 shows wind tests included in the campaign.

Configuration WC2 [0 degrees]												
Wind												
Test	H [m]		T [s]		h [m]	Current [m/s]		Wind [m/s]	Thrust [tonnes]	Direction [°]	Duration [h]	
	1/1	1/55	1/1	1/55		1/1	1/55					
41	0	0	0	0	165	0	0	10.5	236.34	0	1	
42	0	0	0	0	165	0	0	10.5 ETM	170.62	0	1	
43	0	0	0	0	165	0	0	10.5 NTM	192.06	0	1	
44	0	0	0	0	165	0	0	9 NTM	173.92	0	1	
45	0	0	0	0	165	0	0	18 NTM	94.18	0	1	

Table 4-37. Configuration WC2: Wind tests. All values are presented at full scale, except for the wave heights, wave periods and current velocities which are also presented at model scale

Table 4-38 presents the tests combining regular waves and wind.

Configuration WC2 [0 degrees]											
Regular Wave + Wind											
Test	H [m]		T [s]		h [m]	Current [m/s]		Wind [m/s]	Thrust [tonnes]	Direction [°]	Duration [Waves]
	1/1	1/55	1/1	1/55		1/1	1/55				
46	2.75	0.050	7.5	1.011	165	0	0	10.5	234.36	0	200
47	2.75	0.050	9	1.214	165	0	0	10.5	231.73	0	200

48	2.75	0.050	11	1.483	165	0	0	10.5	227.04	0	200
49	2.75	0.050	14	1.888	165	0	0	10.5	218.26	0	200
50	2.75	0.050	17	2.292	165	0	0	10.5	215.72	0	200
51	2.75	0.050	20	2.697	165	0	0	10.5	216.02	0	200

Table 4-38. Configuration WC2: Regular wave and Wind tests. All values are presented at full scale, except for the wave heights, wave periods and current velocities which are also presented at model scale

Table 4-39 shows the tests combining irregular waves and wind.

Configuration WC2 [0 degrees]												
Irregular Wave + Wind												
Test	Hs [m]		Tp [s]		Spectrum	h [m]	Current [m/s]		Wind [m/s]	Thrust [tonnes]	Direction [°]	Duration [h]
	1/1	1/55	1/1	1/55			1/1	1/55				
52	2.75	0.050	9	1.214	JS-3.3	165	0	0	10.5 ETM	174.26	0	3
53	5.11	0.093	9	1.214	JS-1.2	165	0	0	9 NTM	176.71	0	3
54	5.11	0.093	9	1.214	JS-1.2	165	0	0	10.5 NTM	194.76	0	3
55	5.11	0.093	9	1.214	JS-1.2	165	0	0	18 NTM	92.23	0	3
56	2.75	0.050	9	1.214	JS-3.3 s = 6	165	0	0	10.5 ETM	175.29	0	3
57	2.75	0.050	9	1.214	JS-3.3 s = 12	165	0	0	10.5 ETM	175.21	0	3

Table 4-39. Configuration WC2: Irregular wave and Wind tests. All values are presented at full scale, except for the wave significant heights, wave peak periods and current velocities which are also presented at model scale

Table 4-40 shows current tests included in the campaign.

Configuration WC2 [0 degrees]											
Current											
Test	H [m]		T [s]		h [m]	Current [m/s]		Wind [m/s]	Thrust [tonnes]	Direction [°]	Duration [h]
	1/1	1/55	1/1	1/55		1/1	1/55				
58	0	0	0	0	165	1.06	0.143	0	0	0	1

Table 4-40. Configuration WC2: Current tests. All values are presented at full scale, except for the wave heights, wave periods and current velocities which are also presented at model scale

Table 4-41 shows the tests combining irregular waves, wind and current.

Configuration WC2 [0 degrees]												
Irregular Wave + Current + Wind												
Test	Hs [m]		Tp [s]		Spectrum	h [m]	Current [m/s]		Wind [m/s]	Thrust [tonnes]	Direction [°]	Duration [h]
	1/1	1/55	1/1	1/55			1/1	1/55				
59	2.75	0.050	9	1.214	JS-1.0	165	1.06	0.143	10.5 ETM	174.99	0	3

60	5.11	0.093	9	1.214	JS-1.2	165	1.06	0.143	10.5 NTM	193.88	0	3
----	------	-------	---	-------	--------	-----	------	-------	-------------	--------	---	---

Table 4-41. Configuration WC2: Irregular wave, Current and Wind tests. All values are presented at full scale, except for the wave significant heights, wave peak periods and current velocities which are also presented at model scale

WINDCRETE Installation Tests

- Installation tests in horizontal position:**

In order to analyse the behaviour of WINDCRETE concept un-ballasted and without wind turbine in horizontal position, irregular wave with soft mooring is proposed (Table 4-42).

Configuration WC0												
Irregular Wave with soft mooring												
Test	Hs [m]		Tp [s]		Spectrum	h [m]	Current [m/s]		Wind [m/s]	Thrust [tonnes]	Duration [h]	
	1/1	1/55	1/1	1/55			1/1	1/55				
61	2.75	0.050	11	1.483	JS-1.0	165	0	0	0	0	3	
62	2.75	0.050	14	1.888	JS-1.0	165	0	0	0	0	3	

Table 4-42. Configuration WC0: Irregular wave tests. All values are presented at full scale, except for the wave significant heights, wave peak periods and current velocities which are also presented at model scale

- Installation tests of raising up (upending):**

A specific test (#63) of the WINDCRETE with soft mooring replicating its erection from horizontal to vertical position, is conducted to validate the procedure and forces to be sustained during the installation of the spar platform. Besides, another raising-up test is repeated, but this time under a white noise loading (Table 4-43).

Configuration WC0												
White Noise with soft mooring												
Test	Hs [m]		T1 [s]		T2 [s]		h [m]	Current [m/s]		Wind [m/s]	Thrust [tonnes]	Duration [h]
	1/1	1/55	1/1	1/55	1/1	1/55		1/1	1/55			
64	2.75	0.050	7.5	1.011	22	2.967	165	0	0	0	0	3

Table 4-43. Configuration WC0: White noise test. All values are presented at full scale, except for the wave significant heights, wave periods and current velocities which are also presented at model scale

ACTIVEFLOAT Characterization Tests

The characterisation tests are a set of essential tests to validate that the model behaviour reflects the one of the designed full-scale prototype for both the platform and mooring system. Table 4-33 shows the characterisation tests and the parameters obtained in each of them.

- Tilt tests**

The initial stability test is performed by inducing roll/pitch motions by means of different heeling moments generated by masses placed at a certain distance from the vertical axis of the platform. The induced rotations are used to obtain the metacentric height (GM), both longitudinal and transverse in Configuration AF1.

- Decay tests**

Decay tests are carried out in free floating (Configuration AF1) in heave/roll/pitch and in moored conditions (Configuration AF2) in all system DoFs, as well as in surge/pitch with rated wind speed (Configuration AF3). The purpose of these tests is to evaluate the natural periods and the non-dimensional linear damping coefficients of each of the six degrees of freedom of the platform system.

Each test plans to alter the equilibrium position of a single degree of freedom and let the system reach its equilibrium again. The transient of the process is recorded by the tracking motion system and provides the pursued information.

- **Static offset tests**

The aim of these tests is to validate the stiffness of the mooring system. To do this, the platform is progressively displaced along the DoF of interest, measuring both the force required to apply the displacement and the displacement itself. The displacement is measured by the tracking position system, while the applied force is measured by an axial load cell installed in the device used to apply the platform displacement. These tests evaluate the stiffness of the mooring for positive and negative surge displacements in Configuration AF2.

Data analysis of hydrodynamic characterization tests						
Test		Mooring	Configuration	DOF	Results from data	
65	<i>Tilt tests</i>	Free floating	AF1	Roll	Metacentric height	
66				Pitch		
67	<i>Decay tests</i>	Free floating	AF1	Heave	Natural periods and non-dimensional coefficient of linear damping	
68				Roll		
69				Pitch		
70		Moored	AF2	Surge		
71				Sway		
72				Heave		
73				Roll		
74				Pitch		
75				Yaw		
76				AF3		Surge with rated wind
77						Pitch with rated wind
78	<i>Static Offset tests</i>	Moored	AF2	Positive Surge	Mooring system stiffness	
79				Negative Surge		

Table 4-44. Summary of hydrodynamic characterization tests

ACTIVEFLOAT Seakeeping Tests

ACTIVEFLOAT platform has been tested under different metocean conditions: (1) regular wave tests, (2) irregular wave tests, (3) white noise tests, (4) wind tests, (5) regular wave tests with wind, (6) irregular wave tests with wind, (7) current tests, (8) irregular wave tests with wind and with current.

The parameters defining the environmental conditions are the following: water depth (h), draught, regular wave height (H), regular wave period (T), significant wave height (H_s), peak period (T_p), wave spectrum and peakedness (γ in this case), wind velocity (U_w) and current velocity (U_c).

The following sections summarise the test matrix executed during the basin testing campaign. All tests have been classified according to the environmental conditions tested and all the environmental parameters are given in prototype scale. Each table includes the test configuration used in each case and the laboratory identification code.

- **Configuration AF2: Wave direction 0 degrees**

This paragraph resumes the characteristics of the tests executed in Configuration AF2, that is when the wave conditions are aligned with the platform main axis. Table 4-34 lists the tests executed generating regular waves.

Configuration AF2 [0 degrees]											
Regular Wave											
Test	H [m]		T [s]		h [m]	Current [m/s]		Wind [m/s]	Thrust [tonnes]	Direction [°]	Duration [Waves]
	1/1	1/55	1/1	1/40		1/1	1/40				
80	2.75	0.069	7.5	1.186	120	0	0	0	0	0	200
81	2.75	0.069	9	1.423	120	0	0	0	0	0	200
82	2.75	0.069	11	1.739	120	0	0	0	0	0	200
83	2.75	0.069	14	2.214	120	0	0	0	0	0	200
84	2.75	0.069	17	2.688	120	0	0	0	0	0	200
85	2.75	0.069	20	3.162	120	0	0	0	0	0	200
86	5.11	0.093	7.5	1.186	120	0	0	0	0	0	200
87	5.11	0.093	9	1.423	120	0	0	0	0	0	200
88	5.11	0.093	11	1.739	120	0	0	0	0	0	200
89	5.11	0.093	14	2.214	120	0	0	0	0	0	200
90	5.11	0.093	17	2.688	120	0	0	0	0	0	200
91	5.11	0.093	20	3.162	120	0	0	0	0	0	200

Table 4-45. Configuration AF2: Regular wave tests. All values are presented at full scale, except for the wave heights, wave periods and current velocities which are also presented at model scale

Table 4-35 presents the tests executed with irregular waves. The waves are generated based on Jonswap spectrum.

Configuration AF2 [0 degrees]												
Irregular Wave												
Test	Hs [m]		Tp [s]		Spectrum	h [m]	Current [m/s]		Wind [m/s]	Thrust [tonnes]	Direction [°]	Duration [h]
	1/1	1/40	1/1	1/40			1/1	1/40				
92	2.75	0.069	9	1.423	JS-3.3	120	0	0	0	0	0	3
93	2.75	0.069	11	1.739	JS-3.3	120	0	0	0	0	0	3

94	2.75	0.069	14	2.214	JS-3.3	120	0	0	0	0	0	3
95	5.11	0.128	9	1.423	JS-1.2	120	0	0	0	0	0	3
96	5.11	0.128	11	1.739	JS-1.2	120	0	0	0	0	0	3
97	2.75	0.069	9	1.423	JS-3.3 s = 9	120	0	0	0	0	0	3
98	2.75	0.069	9	1.423	JS-3.3 s = 15	120	0	0	0	0	0	3
99	5.11	0.128	11	1.739	JS-1.2 s = 6	120	0	0	0	0	0	3
100	5.11	0.128	11	1.739	JS-1.2 s = 12	120	0	0	0	0	0	3

Table 4-46. Configuration AF2: Irregular wave tests. All values are presented at full scale, except for the wave significant heights, wave peak periods and current velocities which are also presented at model scale

Table 4-36 provides the details of the white noise tests included in the campaign. These tests are used to build the platform RAOs.

Configuration AF2 [0 degrees]													
White Noise													
Test	Hs [m]		T1 [s]		T2 [s]		h [m]	Current [m/s]		Wind [m/s]	Thrust [tonnes]	Direction [°]	Duration [h]
	1/1	1/40	1/1	1/40	1/1	1/40		1/1	1/40				
101	2.75	0.069	7.5	1.186	22	3.479	120	0	0	0	0	0	3
102	5.11	0.128	7.5	1.186	22	3.479	120	0	0	0	0	0	3

Table 4-47. Configuration AF2: White noise tests. All values are presented at full scale, except for the wave significant heights, wave periods and current velocities which are also presented at model scale

- **Configuration AF3: Wave + Wind + Current direction 0 degrees**

This paragraph resumes the characteristics of the tests executed in Configuration AF3, that is when the environmental conditions are aligned with the platform main axis. Table 4-37 shows wind tests included in the campaign.

Configuration AF3 [0 degrees]											
Wind											
Test	H [m]		T [s]		h [m]	Current [m/s]		Wind [m/s]	Thrust [tonnes]	Direction [°]	Duration [h]
	1/1	1/40	1/1	1/40		1/1	1/40				
103	0	0	0	0	120	0	0	10.5	227.86	0	1
104	0	0	0	0	120	0	0	10.5 ETM	171.51	0	1
105	0	0	0	0	120	0	0	10.5 NTM	192.35	0	1

Table 4-48. Configuration AF3: Wind tests. All values are presented at full scale, except for the wave heights, wave periods and current velocities which are also presented at model scale

Table 4-38 presents the tests combining regular waves and wind.

Configuration AF3 [0 degrees]											
-------------------------------	--	--	--	--	--	--	--	--	--	--	--

Regular Wave + Wind											
Test	H [m]		T [s]		h [m]	Current [m/s]		Wind [m/s]	Thrust [tonnes]	Direction [°]	Duration [Waves]
	1/1	1/40	1/1	1/40		1/1	1/40				
106	2.75	0.069	7.5	1.186	120	0	0	10.5	227.44	0	200
107	2.75	0.069	9	1.423	120	0	0	10.5	227.86	0	200
108	2.75	0.069	11	1.739	120	0	0	10.5	226.72	0	200
109	2.75	0.069	14	2.214	120	0	0	10.5	221.35	0	200
110	2.75	0.069	17	2.688	120	0	0	10.5	220.23	0	200
111	2.75	0.069	20	3.162	120	0	0	10.5	216.45	0	200

Table 4-49. Configuration AF3: Regular wave and Wind tests. All values are presented at full scale, except for the wave heights, wave periods and current velocities which are also presented at model scale

Table 4-39 shows the tests combining irregular waves and wind.

Configuration AF3 [0 degrees]												
Irregular Wave + Wind												
Test	Hs [m]		Tp [s]		Spectrum	h [m]	Current [m/s]		Wind [m/s]	Thrust [tonnes]	Direction [°]	Duration [h]
	1/1	1/40	1/1	1/40			1/1	1/40				
112	2.75	0.069	9	1.423	JS-3.3	120	0	0	10.5 ETM	173.58	0	3
113	5.11	0.128	9	1.423	JS-1.2	120	0	0	10.5 NTM	193.29	0	3
114	2.75	0.069	9	1.423	JS-3.3 s = 6	120	0	0	10.5 ETM	173.29	0	3
115	2.75	0.069	9	1.423	JS-3.3 s = 12	120	0	0	10.5 ETM	174.02	0	3

Table 4-50. Configuration AF3: Irregular wave and Wind tests. All values are presented at full scale, except for the wave significant heights, wave peak periods and current velocities which are also presented at model scale

Table 4-40 shows current tests included in the campaign.

Configuration AF3 [0 degrees]											
Current											
Test	H [m]		T [s]		h [m]	Current [m/s]		Wind [m/s]	Thrust [tonnes]	Direction [°]	Duration [h]
	1/1	1/40	1/1	1/40		1/1	1/40				
116	0	0	0	0	120	1.06	0.168	0	0	0	1

Table 4-51. Configuration AF3: Current tests. All values are presented at full scale, except for the wave heights, wave periods and current velocities which are also presented at model scale

Table 4-41 shows the tests combining irregular waves, wind and current.

Configuration AF3 [0 degrees]												
Irregular Wave + Current + Wind												

Test	Hs [m]		Tp [s]		Spectrum	h [m]	Current [m/s]		Wind [m/s]	Thrust [tonnes]	Direction [°]	Duration [h]
	1/1	1/40	1/1	1/40			1/1	1/40				
117	2.75	0.069	9	1.423	JS-1.0	120	1.06	0.168	10.5 ETM	173.99	0	3
118	5.11	0.128	9	1.423	JS-1.2	120	1.06	0.168	10.5 NTM	193.63	0	3

Table 4-52. Configuration AF3: Irregular wave, Current and Wind tests. All values are presented at full scale, except for the wave significant heights, wave peak periods and current velocities which are also presented at model scale

ACTIVEFLOAT Installation Tests

In order to analyse the behaviour of ACTIVEFLOAT concept un-ballasted, irregular wave and white noise tests with soft mooring to obtain the spectral RAOs of motions are proposed (Table 4-42 and Table 4-43).

Configuration AF0											
Irregular Wave with soft mooring											
Test	Hs [m]		Tp [s]		Spectrum	h [m]	Current [m/s]		Wind [m/s]	Thrust [tonnes]	Duration [h]
	1/1	1/40	1/1	1/40			1/1	1/40			
119	2.75	0.069	9	1.423	JS-1.0	120	0	0	0	0	3
120	2.75	0.069	11	1.739	JS-1.0	120	0	0	0	0	3
121	2.75	0.069	14	2.214	JS-1.0	120	0	0	0	0	3

Table 4-53. Configuration AF0: Irregular wave tests. All values are presented at full scale, except for the wave significant heights, wave peak periods and current velocities which are also presented at model scale

Configuration AF0												
White Noise with soft mooring												
Test	Hs [m]		T1 [s]		T2 [s]		h [m]	Current [m/s]		Wind [m/s]	Thrust [tonnes]	Duration [h]
	1/1	1/40	1/1	1/40	1/1	1/40		1/1	1/40			
122	2.75	0.069	7.5	1.186	22	3.479	120	0	0	0	0	3

Table 4-54. Configuration AF0: White noise test. All values are presented at full scale, except for the wave significant heights, wave periods and current velocities which are also presented at model scale

4.7 Experimental Layouts

4.7.1 First round of wave basin tests

The layout of the Multi-fan system on the bench is being designed in order to conduct the prescribed oscillations forced by a linear actuator.

4.7.2 Second round of wave basin tests

The inertial reference system is placed on the free surface, in the vertical of the CoG of both platforms. The placement of the mockups inside the basin is defined by the mooring characteristics and auxiliary devices included in the basin layout.

In both seakeeping tests campaigns, the CoG of WINDCRETE mockup as well as the CoG of ACTIVEFLOAT mockup are placed at the coordinates [N+34, 00] of the CCOB grid. Note there is 1 m of distance between two consecutive letters, beginning to count from wave generation.

In the installation tests campaign of the WINDCRETE, the CoG of the mockup is placed at the coordinates [M+504, 00] of the CCOB grid. In the installation tests campaign of the ACTIVEFLOAT, the CoG of the mockup is placed at the coordinates [N+452, 00] of the CCOB grid.

Calibration Layout

Figure 4-44 shows the layout of the wave gauges and the ADV current sensors during the calibration of wave and/or current sea states.

WINDCRETE Mooring Layout

The layout of the truncated mooring system in Figure 4-45 presents the nomenclature of the main lines, delta connections and delta lines, as well as the location of the three anchors on the basin floor as coordinates of the CCOB grid. Since there is a load cell in the fairlead/connection of each line, we use the same nomenclature to refer load cells.

WINDCRETE Soft-mooring Layouts

The layout of the soft-mooring systems for the installation tests of the WINDCRETE un-ballasted and without the wind turbine presents the nomenclature of the four lines used in horizontal position (Figure 4-46) and the only two lines used in the raising-up tests (Figure 4-47), as well as the location of their corresponding anchors on the basin floor as coordinates of the CCOB grid.

WINDCRETE Bodies Layout

The layout of the bodies in Figure 4-48 presents the nomenclature of the bodies to which the movements are referred and their location in plane XZ for the different configurations, as well as the local axes in plane XY when recording forces and moments from the tri-axis load cell and accelerations at the nacelle.

ACTIVEFLOAT Mooring Layout

The layout of the truncated mooring system in Figure 4-49 presents the nomenclature of the three mooring lines, as well as the location of the three anchors on the basin floor as coordinates of the CCOB grid.

ACTIVEFLOAT Soft-mooring Layout

The layout of the soft-mooring system for the installation tests of the ACTIVEFLOAT un-ballasted presents the nomenclature of the four lines used (Figure 4-50), as well as the location of their corresponding anchors on the basin floor as coordinates of the CCOB grid.

ACTIVEFLOAT Bodies Layout

The layout of the bodies in Figure 4-51 presents the nomenclature of the bodies to which the movements are referred and their location in plane XZ for the different configurations, as well as the local axes in plane XY when recording forces and moments from the tri-axis load cell and accelerations at the nacelle.

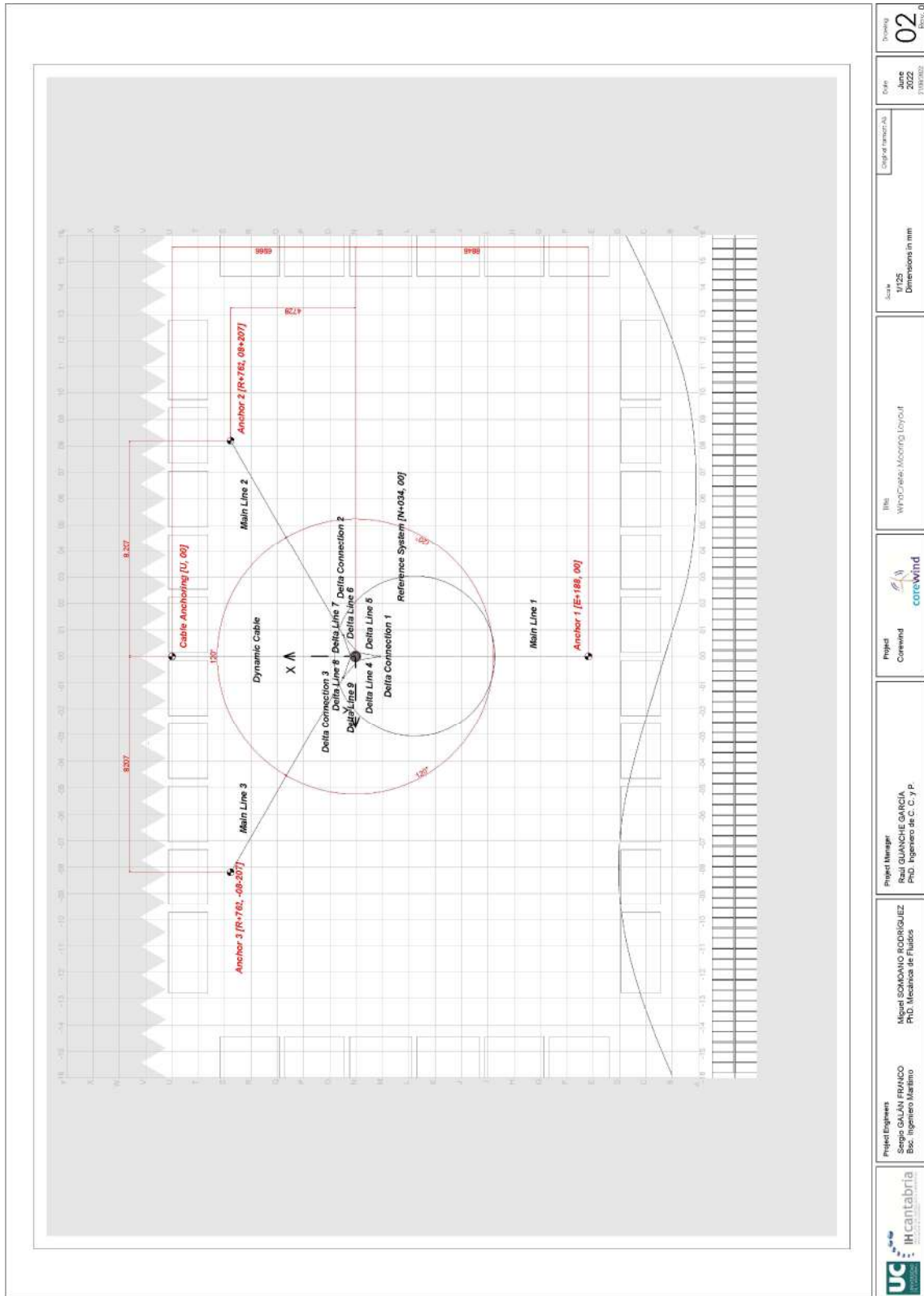


Figure 4-45. WINDCRETE Mooring system and Dynamic cable Layout

		Project Engineers Sergio GALAN FRANCO Ebc. Ingeniero Industrial	Project Manager Raúl GUANICHE GARCÍA PhD. Ingeniero de C. y P.	Project Corewind		Title WINDCRETE Mooring Layout	Scale D1/25 Dimensions in mm	Author Juan José 13/03/2022	Revising 02 13/03/22
---	---	--	---	----------------------------	--	--	---	--	-----------------------------------

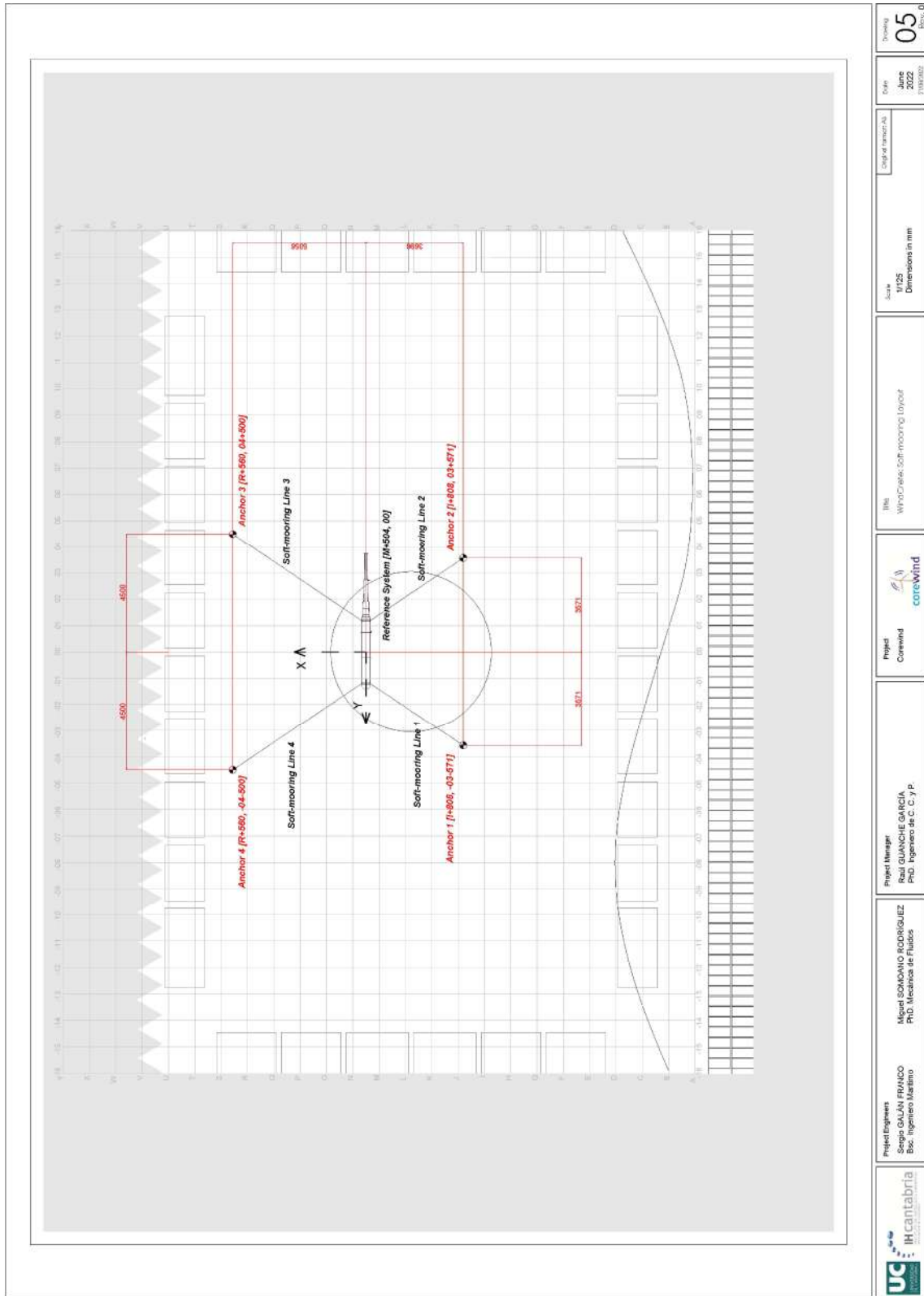


Figure 4-46. WINDCRETE Soft-mooring Layout for installation tests

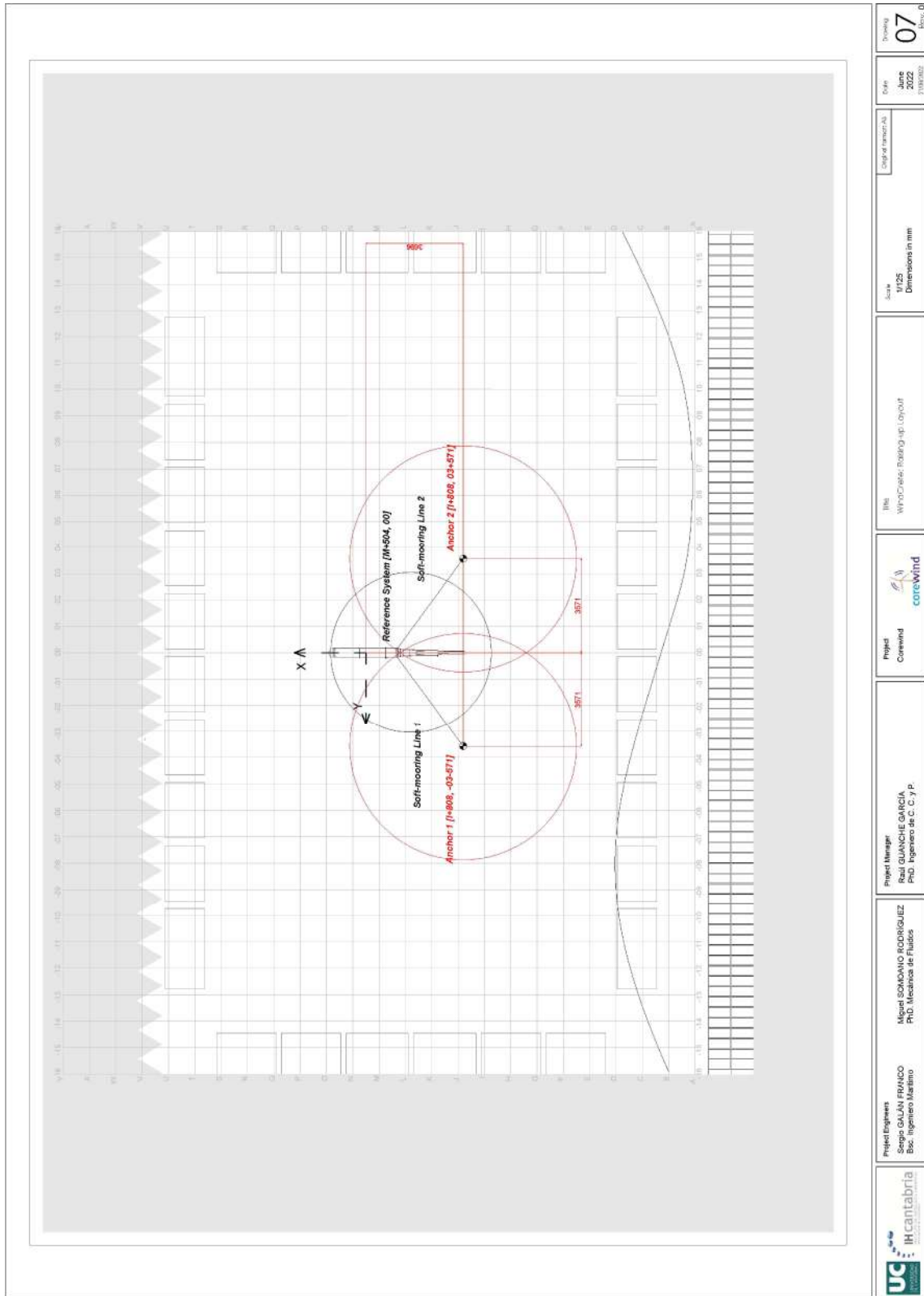


Figure 4-47. WINDCRETE Soft-mooring Layout for raising-up tests

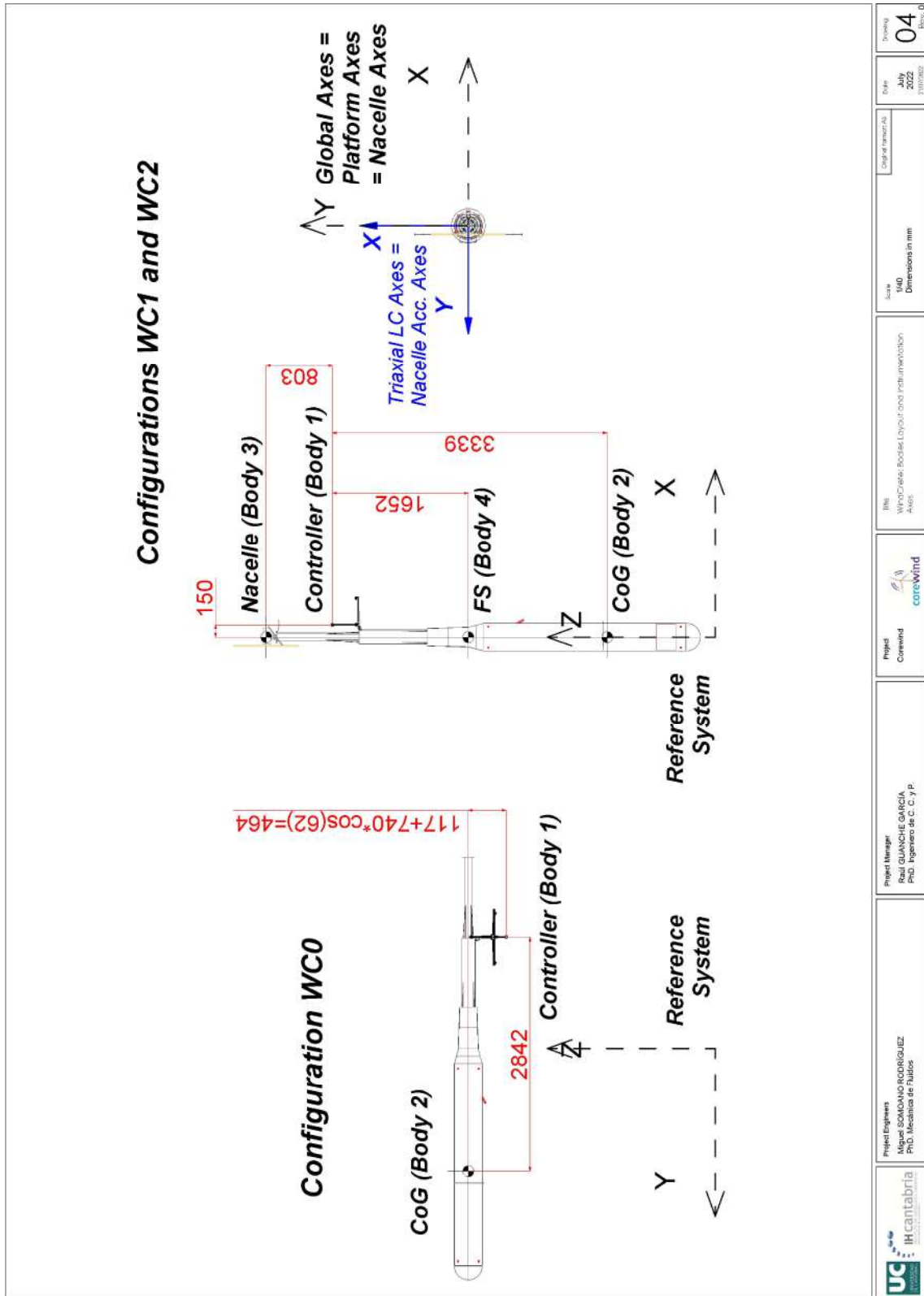


Figure 4-48. WINDCRETE Bodies Layout and Instrumentation Axes

	Project Engineers Alquel SOMOLANO RODRIGUEZ PhD. Mecánica de Fluidos	Project Manager Raúl GUANICHE GARCÍA PhD. Ingeniero de C. C. y P.	Project Corewind		Title WINDCRETE Bodies Layout and Instrumentation PAGE	Scale 1:10 Dimensions in mm	Date July 2013	Drawing 04
---	--	---	---------------------	---	--	-----------------------------------	-------------------	---------------

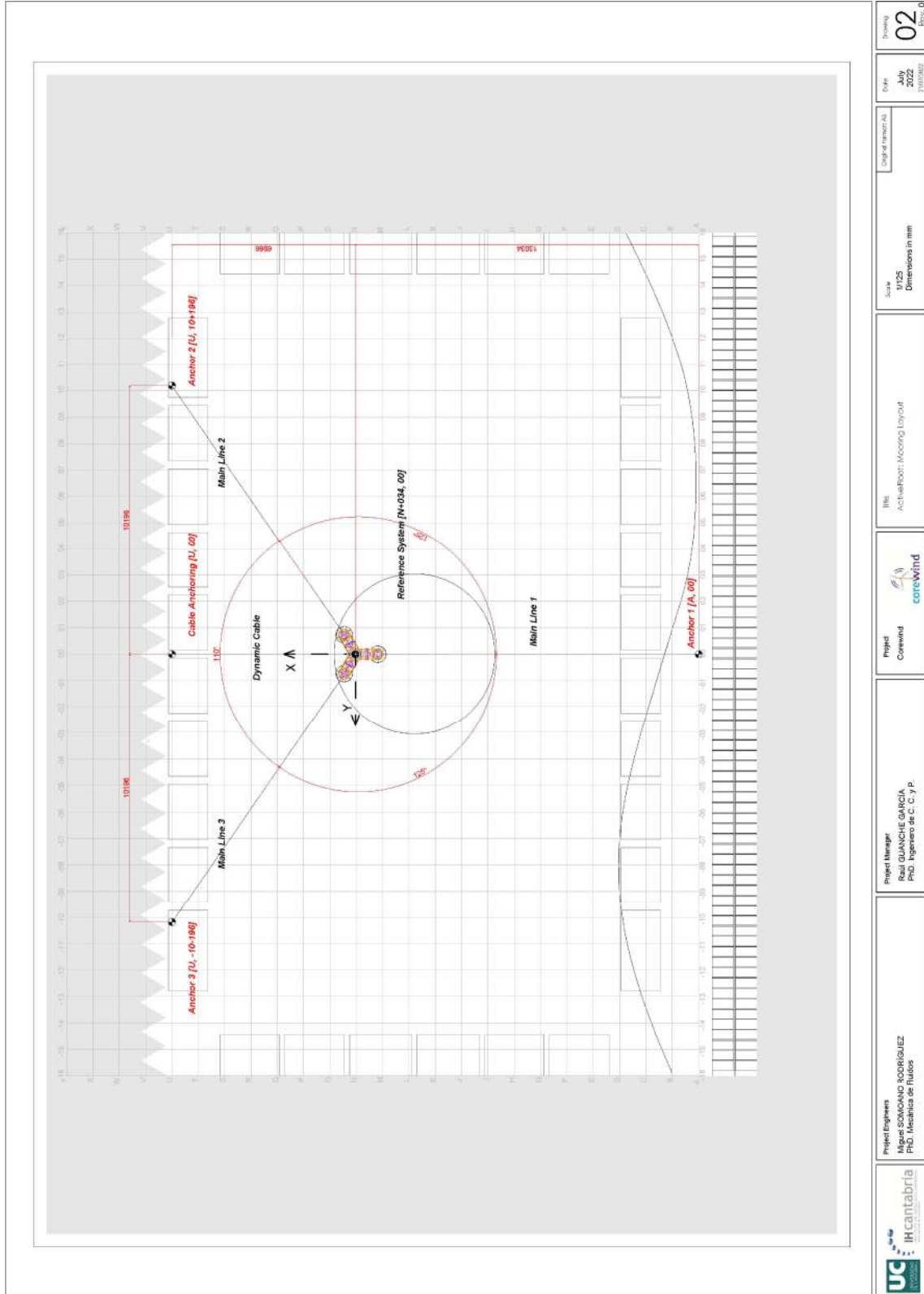


Figure 4-49. ACTIVEFLOAT Mooring system and Dynamic cable Layout

Project Engineers Iñigo DOMÍNGUEZ RODRÍGUEZ PhD - Inicial de Tutores	Project Manager Raúl GUANICHE GARCÍA PhD - Ingeniero de C. y P.	Project Corewind	corewind	File ActiveFloat: Mooring Layout	Scale D1:25 Dimensions in mm	Date July 2023	Drawing 02
--	---	---------------------	----------	-------------------------------------	------------------------------------	----------------------	---------------

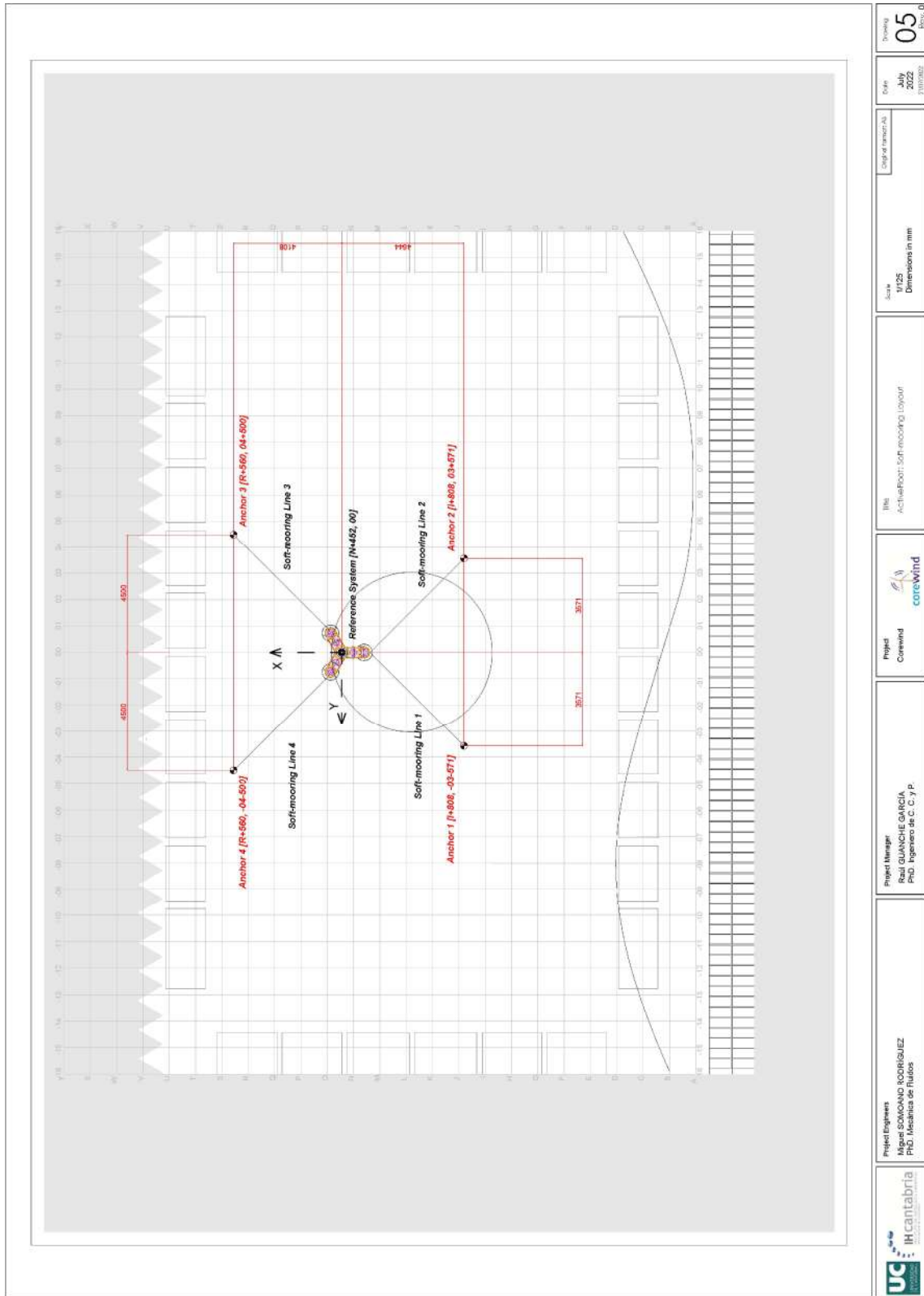


Figure 4-50. ACTIVEFLOAT Soft-mooring Layout for installation tests

Project Engineers Iñigo DOMÍNGUEZ RODRÍGUEZ PhD. Ingeniero de Títulos	Project Manager Raúl GUANACHE GARCÍA PhD. Ingeniero de C. y P.	Project Corewind	corewind	Title ActualPort: Soft-mooring Layout	Scale D1/25 Dimensions in mm	Drawn July 2023 13/07/2023	Revising 05 13/07/2023
---	--	---------------------	----------	--	------------------------------------	----------------------------------	------------------------------

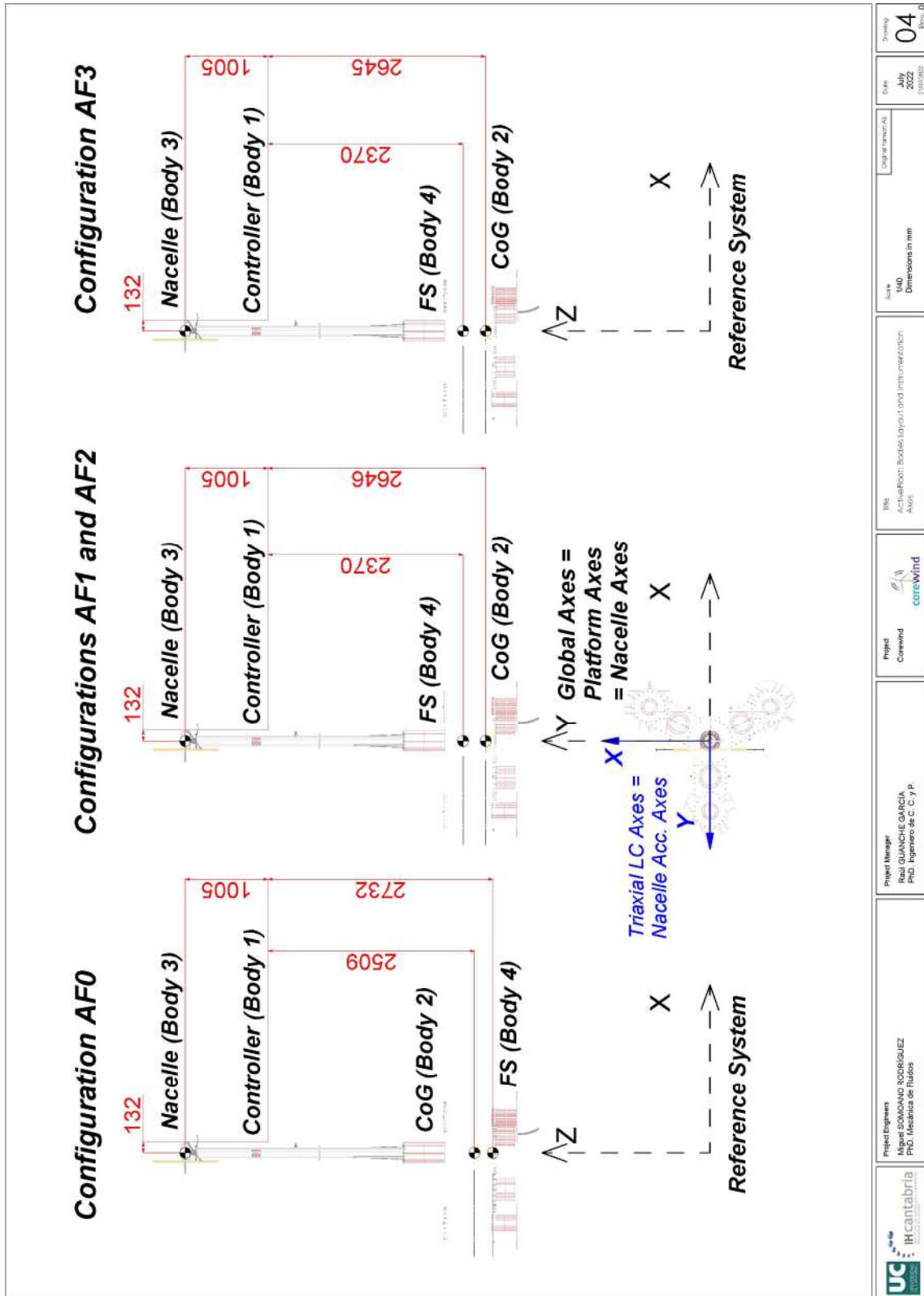


Figure 4-51. ACTIVEFLOAT Bodies Layout for the different configurations

		Project Engineers Igor DOMONICO RODRIGUEZ PhD. Ingeniero de Fluidos	Project Manager Raúl GUANICHE GARCÍA PhD. Ingeniero de C. y P.	Project Corewind		Title Activefloat Bodies layout and instrumentation AF01	Scale 1:100 Dimensions in mm	Date July 2018 13/07/2018	Revisión 04 Rev. 0
---	---	---	--	---------------------	--	--	------------------------------------	---------------------------------	--------------------------

4.8 Data analysis

To ease the understanding of the present report and the results included on it, this paragraph briefly summarizes the variables analysed as well as the statistical analysis carried out and how the results obtained are depicted.

For each test performed, different variables such as loads, motions, accelerations and environmental loads (wave, current and wind/thrust) are recorded. Such data allows to analyse the hydrodynamic and aerodynamic response of the floating platform.

The analysis performed for the different variables commented above are divided in three groups: (1) characterization tests; (2) wind tests; (3) wave, current and coupled tests.

4.8.1 Characterization tests

Table 4-55 summarizes the characterization tests carried out during the basin testing campaign.

Data analysis of hydrodynamic characterization tests		
Tests	Configuration	Results from data
<i>Tilt tests</i>	Free floating (Roll, Pitch)	Metacentric height
<i>Decay tests</i>	Free floating (Heave, Roll, Pitch)	Natural periods and Non-dimensional coefficient of linear damping
	Moored (Surge, Sway, Heave, Roll, Pitch, Yaw, Surge with, below and above rated wind, Pitch with, below and above rated wind)	
<i>Static Offset tests</i>	Moored (Positive Surge, Negative Surge)	Mooring system stiffness

Table 4-55. Data analysis and intended results of characterization test

4.8.2 Wind tests

During the execution of the wind tests, time series of motions, mooring line loads, accelerations and thrust are recorded. Beside them, the rotor thrust calculated by the Hardware-In-the-Loop is analysed. Table 4-56 summarizes all statistical variables obtained from time series for wind tests.

Data analysis: Wind tests		
Variable	Measured	Output
Movements	CoG	Statistical and spectral analysis
	Nacelle	
	MSL	
Mooring system loads	Mooring line fairleads	
Accelerations	Nacelle	
Wind thrust	Tower Top	
Wind thrust – calculated by HIL	Rotor	-

Table 4-56. Data analysis: Wind tests

4.8.3 Wave, current and coupled tests

Wave tests (regular, irregular and white noise), current tests and coupled tests (wave, current and/or wind combinations) are used to check the overall hydrodynamic performance of the floating platform. Time series of motions, mooring system loads, nacelle accelerations, free surface, wind loads (thrust) and current are recorded during each test. Beside them, the rotor thrust calculated by the Hardware in the Loop is also analysed.

Several statistical variables are obtained from these time series. Table 4-57 summarizes them, the position at which the variables are measured, and the analysis carried out for each variable recorded.

Data analysis: Wave and coupled tests		
Variable	Measured	Output
Movements	CoG	Statistical and spectral analysis
	Nacelle	
	MSL	
Mooring system loads	Mooring line fairleads	
Accelerations	Nacelle	
Free Surface	Incident analysis (Control Array)	
Wind thrust	Tower Top	
Current velocity	Control array	Statistical analysis. Mean value
Wind thrust – calculated by HIL	Rotor	-

Table 4-57. Data analysis: Wave, Current and Coupled tests

4.8.4 Statistical analysis

The statistical parameters obtained from time series of variables considered in these tests are broken down below:

- Mean Value.
- Standard Deviation.
- Maximum Value: Maximum peak Value (A^+).
- Minimum Value: Maximum Trough Value (A^-).
- Maximum double Amplitude: Maximum cycle of the time series. Height or difference between peak and trough ($2A_{max}$).
- Mean Peak Value: Mean of all peaks.
- Mean trough Value: Mean of all troughs.
- Significant peak value ($A^{+1/3}$): Mean of the highest third of the crest values.
- Significant trough value ($A^{-1/3}$): Mean of the lowest third of the trough values.
- Significant double amplitude ($2A^{+1/3}$): Mean of the highest third of the distance between crest and trough.

In addition to statistical parameters described previously, the Response Amplitude Operators (RAOs) are obtained for the platform motions (referred to CoG and nacelle) for regular wave tests. The formulation to obtain the regular RAO functions is shown in following equation.

$$RAO \left(\frac{m}{m} \text{ or } \frac{deg}{m} \right) = \frac{2A_{DOF}}{H_{inc}}$$

Where:

- $2A_{DOF}$: For a DOF analysed, it is mean value between peaks and troughs (m or deg).
- H_{inc} : Incident wave height (m).

RAOs for mooring line forces and accelerations at nacelle have been also obtained in order to analyse the response of these variables depending on the period of the regular wave.

Likewise, irregular wave response functions were calculated from spectral densities in the following way. In this case, white noise tests are used to obtain spectral RAOs of motions.

$$\text{Spectral RAO} \left(\frac{m}{m} \text{ or } \frac{\text{deg}}{m} \right) = \sqrt{\frac{S_{mov}(w)}{S_{\eta}(w)}}$$

- $S_{mov}(w)$: For a DOF analysed, spectral density of signal S_{mov} (m^2/s or deg^2/s).
- $S_{\eta}(w)$: Spectral density of incoming waves (m^2/s).

Finally, the tension peaks recorded at the platform fairleads are fitted with a Weibull distribution function. The analysis is done for first and second order forces, as well as for the original time series. Beside the Weibull fitting parameters, the Most Probable Maximum (MPM) is calculated for each of the three series.

5 RESULTS FROM FIRST ROUND OF WAVE BASIN TESTS

To validate the basic aerodynamics of the 15MW Wind Turbine observed in the POLIMI Wind Tunnel, the FIHAC Multi-fan is firstly tested in a fixed condition with several different wind speeds, including different below rated, above rated and wind rated cases. Once the load cases with fixed turbine have been carried out to simulate the aerodynamic response of the IEA 15 MW in the corresponding wind conditions, prescribed movements tests are conducted to validate the control induced effects as well as the unsteady aerodynamic effects,

For the unsteady wind cases to reproduce the performance of a dynamic turbine, the FIHAC Multi-fan is forced to oscillate in surge using different frequencies and amplitudes under the same wind conditions as in the fixed turbine cases. The prescribed movements set by POLIMI are based on the test requirements given for both structures. Thus, the wind turbine control system is validated for a given set of realistic range of movements, and the unsteady aerodynamics are studied in the same range of movements.

Figure 5-1 shows how the linear actuator used to oscillate the FIHAC Multi-fan in surge, is previously calibrated by tracking the motions of the Qualisys super-spherical markers.



Figure 5-1. Calibration of the linear actuator for the prescribed movements

Figure 5-2 presents the experimental setup of the FIHAC Multi-fan when it is forced by the linear actuator to oscillate under the prescribed movements tests.



Figure 5-2. Setup of the FIHAC Multi-fan for the prescribed movements

5.1 WINDCRETE wind turbine

The capability to reproduce aerodynamic loads with high accuracy is guaranteed by an adequate calibration procedure. The result of such practice allows to limit the error of the generated thrust at less than 3% of the target value. Figure 5-3, Figure 5-4 and Figure 5-5 show the comparison between the generated thrust and the target value in the calibration of FIHAC Multi-fan to step wind, to ramp wind and to rated wind (10.5 m/s) with Extreme Turbulence Model (ETM), respectively.

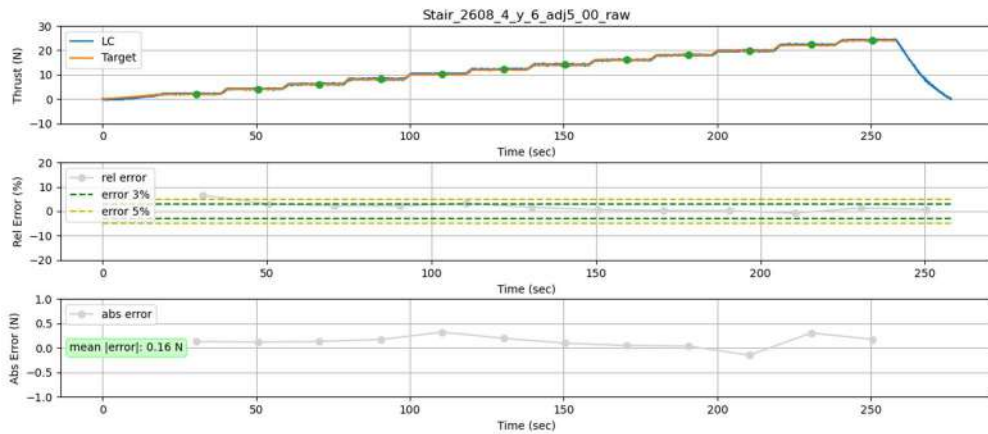


Figure 5-3. Calibration of FIHAC Multi-fan to step wind

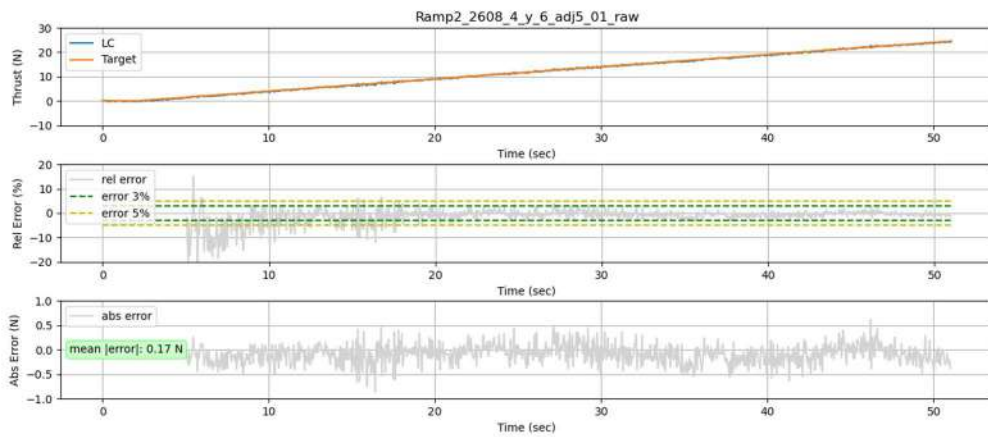


Figure 5-4. Calibration of FIHAC Multi-fan to ramp wind

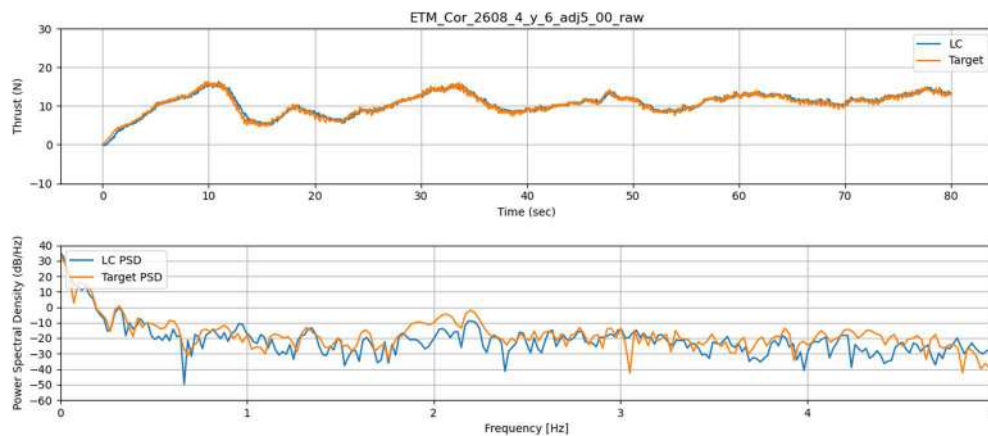


Figure 5-5. Calibration of FIHAC Multi-fan to rated wind (10.5 m/s) with Extreme Turbulence Model (ETM)

5.2 ACTIVEFLOAT wind turbine

The capability to reproduce aerodynamic loads with high accuracy is guaranteed by an adequate calibration procedure. The result of such practice allows to limit the error of the generated thrust at less than 3% of the target value. Figure 5-6, Figure 5-7 and Figure 5-8 show the comparison between the generated thrust and the target value in the calibration of FIHAC Multi-fan to step wind, to ramp wind and to rated wind (10.5 m/s) with Extreme Turbulence Model (ETM), respectively.

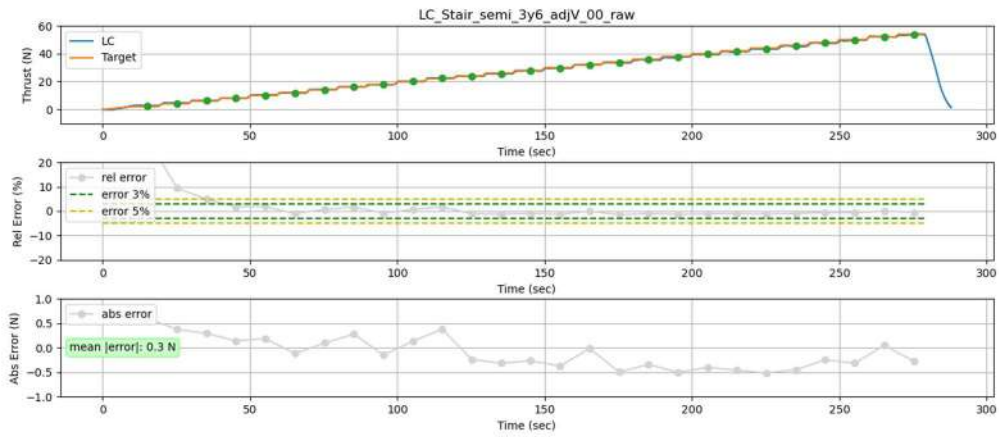


Figure 5-6. Calibration of FIHAC Multi-fan to step wind

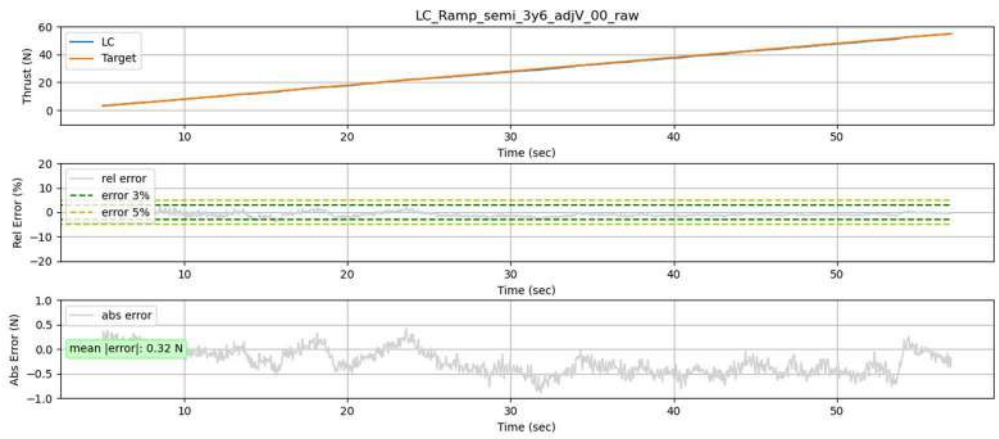


Figure 5-7. Calibration of FIHAC Multi-fan to ramp wind

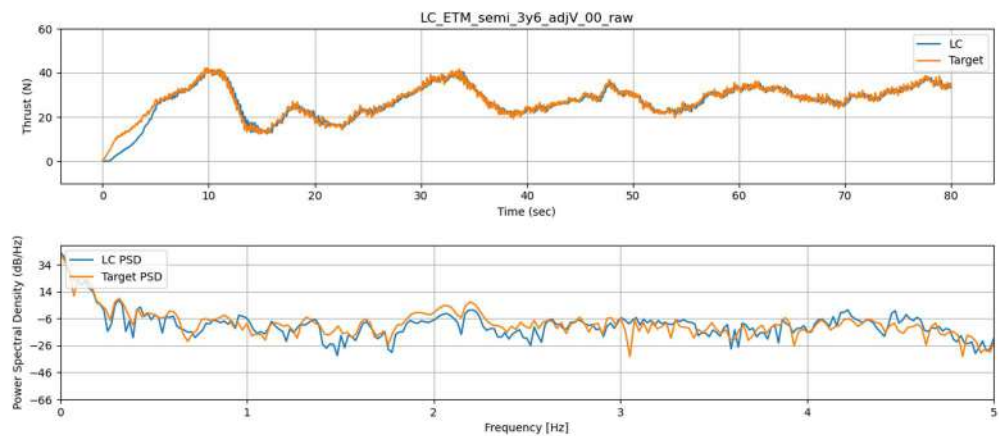


Figure 5-8. Calibration of FIHAC Multi-fan to rated wind (10.5 m/s) with Extreme Turbulence Model (ETM)

6 RESULTS FROM SECOND ROUND OF WAVE BASIN TESTS

During this section, the results obtained from the physical experiments are widely described and discussed. For each platform, the results section is organized as follow: (1) a summary of the wave calibration, (2) the hydrodynamic characterization outcome and (3) the more relevant statistics of the measurements recorded during the seakeeping tests.

6.1 WINDCRETE spar-based wind concept

As aforementioned, the test set-ups or configurations tested are the followings:

- **Configuration WC0:** Free floating WINDCRETE without wind turbine and without ballast for installation tests.
- **Configuration WC1:** Free floating WINDCRETE.
- **Configuration WC2:** Moored WINDCRETE with environmental loads aligned at 0°.

6.1.1 Wave calibration

To correctly reproduce the target sea-state conditions during the seakeeping tests, regular waves (Table 6-1), irregular waves (Table 6-2), white noise (Table 6-3), current (Table 6-4) and irregular waves with current (Table 6-5) were previously calibrated in absence of the model in the flume. From the surface measurements, the incident wave was obtained using WaveLab 3 software from Aalborg University and presented for the control and the calibration arrays. The calibration array is used only during this wave calibration phase; and the control array provides a reference to verify the validity of the generated sea-state conditions during the seakeeping tests.

Calibration: Regular Wave					
Test/Laboratory Code	h [m]	H [m]	T [s]	Calibration Array	
				Hinc [m]	Tinc [s]
'FIH18-00014_CAL_RW_H2p75_T7p5_ABS_05'	165	2.75	7.5	2.73	7.50
'FIH18-00014_CAL_RW_H2p75_T9_ABS_05'	165	2.75	9	2.69	9.00
'FIH18-00014_CAL_RW_H2p75_T11_ABS_05'	165	2.75	11	2.80	11.01
'FIH18-00014_CAL_RW_H2p75_T14_ABS_05'	165	2.75	14	2.63	13.95
'FIH18-00014_CAL_RW_H2p75_T17_ABS_02'	165	2.75	17	2.83	16.98
'FIH18-00014_CAL_RW_H2p75_T20_ABS_04'	165	2.75	20	2.78	19.93
'FIH18-00014_CAL_RW_H5p11_T7p5_ABS_07'	165	5.11	7.5	5.04	7.46
'FIH18-00014_CAL_RW_H5p11_T9_ABS_04'	165	5.11	9	5.01	9.00
'FIH18-00014_CAL_RW_H5p11_T11_ABS_02'	165	5.11	11	5.01	10.95
'FIH18-00014_CAL_RW_H5p11_T14_ABS_02'	165	5.11	14	4.90	13.99
'FIH18-00014_CAL_RW_H5p11_T17_ABS_02'	165	5.11	17	4.99	16.95
'FIH18-00014_CAL_RW_H5p11_T20_ABS_01'	165	5.11	20	5.10	20.00

Table 6-1. Calibration: Regular Wave. Incident Analysis

Calibration: Irregular Wave								
Test/Laboratory Code	h [m]	Hs [m]	Tp [s]	Spectrum	Gamma	Spread	Calibration Array	
							Hinc [m]	Tinc [s]
'FIH18-00014_CAL_JS_H2p75_T9_G3p3_ABS_01'	165	2.75	9	'JS'	3.3	-	2.66	9.34
'FIH18-00014_CAL_JS_H2p75_T11_G3p3_ABS_00'	165	2.75	11	'JS'	3.3	-	2.74	11.04
'FIH18-00014_CAL_JS_H2p75_T14_G3p3_ABS_00'	165	2.75	14	'JS'	3.3	-	2.77	14.13
'FIH18-00014_CAL_JS_H5p11_T9_G1p2_ABS_01'	165	5.11	9	'JS'	1.2	-	5.23	8.44
'FIH18-00014_CAL_JS_H5p11_T11_G1p2_ABS_01'	165	5.11	11	'JS'	1.2	-	5.26	11.47
'FIH18-00014_CAL_JS_H2p75_T9_G3p3_S6_ABS_02'	165	2.75	9	'JS'	3.3	6	2.71	9.11
'FIH18-00014_CAL_JS_H2p75_T9_G3p3_S12_ABS_01'	165	2.75	9	'JS'	3.3	12	2.87	8.94
'FIH18-00014_CAL_JS_H5p11_T11_G1p2_S6_ABS_02'	165	5.11	11	'JS'	1.2	6	5.19	10.60
'FIH18-00014_CAL_JS_H5p11_T11_G1p2_S12_ABS_01'	165	5.11	11	'JS'	1.2	12	5.29	11.12

Table 6-2. Calibration: Irregular Wave. Incident Analysis

Calibration: White Noise					
Test/Laboratory Code	h [m]	Hs [m]	T1 [s]	T2 [s]	Calibration Array Hinc [m]
'FIH18-00014_CAL_TH_H2p75_T11p19_DF0p088_ABS_02'	165	2.75	7.5	22	2.81
'FIH18-00014_CAL_TH_H5p11_T11p19_DF0p088_ABS_01'	165	5.11	7.5	22	5.10

Table 6-3. Calibration: White Noise. Incident Analysis

Calibration: Current			
Test/Laboratory Code	h [m]	Current [m/s]	Calibration Array Current [m/s]
'FIH18-00014_CAL_SN0p143_23Hz_00'	165	1.06	1.07

Table 6-4. Calibration: Current

Calibration: Irregular Wave + Current								
Test/Laboratory Code	h [m]	Hs [m]	Tp [s]	Spectrum	Gamma	Current [m/s]	Calibration Array	
							Hinc [m]	Current [m/s]
'FIH18-00014_CAL_JS_H2p75_T9_G1_SN0p143_00'	165	2.75	9	'JS'	1.0	1.06	2.70	0.98
'FIH18-00014_CAL_JS_H5p11_T9_G1p2_SN0p143_00'	165	2.75	9	'JS'	1.2	1.06	5.04	1.03

Table 6-5. Calibration: Irregular Wave with Current. Incident Analysis

6.1.2 Characterization Tests Results

GM analysis

Once the mockup is moored (Configuration WC2), it shows the expected draft, i.e. 156.650 m instead of 155 m due to the negative deviation in the diameter and the positive deviation in weight when manufactured.

To obtain the GM, in this case we cannot conduct the tilt tests. Thus, we carry out a hydrostatic analysis with AQWA software taking into account all deviations aforementioned. The actual GM is 14.890 m, what involved a deviation of -4.31%. However, note that this analytical approach may introduce uncertainty in the result.

The mooring line also have the expected pretensions for this draft in the static position, i.e. 296 tonnes in main lines 1-3 for the actual draft of 156.650 m (instead of 330 tonnes for a draft of 155 m) and 156 tonnes in delta lines 4-9 for the actual draft of 156.650 m (instead of 174 tonnes for a draft of 155 m).

When the WINDCRETE platform is moored, the static position of its CoG has a $X < 0$ because it was the inertial reference for the preliminary but not for the optimized mooring system.

Decay tests

The decays tests are executed with the platform in free floating (Configuration WC1) and moored (Configuration WC2) conditions. When executed in free floating condition, clump weights are added at the fairleads to replicate the vertical tensions of the delta mooring lines. Table 6-6 summarizes the tests conducted.

Tests	Mooring	Tested DoF	Repetitions
Decay Tests	Free Floating	Heave, Roll, Pitch	5
	Moored	Surge, Sway, Heave, Roll, Pitch, Yaw	5
		Surge with, below and above rated wind, Pitch with, below and above rated wind	5

Table 6-6. Decay Tests executed

Each test is repeated five times to ensure the statistical representativeness of the results. Therefore, the results shown in the following tables are the mean values of the trials performed for each DoF. Figure 6-1 shows a

picture of the decay test procedure. The average values of the natural period and the non-dimensional damping coefficient for each cycle [15], are shown on the top. Assuming the damping is linear and so the logarithmic decrement is constant, the non-dimensional damping coefficient may also be calculated by linear regression (on the left).

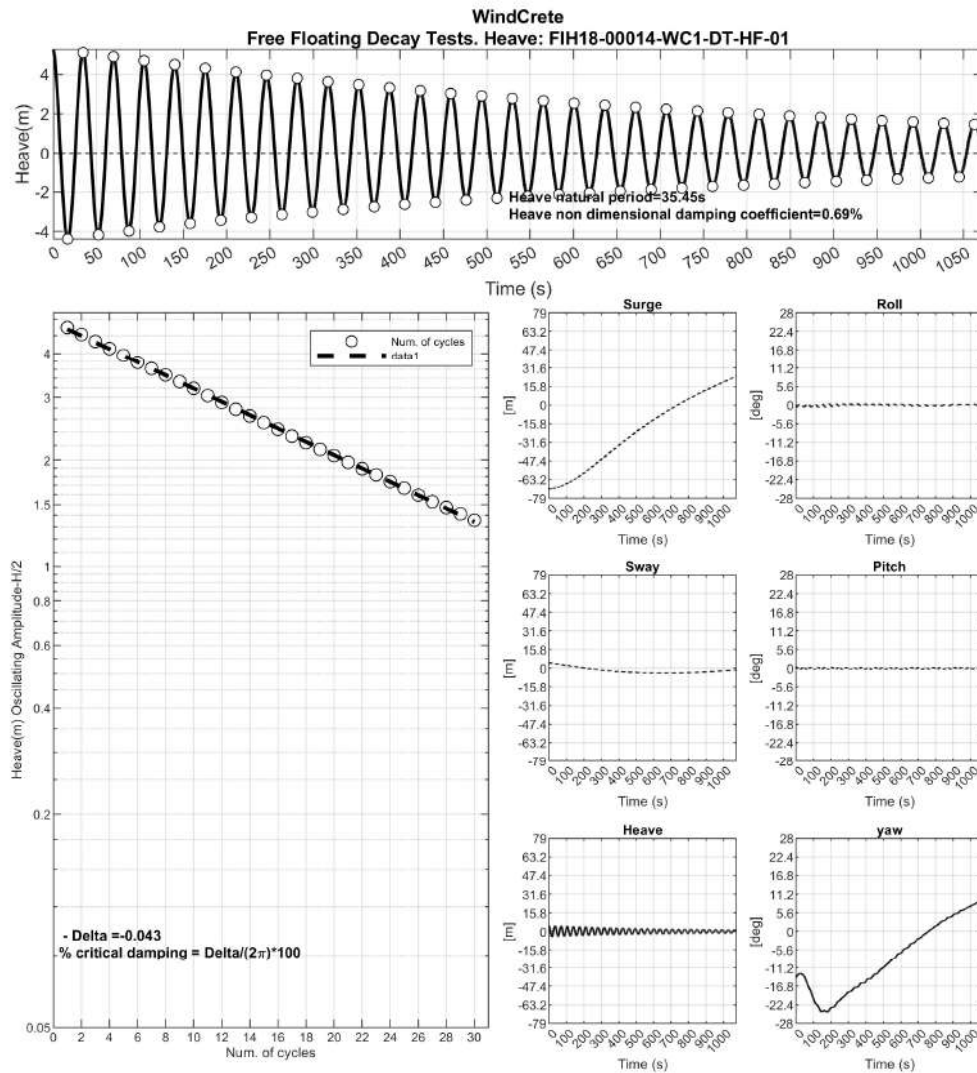


Figure 6-1. Example of a free-floating decay test analysis (Heave)

The decay tests results are shown in Table 6-7. The average non-dimensional linear damping presented in the tables is related to critical damping of the specific DoF.

	DOF	Damping [%]	Measured Natural Period [s]	Target Natural Period [s]	Deviation [s]
Free-floating Decay Tests	Heave	0.69	35.41		
	Roll	0.90	41.42		
	Pitch	0.79	41.10		
	Surge	7.40	79.23	84.10	-4.87

Moored Decay Tests	<i>Sway</i>	6.02	82.94		
	<i>Heave</i>	1.60	34.73	33.97	0.76
	<i>Roll</i>	0.64	41.30		
	<i>Pitch</i>	0.89	41.02	42.46	-1.44
	<i>Yaw</i>	6.37	16.18	11.76	4.42
	<i>Surge with rated wind</i>	14.30	66.63		
	<i>Pitch with rated wind</i>	9.53	44.78		
	<i>Surge below rated wind</i>	15.20	66.48		
	<i>Pitch below rated wind</i>	19.83	48.74		
	<i>Surge above rated wind</i>	10.51	75.55		
	<i>Pitch above rated wind</i>	6.23	42.30		

Table 6-7. Natural periods and Damping coefficients obtained during the decay tests

Mooring system decreases natural periods in heave, roll and pitch. Besides, there is a negative deviation in surge and in pitch with respect to the target values, what may be explained by using a stiffer mooring system. However, since the actual draft is 156.650 m, the free-surface section is smaller, and this means a negative deviation of the hydrostatic stiffness. Together with a positive deviation in weight of the manufactured mockup, this causes the positive deviation in the natural period of heave with respect to the target value.

Static Offset Tests

The static offset tests are performed to assess the stiffness of the mooring system in Configuration WC2. Those tests are executed in positive and negative surge directions.

Figure 6-2 shows the relation between the platform surge and the force applied for achieving those displacements during the three repetitions executed pulling the platform at 0° in the positive surge direction.

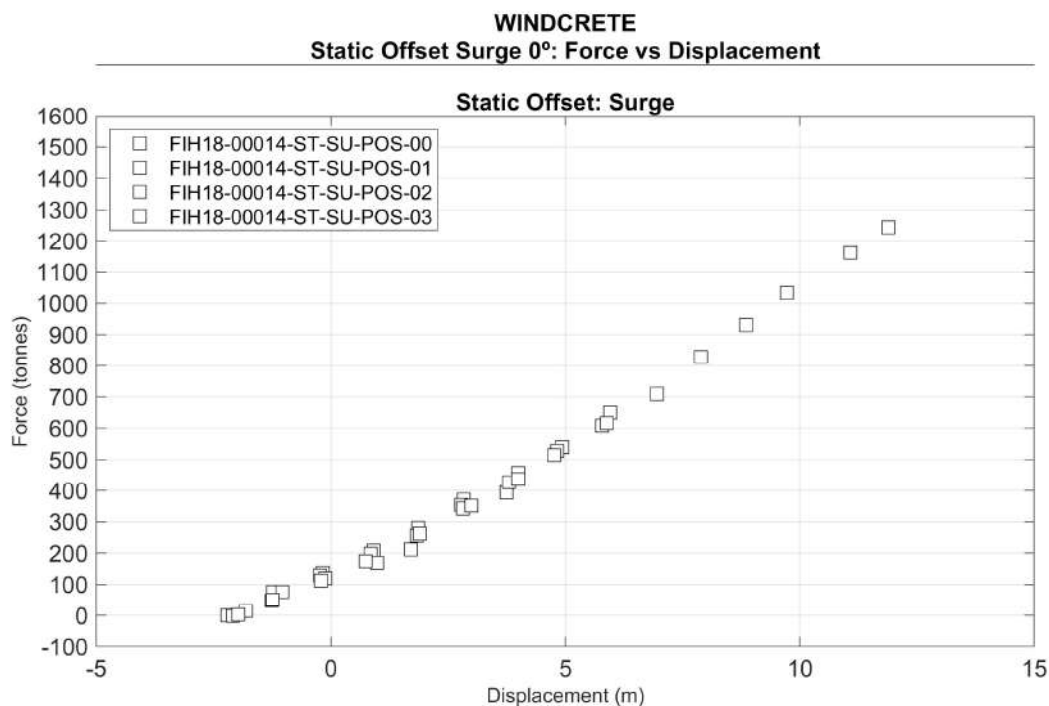


Figure 6-2. Applied force vs platform displacements in surge (0°)

Figure 6-3 presents the relation between the platform surge and mooring forces in the same set of trials. The results of the truncated main line 1 are compared to those from numerically obtained with a draft of 156.650 m drawn in red circles.

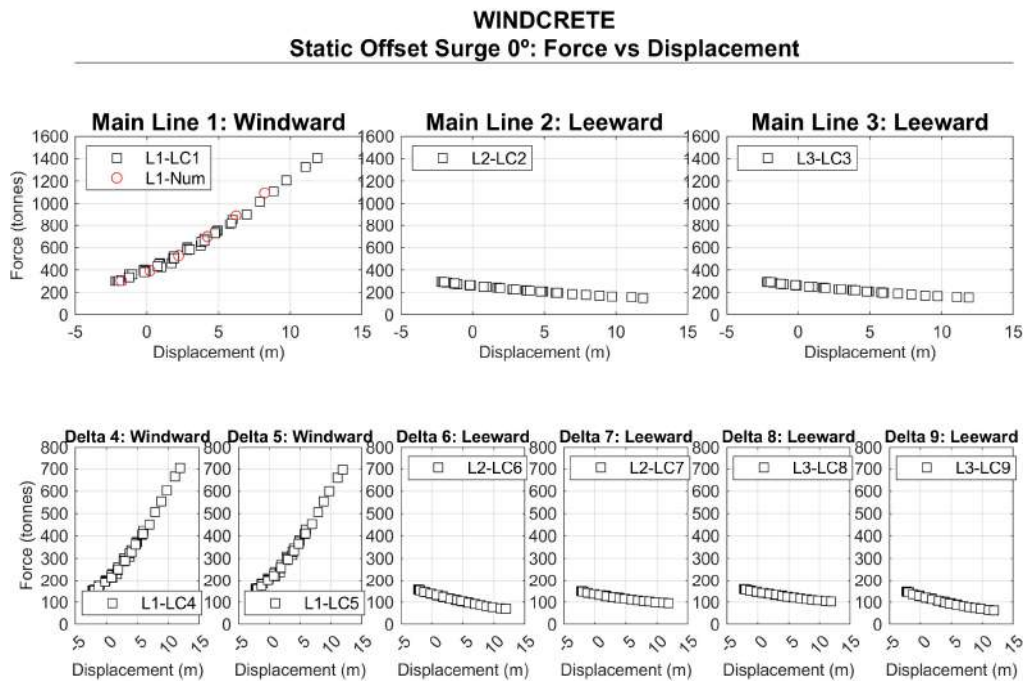


Figure 6-3. Mooring forces vs platform displacements in surge (0°)

Figure 6-3 shows the relation between the platform surge and the force applied for achieving those displacements during the three repetitions executed pulling the platform at 0° in the positive negative direction.

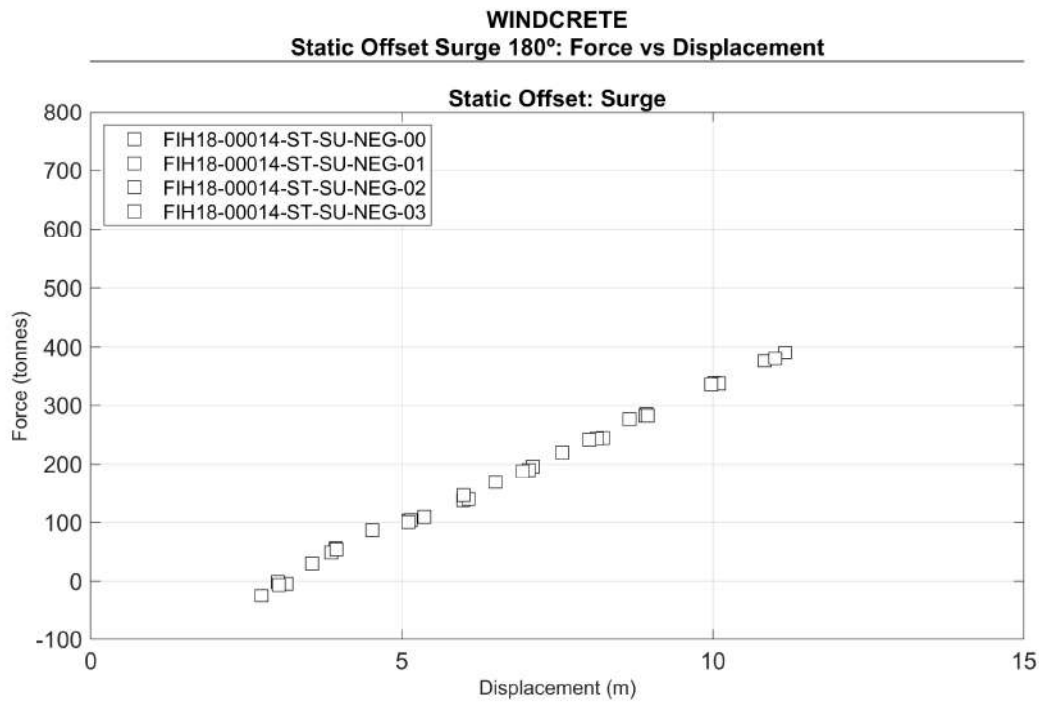


Figure 6-4. Applied force vs platform displacements in surge (0°)

Figure 6-4 presents the relation between the platform surge and mooring forces in the same set of trials. The results of the truncated main line 1 are compared to those from numerically obtained with a draft of 156.650 m drawn in red circles.

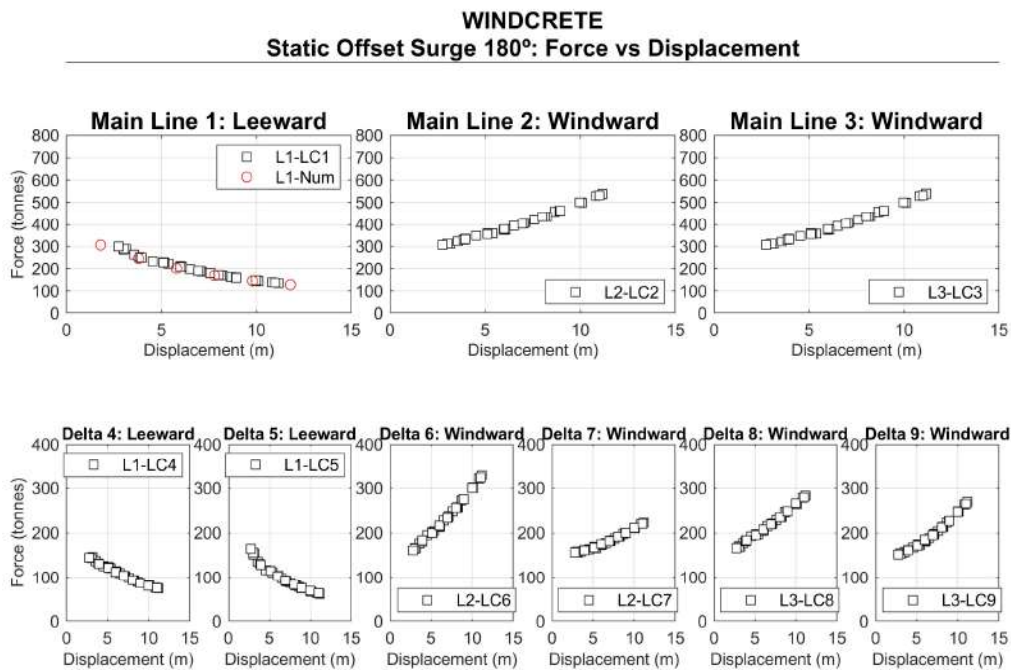


Figure 6-5. Mooring forces vs platform displacements in surge (180°)

6.1.3 Seakeeping tests results

To show a preliminary understanding of the system behaviour and its dynamics, the present section provides a summary of the variables recorded during the tests execution. The tables on the following pages report the motions and accelerations of the platform and mooring system loads for the wave, current and wind tests, in case of application of singular and coupled environmental conditions.

This information provides an understanding of seakeeping of the WINDCRETE floating wind turbine. The next sections include a selection of statistical results obtained from the measurements recorded during the tests, as well as some examples of graphics built based on the post processing analysis.

The presented data is summarized in the following list:

- Incident Wave characteristics, which are included in the first table defined by their wave height and period (Regular Wave) or by their significant height, peak period and spectral definition (Irregular Wave).
- Mean incident current.
- To ease the interpretation of the tank testing results, the static condition data shows the initial value of each measured parameter. Such data is defined as the average of the measured parameters calculated over a period where the model is not subjected to environmental loads.
- Mean, maximum and minimum values of motions, which are obtained for CoG, for the Nacelle and for the MSL.
- Mean and dynamic maximum and minimum mooring loads.
- Mean, maximum and minimum nacelle accelerations.
- Mean calculated rotor thrust.
- Spectral RAOs obtained through Regular Wave, Irregular Wave and White Noise tests.

Configuration WC2: Regular Wave at 0 deg

Table 6-8 summarizes the main characteristics of the incident sea states considered.

Configuration WC2 - Regular Wave at 0 deg						
#	Test/Laboratory Code	h [m]	H [m]	T [s]	Hinc [m]	Tinc [s]
18	'FIH18-00014_WC2_RW_H2p75_T7p5_ABS_00'	165	2.75	7.5	2.73	7.50
19	'FIH18-00014_WC2_RW_H2p75_T9_ABS_00'	165	2.75	9	2.69	9.00
20	'FIH18-00014_WC2_RW_H2p75_T11_ABS_01'	165	2.75	11	2.80	11.01
21	'FIH18-00014_WC2_RW_H2p75_T14_ABS_00'	165	2.75	14	2.63	13.95
22	'FIH18-00014_WC2_RW_H2p75_T17_ABS_00'	165	2.75	17	2.83	16.98
23	'FIH18-00014_WC2_RW_H2p75_T20_ABS_00'	165	2.75	20	2.78	19.93
24	'FIH18-00014_WC2_RW_H5p11_T7p5_ABS_00'	165	5.11	7.5	5.04	7.46
25	'FIH18-00014_WC2_RW_H5p11_T9_ABS_00'	165	5.11	9	5.01	9.00
26	'FIH18-00014_WC2_RW_H5p11_T11_ABS_00'	165	5.11	11	5.01	10.95
27	'FIH18-00014_WC2_RW_H5p11_T14_ABS_00'	165	5.11	14	4.90	13.99
28	'FIH18-00014_WC2_RW_H5p11_T17_ABS_00'	165	5.11	17	4.99	16.95
29	'FIH18-00014_WC2_RW_H5p11_T20_ABS_00'	165	5.11	20	5.10	20.00

Table 6-8. Configuration WC2: Regular Wave. Incident Analysis

Next, on Table 6-9 a summary of the initial position of the FOWT. Moreover, on Table 6-10 the pretensions registered are also shown. As aforementioned, the static position of WINDCRETE CoG has a Z of -1.65 m due to the actual draft, and a X lower than -1.75 m for a positive pitch because the inertial reference is at the fairlead's depth for a non-optimized mooring system.

Configuration WC2 - Regular Wave at 0 deg				
#	Equilibrium Condition	Motions - CoG: Initial Position	Motions - Nacelle: Initial Position	Motions - MSL: Initial Position

	Test/Laboratory Code	X [m]	Y [m]	Z [m]	roll [deg]	pitch [deg]	yaw [deg]	X [m]	Y [m]	Z [m]	X [m]	Y [m]	Z [m]
18	'FIH18-00014_WC2_RW_H2p75_T7p5_ABS_00'	-2.03	1.38	-1.69	0.23	0.53	1.12	0.10	0.49	-1.70	-1.16	1.02	-1.69
19	'FIH18-00014_WC2_RW_H2p75_T9_ABS_00'	-2.02	1.37	-1.67	0.24	0.53	1.14	0.08	0.47	-1.68	-1.16	1.00	-1.68
20	'FIH18-00014_WC2_RW_H2p75_T11_ABS_01'	-1.96	1.30	-1.75	0.22	0.51	1.18	0.10	0.45	-1.76	-1.12	0.96	-1.75
21	'FIH18-00014_WC2_RW_H2p75_T14_ABS_00'	-2.04	1.37	-1.68	0.24	0.52	1.14	0.04	0.47	-1.69	-1.20	1.00	-1.69
22	'FIH18-00014_WC2_RW_H2p75_T17_ABS_00'	-2.03	1.37	-1.68	0.23	0.52	1.14	0.06	0.48	-1.69	-1.18	1.00	-1.68
23	'FIH18-00014_WC2_RW_H2p75_T20_ABS_00'	-2.05	1.40	-1.69	0.24	0.53	1.12	0.07	0.47	-1.70	-1.19	1.02	-1.69
24	'FIH18-00014_WC2_RW_H5p11_T7p5_ABS_00'	-2.01	1.42	-1.69	0.24	0.52	1.09	0.08	0.50	-1.70	-1.16	1.04	-1.69
25	'FIH18-00014_WC2_RW_H5p11_T9_ABS_00'	-2.04	1.37	-1.69	0.23	0.53	1.10	0.10	0.51	-1.70	-1.17	1.02	-1.70
26	'FIH18-00014_WC2_RW_H5p11_T11_ABS_00'	-2.02	1.37	-1.70	0.23	0.53	1.11	0.10	0.50	-1.71	-1.16	1.02	-1.70
27	'FIH18-00014_WC2_RW_H5p11_T14_ABS_00'	-2.06	1.40	-1.70	0.24	0.54	1.08	0.12	0.49	-1.71	-1.17	1.03	-1.70
28	'FIH18-00014_WC2_RW_H5p11_T17_ABS_00'	-2.06	1.37	-1.69	0.23	0.54	1.09	0.10	0.49	-1.71	-1.18	1.01	-1.70
29	'FIH18-00014_WC2_RW_H5p11_T20_ABS_00'	-2.06	1.37	-1.70	0.23	0.53	1.12	0.05	0.49	-1.71	-1.20	1.01	-1.70

Table 6-9. Configuration WC2: Regular Wave. Motions initial positions

Configuration WC2 - Regular Wave at 0 deg										
#	Equilibrium Condition Test/Laboratory Code	Mooring Lines - Pretension [tonnes]								
		LC1	LC2	LC3	LC4	LC5	LC6	LC7	LC8	LC9
18	'FIH18-00014_WC2_RW_H2p75_T7p5_ABS_00'	294.83	280.64	281.85	146.53	153.65	149.65	142.96	154.33	137.33
19	'FIH18-00014_WC2_RW_H2p75_T9_ABS_00'	294.97	280.59	281.95	146.62	153.79	149.60	142.85	154.29	137.38
20	'FIH18-00014_WC2_RW_H2p75_T11_ABS_01'	296.31	278.49	280.41	147.90	151.27	147.44	142.45	152.62	133.43
21	'FIH18-00014_WC2_RW_H2p75_T14_ABS_00'	295.21	280.80	282.12	146.79	153.83	149.75	142.91	154.31	137.49
22	'FIH18-00014_WC2_RW_H2p75_T17_ABS_00'	295.22	280.73	282.05	146.82	153.83	149.74	142.88	154.25	137.44
23	'FIH18-00014_WC2_RW_H2p75_T20_ABS_00'	295.36	280.74	282.13	146.94	153.87	149.75	142.91	154.32	137.49
24	'FIH18-00014_WC2_RW_H5p11_T7p5_ABS_00'	294.65	280.33	281.93	147.06	153.10	149.20	142.98	154.00	137.65
25	'FIH18-00014_WC2_RW_H5p11_T9_ABS_00'	294.78	280.31	281.77	147.04	153.13	149.17	142.95	153.96	137.61
26	'FIH18-00014_WC2_RW_H5p11_T11_ABS_00'	294.75	280.26	281.75	146.99	153.10	149.15	142.97	153.98	137.64
27	'FIH18-00014_WC2_RW_H5p11_T14_ABS_00'	294.67	280.18	281.62	146.96	152.93	149.16	142.85	153.87	137.66
28	'FIH18-00014_WC2_RW_H5p11_T17_ABS_00'	295.03	280.14	281.61	147.05	153.14	149.10	142.90	154.01	137.54
29	'FIH18-00014_WC2_RW_H5p11_T20_ABS_00'	295.40	280.80	281.79	146.94	153.82	149.76	142.95	154.29	137.30

Table 6-10. Configuration WC2: Regular Wave. Mooring system pretensions

Table 6-11, Table 6-12, Table 6-13 and Table 6-14 report the mean, maximum and minimum values of the platform motions.

Configuration WC2 - Regular Wave at 0 deg										
#	Test/Laboratory Code	Motions - CoG: Position								
		X [m]			Y [m]			Z [m]		
		mean	max	min	mean	max	min	mean	max	min
18	'FIH18-00014_WC2_RW_H2p75_T7p5_ABS_00'	-2.03	-1.87	-2.21	1.37	1.46	1.29	-1.66	-1.60	-1.73
19	'FIH18-00014_WC2_RW_H2p75_T9_ABS_00'	-2.01	-1.76	-2.21	1.35	1.45	1.24	-1.67	-1.58	-1.75
20	'FIH18-00014_WC2_RW_H2p75_T11_ABS_01'	-1.90	-1.60	-2.20	1.29	1.40	1.17	-1.74	-1.60	-1.89
21	'FIH18-00014_WC2_RW_H2p75_T14_ABS_00'	-2.06	-1.55	-2.54	1.36	1.46	1.27	-1.68	-1.47	-1.89
22	'FIH18-00014_WC2_RW_H2p75_T17_ABS_00'	-2.05	-1.47	-2.67	1.36	1.45	1.26	-1.69	-1.40	-1.96
23	'FIH18-00014_WC2_RW_H2p75_T20_ABS_00'	-2.09	-1.17	-2.98	1.36	1.47	1.26	-1.69	-1.45	-1.94
24	'FIH18-00014_WC2_RW_H5p11_T7p5_ABS_00'	-1.76	-1.47	-2.09	1.41	1.51	1.30	-1.59	-1.40	-1.76
25	'FIH18-00014_WC2_RW_H5p11_T9_ABS_00'	-1.96	-1.58	-2.33	1.38	1.50	1.22	-1.62	-1.47	-1.78
26	'FIH18-00014_WC2_RW_H5p11_T11_ABS_00'	-2.00	-1.54	-2.51	1.39	1.51	1.26	-1.66	-1.43	-1.89
27	'FIH18-00014_WC2_RW_H5p11_T14_ABS_00'	-2.02	-1.24	-2.81	1.38	1.52	1.25	-1.68	-1.29	-2.07
28	'FIH18-00014_WC2_RW_H5p11_T17_ABS_00'	-2.05	-0.95	-3.13	1.39	1.52	1.24	-1.69	-1.24	-2.14
29	'FIH18-00014_WC2_RW_H5p11_T20_ABS_00'	-2.08	-0.51	-3.67	1.38	1.52	1.24	-1.69	-1.26	-2.12

Table 6-11. Configuration WC2: Regular Wave. Displacements results in the CoG Position

Configuration WC2 - Regular Wave at 0 deg										
#	Test/Laboratory Code	Motions - CoG: Position								
		roll [deg]			pitch [deg]			yaw [deg]		
		mean	max	min	mean	max	min	mean	max	min
18	'FIH18-00014_WC2_RW_H2p75_T7p5_ABS_00'	0.23	0.27	0.19	0.57	0.72	0.42	1.13	1.19	1.07
19	'FIH18-00014_WC2_RW_H2p75_T9_ABS_00'	0.23	0.28	0.19	0.53	0.75	0.32	1.14	1.20	1.08
20	'FIH18-00014_WC2_RW_H2p75_T11_ABS_01'	0.22	0.27	0.17	0.52	0.76	0.25	1.19	1.27	1.11
21	'FIH18-00014_WC2_RW_H2p75_T14_ABS_00'	0.24	0.27	0.20	0.52	0.86	0.19	1.14	1.36	0.93
22	'FIH18-00014_WC2_RW_H2p75_T17_ABS_00'	0.23	0.27	0.20	0.53	0.83	0.21	1.14	1.29	0.99

23	'FIH18-00014_WC2_RW_H2p75_T20_ABS_00'	0.23	0.29	0.17	0.53	0.91	0.09	1.12	1.24	1.01
24	'FIH18-00014_WC2_RW_H5p11_T7p5_ABS_00'	0.23	0.29	0.17	0.66	1.00	0.32	1.09	1.16	1.01
25	'FIH18-00014_WC2_RW_H5p11_T9_ABS_00'	0.23	0.28	0.17	0.59	0.98	0.21	1.10	1.18	1.03
26	'FIH18-00014_WC2_RW_H5p11_T11_ABS_00'	0.23	0.28	0.18	0.56	1.01	0.12	1.10	1.23	0.99
27	'FIH18-00014_WC2_RW_H5p11_T14_ABS_00'	0.23	0.27	0.19	0.54	1.15	-0.06	1.09	1.41	0.79
28	'FIH18-00014_WC2_RW_H5p11_T17_ABS_00'	0.24	0.29	0.17	0.54	1.12	-0.07	1.08	1.24	0.91
29	'FIH18-00014_WC2_RW_H5p11_T20_ABS_00'	0.23	0.29	0.17	0.54	1.29	-0.24	1.11	1.34	0.92

Table 6-12. Configuration WC2: Regular Wave. Rotations results in the CoG Position

Configuration WC2 - Regular Wave at 0 deg										
#	Test/Laboratory Code	Motions - Nacelle: Position								
		X [m]			Y [m]			Z [m]		
		mean	max	min	mean	max	min	mean	max	min
18	'FIH18-00014_WC2_RW_H2p75_T7p5_ABS_00'	0.25	0.86	-0.39	0.50	0.62	0.36	-1.68	-1.61	-1.74
19	'FIH18-00014_WC2_RW_H2p75_T9_ABS_00'	0.13	1.02	-0.79	0.47	0.62	0.32	-1.68	-1.59	-1.77
20	'FIH18-00014_WC2_RW_H2p75_T11_ABS_01'	0.17	1.31	-1.04	0.45	0.65	0.25	-1.76	-1.61	-1.90
21	'FIH18-00014_WC2_RW_H2p75_T14_ABS_00'	0.03	1.68	-1.59	0.46	0.57	0.36	-1.69	-1.48	-1.90
22	'FIH18-00014_WC2_RW_H2p75_T17_ABS_00'	0.07	1.69	-1.62	0.46	0.59	0.33	-1.70	-1.41	-1.98
23	'FIH18-00014_WC2_RW_H2p75_T20_ABS_00'	0.04	2.31	-2.38	0.47	0.68	0.29	-1.71	-1.47	-1.95
24	'FIH18-00014_WC2_RW_H5p11_T7p5_ABS_00'	0.87	2.37	-0.60	0.55	0.78	0.29	-1.60	-1.41	-1.78
25	'FIH18-00014_WC2_RW_H5p11_T9_ABS_00'	0.43	2.06	-1.23	0.52	0.68	0.39	-1.64	-1.49	-1.80
26	'FIH18-00014_WC2_RW_H5p11_T11_ABS_00'	0.25	2.30	-1.81	0.51	0.67	0.37	-1.67	-1.45	-1.90
27	'FIH18-00014_WC2_RW_H5p11_T14_ABS_00'	0.14	3.15	-2.80	0.51	0.60	0.41	-1.70	-1.30	-2.08
28	'FIH18-00014_WC2_RW_H5p11_T17_ABS_00'	0.11	3.28	-3.19	0.49	0.63	0.36	-1.71	-1.26	-2.15
29	'FIH18-00014_WC2_RW_H5p11_T20_ABS_00'	0.06	4.38	-4.34	0.50	0.67	0.35	-1.71	-1.28	-2.13

Table 6-13. Configuration WC2: Regular Wave. Motions results in the Nacelle Position

Configuration WC2 - Regular Wave at 0 deg										
#	Test/Laboratory Code	Motions - MSL: Position								
		X [m]			Y [m]			Z [m]		
		mean	max	min	mean	max	min	mean	max	min
18	'FIH18-00014_WC2_RW_H2p75_T7p5_ABS_00'	-1.10	-0.79	-1.43	1.02	1.10	0.93	-1.67	-1.61	-1.73
19	'FIH18-00014_WC2_RW_H2p75_T9_ABS_00'	-1.13	-0.65	-1.60	0.99	1.09	0.90	-1.67	-1.59	-1.76
20	'FIH18-00014_WC2_RW_H2p75_T11_ABS_01'	-1.06	-0.43	-1.71	0.94	1.06	0.83	-1.75	-1.61	-1.89
21	'FIH18-00014_WC2_RW_H2p75_T14_ABS_00'	-1.21	-0.28	-2.13	1.00	1.08	0.92	-1.69	-1.47	-1.90
22	'FIH18-00014_WC2_RW_H2p75_T17_ABS_00'	-1.19	-0.21	-2.22	0.99	1.08	0.91	-1.69	-1.40	-1.97
23	'FIH18-00014_WC2_RW_H2p75_T20_ABS_00'	-1.22	0.21	-2.67	1.00	1.11	0.89	-1.70	-1.46	-1.94
24	'FIH18-00014_WC2_RW_H5p11_T7p5_ABS_00'	-0.69	0.03	-1.42	1.06	1.18	0.91	-1.59	-1.41	-1.77
25	'FIH18-00014_WC2_RW_H5p11_T9_ABS_00'	-0.99	-0.13	-1.85	1.03	1.13	0.93	-1.63	-1.48	-1.79
26	'FIH18-00014_WC2_RW_H5p11_T11_ABS_00'	-1.09	-0.01	-2.18	1.03	1.14	0.92	-1.67	-1.44	-1.90
27	'FIH18-00014_WC2_RW_H5p11_T14_ABS_00'	-1.14	0.51	-2.75	1.02	1.11	0.94	-1.69	-1.30	-2.08
28	'FIH18-00014_WC2_RW_H5p11_T17_ABS_00'	-1.17	0.72	-3.11	1.02	1.13	0.91	-1.70	-1.25	-2.14
29	'FIH18-00014_WC2_RW_H5p11_T20_ABS_00'	-1.21	1.43	-3.89	1.02	1.15	0.91	-1.70	-1.27	-2.12

Table 6-14. Configuration WC2: Regular Wave. Motions results in the MSL Position

This set of tests provided the data necessary to obtain the Amplitude Response Operators (RAOs), which are illustrated in Figure 6-6, Figure 6-7 and Figure 6-8. As mentioned in Section 4.8.4, these RAOs are obtained as the mean value of the distance between peaks and troughs over incident wave height. RAOs in Yaw present resonant peaks at $T = 14$ s, in agreement with the natural period of WINDCRETE platform in this DOF of 16s (Table 6-7), as the next assessed period is 17s, over the resonant period. In the next section, the spectral RAO assessment shows the actual peak response of the platform at a period of 16s in the Yaw DOF.

WINDCRETE Configuration WC2: Regular Wave - CoG

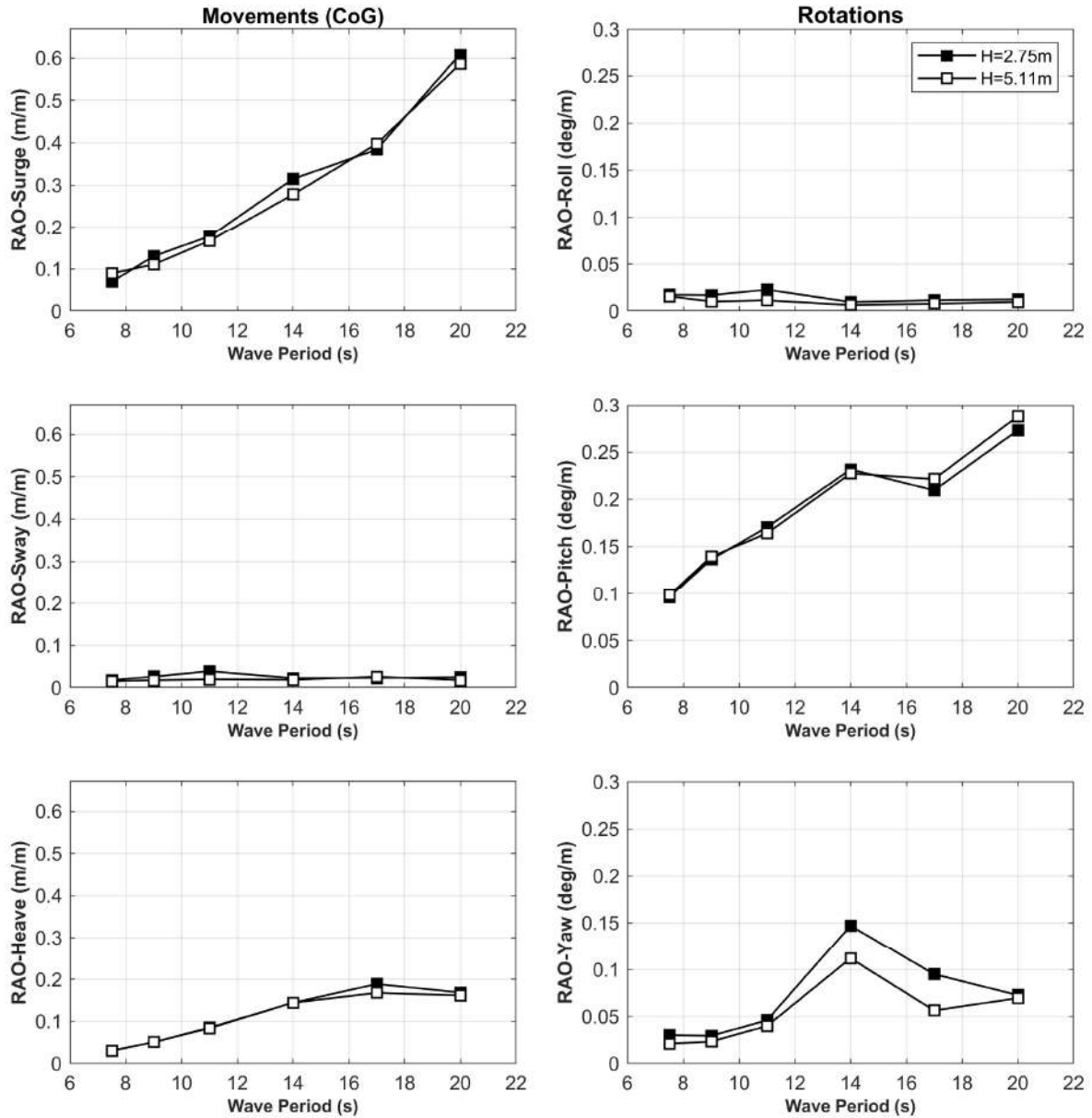


Figure 6-6. Configuration WC2: Regular Wave. RAO of motions (CoG)

WINDCRETE Configuration WC2: Regular Wave - Nacelle

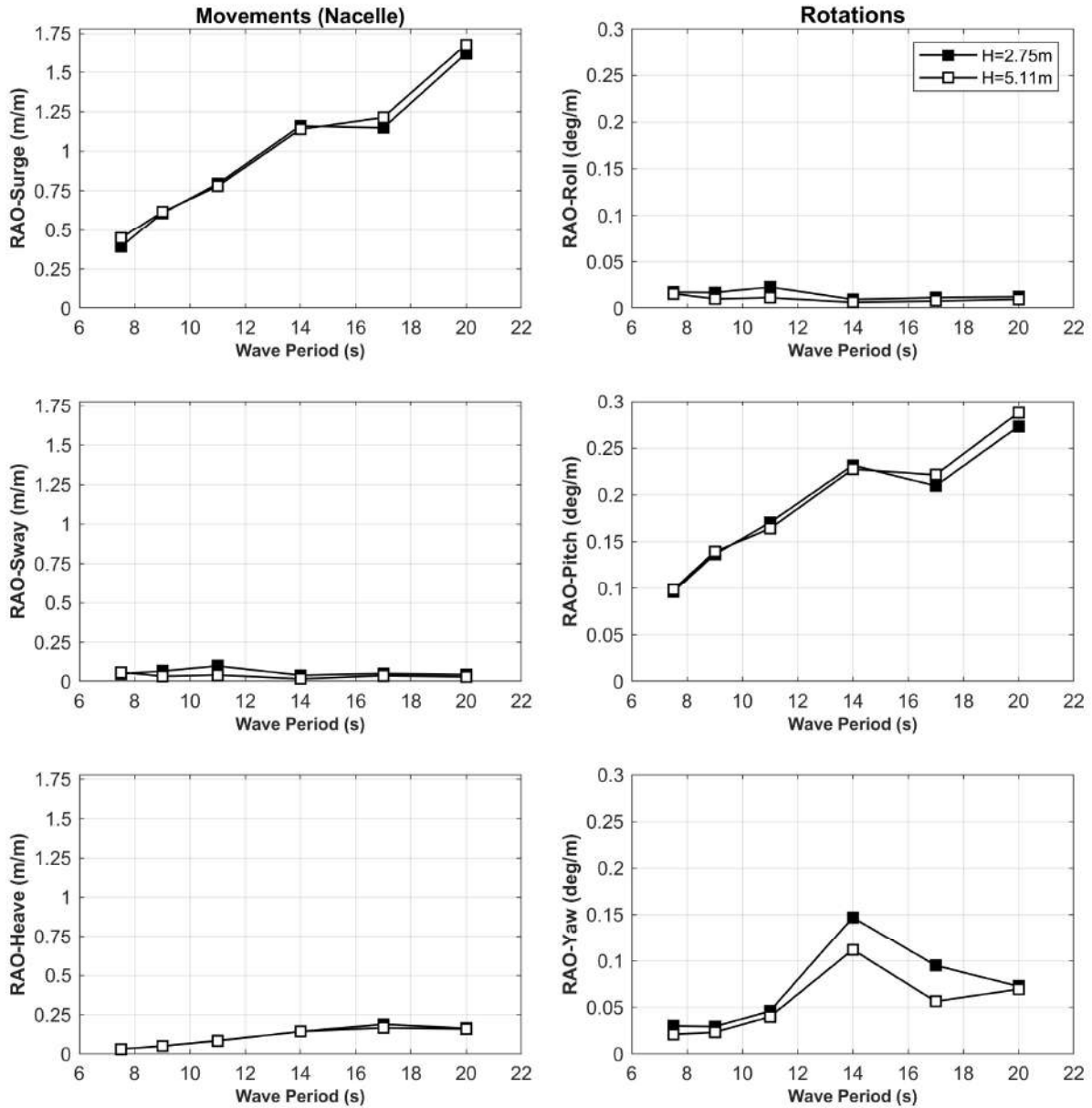


Figure 6-7. Configuration WC2: Regular Wave. RAO of motions (Nacelle)

WINDCRETE Configuration WC2: Regular Wave - MSL

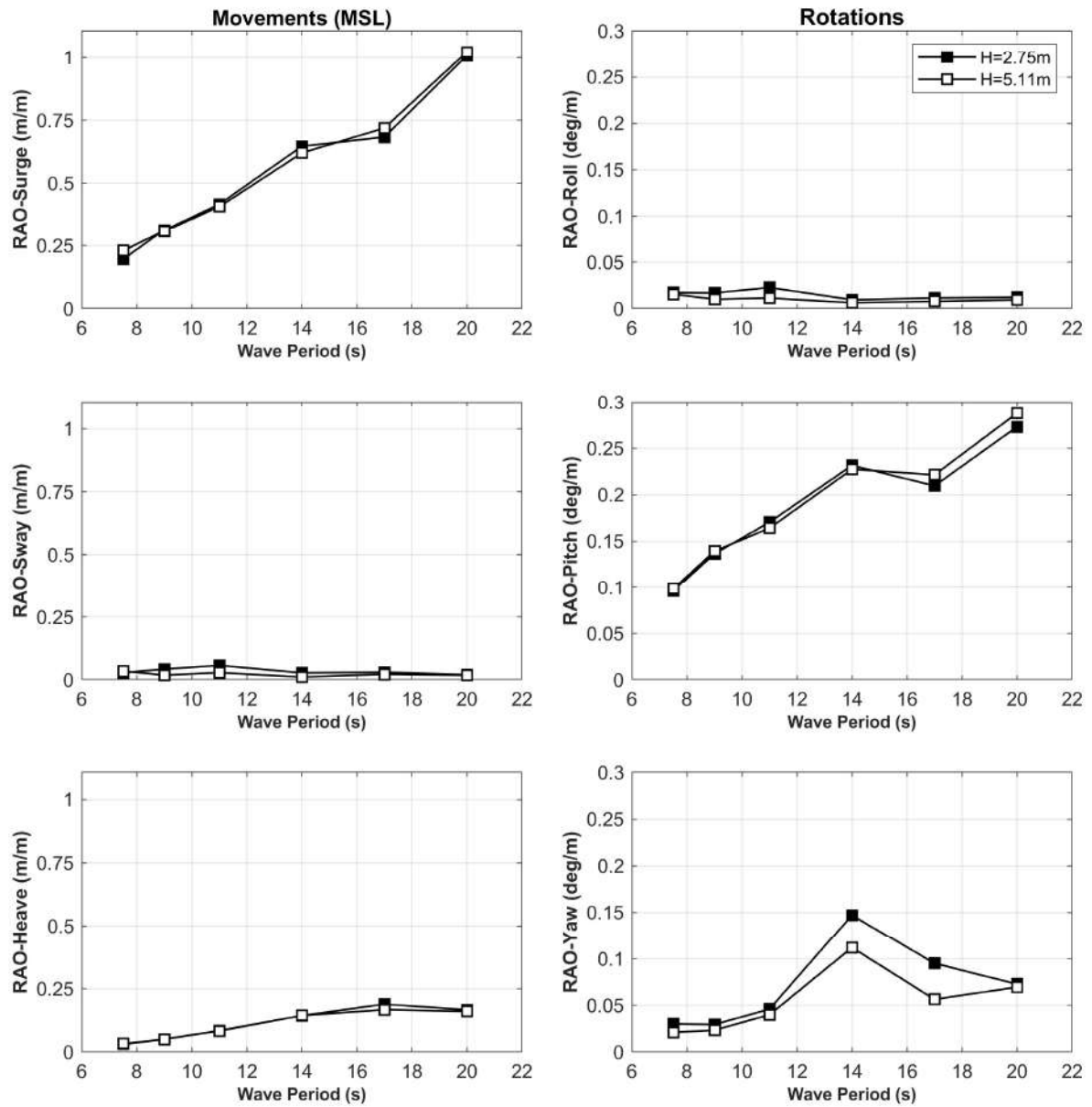


Figure 6-8. Configuration WC2: Regular Wave. RAO of motions (MSL)

Table 6-15, Table 6-16 and Table 6-17 contain the information regarding the tensions recorded during the tests.

Configuration WC2 - Regular Wave at 0 deg										
#	Test/Laboratory Code	Mooring Line 1 - Load [tonnes]								
		LC1			LC4			LC5		
		mean	max	min	mean	max	min	mean	max	min
18	'FIH18-00014_WC2_RW_H2p75_T7p5_ABS_00'	296.73	301.47	292.03	147.67	150.33	145.23	154.74	157.54	151.99
19	'FIH18-00014_WC2_RW_H2p75_T9_ABS_00'	295.70	299.03	292.17	147.22	148.06	146.51	154.19	157.23	150.89
20	'FIH18-00014_WC2_RW_H2p75_T11_ABS_01'	297.06	300.06	292.85	148.50	149.44	147.44	151.66	154.15	148.76
21	'FIH18-00014_WC2_RW_H2p75_T14_ABS_00'	295.49	303.42	288.15	147.31	150.79	143.81	153.98	158.78	149.10
22	'FIH18-00014_WC2_RW_H2p75_T17_ABS_00'	295.58	309.42	283.33	147.54	154.39	141.44	153.90	160.78	148.74

23	'FIH18-00014_WC2_RW_H2p75_T20_ABS_00'	296.03	321.31	273.97	147.88	159.54	138.30	154.05	167.16	143.10
24	'FIH18-00014_WC2_RW_H5p11_T7p5_ABS_00'	306.19	315.05	295.41	152.83	157.69	147.95	158.67	164.45	151.86
25	'FIH18-00014_WC2_RW_H5p11_T9_ABS_00'	299.35	307.06	291.31	149.40	151.74	147.31	155.39	161.45	149.12
26	'FIH18-00014_WC2_RW_H5p11_T11_ABS_00'	297.16	304.59	290.09	148.39	150.69	146.20	154.21	159.74	149.29
27	'FIH18-00014_WC2_RW_H5p11_T14_ABS_00'	296.68	314.20	282.65	148.39	156.19	141.70	153.85	164.14	144.60
28	'FIH18-00014_WC2_RW_H5p11_T17_ABS_00'	296.67	323.23	273.03	148.43	162.80	136.14	153.86	165.33	142.90
29	'FIH18-00014_WC2_RW_H5p11_T20_ABS_00'	298.26	355.79	244.74	149.55	178.41	125.20	154.63	182.64	126.92

Table 6-15. Configuration WC2: Regular Waves. Mooring system results: Line 1

Configuration WC2 - Regular Wave at 0 deg										
#	Test/Laboratory Code	Mooring Line 2 - Load [tonnes]								
		LC2			LC6			LC7		
		mean	max	min	mean	max	min	mean	max	min
18	'FIH18-00014_WC2_RW_H2p75_T7p5_ABS_00'	280.06	282.98	277.06	149.36	153.13	145.73	142.62	144.35	140.71
19	'FIH18-00014_WC2_RW_H2p75_T9_ABS_00'	280.22	282.69	277.51	149.40	154.75	144.14	142.68	146.40	138.95
20	'FIH18-00014_WC2_RW_H2p75_T11_ABS_01'	278.19	281.86	275.13	147.28	150.94	143.29	142.37	145.89	138.72
21	'FIH18-00014_WC2_RW_H2p75_T14_ABS_00'	280.93	285.58	275.89	149.81	154.49	145.32	142.96	149.18	137.07
22	'FIH18-00014_WC2_RW_H2p75_T17_ABS_00'	280.89	288.92	273.04	149.78	151.75	148.01	142.98	149.75	136.27
23	'FIH18-00014_WC2_RW_H2p75_T20_ABS_00'	281.37	293.89	269.95	150.03	153.67	146.34	143.15	152.46	134.71
24	'FIH18-00014_WC2_RW_H5p11_T7p5_ABS_00'	276.84	282.26	272.32	147.65	155.17	140.56	140.84	143.73	137.85
25	'FIH18-00014_WC2_RW_H5p11_T9_ABS_00'	278.60	283.02	274.35	148.24	156.58	139.34	142.08	147.37	136.58
26	'FIH18-00014_WC2_RW_H5p11_T11_ABS_00'	279.62	285.79	273.66	148.65	155.46	142.40	142.72	148.46	136.86
27	'FIH18-00014_WC2_RW_H5p11_T14_ABS_00'	280.49	290.35	270.66	149.20	156.73	141.92	143.08	153.52	133.04
28	'FIH18-00014_WC2_RW_H5p11_T17_ABS_00'	280.92	295.39	268.27	149.52	153.85	145.65	143.17	156.43	131.64
29	'FIH18-00014_WC2_RW_H5p11_T20_ABS_00'	282.80	308.55	261.16	150.27	157.02	143.09	144.26	164.85	126.62

Table 6-16. Configuration WC2: Regular Waves. Mooring system results: Line 2

Configuration WC2 - Regular Wave at 0 deg										
#	Test/Laboratory Code	Mooring Line 3 - Load [tonnes]								
		LC3			LC8			LC9		
		mean	max	min	mean	max	min	mean	max	min
18	'FIH18-00014_WC2_RW_H2p75_T7p5_ABS_00'	280.73	284.09	277.59	153.66	155.14	152.17	136.99	139.25	134.88
19	'FIH18-00014_WC2_RW_H2p75_T9_ABS_00'	281.62	284.30	279.15	154.05	156.70	151.29	137.37	141.47	133.39
20	'FIH18-00014_WC2_RW_H2p75_T11_ABS_01'	280.12	284.05	277.07	152.46	155.62	149.05	133.49	136.03	130.63
21	'FIH18-00014_WC2_RW_H2p75_T14_ABS_00'	282.37	287.76	276.62	154.40	159.44	149.13	137.84	138.60	136.90
22	'FIH18-00014_WC2_RW_H2p75_T17_ABS_00'	282.46	291.49	274.79	154.40	160.95	148.80	137.84	141.52	134.70
23	'FIH18-00014_WC2_RW_H2p75_T20_ABS_00'	282.90	296.35	271.78	154.76	164.30	145.40	137.96	143.27	133.90
24	'FIH18-00014_WC2_RW_H5p11_T7p5_ABS_00'	276.77	282.14	272.17	151.05	152.94	148.79	135.52	140.32	131.03
25	'FIH18-00014_WC2_RW_H5p11_T9_ABS_00'	280.00	284.47	275.44	152.76	156.77	148.51	137.20	144.07	130.71
26	'FIH18-00014_WC2_RW_H5p11_T11_ABS_00'	280.93	286.80	275.81	153.36	158.55	147.69	137.65	142.82	132.90
27	'FIH18-00014_WC2_RW_H5p11_T14_ABS_00'	281.96	294.62	268.66	154.05	163.70	144.80	138.03	141.52	133.19
28	'FIH18-00014_WC2_RW_H5p11_T17_ABS_00'	282.70	298.26	269.29	154.45	164.47	144.28	138.29	146.11	129.74
29	'FIH18-00014_WC2_RW_H5p11_T20_ABS_00'	283.87	307.39	263.36	155.30	171.74	137.97	138.55	149.89	128.56

Table 6-17. Configuration WC2: Regular Waves. Mooring system results: Line 3

The tensions as a function of wave period are shown in Figure 6-9, Figure 6-10 and Figure 6-11.

WINDCRETE Configuration WC2: Regular Wave - Mooring Line 1

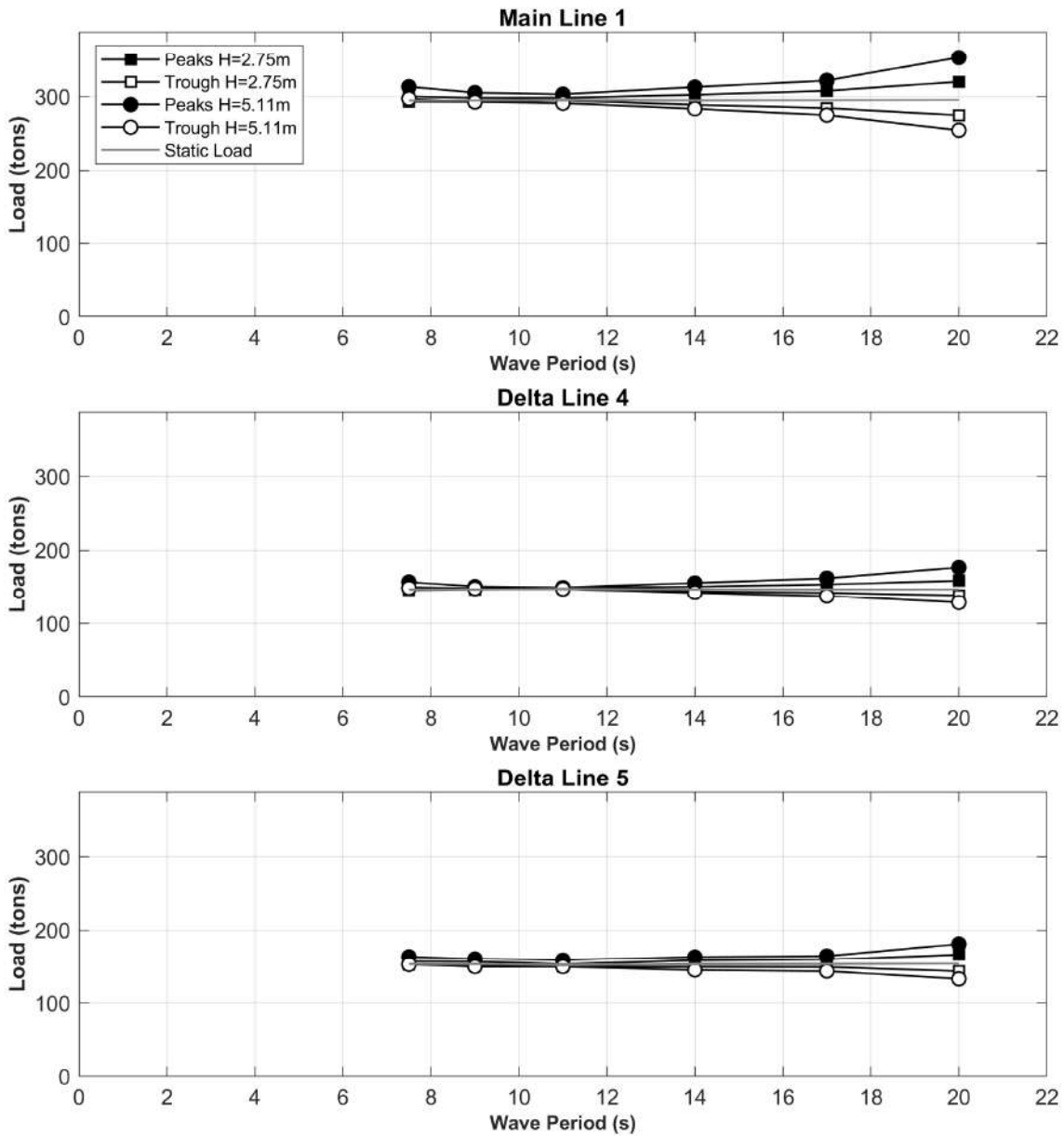


Figure 6-9. Configuration WC2: Regular Wave. Positive and Negative mean values of dynamic mooring loads: Line 1

WINDCRETE Configuration WC2: Regular Wave - Mooring Line 2

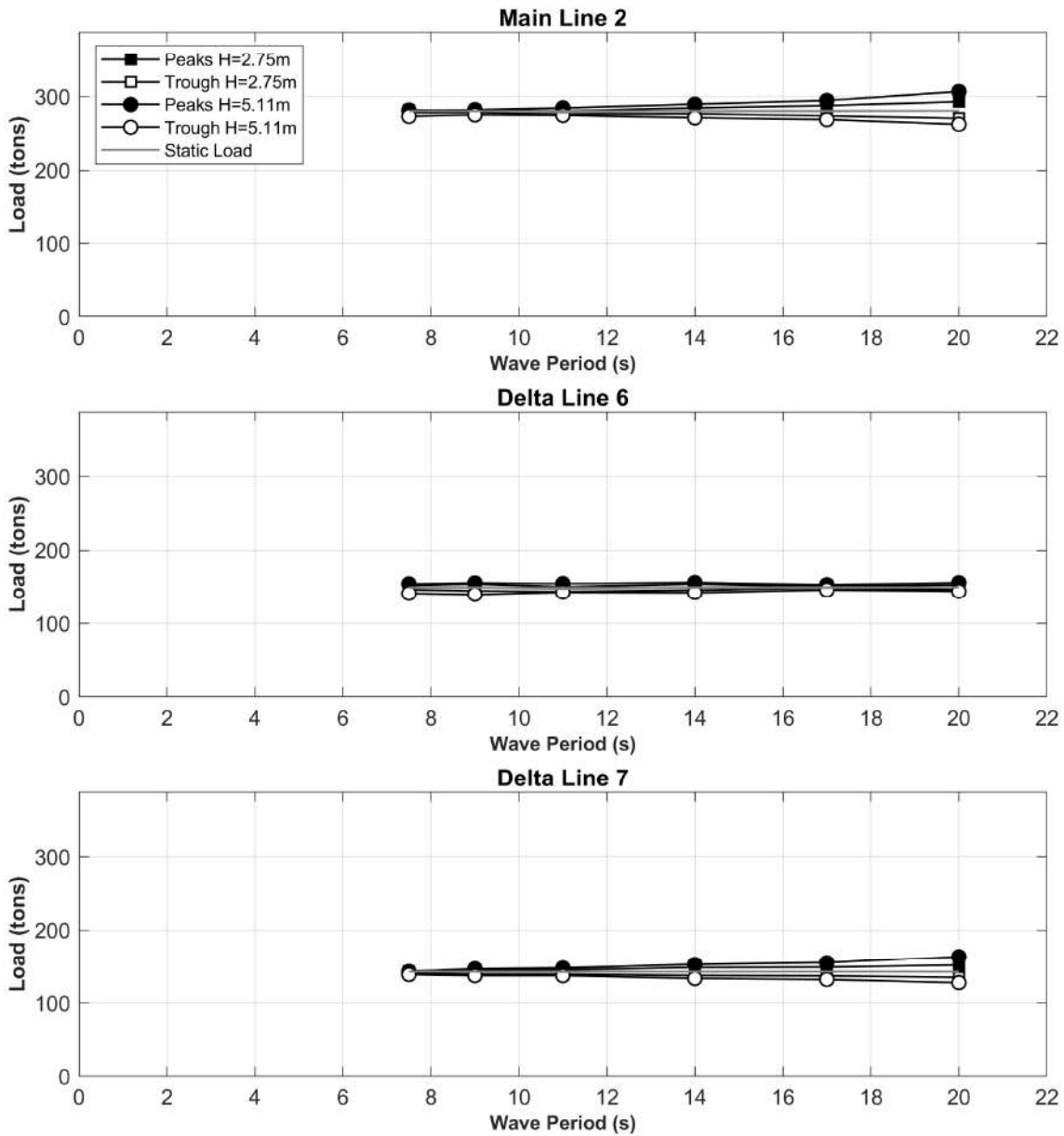


Figure 6-10. Configuration WC2: Regular Wave. Positive and Negative mean values of dynamic mooring loads: Line 2

WINDCRETE Configuration WC2: Regular Wave - Mooring Line 3

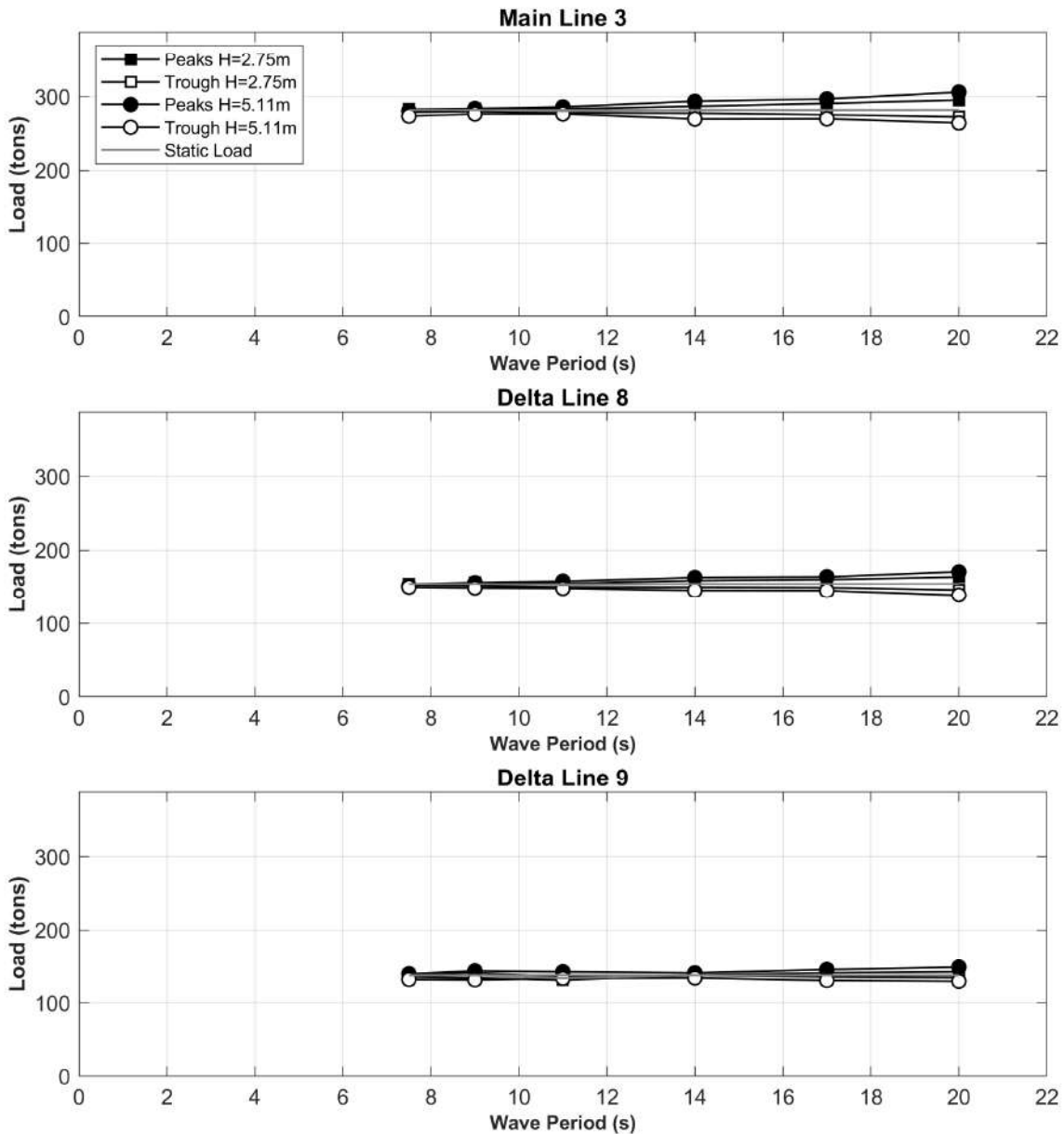


Figure 6-11. Configuration WC2: Regular Wave. Positive and Negative mean values of dynamic mooring loads: Line 3

Table 6-18 and Figure 6-12 show the accelerations at the nacelle.

Configuration WC2 - Regular Wave at 0 deg							
#	Test/Laboratory Code	Accelerations - Nacelle [m/s ²]					
		Acc. X		Acc. Y		Acc. Z	
		max	min	max	min	max	min
18	'FIH18-00014_WC2_RW_H2p75_T7p5_ABS_00'	0.40	-0.37	0.06	-0.07	0.03	-0.03
19	'FIH18-00014_WC2_RW_H2p75_T9_ABS_00'	0.45	-0.43	0.05	-0.05	0.04	-0.04
20	'FIH18-00014_WC2_RW_H2p75_T11_ABS_01'	0.43	-0.32	0.05	-0.06	0.05	-0.05
21	'FIH18-00014_WC2_RW_H2p75_T14_ABS_00'	0.34	-0.35	0.02	-0.02	0.05	-0.05
22	'FIH18-00014_WC2_RW_H2p75_T17_ABS_00'	0.27	-0.22	0.03	-0.02	0.04	-0.04

23	'FIH18-00014_WC2_RW_H2p75_T20_ABS_00'	0.27	-0.22	0.03	-0.03	0.03	-0.03
24	'FIH18-00014_WC2_RW_H5p11_T7p5_ABS_00'	0.83	-0.86	0.16	-0.13	0.05	-0.06
25	'FIH18-00014_WC2_RW_H5p11_T9_ABS_00'	0.81	-0.75	0.04	-0.07	0.06	-0.07
26	'FIH18-00014_WC2_RW_H5p11_T11_ABS_00'	0.70	-0.66	0.06	-0.06	0.07	-0.08
27	'FIH18-00014_WC2_RW_H5p11_T14_ABS_00'	0.57	-0.65	0.05	-0.02	0.08	-0.08
28	'FIH18-00014_WC2_RW_H5p11_T17_ABS_00'	0.51	-0.48	0.04	-0.05	0.06	-0.07
29	'FIH18-00014_WC2_RW_H5p11_T20_ABS_00'	0.48	-0.44	0.03	-0.04	0.04	-0.05

Table 6-18. Configuration WC2: Regular Wave. Accelerations results in the Nacelle Position

WINDCRETE Configuration WC2: Regular Wave - Nacelle Accelerations

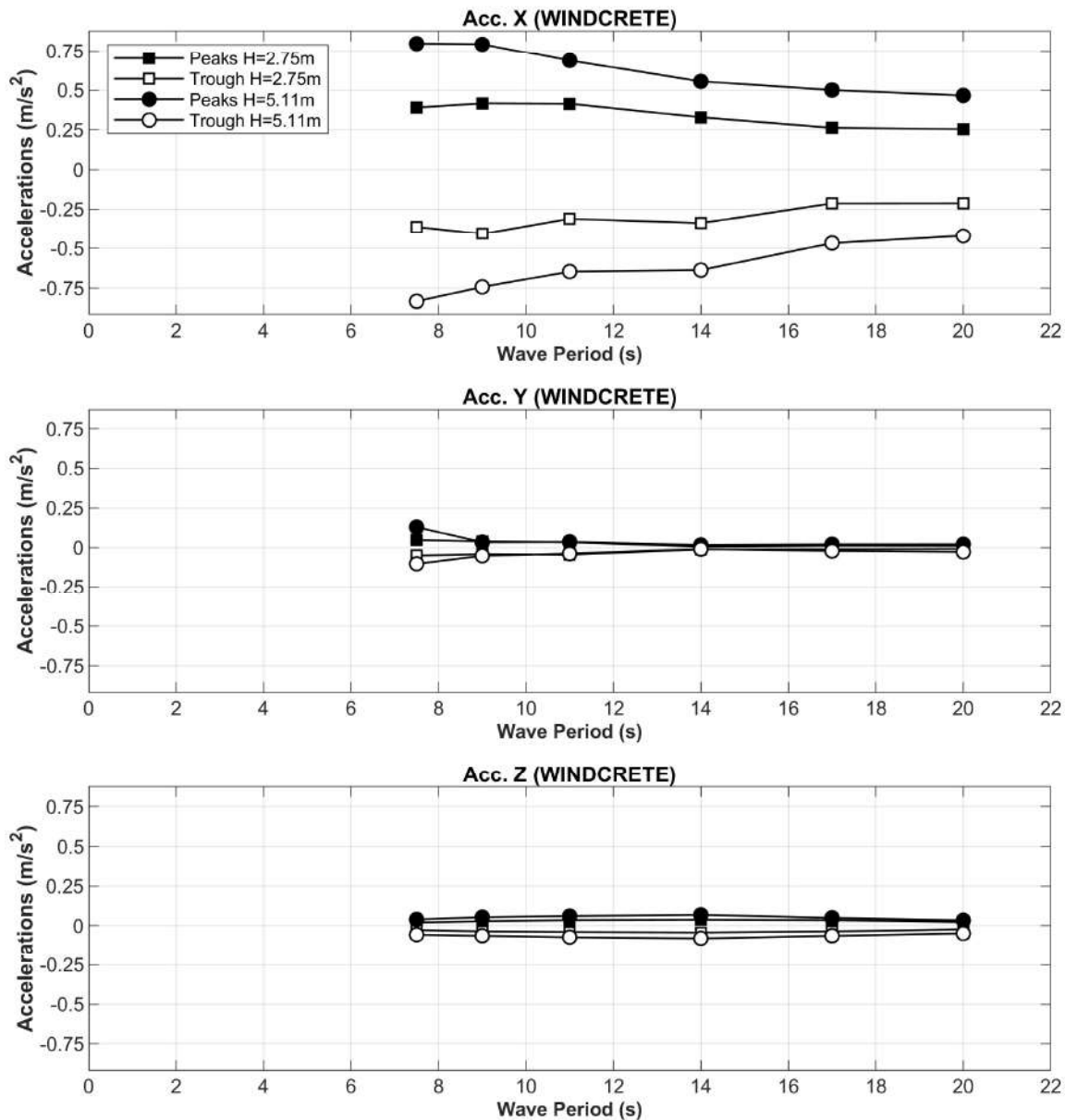


Figure 6-12. Configuration WC2: Regular Waves. Positive and Negative mean values of nacelle accelerations

Configuration WC2: Irregular Wave at 0°

Table 6-19 summarizes the main statistics of the incident sea states considered.

Configuration WC2 - Irregular Wave at 0 deg									
#	Test/Laboratory Code	h [m]	Hs [m]	Tp [s]	Spectrum	Gamma	Spread	Hinc [m]	Tinc [s]
30	'FIH18-00014_WC2_JS_H2p75_T9_G3p3_ABS_00'	165	2.75	9	JS	3.3	-	2.66	9.34
31	'FIH18-00014_WC2_JS_H2p75_T11_G3p3_ABS_00'	165	2.75	11	JS	3.3	-	2.74	11.04
32	'FIH18-00014_WC2_JS_H2p75_T14_G3p3_ABS_00'	165	2.75	14	JS	3.3	-	2.77	14.13
33	'FIH18-00014_WC2_JS_H5p11_T9_G1p2_ABS_00'	165	5.11	9	JS	1.2	-	5.23	8.44
34	'FIH18-00014_WC2_JS_H5p11_T11_G1p2_ABS_00'	165	5.11	11	JS	1.2	-	5.26	11.47
35	'FIH18-00014_WC2_JS_H2p75_T9_G3p3_S6_ABS_01'	165	2.75	9	JS	3.3	6	2.71	9.11
36	'FIH18-00014_WC2_JS_H2p75_T9_G3p3_S12_ABS_00'	165	2.75	9	JS	3.3	12	2.87	8.94
37	'FIH18-00014_WC2_JS_H5p11_T11_G1p2_S6_ABS_00'	165	5.11	11	JS	1.2	6	5.19	10.60
38	'FIH18-00014_WC2_JS_H5p11_T11_G1p2_S12_ABS_00'	165	5.11	11	JS	1.2	12	5.29	11.12

Table 6-19. Configuration WC2: Irregular Wave. Incident Analysis

The initial position as well as the mooring line pretensions are summarized on the next two tables (see Table 6-20 and Table 6-21). As aforementioned, the static position of WINDCRETE CoG has a Z of -1.65 m due to the actual draft, and a X lower than -1.75 m for a positive pitch because the inertial reference is at the fairlead's depth for a non-optimized mooring system.

Configuration WC2 - Irregular Wave at 0 deg													
#	Equilibrium Condition	Motions - CoG: Initial Position						Motions - Nacelle: Initial Position			Motions - MSL: Initial Position		
	Test/Laboratory Code	X [m]	Y [m]	Z [m]	roll [deg]	pitch [deg]	yaw [deg]	X [m]	Y [m]	Z [m]	X [m]	Y [m]	Z [m]
30	'FIH18-00014_WC2_JS_H2p75_T9_G3p3_ABS_00'	-1.99	1.32	-1.62	0.23	0.50	1.12	0.02	0.44	-1.63	-1.17	0.96	-1.63
31	'FIH18-00014_WC2_JS_H2p75_T11_G3p3_ABS_00'	-2.01	1.34	-1.65	0.24	0.52	1.10	0.06	0.44	-1.66	-1.16	0.97	-1.66
32	'FIH18-00014_WC2_JS_H2p75_T14_G3p3_ABS_00'	-2.03	1.37	-1.66	0.23	0.51	1.11	0.03	0.48	-1.68	-1.19	1.01	-1.67
33	'FIH18-00014_WC2_JS_H5p11_T9_G1p2_ABS_00'	-2.05	1.39	-1.68	0.24	0.52	1.09	0.05	0.47	-1.69	-1.20	1.02	-1.68
34	'FIH18-00014_WC2_JS_H5p11_T11_G1p2_ABS_00'	-2.02	1.38	-1.68	0.23	0.53	1.10	0.10	0.49	-1.69	-1.15	1.01	-1.69
35	'FIH18-00014_WC2_JS_H2p75_T9_G3p3_S6_ABS_01'	-1.93	1.33	-1.67	0.24	0.53	1.14	0.17	0.43	-1.69	-1.07	0.97	-1.68
36	'FIH18-00014_WC2_JS_H2p75_T9_G3p3_S12_ABS_00'	-2.06	1.36	-1.68	0.23	0.55	1.12	0.13	0.50	-1.69	-1.17	1.01	-1.69
37	'FIH18-00014_WC2_JS_H5p11_T11_G1p2_S6_ABS_00'	-2.04	1.39	-1.70	0.23	0.54	1.10	0.12	0.51	-1.71	-1.16	1.03	-1.70
38	'FIH18-00014_WC2_JS_H5p11_T11_G1p2_S12_ABS_00'	-2.07	1.39	-1.69	0.24	0.55	1.11	0.13	0.49	-1.70	-1.17	1.03	-1.69

Table 6-20. Configuration WC2: Irregular Wave. Motions initial positions

Configuration WC2 - Irregular Wave at 0 deg										
#	Equilibrium Condition	Mooring Lines - Pretension [tonnes]								
	Test/Laboratory Code	LC1	LC2	LC3	LC4	LC5	LC6	LC7	LC8	LC9
30	'FIH18-00014_WC2_JS_H2p75_T9_G3p3_ABS_00'	292.94	280.46	281.71	145.92	152.95	150.09	142.38	154.45	137.17
31	'FIH18-00014_WC2_JS_H2p75_T11_G3p3_ABS_00'	293.51	280.34	281.65	146.49	153.19	149.92	142.45	154.38	137.16
32	'FIH18-00014_WC2_JS_H2p75_T14_G3p3_ABS_00'	293.17	280.03	281.12	146.19	152.99	149.65	142.34	154.11	136.98
33	'FIH18-00014_WC2_JS_H5p11_T9_G1p2_ABS_00'	293.32	280.19	281.45	146.47	153.08	149.76	142.43	154.22	137.06
34	'FIH18-00014_WC2_JS_H5p11_T11_G1p2_ABS_00'	294.28	280.58	281.71	146.38	153.66	149.67	142.94	154.18	137.40
35	'FIH18-00014_WC2_JS_H2p75_T9_G3p3_S6_ABS_01'	297.32	279.09	280.89	147.82	153.30	148.30	142.05	153.69	136.30
36	'FIH18-00014_WC2_JS_H2p75_T9_G3p3_S12_ABS_00'	294.53	280.48	281.80	146.68	153.68	149.53	142.92	154.08	137.33
37	'FIH18-00014_WC2_JS_H5p11_T11_G1p2_S6_ABS_00'	294.46	280.57	281.87	146.76	153.53	149.62	143.01	154.15	137.34
38	'FIH18-00014_WC2_JS_H5p11_T11_G1p2_S12_ABS_00'	294.41	280.23	281.70	146.80	153.47	149.45	142.87	154.19	137.34

Table 6-21. Configuration WC2: Irregular Wave. Mooring system pretensions

Table 6-22, Table 6-23, Table 6-24 and Table 6-25 show mean, maximum and minimum values of motions related to the CoG, Nacelle and MSL positions.

Configuration WC2 - Irregular Wave at 0 deg										
#	Test/Laboratory Code	Motions - CoG: Position								
		X [m]			Y [m]			Z [m]		
		mean	max	min	mean	max	min	mean	max	min

30	'FIH18-00014_WC2_JS_H2p75_T9_G3p3_ABS_00'	-1.96	-1.18	-2.87	1.31	1.48	1.13	-1.63	-1.20	-2.01
31	'FIH18-00014_WC2_JS_H2p75_T11_G3p3_ABS_00'	-2.03	-1.23	-2.73	1.33	1.49	1.17	-1.65	-1.14	-2.15
32	'FIH18-00014_WC2_JS_H2p75_T14_G3p3_ABS_00'	-2.06	-1.21	-2.92	1.36	1.51	1.23	-1.67	-1.21	-2.08
33	'FIH18-00014_WC2_JS_H5p11_T9_G1p2_ABS_00'	-1.89	-0.49	-3.51	1.37	1.58	1.17	-1.65	-0.39	-2.72
34	'FIH18-00014_WC2_JS_H5p11_T11_G1p2_ABS_00'	-1.92	-0.50	-3.25	1.37	1.57	1.18	-1.66	-0.72	-2.60
35	'FIH18-00014_WC2_JS_H2p75_T9_G3p3_S6_ABS_01'	-1.89	-1.51	-2.28	1.31	1.56	1.06	-1.68	-1.33	-1.96
36	'FIH18-00014_WC2_JS_H2p75_T9_G3p3_S12_ABS_00'	-2.01	-1.52	-2.42	1.35	1.66	1.03	-1.68	-1.33	-2.01
37	'FIH18-00014_WC2_JS_H5p11_T11_G1p2_S6_ABS_00'	-1.92	-0.89	-3.06	1.38	1.96	0.82	-1.67	-0.81	-2.44
38	'FIH18-00014_WC2_JS_H5p11_T11_G1p2_S12_ABS_00'	-1.92	-0.82	-2.93	1.40	1.91	0.75	-1.67	-0.92	-2.46

Table 6-22. Configuration WC2: Irregular Wave. Displacements results in the CoG Position

Configuration WC2 - Irregular Wave at 0 deg										
#	Test/Laboratory Code	Motions - CoG: Position								
		roll [deg]			pitch [deg]			yaw [deg]		
		mean	max	min	mean	max	min	mean	max	min
30	'FIH18-00014_WC2_JS_H2p75_T9_G3p3_ABS_00'	0.23	0.32	0.15	0.52	0.97	0.11	1.12	1.21	1.03
31	'FIH18-00014_WC2_JS_H2p75_T11_G3p3_ABS_00'	0.23	0.32	0.16	0.53	1.01	0.06	1.11	1.26	0.95
32	'FIH18-00014_WC2_JS_H2p75_T14_G3p3_ABS_00'	0.23	0.29	0.17	0.53	1.09	0.00	1.10	1.40	0.80
33	'FIH18-00014_WC2_JS_H5p11_T9_G1p2_ABS_00'	0.23	0.44	0.02	0.60	1.70	-0.46	1.10	1.27	0.94
34	'FIH18-00014_WC2_JS_H5p11_T11_G1p2_ABS_00'	0.24	0.47	0.01	0.59	1.84	-0.87	1.10	1.33	0.85
35	'FIH18-00014_WC2_JS_H2p75_T9_G3p3_S6_ABS_01'	0.23	0.43	0.03	0.53	0.89	0.20	1.14	1.25	1.05
36	'FIH18-00014_WC2_JS_H2p75_T9_G3p3_S12_ABS_00'	0.22	0.46	0.00	0.56	1.01	0.16	1.11	1.21	1.02
37	'FIH18-00014_WC2_JS_H5p11_T11_G1p2_S6_ABS_00'	0.23	0.71	-0.24	0.58	1.52	-0.24	1.10	1.36	0.85
38	'FIH18-00014_WC2_JS_H5p11_T11_G1p2_S12_ABS_00'	0.24	0.74	-0.27	0.59	1.46	-0.29	1.10	1.36	0.82

Table 6-23. Configuration WC2: Irregular Wave. Rotations results in the CoG Position

Configuration WC2 - Irregular Wave at 0 deg										
#	Test/Laboratory Code	Motions - Nacelle: Position								
		X [m]			Y [m]			Z [m]		
		mean	max	min	mean	max	min	mean	max	min
30	'FIH18-00014_WC2_JS_H2p75_T9_G3p3_ABS_00'	0.14	2.30	-1.70	0.43	0.75	0.11	-1.64	-1.21	-2.03
31	'FIH18-00014_WC2_JS_H2p75_T11_G3p3_ABS_00'	0.11	2.21	-2.24	0.44	0.72	0.13	-1.67	-1.15	-2.17
32	'FIH18-00014_WC2_JS_H2p75_T14_G3p3_ABS_00'	0.08	2.65	-2.65	0.47	0.68	0.24	-1.68	-1.22	-2.10
33	'FIH18-00014_WC2_JS_H5p11_T9_G1p2_ABS_00'	0.50	5.55	-4.30	0.48	1.29	-0.28	-1.67	-0.42	-2.73
34	'FIH18-00014_WC2_JS_H5p11_T11_G1p2_ABS_00'	0.42	6.29	-5.84	0.48	1.33	-0.35	-1.68	-0.74	-2.60
35	'FIH18-00014_WC2_JS_H2p75_T9_G3p3_S6_ABS_01'	0.25	1.77	-1.23	0.43	1.22	-0.47	-1.69	-1.34	-1.97
36	'FIH18-00014_WC2_JS_H2p75_T9_G3p3_S12_ABS_00'	0.22	2.13	-1.52	0.50	1.46	-0.44	-1.69	-1.34	-2.02
37	'FIH18-00014_WC2_JS_H5p11_T11_G1p2_S6_ABS_00'	0.40	4.46	-3.04	0.51	2.56	-1.57	-1.69	-0.82	-2.45
38	'FIH18-00014_WC2_JS_H5p11_T11_G1p2_S12_ABS_00'	0.42	4.19	-3.28	0.51	2.76	-1.53	-1.68	-0.94	-2.48

Table 6-24. Configuration WC2: Irregular Wave. Motions results in the Nacelle Position

Configuration WC2 - Irregular Wave at 0 deg										
#	Test/Laboratory Code	Motions - MSL: Position								
		X [m]			Y [m]			Z [m]		
		mean	max	min	mean	max	min	mean	max	min
30	'FIH18-00014_WC2_JS_H2p75_T9_G3p3_ABS_00'	-1.11	0.09	-2.33	0.95	1.13	0.76	-1.63	-1.21	-2.02
31	'FIH18-00014_WC2_JS_H2p75_T11_G3p3_ABS_00'	-1.16	0.12	-2.42	0.97	1.15	0.79	-1.66	-1.14	-2.16
32	'FIH18-00014_WC2_JS_H2p75_T14_G3p3_ABS_00'	-1.19	0.32	-2.79	1.00	1.13	0.85	-1.67	-1.21	-2.09
33	'FIH18-00014_WC2_JS_H5p11_T9_G1p2_ABS_00'	-0.92	1.61	-3.30	1.01	1.38	0.64	-1.66	-0.40	-2.72
34	'FIH18-00014_WC2_JS_H5p11_T11_G1p2_ABS_00'	-0.97	2.25	-3.83	1.01	1.37	0.61	-1.66	-0.73	-2.60
35	'FIH18-00014_WC2_JS_H2p75_T9_G3p3_S6_ABS_01'	-1.02	-0.27	-1.76	0.95	1.39	0.49	-1.68	-1.34	-1.97
36	'FIH18-00014_WC2_JS_H2p75_T9_G3p3_S12_ABS_00'	-1.11	-0.15	-1.93	1.01	1.49	0.51	-1.68	-1.34	-2.02
37	'FIH18-00014_WC2_JS_H5p11_T11_G1p2_S6_ABS_00'	-0.98	1.11	-2.75	1.02	2.13	-0.08	-1.68	-0.81	-2.44
38	'FIH18-00014_WC2_JS_H5p11_T11_G1p2_S12_ABS_00'	-0.97	1.09	-2.88	1.04	2.14	0.01	-1.68	-0.93	-2.47

Table 6-25. Configuration WC2: Irregular Wave. Motions results in the MSL Position

The spectral RAOs are obtained through the irregular wave tests, using the equation presented in previous section 4.8.4 Statistical analysis. The spectral RAOs shown in Figure 6-13, Figure 6-14 and Figure 6-15, are in good agreement with the ones obtained through the regular wave tests (Figure 6-6, Figure 6-7 and Figure 6-8). RAOs in Yaw present resonant peaks at $T = 16$ s, in agreement with the natural period of WINDCRETE platform in this DOF (Table 6-7).

WINDCRETE Configuration WC2: Irregular Wave - CoG

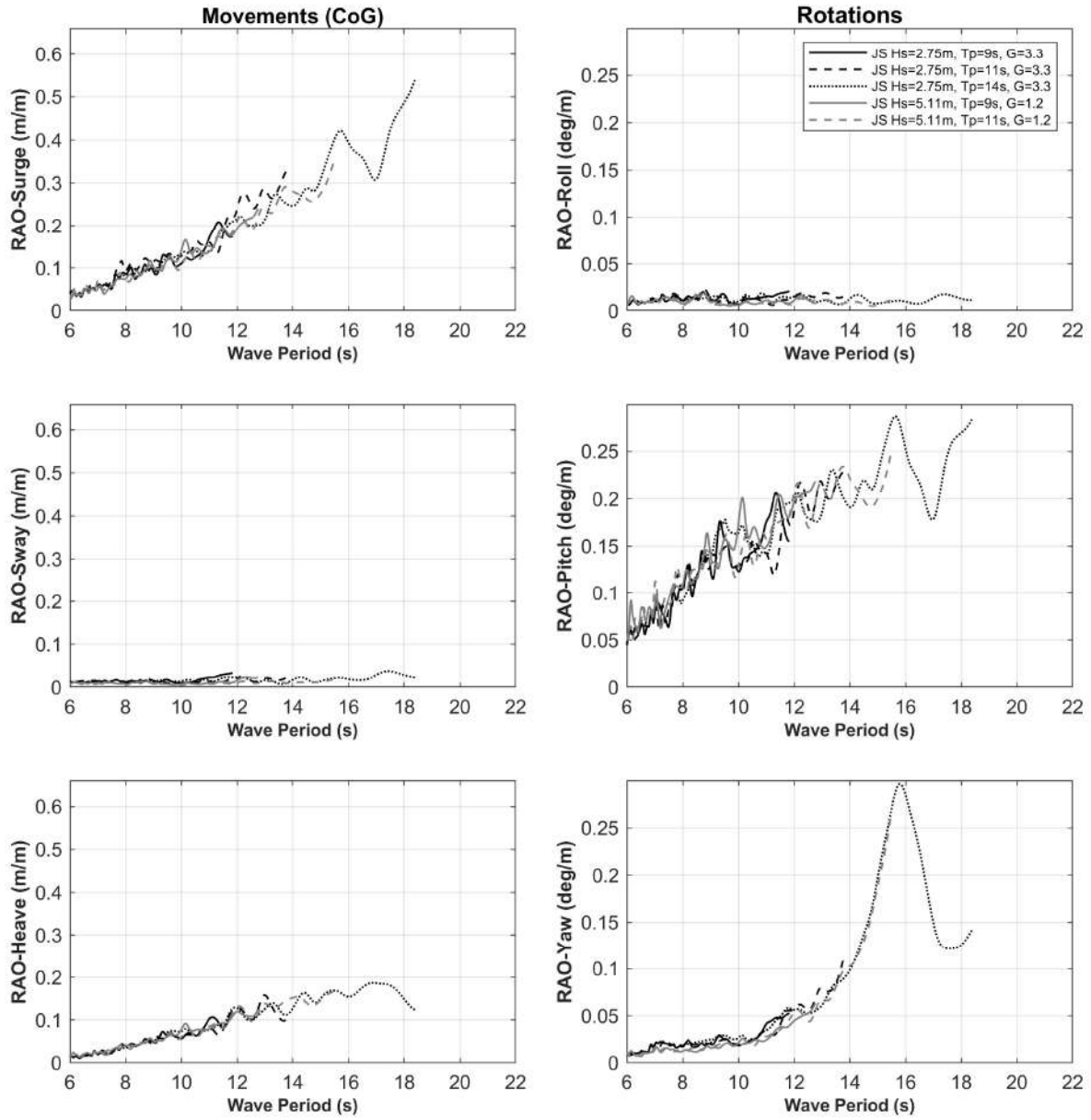


Figure 6-13. Configuration WC2: Irregular Wave. RAO of motions (CoG)

WINDCRETE Configuration WC2: Irregular Wave - Nacelle

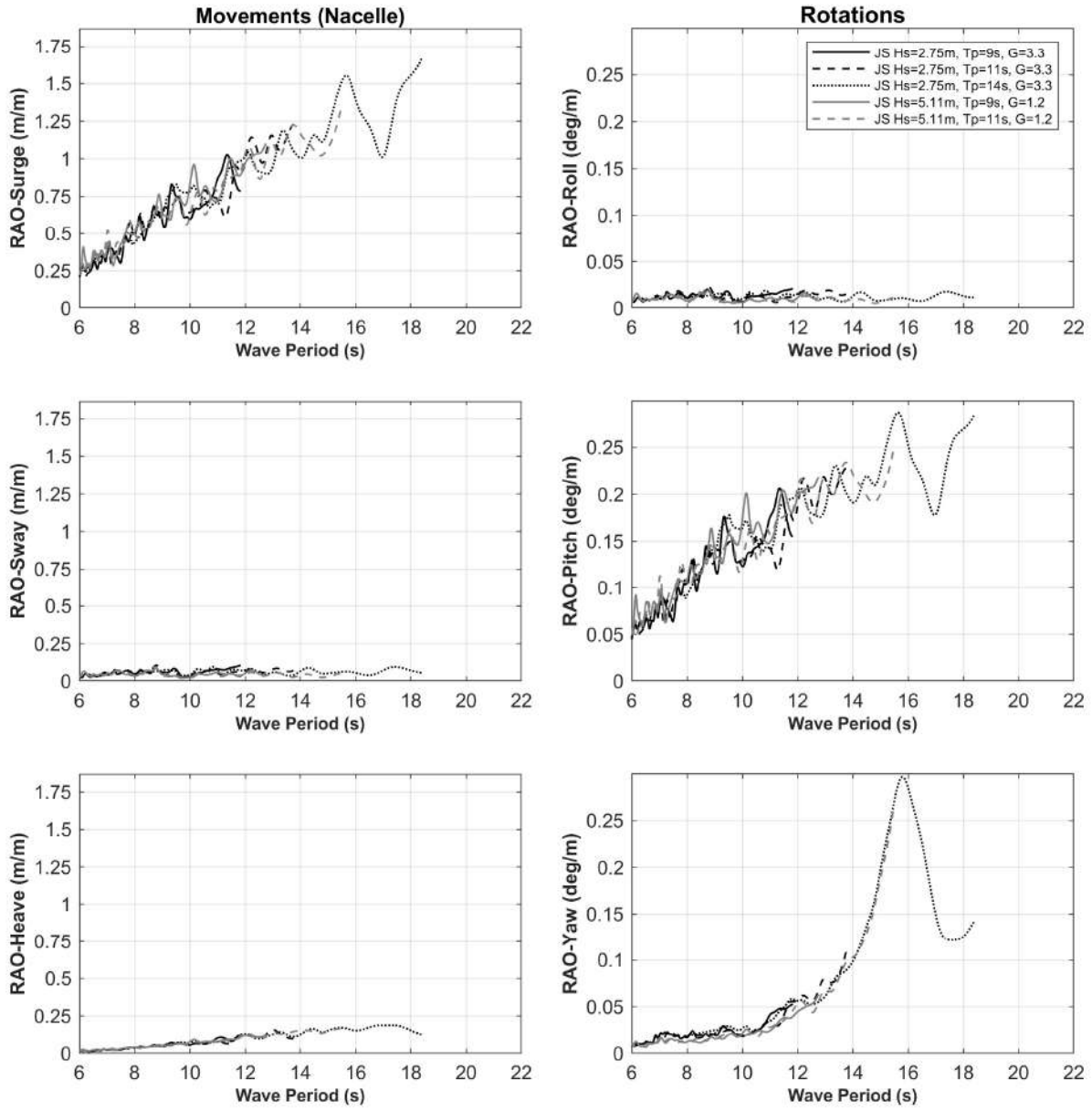


Figure 6-14. Configuration WC2: Irregular Wave. RAO of motions (Nacelle)

WINDCRETE Configuration WC2: Irregular Wave - MSL

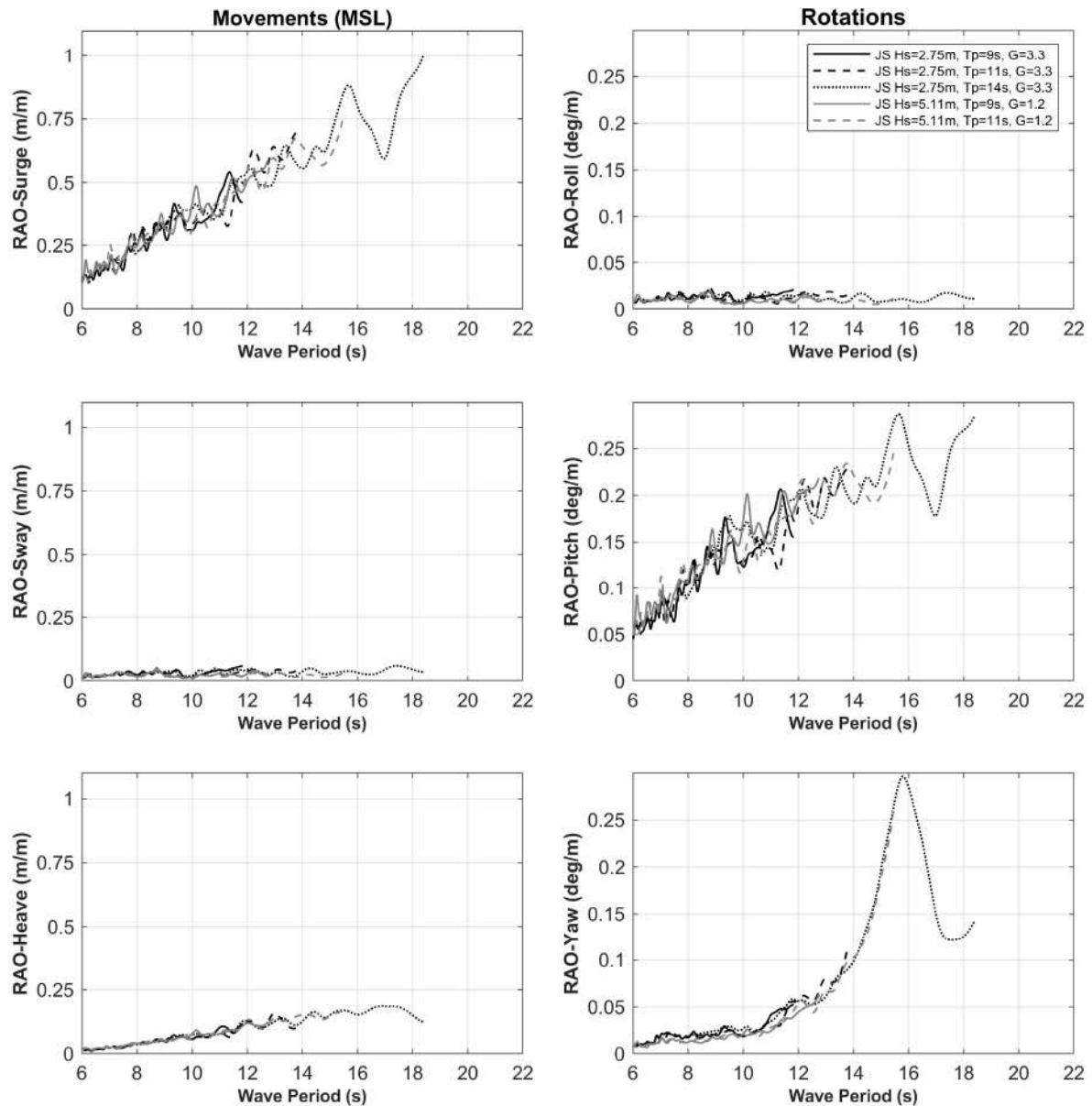


Figure 6-15. Configuration WC2: Irregular Wave. RAO of motions (MSL)

Table 6-26, Table 6-27 and Table 6-28 indicate the tensions obtained during the tests carried out.

Configuration WC2 - Irregular Wave at 0 deg										
#	Test/Laboratory Code	Mooring Line 1 - Load [tonnes]								
		LC1			LC4			LC5		
		mean	max	min	mean	max	min	mean	max	min
30	'FIH18-00014_WC2_JS_H2p75_T9_G3p3_ABS_00'	294.58	322.81	269.34	147.26	160.92	136.10	153.77	168.64	140.74
31	'FIH18-00014_WC2_JS_H2p75_T11_G3p3_ABS_00'	294.34	317.98	273.74	147.34	158.54	138.97	153.57	165.31	142.73
32	'FIH18-00014_WC2_JS_H2p75_T14_G3p3_ABS_00'	293.64	317.69	274.35	146.88	159.10	137.43	153.18	164.49	142.24
33	'FIH18-00014_WC2_JS_H5p11_T9_G1p2_ABS_00'	300.84	360.71	252.51	150.27	179.27	128.15	156.65	186.86	131.02
34	'FIH18-00014_WC2_JS_H5p11_T11_G1p2_ABS_00'	299.30	360.46	258.77	149.36	179.54	131.35	155.87	185.65	135.56

35	'FIH18-00014_WC2_JS_H2p75_T9_G3p3_S6_ABS_01'	298.11	308.26	286.99	148.51	153.52	144.26	153.77	160.96	146.50
36	'FIH18-00014_WC2_JS_H2p75_T9_G3p3_S12_ABS_00'	295.67	307.48	283.91	147.53	153.16	142.60	154.19	161.48	146.73
37	'FIH18-00014_WC2_JS_H5p11_T11_G1p2_S6_ABS_00'	298.79	331.07	273.02	149.18	164.82	137.59	155.54	173.22	138.88
38	'FIH18-00014_WC2_JS_H5p11_T11_G1p2_S12_ABS_00'	299.01	336.84	269.06	149.33	166.32	134.60	155.62	177.69	139.98

Table 6-26. Configuration WC2: Irregular Wave. Mooring system results: Line 1

Configuration WC2 - Irregular Wave at 0 deg										
#	Test/Laboratory Code	Mooring Line 2 - Load [tonnes]								
		LC2			LC6			LC7		
		mean	max	min	mean	max	min	mean	max	min
30	'FIH18-00014_WC2_JS_H2p75_T9_G3p3_ABS_00'	279.86	295.88	267.91	149.79	159.97	140.82	142.06	150.01	134.96
31	'FIH18-00014_WC2_JS_H2p75_T11_G3p3_ABS_00'	280.15	292.10	269.07	149.85	159.21	141.15	142.30	150.75	133.36
32	'FIH18-00014_WC2_JS_H2p75_T14_G3p3_ABS_00'	280.03	294.82	269.17	149.66	160.54	140.96	142.32	155.19	133.51
33	'FIH18-00014_WC2_JS_H5p11_T9_G1p2_ABS_00'	278.69	304.73	253.44	148.98	170.44	132.13	141.59	155.86	127.57
34	'FIH18-00014_WC2_JS_H5p11_T11_G1p2_ABS_00'	278.75	301.96	259.72	148.81	166.74	133.06	141.84	156.93	125.70
35	'FIH18-00014_WC2_JS_H2p75_T9_G3p3_S6_ABS_01'	278.81	286.92	269.29	148.18	155.73	140.65	141.85	147.72	136.18
36	'FIH18-00014_WC2_JS_H2p75_T9_G3p3_S12_ABS_00'	279.96	289.34	270.92	149.32	157.90	140.59	142.61	149.82	135.86
37	'FIH18-00014_WC2_JS_H5p11_T11_G1p2_S6_ABS_00'	278.99	299.82	258.60	148.85	163.61	133.71	142.11	155.31	126.08
38	'FIH18-00014_WC2_JS_H5p11_T11_G1p2_S12_ABS_00'	278.81	297.58	258.41	148.73	164.99	135.45	142.05	156.23	128.53

Table 6-27. Configuration WC2: Irregular Wave. Mooring system results: Line 2

Configuration WC2 - Irregular Wave at 0 deg										
#	Test/Laboratory Code	Mooring Line 3 - Load [tonnes]								
		LC3			LC8			LC9		
		mean	max	min	mean	max	min	mean	max	min
30	'FIH18-00014_WC2_JS_H2p75_T9_G3p3_ABS_00'	281.35	298.57	269.36	154.26	162.70	147.58	137.09	147.17	128.52
31	'FIH18-00014_WC2_JS_H2p75_T11_G3p3_ABS_00'	281.51	293.80	269.56	154.27	161.10	146.74	137.25	145.76	129.07
32	'FIH18-00014_WC2_JS_H2p75_T14_G3p3_ABS_00'	281.23	295.75	270.02	154.15	163.97	147.47	137.14	144.70	130.77
33	'FIH18-00014_WC2_JS_H5p11_T9_G1p2_ABS_00'	279.97	309.66	257.62	153.44	166.36	141.33	136.62	158.77	122.36
34	'FIH18-00014_WC2_JS_H5p11_T11_G1p2_ABS_00'	280.30	304.98	261.86	153.51	168.46	135.68	136.89	153.88	123.24
35	'FIH18-00014_WC2_JS_H2p75_T9_G3p3_S6_ABS_01'	280.55	290.35	272.27	153.48	159.37	148.06	136.28	141.76	131.46
36	'FIH18-00014_WC2_JS_H2p75_T9_G3p3_S12_ABS_00'	281.34	291.98	272.07	153.88	159.98	146.70	137.23	144.75	130.06
37	'FIH18-00014_WC2_JS_H5p11_T11_G1p2_S6_ABS_00'	280.33	302.55	260.81	153.43	168.92	139.79	136.88	150.21	124.20
38	'FIH18-00014_WC2_JS_H5p11_T11_G1p2_S12_ABS_00'	280.17	302.22	261.52	153.31	167.82	141.88	136.86	151.05	124.09

Table 6-28. Configuration WC2: Irregular Wave. Mooring system results: Line 3

Table 6-29 shows the accelerations at the nacelle.

Configuration WC2 - Irregular Wave at 0 deg								
#	Test/Laboratory Code	Accelerations - Nacelle [m/s ²]						
		Acc. X		Acc. Y		Acc. Z		
		max	min	max	min	max	min	min
30	'FIH18-00014_WC2_JS_H2p75_T9_G3p3_ABS_00'	0.78	-0.76	0.10	-0.09	0.05	-0.06	
31	'FIH18-00014_WC2_JS_H2p75_T11_G3p3_ABS_00'	0.91	-0.83	0.09	-0.07	0.07	-0.07	
32	'FIH18-00014_WC2_JS_H2p75_T14_G3p3_ABS_00'	0.80	-0.78	0.08	-0.07	0.07	-0.08	
33	'FIH18-00014_WC2_JS_H5p11_T9_G1p2_ABS_00'	1.42	-1.35	0.18	-0.17	0.10	-0.13	
34	'FIH18-00014_WC2_JS_H5p11_T11_G1p2_ABS_00'	1.44	-1.32	0.14	-0.14	0.11	-0.13	
35	'FIH18-00014_WC2_JS_H2p75_T9_G3p3_S6_ABS_01'	0.73	-0.63	0.25	-0.29	0.04	-0.08	
36	'FIH18-00014_WC2_JS_H2p75_T9_G3p3_S12_ABS_00'	0.87	-0.81	0.35	-0.32	0.07	-0.07	
37	'FIH18-00014_WC2_JS_H5p11_T11_G1p2_S6_ABS_00'	1.35	-1.23	0.73	-0.66	0.12	-0.12	
38	'FIH18-00014_WC2_JS_H5p11_T11_G1p2_S12_ABS_00'	1.58	-1.22	0.53	-0.61	0.12	-0.14	

Table 6-29. Configuration WC2: Irregular Wave. Accelerations results in the Nacelle Position

Configuration WC2: White Noise at 0°

Spectral RAOs are also obtained through white noise tests whose wave spectrum characteristics are presented in Table 6-30. During these tests, the platform is hit by irregular waves defined by a limited white noise spectrum between the periods of 7.5 and 22 seconds.

Configuration WC2 – White Noise at 0 deg						
#	Test/Laboratory Code	h [m]	Hs [m]	T1 [s]	T2 [s]	Hinc [m]

39	FIH18-00014_WC2_TH_H2p75_T11p19_DF0p088_ABS_00	165	2.75	7.5	22	2.81
40	FIH18-00014_WC2_TH_H5p11_T11p19_DF0p088_ABS_00	165	5.11	7.5	22	5.10

Table 6-30. Configuration WC2: White Noise

The spectral RAOs obtained through the white noise test is shown in Figure 6-16, Figure 6-17 and Figure 6-18. These RAOs are in good agreement with the ones obtained through the irregular waves tests (Figure 6-13, Figure 6-14 and Figure 6-15). RAOs in Yaw present resonant peaks at $T = 16$ s, in agreement with the natural period of WINDCRETE platform in this DOF (Table 6-7).

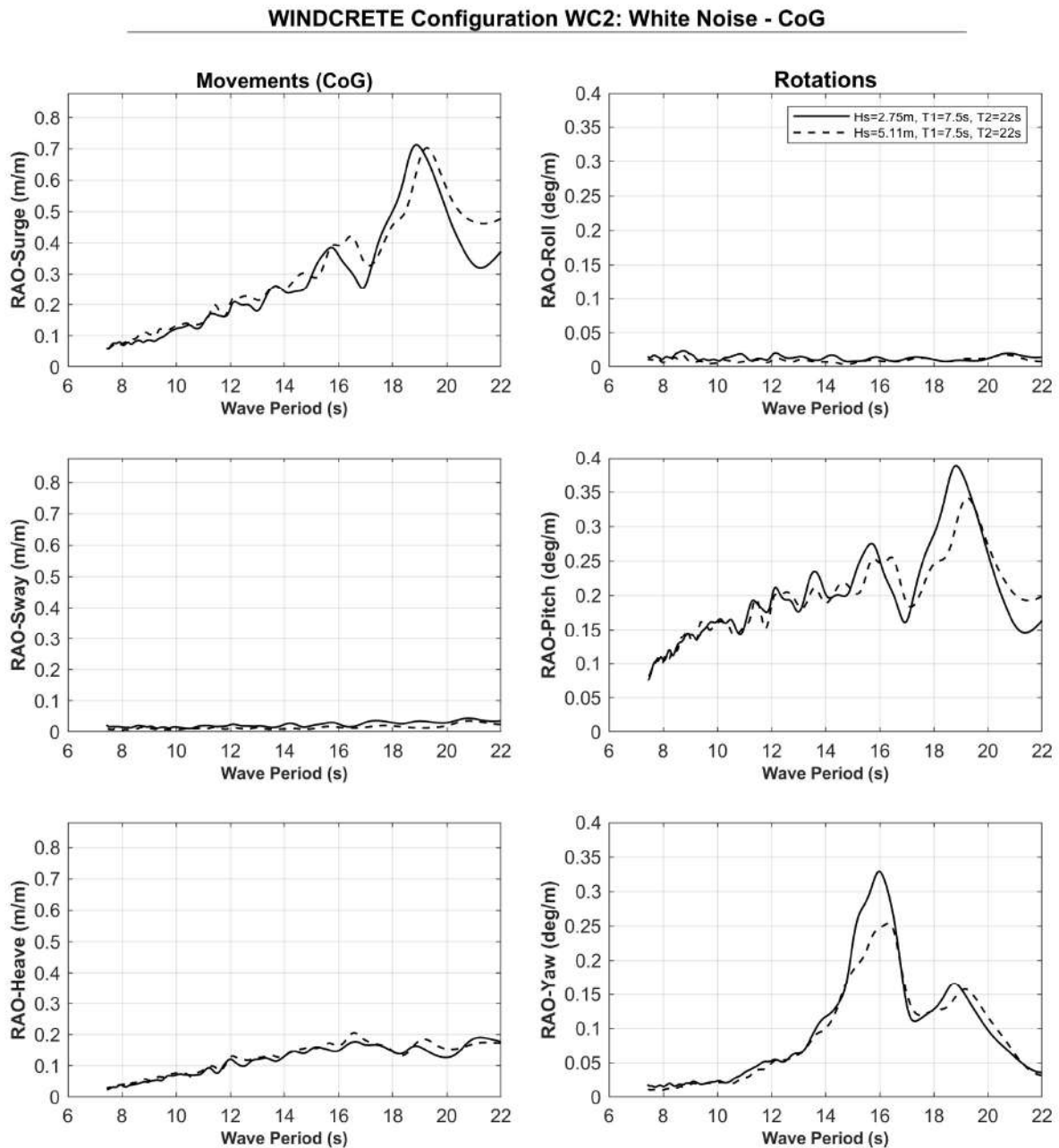


Figure 6-16. Configuration WC2: White Noise. RAO of motions (CoG)

WINDCRETE Configuration WC2: White Noise - Nacelle

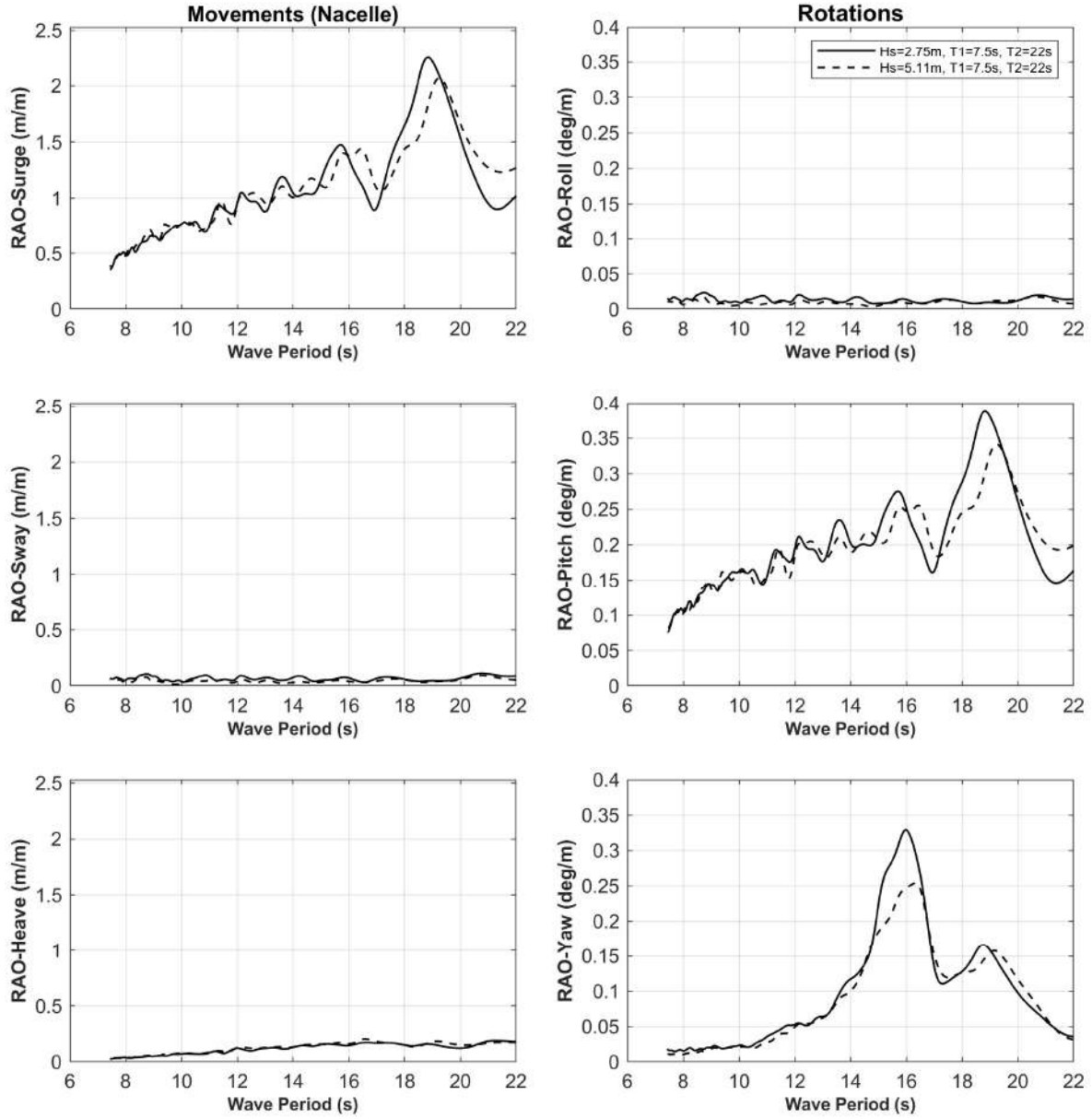


Figure 6-17. Configuration WC2: White Noise. RAO of motions (Nacelle)

WINDCRETE Configuration WC2: White Noise - MSL

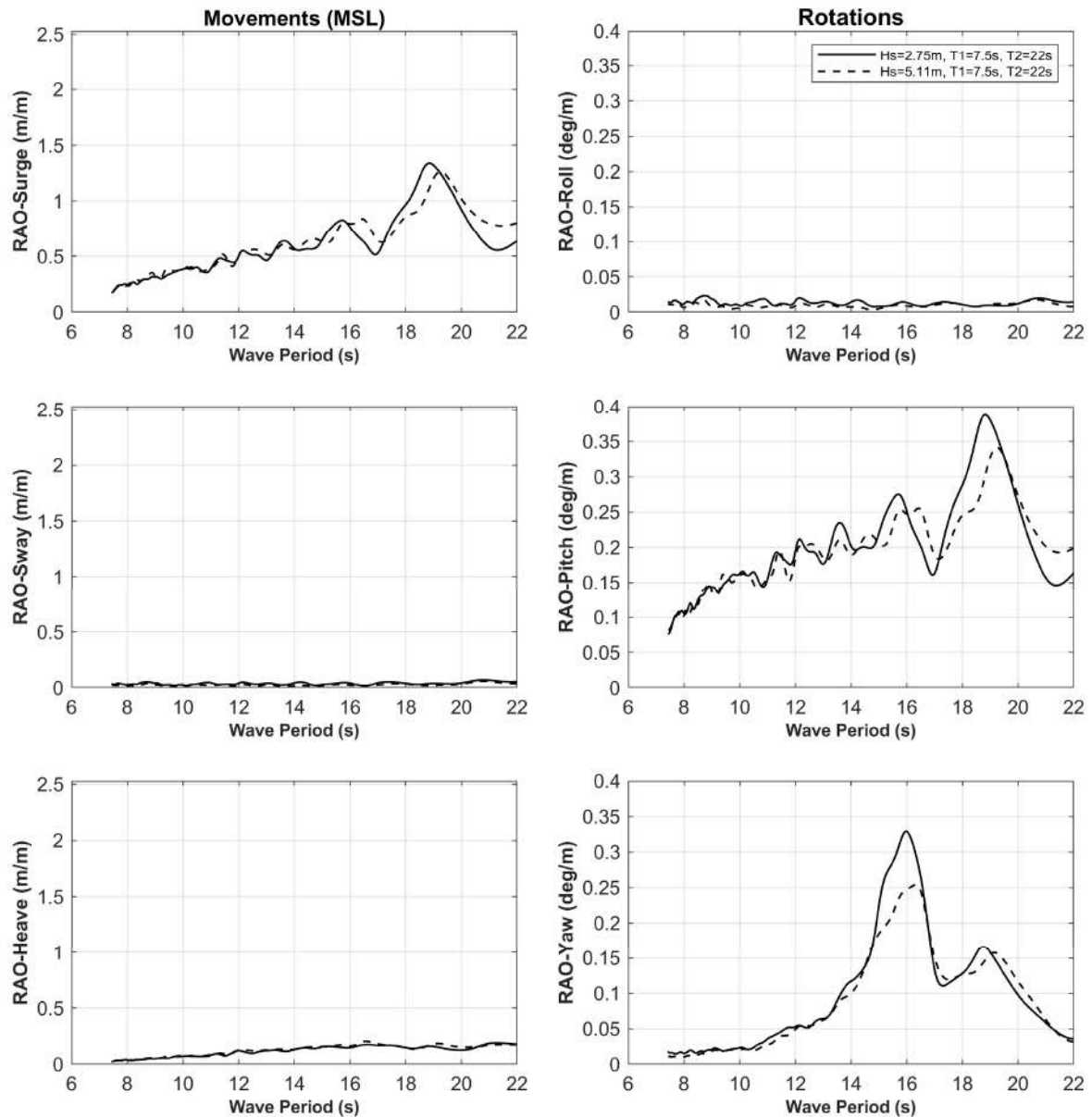


Figure 6-18. Configuration WC2: White Noise. RAO of motions (MSL)

Configuration WC2: Wind at 0°

Table 6-31 provides the wind characteristics reproduced during these tests, the average values of the thrust force measured by the triaxial load cell placed at the base of the multi-fan.

Configuration WC2 – Wind at 0 deg					
#	Test/Laboratory Code	h [m]	Wind [m/s]	Thrust [tonnes]	Measured Thrust [tonnes]
41	'FIH18-00014_WC2_WDC10p5_00'	165	10.5	236.34	234.09
42	'FIH18-00014_WC2_WDT10p5_TMETM_00'	165	10.5 ETM	170.62	172.25
43	'FIH18-00014_WC2_WDT10p5_TMNTM_01'	165	10.5 NTM	192.06	191.67
44	'FIH18-00014_WC2_WDT9_TMNTM_00'	165	9 NTM	173.92	175.60

45	'FIH18-00014_WC2_WDT18_TMNTM_00'	165	18 NTM	94.18	97.01
----	----------------------------------	-----	--------	-------	-------

Table 6-31. Configuration WC2: Wind. Incident Analysis

The data provided in the following Table 6-32 and Table 6-33 report information about the initial position for each degree of freedom, as well as the mooring loads recorded.

Configuration WC2 – Wind at 0 deg													
#	Equilibrium Condition Test/Laboratory Code	Motions - CoG: Initial Position						Motions - Nacelle: Initial Position			Motions - MSL: Initial Position		
		X [m]	Y [m]	Z [m]	roll [deg]	pitch [deg]	yaw [deg]	X [m]	Y [m]	Z [m]	X [m]	Y [m]	Z [m]
41	'FIH18-00014_WC2_WDC10p5_00'	-1.91	1.23	-1.62	0.22	0.49	1.15	0.07	0.40	-1.63	-1.10	0.89	-1.62
42	'FIH18-00014_WC2_WDT10p5_TMETM_00'	-1.85	1.26	-1.63	0.23	0.49	1.14	0.13	0.39	-1.64	-1.05	0.90	-1.63
43	'FIH18-00014_WC2_WDT10p5_TMNTM_01'	-1.93	1.31	-1.67	0.23	0.51	1.13	0.12	0.44	-1.69	-1.10	0.96	-1.68
44	'FIH18-00014_WC2_WDT9_TMNTM_00'	-2.00	1.29	-1.68	0.23	0.52	1.13	0.08	0.42	-1.69	-1.15	0.94	-1.68
45	'FIH18-00014_WC2_WDT18_TMNTM_00'	-1.98	1.31	-1.68	0.23	0.53	1.12	0.15	0.42	-1.69	-1.11	0.95	-1.68

Table 6-32. Configuration WC2: Wind. Motions initial positions

Configuration WC2 – Wind at 0 deg										
#	Equilibrium Condition Test/Laboratory Code	Mooring Lines - Pretension [tonnes]								
		LC1	LC2	LC3	LC4	LC5	LC6	LC7	LC8	LC9
41	'FIH18-00014_WC2_WDC10p5_00'	295.35	280.82	282.20	147.10	153.33	149.25	143.19	154.26	137.42
42	'FIH18-00014_WC2_WDT10p5_TMETM_00'	295.41	279.95	281.75	147.48	153.24	148.94	142.83	153.98	137.20
43	'FIH18-00014_WC2_WDT10p5_TMNTM_01'	295.51	279.95	281.18	148.29	152.89	148.91	142.80	153.91	136.83
44	'FIH18-00014_WC2_WDT9_TMNTM_00'	295.97	280.48	281.68	148.62	152.94	149.22	143.02	154.18	137.16
45	'FIH18-00014_WC2_WDT18_TMNTM_00'	295.76	280.08	281.38	148.44	152.79	148.97	142.88	154.08	136.93

Table 6-33. Configuration WC2: Wind. Mooring system pretensions

Table 6-34, Table 6-35, Table 6-36 and Table 6-37 show mean, maximum and minimum values of motions related to the CoG, Nacelle and MSL positions. Surge and pitch values are higher as rotor thrust is increased. Taking into account the initial position, the constant rated wind causes a mean pitch over 4 degrees; the rated wind with both Extreme Turbulence Model and Normal Turbulence Model as well as the below rated wind with Normal Turbulence Model result in a maximum pitch over 5.5 degrees.

Configuration WC2 – Wind at 0 deg										
#	Test/Laboratory Code	Motions - CoG: Position								
		X [m]			Y [m]			Z [m]		
		mean	max	min	mean	max	min	mean	max	min
41	'FIH18-00014_WC2_WDC10p5_00'	1.46	1.62	1.31	0.94	1.05	0.83	-1.57	-1.49	-1.64
42	'FIH18-00014_WC2_WDT10p5_TMETM_00'	0.92	3.58	-1.86	1.05	1.36	0.77	-1.61	-0.83	-2.39
43	'FIH18-00014_WC2_WDT10p5_TMNTM_01'	1.15	2.44	-0.53	1.08	1.35	0.82	-1.64	-1.13	-2.18
44	'FIH18-00014_WC2_WDT9_TMNTM_00'	0.91	2.12	-0.53	1.09	1.30	0.83	-1.66	-1.23	-2.07
45	'FIH18-00014_WC2_WDT18_TMNTM_00'	-0.20	1.80	-2.32	1.17	1.38	0.91	-1.68	-0.82	-2.52

Table 6-34. Configuration WC2: Wind. Displacements results in the CoG Position

Configuration WC2 – Wind at 0 deg										
#	Test/Laboratory Code	Motions - CoG: Position								
		roll [deg]			pitch [deg]			yaw [deg]		
		mean	max	min	mean	max	min	mean	max	min
41	'FIH18-00014_WC2_WDC10p5_00'	0.50	0.54	0.45	4.77	4.88	4.63	1.02	1.13	0.92
42	'FIH18-00014_WC2_WDT10p5_TMETM_00'	0.44	0.65	0.24	3.67	6.26	1.15	1.07	1.32	0.78
43	'FIH18-00014_WC2_WDT10p5_TMNTM_01'	0.46	0.58	0.32	4.03	5.78	2.28	1.06	1.30	0.80
44	'FIH18-00014_WC2_WDT9_TMNTM_00'	0.44	0.58	0.27	3.70	5.65	1.69	1.04	1.28	0.81
45	'FIH18-00014_WC2_WDT18_TMNTM_00'	0.34	0.52	0.19	2.29	4.15	0.55	1.06	1.19	0.93

Table 6-35. Configuration WC2: Wind. Rotations results in the CoG Position

Configuration WC2 – Wind at 0 deg										
#	Test/Laboratory Code	Motions - Nacelle: Position								
		X [m]			Y [m]			Z [m]		
		mean	max	min	mean	max	min	mean	max	min
41	'FIH18-00014_WC2_WDC10p5_00'	20.42	20.85	19.93	-0.70	-0.55	-0.87	-2.37	-2.29	-2.45

42	'FIH18-00014_WC2_WDT10p5_TMETM_00'	15.54	26.16	5.52	-0.43	0.21	-1.10	-2.11	-1.53	-2.90
43	'FIH18-00014_WC2_WDT10p5_TMNTM_01'	17.19	24.63	10.12	-0.45	0.07	-0.85	-2.23	-1.76	-2.75
44	'FIH18-00014_WC2_WDT9_TMNTM_00'	15.63	23.59	7.13	-0.39	0.12	-0.87	-2.16	-1.67	-2.77
45	'FIH18-00014_WC2_WDT18_TMNTM_00'	8.91	16.24	2.29	-0.03	0.58	-0.87	-1.88	-1.05	-3.00

Table 6-36. Configuration WC2: Wind. Motions results in the Nacelle Position

Configuration WC2 – Wind at 0 deg										
#	Test/Laboratory Code	Motions - MSL: Position								
		X [m]			Y [m]			Z [m]		
		mean	max	min	mean	max	min	mean	max	min
41	'FIH18-00014_WC2_WDC10p5_00'	9.18	9.40	8.93	0.27	0.38	0.15	-1.90	-1.82	-1.97
42	'FIH18-00014_WC2_WDT10p5_TMETM_00'	6.87	12.15	1.87	0.45	0.80	0.10	-1.81	-1.20	-2.44
43	'FIH18-00014_WC2_WDT10p5_TMNTM_01'	7.68	11.12	4.30	0.46	0.81	0.19	-1.88	-1.44	-2.31
44	'FIH18-00014_WC2_WDT9_TMNTM_00'	6.91	10.39	2.99	0.49	0.76	0.20	-1.86	-1.50	-2.30
45	'FIH18-00014_WC2_WDT18_TMNTM_00'	3.51	6.72	0.40	0.68	1.01	0.26	-1.76	-0.96	-2.56

Table 6-37. Configuration WC2: Wind. Motions results in the MSL Position

Table 6-38, Table 6-39 and Table 6-40 indicate the tensions obtained during the tests. In agreement with static offset tests in surge (Figure 6-3), mooring tensions are higher on windward lines and lower on leeward lines as rotor thrust is increased. The higher mean load in the main line 1 equal to 471 tonnes is obtained with the constant rated wind since it is directly related to the thrust value. The maximum tension in the main line 1 equal to 641 tonnes is reached in the case of rated wind with Extreme Turbulence Model.

Configuration WC2 – Wind at 0 deg										
#	Test/Laboratory Code	Mooring Line 1 - Load [tonnes]								
		LC1			LC4			LC5		
		mean	max	min	mean	max	min	mean	max	min
41	'FIH18-00014_WC2_WDC10p5_00'	470.51	480.38	462.19	235.65	240.87	230.75	236.41	241.64	231.38
42	'FIH18-00014_WC2_WDT10p5_TMETM_00'	422.33	640.53	290.52	210.17	323.21	147.15	214.39	319.47	148.56
43	'FIH18-00014_WC2_WDT10p5_TMNTM_01'	436.76	551.31	334.31	217.24	276.10	166.18	221.24	279.93	170.54
44	'FIH18-00014_WC2_WDT9_TMNTM_00'	422.48	533.59	328.46	210.36	263.58	163.72	213.99	271.52	167.23
45	'FIH18-00014_WC2_WDT18_TMNTM_00'	362.70	493.35	276.72	180.97	244.88	142.04	184.69	250.49	141.20

Table 6-38. Configuration WC2: Wind. Mooring system results: Line 1

Configuration WC2 – Wind at 0 deg										
#	Test/Laboratory Code	Mooring Line 2 - Load [tonnes]								
		LC2			LC6			LC7		
		mean	max	min	mean	max	min	mean	max	min
41	'FIH18-00014_WC2_WDC10p5_00'	230.40	232.02	228.88	138.63	140.05	137.51	100.70	102.40	99.24
42	'FIH18-00014_WC2_WDT10p5_TMETM_00'	238.60	281.16	204.04	139.23	162.90	117.00	110.85	130.78	90.61
43	'FIH18-00014_WC2_WDT10p5_TMNTM_01'	233.99	263.07	215.17	137.98	152.26	124.02	107.46	124.71	93.83
44	'FIH18-00014_WC2_WDT9_TMNTM_00'	237.77	260.38	218.27	138.91	147.89	129.20	110.39	126.42	95.80
45	'FIH18-00014_WC2_WDT18_TMNTM_00'	253.59	277.19	231.59	142.28	157.88	123.95	123.04	135.80	112.69

Table 6-39. Configuration WC2: Wind. Mooring system results: Line 2

Configuration WC2 – Wind at 0 deg										
#	Test/Laboratory Code	Mooring Line 3 - Load [tonnes]								
		LC3			LC8			LC9		
		mean	max	min	mean	max	min	mean	max	min
41	'FIH18-00014_WC2_WDC10p5_00'	244.76	245.96	243.85	119.31	120.56	117.78	132.02	132.97	130.76
42	'FIH18-00014_WC2_WDT10p5_TMETM_00'	249.59	283.35	221.62	126.70	147.65	108.66	132.25	153.32	113.67
43	'FIH18-00014_WC2_WDT10p5_TMNTM_01'	245.49	264.76	231.71	123.46	136.09	110.07	131.57	144.46	120.18
44	'FIH18-00014_WC2_WDT9_TMNTM_00'	248.31	266.99	235.43	126.42	142.08	114.16	131.53	140.17	124.04
45	'FIH18-00014_WC2_WDT18_TMNTM_00'	260.11	295.25	235.59	137.59	153.49	126.17	132.17	148.33	112.96

Table 6-40. Configuration WC2: Wind. Mooring system results: Line 3

Table 6-41 shows the accelerations at the nacelle with wind.

Configuration WC2 – Wind at 0 deg		
#	Test/Laboratory Code	Accelerations - Nacelle [m/s ²]

		Acc. X		Acc. Y		Acc. Z	
		max	min	max	min	max	min
41	'FIH18-00014_WC2_WDC10p5_00'	0.02	-0.02	0.02	-0.01	0.01	-0.01
42	'FIH18-00014_WC2_WDT10p5_TMETM_00'	0.20	-0.21	0.03	-0.03	0.01	-0.04
43	'FIH18-00014_WC2_WDT10p5_TMNTM_01'	0.12	-0.12	0.02	-0.02	0.01	-0.03
44	'FIH18-00014_WC2_WDT9_TMNTM_00'	0.09	-0.09	0.02	-0.01	0.01	-0.02
45	'FIH18-00014_WC2_WDT18_TMNTM_00'	0.15	-0.20	0.04	-0.02	0.03	-0.05

Table 6-41. Configuration WC2: Wind. Accelerations results in the Nacelle Position

Configuration WC2: Combined Regular Wave and Constant Wind at 0°

Table 6-42 summarizes the main characteristics of the incident sea state and rotor thrust force measured during the combined regular waves and constant wind tests.

Configuration WC2 - Regular Wave + Constant Wind at 0 deg									
#	Test/Laboratory Code	h [m]	H [m]	T [s]	Wind [m/s]	Thrust [tonnes]	Hinc [m]	Tinc [s]	Measured Thrust [tonnes]
46	'FIH18-00014_WC2_RW_H2p75_T7p5_ABS_WDC10p5_02'	165	2.75	7.5	10.5	234.36	2.73	7.50	236.22
47	'FIH18-00014_WC2_RW_H2p75_T9_ABS_WDC10p5_00'	165	2.75	9	10.5	231.73	2.69	9.00	233.08
48	'FIH18-00014_WC2_RW_H2p75_T11_ABS_WDC10p5_01'	165	2.75	11	10.5	227.04	2.80	11.01	227.15
49	'FIH18-00014_WC2_RW_H2p75_T14_ABS_WDC10p5_00'	165	2.75	14	10.5	218.26	2.63	13.95	221.08
50	'FIH18-00014_WC2_RW_H2p75_T17_ABS_WDC10p5_00'	165	2.75	17	10.5	215.72	2.83	16.98	218.97
51	'FIH18-00014_WC2_RW_H2p75_T20_ABS_WDC10p5_00'	165	2.75	20	10.5	216.02	2.78	19.93	218.96

Table 6-42. Configuration WC2: Combined Regular Wave and Constant Wind. Incident Analysis

The data provided in the following tables (see Table 6-43 and Table 6-44) report information about the initial position for each degree of freedom and mooring loads on the WINDCRETE floating wind turbine.

Configuration WC2 - Regular Wave + Constant Wind at 0 deg													
#	Equilibrium Condition	Motions - CoG: Initial Position						Motions - Nacelle: Initial Position			Motions - MSL: Initial Position		
	Test/Laboratory Code	X [m]	Y [m]	Z [m]	roll [deg]	pitch [deg]	yaw [deg]	X [m]	Y [m]	Z [m]	X [m]	Y [m]	Z [m]
46	'FIH18-00014_WC2_RW_H2p75_T7p5_ABS_WDC10p5_02'	-1.83	1.30	-1.78	0.22	0.51	1.17	0.22	0.45	-1.79	-1.00	0.95	-1.79
47	'FIH18-00014_WC2_RW_H2p75_T9_ABS_WDC10p5_00'	-1.96	1.34	-1.71	0.23	0.53	1.13	0.16	0.46	-1.72	-1.09	0.98	-1.71
48	'FIH18-00014_WC2_RW_H2p75_T11_ABS_WDC10p5_01'	-1.92	1.30	-1.76	0.22	0.51	1.18	0.11	0.47	-1.78	-1.10	0.96	-1.77
49	'FIH18-00014_WC2_RW_H2p75_T14_ABS_WDC10p5_00'	-1.95	1.35	-1.71	0.24	0.52	1.13	0.15	0.46	-1.72	-1.09	0.99	-1.71
50	'FIH18-00014_WC2_RW_H2p75_T17_ABS_WDC10p5_00'	-1.93	1.31	-1.70	0.23	0.53	1.13	0.20	0.45	-1.72	-1.06	0.96	-1.71
51	'FIH18-00014_WC2_RW_H2p75_T20_ABS_WDC10p5_00'	-1.90	1.31	-1.71	0.23	0.52	1.13	0.17	0.44	-1.73	-1.05	0.96	-1.72

Table 6-43. Configuration WC2: Combined Regular Wave and Constant Wind. Motions initial positions

Configuration WC2 - Regular Wave + Constant Wind at 0 deg										
#	Equilibrium Condition	Mooring Lines - Pretension [tonnes]								
	Test/Laboratory Code	LC1	LC2	LC3	LC4	LC5	LC6	LC7	LC8	LC9
46	'FIH18-00014_WC2_RW_H2p75_T7p5_ABS_WDC10p5_02'	296.22	277.54	279.77	148.19	151.47	146.92	142.22	152.45	132.90
47	'FIH18-00014_WC2_RW_H2p75_T9_ABS_WDC10p5_00'	297.71	279.35	281.22	148.11	153.10	148.46	142.14	153.90	136.30
48	'FIH18-00014_WC2_RW_H2p75_T11_ABS_WDC10p5_01'	296.50	278.42	280.38	148.01	151.63	147.43	142.45	152.59	133.44
49	'FIH18-00014_WC2_RW_H2p75_T14_ABS_WDC10p5_00'	298.16	279.58	281.45	148.28	153.12	148.63	142.20	154.01	136.45
50	'FIH18-00014_WC2_RW_H2p75_T17_ABS_WDC10p5_00'	297.75	279.18	280.95	148.02	152.92	148.36	142.07	153.93	136.14
51	'FIH18-00014_WC2_RW_H2p75_T20_ABS_WDC10p5_00'	297.91	278.94	280.83	148.18	152.77	148.33	141.88	153.62	136.27

Table 6-44. Configuration WC2: Combined Regular Wave and Constant Wind. Mooring system pretensions

Table 4-47, Table 4-48, Table 4-49 and Table 4-50 report the mean, maximum and minimum values of the platform motions. Considering the initial position, regular wave with constant rated wind and low periods ≤ 11 s causes a mean pitch over 4 degrees.

Configuration WC2 - Regular Wave + Constant Wind at 0 deg										
#	Test/Laboratory Code	Motions - CoG: Position								
		X [m]			Y [m]			Z [m]		
		mean	max	min	mean	max	min	mean	max	min

46	'FIH18-00014_WC2_RW_H2p75_T7p5_ABS_WDC10p5_02'	1.51	1.69	1.34	1.09	1.18	0.99	-1.70	-1.61	-1.78
47	'FIH18-00014_WC2_RW_H2p75_T9_ABS_WDC10p5_00'	1.48	1.69	1.26	1.04	1.14	0.95	-1.64	-1.54	-1.74
48	'FIH18-00014_WC2_RW_H2p75_T11_ABS_WDC10p5_01'	1.48	1.75	1.20	1.07	1.16	0.98	-1.71	-1.57	-1.86
49	'FIH18-00014_WC2_RW_H2p75_T14_ABS_WDC10p5_00'	1.50	1.96	0.98	1.04	1.16	0.93	-1.66	-1.44	-1.89
50	'FIH18-00014_WC2_RW_H2p75_T17_ABS_WDC10p5_00'	1.52	2.08	0.89	1.05	1.15	0.94	-1.66	-1.37	-1.95
51	'FIH18-00014_WC2_RW_H2p75_T20_ABS_WDC10p5_00'	1.45	2.42	0.50	1.08	1.20	0.97	-1.68	-1.41	-1.95

Table 6-45. Configuration WC2: Combined Regular Wave and Constant Wind. Displacements results in the CoG Position

Configuration WC2 - Regular Wave + Constant Wind at 0 deg										
#	Test/Laboratory Code	Motions - CoG: Position								
		roll [deg]			pitch [deg]			yaw [deg]		
		mean	max	min	mean	max	min	mean	max	min
46	'FIH18-00014_WC2_RW_H2p75_T7p5_ABS_WDC10p5_02'	0.48	0.51	0.44	4.84	5.01	4.65	1.17	1.27	1.09
47	'FIH18-00014_WC2_RW_H2p75_T9_ABS_WDC10p5_00'	0.51	0.57	0.45	4.77	5.03	4.52	1.07	1.17	0.97
48	'FIH18-00014_WC2_RW_H2p75_T11_ABS_WDC10p5_01'	0.47	0.51	0.44	4.66	4.97	4.36	1.19	1.31	1.08
49	'FIH18-00014_WC2_RW_H2p75_T14_ABS_WDC10p5_00'	0.50	0.59	0.41	4.54	4.96	4.11	1.05	1.69	0.42
50	'FIH18-00014_WC2_RW_H2p75_T17_ABS_WDC10p5_00'	0.49	0.56	0.43	4.51	4.88	4.13	1.05	1.41	0.69
51	'FIH18-00014_WC2_RW_H2p75_T20_ABS_WDC10p5_00'	0.49	0.58	0.40	4.50	4.85	4.15	1.07	1.28	0.85

Table 6-46. Configuration WC2: Combined Regular Wave and Constant Wind. Rotations results in the CoG Position

Configuration WC2 - Regular Wave + Constant Wind at 0 deg										
#	Test/Laboratory Code	Motions - Nacelle: Position								
		X [m]			Y [m]			Z [m]		
		mean	max	min	mean	max	min	mean	max	min
46	'FIH18-00014_WC2_RW_H2p75_T7p5_ABS_WDC10p5_02'	20.76	21.47	20.00	-0.41	-0.27	-0.56	-2.52	-2.42	-2.62
47	'FIH18-00014_WC2_RW_H2p75_T9_ABS_WDC10p5_00'	20.47	21.55	19.34	-0.63	-0.43	-0.83	-2.44	-2.31	-2.57
48	'FIH18-00014_WC2_RW_H2p75_T11_ABS_WDC10p5_01'	20.04	21.38	18.65	-0.42	-0.27	-0.59	-2.48	-2.30	-2.65
49	'FIH18-00014_WC2_RW_H2p75_T14_ABS_WDC10p5_00'	19.55	21.52	17.50	-0.61	-0.41	-0.79	-2.38	-2.16	-2.62
50	'FIH18-00014_WC2_RW_H2p75_T17_ABS_WDC10p5_00'	19.45	21.40	17.48	-0.58	-0.44	-0.78	-2.38	-2.07	-2.65
51	'FIH18-00014_WC2_RW_H2p75_T20_ABS_WDC10p5_00'	19.37	21.33	17.24	-0.52	-0.25	-0.81	-2.39	-2.20	-2.59

Table 6-47. Configuration WC2: Combined Regular Wave and Constant Wind. Motions results in the Nacelle Position

Configuration WC2 - Regular Wave + Constant Wind at 0 deg										
#	Test/Laboratory Code	Motions - MSL: Position								
		X [m]			Y [m]			Z [m]		
		mean	max	min	mean	max	min	mean	max	min
46	'FIH18-00014_WC2_RW_H2p75_T7p5_ABS_WDC10p5_02'	9.35	9.71	8.99	0.48	0.58	0.38	-2.03	-1.94	-2.12
47	'FIH18-00014_WC2_RW_H2p75_T9_ABS_WDC10p5_00'	9.22	9.74	8.65	0.36	0.49	0.24	-1.97	-1.87	-2.07
48	'FIH18-00014_WC2_RW_H2p75_T11_ABS_WDC10p5_01'	9.04	9.71	8.32	0.46	0.55	0.37	-2.02	-1.87	-2.18
49	'FIH18-00014_WC2_RW_H2p75_T14_ABS_WDC10p5_00'	8.85	9.88	7.74	0.37	0.50	0.25	-1.96	-1.73	-2.18
50	'FIH18-00014_WC2_RW_H2p75_T17_ABS_WDC10p5_00'	8.82	9.93	7.70	0.38	0.48	0.26	-1.95	-1.66	-2.22
51	'FIH18-00014_WC2_RW_H2p75_T20_ABS_WDC10p5_00'	8.75	10.06	7.41	0.43	0.56	0.28	-1.97	-1.73	-2.21

Table 6-48. Configuration WC2: Combined Regular Wave and Constant Wind. Motions results in the MSL Position

This set of tests provided the data necessary to obtain the Amplitude Response Operators (RAOs), which are illustrated in Figure 6-19, Figure 6-20 and Figure 6-21. RAOs in Yaw present resonant peaks at $T = 14$ s, in agreement with the natural period of WINDCRETE platform in this DOF (Table 6-7).

WINDCRETE Configuration WC2: Regular Wave and Constant Wind - CoG

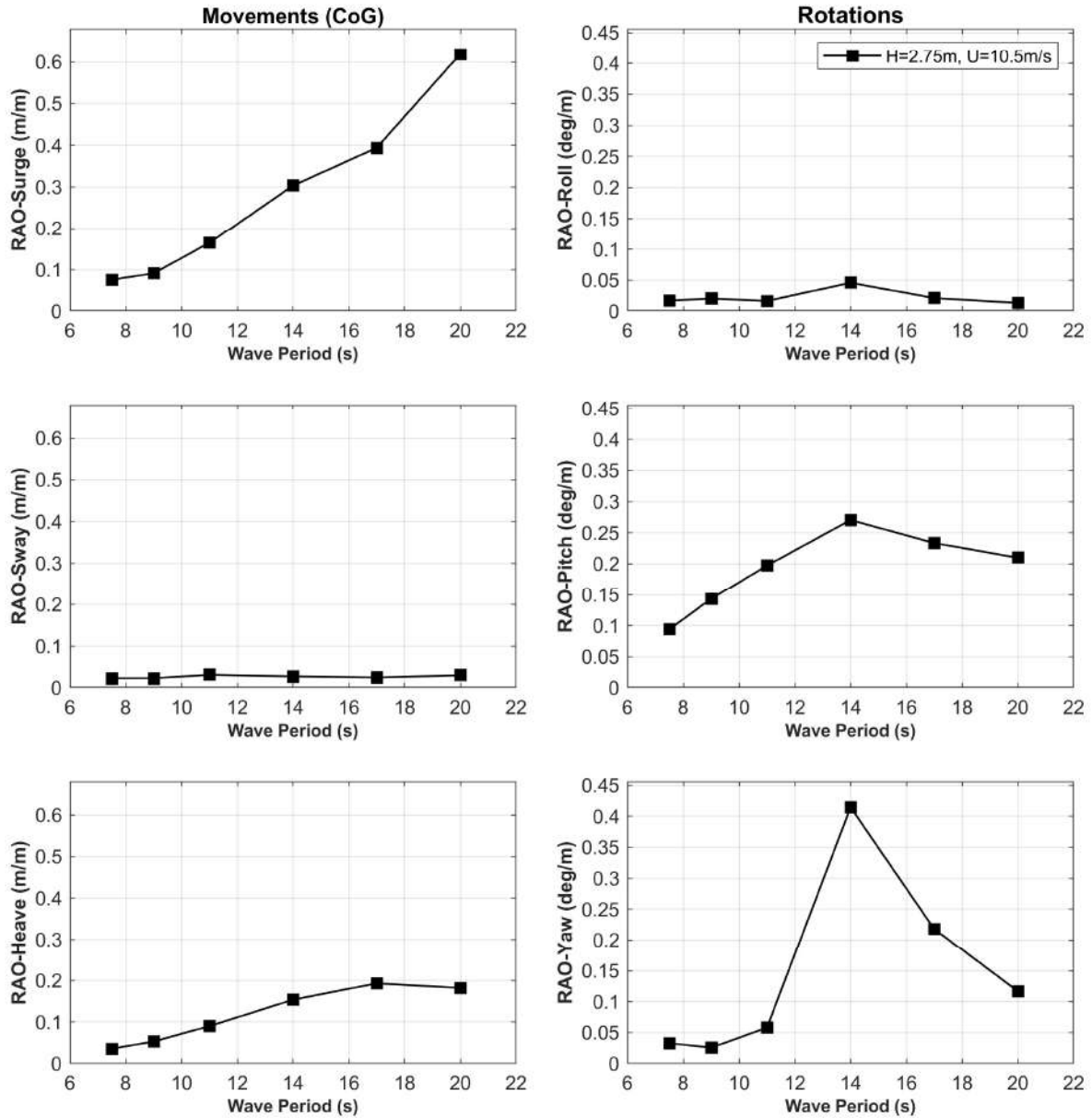


Figure 6-19. Configuration WC2: Combined Regular Wave and Constant Wind. RAO of motions (CoG)

WINDCRETE Configuration WC2: Regular Wave and Constant Wind - Nacelle

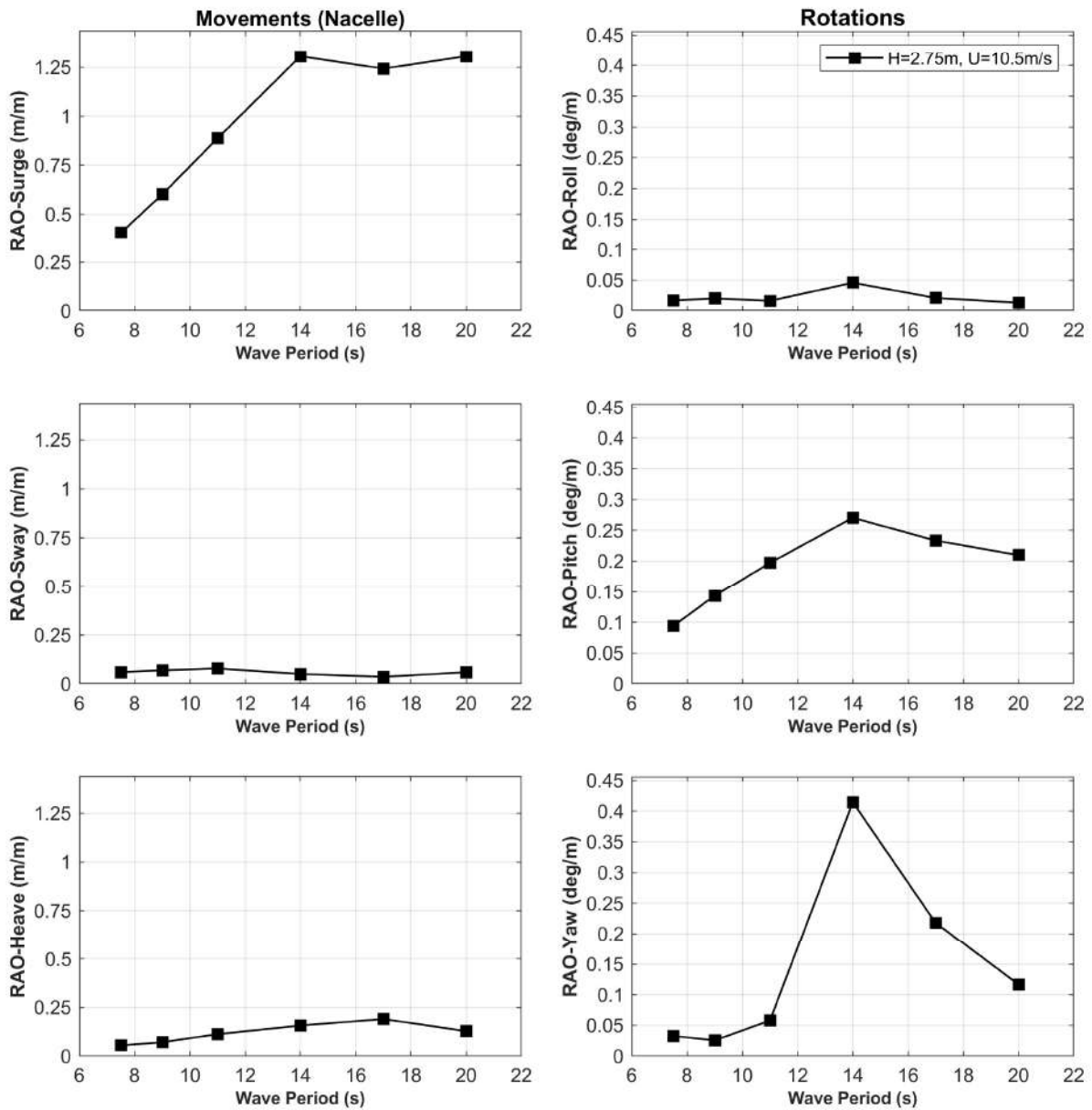


Figure 6-20. Configuration WC2: Combined Regular Wave and Constant Wind. RAO of motions (Nacelle)

WINDCRETE Configuration WC2: Regular Wave and Constant Wind - MSL

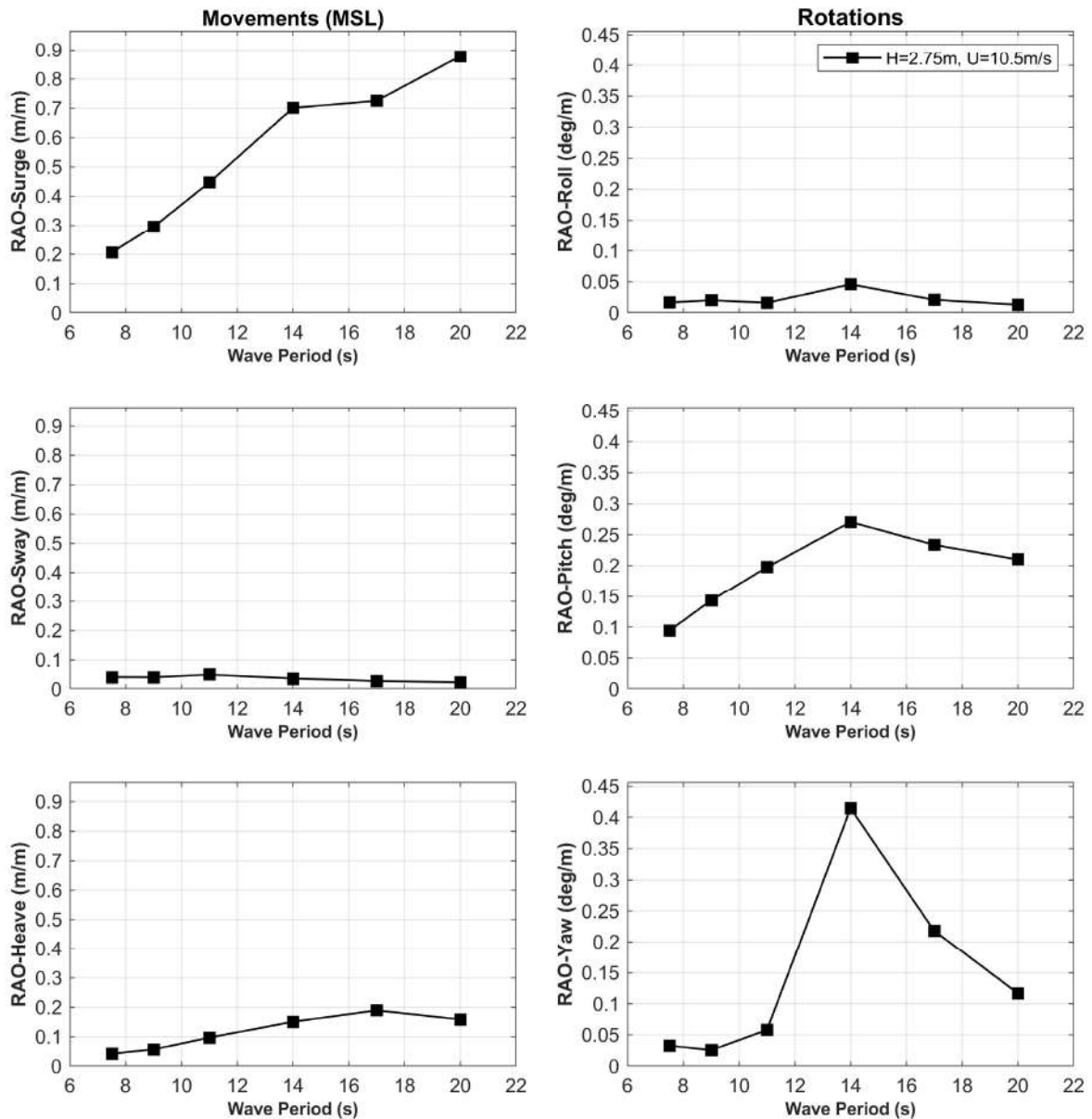


Figure 6-21. Configuration WC2: Combined Regular Wave and Constant Wind. RAO of motions (MSL)

Table 6-49, Table 6-50 and Table 6-51 contain the information regarding the tensions recorded during the tests. The maximum tension in the main line 1 equal to 557 tonnes is reached in the case of $H = 2.75\text{ m}$ and $T = 20\text{ s}$ with constant rated wind.

Configuration WC2 - Regular Wave + Constant Wind at 0 deg										
#	Test/Laboratory Code	Mooring Line 1 - Load [tonnes]								
		LC1			LC4			LC5		
		mean	max	min	mean	max	min	mean	max	min
46	'FIH18-00014_WC2_RW_H2p75_T7p5_ABS_WDC10p5_02'	477.07	486.08	467.07	233.66	238.06	229.73	241.54	247.78	235.38
47	'FIH18-00014_WC2_RW_H2p75_T9_ABS_WDC10p5_00'	471.81	482.72	460.37	234.06	240.46	227.64	237.96	243.89	230.56
48	'FIH18-00014_WC2_RW_H2p75_T11_ABS_WDC10p5_01'	467.06	486.93	449.37	228.58	237.18	221.36	236.75	247.73	225.92

49	'FIH18-00014_WC2_RW_H2p75_T14_ABS_WDC10p5_00'	460.31	513.59	411.67	228.88	254.79	203.23	231.58	260.34	200.10
50	'FIH18-00014_WC2_RW_H2p75_T17_ABS_WDC10p5_00'	459.00	524.54	402.34	228.67	264.25	196.97	230.51	260.28	204.50
51	'FIH18-00014_WC2_RW_H2p75_T20_ABS_WDC10p5_00'	459.22	557.42	382.78	227.97	275.82	190.00	231.18	281.89	191.94

Table 6-49. Configuration WC2: Combined Regular Wave and Constant Wind. Mooring system results: Line 1

Configuration WC2 - Regular Wave + Constant Wind at 0 deg										
#	Test/Laboratory Code	Mooring Line 2 - Load [tonnes]								
		LC2			LC6			LC7		
		mean	max	min	mean	max	min	mean	max	min
46	'FIH18-00014_WC2_RW_H2p75_T7p5_ABS_WDC10p5_02'	225.79	228.35	222.98	135.70	140.39	130.78	101.55	104.75	98.60
47	'FIH18-00014_WC2_RW_H2p75_T9_ABS_WDC10p5_00'	227.52	229.28	225.56	136.54	140.97	131.49	100.68	105.21	96.78
48	'FIH18-00014_WC2_RW_H2p75_T11_ABS_WDC10p5_01'	226.93	229.20	225.00	135.37	138.23	132.07	102.95	106.33	99.67
49	'FIH18-00014_WC2_RW_H2p75_T14_ABS_WDC10p5_00'	228.55	233.09	224.37	136.30	143.50	129.29	101.85	111.20	93.42
50	'FIH18-00014_WC2_RW_H2p75_T17_ABS_WDC10p5_00'	229.39	235.89	223.13	136.50	140.29	132.69	102.57	111.23	95.24
51	'FIH18-00014_WC2_RW_H2p75_T20_ABS_WDC10p5_00'	229.79	240.97	220.18	136.56	141.21	131.60	102.90	111.00	95.23

Table 6-50. Configuration WC2: Combined Regular Wave and Constant Wind. Mooring system results: Line 2

Configuration WC2 - Regular Wave + Constant Wind at 0 deg										
#	Test/Laboratory Code	Mooring Line 3 - Load [tonnes]								
		LC3			LC8			LC9		
		mean	max	min	mean	max	min	mean	max	min
46	'FIH18-00014_WC2_RW_H2p75_T7p5_ABS_WDC10p5_02'	237.89	239.87	235.70	114.71	115.63	113.34	128.68	130.32	126.95
47	'FIH18-00014_WC2_RW_H2p75_T9_ABS_WDC10p5_00'	240.34	242.61	238.20	117.70	120.36	115.01	131.43	134.38	128.39
48	'FIH18-00014_WC2_RW_H2p75_T11_ABS_WDC10p5_01'	239.00	241.36	237.41	115.80	118.17	112.60	128.85	131.39	126.01
49	'FIH18-00014_WC2_RW_H2p75_T14_ABS_WDC10p5_00'	241.52	245.21	238.01	119.45	125.44	113.74	131.02	133.76	128.97
50	'FIH18-00014_WC2_RW_H2p75_T17_ABS_WDC10p5_00'	242.06	246.69	237.41	119.63	124.42	114.88	131.35	134.83	128.13
51	'FIH18-00014_WC2_RW_H2p75_T20_ABS_WDC10p5_00'	241.99	251.67	233.77	119.21	127.42	110.53	131.63	135.87	127.88

Table 6-51. Configuration WC2: Combined Regular Wave and Constant Wind. Mooring system results: Line 3

The tensions as a function of wave period are shown in Figure 6-22, Figure 6-23 and Figure 6-24.

WINDCRETE Configuration WC2: Regular Wave and Constant Wind - Mooring Line 1

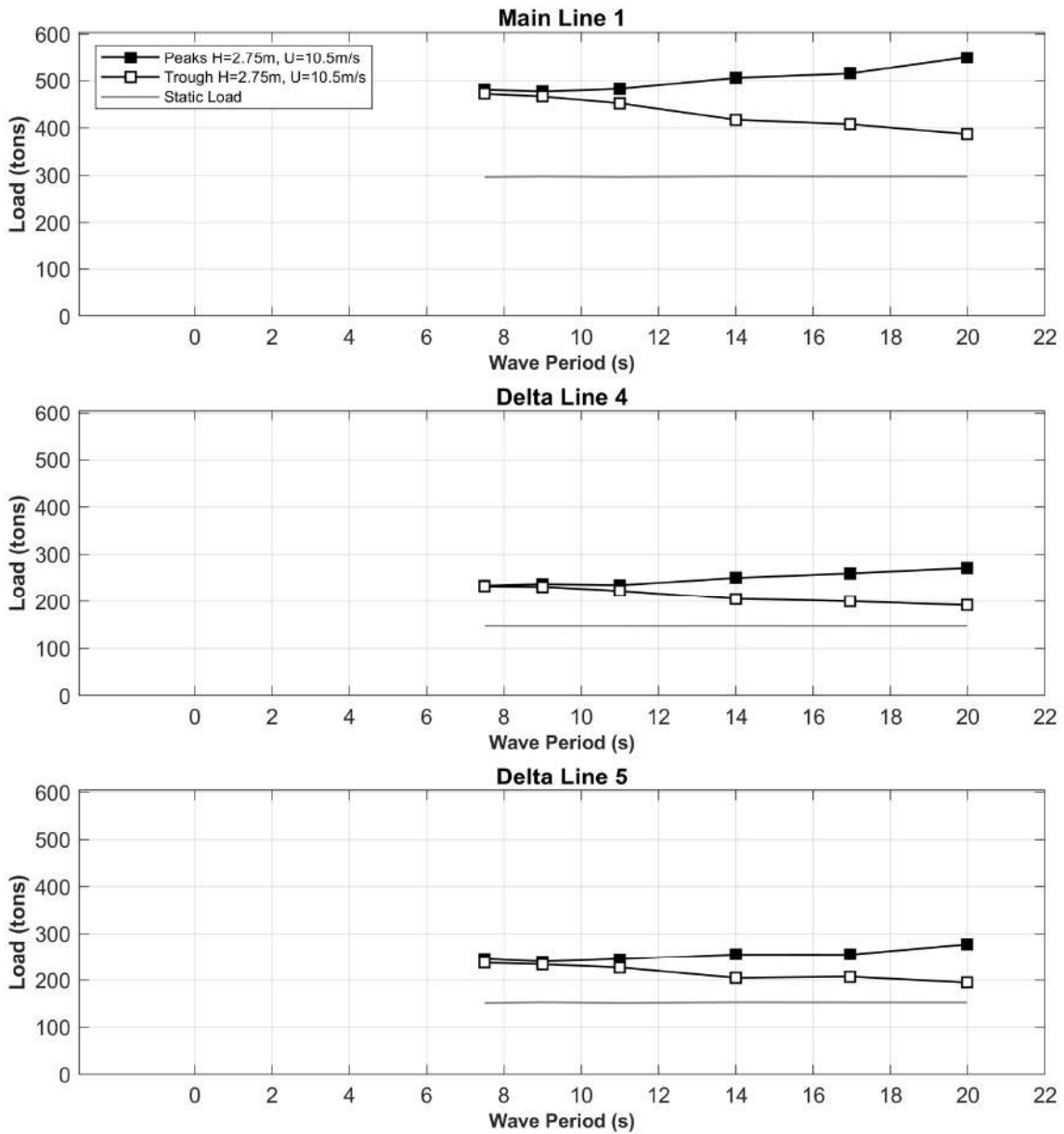


Figure 6-22. Configuration WC2: Combined Regular Wave and Constant Wind. Positive and Negative mean values of dynamic mooring loads: Line 1

WINDCRETE Configuration WC2: Regular Wave and Constant Wind - Mooring Line 2

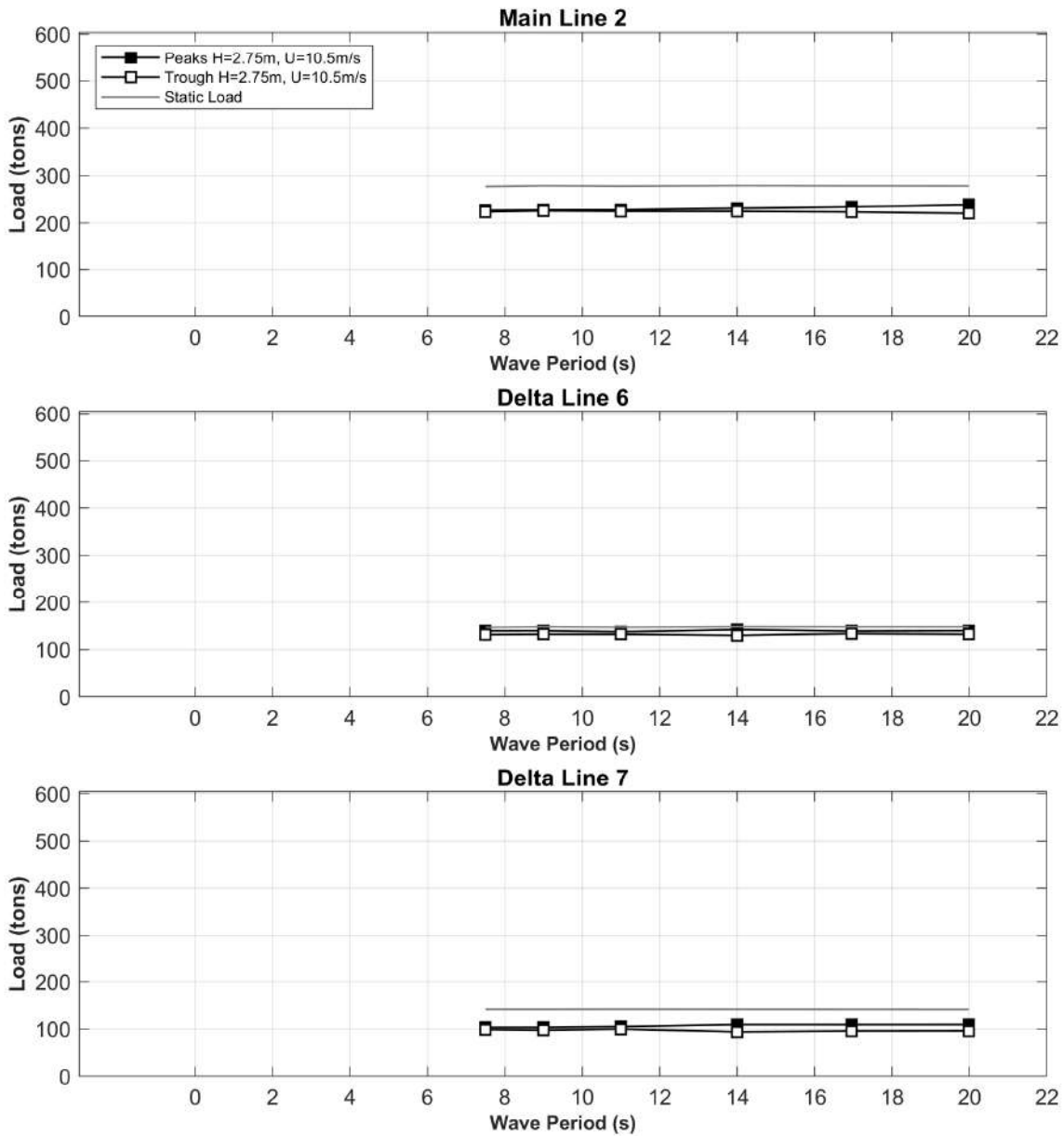


Figure 6-23. Configuration WC2: Combined Regular Wave and Constant Wind. Positive and Negative mean values of dynamic mooring loads: Line 2

WINDCRETE Configuration WC2: Regular Wave and Constant Wind - Mooring Line 3

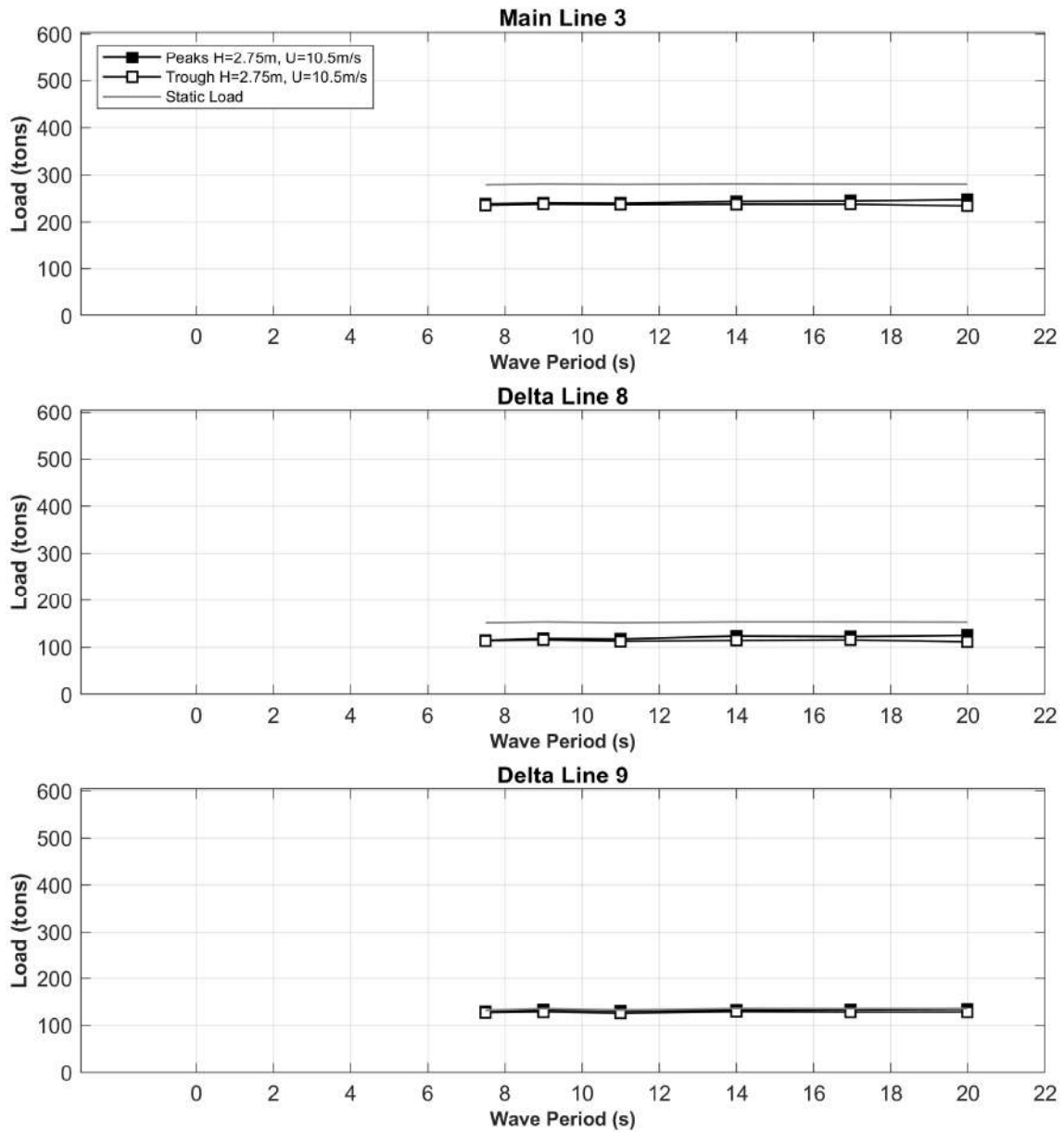


Figure 6-24. Configuration WC2: Combined Regular Wave and Constant Wind. Positive and Negative mean values of dynamic mooring loads: Line 3

Table 6-52 and Figure 6-25 show the accelerations at the nacelle.

Configuration WC2 - Regular Wave + Constant Wind at 0 deg							
#	Test/Laboratory Code	Accelerations - Nacelle [m/s ²]					
		Acc. X		Acc. Y		Acc. Z	
		max	min	max	min	max	min
46	'FIH18-00014_WC2_RW_H2p75_T7p5_ABS_WDC10p5_02'	0.41	-0.41	0.10	-0.08	0.02	-0.05
47	'FIH18-00014_WC2_RW_H2p75_T9_ABS_WDC10p5_00'	0.42	-0.41	0.07	-0.06	0.03	-0.05
48	'FIH18-00014_WC2_RW_H2p75_T11_ABS_WDC10p5_01'	0.47	-0.37	0.05	-0.04	0.05	-0.05
49	'FIH18-00014_WC2_RW_H2p75_T14_ABS_WDC10p5_00'	0.40	-0.36	0.03	-0.02	0.05	-0.05

50	'FIH18-00014_WC2_RW_H2p75_T17_ABS_WDC10p5_00'	0.26	-0.24	0.04	-0.02	0.04	-0.05
51	'FIH18-00014_WC2_RW_H2p75_T20_ABS_WDC10p5_00'	0.18	-0.15	0.04	-0.03	0.03	-0.04

Table 6-52. Configuration WC2: Combined Regular Wave and Constant Wind. Accelerations results in the Nacelle Position

WINDCRETE Configuration WC2: Regular Wave and Constant Wind - Nacelle Accelerations

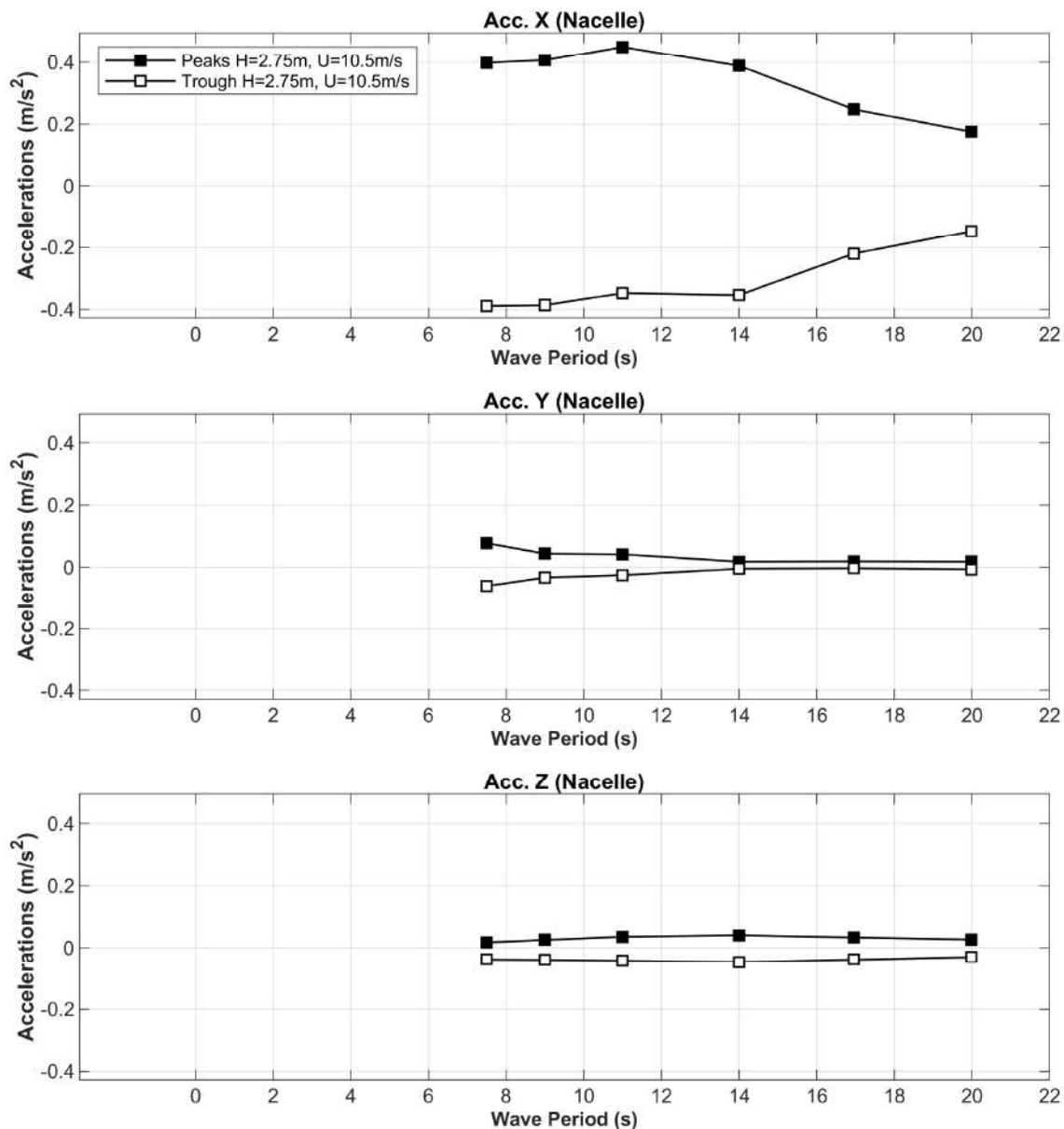


Figure 6-25. Configuration WC2: Combined Regular Wave and Constant Wind. Positive and Negative mean values of nacelle accelerations

Configuration WC2: Combined Irregular Wave and Wind at 0°

Table 6-53 summarizes the main characteristics of the incident sea state and rotor thrust force measured during the combined irregular wave and wind tests.

Configuration WC2 - Irregular Wave + Wind at 0 deg												
#	Test/Laboratory Code	h [m]	Hs [m]	Tp [s]	Spectrum	Gamma	Spread	Wind [m/s]	Thrust [tonnes]	Hinc [m]	Tinc [s]	Measured Thrust [tonnes]
52	'FIH18-00014_WC2_JS_H2p75_T9_G3p3_ABS_WDT10p5_TMETM_00'	165	2.75	9	JS	3.3	-	10.5 ETM	174.26	2.66	9.34	177.25
53	'FIH18-00014_WC2_JS_H5p11_T9_G1p2_ABS_WDT9_TMNTM_00'	165	5.11	9	JS	1.2	-	9 NTM	176.71	5.23	8.44	177.04
54	'FIH18-00014_WC2_JS_H5p11_T9_G1p2_ABS_WDT10p5_TMNTM_00'	165	5.11	9	JS	1.2	-	10.5 NTM	194.76	5.23	8.44	196.82
55	'FIH18-00014_WC2_JS_H5p11_T9_G1p2_ABS_WDT18_TMNTM_01'	165	5.11	9	JS	1.2	-	18 NTM	92.23	5.23	8.44	97.13
56	'FIH18-00014_WC2_JS_H2p75_T9_G3p3_S6_ABS_WDT10p5_TMETM_00'	165	2.75	9	JS	3.3	6	10.5 ETM	175.29	2.71	9.11	178.34
57	'FIH18-00014_WC2_JS_H2p75_T9_G3p3_S12_ABS_WDT10p5_TMETM_00'	165	2.75	9	JS	3.3	12	10.5 ETM	175.21	2.87	8.94	178.88

Table 6-53. Configuration WC2: Combined Irregular Wave and Wind. Incident Analysis

The data summarized in the following two tables report the information about the initial position for each degree of freedom and mooring loads on the WINDCRETE floating wind turbine.

Configuration WC2 - Irregular Wave + Wind at 0 deg													
#	Equilibrium Condition	Motions - CoG: Initial Position						Motions - Nacelle: Initial Position			Motions - MSL: Initial Position		
	Test/Laboratory Code	X [m]	Y [m]	Z [m]	roll [deg]	pitch [deg]	yaw [deg]	X [m]	Y [m]	Z [m]	X [m]	Y [m]	Z [m]
52	'FIH18-00014_WC2_JS_H2p75_T9_G3p3_ABS_WDT10p5_TMETM_00'	-2.02	1.33	-1.68	0.23	0.52	1.12	0.08	0.46	-1.69	-1.17	0.97	-1.68
53	'FIH18-00014_WC2_JS_H5p11_T9_G1p2_ABS_WDT9_TMNTM_00'	-2.00	1.31	-1.70	0.23	0.52	1.13	0.10	0.45	-1.71	-1.15	0.96	-1.70
54	'FIH18-00014_WC2_JS_H5p11_T9_G1p2_ABS_WDT10p5_TMNTM_00'	-2.08	1.33	-1.68	0.23	0.53	1.12	0.05	0.43	-1.69	-1.21	0.96	-1.69
55	'FIH18-00014_WC2_JS_H5p11_T9_G1p2_ABS_WDT18_TMNTM_01'	-1.88	1.31	-1.67	0.22	0.52	1.14	0.20	0.47	-1.68	-1.03	0.97	-1.67
56	'FIH18-00014_WC2_JS_H2p75_T9_G3p3_S6_ABS_WDT10p5_TMETM_00'	-1.84	1.30	-1.64	0.23	0.52	1.16	0.24	0.44	-1.65	-1.00	0.95	-1.64
57	'FIH18-00014_WC2_JS_H2p75_T9_G3p3_S12_ABS_WDT10p5_TMETM_00'	-1.96	1.34	-1.70	0.23	0.53	1.13	0.15	0.45	-1.71	-1.10	0.98	-1.70

Table 6-54. Configuration WC2: Combined Irregular Wave and Wind. Motions initial positions

Configuration WC2 - Irregular Wave + Wind at 0 deg										
#	Equilibrium Condition	Mooring Lines - Pretension [tonnes]								
	Test/Laboratory Code	LC1	LC2	LC3	LC4	LC5	LC6	LC7	LC8	LC9
52	'FIH18-00014_WC2_JS_H2p75_T9_G3p3_ABS_WDT10p5_TMETM_00'	295.66	279.91	281.34	148.34	152.81	148.89	142.80	154.06	136.71
53	'FIH18-00014_WC2_JS_H5p11_T9_G1p2_ABS_WDT9_TMNTM_00'	296.16	279.66	281.01	147.73	152.68	148.65	142.58	153.82	136.47
54	'FIH18-00014_WC2_JS_H5p11_T9_G1p2_ABS_WDT10p5_TMNTM_00'	296.59	280.49	281.90	148.01	153.18	149.19	142.88	154.19	136.97
55	'FIH18-00014_WC2_JS_H5p11_T9_G1p2_ABS_WDT18_TMNTM_01'	296.14	279.30	280.84	147.78	152.74	148.34	142.38	153.72	135.96
56	'FIH18-00014_WC2_JS_H2p75_T9_G3p3_S6_ABS_WDT10p5_TMETM_00'	296.88	279.13	280.84	147.48	153.33	148.27	142.21	153.75	135.94
57	'FIH18-00014_WC2_JS_H2p75_T9_G3p3_S12_ABS_WDT10p5_TMETM_00'	297.22	279.28	281.01	147.90	153.22	148.39	142.14	153.77	136.29

Table 6-55. Configuration WC2: Combined Irregular Wave and Wind. Mooring system pretensions

Table 6-56, Table 6-57, Table 6-58 and Table 6-59 report the mean, minimum and maximum values of the platform motions for each degree of freedom recorded during the tests. Taking into account the initial position, irregular wave with rated wind with both Extreme Turbulence Model and Normal Turbulence Model as well as irregular wave with below rated wind with Normal Turbulence Model result in a maximum pitch over 5.5 degrees.

Configuration WC2 - Irregular Wave + Wind at 0 deg										
#	Test/Laboratory Code	Motions - CoG: Position								
		X [m]			Y [m]			Z [m]		
		mean	max	min	mean	max	min	mean	max	min
52	'FIH18-00014_WC2_JS_H2p75_T9_G3p3_ABS_WDT10p5_TMETM_00'	0.97	3.79	-1.53	1.10	1.41	0.85	-1.65	-0.86	-2.44
53	'FIH18-00014_WC2_JS_H5p11_T9_G1p2_ABS_WDT9_TMNTM_00'	1.09	2.75	-1.01	1.13	1.45	0.85	-1.64	-0.65	-2.75
54	'FIH18-00014_WC2_JS_H5p11_T9_G1p2_ABS_WDT10p5_TMNTM_00'	1.32	2.89	-0.66	1.09	1.32	0.84	-1.62	-0.62	-2.57
55	'FIH18-00014_WC2_JS_H5p11_T9_G1p2_ABS_WDT18_TMNTM_01'	0.04	1.63	-1.52	1.18	1.44	0.92	-1.65	-0.54	-2.65
56	'FIH18-00014_WC2_JS_H2p75_T9_G3p3_S6_ABS_WDT10p5_TMETM_00'	1.12	3.79	-1.45	1.10	1.42	0.78	-1.63	-0.80	-2.53
57	'FIH18-00014_WC2_JS_H2p75_T9_G3p3_S12_ABS_WDT10p5_TMETM_00'	1.06	3.85	-1.60	1.11	1.44	0.80	-1.67	-0.85	-2.55

Table 6-56. Configuration WC2: Combined Irregular Wave and Wind. Displacements results in the CoG Position

Configuration WC2 - Irregular Wave + Wind at 0 deg										
--	--	--	--	--	--	--	--	--	--	--

#	Test/Laboratory Code	Motions - CoG: Position								
		roll [deg]			pitch [deg]			yaw [deg]		
		mean	max	min	mean	max	min	mean	max	min
52	'FIH18-00014_WC2_JS_H2p75_T9_G3p3_ABS_WDT10p5_TMETM_00'	0.45	0.69	0.16	3.76	6.43	0.91	1.04	1.32	0.76
53	'FIH18-00014_WC2_JS_H5p11_T9_G1p2_ABS_WDT9_TMNTM_00'	0.45	0.76	0.11	3.84	6.17	1.39	1.04	1.30	0.78
54	'FIH18-00014_WC2_JS_H5p11_T9_G1p2_ABS_WDT10p5_TMNTM_00'	0.47	0.68	0.25	4.17	6.20	1.83	1.04	1.32	0.77
55	'FIH18-00014_WC2_JS_H5p11_T9_G1p2_ABS_WDT18_TMNTM_01'	0.34	0.56	0.12	2.34	4.56	0.41	1.08	1.28	0.91
56	'FIH18-00014_WC2_JS_H2p75_T9_G3p3_S6_ABS_WDT10p5_TMETM_00'	0.44	0.76	0.19	3.78	6.41	0.70	1.09	1.41	0.84
57	'FIH18-00014_WC2_JS_H2p75_T9_G3p3_S12_ABS_WDT10p5_TMETM_00'	0.45	0.79	0.12	3.80	6.51	0.73	1.07	1.41	0.71

Table 6-57. Configuration WC2: Combined Irregular Wave and Wind. Rotations results in the CoG Position

Configuration WC2 - Irregular Wave + Wind at 0 deg										
#	Test/Laboratory Code	Motions - Nacelle: Position								
		X [m]			Y [m]			Z [m]		
		mean	max	min	mean	max	min	mean	max	min
52	'FIH18-00014_WC2_JS_H2p75_T9_G3p3_ABS_WDT10p5_TMETM_00'	15.94	27.52	3.37	-0.40	0.63	-1.13	-2.18	-1.26	-3.10
53	'FIH18-00014_WC2_JS_H5p11_T9_G1p2_ABS_WDT9_TMNTM_00'	16.39	26.12	5.44	-0.38	0.97	-1.56	-2.18	-0.99	-3.33
54	'FIH18-00014_WC2_JS_H5p11_T9_G1p2_ABS_WDT10p5_TMNTM_00'	17.94	26.14	7.66	-0.47	0.34	-1.23	-2.25	-1.09	-3.39
55	'FIH18-00014_WC2_JS_H5p11_T9_G1p2_ABS_WDT18_TMNTM_01'	9.35	18.14	1.35	0.00	0.83	-0.76	-1.85	-0.75	-2.83
56	'FIH18-00014_WC2_JS_H2p75_T9_G3p3_S6_ABS_WDT10p5_TMETM_00'	16.15	27.57	3.15	-0.37	0.65	-1.40	-2.16	-1.30	-3.17
57	'FIH18-00014_WC2_JS_H2p75_T9_G3p3_S12_ABS_WDT10p5_TMETM_00'	16.17	28.06	3.44	-0.39	0.79	-1.73	-2.20	-1.39	-3.11

Table 6-58. Configuration WC2: Combined Irregular Wave and Wind. Motions results in the Nacelle Position

Configuration WC2 - Irregular Wave + Wind at 0 deg										
#	Test/Laboratory Code	Motions - MSL: Position								
		X [m]			Y [m]			Z [m]		
		mean	max	min	mean	max	min	mean	max	min
52	'FIH18-00014_WC2_JS_H2p75_T9_G3p3_ABS_WDT10p5_TMETM_00'	7.07	12.74	0.73	0.49	1.01	0.07	-1.86	-1.11	-2.65
53	'FIH18-00014_WC2_JS_H5p11_T9_G1p2_ABS_WDT9_TMNTM_00'	7.32	11.95	2.08	0.51	1.13	-0.04	-1.86	-0.83	-2.86
54	'FIH18-00014_WC2_JS_H5p11_T9_G1p2_ABS_WDT10p5_TMNTM_00'	8.09	11.87	3.29	0.46	0.87	0.02	-1.88	-0.85	-2.83
55	'FIH18-00014_WC2_JS_H5p11_T9_G1p2_ABS_WDT18_TMNTM_01'	3.83	7.41	0.37	0.70	1.13	0.33	-1.73	-0.63	-2.69
56	'FIH18-00014_WC2_JS_H2p75_T9_G3p3_S6_ABS_WDT10p5_TMETM_00'	7.24	12.66	0.62	0.50	1.08	-0.05	-1.84	-1.06	-2.74
57	'FIH18-00014_WC2_JS_H2p75_T9_G3p3_S12_ABS_WDT10p5_TMETM_00'	7.21	12.82	0.86	0.50	1.05	-0.17	-1.89	-1.18	-2.77

Table 6-59. Configuration WC2: Combined Irregular Wave and Wind. Motions results in the MSL Position

The spectral RAOs obtained through the coupled tests with irregular wave are shown in Figure 6-26, Figure 6-27 and Figure 6-28. These RAOs are in good agreement with the ones obtained through the coupled tests with regular wave tests (Figure 6-19, Figure 6-20 and Figure 6-21).

WINDCRETE Configuration WC2: Irregular Wave and Wind - CoG

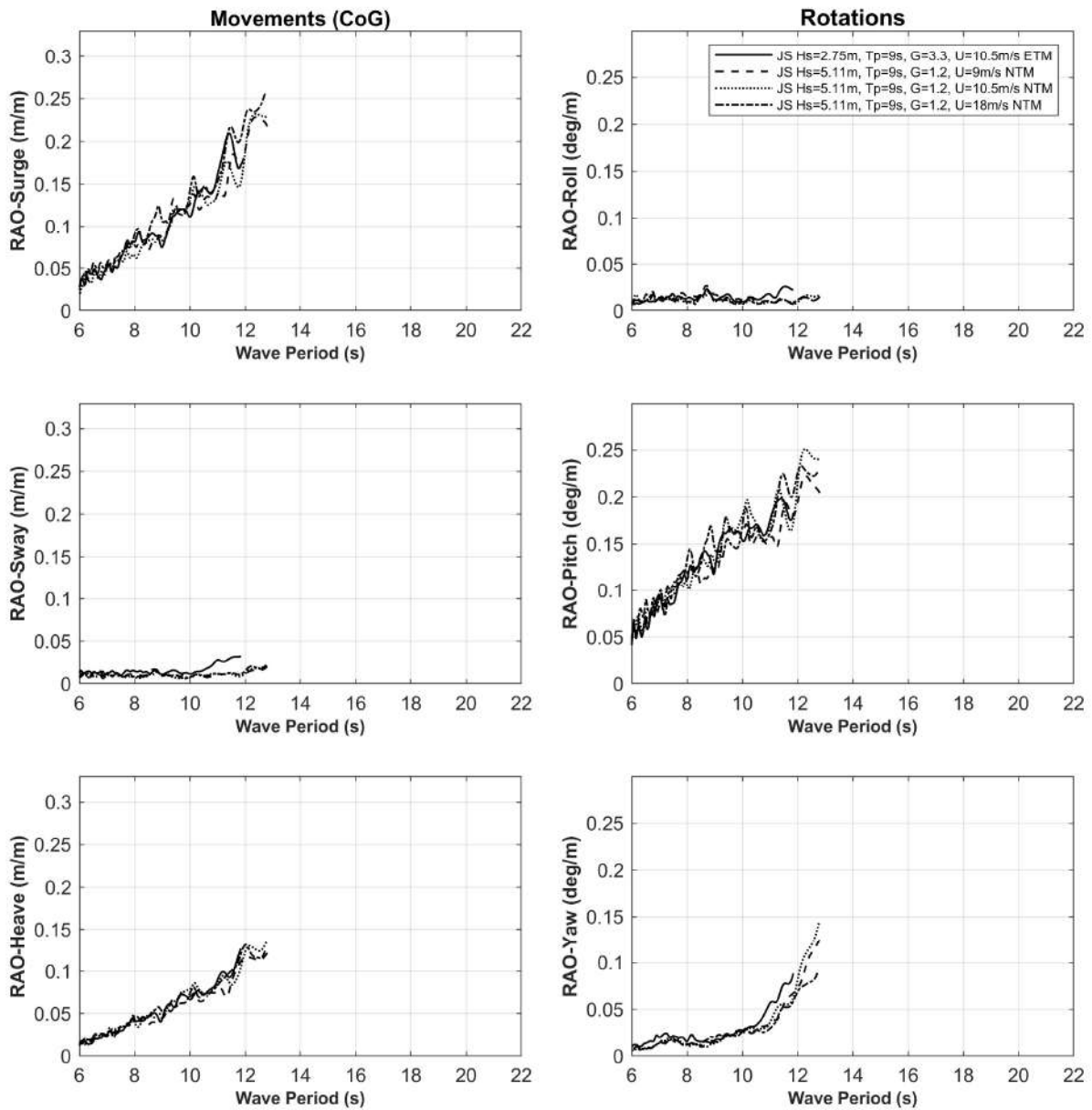


Figure 6-26. Configuration WC2: Combined Irregular Wave and Wind. RAO of motions (CoG)

WINDCRETE Configuration WC2: Irregular Wave and Wind - Nacelle

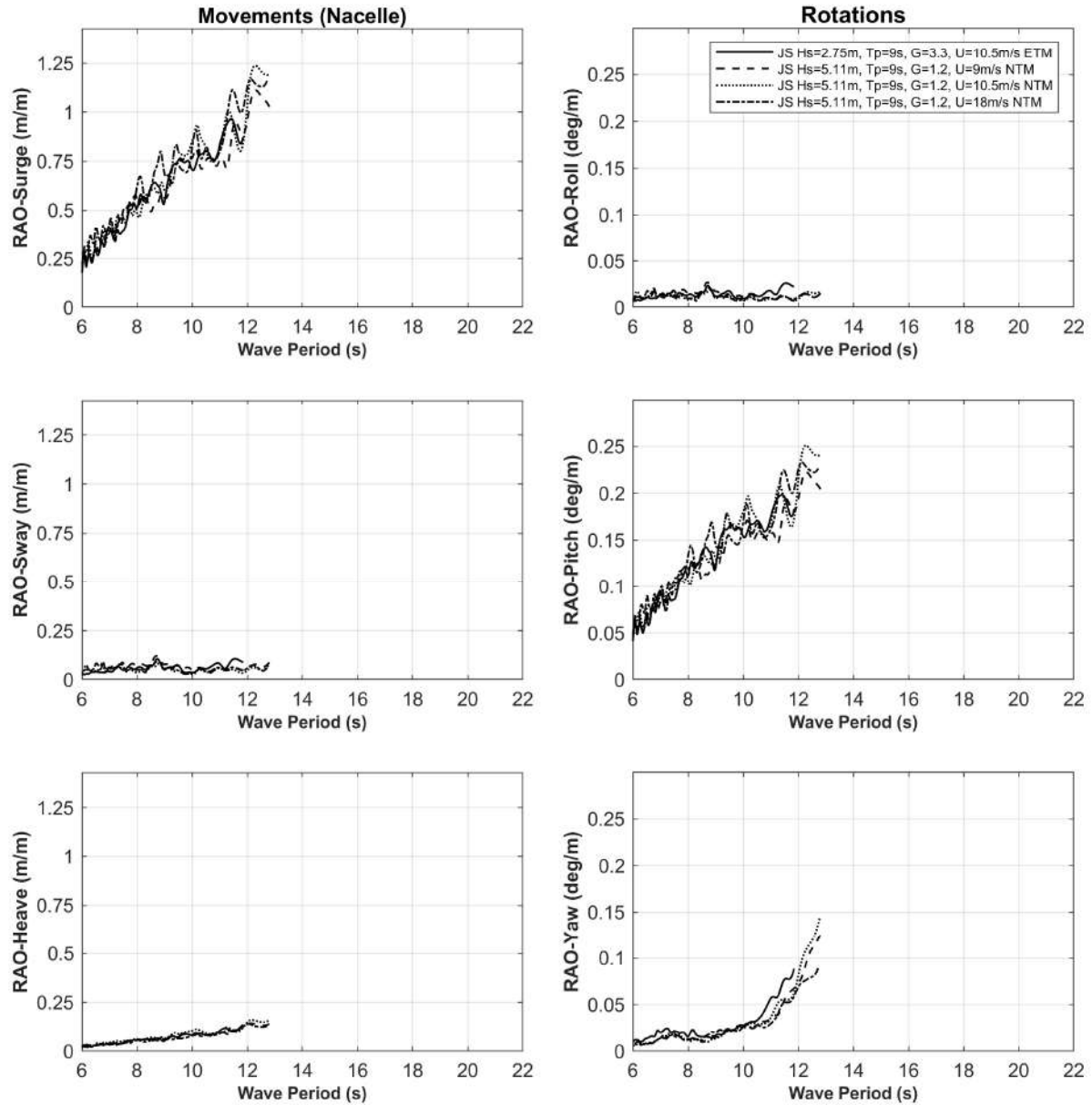


Figure 6-27. Configuration WC2: Combined Irregular Wave and Wind. RAO of motions (Nacelle)

WINDCRETE Configuration WC2: Irregular Wave and Wind - MSL

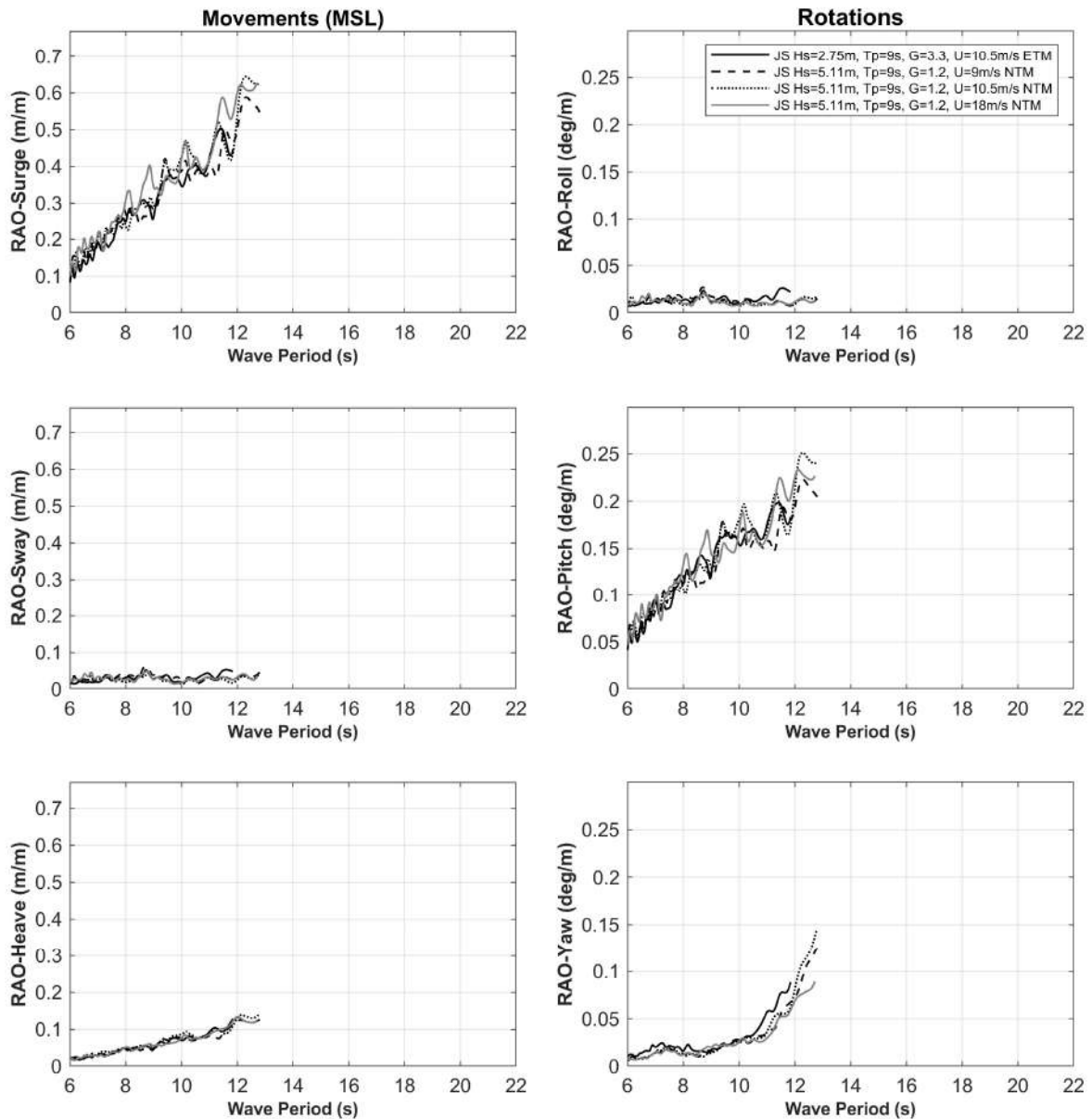


Figure 6-28. Configuration WC2: Combined Irregular Wave and Wind. RAO of motions (MSL)

Table 6-60, Table 6-61 and Table 6-62 contain the information related to the tensions obtained during the execution of the tests. The maximum tension in the main line 1 equal to 663 tonnes is reached in the case of $H_s = 2.75\text{ m}$, $T_p = 9\text{ s}$ and $\gamma = 3.3$ with rated wind with Extreme Turbulence Model.

Configuration WC2 - Irregular Wave + Wind at 0 deg										
#	Test/Laboratory Code	Mooring Line 1 - Load [tonnes]								
		LC1			LC4			LC5		
		mean	max	min	mean	max	min	mean	max	min
52	'FIH18-00014_WC2_JS_H2p75_T9_G3p3_ABS_WDT10p5_TMETM_00'	426.29	662.70	299.80	212.57	329.93	152.98	215.58	333.31	150.91
53	'FIH18-00014_WC2_JS_H5p11_T9_G1p2_ABS_WDT9_TMNTM_00'	433.52	572.99	318.21	215.93	283.95	161.44	218.86	289.85	160.02
54	'FIH18-00014_WC2_JS_H5p11_T9_G1p2_ABS_WDT10p5_TMNTM_00'	448.20	584.63	335.74	223.29	291.80	167.92	226.15	293.36	170.74

55	'FIH18-00014_WC2_JS_H5p11_T9_G1p2_ABS_WDT18_TMNTM_01'	370.66	484.34	292.83	184.62	240.40	147.57	188.44	245.20	150.00
56	'FIH18-00014_WC2_JS_H2p75_T9_G3p3_S6_ABS_WDT10p5_TMETM_00'	428.44	649.66	303.94	212.42	326.02	152.57	217.17	324.37	153.43
57	'FIH18-00014_WC2_JS_H2p75_T9_G3p3_S12_ABS_WDT10p5_TMETM_00'	429.57	660.58	303.60	213.37	330.40	153.61	217.08	329.99	150.49

Table 6-60. Configuration WC2: Combined Irregular Wave and Wind. Mooring system results: Line 1

Configuration WC2 - Irregular Wave + Wind at 0 deg										
#	Test/Laboratory Code	Mooring Line 2 - Load [tonnes]								
		LC2			LC6			LC7		
		mean	max	min	mean	max	min	mean	max	min
52	'FIH18-00014_WC2_JS_H2p75_T9_G3p3_ABS_WDT10p5_TMETM_00'	236.86	271.94	199.85	138.52	167.39	115.00	109.75	136.39	89.49
53	'FIH18-00014_WC2_JS_H5p11_T9_G1p2_ABS_WDT9_TMNTM_00'	235.12	268.28	208.99	137.54	156.01	120.53	108.82	130.34	88.78
54	'FIH18-00014_WC2_JS_H5p11_T9_G1p2_ABS_WDT10p5_TMNTM_00'	231.87	261.15	207.68	137.08	156.71	116.83	106.01	126.29	88.71
55	'FIH18-00014_WC2_JS_H5p11_T9_G1p2_ABS_WDT18_TMNTM_01'	251.81	277.77	227.01	141.08	162.42	119.31	122.14	137.33	107.24
56	'FIH18-00014_WC2_JS_H2p75_T9_G3p3_S6_ABS_WDT10p5_TMETM_00'	237.44	274.49	203.18	138.11	170.38	112.82	109.68	138.67	88.75
57	'FIH18-00014_WC2_JS_H2p75_T9_G3p3_S12_ABS_WDT10p5_TMETM_00'	236.77	275.66	202.25	138.03	171.50	113.69	109.13	135.14	87.83

Table 6-61. Configuration WC2: Combined Irregular Wave and Wind. Mooring system results: Line 2

Configuration WC2 - Irregular Wave + Wind at 0 deg										
#	Test/Laboratory Code	Mooring Line 3 - Load [tonnes]								
		LC3			LC8			LC9		
		mean	max	min	mean	max	min	mean	max	min
52	'FIH18-00014_WC2_JS_H2p75_T9_G3p3_ABS_WDT10p5_TMETM_00'	247.66	283.83	217.94	125.99	149.80	105.91	131.14	158.63	111.27
53	'FIH18-00014_WC2_JS_H5p11_T9_G1p2_ABS_WDT9_TMNTM_00'	245.89	274.27	228.56	124.87	144.23	109.72	130.54	145.74	118.49
54	'FIH18-00014_WC2_JS_H5p11_T9_G1p2_ABS_WDT10p5_TMNTM_00'	243.81	272.38	226.00	122.59	141.92	108.34	130.67	148.80	116.19
55	'FIH18-00014_WC2_JS_H5p11_T9_G1p2_ABS_WDT18_TMNTM_01'	258.35	285.17	237.56	136.57	150.64	124.75	130.88	153.27	112.41
56	'FIH18-00014_WC2_JS_H2p75_T9_G3p3_S6_ABS_WDT10p5_TMETM_00'	247.50	280.71	220.52	125.40	150.38	106.63	131.27	153.30	114.37
57	'FIH18-00014_WC2_JS_H2p75_T9_G3p3_S12_ABS_WDT10p5_TMETM_00'	247.35	281.62	217.00	125.46	150.64	105.87	131.17	154.49	113.58

Table 6-62. Configuration WC2: Combined Irregular Wave and Wind. Mooring system results: Line 3

The accelerations at the nacelle are shown in Table 6-63.

Configuration WC2 - Irregular Wave + Wind at 0 deg									
#	Test/Laboratory Code	Accelerations - Nacelle [m/s ²]							
		Acc. X		Acc. Y		Acc. Z			
		max	min	max	min	max	min		
52	'FIH18-00014_WC2_JS_H2p75_T9_G3p3_ABS_WDT10p5_TMETM_00'	0.83	-0.74	0.10	-0.10	0.06	-0.08		
53	'FIH18-00014_WC2_JS_H5p11_T9_G1p2_ABS_WDT9_TMNTM_00'	1.52	-1.37	0.22	-0.29	0.10	-0.13		
54	'FIH18-00014_WC2_JS_H5p11_T9_G1p2_ABS_WDT10p5_TMNTM_00'	1.51	-1.34	0.19	-0.19	0.09	-0.15		
55	'FIH18-00014_WC2_JS_H5p11_T9_G1p2_ABS_WDT18_TMNTM_01'	1.47	-1.39	0.19	-0.19	0.10	-0.13		
56	'FIH18-00014_WC2_JS_H2p75_T9_G3p3_S6_ABS_WDT10p5_TMETM_00'	0.75	-0.67	0.29	-0.28	0.08	-0.07		
57	'FIH18-00014_WC2_JS_H2p75_T9_G3p3_S12_ABS_WDT10p5_TMETM_00'	0.82	-0.80	0.35	-0.30	0.08	-0.07		

Table 6-63. Configuration WC2: Combined Irregular Wave and Wind. Accelerations results in the Nacelle Position

Configuration WC2: Current at 0°

Table 6-64 provides the current characteristics reproduced during these tests, the average velocity value measured by the ADV placed at 60% of the basin depth from free surface.

Configuration WC2 - Current at 0 deg				
#	Test/Laboratory Code	h [m]	Current [m/s]	M. Current [m/s]
58	'FIH18-00014_WC2_SN0p143_23Hz_00'	165	1.06	1.07

Table 6-64. Configuration WC2: Current. Incident Analysis

The data provided in the following Table 6-65 and Table 6-66 report information about the initial position for each degree of freedom, as well as the mooring loads recorded.

Configuration WC2 - Current at 0 deg				
#	Equilibrium Condition	Motions - CoG: Initial Position	Motions - Nacelle: Initial Position	Motions - MSL: Initial Position

	Test/Laboratory Code	X [m]	Y [m]	Z [m]	roll [deg]	pitch [deg]	yaw [deg]	X [m]	Y [m]	Z [m]	X [m]	Y [m]	Z [m]
58	'FIH18-00014_WC2_SNOp143_23Hz_00'	-2.80	2.46	-1.75	0.17	0.42	0.93	-1.13	1.82	-1.76	-2.12	2.20	-1.76

Table 6-65. Configuration WC2: Current. Motions initial positions

Configuration WC2 – Current at 0 deg										
#	Equilibrium Condition	Mooring Lines - Pretension [tonnes]								
	Test/Laboratory Code	LC1	LC2	LC3	LC4	LC5	LC6	LC7	LC8	LC9
58	'FIH18-00014_WC2_SNOp143_23Hz_00'	323.75	313.73	310.94	176.06	156.23	161.23	166.73	156.91	171.61

Table 6-66. Configuration WC2: Current. Mooring system pretensions

Table 6-67, Table 6-68, Table 6-69 and Table 6-70 show mean, maximum and minimum values of motions related to the CoG, Nacelle and MSL positions. Surge values are higher when acting current.

Configuration WC2 – Current at 0 deg										
#	Test/Laboratory Code	Motions - CoG: Position								
		X [m]			Y [m]			Z [m]		
		mean	max	min	mean	max	min	mean	max	min
58	'FIH18-00014_WC2_SNOp143_23Hz_00'	-1.89	-1.12	-2.60	2.42	4.11	0.27	-1.75	-1.67	-1.84

Table 6-67. Configuration WC2: Current. Displacements results in the CoG Position

Configuration WC2 – Current at 0 deg										
#	Test/Laboratory Code	Motions - CoG: Position								
		roll [deg]			pitch [deg]			yaw [deg]		
		mean	max	min	mean	max	min	mean	max	min
58	'FIH18-00014_WC2_SNOp143_23Hz_00'	0.16	0.52	-0.15	0.59	1.05	0.30	0.98	1.11	0.89

Table 6-68. Configuration WC2: Current. Rotations results in the CoG Position

Configuration WC2 – Current at 0 deg										
#	Test/Laboratory Code	Motions - Nacelle: Position								
		X [m]			Y [m]			Z [m]		
		mean	max	min	mean	max	min	mean	max	min
58	'FIH18-00014_WC2_SNOp143_23Hz_00'	0.49	2.58	-0.99	1.84	3.76	-1.39	-1.77	-1.68	-1.86

Table 6-69. Configuration WC2: Current. Motions results in the Nacelle Position

Configuration WC2 – Current at 0 deg										
#	Test/Laboratory Code	Motions - MSL: Position								
		X [m]			Y [m]			Z [m]		
		mean	max	min	mean	max	min	mean	max	min
58	'FIH18-00014_WC2_SNOp143_23Hz_00'	-0.92	0.18	-1.82	2.18	3.78	-0.37	-1.76	-1.67	-1.85

Table 6-70. Configuration WC2: Current. Motions results in the MSL Position

Table 6-71, Table 6-72 and Table 6-73 indicate the tensions obtained during the tests execution. In agreement with static offset tests in surge (Figure 6-3), mooring tensions are higher on windward lines and lower on leeward lines when acting current. Although the higher mean load equal to 432 tonnes is obtained in the main line 1, the maximum tensions over 683 tonnes take place in main lines 2 and 3.

Configuration WC2 – Current at 0 deg										
#	Test/Laboratory Code	Mooring Line 1 - Load [tonnes]								
		LC1			LC4			LC5		
		mean	max	min	mean	max	min	mean	max	min
58	'FIH18-00014_WC2_SNOp143_23Hz_00'	361.09	402.54	327.15	194.93	214.32	174.22	174.79	197.15	159.61

Table 6-71. Configuration WC2: Current. Mooring system results: Line 1

Configuration WC2 – Current at 0 deg										
#	Test/Laboratory Code	Mooring Line 2 - Load [tonnes]								
		LC2			LC6			LC7		
		mean	max	min	mean	max	min	mean	max	min
58	'FIH18-00014_WC2_SNOp143_23Hz_00'	301.66	361.08	242.23	157.25	183.73	128.75	158.71	192.31	127.27

Table 6-72. Configuration WC2: Current. Mooring system results: Line 2

Configuration WC2 – Current at 0 deg										
#	Test/Laboratory Code	Mooring Line 3 - Load [tonnes]								
		LC3			LC8			LC9		
		mean	max	min	mean	max	min	mean	max	min
58	'FIH18-00014_WC2_SNOp143_23Hz_00'	300.27	372.23	251.20	148.84	182.64	124.20	169.32	207.70	145.16

Table 6-73. Configuration WC2: Current. Mooring system results: Line 3

Table 6-74 shows the accelerations at the nacelle with wind.

Configuration WC2 – Current at 0 deg							
#	Test/Laboratory Code	Accelerations - Nacelle [m/s ²]					
		Acc. X		Acc. Y		Acc. Z	
		max	min	max	min	max	min
58	'FIH18-00014_WC2_SNOp143_23Hz_00'	0.03	-0.03	0.04	-0.03	0.01	-0.01

Table 6-74. Configuration WC2: Current. Accelerations results in the Nacelle Position

Configuration WC2: Combined Irregular Wave and Current and Wind at 0°

Table 6-75 summarizes the main characteristics of the incident sea state and rotor thrust force measured during the combined irregular wave and current and wind tests.

Configuration WC2 - Irregular Wave + Current + Wind at 0 deg												
#	Test/Laboratory Code	h [m]	Hs [m]	Tp [s]	Spectrum	Gamma	Current [m/s]	Wind [m/s]	Thrust [tonnes]	Hinc [m]	Measured Current [m/s]	Measured Thrust [tonnes]
59	'FIH18-00014_WC2_JS_H2p75_T9_G1_SNOp143_WDT10p5_TCETM_23Hz_00'	165	2.75	9	'JS'	1.0	1.06	10.5	174.99	2.70	0.98	152.67
60	'FIH18-00014_WC2_JS_H5p11_T9_G1p2_SNOp143_WDT10p5_TCNTM_23Hz_00'	165	5.11	9	'JS'	1.2	1.06	10.5	193.88	5.04	1.03	156.99

Table 6-75. Configuration WC2: Combined Irregular Wave and Current and Wind. Incident Analysis

The data provided in the following two tables (see Table 6-76 and Table 6-77) report information about the initial position for each degree of freedom and mooring loads on the WINDCRETE floating wind turbine.

Configuration WC2 - Irregular Wave + Current + Wind at 0 deg													
#	Equilibrium Condition	Motions - CoG: Initial Position						Motions - Nacelle: Initial Position			Motions - MSL: Initial Position		
	Test/Laboratory Code	X [m]	Y [m]	Z [m]	roll [deg]	pitch [deg]	yaw [deg]	X [m]	Y [m]	Z [m]	X [m]	Y [m]	Z [m]
59	'FIH18-00014_WC2_JS_H2p75_T9_G1_SNOp143_WDT10p5_TCETM_23Hz_00'	-3.24	1.44	-1.72	-0.10	0.54	1.51	-1.09	1.91	-1.73	-2.36	1.63	-1.72
60	'FIH18-00014_WC2_JS_H5p11_T9_G1p2_SNOp143_WDT10p5_TCNTM_23Hz_00'	-2.84	2.39	-1.71	0.16	0.50	0.91	-0.84	1.79	-1.72	-2.02	2.15	-1.72

Table 6-76. Configuration WC2: Combined Irregular Wave and Current and Wind. Motions initial positions

Configuration WC2 - Irregular Wave + Current + Wind at 0 deg										
#	Equilibrium Condition	Mooring Lines - Pretension [tonnes]								
	Test/Laboratory Code	LC1	LC2	LC3	LC4	LC5	LC6	LC7	LC8	LC9
59	'FIH18-00014_WC2_JS_H2p75_T9_G1_SNOp143_WDT10p5_TCETM_23Hz_00'	324.54	311.77	312.13	176.98	155.07	160.40	165.19	157.19	172.47
60	'FIH18-00014_WC2_JS_H5p11_T9_G1p2_SNOp143_WDT10p5_TCNTM_23Hz_00'	327.89	313.80	303.35	178.80	151.11	162.19	165.09	151.49	169.27

Table 6-77. Configuration WC2: Combined Irregular Wave and Current and Wind. Mooring system pretensions

Table 6-78, Table 6-79, Table 6-80 and Table 6-81 report the mean, minimum and maximum values of the platform motions for each degree of freedom recorded during the tests. Considering the initial position, irregular wave with current and with rated wind with both Extreme Turbulence Model and Normal Turbulence Model result in a maximum pitch over 5.5 degrees.

Configuration WC2 - Irregular Wave + Current + Wind at 0 deg										
#	Test/Laboratory Code	Motions - CoG: Position								
		X [m]			Y [m]			Z [m]		
		mean	max	min	mean	max	min	mean	max	min
59	'FIH18-00014_WC2_JS_H2p75_T9_G1_SNOp143_WDT10p5_TCETM_23Hz_00'	1.05	3.31	-1.42	2.15	11.68	-7.49	-1.80	-0.90	-2.72

60	'FIH18-00014_WC2_JS_H5p11_T9_G1p2_SNOp143_WDT10p5_TCNTM_23Hz_00'	1.18	3.32	-0.60	1.97	10.29	-6.85	-1.77	-0.83	-2.73
----	--	------	------	-------	------	-------	-------	-------	-------	-------

Table 6-78. Configuration WC2: Combined Irregular Wave and Current and Wind. Displacements results in the CoG Position

Configuration WC2 - Irregular Wave + Current + Wind at 0 deg										
#	Test/Laboratory Code	Motions - CoG: Position								
		roll [deg]			pitch [deg]			yaw [deg]		
		mean	max	min	mean	max	min	mean	max	min
59	'FIH18-00014_WC2_JS_H2p75_T9_G1_SNOp143_WDT10p5_TCETM_23Hz_00'	0.40	1.50	-0.57	3.94	6.74	0.97	1.06	1.65	0.57
60	'FIH18-00014_WC2_JS_H5p11_T9_G1p2_SNOp143_WDT10p5_TCNTM_23Hz_00'	0.45	1.64	-0.95	4.39	6.34	2.18	1.07	1.63	0.42

Table 6-79. Configuration WC2: Combined Irregular Wave and Current and Wind. Rotations results in the CoG Position

Configuration WC2 - Irregular Wave + Current + Wind at 0 deg										
#	Test/Laboratory Code	Motions - Nacelle: Position								
		X [m]			Y [m]			Z [m]		
		mean	max	min	mean	max	min	mean	max	min
59	'FIH18-00014_WC2_JS_H2p75_T9_G1_SNOp143_WDT10p5_TCETM_23Hz_00'	16.71	28.87	5.47	0.85	11.87	-10.68	-2.37	-1.37	-3.58
60	'FIH18-00014_WC2_JS_H5p11_T9_G1p2_SNOp143_WDT10p5_TCNTM_23Hz_00'	18.64	26.92	8.91	0.51	12.53	-10.31	-2.47	-1.49	-3.59

Table 6-80. Configuration WC2: Combined Irregular Wave and Current and Wind. Motions results in the Nacelle Position

Configuration WC2 - Irregular Wave + Current + Wind at 0 deg										
#	Test/Laboratory Code	Motions - MSL: Position								
		X [m]			Y [m]			Z [m]		
		mean	max	min	mean	max	min	mean	max	min
59	'FIH18-00014_WC2_JS_H2p75_T9_G1_SNOp143_WDT10p5_TCETM_23Hz_00'	7.42	13.06	2.10	1.62	11.75	-8.72	-2.03	-1.09	-2.92
60	'FIH18-00014_WC2_JS_H5p11_T9_G1p2_SNOp143_WDT10p5_TCNTM_23Hz_00'	8.29	12.34	3.68	1.38	10.68	-7.88	-2.06	-1.15	-3.07

Table 6-81. Configuration WC2: Combined Irregular Wave and Current and Wind. Motions results in the MSL Position

The spectral RAOs obtained through the coupled tests with irregular wave are shown in Figure 6-29, Figure 6-30 and Figure 6-31.

WINDCRETE Configuration WC2: Irregular Wave and Current and Wind - CoG

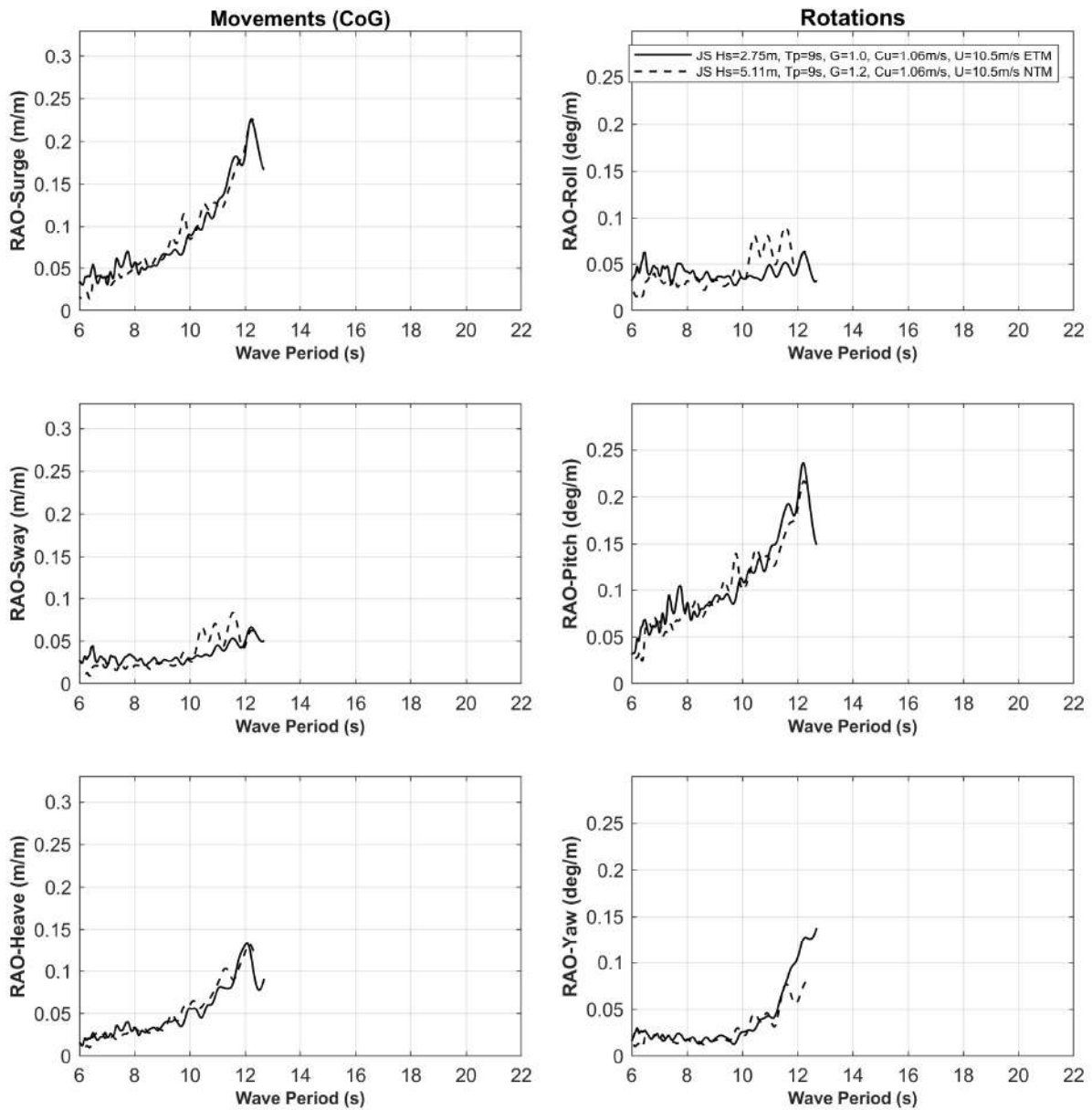


Figure 6-29. Configuration WC2: Combined Irregular and Current Wave and Wind. RAO of motions (CoG)

WINDCRETE Configuration WC2: Irregular Wave and Current and Wind - Nacelle

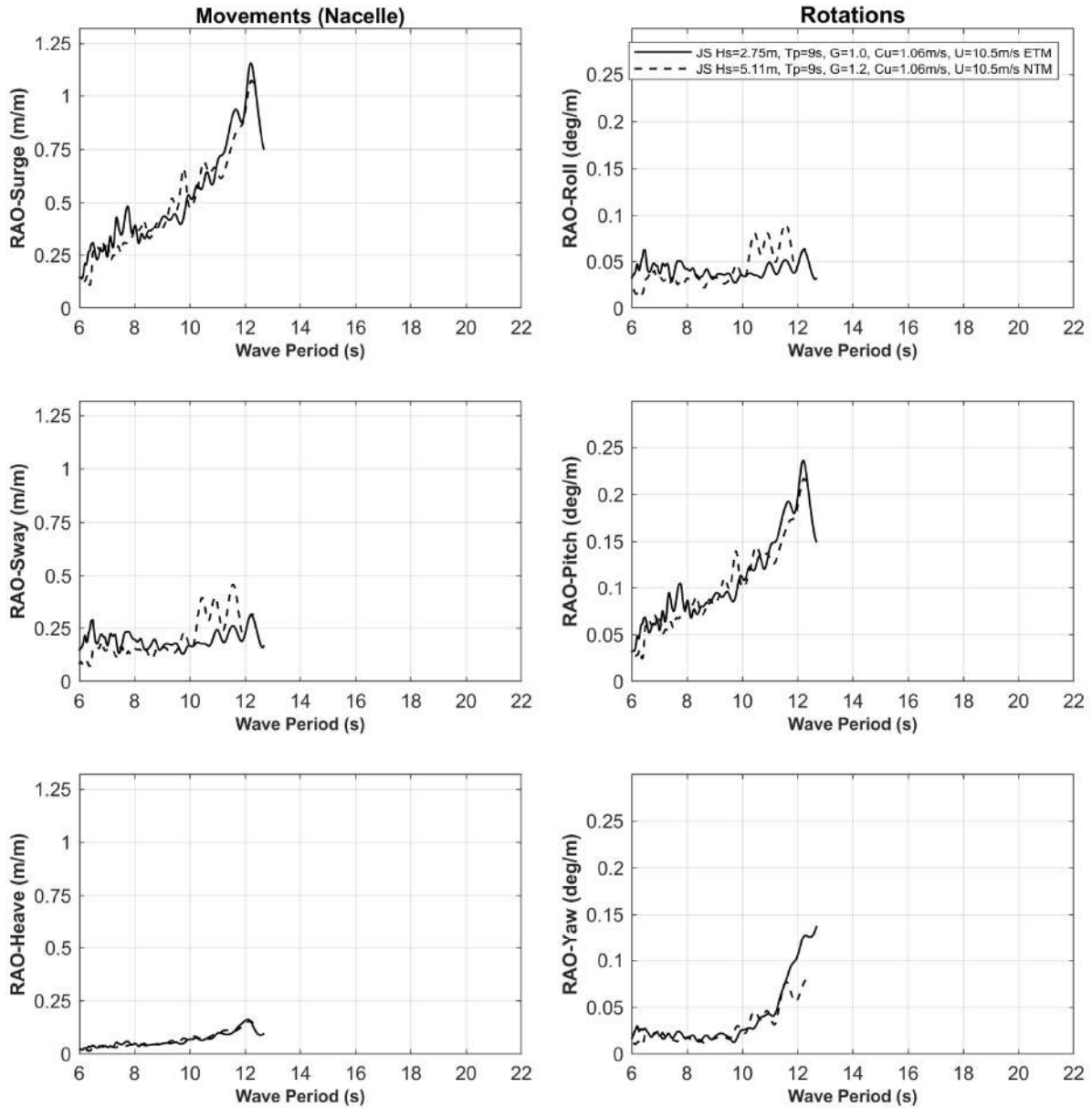


Figure 6-30. Configuration WC2: Combined Irregular Wave and Current and Wind. RAO of motions (Nacelle)

WINDCRETE Configuration WC2: Irregular Wave and Current and Wind - MSL

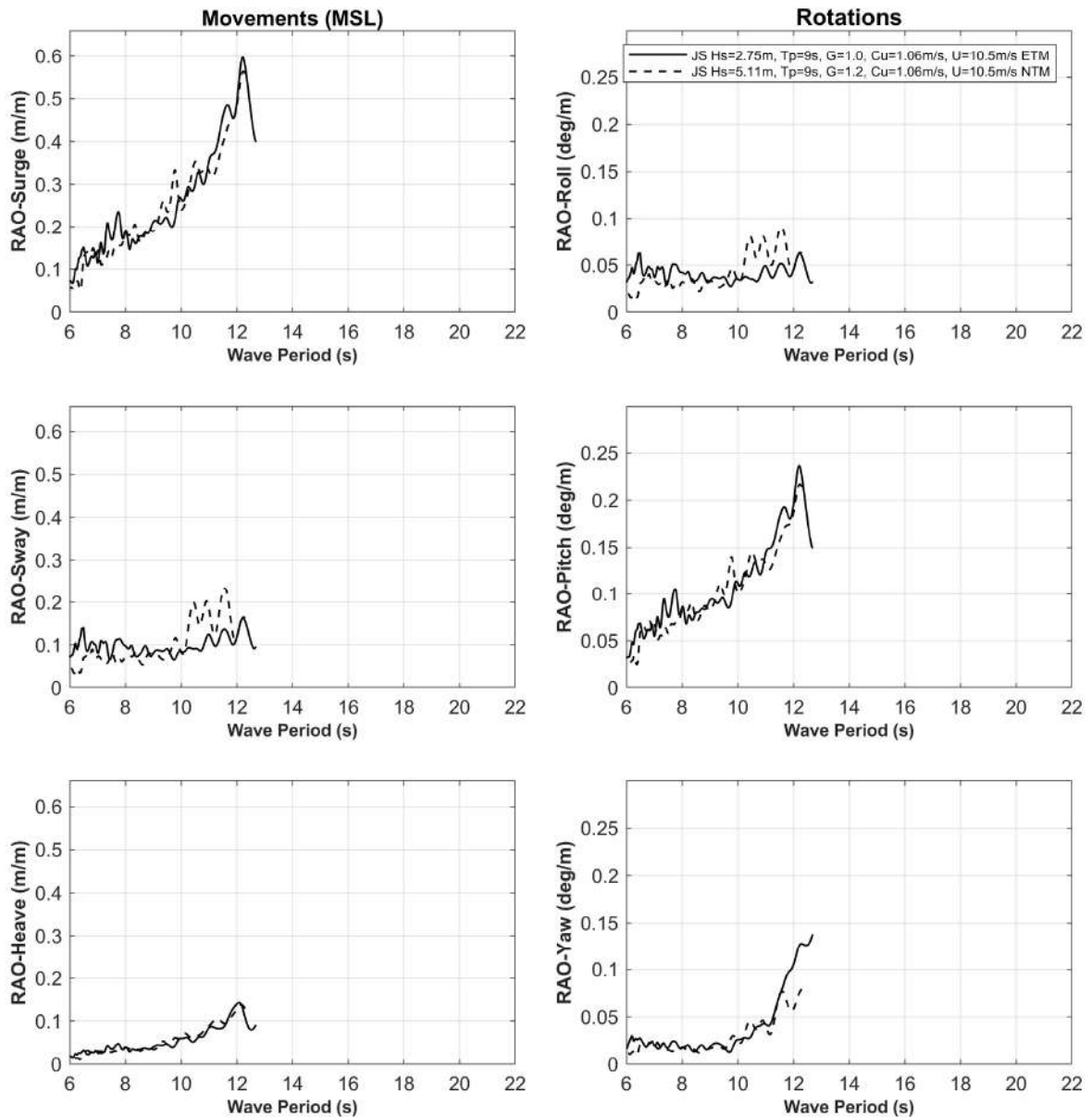


Figure 6-31. Configuration WC2: Combined Irregular Wave and Current and Wind. RAO of motions (MSL)

Table 6-82, Table 6-83 and Table 6-84 contain the information related to the tensions obtained during the execution of the tests. The maximum tension in the main line 1 equal to 816 tonnes is reached in the case of $H_s = 5.11\text{ m}$, $T_p = 9\text{ s}$, $\gamma = 1.2$ with current and rated wind with Normal Turbulence Model.

Configuration WC2 - Irregular Wave + Current + Wind at 0 deg										
#	Test/Laboratory Code	Mooring Line 1 - Load [tonnes]								
		LC1			LC4			LC5		
		mean	max	min	mean	max	min	mean	max	min
59	'FIH18-00014_WC2_JS_H2p75_T9_G1_SN0p143_WDT10p5_TCETM_23Hz_00'	539.79	800.37	379.68	288.38	446.06	204.59	259.10	395.66	182.06
60	'FIH18-00014_WC2_JS_H5p11_T9_G1p2_SN0p143_WDT10p5_TCNTM_23Hz_00'	561.06	815.77	423.74	300.44	447.82	227.43	260.54	385.95	194.61

Table 6-82. Configuration WC2: Combined Irregular Wave and Current and Wind. Mooring system results: Line 1

Configuration WC2 - Irregular Wave + Current + Wind at 0 deg										
#	Test/Laboratory Code	Mooring Line 2 - Load [tonnes]								
		LC2			LC6			LC7		
		mean	max	min	mean	max	min	mean	max	min
59	'FIH18-00014_WC2_JS_H2p75_T9_G1_SNOp143_WDT10p5_TCETM_23Hz_00'	260.60	641.54	110.65	148.31	315.90	74.98	126.96	359.92	54.00
60	'FIH18-00014_WC2_JS_H5p11_T9_G1p2_SNOp143_WDT10p5_TCNTM_23Hz_00'	254.31	557.03	124.57	146.50	275.97	82.49	121.49	301.78	50.63

Table 6-83. Configuration WC2: Combined Irregular Wave and Current and Wind. Mooring system results: Line 2

Configuration WC2 - Irregular Wave + Current + Wind at 0 deg										
#	Test/Laboratory Code	Mooring Line 3 - Load [tonnes]								
		LC3			LC8			LC9		
		mean	max	min	mean	max	min	mean	max	min
59	'FIH18-00014_WC2_JS_H2p75_T9_G1_SNOp143_WDT10p5_TCETM_23Hz_00'	271.44	663.75	123.04	121.86	344.23	44.07	167.63	341.70	83.43
60	'FIH18-00014_WC2_JS_H5p11_T9_G1p2_SNOp143_WDT10p5_TCNTM_23Hz_00'	267.14	633.09	137.12	117.13	323.14	45.73	167.36	329.36	91.26

Table 6-84. Configuration WC2: Combined Irregular Wave and Current and Wind. Mooring system results: Line 3

The accelerations at the nacelle are shown in Table 6-85.

Configuration WC2 - Irregular Wave + Current + Wind at 0 deg										
#	Test/Laboratory Code	Accelerations - Nacelle [m/s ²]								
		Acc. X		Acc. Y		Acc. Z				
		max	min	max	min	max	min			
59	'FIH18-00014_WC2_JS_H2p75_T9_G1_SNOp143_WDT10p5_TCETM_23Hz_00'	0.98	-0.90	0.52	-0.52	0.08	-0.08			
60	'FIH18-00014_WC2_JS_H5p11_T9_G1p2_SNOp143_WDT10p5_TCNTM_23Hz_00'	1.74	-1.48	0.70	-0.65	0.14	-0.15			

Table 6-85. Configuration WC2: Combined Irregular Wave and Current and Wind. Accelerations results in the Nacelle Position

6.1.4 Installation Tests

Configuration WC0: Irregular Wave during Installation

Table 6-86 summarizes the main statistics of the incident sea states considered.

Configuration WC0 - Irregular Wave during Installation									
#	Test/Laboratory Code	h [m]	Hs [m]	Tp [s]	Spectrum	Gamma	Spread	Hinc [m]	Tinc [s]
61	'FIH18-00014_WC0_JS_H2p75_T11_G1_ABS_00'	165	2.75	11	JS	1.0	-	2.74	11.04
62	'FIH18-00014_WC0_JS_H2p75_T14_G1_ABS_00'	165	2.75	14	JS	1.0	-	2.77	14.13

Table 6-86. Configuration WC0: Irregular Wave during Installation. Incident Analysis

The initial position as well as the soft-mooring line pretensions are summarized on the next two tables (see Table 6-87 and Table 6-8). The static position of the CoG of WINDCRETE with no wind turbine and with only 55 kg of the ballast has a Z around -8.35 m because the spar was not stable in yaw in horizontal position, and we have to introduce 28.7 kg extra into the hemisphere (already included in Table 4-7) to stabilize it. The tensions of soft-mooring lines 1 and 4 are not equal to those of lines 2 and 3 because of the resulting extra Roll of 11.25 deg.

Configuration WC0 - Irregular Wave during Installation							
#	Equilibrium Condition	Motions - CoG: Initial Position					
	Test/Laboratory Code	X [m]	Y [m]	Z [m]	roll [deg]	pitch [deg]	yaw [deg]
61	'FIH18-00014_WC0_JS_H2p75_T11_G1_ABS_00'	1.39	0.46	-8.29	-78.73	-2.43	125.05
62	'FIH18-00014_WC0_JS_H2p75_T14_G1_ABS_00'	0.83	1.03	-8.41	-78.77	-2.38	-179.91

Table 6-87. Configuration WC0: Irregular Wave during Installation. Motions initial positions

Configuration WC0 - Irregular Wave during Installation					
#	Equilibrium Condition	Mooring Lines - Pretension [tonnes]			
	Test/Laboratory Code	LC1	LC2	LC3	LC4
61	'FIH18-00014_WC0_JS_H2p75_T11_G1_ABS_00'	17.07	19.50	19.39	17.40
62	'FIH18-00014_WC0_JS_H2p75_T14_G1_ABS_00'	17.08	19.16	19.18	17.28

Table 6-88. Configuration WC0: Irregular Wave during Installation. Mooring system pretensions

Figure 6-32 shows this initial position of the platform in the wave basin for Installation tests.

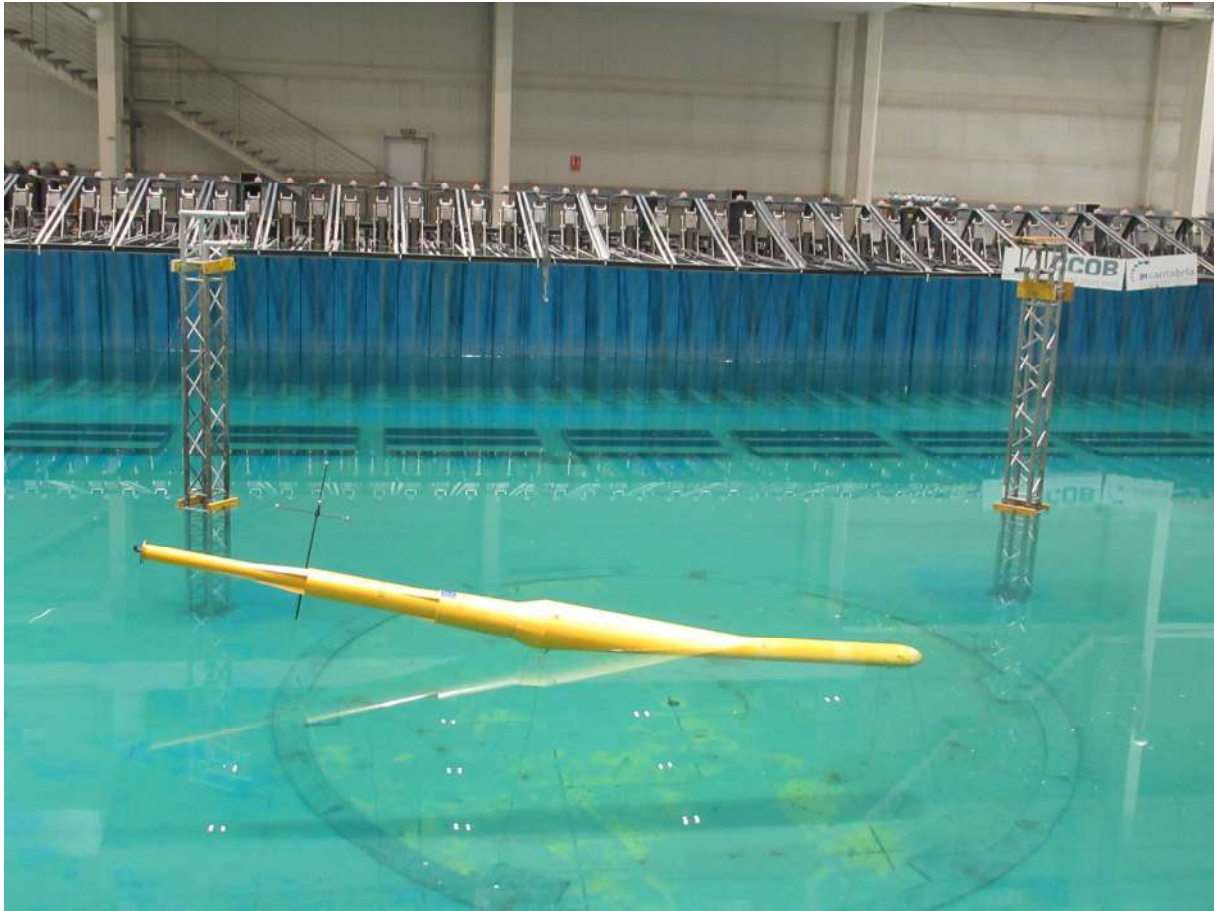


Figure 6-32. Initial position for Installation tests

Table 6-89 and Table 6-90 show mean, maximum and minimum values of motions related to the CoG position.

Configuration WC0 - Irregular Wave during Installation										
#	Test/Laboratory Code	Motions - CoG: Position								
		X [m]			Y [m]			Z [m]		
		mean	max	min	mean	max	min	mean	max	min
61	'FIH18-00014_WCO_JS_H2p75_T11_G1_ABS_00'	6.71	13.98	0.89	2.27	6.66	-0.77	-8.34	-6.64	-10.15
62	'FIH18-00014_WCO_JS_H2p75_T14_G1_ABS_00'	4.01	8.60	-0.40	1.48	3.49	-1.21	-8.34	-6.23	-10.40

Table 6-89. Configuration WC0: Irregular Wave during Installation. Displacements results in the CoG Position

Configuration WC0 - Irregular Wave during Installation										
#	Test/Laboratory Code	Motions - CoG: Position								
		roll [deg]			pitch [deg]			yaw [deg]		
		mean	max	min	mean	max	min	mean	max	min
61	'FIH18-00014_WCO_JS_H2p75_T11_G1_ABS_00'	-78.69	-77.42	-79.62	-3.32	-0.95	-6.62	-175.45	-167.97	-180.00
62	'FIH18-00014_WCO_JS_H2p75_T14_G1_ABS_00'	-78.76	-77.66	-79.71	-2.90	-1.52	-5.10	-175.51	-172.56	-180.00

Table 6-90. Configuration WC0: Irregular Wave during Installation. Rotations results in the CoG Position

Table 6-13 indicates the tensions obtained during the tests carried out. The maximum tensions are reached in soft-mooring line 2 because it is the one on the upstream side anchored to the lighter part of the platform.

Configuration WC0 - Irregular Wave during Installation					
#	Test/Laboratory Code	Mooring Lines - Load [tonnes]			
		LC1	LC2	LC3	LC4

		mean	max	min									
61	'FIH18-00014_WCO_JS_H2p75_T11_G1_ABS_00'	17.47	27.70	10.83	23.75	34.30	16.36	16.18	26.65	10.32	16.55	23.17	11.09
62	'FIH18-00014_WCO_JS_H2p75_T14_G1_ABS_00'	17.09	27.15	10.68	21.88	30.01	15.13	17.09	27.20	11.74	17.10	27.08	11.72

Table 6-91. Configuration WCO: Irregular Wave during Installation. Mooring system results

Configuration WCO: Raising up (Up-ending)

Two tests of the WINDCRETE with soft mooring are conducted during its erection from horizontal to vertical position. The first one #63 is executed without any external loads. The second one is carried out while the platform is hit by irregular waves defined by a limited white noise spectrum between the periods of 7.5 and 22 seconds, whose wave spectrum characteristics are presented in Table 6-92.

Configuration WCO - White Noise during Raising up						
#	Test/Laboratory Code	h [m]	Hs [m]	T1 [s]	T2 [s]	Hinc [m]
64	'FIH18-00014_WCO_TH_H2p75_T11p19_DF0p088_ABS_izado_00'	165	2.75	7.5	22	2.81

Table 6-92. Configuration WCO during Raising up: White Noise

The initial position as well as the soft-mooring line pretensions are summarized on the next two tables (see Table 6-93 and Table 6-94). The static position of the CoG of WINDCRETE with no wind turbine and with only 55 kg of the ballast and 28.7 kg extra introduced into the hemisphere (already included in Table 4-7) has an $X < 0$ in case #63 because there are no soft-mooring lines on the downstream side anymore. However, in case #64 the static position of the CoG has an $X > 0$ because the white noise is already acting on the platform. For the same reason, the soft-mooring lines in case #64 are higher. In both cases, the tensions of soft-mooring line 1 are not equal to those of line 2 because of the resulting extra Roll. This resulting extra roll is lower in case #64 because the initial ballast has 5 litres less of still water.

Configuration WCO - Raising up							
#	Equilibrium Condition	Motions - CoG: Initial Position					
	Test/Laboratory Code	X [m]	Y [m]	Z [m]	roll [deg]	pitch [deg]	yaw [deg]
63	'FIH18-00014_WCO_izado_00'	-57.46	2.72	-9.28	-78.37	-3.61	93.90
64	'FIH18-00014_WCO_TH_H2p75_T11p19_DF0p088_ABS_izado_00'	6.73	-1.90	-5.97	-82.22	-2.91	91.41

Table 6-93. Configuration WCO: Raising up. Motions initial positions

Configuration WCO - Raising up			
#	Equilibrium Condition	Mooring Lines - Pretension [tonnes]	
	Test/Laboratory Code	LC1	LC2
63	'FIH18-00014_WCO_izado_00'	6.23	7.88
64	'FIH18-00014_WCO_TH_H2p75_T11p19_DF0p088_ABS_izado_00'	16.58	18.00

Table 6-94. Configuration WCO: Raising up. Mooring system pretensions

Figure 6-33 shows this initial and the final positions of the platform in the wave basin for Raising up tests.

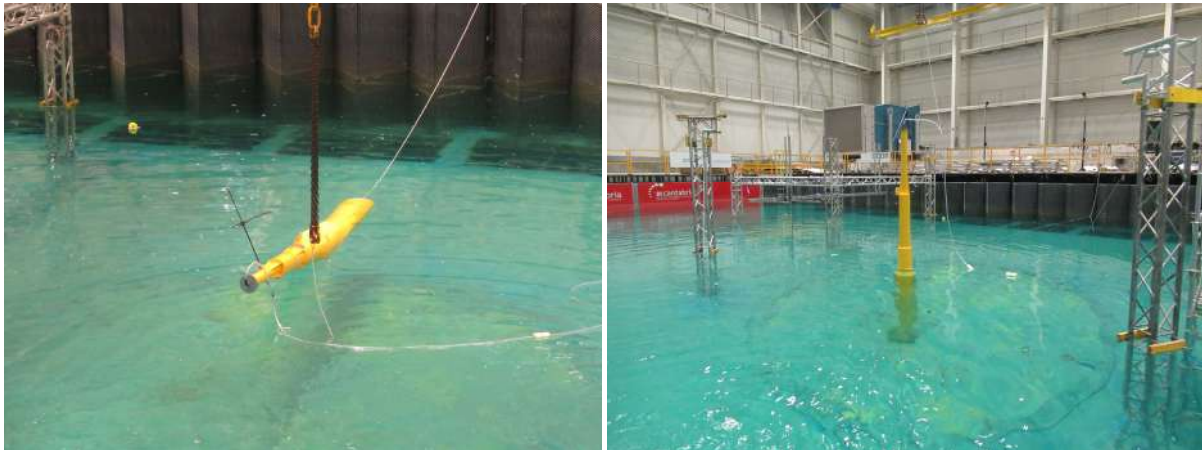


Figure 6-33. Initial position (left) and final position (right) for Raising up tests

Figure 6-34 and Figure 6-35 shows Heave motion and Roll rotation in Raising up tests while increasing the weight of the ballast with still water with a flow of 4.6 litres/min. As can be seen, the Roll rotation from the initial to the final values is very quick, above all between -70 and -20 degrees. Most of the time of filling up the ballast takes place with the WINDCRETE platform already raised.

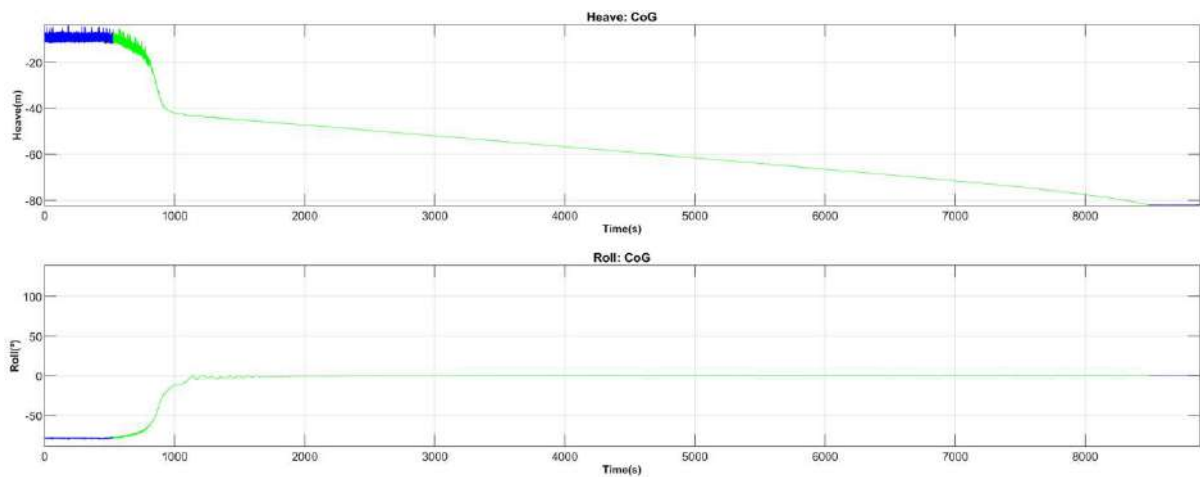


Figure 6-34. Heave motion and Roll rotation in Raising up test without any external loads

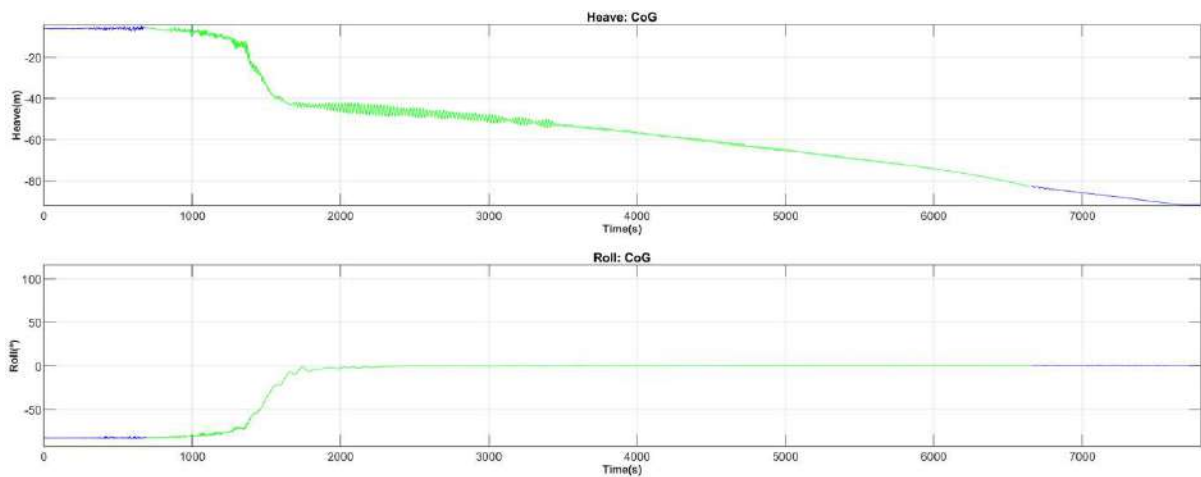


Figure 6-35. Heave motion and Roll rotation in White Noise test during Raising up

Table 6-95 and Table 6-96 show mean, maximum and minimum values of motions related to the CoG position. The raising up is conducted on Roll rotation.

Configuration WC0 - Raising up										
#	Test/Laboratory Code	Motions - CoG: Position								
		X [m]			Y [m]			Z [m]		
		mean	max	min	mean	max	min	mean	max	min
63	'FIH18-00014_WCO_izado_00'	-131.00	-53.50	-142.31	-0.83	10.48	-11.68	-58.29	-5.54	-81.46
64	'FIH18-00014_WCO_TH_H2p75_T11p19_DF0p088_ABS_izado_00'	-129.96	-14.78	-156.65	-2.52	17.20	-20.02	-52.39	-5.23	-82.52

Table 6-95. Configuration WC0: Raising up. Displacements results in the CoG Position

Configuration WC0 - Raising up										
#	Test/Laboratory Code	Motions - CoG: Position								
		roll [deg]			pitch [deg]			yaw [deg]		
		mean	max	min	mean	max	min	mean	max	min
63	'FIH18-00014_WCO_izado_00'	-3.46	0.72	-78.73	-0.61	3.15	-9.21	110.16	126.59	67.10
64	'FIH18-00014_WCO_TH_H2p75_T11p19_DF0p088_ABS_izado_00'	-10.65	1.27	-82.47	-0.85	2.52	-11.28	85.35	104.95	51.56

Table 6-96. Configuration WC0: Raising up. Rotations results in the CoG Position

Table 6-97 indicates the tensions obtained during the tests carried out.

Configuration WC0 - Raising up							
#	Test/Laboratory Code	Mooring Lines - Load [tonnes]					
		LC1			LC2		
		mean	max	min	mean	max	min
63	'FIH18-00014_WCO_izado_00'	7.72	24.26	5.71	7.21	16.74	5.51
64	'FIH18-00014_WCO_TH_H2p75_T11p19_DF0p088_ABS_izado_00'	6.35	21.23	3.24	7.14	21.35	4.70

Table 6-97. Configuration WC0: Raising up. Mooring system results

6.2 ACTIVEFLOAT semisub-based wind concept

As aforementioned, the test set-ups or configurations tested are the followings:

- **Configuration AF0:** Free floating ACTIVEFLOAT without ballast for installation tests.
- **Configuration AF1:** Free floating ACTIVEFLOAT.
- **Configuration AF2:** Moored ACTIVEFLOAT with wave loads at 0°.
- **Configuration AF3:** Moored ACTIVEFLOAT with environmental loads aligned at 0°.

6.2.1 Wave calibration

To correctly reproduce the target sea-state conditions during the seakeeping tests, regular waves (Table 6-98), irregular waves (Table 6-99), white noise (Table 6-100), current (Table 6-101) and irregular waves with current (Table 6-102) were previously calibrated in absence of the model in the flume. From the surface measurements, the incident wave was obtained using WaveLab 3 software from Aalborg University and presented for the control and the calibration arrays. The calibration array is used only during this wave calibration phase; and the control array provides a reference to verify the validity of the generated sea-state conditions during the seakeeping tests.

Calibration: Regular Wave					
Test/Laboratory Code	h [m]	H [m]	T [s]	Calibration Array	
				Hinc [m]	Tinc [s]
'FIH18-00014_CAL_RW_H2p75_T7p5_ABS_03'	120	2.75	7.5	2.74	7.48
'FIH18-00014_CAL_RW_H2p75_T9_ABS_04'	120	2.75	9	2.63	8.82
'FIH18-00014_CAL_RW_H2p75_T11_ABS_02'	120	2.7	11	2.65	11.00
'FIH18-00014_CAL_RW_H2p75_T14_ABS_03'	120	2.75	14	2.73	14.00
'FIH18-00014_CAL_RW_H2p75_T17_ABS_03'	120	2.75	17	2.77	16.99
'FIH18-00014_CAL_RW_H2p75_T20_ABS_01'	120	2.75	20	2.75	19.90
'FIH18-00014_CAL_RW_H5p11_T7p5_ABS_04'	120	5.11	7.5	5.02	7.49
'FIH18-00014_CAL_RW_H5p11_T9_ABS_02'	120	5.11	9	5.03	8.92
'FIH18-00014_CAL_RW_H5p11_T11_ABS_02'	120	5.11	11	5.30	11.00
'FIH18-00014_CAL_RW_H5p11_T14_ABS_02'	120	5.11	14	4.88	14.00
'FIH18-00014_CAL_RW_H5p11_T17_ABS_02'	120	5.11	17	5.06	17.00
'FIH18-00014_CAL_RW_H5p11_T20_ABS_02'	120	5.11	20	5.11	20.00

Table 6-98. Calibration: Regular Wave. Incident Analysis

Calibration: Irregular Wave								
Test/Laboratory Code	h [m]	Hs [m]	Tp [s]	Spectrum	Gamma	Spread	Calibration Array	
							Hinc [m]	Tinc [s]
'FIH18-00014_CAL_JS_H2p75_T9_G3p3_ABS_00'	120	2.75	9	'JS'	3.3	-	2.74	8.93
'FIH18-00014_CAL_JS_H2p75_T11_G3p3_ABS_00'	120	2.75	11	'JS'	3.3	-	2.77	11.02
'FIH18-00014_CAL_JS_H2p75_T14_G3p3_ABS_01'	120	2.75	14	'JS'	3.3	-	2.80	14.00
'FIH18-00014_CAL_JS_H5p11_T9_G1p2_ABS_01'	120	5.11	9	'JS'	1.2	-	5.04	8.22
'FIH18-00014_CAL_JS_H5p11_T11_G1p2_ABS_01'	120	5.11	11	'JS'	1.2	-	5.04	10.57
'FIH18-00014_CAL_JS_H2p75_T9_G3p3_S6_ABS_00'	120	2.75	9	'JS'	3.3	6	2.80	9.04
'FIH18-00014_CAL_JS_H2p75_T9_G3p3_S12_ABS_00'	120	2.75	9	'JS'	3.3	12	2.68	8.63
'FIH18-00014_CAL_JS_H5p11_T11_G1p2_S6_ABS_02'	120	5.11	11	'JS'	1.2	6	5.26	11.10
'FIH18-00014_CAL_JS_H5p11_T11_G1p2_S12_ABS_01'	120	5.1	11	'JS'	1.2	12	5.09	11.43

Table 6-99. Calibration: Irregular Wave. Incident Analysis

Calibration: White Noise					
Test/Laboratory Code	h [m]	Hs [m]	T1 [s]	T2 [s]	Calibration Array
					Hinc [m]
'FIH18-00014_CAL_TH_H2p75_T11p19_DF0p088_ABS_01'	120	2.75	7.5	22	2.68
'FIH18-00014_CAL_TH_H5p11_T11p19_DF0p088_ABS_02'	120	5.11	7.5	22	5.13

Table 6-100. Calibration: White Noise. Incident Analysis

Calibration: Current			
Test/Laboratory Code	h [m]	Current [m/s]	Calibration Array
			Current [m/s]
'FIH18-00014_CAL_SN0p168_26Hz_00'	120	1.06	1.05

Table 6-101. Calibration: Current

Calibration: Irregular Wave + Current									
Test/Laboratory Code	h [m]	Hs [m]	Tp [s]	Spectrum	Gamma	Current [m/s]	Calibration Array		
							Hinc [m]	Current [m/s]	
'FIH18-00014_CAL_JS_H2p75_T9_G1_SN0p168_26Hz_00'	120	2.75	9	'JS'	1.0	1.06	2.76	1.10	
'FIH18-00014_CAL_JS_H5p11_T9_G1p2_SN0p168_26Hz_00'	120	2.75	9	'JS'	3.2	1.06	5.28	1.03	

Table 6-102. Calibration: Irregular Wave with Current. Incident Analysis

6.2.2 Characterization Tests Results

Tilt tests

The tilt tests are executed in three repetitions for both pitch and roll rotations in free-floating condition (Configuration AF1). The inclination tests in negative Pitch are performed by applying a weight on the windward floater, such that its eccentricity with respect to the platform applies a moment in the pitch (Figure 6-36 on the left). These tests are conducted without mooring system and clump weights are not added at the fairleads, thus the expected draft is 25.75 m (instead of 26.5 m). The resulting GM is draw in Figure 6-37.

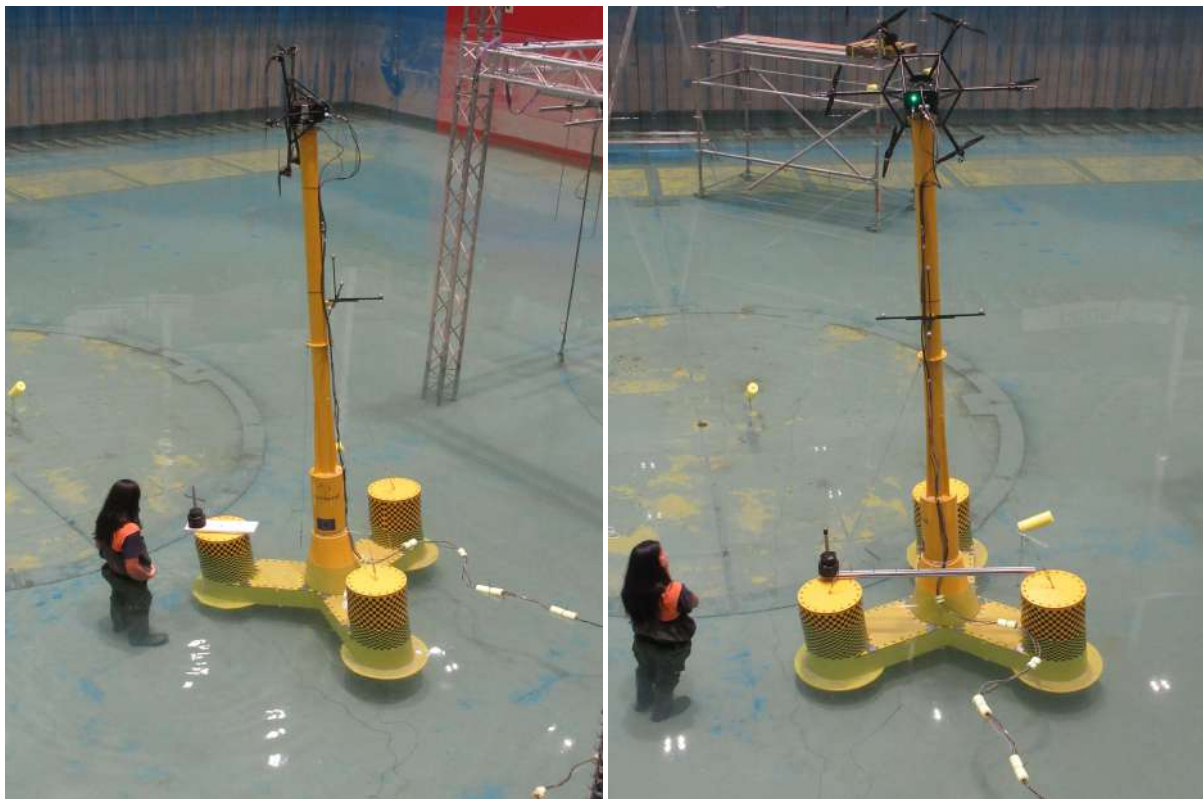


Figure 6-36. Inclination tests in negative Pitch (left) and in positive Roll (right)

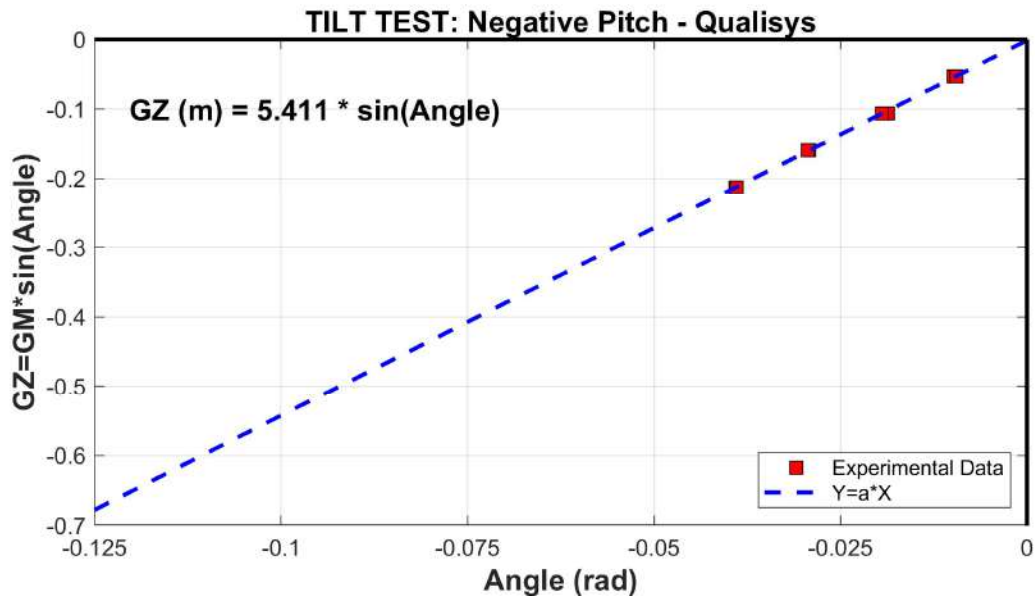


Figure 6-37. Inclination test analysis in negative Pitch

The inclination tests in positive Roll are performed by applying a weight on one of the leeward floaters, such that its eccentricity with respect to the platform applies a moment in the roll (Figure 6-36 on the right). These tests are conducted without mooring system and clump weights are not added at the fairleads, thus the expected draft is 25.75 m (instead of 26.5 m). The resulting GM is draw in Figure 6-38.

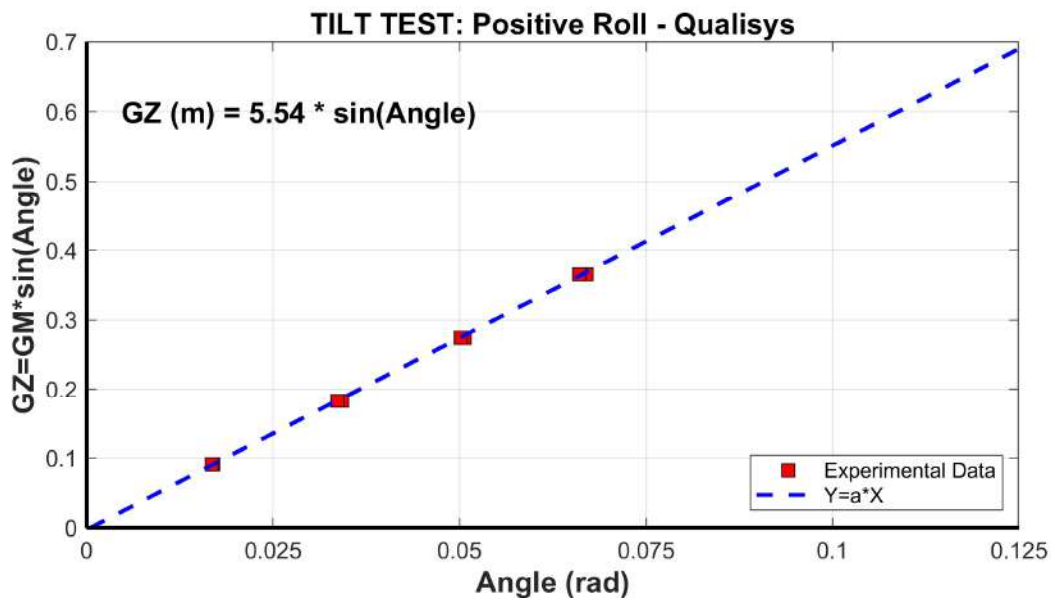


Figure 6-38. Inclination test analysis in positive Roll

In order to consider the influence of the added weights used to force the tilt over the output of the tests, the GM distance obtained during the tilt tests is corrected considering the mass of the added weight. Table 6-103 reports the corrected GM values.

GM corrected values	
DOF	GM [m]
<i>Pitch</i>	5.596
<i>Roll</i>	5.901

Table 6-103 GM corrected value

The corrected GM target is 6.07 m, hence the deviation with respect to this value is -2.80%.

Decay tests

The decays tests are executed with the platform in free floating (Configuration AF1) and moored (Configuration AF2 without wind and Configuration AF3 with rated wind) conditions. For this platform, when executed in free floating condition, clump weights are not added at the fairleads and the expected draft is 25.75 m (instead of 26.5 m). Table 6-6 summarizes the tests conducted.

Tests	Mooring	Tested DoF	Repetitions
Decay Tests	Free Floating	Heave, Roll, Pitch	5
	Moored	Surge, Sway, Heave, Roll, Pitch, Yaw	5
		Surge with rated wind, Pitch with rated wind	5

Table 6-104. Decay Tests executed

Each test is repeated five times to ensure the statistical representativeness of the results. Therefore, the results shown in the following tables are the mean values of the trials performed for each DoF. Figure 6-1 shows a picture of the decay test procedure. The average values of the natural period and the non-dimensional damping coefficient for each cycle [15], are shown on the top. Assuming the damping is linear and so the logarithmic decrement is constant, the non-dimensional damping coefficient may also be calculated by linear regression (on the left).

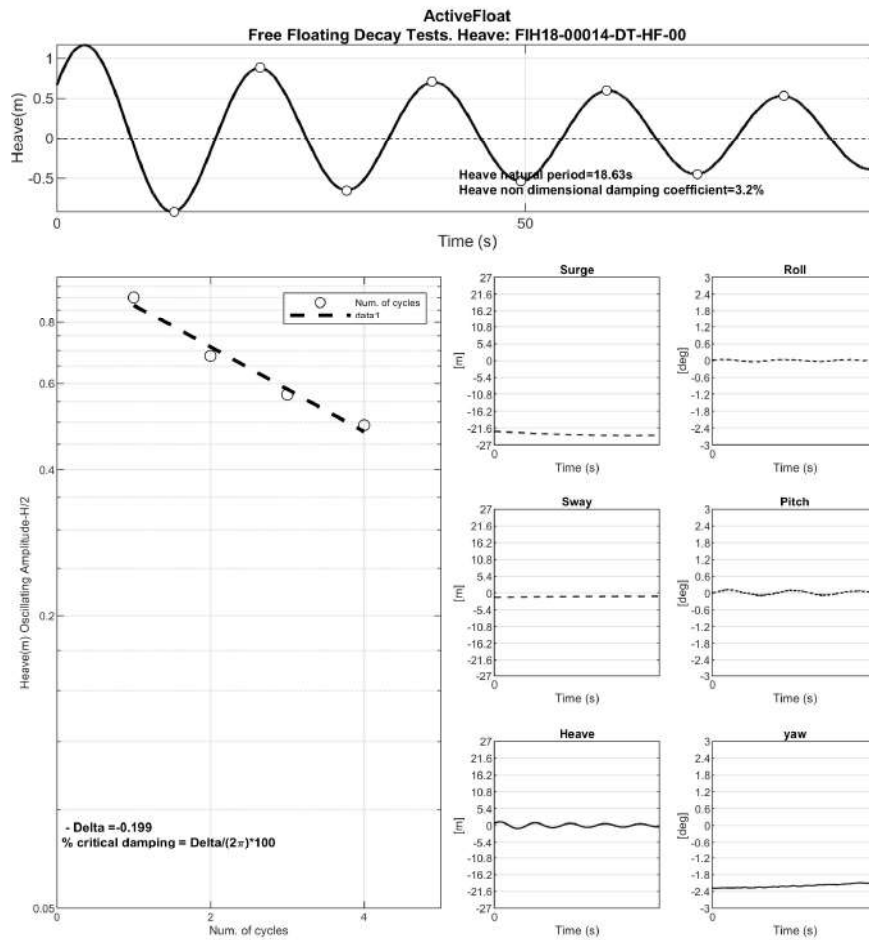


Figure 6-39. Example of a free-floating decay test analysis (Heave)

The decay tests results are shown in Table 6-7. The average non-dimensional linear damping presented in the tables is related to critical damping of the specific DoF.

	DOF	Damping [%]	Measured Natural Period [s]	Target Natural Period [s]	Deviation [s]
Free-floating Decay Tests	Heave	3.99	18.55		
	Roll	3.83	32.98		
	Pitch	3.55	32.97		
Moored Decay Tests	Surge	6.34	227.80	299.40	-71.6
	Sway	10.05	260.72		
	Heave	4.29	18.61	18.28	0.33
	Roll	3.49	32.59		
	Pitch	3.43	32.50	30.60	1.90
	Yaw	4.43	166.84	187.27	-20.43
	Pitch with rated wind	5.95	101.36		
Pitch with rated wind	20.16	41.40			

Table 6-105. Natural periods and Damping coefficients obtained during the decay tests

Static Offset Tests

The static offset tests are performed to assess the stiffness of the mooring system in Configuration AF2. Those tests are executed in positive and negative surge directions.

Figure 6-40 shows the relation between the platform surge and the force applied for achieving those displacements during the three repetitions executed pulling the platform at 0° in the positive surge direction. The static tension effect of the mooring line is clearly shown in the beginning of the first repetition, where the tensions are higher. Initially for the first 10-15 meters, the section of mooring line 1 lying on the seabed is not slipping as the fairlead moves because the static friction is holding the line.

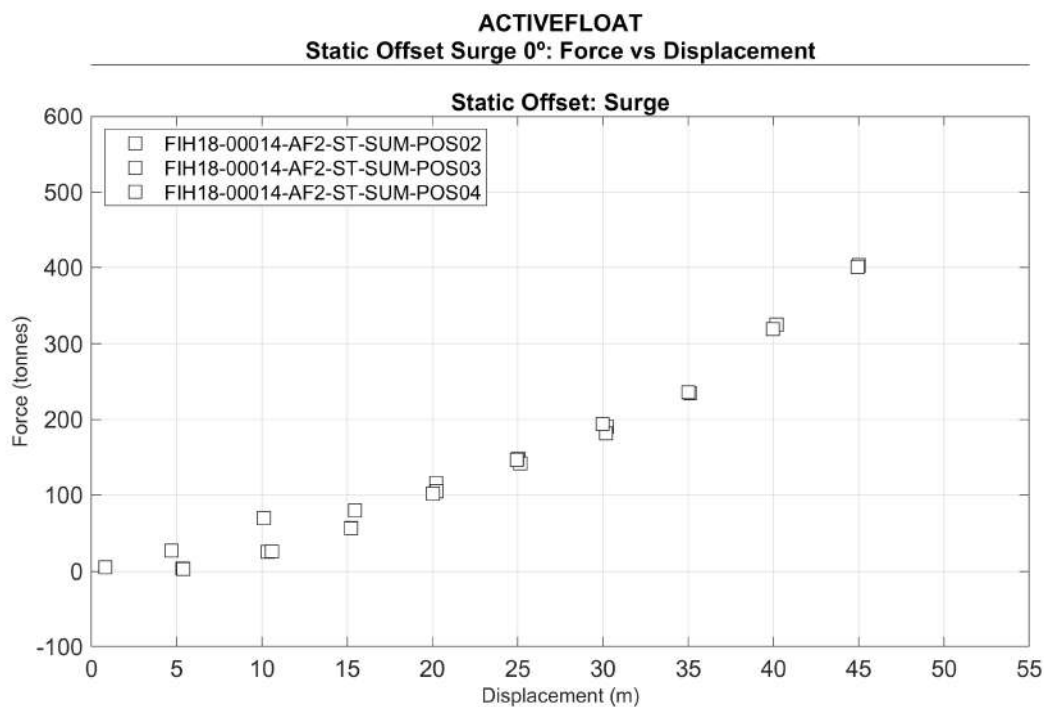


Figure 6-40. Applied force vs platform displacements in surge (0°)

Figure 6-41 presents the relation between the platform surge and mooring forces in the same set of trials. The results of the truncated main line 1 are compared to those from numerically obtained drawn in red circles.

ACTIVEFLOAT
Static Offset Surge 0°: Force vs Displacement

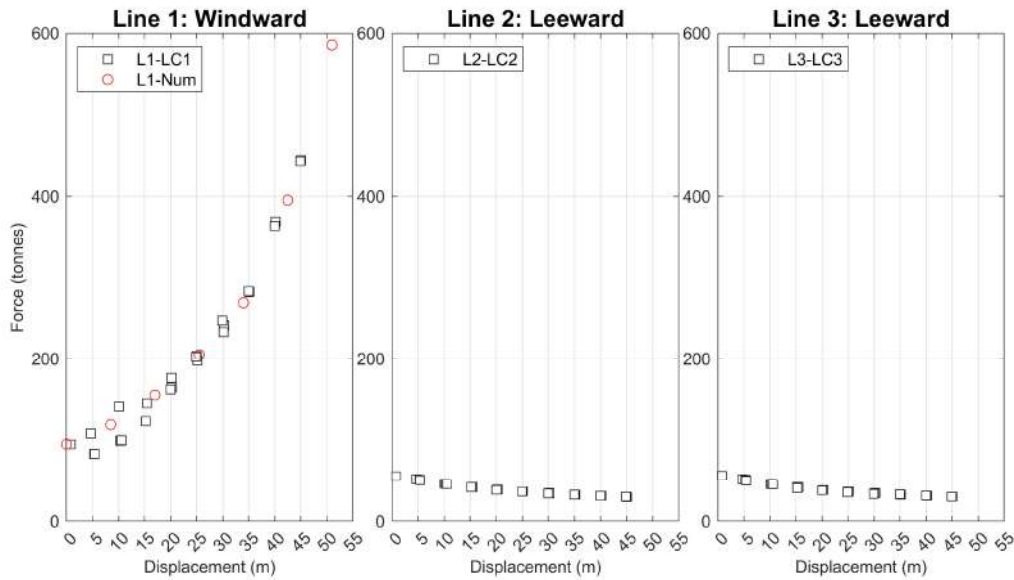


Figure 6-41. Mooring forces vs platform displacements in surge (0°)

Figure 6-42 shows the relation between the platform surge and the force applied for achieving those displacements during the three repetitions executed pulling the platform at 0° in the positive negative direction.

ACTIVEFLOAT
Static Offset Surge 180°: Force vs Displacement

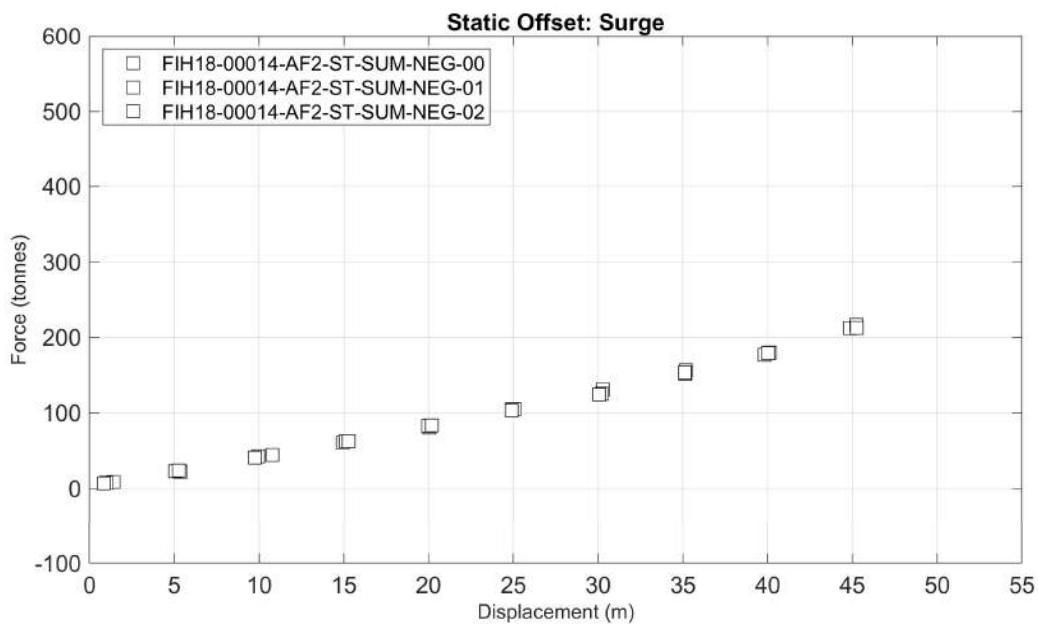


Figure 6-42. Applied force vs platform displacements in surge (0°)

Figure 6-43 presents the relation between the platform surge and mooring forces in the same set of trials. The results of the truncated main line 1 are compared to those from numerically obtained drawn in red circles.

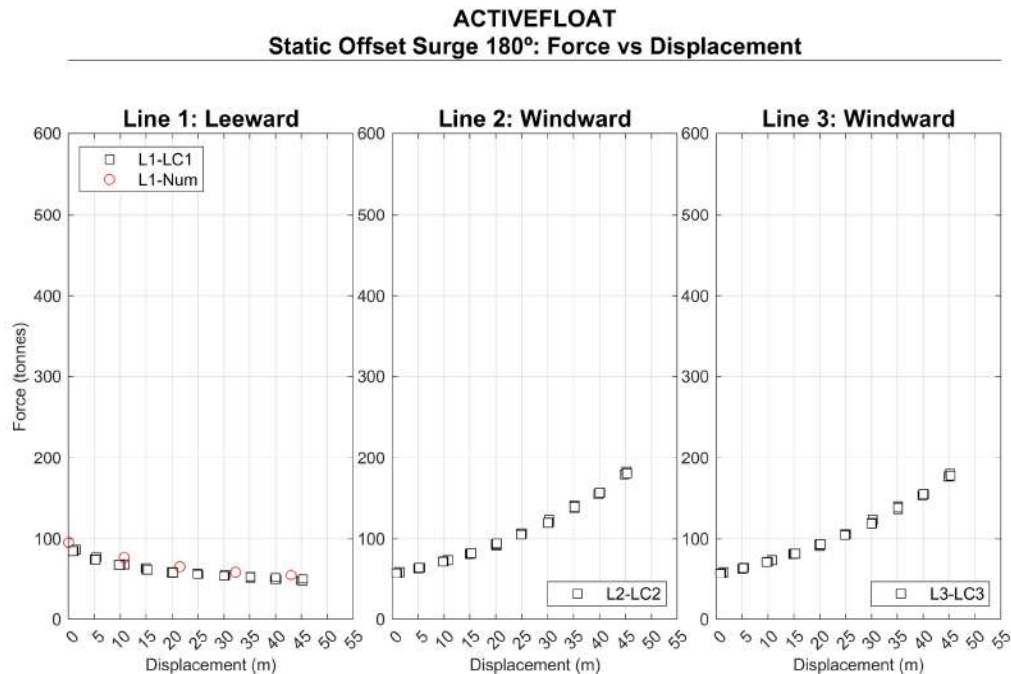


Figure 6-43. Mooring forces vs platform displacements in surge (180°)

6.2.3 Seakeeping tests results

To show a preliminary understanding of the system behaviour and its dynamics, the present section provides a summary of the variables recorded during the tests execution. The tables on the following pages report the motions and accelerations of the platform and mooring system loads for the wave, current and wind tests, in case of application of singular and coupled environmental conditions.

This information provides an understanding of seakeeping of the ACTIVEFLOAT floating wind turbine. The next sections include a selection of statistical results obtained from the measurements recorded during the tests, as well as some examples of graphics built based on the post processing analysis.

The presented data is summarized in the following list:

- Incident Wave characteristics, which are included in the first table defined by their wave height and period (Regular Wave) or by their significant height, peak period and spectral definition (Irregular Wave).
- Mean incident current.
- To ease the interpretation of the tank testing results, the static condition data shows the initial value of each measured parameter. Such data is defined as the average of the measured parameters calculated over a period where the model is not subjected to environmental loads.
- Mean, maximum and minimum values of motions, which are obtained for CoG, for the Nacelle and for the MSL.
- Mean and dynamic maximum and minimum mooring loads.
- Mean, maximum and minimum nacelle accelerations.

- Mean calculated rotor thrust.
- Spectral RAOs obtained through Regular Wave, Irregular Wave and White Noise tests.

Configuration AF2 - Regular Wave at 0 deg

Table 6-106 summarizes the main characteristics of the incident sea states considered.

Configuration AF2 - Regular Wave at 0 deg						
#	Test/Laboratory Code	h [m]	H [m]	T [s]	Hinc [m]	Tinc [s]
80	'FIH18-00014_AF2_RW_H2p75_T7p5_ABS_00'	120	2.75	7.5	2.74	7.48
81	'FIH18-00014_AF2_RW_H2p75_T9_ABS_00'	120	2.75	9	2.63	8.82
82	'FIH18-00014_AF2_RW_H2p75_T11_ABS_01'	120	2.75	11	2.65	11.00
83	'FIH18-00014_AF2_RW_H2p75_T14_ABS_00'	120	2.75	14	2.73	14.00
84	'FIH18-00014_AF2_RW_H2p75_T17_ABS_00'	120	2.75	17	2.77	16.99
85	'FIH18-00014_AF2_RW_H2p75_T20_ABS_00'	120	2.75	20	2.75	19.90
86	'FIH18-00014_AF2_RW_H5p11_T7p5_ABS_00'	120	5.11	7.5	5.02	7.49
87	'FIH18-00014_AF2_RW_H5p11_T9_ABS_00'	120	5.11	9	5.03	8.92
88	'FIH18-00014_AF2_RW_H5p11_T11_ABS_00'	120	5.11	11	5.30	11.00
89	'FIH18-00014_AF2_RW_H5p11_T14_ABS_00'	120	5.11	14	4.88	14.00
90	'FIH18-00014_AF2_RW_H5p11_T17_ABS_00'	120	5.11	17	5.06	17.00
91	'FIH18-00014_AF2_RW_H5p11_T20_ABS_00'	120	5.11	20	5.11	20.00

Table 6-106. Configuration AF2: Regular Wave. Incident Analysis

Next, on Table 6-107 a summary of the initial position of the FOWT. Moreover, on Table 6-108 the pretensions registered are also shown. As aforementioned, the static position of ACTIVEFLOAT CoG has a positive X due to the static friction, and a Z around 0.5 m because of the actual lower draft. The tension in mooring line 1 is higher than the tensions in mooring lines 2 and 3, as shown in Figure 6-41 and Figure 6-43.

Configuration AF2 - Regular Wave at 0 deg													
#	Equilibrium Condition	Motions - CoG: Initial Position						Motions - Nacelle: Initial Position			Motions - MSL: Initial Position		
	Test/Laboratory Code	X [m]	Y [m]	Z [m]	roll [deg]	pitch [deg]	yaw [deg]	X [m]	Y [m]	Z [m]	X [m]	Y [m]	Z [m]
80	'FIH18-00014_AF2_RW_H2p75_T7p5_ABS_00'	2.50	0.08	0.51	0.15	-0.46	0.40	1.33	-0.32	0.50	2.41	0.05	0.51
81	'FIH18-00014_AF2_RW_H2p75_T9_ABS_00'	1.93	0.03	0.54	0.16	-0.45	0.28	0.79	-0.37	0.53	1.84	0.00	0.54
82	'FIH18-00014_AF2_RW_H2p75_T11_ABS_01'	2.43	0.07	0.51	0.15	-0.46	0.38	1.26	-0.32	0.50	2.34	0.04	0.51
83	'FIH18-00014_AF2_RW_H2p75_T14_ABS_00'	2.35	-0.18	0.51	0.14	-0.45	0.37	1.21	-0.54	0.50	2.27	-0.21	0.51
84	'FIH18-00014_AF2_RW_H2p75_T17_ABS_00'	2.37	-0.22	0.48	0.15	-0.46	0.38	1.21	-0.60	0.47	2.28	-0.24	0.48
85	'FIH18-00014_AF2_RW_H2p75_T20_ABS_00'	2.64	0.10	0.46	0.14	-0.48	0.40	1.43	-0.28	0.46	2.55	0.07	0.46
86	'FIH18-00014_AF2_RW_H5p11_T7p5_ABS_00'	1.60	0.03	0.53	0.15	-0.45	0.23	0.46	-0.37	0.53	1.51	0.00	0.53
87	'FIH18-00014_AF2_RW_H5p11_T9_ABS_00'	1.93	0.07	0.54	0.15	-0.44	0.31	0.82	-0.32	0.53	1.84	0.04	0.54
88	'FIH18-00014_AF2_RW_H5p11_T11_ABS_00'	2.57	0.07	0.50	0.15	-0.47	0.38	1.37	-0.32	0.50	2.48	0.04	0.50
89	'FIH18-00014_AF2_RW_H5p11_T14_ABS_00'	1.82	-0.27	0.57	0.16	-0.43	0.29	0.72	-0.69	0.56	1.74	-0.30	0.57
90	'FIH18-00014_AF2_RW_H5p11_T17_ABS_00'	1.74	-0.22	0.56	0.16	-0.43	0.30	0.64	-0.63	0.55	1.65	-0.25	0.56
91	'FIH18-00014_AF2_RW_H5p11_T20_ABS_00'	1.87	-0.17	0.55	0.15	-0.44	0.31	0.75	-0.57	0.54	1.79	-0.19	0.55

Table 6-107. Configuration AF2: Regular Wave. Motions initial positions

Configuration AF2 - Regular Wave at 0 deg				
#	Equilibrium Condition	Mooring Lines - Pretension [tonnes]		
	Test/Laboratory Code	LC1	LC2	LC3
80	'FIH18-00014_AF2_RW_H2p75_T7p5_ABS_00'	90.77	54.73	53.95
81	'FIH18-00014_AF2_RW_H2p75_T9_ABS_00'	92.50	54.95	55.63
82	'FIH18-00014_AF2_RW_H2p75_T11_ABS_01'	90.74	54.64	53.88
83	'FIH18-00014_AF2_RW_H2p75_T14_ABS_00'	90.38	54.36	53.59
84	'FIH18-00014_AF2_RW_H2p75_T17_ABS_00'	90.71	54.23	53.59
85	'FIH18-00014_AF2_RW_H2p75_T20_ABS_00'	91.16	54.56	53.71
86	'FIH18-00014_AF2_RW_H5p11_T7p5_ABS_00'	91.72	54.41	54.87
87	'FIH18-00014_AF2_RW_H5p11_T9_ABS_00'	92.37	55.03	55.50
88	'FIH18-00014_AF2_RW_H5p11_T11_ABS_00'	90.82	54.53	53.74
89	'FIH18-00014_AF2_RW_H5p11_T14_ABS_00'	92.32	54.47	55.22
90	'FIH18-00014_AF2_RW_H5p11_T17_ABS_00'	92.05	54.73	55.29
91	'FIH18-00014_AF2_RW_H5p11_T20_ABS_00'	92.35	54.86	55.41

Table 6-108. Configuration AF2: Regular Wave. Mooring system pretensions

Table 6-109, Table 6-110, Table 6-111 and Table 6-112 report the mean, maximum and minimum values of the platform motions. It can be observed a high mean drift for low periods ≤ 9 s. Considering the initial position, this mean drift with a height of 5.11 m and a period of 7.5 s results in a mean excursion over 15 m in surge.

Configuration AF2 - Regular Wave at 0 deg										
#	Test/Laboratory Code	Motions - CoG: Position								
		X [m]			Y [m]			Z [m]		
		mean	max	min	mean	max	min	mean	max	min
80	'FIH18-00014_AF2_RW_H2p75_T7p5_ABS_00'	5.90	6.24	5.53	-0.02	0.06	-0.15	0.51	0.66	0.37
81	'FIH18-00014_AF2_RW_H2p75_T9_ABS_00'	4.55	5.10	4.01	0.27	0.40	0.13	0.54	0.84	0.24
82	'FIH18-00014_AF2_RW_H2p75_T11_ABS_01'	2.89	3.64	2.15	0.11	0.19	0.03	0.52	0.97	0.06
83	'FIH18-00014_AF2_RW_H2p75_T14_ABS_00'	2.53	3.48	1.60	-0.14	-0.04	-0.23	0.51	0.89	0.14
84	'FIH18-00014_AF2_RW_H2p75_T17_ABS_00'	2.58	3.73	1.35	-0.10	0.17	-0.27	0.49	1.07	-0.07
85	'FIH18-00014_AF2_RW_H2p75_T20_ABS_00'	2.84	4.70	0.89	0.05	0.54	-0.33	0.48	2.76	-1.80
86	'FIH18-00014_AF2_RW_H5p11_T7p5_ABS_00'	17.26	18.08	16.67	-0.86	-0.05	-1.66	0.53	0.80	0.27
87	'FIH18-00014_AF2_RW_H5p11_T9_ABS_00'	14.85	15.75	13.96	-0.18	0.33	-0.64	0.52	1.13	-0.08
88	'FIH18-00014_AF2_RW_H5p11_T11_ABS_00'	4.03	5.54	2.54	0.17	0.32	-0.01	0.53	1.40	-0.34
89	'FIH18-00014_AF2_RW_H5p11_T14_ABS_00'	2.19	3.96	0.43	-0.20	-0.06	-0.35	0.57	1.24	-0.11
90	'FIH18-00014_AF2_RW_H5p11_T17_ABS_00'	3.32	5.61	0.77	-0.20	0.28	-0.56	0.55	1.56	-0.50
91	'FIH18-00014_AF2_RW_H5p11_T20_ABS_00'	3.98	7.13	0.89	0.20	0.99	-0.36	0.55	3.67	-2.58

Table 6-109. Configuration AF2: Regular Wave. Displacements results in the CoG Position

Configuration AF2 - Regular Wave at 0 deg										
#	Test/Laboratory Code	Motions - CoG: Position								
		roll [deg]			pitch [deg]			yaw [deg]		
		mean	max	min	mean	max	min	mean	max	min
80	'FIH18-00014_AF2_RW_H2p75_T7p5_ABS_00'	0.16	0.20	0.12	-0.47	-0.29	-0.64	0.11	0.29	-0.12
81	'FIH18-00014_AF2_RW_H2p75_T9_ABS_00'	0.14	0.18	0.10	-0.45	-0.24	-0.66	0.29	0.42	0.14
82	'FIH18-00014_AF2_RW_H2p75_T11_ABS_01'	0.15	0.17	0.12	-0.47	-0.28	-0.65	0.43	0.48	0.38
83	'FIH18-00014_AF2_RW_H2p75_T14_ABS_00'	0.14	0.18	0.11	-0.46	-0.31	-0.60	0.39	0.45	0.33
84	'FIH18-00014_AF2_RW_H2p75_T17_ABS_00'	0.15	0.20	0.09	-0.45	-0.23	-0.67	0.39	0.72	0.00
85	'FIH18-00014_AF2_RW_H2p75_T20_ABS_00'	0.14	0.22	0.07	-0.45	-0.18	-0.74	0.43	0.77	0.04
86	'FIH18-00014_AF2_RW_H5p11_T7p5_ABS_00'	0.17	0.25	0.09	-0.39	-0.07	-0.70	1.18	1.69	0.39
87	'FIH18-00014_AF2_RW_H5p11_T9_ABS_00'	0.15	0.20	0.11	-0.46	-0.10	-0.80	0.42	0.75	-0.10
88	'FIH18-00014_AF2_RW_H5p11_T11_ABS_00'	0.15	0.20	0.11	-0.53	-0.17	-0.88	0.47	0.79	0.17
89	'FIH18-00014_AF2_RW_H5p11_T14_ABS_00'	0.17	0.20	0.14	-0.45	-0.20	-0.69	0.28	0.48	0.14
90	'FIH18-00014_AF2_RW_H5p11_T17_ABS_00'	0.17	0.24	0.09	-0.36	0.08	-0.84	0.27	1.10	-0.52
91	'FIH18-00014_AF2_RW_H5p11_T20_ABS_00'	0.17	0.27	0.08	-0.37	0.17	-0.91	0.54	1.28	-0.25

Table 6-110. Configuration AF2: Regular Wave. Rotations results in the CoG Position

Configuration AF2 - Regular Wave at 0 deg										
#	Test/Laboratory Code	Motions - Nacelle: Position								
		X [m]			Y [m]			Z [m]		
		mean	max	min	mean	max	min	mean	max	min
80	'FIH18-00014_AF2_RW_H2p75_T7p5_ABS_00'	4.71	5.12	4.26	-0.42	-0.32	-0.58	0.50	0.65	0.36
81	'FIH18-00014_AF2_RW_H2p75_T9_ABS_00'	3.41	3.64	3.20	-0.10	0.00	-0.20	0.54	0.84	0.24
82	'FIH18-00014_AF2_RW_H2p75_T11_ABS_01'	1.69	2.08	1.28	-0.27	-0.21	-0.33	0.51	0.97	0.05
83	'FIH18-00014_AF2_RW_H2p75_T14_ABS_00'	1.35	2.28	0.46	-0.51	-0.45	-0.57	0.51	0.89	0.13
84	'FIH18-00014_AF2_RW_H2p75_T17_ABS_00'	1.42	2.86	0.02	-0.48	-0.22	-0.66	0.49	1.07	-0.08
85	'FIH18-00014_AF2_RW_H2p75_T20_ABS_00'	1.70	3.96	-0.64	-0.33	0.15	-0.73	0.47	2.76	-1.81
86	'FIH18-00014_AF2_RW_H5p11_T7p5_ABS_00'	16.28	17.27	15.44	-1.33	-0.44	-2.21	0.52	0.79	0.27
87	'FIH18-00014_AF2_RW_H5p11_T9_ABS_00'	13.69	13.95	13.39	-0.57	-0.11	-1.04	0.51	1.13	-0.09
88	'FIH18-00014_AF2_RW_H5p11_T11_ABS_00'	2.69	3.54	1.89	-0.22	-0.10	-0.40	0.52	1.40	-0.35
89	'FIH18-00014_AF2_RW_H5p11_T14_ABS_00'	1.05	2.73	-0.64	-0.64	-0.51	-0.78	0.56	1.24	-0.12
90	'FIH18-00014_AF2_RW_H5p11_T17_ABS_00'	2.40	5.12	-0.60	-0.63	-0.18	-1.07	0.55	1.56	-0.51
91	'FIH18-00014_AF2_RW_H5p11_T20_ABS_00'	3.03	6.61	-0.58	-0.24	0.57	-0.90	0.54	3.67	-2.60

Table 6-111. Configuration AF2: Regular Wave. Motions results in the Nacelle Position

Configuration AF2 - Regular Wave at 0 deg										
#	Test/Laboratory Code	Motions - MSL: Position								
		X [m]			Y [m]			Z [m]		
		mean	max	min	mean	max	min	mean	max	min
80	'FIH18-00014_AF2_RW_H2p75_T7p5_ABS_00'	5.81	6.14	5.45	-0.05	0.03	-0.17	0.51	0.66	0.37
81	'FIH18-00014_AF2_RW_H2p75_T9_ABS_00'	4.46	4.98	3.96	0.24	0.37	0.11	0.54	0.84	0.24
82	'FIH18-00014_AF2_RW_H2p75_T11_ABS_01'	2.80	3.52	2.08	0.08	0.16	0.01	0.51	0.97	0.06
83	'FIH18-00014_AF2_RW_H2p75_T14_ABS_00'	2.44	3.38	1.51	-0.17	-0.07	-0.26	0.51	0.89	0.14
84	'FIH18-00014_AF2_RW_H2p75_T17_ABS_00'	2.49	3.66	1.26	-0.12	0.14	-0.30	0.49	1.07	-0.07
85	'FIH18-00014_AF2_RW_H2p75_T20_ABS_00'	2.76	4.63	0.78	0.02	0.51	-0.36	0.48	2.76	-1.80
86	'FIH18-00014_AF2_RW_H5p11_T7p5_ABS_00'	17.19	17.96	16.62	-0.90	-0.09	-1.68	0.53	0.80	0.27
87	'FIH18-00014_AF2_RW_H5p11_T9_ABS_00'	14.76	15.60	13.94	-0.20	0.30	-0.67	0.52	1.13	-0.08
88	'FIH18-00014_AF2_RW_H5p11_T11_ABS_00'	3.93	5.38	2.50	0.14	0.28	-0.03	0.53	1.40	-0.34
89	'FIH18-00014_AF2_RW_H5p11_T14_ABS_00'	2.10	3.85	0.36	-0.23	-0.09	-0.38	0.57	1.24	-0.11
90	'FIH18-00014_AF2_RW_H5p11_T17_ABS_00'	3.24	5.56	0.67	-0.23	0.24	-0.59	0.55	1.56	-0.50
91	'FIH18-00014_AF2_RW_H5p11_T20_ABS_00'	3.91	7.05	0.80	0.17	0.96	-0.40	0.54	3.67	-2.58

Table 6-112. Configuration AF2: Regular Wave. Motions results in the MSL Position

This set of tests provided the data necessary to obtain the Amplitude Response Operators (RAOs), which are illustrated in Figure 6-44, Figure 6-45 and Figure 6-46. As mentioned in Section 4.8.4, these RAOs are obtained as the mean value of the distance between peaks and troughs over incident wave height. RAOs in Heave present resonant peaks at $T = 20$ s, in agreement with the natural period of ACTIVEFLOAT platform in this DOF (Table 6-105).

ACTIVEFLOAT Configuration AF2: Regular Wave - CoG

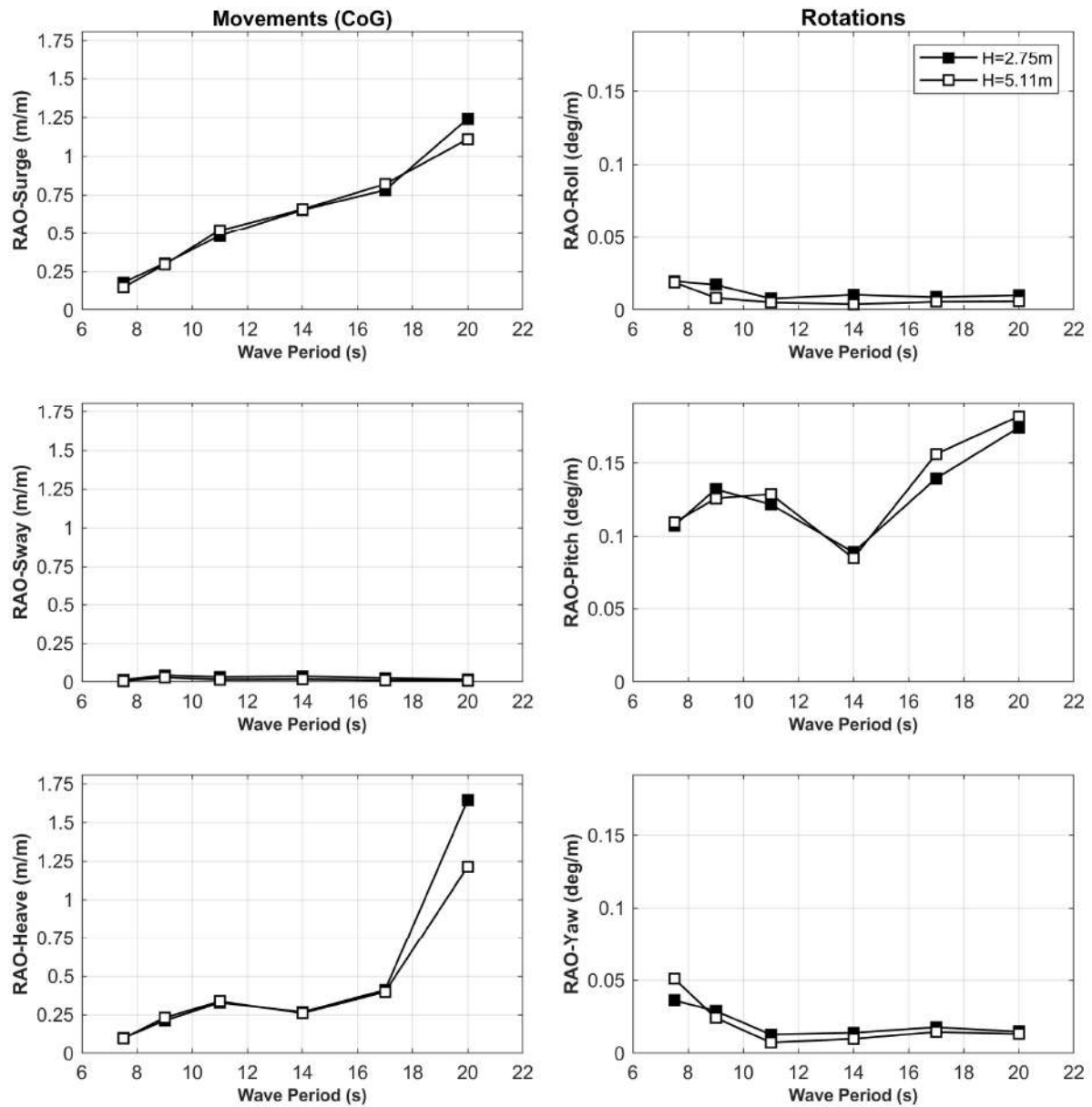


Figure 6-44. Configuration AF2: Regular Wave. RAO of motions (CoG)

ACTIVEFLOAT Configuration AF2: Regular Wave - Nacelle

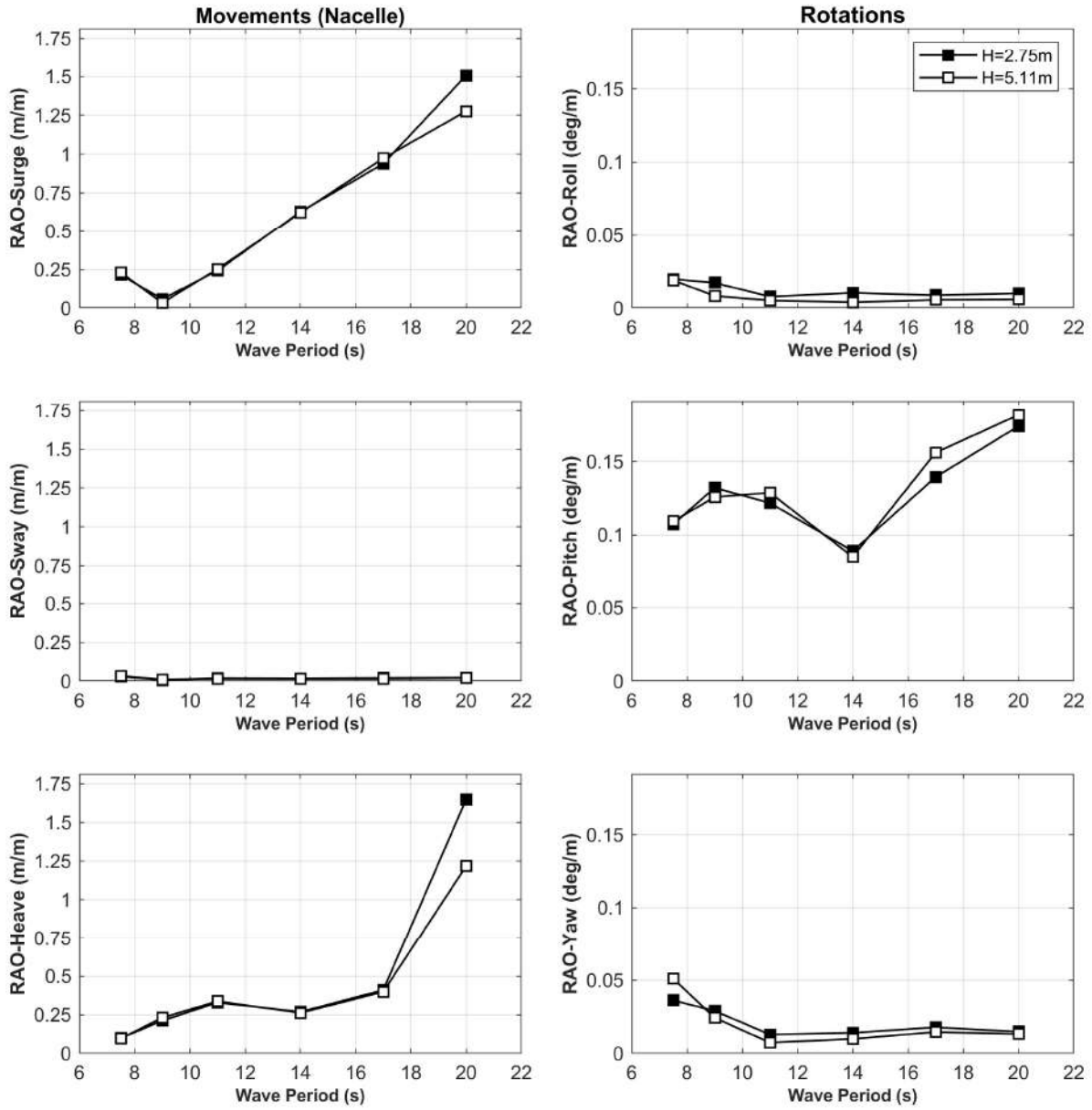


Figure 6-45. Configuration AF2: Regular Wave. RAO of motions (Nacelle)

ACTIVEFLOAT Configuration AF2: Regular Wave - MSL

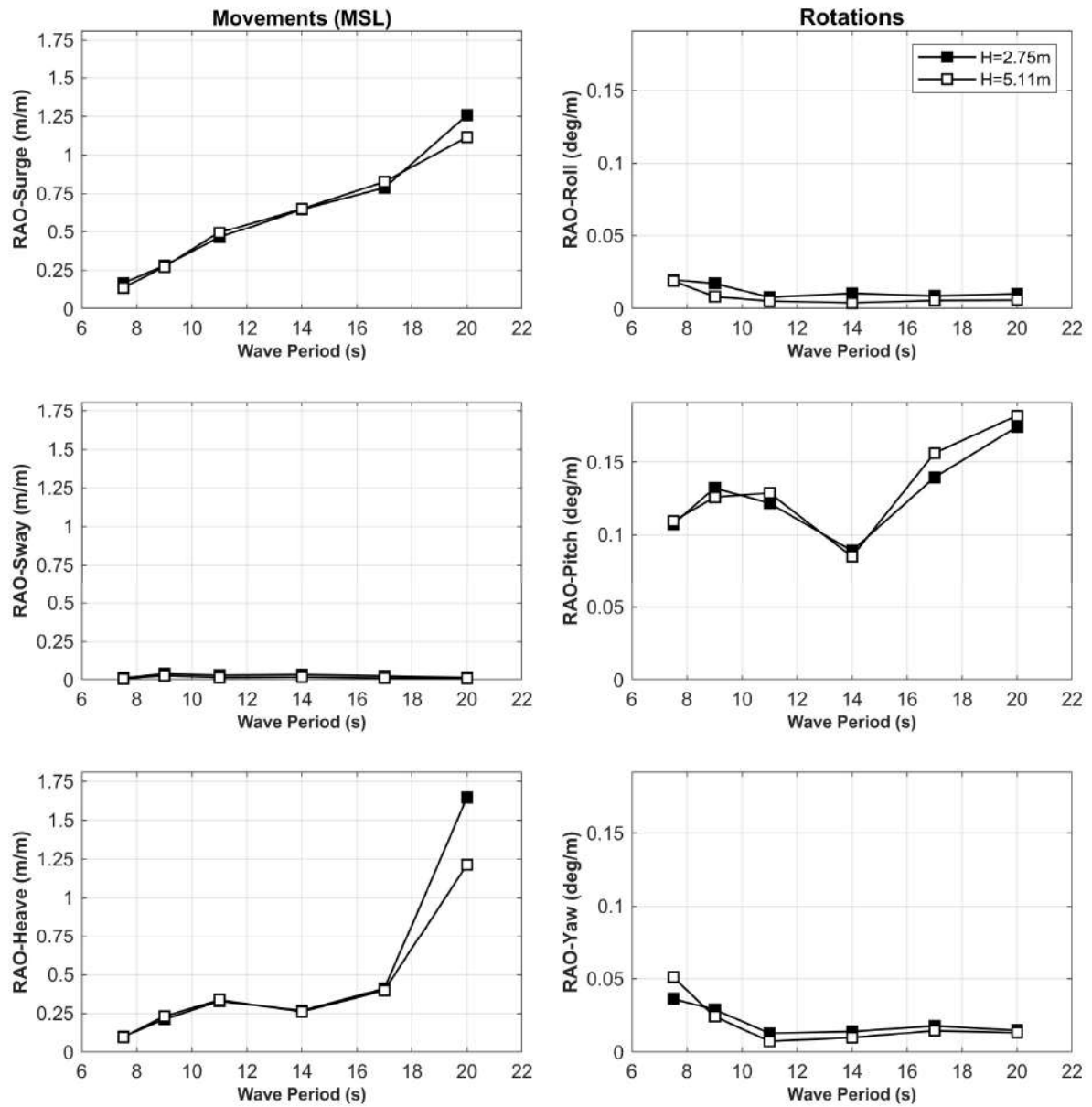


Figure 6-46. Configuration AF2: Regular Wave. RAO of motions (MSL)

Table 6-113 contains the information regarding the tensions recorded during the tests.

Configuration AF2 - Regular Wave at 0 deg										
#	Test/Laboratory Code	Mooring Lines - Load [tonnes]								
		LC1			LC2			LC3		
		mean	max	min	mean	max	min	mean	max	min
80	'FIH18-00014_AF2_RW_H2p75_T7p5_ABS_00'	102.77	103.63	101.91	50.63	51.65	49.63	50.21	51.39	49.01
81	'FIH18-00014_AF2_RW_H2p75_T9_ABS_00'	101.56	103.50	99.85	51.75	53.04	50.09	52.23	53.78	50.70
82	'FIH18-00014_AF2_RW_H2p75_T11_ABS_01'	92.60	93.87	91.29	54.09	55.43	52.73	53.27	54.96	51.68
83	'FIH18-00014_AF2_RW_H2p75_T14_ABS_00'	91.50	92.33	90.75	54.18	55.54	52.73	53.43	54.75	52.01
84	'FIH18-00014_AF2_RW_H2p75_T17_ABS_00'	91.52	94.24	88.83	54.20	55.34	53.15	53.33	54.40	52.11
85	'FIH18-00014_AF2_RW_H2p75_T20_ABS_00'	92.38	95.12	89.09	54.01	60.15	48.63	53.22	57.92	48.88
86	'FIH18-00014_AF2_RW_H5p11_T7p5_ABS_00'	149.23	155.26	145.25	39.84	41.84	37.73	42.95	45.52	40.43
87	'FIH18-00014_AF2_RW_H5p11_T9_ABS_00'	143.43	148.88	137.58	42.20	44.53	39.61	43.22	45.79	40.47
88	'FIH18-00014_AF2_RW_H5p11_T11_ABS_00'	96.27	99.44	92.76	52.92	56.88	48.55	51.95	55.93	47.84
89	'FIH18-00014_AF2_RW_H5p11_T14_ABS_00'	93.89	96.41	91.74	54.16	58.31	50.29	54.92	58.55	51.44
90	'FIH18-00014_AF2_RW_H5p11_T17_ABS_00'	97.06	104.79	89.17	52.65	56.05	49.99	53.60	56.91	50.82
91	'FIH18-00014_AF2_RW_H5p11_T20_ABS_00'	99.09	112.41	86.52	52.53	60.11	46.18	53.14	59.72	46.73

Table 6-113. Configuration AF2: Regular Waves. Mooring system results

The tensions as a function of wave period are shown in Figure 6-47.

ACTIVEFLOAT Configuration AF2: Regular Wave - Mooring Lines

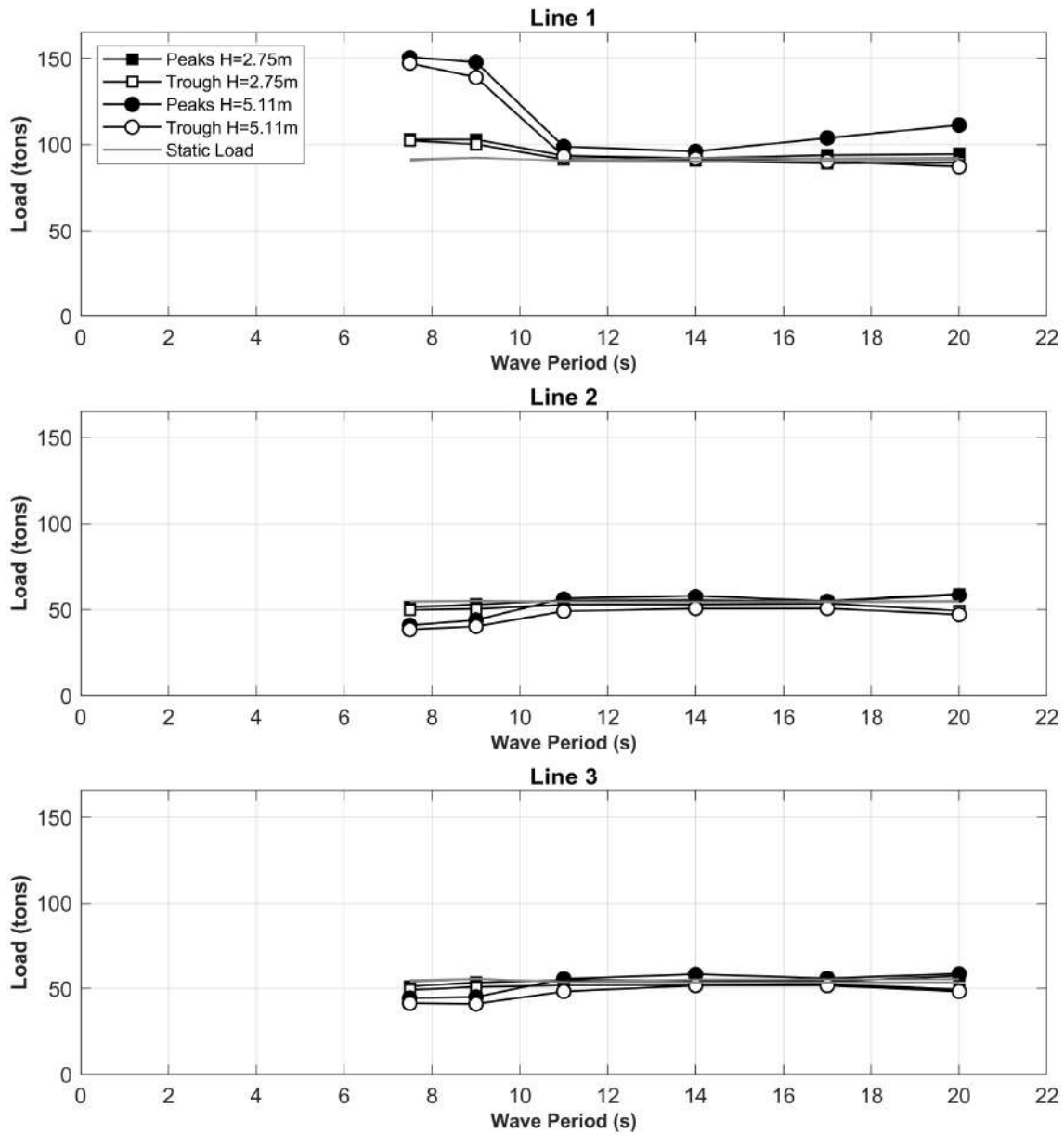


Figure 6-47. Configuration AF2: Regular Wave. Positive and Negative mean values of dynamic mooring loads

Table 6-114 and Figure 6-48 show the accelerations at the nacelle.

Configuration AF2 - Regular Wave at 0 deg							
#	Test/Laboratory Code	Accelerations - Nacelle [m/s ²]					
		Acc. X		Acc. Y		Acc. Z	
		max	min	max	min	max	min
80	'FIH18-00014_AF2_RW_H2p75_T7p5_ABS_00'	0.22	-0.23	0.04	-0.03	0.09	-0.11
81	'FIH18-00014_AF2_RW_H2p75_T9_ABS_00'	0.04	-0.08	0.02	-0.02	0.14	-0.15
82	'FIH18-00014_AF2_RW_H2p75_T11_ABS_01'	0.13	-0.10	0.02	-0.01	0.15	-0.16
83	'FIH18-00014_AF2_RW_H2p75_T14_ABS_00'	0.19	-0.19	0.02	-0.02	0.08	-0.09
84	'FIH18-00014_AF2_RW_H2p75_T17_ABS_00'	0.18	-0.19	0.02	-0.02	0.08	-0.09
85	'FIH18-00014_AF2_RW_H2p75_T20_ABS_00'	0.25	-0.24	0.02	-0.02	0.23	-0.24
86	'FIH18-00014_AF2_RW_H5p11_T7p5_ABS_00'	0.47	-0.52	0.11	-0.12	0.17	-0.20
87	'FIH18-00014_AF2_RW_H5p11_T9_ABS_00'	0.13	-0.14	0.08	-0.06	0.28	-0.31
88	'FIH18-00014_AF2_RW_H5p11_T11_ABS_00'	0.25	-0.24	0.03	-0.02	0.28	-0.30
89	'FIH18-00014_AF2_RW_H5p11_T14_ABS_00'	0.37	-0.35	0.02	-0.02	0.14	-0.14
90	'FIH18-00014_AF2_RW_H5p11_T17_ABS_00'	0.40	-0.37	0.03	-0.03	0.16	-0.14
91	'FIH18-00014_AF2_RW_H5p11_T20_ABS_00'	0.43	-0.35	0.02	-0.03	0.32	-0.33

Table 6-114. Configuration AF2: Regular Wave. Accelerations results in the Nacelle Position

ACTIVEFLOAT Configuration AF2: Regular Wave - Nacelle Accelerations

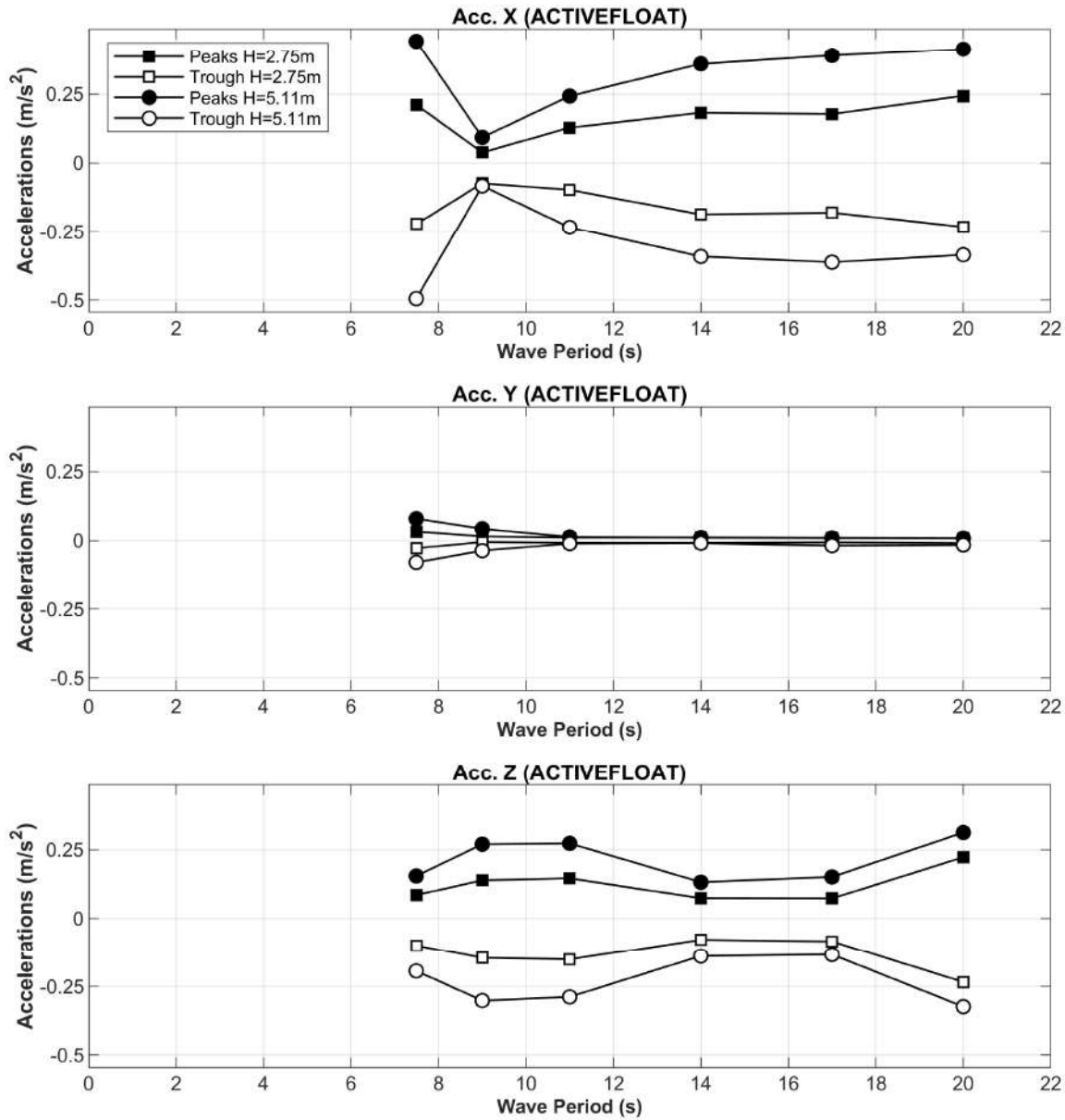


Figure 6-48. Configuration AF2: Regular Waves. Positive and Negative mean values of nacelle accelerations

Configuration AF2: Irregular Wave at 0°

Table 6-115 summarizes the main statistics of the incident sea states considered.

Configuration AF2 - Irregular Wave at 0 deg									
#	Test/Laboratory Code	h [m]	Hs [m]	Tp [s]	Spectrum	Gamma	Spread	Hinc [m]	Tinc [s]
92	'FIH18-00014_AF2_JS_H2p75_T9_G3p3_ABS_00'	120	2.75	9	JS	3.3	-	2.74	8.93
93	'FIH18-00014_AF2_JS_H2p75_T11_G3p3_ABS_00'	120	2.75	11	JS	3.3	-	2.77	11.02
94	'FIH18-00014_AF2_JS_H2p75_T14_G3p3_ABS_00'	120	2.75	14	JS	3.3	-	2.80	14.00
95	'FIH18-00014_AF2_JS_H5p11_T9_G1p2_ABS_01'	120	5.11	9	JS	1.2	-	5.04	8.22
96	'FIH18-00014_AF2_JS_H5p11_T11_G1p2_ABS_01'	120	5.11	11	JS	1.2	-	5.04	10.57
97	'FIH18-00014_AF2_JS_H2p75_T9_G3p3_S6_ABS_00'	120	2.75	9	JS	3.3	6	2.80	9.04
98	'FIH18-00014_AF2_JS_H2p75_T9_G3p3_S12_ABS_00'	120	2.75	9	JS	3.3	12	2.68	8.63
99	'FIH18-00014_AF2_JS_H5p11_T11_G1p2_S6_ABS_00'	120	5.11	11	JS	1.2	6	5.26	11.10
100	'FIH18-00014_AF2_JS_H5p11_T11_G1p2_S12_ABS_00'	120	5.11	11	JS	1.2	12	5.09	11.43

Table 6-115. Configuration AF2: Irregular Wave. Incident Analysis

The initial position as well as the mooring line pretensions are summarized on the next two tables (see Table 6-116 and Table 6-117).

Configuration AF2 - Irregular Wave at 0 deg													
#	Equilibrium Condition Test/Laboratory Code	Motions - CoG: Initial Position					Motions - Nacelle: Initial Position			Motions - MSL: Initial Position			
		X [m]	Y [m]	Z [m]	roll [deg]	pitch [deg]	yaw [deg]	X [m]	Y [m]	Z [m]	X [m]	Y [m]	Z [m]
92	'FIH18-00014_AF2_JS_H2p75_T9_G3p3_ABS_00'	2.92	0.09	0.40	0.16	-0.47	0.39	1.73	-0.33	0.39	2.82	0.06	0.40
93	'FIH18-00014_AF2_JS_H2p75_T11_G3p3_ABS_00'	2.90	-0.29	0.39	0.14	-0.46	0.34	1.72	-0.65	0.39	2.80	-0.32	0.39
94	'FIH18-00014_AF2_JS_H2p75_T14_G3p3_ABS_00'	2.51	-0.17	0.39	0.16	-0.44	0.30	1.39	-0.58	0.39	2.42	-0.20	0.39
95	'FIH18-00014_AF2_JS_H5p11_T9_G1p2_ABS_01'	2.53	-0.09	0.40	0.14	-0.43	0.29	1.43	-0.45	0.39	2.45	-0.12	0.40
96	'FIH18-00014_AF2_JS_H5p11_T11_G1p2_ABS_01'	2.30	-0.17	0.39	0.15	-0.42	0.36	1.23	-0.55	0.39	2.22	-0.20	0.39
97	'FIH18-00014_AF2_JS_H2p75_T9_G3p3_S6_ABS_00'	2.79	-0.11	0.48	0.16	-0.45	0.36	1.65	-0.53	0.48	2.70	-0.14	0.48
98	'FIH18-00014_AF2_JS_H2p75_T9_G3p3_S12_ABS_00'	2.00	-0.29	0.55	0.15	-0.42	0.40	0.94	-0.69	0.54	1.92	-0.32	0.55
99	'FIH18-00014_AF2_JS_H5p11_T11_G1p2_S6_ABS_00'	1.99	-0.24	0.59	0.15	-0.43	0.34	0.90	-0.64	0.59	1.91	-0.27	0.59
100	'FIH18-00014_AF2_JS_H5p11_T11_G1p2_S12_ABS_00'	2.41	-0.21	0.58	0.15	-0.46	0.37	1.24	-0.61	0.57	2.32	-0.24	0.58

Table 6-116. Configuration AF2: Irregular Wave. Motions initial positions

Configuration AF2 - Irregular Wave at 0 deg				
#	Equilibrium Condition Test/Laboratory Code	Mooring Lines - Pretension [tonnes]		
		LC1	LC2	LC3
92	'FIH18-00014_AF2_JS_H2p75_T9_G3p3_ABS_00'	91.21	54.24	54.68
93	'FIH18-00014_AF2_JS_H2p75_T11_G3p3_ABS_00'	90.84	53.56	53.98
94	'FIH18-00014_AF2_JS_H2p75_T14_G3p3_ABS_00'	89.96	54.01	54.68
95	'FIH18-00014_AF2_JS_H5p11_T9_G1p2_ABS_01'	90.46	54.10	54.74
96	'FIH18-00014_AF2_JS_H5p11_T11_G1p2_ABS_01'	90.49	54.18	54.93
97	'FIH18-00014_AF2_JS_H2p75_T9_G3p3_S6_ABS_00'	90.89	54.04	53.67
98	'FIH18-00014_AF2_JS_H2p75_T9_G3p3_S12_ABS_00'	91.37	54.49	54.30
99	'FIH18-00014_AF2_JS_H5p11_T11_G1p2_S6_ABS_00'	91.14	54.72	54.23
100	'FIH18-00014_AF2_JS_H5p11_T11_G1p2_S12_ABS_00'	91.06	54.42	53.80

Table 6-117. Configuration AF2: Irregular Wave. Mooring system pretensions

Table 6-118, Table 6-119, Table 6-120 and Table 6-121 show mean, maximum and minimum values of motions related to the CoG, Nacelle and MSL positions.

Configuration AF2 - Irregular Wave at 0 deg										
#	Test/Laboratory Code	Motions - CoG: Position								
		X [m]			Y [m]			Z [m]		
		mean	max	min	mean	max	min	mean	max	min
92	'FIH18-00014_AF2_JS_H2p75_T9_G3p3_ABS_00'	4.45	9.23	-0.68	0.11	0.62	-0.38	0.40	1.02	-0.17
93	'FIH18-00014_AF2_JS_H2p75_T11_G3p3_ABS_00'	3.81	7.52	0.67	0.11	0.46	-0.31	0.39	1.17	-0.34
94	'FIH18-00014_AF2_JS_H2p75_T14_G3p3_ABS_00'	3.21	5.54	0.66	-0.05	0.29	-0.39	0.39	1.75	-1.10
95	'FIH18-00014_AF2_JS_H5p11_T9_G1p2_ABS_01'	8.51	17.50	-0.60	0.07	1.32	-1.39	0.38	1.65	-0.80
96	'FIH18-00014_AF2_JS_H5p11_T11_G1p2_ABS_01'	6.76	16.39	-2.45	0.15	0.99	-0.74	0.38	1.86	-1.05
97	'FIH18-00014_AF2_JS_H2p75_T9_G3p3_S6_ABS_00'	4.26	8.15	0.56	0.09	2.61	-2.42	0.46	1.07	-0.05
98	'FIH18-00014_AF2_JS_H2p75_T9_G3p3_S12_ABS_00'	3.43	8.07	-0.39	-0.12	1.67	-1.95	0.55	1.12	0.06
99	'FIH18-00014_AF2_JS_H5p11_T11_G1p2_S6_ABS_00'	5.95	11.65	0.90	0.01	4.18	-4.15	0.58	1.91	-0.79
100	'FIH18-00014_AF2_JS_H5p11_T11_G1p2_S12_ABS_00'	6.11	13.77	-1.21	0.21	3.52	-3.11	0.58	1.89	-0.65

Table 6-118. Configuration AF2: Irregular Wave. Displacements results in the CoG Position

Configuration AF2 - Irregular Wave at 0 deg										
#	Test/Laboratory Code	Motions - CoG: Position								
		roll [deg]			pitch [deg]			yaw [deg]		
		mean	max	min	mean	max	min	mean	max	min
92	'FIH18-00014_AF2_JS_H2p75_T9_G3p3_ABS_00'	0.16	0.27	0.03	-0.44	0.35	-1.22	0.36	0.94	-0.28
93	'FIH18-00014_AF2_JS_H2p75_T11_G3p3_ABS_00'	0.16	0.26	0.05	-0.44	0.24	-1.12	0.35	0.86	-0.13
94	'FIH18-00014_AF2_JS_H2p75_T14_G3p3_ABS_00'	0.16	0.25	0.07	-0.45	0.20	-1.02	0.35	0.73	0.00
95	'FIH18-00014_AF2_JS_H5p11_T9_G1p2_ABS_01'	0.15	0.42	-0.14	-0.44	1.98	-2.51	0.43	1.88	-1.14
96	'FIH18-00014_AF2_JS_H5p11_T11_G1p2_ABS_01'	0.15	0.38	-0.06	-0.43	1.53	-2.37	0.35	1.91	-0.86
97	'FIH18-00014_AF2_JS_H2p75_T9_G3p3_S6_ABS_00'	0.17	0.62	-0.30	-0.44	0.28	-1.15	0.39	4.96	-4.36
98	'FIH18-00014_AF2_JS_H2p75_T9_G3p3_S12_ABS_00'	0.15	0.49	-0.18	-0.42	0.33	-1.11	0.41	5.22	-3.86
99	'FIH18-00014_AF2_JS_H5p11_T11_G1p2_S6_ABS_00'	0.15	1.65	-0.95	-0.46	0.84	-1.69	0.35	7.05	-7.23
100	'FIH18-00014_AF2_JS_H5p11_T11_G1p2_S12_ABS_00'	0.15	1.37	-1.00	-0.46	0.97	-1.62	0.37	6.14	-6.47

Table 6-119. Configuration AF2: Irregular Wave. Rotations results in the CoG Position

Configuration AF2 - Irregular Wave at 0 deg										
#	Test/Laboratory Code	Motions - Nacelle: Position								
		X [m]			Y [m]			Z [m]		
		mean	max	min	mean	max	min	mean	max	min
92	'FIH18-00014_AF2_JS_H2p75_T9_G3p3_ABS_00'	3.34	8.96	-1.97	-0.29	0.28	-0.83	0.39	1.00	-0.17
93	'FIH18-00014_AF2_JS_H2p75_T11_G3p3_ABS_00'	2.68	6.43	-0.98	-0.29	0.05	-0.71	0.39	1.16	-0.35
94	'FIH18-00014_AF2_JS_H2p75_T14_G3p3_ABS_00'	2.07	4.85	-0.58	-0.46	-0.11	-0.80	0.38	1.75	-1.11
95	'FIH18-00014_AF2_JS_H5p11_T9_G1p2_ABS_01'	7.40	17.38	-3.13	-0.32	1.21	-2.08	0.37	1.65	-0.83
96	'FIH18-00014_AF2_JS_H5p11_T11_G1p2_ABS_01'	5.67	17.52	-4.93	-0.25	0.78	-1.17	0.37	1.84	-1.05
97	'FIH18-00014_AF2_JS_H2p75_T9_G3p3_S6_ABS_00'	3.13	7.67	-0.81	-0.35	2.45	-3.07	0.46	1.06	-0.06
98	'FIH18-00014_AF2_JS_H2p75_T9_G3p3_S12_ABS_00'	2.37	7.63	-1.57	-0.52	1.86	-2.64	0.55	1.11	0.06
99	'FIH18-00014_AF2_JS_H5p11_T11_G1p2_S6_ABS_00'	4.77	10.67	-0.82	-0.38	4.83	-5.39	0.57	1.90	-0.80
100	'FIH18-00014_AF2_JS_H5p11_T11_G1p2_S12_ABS_00'	4.94	13.75	-2.50	-0.17	4.66	-4.10	0.57	1.88	-0.68

Table 6-120. Configuration AF2: Irregular Wave. Motions results in the Nacelle Position

Configuration AF2 - Irregular Wave at 0 deg										
#	Test/Laboratory Code	Motions - MSL: Position								
		X [m]			Y [m]			Z [m]		
		mean	max	min	mean	max	min	mean	max	min
92	'FIH18-00014_AF2_JS_H2p75_T9_G3p3_ABS_00'	4.36	9.14	-0.64	0.09	0.58	-0.40	0.40	1.02	-0.17
93	'FIH18-00014_AF2_JS_H2p75_T11_G3p3_ABS_00'	3.72	7.41	0.56	0.08	0.43	-0.34	0.39	1.17	-0.34
94	'FIH18-00014_AF2_JS_H2p75_T14_G3p3_ABS_00'	3.12	5.48	0.59	-0.08	0.26	-0.41	0.39	1.75	-1.10
95	'FIH18-00014_AF2_JS_H5p11_T9_G1p2_ABS_01'	8.43	17.26	-0.46	0.04	1.27	-1.42	0.38	1.65	-0.80
96	'FIH18-00014_AF2_JS_H5p11_T11_G1p2_ABS_01'	6.67	16.44	-2.54	0.13	0.95	-0.75	0.38	1.85	-1.05
97	'FIH18-00014_AF2_JS_H2p75_T9_G3p3_S6_ABS_00'	4.17	8.10	0.46	0.05	2.58	-2.40	0.46	1.07	-0.05
98	'FIH18-00014_AF2_JS_H2p75_T9_G3p3_S12_ABS_00'	3.35	8.03	-0.38	-0.15	1.67	-1.99	0.55	1.12	0.06
99	'FIH18-00014_AF2_JS_H5p11_T11_G1p2_S6_ABS_00'	5.86	11.52	0.77	-0.02	4.20	-4.11	0.58	1.91	-0.79
100	'FIH18-00014_AF2_JS_H5p11_T11_G1p2_S12_ABS_00'	6.02	13.77	-1.29	0.19	3.61	-3.11	0.58	1.89	-0.65

Table 6-121. Configuration AF2: Irregular Wave. Motions results in the MSL Position

The spectral RAOs are obtained through the irregular wave tests, using the equation presented in previous section 4.8.4 Statistical analysis. The spectral RAOs shown in Figure 6-49, Figure 6-50 and Figure 6-51, are in good agreement with the ones obtained through the regular wave tests (Figure 6-44, Figure 6-45 and Figure 6-46). RAOs in Heave present resonant peaks at $T = 18.6 s$, in agreement with the natural period of ACTIVEFLOAT platform in this DOF (Table 6-105).

ACTIVEFLOAT Configuration AF2: Irregular Wave - CoG

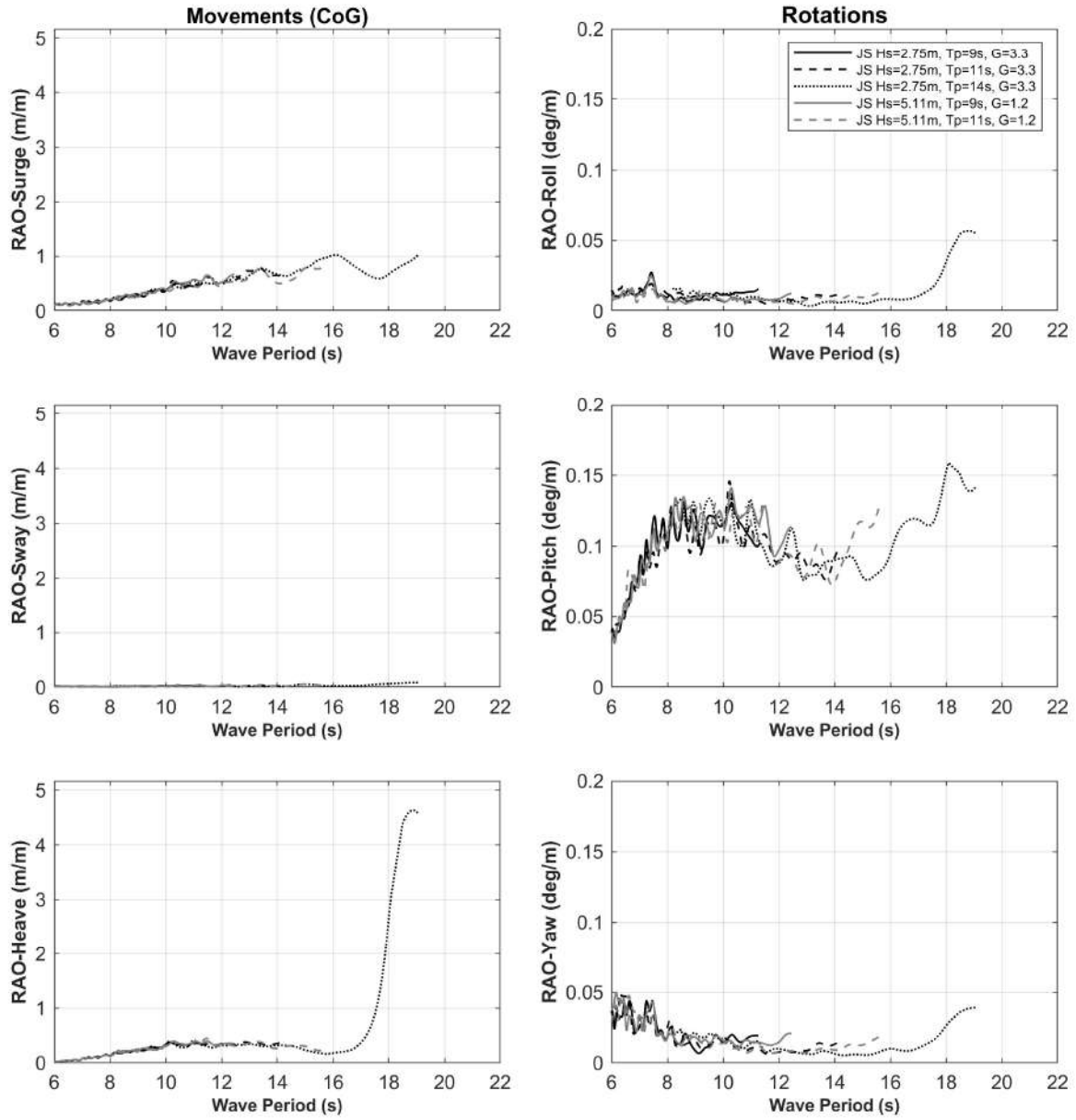


Figure 6-49. Configuration AF2: Irregular Wave. RAO of motions (CoG)

ACTIVEFLOAT Configuration AF2: Irregular Wave - Nacelle

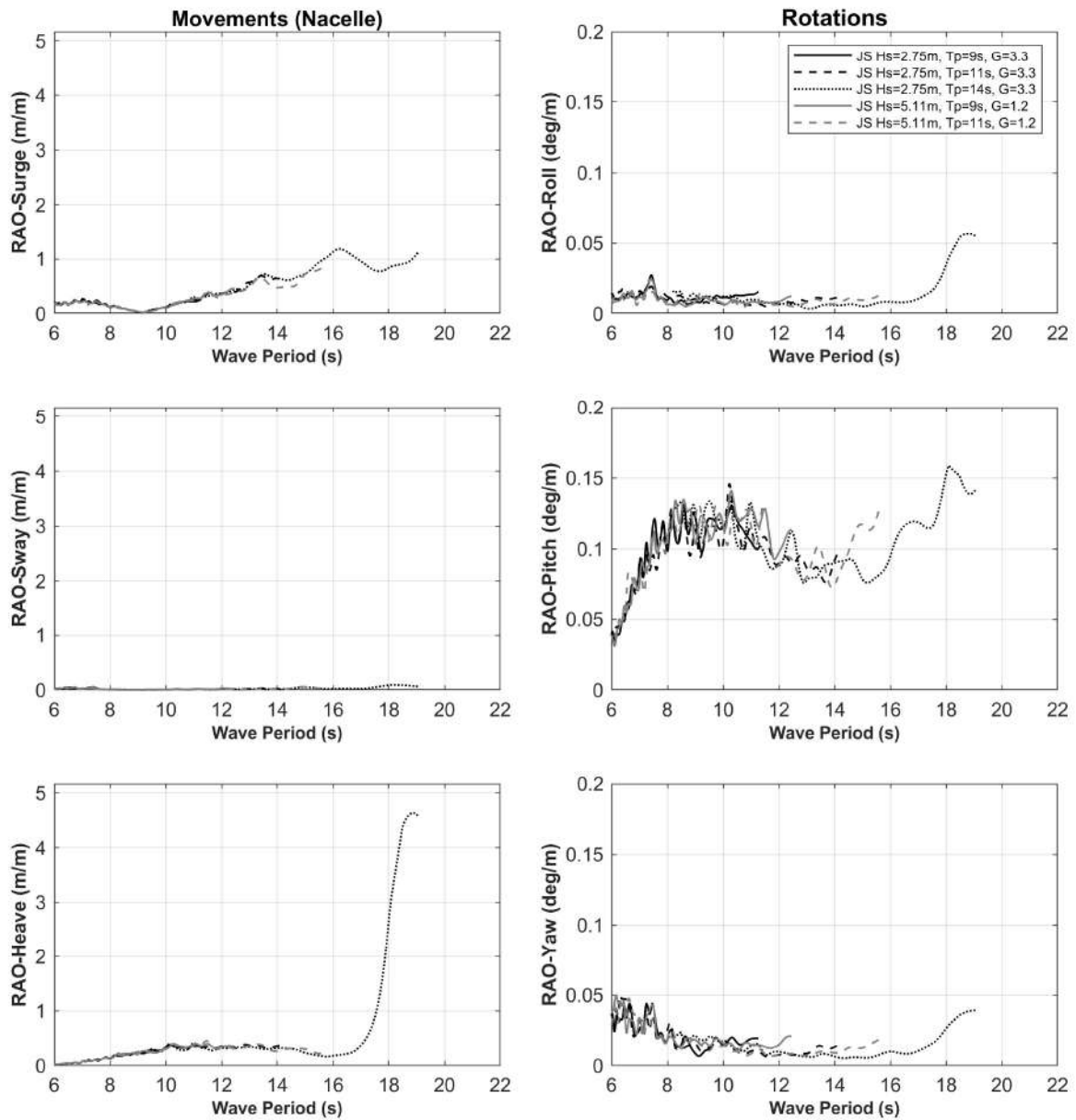


Figure 6-50. Configuration AF2: Irregular Wave. RAO of motions (Nacelle)

ACTIVEFLOAT Configuration AF2: Irregular Wave - MSL

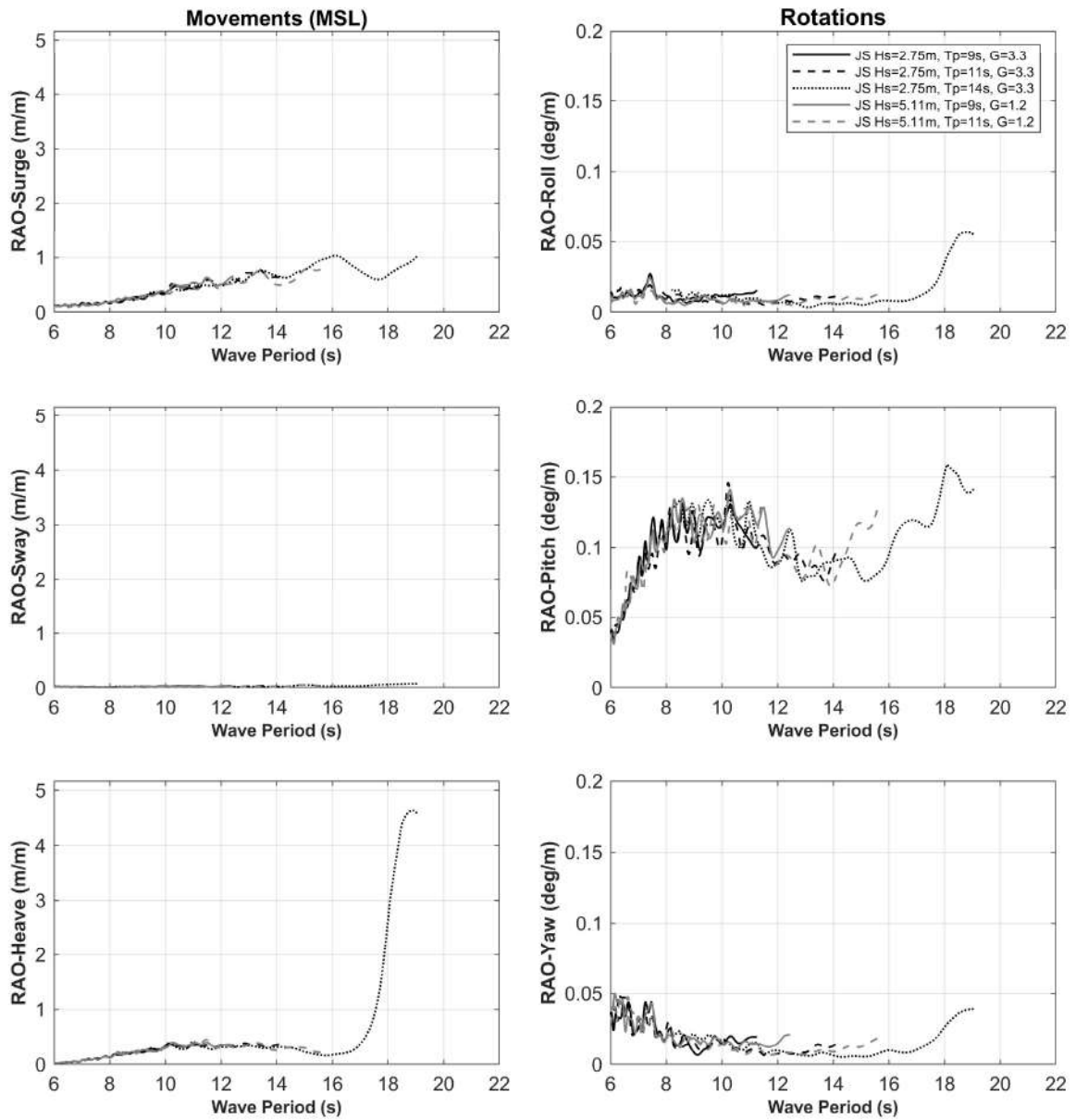


Figure 6-51. Configuration AF2: Irregular Wave. RAO of motions (MSL)

Table 6-122 indicates the tensions obtained during the tests carried out.

Configuration AF2 - Irregular Wave at 0 deg										
#	Test/Laboratory Code	Mooring Lines - Load [tonnes]								
		LC1			LC2			LC3		
		mean	max	min	mean	max	min	mean	max	min
92	'FIH18-00014_AF2_JS_H2p75_T9_G3p3_ABS_00'	96.99	115.58	81.63	52.15	60.23	46.15	52.75	59.63	47.01
93	'FIH18-00014_AF2_JS_H2p75_T11_G3p3_ABS_00'	94.66	107.99	85.78	52.91	58.21	47.90	53.48	58.09	48.74
94	'FIH18-00014_AF2_JS_H2p75_T14_G3p3_ABS_00'	92.73	100.23	85.83	53.28	58.26	48.90	53.93	57.83	50.30
95	'FIH18-00014_AF2_JS_H5p11_T9_G1p2_ABS_01'	113.56	170.51	82.45	48.30	59.84	39.48	48.95	60.71	39.91
96	'FIH18-00014_AF2_JS_H5p11_T11_G1p2_ABS_01'	106.63	162.21	79.16	49.94	62.49	40.87	50.65	63.41	41.79
97	'FIH18-00014_AF2_JS_H2p75_T9_G3p3_S6_ABS_00'	96.06	111.00	84.69	52.55	59.93	45.82	52.32	57.63	46.13
98	'FIH18-00014_AF2_JS_H2p75_T9_G3p3_S12_ABS_00'	96.52	116.19	84.72	53.13	59.78	45.16	52.91	58.70	46.50
99	'FIH18-00014_AF2_JS_H5p11_T11_G1p2_S6_ABS_00'	105.73	134.91	88.64	50.89	62.01	41.09	50.57	61.60	39.50
100	'FIH18-00014_AF2_JS_H5p11_T11_G1p2_S12_ABS_00'	104.82	146.61	82.17	50.98	61.95	41.32	50.08	60.49	37.63

Table 6-122. Configuration AF2: Irregular Wave. Mooring system results

Table 6-123 shows the accelerations at the nacelle.

Configuration AF2 - Irregular Wave at 0 deg								
#	Test/Laboratory Code	Accelerations - Nacelle [m/s ²]						
		Acc. X		Acc. Y		Acc. Z		
		max	min	max	min	max	min	
92	'FIH18-00014_AF2_JS_H2p75_T9_G3p3_ABS_00'	0.34	-0.34	0.06	-0.06	0.24	-0.26	
93	'FIH18-00014_AF2_JS_H2p75_T11_G3p3_ABS_00'	0.33	-0.35	0.04	-0.04	0.25	-0.25	
94	'FIH18-00014_AF2_JS_H2p75_T14_G3p3_ABS_00'	0.32	-0.38	0.04	-0.04	0.27	-0.24	
95	'FIH18-00014_AF2_JS_H5p11_T9_G1p2_ABS_01'	0.66	-0.72	0.13	-0.17	0.37	-0.43	
96	'FIH18-00014_AF2_JS_H5p11_T11_G1p2_ABS_01'	0.63	-0.64	0.09	-0.12	0.45	-0.53	
97	'FIH18-00014_AF2_JS_H2p75_T9_G3p3_S6_ABS_00'	0.29	-0.28	0.21	-0.22	0.26	-0.27	
98	'FIH18-00014_AF2_JS_H2p75_T9_G3p3_S12_ABS_00'	0.28	-0.29	0.17	-0.21	0.20	-0.24	
99	'FIH18-00014_AF2_JS_H5p11_T11_G1p2_S6_ABS_00'	0.56	-0.56	0.39	-0.40	0.45	-0.44	
100	'FIH18-00014_AF2_JS_H5p11_T11_G1p2_S12_ABS_00'	0.61	-0.51	0.37	-0.35	0.39	-0.48	

Table 6-123. Configuration AF2: Irregular Wave. Accelerations results in the Nacelle Position

Configuration AF2: White Noise at 0°

Spectral RAOs are also obtained through white noise tests whose wave spectrum characteristics are presented in Table 6-124. During these tests, the platform is hit by irregular waves defined by a limited white noise spectrum between the periods of 7.5 and 22 seconds.

Configuration AF2 – White Noise at 0 deg						
#	Test/Laboratory Code	h [m]	Hs [m]	T1 [s]	T2 [s]	Hinc [m]
101	'FIH18-00014_AF2_TH_H2p75_T11p19_DF0p088_ABS_00'	120	2.75	7.5	22	2.68
102	'FIH18-00014_AF2_TH_H5p11_T11p19_DF0p088_ABS_00'	120	5.11	7.5	22	5.13

Table 6-124. Configuration AF2: White Noise

The spectral RAOs obtained through the white noise test is shown in Figure 6-52, Figure 6-53 and Figure 6-54. These RAOs are in good agreement with the ones obtained through the irregular waves tests (Figure 6-49, Figure 6-50 and Figure 6-51). RAOs in Heave present resonant peaks at $T = 18.6 s$, in agreement with the natural period of ACTIVEFLOAT platform in this DOF (Table 6-105).

ACTIVEFLOAT Configuration AF2: White Noise - CoG

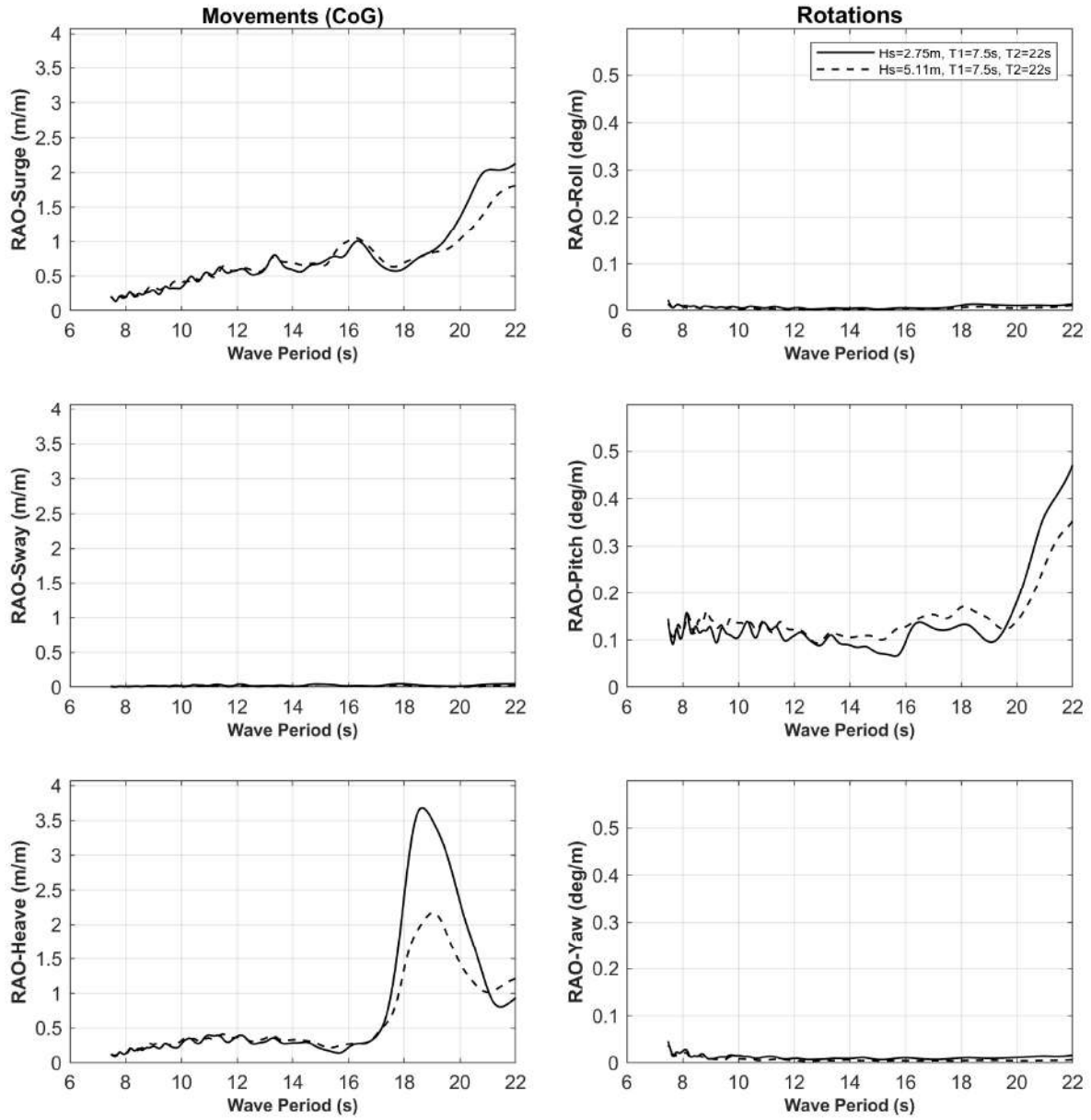


Figure 6-52. Configuration AF2: White Noise. RAO of motions (CoG)

ACTIVEFLOAT Configuration AF2: White Noise - Nacelle

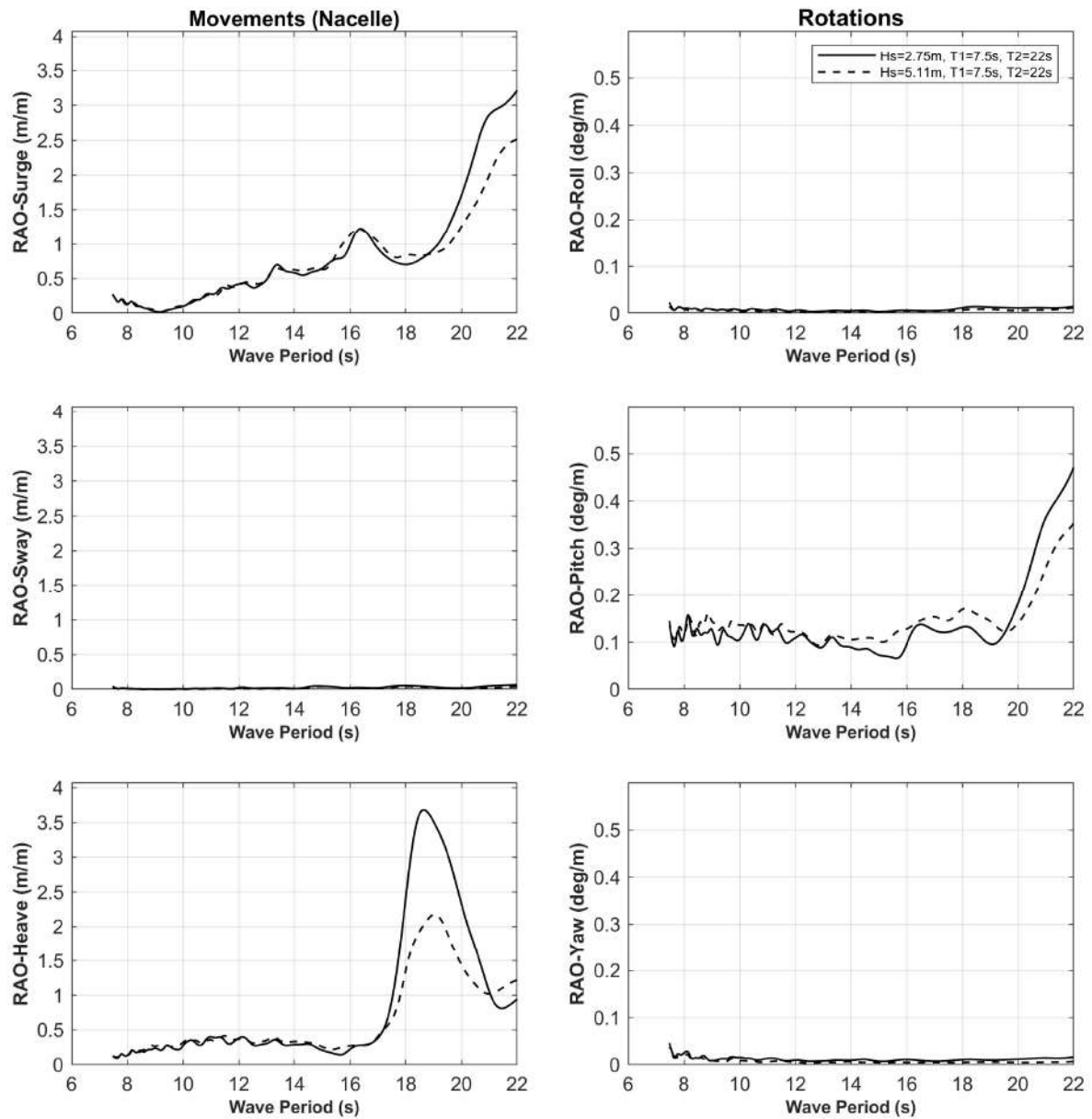


Figure 6-53. Configuration AF2: White Noise. RAO of motions (Nacelle)

ACTIVEFLOAT Configuration AF2: White Noise - MSL

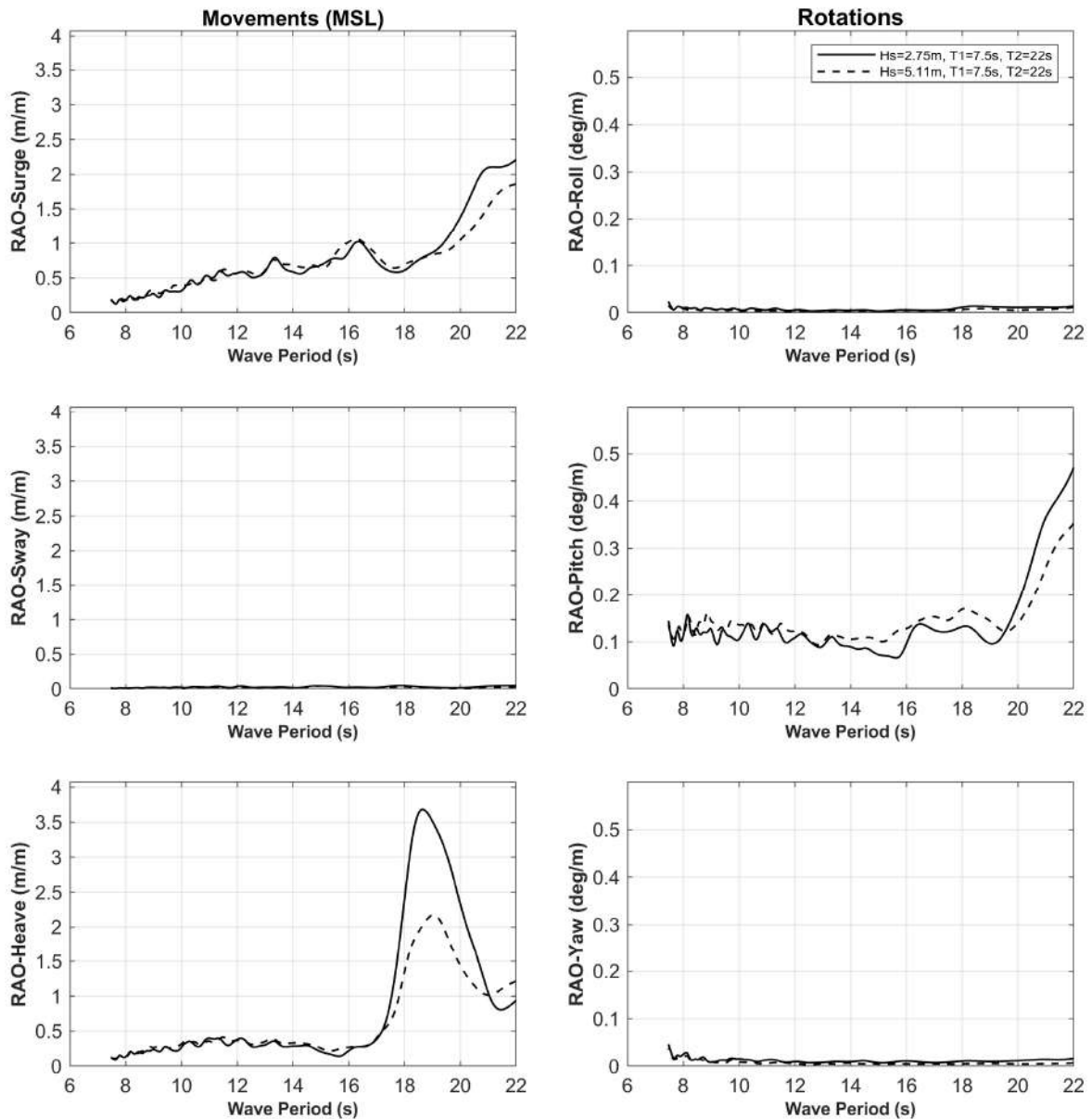


Figure 6-54. Configuration AF2: White Noise. RAO of motions (MSL)

Configuration AF3: Wind at 0°

Table 6-125 provides the wind characteristics reproduced during these tests, the average values of the thrust force measured by the triaxial load cell placed at the base of the multi-fan.

Configuration AF3 – Wind at 0 deg					
#	Test/Laboratory Code	h [m]	Wind [m/s]	Thrust [tonnes]	Measured Thrust [tonnes]
103	'FIH18-00014_AF3_WDC10p5_00'	120	10.5	227.86	228.01
104	'FIH18-00014_AF3_WDT10p5_TCETM_00'	120	10.5 ETM	171.51	171.66
105	'FIH18-00014_AF3_WDT10p5_TCNTM_00'	120	10.5 NTM	192.35	193.26

Table 6-125. Configuration AF3: Wind. Incident Analysis

The data provided in the following Table 6-126 and Table 6-127 report information about the initial position for each degree of freedom, as well as the mooring loads recorded. The Pitch is around -7.8 degrees to reach 0 degrees when the thrust associated to constant rated wind is acting on. The tension in mooring line 1 is higher than the tensions in mooring lines 2 and 3.

Configuration AF3 – Wind at 0 deg													
#	Equilibrium Condition	Motions - CoG: Initial Position						Motions - Nacelle: Initial Position			Motions - MSL: Initial Position		
	Test/Laboratory Code	X [m]	Y [m]	Z [m]	roll [deg]	pitch [deg]	yaw [deg]	X [m]	Y [m]	Z [m]	X [m]	Y [m]	Z [m]
103	'FIH18-00014_AF3_WDC10p5_00'	3.29	-0.05	1.48	0.15	-7.80	0.26	-16.51	-0.52	0.13	1.80	-0.08	1.37
104	'FIH18-00014_AF3_WDT10p5_TCETM_00'	3.50	0.26	0.56	0.29	-7.82	0.23	-16.36	-0.56	-0.80	2.01	0.20	0.46
105	'FIH18-00014_AF3_WDT10p5_TCNTM_00'	4.38	0.39	0.54	0.29	-7.81	0.29	-15.45	-0.44	-0.81	2.88	0.33	0.44

Table 6-126. Configuration AF3: Wind. Motions initial positions

Configuration AF3 – Wind at 0 deg				
#	Equilibrium Condition	Mooring Lines - Pretension [tonnes]		
	Test/Laboratory Code	LC1	LC2	LC3
103	'FIH18-00014_AF3_WDC10p5_00'	91.98	54.49	54.88
104	'FIH18-00014_AF3_WDT10p5_TCETM_00'	91.61	54.27	54.13
105	'FIH18-00014_AF3_WDT10p5_TCNTM_00'	88.06	53.67	53.29

Table 6-127. Configuration AF3: Wind. Mooring system pretensions

Figure 6-55 shows this initial position of the platform in the wave basin before acting wind loads.



Figure 6-55. Initial position before acting wind loads

Table 6-128, Table 6-129, Table 6-130 and Table 6-131 show mean, maximum and minimum values of motions related to the CoG, Nacelle and MSL positions. Surge and pitch values are higher as rotor thrust is increased. Considering the initial position, all wind cases cause a mean excursion over 15 m and a maximum excursion over 30 m in surge.

Configuration AF3 – Wind at 0 deg										
#	Test/Laboratory Code	Motions - CoG: Position								
		X [m]			Y [m]			Z [m]		
		mean	max	min	mean	max	min	mean	max	min
103	'FIH18-00014_AF3_WDC10p5_00'	34.12	34.39	33.85	-0.95	-0.41	-1.62	1.26	1.28	1.25
104	'FIH18-00014_AF3_WDT10p5_TCETM_00'	28.71	40.25	18.27	-0.50	1.13	-1.61	0.38	0.49	0.29
105	'FIH18-00014_AF3_WDT10p5_TCNTM_00'	30.88	39.12	23.10	-0.31	0.87	-1.36	0.35	0.43	0.29

Table 6-128. Configuration AF3: Wind. Displacements results in the CoG Position

Configuration AF3 – Wind at 0 deg										
#	Test/Laboratory Code	Motions - CoG: Position								
		roll [deg]			pitch [deg]			yaw [deg]		
		mean	max	min	mean	max	min	mean	max	min
103	'FIH18-00014_AF3_WDC10p5_00'	0.42	0.46	0.37	-0.04	0.07	-0.15	0.74	1.13	0.32
104	'FIH18-00014_AF3_WDT10p5_TCETM_00'	0.49	0.70	0.31	-2.02	2.43	-6.16	0.83	2.98	-1.36
105	'FIH18-00014_AF3_WDT10p5_TCNTM_00'	0.51	0.66	0.36	-1.30	1.79	-4.53	0.96	2.68	-0.81

Table 6-129. Configuration AF3: Wind. Rotations results in the CoG Position

Configuration AF3 – Wind at 0 deg										
#	Test/Laboratory Code	Motions - Nacelle: Position								
		X [m]			Y [m]			Z [m]		
		mean	max	min	mean	max	min	mean	max	min
103	'FIH18-00014_AF3_WDC10p5_00'	34.05	34.34	33.66	-2.01	-1.46	-2.72	1.26	1.27	1.25
104	'FIH18-00014_AF3_WDT10p5_TCETM_00'	23.59	38.77	6.85	-1.81	-0.03	-2.96	0.23	0.41	-0.38
105	'FIH18-00014_AF3_WDT10p5_TCNTM_00'	27.61	38.83	16.52	-1.66	-0.26	-2.82	0.28	0.37	-0.04

Table 6-130. Configuration AF3: Wind. Motions results in the Nacelle Position

Configuration AF3 – Wind at 0 deg										
#	Test/Laboratory Code	Motions - MSL: Position								
		X [m]			Y [m]			Z [m]		
		mean	max	min	mean	max	min	mean	max	min
103	'FIH18-00014_AF3_WDC10p5_00'	34.11	34.37	33.85	-1.03	-0.48	-1.70	1.26	1.27	1.25
104	'FIH18-00014_AF3_WDT10p5_TCETM_00'	28.33	39.90	17.78	-0.59	1.03	-1.71	0.36	0.45	0.29
105	'FIH18-00014_AF3_WDT10p5_TCNTM_00'	30.64	38.88	22.74	-0.41	0.78	-1.46	0.35	0.40	0.28

Table 6-131. Configuration AF3: Wind. Motions results in the MSL Position

Table 6-132 indicates the tensions obtained during the tests execution. In agreement with static offset tests in surge (Figure 6-41), mooring tensions are higher on the windward line and lower on leeward lines as rotor thrust is increased. The higher mean load in the main line 1 equal to 268 tonnes is obtained with the constant rated wind since it is directly related to the thrust value. The maximum tension in the main line 1 equal to 373 tonnes is reached in the case of rated wind with Extreme Turbulence Model.

Configuration AF3 – Wind at 0 deg										
#	Test/Laboratory Code	Mooring Lines - Load [tonnes]								
		LC1			LC2			LC3		
		mean	max	min	mean	max	min	mean	max	min
103	'FIH18-00014_AF3_WDC10p5_00'	267.88	274.19	261.92	32.24	32.57	31.85	33.99	34.52	33.52
104	'FIH18-00014_AF3_WDT10p5_TCETM_00'	220.03	372.64	132.30	34.95	40.75	30.44	36.30	43.81	31.10
105	'FIH18-00014_AF3_WDT10p5_TCNTM_00'	237.69	359.76	161.38	33.92	37.48	30.76	35.13	40.21	31.45

Table 6-132. Configuration AF3: Wind. Mooring system results

Table 6-133 shows the accelerations at the nacelle with wind.

Configuration AF3 – Wind at 0 deg										
#	Test/Laboratory Code	Accelerations - Nacelle [m/s ²]								
		Acc. X		Acc. Y		Acc. Z				
		max	min	max	min	max	min			
103	'FIH18-00014_AF3_WDC10p5_00'	0.00	-0.03	0.08	0.05	0.00	-0.03			
104	'FIH18-00014_AF3_WDT10p5_TCETM_00'	0.92	-0.56	0.10	-0.05	-0.01	-0.10			
105	'FIH18-00014_AF3_WDT10p5_TCNTM_00'	0.23	-0.21	0.09	0.01	0.00	-0.04			

Table 6-133. Configuration AF3: Wind. Accelerations results in the Nacelle Position

Configuration AF3: Combined Regular Wave and Constant Wind at 0°

Table 6-134 summarizes the main characteristics of the incident sea state and rotor thrust force measured during the combined regular waves and constant wind tests.

Configuration AF3 - Regular Wave + Constant Wind at 0 deg									
#	Test/Laboratory Code	h [m]	H [m]	T [s]	Wind [m/s]	Thrust [tonnes]	Hinc [m]	Tinc [s]	Measured Thrust [tonnes]
106	'FIH18-00014_AF3_RW_H2p75_T7p5_ABS_WDC10p5_01'	120	2.75	7.5	10.5	227.44	2.74	7.48	227.61
107	'FIH18-00014_AF3_RW_H2p75_T9_ABS_WDC10p5_00'	120	2.75	9	10.5	227.86	2.63	8.82	226.96
108	'FIH18-00014_AF3_RW_H2p75_T11_ABS_WDC10p5_00'	120	2.75	11	10.5	226.72	2.65	11.00	226.74
109	'FIH18-00014_AF3_RW_H2p75_T14_ABS_WDC10p5_00'	120	2.75	14	10.5	221.35	2.73	14.00	220.81
110	'FIH18-00014_AF3_RW_H2p75_T17_ABS_WDC10p5_00'	120	2.75	17	10.5	220.23	2.77	16.99	219.99
111	'FIH18-00014_AF3_RW_H2p75_T20_ABS_WDC10p5_00'	120	2.75	20	10.5	216.45	2.75	19.90	216.01

Table 6-134. Configuration AF3: Combined Regular Wave and Constant Wind. Incident Analysis

The data provided in the following tables (see Table 6-135 and Table 6-136) report information about the initial position for each degree of freedom and mooring loads on the ACTIVEFLOAT floating wind turbine. The Pitch is around -7.8 degrees to reach 0 degrees when the thrust associated to constant rated wind is acting on. The tension in mooring line 1 is higher than the tensions in mooring lines 2 and 3.

Configuration AF3 - Regular Wave + Constant Wind at 0 deg													
#	Equilibrium Condition	Motions - CoG: Initial Position						Motions - Nacelle: Initial Position			Motions - MSL: Initial Position		
	Test/Laboratory Code	X [m]	Y [m]	Z [m]	roll [deg]	pitch [deg]	yaw [deg]	X [m]	Y [m]	Z [m]	X [m]	Y [m]	Z [m]
106	'FIH18-00014_AF3_RW_H2p75_T7p5_ABS_WDC10p5_01'	3.71	-0.02	0.53	0.29	-7.82	0.15	-16.14	-0.80	-0.83	2.22	-0.08	0.43
107	'FIH18-00014_AF3_RW_H2p75_T9_ABS_WDC10p5_00'	3.52	0.02	0.53	0.29	-7.82	0.21	-16.32	-0.80	-0.82	2.03	-0.04	0.43
108	'FIH18-00014_AF3_RW_H2p75_T11_ABS_WDC10p5_00'	3.50	0.00	0.53	0.28	-7.82	0.21	-16.36	-0.79	-0.82	2.00	-0.06	0.43
109	'FIH18-00014_AF3_RW_H2p75_T14_ABS_WDC10p5_00'	3.94	0.29	0.54	0.29	-7.83	0.21	-15.93	-0.52	-0.82	2.45	0.23	0.43
110	'FIH18-00014_AF3_RW_H2p75_T17_ABS_WDC10p5_00'	3.30	0.01	0.53	0.28	-7.84	0.19	-16.59	-0.79	-0.83	1.81	-0.05	0.43
111	'FIH18-00014_AF3_RW_H2p75_T20_ABS_WDC10p5_00'	4.00	0.25	0.51	0.29	-7.82	0.19	-15.84	-0.56	-0.84	2.51	0.19	0.41

Table 6-135. Configuration AF3: Combined Regular Wave and Constant Wind. Motions initial positions

Configuration AF3 - Regular Wave + Constant Wind at 0 deg				
#	Equilibrium Condition	Mooring Lines - Pretension [tonnes]		
	Test/Laboratory Code	LC1	LC2	LC3
106	'FIH18-00014_AF3_RW_H2p75_T7p5_ABS_WDC10p5_01'	90.81	53.41	52.91
107	'FIH18-00014_AF3_RW_H2p75_T9_ABS_WDC10p5_00'	90.40	53.66	53.17
108	'FIH18-00014_AF3_RW_H2p75_T11_ABS_WDC10p5_00'	90.47	53.60	53.08
109	'FIH18-00014_AF3_RW_H2p75_T14_ABS_WDC10p5_00'	90.88	53.67	53.35
110	'FIH18-00014_AF3_RW_H2p75_T17_ABS_WDC10p5_00'	91.12	53.97	53.32
111	'FIH18-00014_AF3_RW_H2p75_T20_ABS_WDC10p5_00'	90.19	53.53	53.65

Table 6-136. Configuration AF3: Combined Regular Wave and Constant Wind. Mooring system pretensions

Table 6-137, Table 6-138, Table 6-139 and Table 6-140 report the mean, maximum and minimum values of the platform motions. Considering the initial position, all cases with regular wave and constant rated wind result in a mean excursion over 15 m and a maximum excursion over 30 m in surge.

Configuration AF3 - Regular Wave + Constant Wind at 0 deg										
#	Test/Laboratory Code	Motions - CoG: Position								
		X [m]			Y [m]			Z [m]		
		mean	max	min	mean	max	min	mean	max	min
106	'FIH18-00014_AF3_RW_H2p75_T7p5_ABS_WDC10p5_01'	36.31	36.72	35.94	-0.68	-0.18	-1.06	0.32	0.50	0.16
107	'FIH18-00014_AF3_RW_H2p75_T9_ABS_WDC10p5_00'	35.41	35.93	34.91	-0.25	0.12	-0.69	0.33	0.66	-0.01
108	'FIH18-00014_AF3_RW_H2p75_T11_ABS_WDC10p5_00'	34.40	35.10	33.70	-0.32	-0.01	-0.54	0.33	0.79	-0.14
109	'FIH18-00014_AF3_RW_H2p75_T14_ABS_WDC10p5_00'	34.14	35.10	33.17	-0.67	-0.15	-1.02	0.33	0.74	-0.08
110	'FIH18-00014_AF3_RW_H2p75_T17_ABS_WDC10p5_00'	34.17	35.17	33.16	-0.77	-0.21	-1.28	0.32	0.93	-0.28
111	'FIH18-00014_AF3_RW_H2p75_T20_ABS_WDC10p5_00'	33.85	35.82	31.82	0.03	0.49	-0.50	0.32	2.06	-1.41

Table 6-137. Configuration AF3: Combined Regular Wave and Constant Wind. Displacements results in the CoG Position

Configuration AF3 - Regular Wave + Constant Wind at 0 deg										
#	Test/Laboratory Code	Motions - CoG: Position								
		roll [deg]			pitch [deg]			yaw [deg]		
		mean	max	min	mean	max	min	mean	max	min
106	'FIH18-00014_AF3_RW_H2p75_T7p5_ABS_WDC10p5_01'	0.55	0.61	0.50	-0.06	0.16	-0.29	0.82	1.43	0.26
107	'FIH18-00014_AF3_RW_H2p75_T9_ABS_WDC10p5_00'	0.56	0.63	0.50	-0.10	0.13	-0.32	0.98	1.35	0.57
108	'FIH18-00014_AF3_RW_H2p75_T11_ABS_WDC10p5_00'	0.55	0.59	0.52	-0.15	0.06	-0.35	1.09	1.54	0.66
109	'FIH18-00014_AF3_RW_H2p75_T14_ABS_WDC10p5_00'	0.55	0.62	0.50	-0.36	0.04	-0.76	1.00	1.38	0.68
110	'FIH18-00014_AF3_RW_H2p75_T17_ABS_WDC10p5_00'	0.55	0.62	0.47	-0.38	0.08	-0.89	0.94	1.22	0.64
111	'FIH18-00014_AF3_RW_H2p75_T20_ABS_WDC10p5_00'	0.51	0.57	0.46	-0.50	0.15	-1.18	1.03	1.27	0.79

Table 6-138. Configuration AF3: Combined Regular Wave and Constant Wind. Rotations results in the CoG Position

Configuration AF3 - Regular Wave + Constant Wind at 0 deg										
#	Test/Laboratory Code	Motions - Nacelle: Position								
		X [m]			Y [m]			Z [m]		
		mean	max	min	mean	max	min	mean	max	min
106	'FIH18-00014_AF3_RW_H2p75_T7p5_ABS_WDC10p5_01'	36.19	36.77	35.69	-2.09	-1.50	-2.50	0.32	0.49	0.15
107	'FIH18-00014_AF3_RW_H2p75_T9_ABS_WDC10p5_00'	35.20	35.42	35.00	-1.67	-1.34	-2.08	0.32	0.65	-0.01
108	'FIH18-00014_AF3_RW_H2p75_T11_ABS_WDC10p5_00'	34.06	34.66	33.54	-1.73	-1.46	-1.95	0.32	0.79	-0.15
109	'FIH18-00014_AF3_RW_H2p75_T14_ABS_WDC10p5_00'	33.27	34.53	31.95	-2.09	-1.56	-2.48	0.32	0.73	-0.10
110	'FIH18-00014_AF3_RW_H2p75_T17_ABS_WDC10p5_00'	33.24	34.30	32.20	-2.18	-1.57	-2.73	0.31	0.92	-0.28
111	'FIH18-00014_AF3_RW_H2p75_T20_ABS_WDC10p5_00'	32.60	34.23	30.82	-1.31	-0.82	-1.87	0.30	2.06	-1.43

Table 6-139. Configuration AF3: Combined Regular Wave and Constant Wind. Motions results in the Nacelle Position

Configuration AF3 - Regular Wave + Constant Wind at 0 deg										
#	Test/Laboratory Code	Motions - MSL: Position								
		X [m]			Y [m]			Z [m]		
		mean	max	min	mean	max	min	mean	max	min
106	'FIH18-00014_AF3_RW_H2p75_T7p5_ABS_WDC10p5_01'	36.30	36.69	35.96	-0.78	-0.29	-1.16	0.32	0.50	0.16
107	'FIH18-00014_AF3_RW_H2p75_T9_ABS_WDC10p5_00'	35.40	35.89	34.94	-0.36	0.01	-0.79	0.32	0.66	-0.01
108	'FIH18-00014_AF3_RW_H2p75_T11_ABS_WDC10p5_00'	34.38	35.06	33.70	-0.42	-0.12	-0.64	0.33	0.79	-0.14
109	'FIH18-00014_AF3_RW_H2p75_T14_ABS_WDC10p5_00'	34.08	35.03	33.10	-0.77	-0.26	-1.13	0.33	0.74	-0.08
110	'FIH18-00014_AF3_RW_H2p75_T17_ABS_WDC10p5_00'	34.10	35.05	33.14	-0.87	-0.31	-1.38	0.32	0.93	-0.28
111	'FIH18-00014_AF3_RW_H2p75_T20_ABS_WDC10p5_00'	33.75	35.66	31.80	-0.07	0.38	-0.60	0.32	2.06	-1.41

Table 6-140. Configuration AF3: Combined Regular Wave and Constant Wind. Motions results in the MSL Position

This set of tests provided the data necessary to obtain the Amplitude Response Operators (RAOs), which are illustrated in Figure 6-56, Figure 6-57 and Figure 6-58. RAOs in Heave present resonant peaks at $T = 20$ s, in agreement with the natural period of ACTIVEFLOAT platform in this DOF (Table 6-105).

ACTIVEFLOAT Configuration AF3: Regular Wave and Constant Wind - CoG

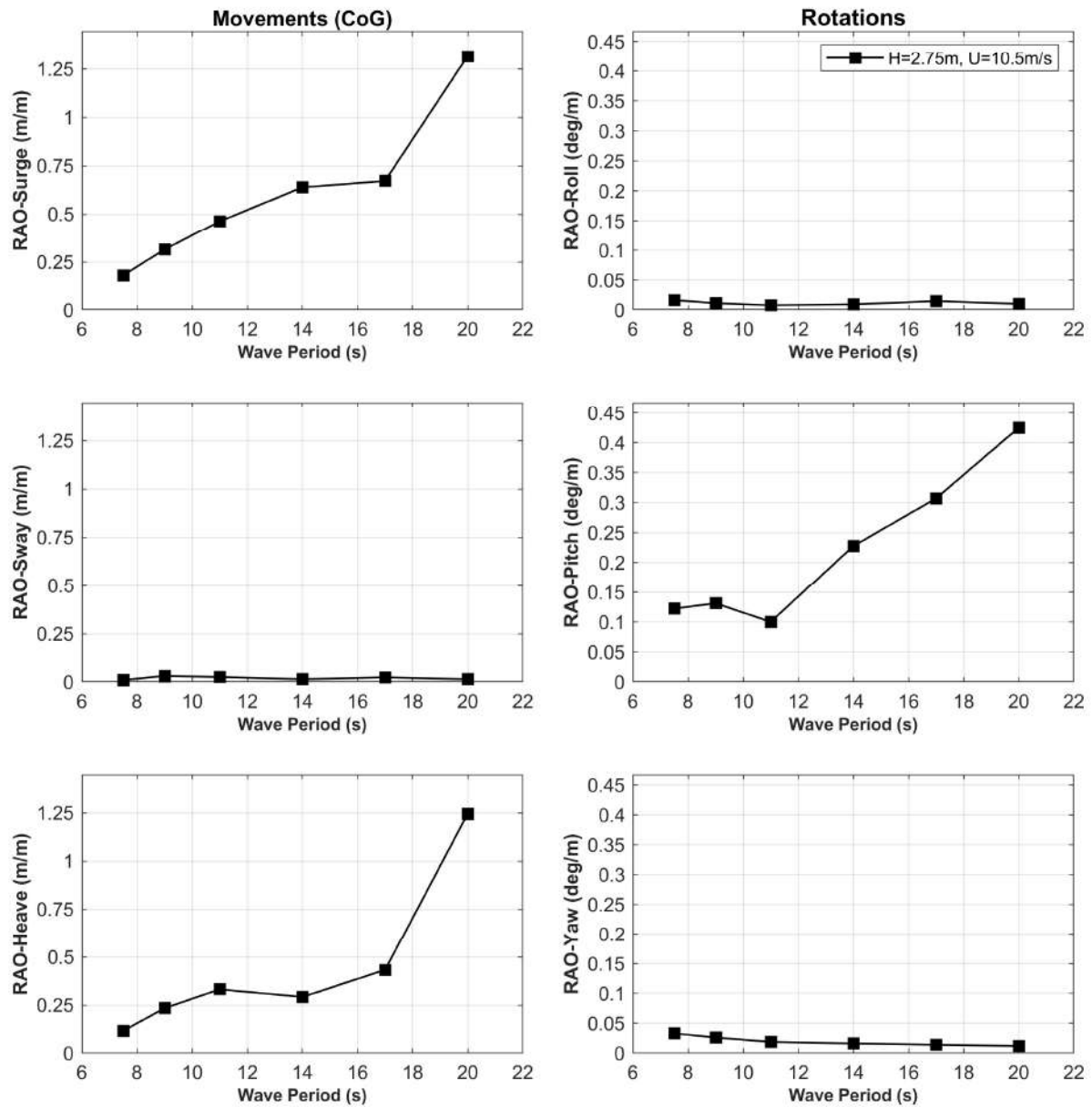


Figure 6-56. Configuration AF3: Combined Regular Wave and Constant Wind. RAO of motions (CoG)

ACTIVEFLOAT Configuration AF3: Regular Wave and Constant Wind - Nacelle

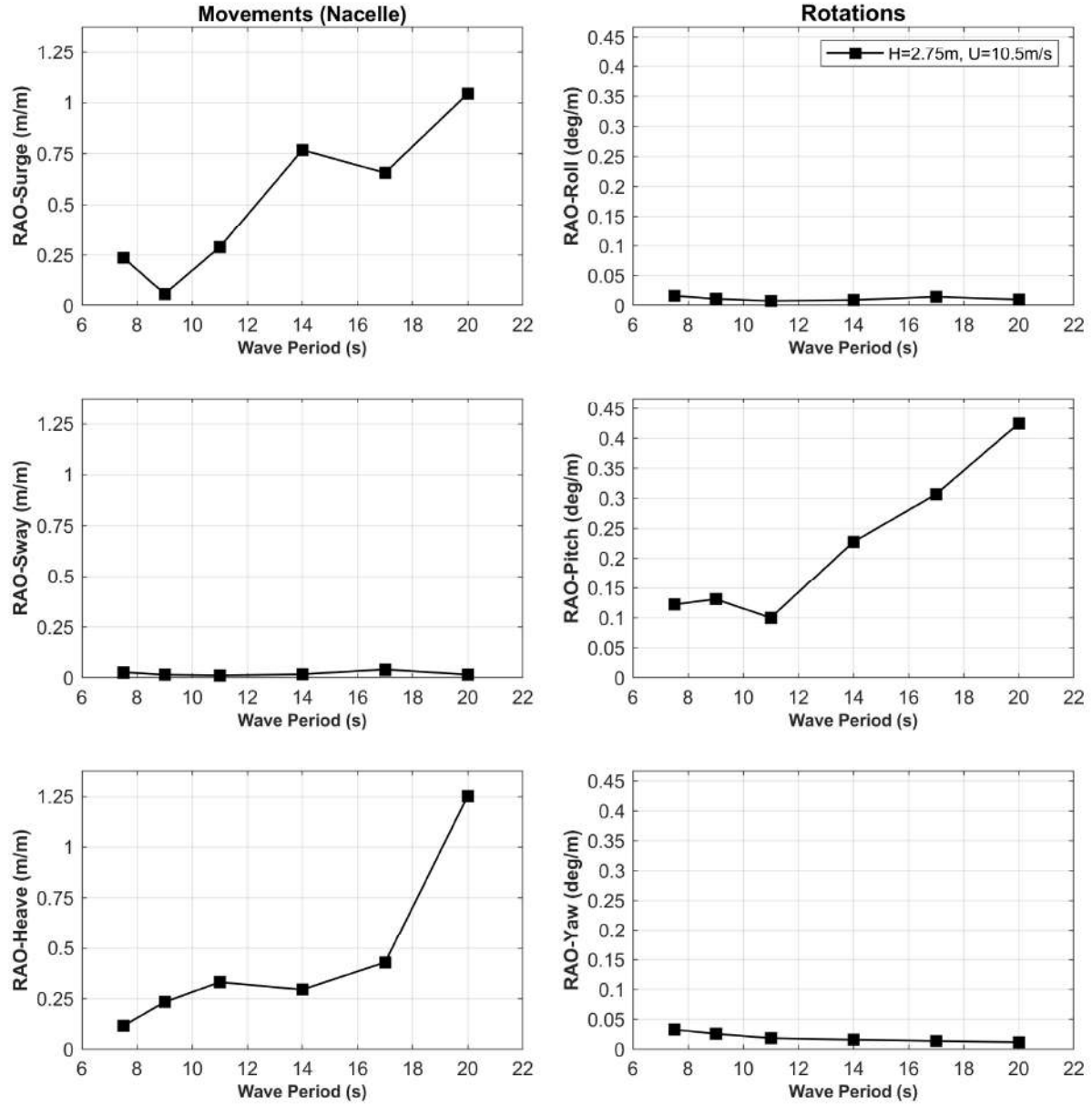


Figure 6-57. Configuration AF3: Combined Regular Wave and Constant Wind. RAO of motions (Nacelle)

ACTIVEFLOAT Configuration AF3: Regular Wave and Constant Wind - MSL

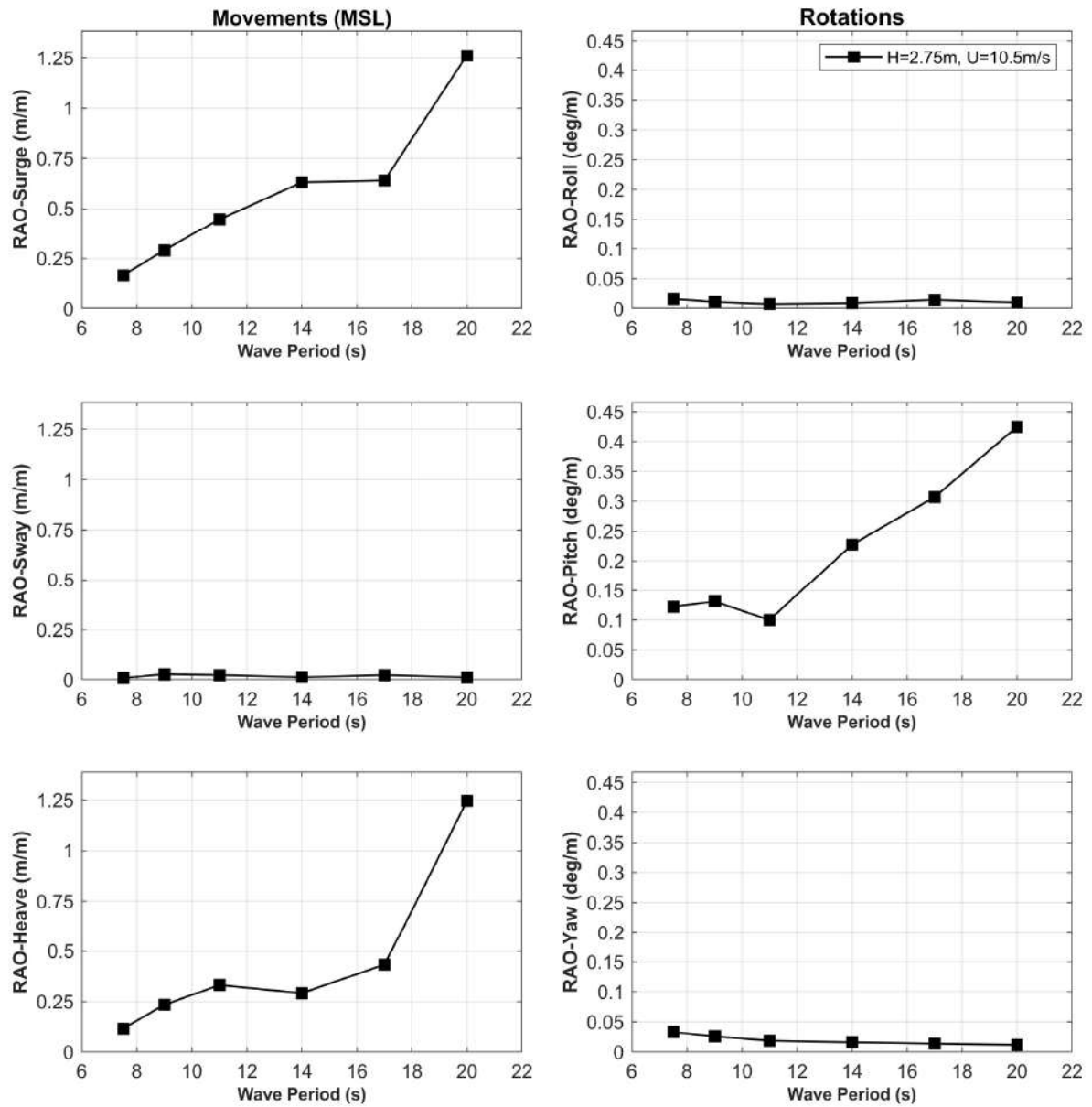


Figure 6-58. Configuration AF3: Combined Regular Wave and Constant Wind. RAO of motions (MSL)

Table 6-141 contains the information regarding the tensions recorded during the tests. The maximum tension in the main line 1 equal to 308 tonnes is reached in the case of $H = 2.75\text{ m}$ and $T = 7.5\text{ s}$ with constant rated wind.

Configuration AF3 - Regular Wave + Constant Wind at 0 deg										
#	Test/Laboratory Code	Mooring Lines - Load [tonnes]								
		LC1			LC2			LC3		
		mean	max	min	mean	max	min	mean	max	min
106	'FIH18-00014_AF3_RW_H2p75_T7p5_ABS_WDC10p5_01'	295.33	307.99	283.97	31.30	32.10	30.58	32.31	33.19	31.30
107	'FIH18-00014_AF3_RW_H2p75_T9_ABS_WDC10p5_00'	279.30	291.17	267.78	31.86	32.73	30.90	32.54	33.50	31.52
108	'FIH18-00014_AF3_RW_H2p75_T11_ABS_WDC10p5_00'	267.16	280.62	256.16	32.20	32.92	31.47	33.00	33.85	32.14
109	'FIH18-00014_AF3_RW_H2p75_T14_ABS_WDC10p5_00'	261.38	278.25	246.57	32.09	32.68	31.61	33.33	33.95	32.55
110	'FIH18-00014_AF3_RW_H2p75_T17_ABS_WDC10p5_00'	261.12	282.32	241.11	32.05	32.59	31.56	33.42	34.04	32.76
111	'FIH18-00014_AF3_RW_H2p75_T20_ABS_WDC10p5_00'	258.19	296.30	230.13	32.60	33.86	31.57	33.54	35.20	32.20

Table 6-141. Configuration WC2: Combined Regular Wave and Constant Wind. Mooring system results

The tensions as a function of wave period are shown in Figure 6-59.

ACTIVEFLOAT Configuration AF3: Regular Wave and Constant Wind - Mooring Lines

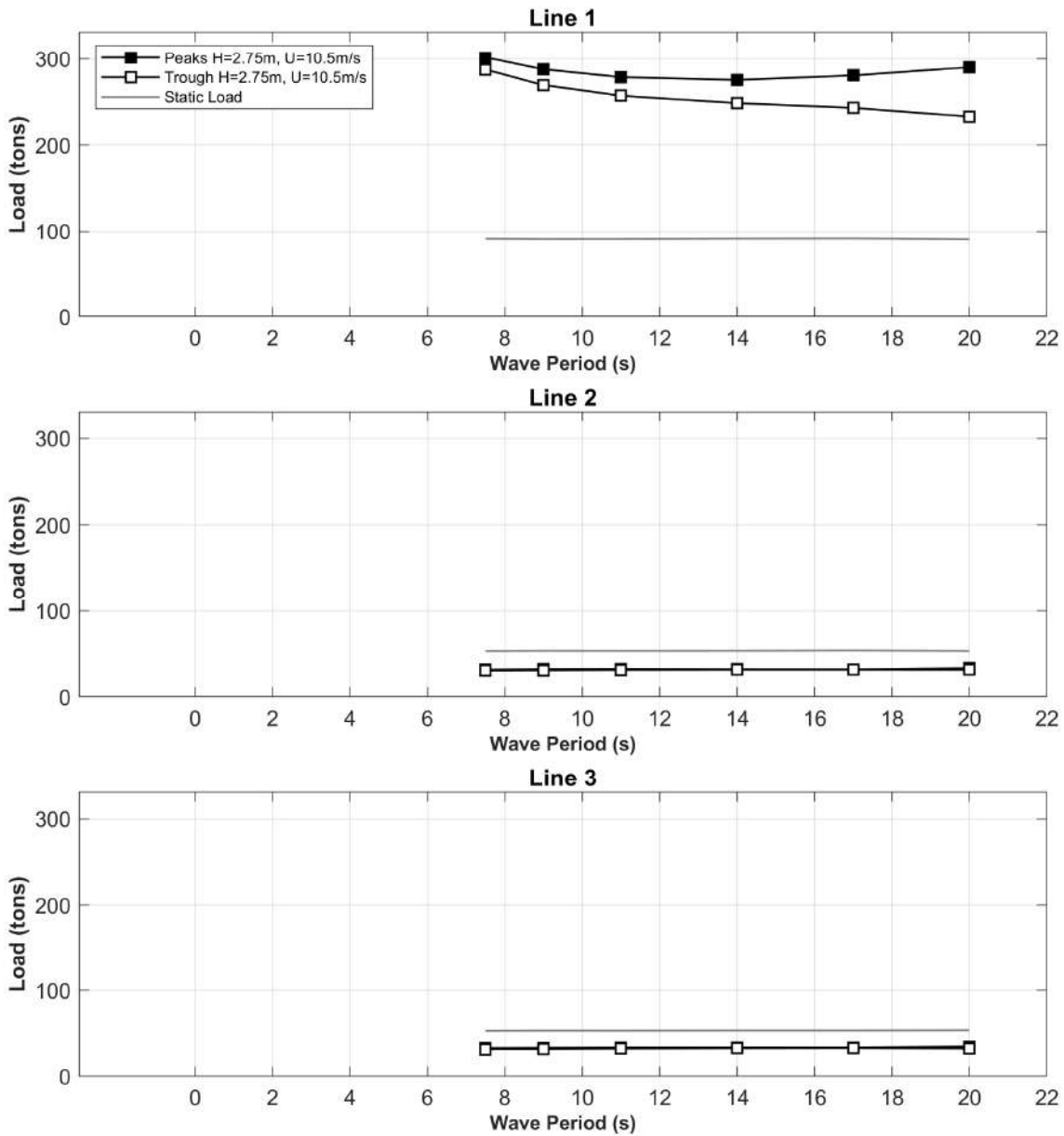


Figure 6-59. Configuration AF3: Combined Regular Wave and Constant Wind. Positive and Negative mean values of dynamic mooring loads

Table 6-142 and Figure 6-60 show the accelerations at the nacelle.

Configuration AF3 - Regular Wave + Constant Wind at 0 deg							
#	Test/Laboratory Code	Accelerations - Nacelle [m/s ²]					
		Acc. X		Acc. Y		Acc. Z	
		max	min	max	min	max	min
106	'FIH18-00014_AF3_RW_H2p75_T7p5_ABS_WDC10p5_01'	0.22	-0.28	0.11	0.01	0.08	-0.15
107	'FIH18-00014_AF3_RW_H2p75_T9_ABS_WDC10p5_00'	0.05	-0.08	0.07	0.03	0.13	-0.20
108	'FIH18-00014_AF3_RW_H2p75_T11_ABS_WDC10p5_00'	0.11	-0.18	0.06	0.03	0.13	-0.20
109	'FIH18-00014_AF3_RW_H2p75_T14_ABS_WDC10p5_00'	0.25	-0.25	0.08	0.02	0.06	-0.13
110	'FIH18-00014_AF3_RW_H2p75_T17_ABS_WDC10p5_00'	0.14	-0.19	0.08	0.02	0.05	-0.12
111	'FIH18-00014_AF3_RW_H2p75_T20_ABS_WDC10p5_00'	0.23	-0.22	0.07	0.00	0.14	-0.25

Table 6-142. Configuration AF3: Combined Regular Wave and Constant Wind. Accelerations results in the Nacelle Position

ACTIVEFLOAT Configuration AF3: Regular Wave and Constant Wind - Nacelle Accelerations

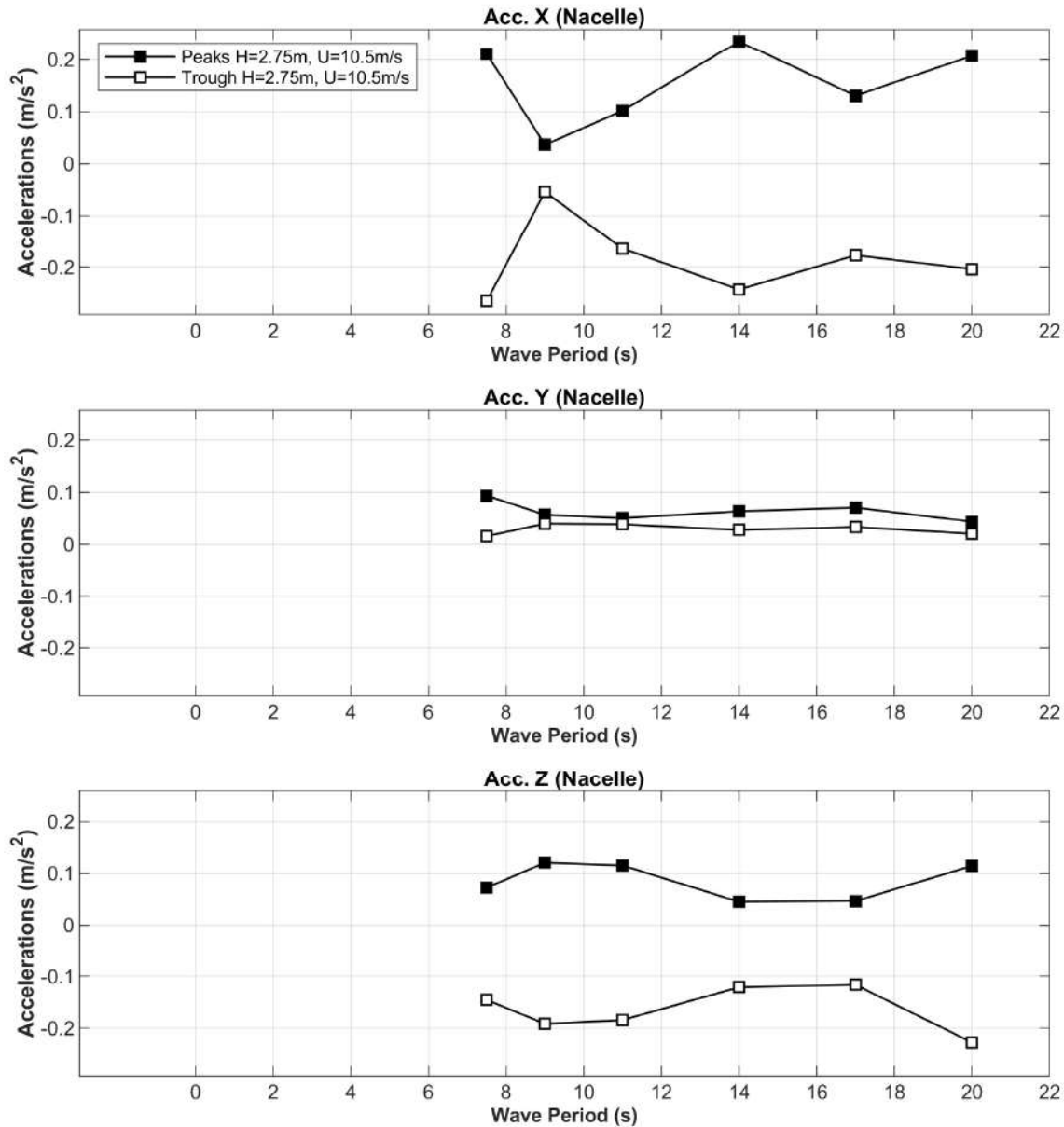


Figure 6-60. Configuration AF3: Combined Regular Wave and Constant Wind. Positive and Negative mean values of nacelle accelerations

Configuration AF3: Combined Irregular Wave and Wind at 0°

Table 6-143 summarizes the main characteristics of the incident sea state and rotor thrust force measured during the combined irregular wave and wind tests.

Configuration AF3 - Irregular Wave + Wind at 0 deg												
#	Test/Laboratory Code	h [m]	Hs [m]	Tp [s]	Spectrum	Gamma	Spread	Wind [m/s]	Thrust [tonnes]	Hinc [m]	Tinc [s]	Measured Thrust [tonnes]
112	'FIH18-00014_AF3_JS_H2p75_T9_G3p3_ABS_WDT10p5_TCETM_00'	120	2.75	9	JS	3.3	-	10.5 ETM	173.58	2.74	8.93	175.28
113	'FIH18-00014_AF3_JS_H5p11_T9_G1p2_ABS_WDT10p5_TCNTM_00'	120	5.11	9	JS	1.2	-	10.5 NTM	193.29	5.04	8.22	193.77
114	'FIH18-00014_AF3_JS_H2p75_T9_G3p3_S6_ABS_WDT10p5_TCETM_00'	120	2.75	9	JS	3.3	6	10.5 ETM	173.29	2.80	9.04	174.59
115	'FIH18-00014_AF3_JS_H2p75_T9_G3p3_S12_ABS_WDT10p5_TCETM_00'	120	2.75	9	JS	3.3	12	10.5 NTM	174.02	2.68	8.63	174.71

Table 6-143. Configuration AF3: Combined Irregular Wave and Wind. Incident Analysis

The data provided in the following two tables (see Table 6-144 and Table 6-145) report information about the initial position for each degree of freedom and mooring loads on the ACTIVEFLOAT floating wind turbine. The Pitch is around -7.8 degrees to reach 0 degrees when the thrust associated to constant rated wind is acting on. The tension in mooring line 1 is higher than the tensions in mooring lines 2 and 3.

Configuration AF3 - Irregular Wave + Wind at 0 deg													
#	Equilibrium Condition	Motions - CoG: Initial Position						Motions - Nacelle: Initial Position			Motions - MSL: Initial Position		
	Test/Laboratory Code	X [m]	Y [m]	Z [m]	roll [deg]	pitch [deg]	yaw [deg]	X [m]	Y [m]	Z [m]	X [m]	Y [m]	Z [m]
112	'FIH18-00014_AF3_JS_H2p75_T9_G3p3_ABS_WDT10p5_TCETM_00'	3.58	0.24	0.54	0.29	-7.81	0.25	-16.25	-0.58	-0.82	2.09	0.18	0.43
113	'FIH18-00014_AF3_JS_H5p11_T9_G1p2_ABS_WDT10p5_TCNTM_00'	3.83	0.29	0.53	0.28	-7.83	0.22	-16.04	-0.51	-0.83	2.34	0.23	0.43
114	'FIH18-00014_AF3_JS_H2p75_T9_G3p3_S6_ABS_WDT10p5_TCETM_00'	3.73	0.21	0.52	0.28	-7.81	0.21	-16.11	-0.58	-0.84	2.23	0.15	0.41
115	'FIH18-00014_AF3_JS_H2p75_T9_G3p3_S12_ABS_WDT10p5_TCETM_00'	3.84	0.24	0.52	0.28	-7.81	0.18	-15.99	-0.53	-0.84	2.35	0.19	0.42

Table 6-144. Configuration AF3: Combined Irregular Wave and Wind. Motions initial positions

Configuration AF3 - Irregular Wave + Wind at 0 deg					
#	Equilibrium Condition	Mooring Lines - Pretension [tonnes]			
	Test/Laboratory Code	LC1	LC2	LC3	
112	'FIH18-00014_AF3_JS_H2p75_T9_G3p3_ABS_WDT10p5_TCETM_00'	90.13	54.28	54.22	
113	'FIH18-00014_AF3_JS_H5p11_T9_G1p2_ABS_WDT10p5_TCNTM_00'	91.08	53.79	53.73	
114	'FIH18-00014_AF3_JS_H2p75_T9_G3p3_S6_ABS_WDT10p5_TCETM_00'	91.48	53.88	53.98	
115	'FIH18-00014_AF3_JS_H2p75_T9_G3p3_S12_ABS_WDT10p5_TCETM_00'	90.19	53.86	53.70	

Table 6-145. Configuration AF3: Combined Irregular Wave and Wind. Mooring system pretensions

Table 6-146, Table 6-147, Table 6-148 and Table 6-149 report the mean, minimum and maximum values of the platform motions for each degree of freedom recorded during the tests. Considering the initial position, all cases of combined irregular wave and wind result in a mean excursion over 15 m and a maximum excursion over 30 m in surge.

Configuration AF3 - Irregular Wave + Wind at 0 deg										
#	Test/Laboratory Code	Motions - CoG: Position								
		X [m]			Y [m]			Z [m]		
		mean	max	min	mean	max	min	mean	max	min
112	'FIH18-00014_AF3_JS_H2p75_T9_G3p3_ABS_WDT10p5_TCETM_00'	30.17	43.45	12.62	-0.14	1.37	-1.39	0.36	0.98	-0.19
113	'FIH18-00014_AF3_JS_H5p11_T9_G1p2_ABS_WDT10p5_TCNTM_00'	34.16	41.72	22.15	0.59	2.71	-1.37	0.33	1.44	-0.66
114	'FIH18-00014_AF3_JS_H2p75_T9_G3p3_S6_ABS_WDT10p5_TCETM_00'	30.06	43.70	11.83	-0.16	2.54	-3.37	0.35	1.04	-0.21
115	'FIH18-00014_AF3_JS_H2p75_T9_G3p3_S12_ABS_WDT10p5_TCETM_00'	30.09	43.74	11.36	-0.03	2.27	-2.96	0.34	0.86	-0.12

Table 6-146. Configuration AF3: Combined Irregular Wave and Wind. Displacements results in the CoG Position

Configuration AF3 - Irregular Wave + Wind at 0 deg										
#	Test/Laboratory Code	Motions - CoG: Position								
		roll [deg]			pitch [deg]			yaw [deg]		
		mean	max	min	mean	max	min	mean	max	min
112	'FIH18-00014_AF3_JS_H2p75_T9_G3p3_ABS_WDT10p5_TCETM_00'	0.48	0.69	0.21	-1.92	3.01	-7.69	0.93	2.96	-1.18
113	'FIH18-00014_AF3_JS_H5p11_T9_G1p2_ABS_WDT10p5_TCNTM_00'	0.49	0.84	0.17	-1.28	2.24	-5.21	1.04	2.43	-0.69
114	'FIH18-00014_AF3_JS_H2p75_T9_G3p3_S6_ABS_WDT10p5_TCETM_00'	0.46	0.96	0.03	-1.94	3.20	-8.01	0.91	4.24	-1.88
115	'FIH18-00014_AF3_JS_H2p75_T9_G3p3_S12_ABS_WDT10p5_TCETM_00'	0.46	0.86	0.11	-1.93	3.03	-7.86	0.89	3.95	-2.40

Table 6-147. Configuration AF3: Combined Irregular Wave and Wind. Rotations results in the CoG Position

Configuration AF3 - Irregular Wave + Wind at 0 deg										
#	Test/Laboratory Code	Motions - Nacelle: Position								
		X [m]			Y [m]			Z [m]		
		mean	max	min	mean	max	min	mean	max	min
112	'FIH18-00014_AF3_JS_H2p75_T9_G3p3_ABS_WDT10p5_TCETM_00'	25.32	41.88	0.84	-1.45	0.24	-2.86	0.22	0.91	-1.16
113	'FIH18-00014_AF3_JS_H5p11_T9_G1p2_ABS_WDT10p5_TCNTM_00'	30.93	42.34	13.60	-0.73	1.84	-3.10	0.26	1.44	-0.87
114	'FIH18-00014_AF3_JS_H2p75_T9_G3p3_S6_ABS_WDT10p5_TCETM_00'	25.14	42.55	-0.33	-1.42	1.67	-4.83	0.20	0.87	-1.00
115	'FIH18-00014_AF3_JS_H2p75_T9_G3p3_S12_ABS_WDT10p5_TCETM_00'	25.20	41.81	-0.48	-1.28	1.23	-4.46	0.20	0.77	-0.89

Table 6-148. Configuration AF3: Combined Irregular Wave and Wind. Motions results in the Nacelle Position

Configuration AF3 - Irregular Wave + Wind at 0 deg										
#	Test/Laboratory Code	Motions - MSL: Position								
		X [m]			Y [m]			Z [m]		
		mean	max	min	mean	max	min	mean	max	min
112	'FIH18-00014_AF3_JS_H2p75_T9_G3p3_ABS_WDT10p5_TCETM_00'	29.80	43.31	11.82	-0.24	1.29	-1.50	0.35	0.97	-0.22
113	'FIH18-00014_AF3_JS_H5p11_T9_G1p2_ABS_WDT10p5_TCNTM_00'	33.92	41.34	21.52	0.49	2.60	-1.47	0.33	1.44	-0.66
114	'FIH18-00014_AF3_JS_H2p75_T9_G3p3_S6_ABS_WDT10p5_TCETM_00'	29.69	43.45	10.99	-0.25	2.46	-3.47	0.34	1.01	-0.23
115	'FIH18-00014_AF3_JS_H2p75_T9_G3p3_S12_ABS_WDT10p5_TCETM_00'	29.72	43.50	10.57	-0.12	2.19	-3.05	0.33	0.85	-0.14

Table 6-149. Configuration AF3: Combined Irregular Wave and Wind. Motions results in the MSL Position

The spectral RAOs obtained through the coupled tests with irregular wave are shown in Figure 6-61, Figure 6-62 and Figure 6-63. These RAOs are in good agreement with the ones obtained through the coupled tests with regular wave tests (Figure 6-56, Figure 6-57 and Figure 6-58).

ACTIVEFLOAT Configuration AF3: Irregular Wave and Wind - CoG

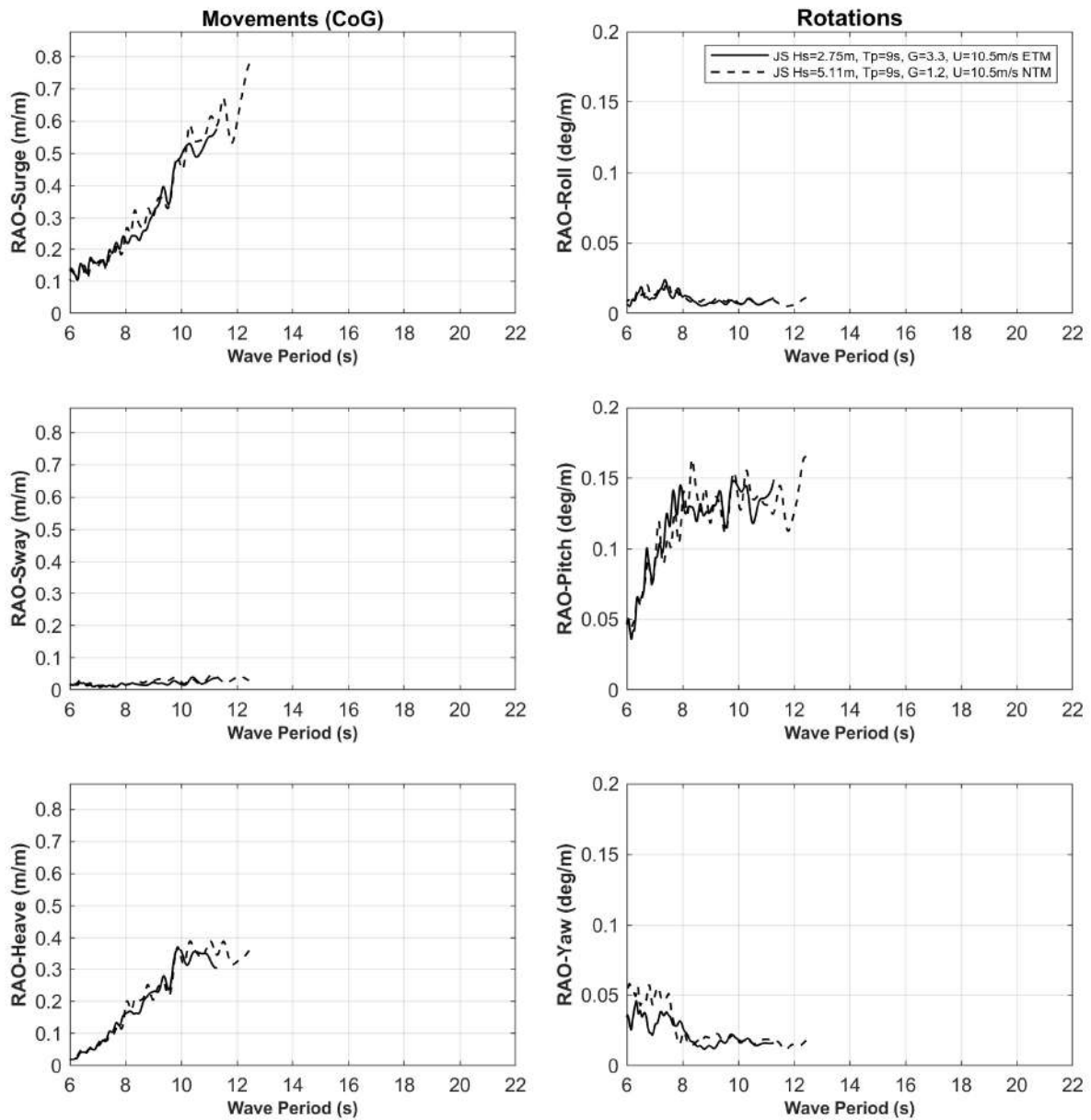


Figure 6-61. Configuration AF3: Combined Irregular Wave and Wind. RAO of motions (CoG)

ACTIVEFLOAT Configuration AF3: Irregular Wave and Wind - Nacelle

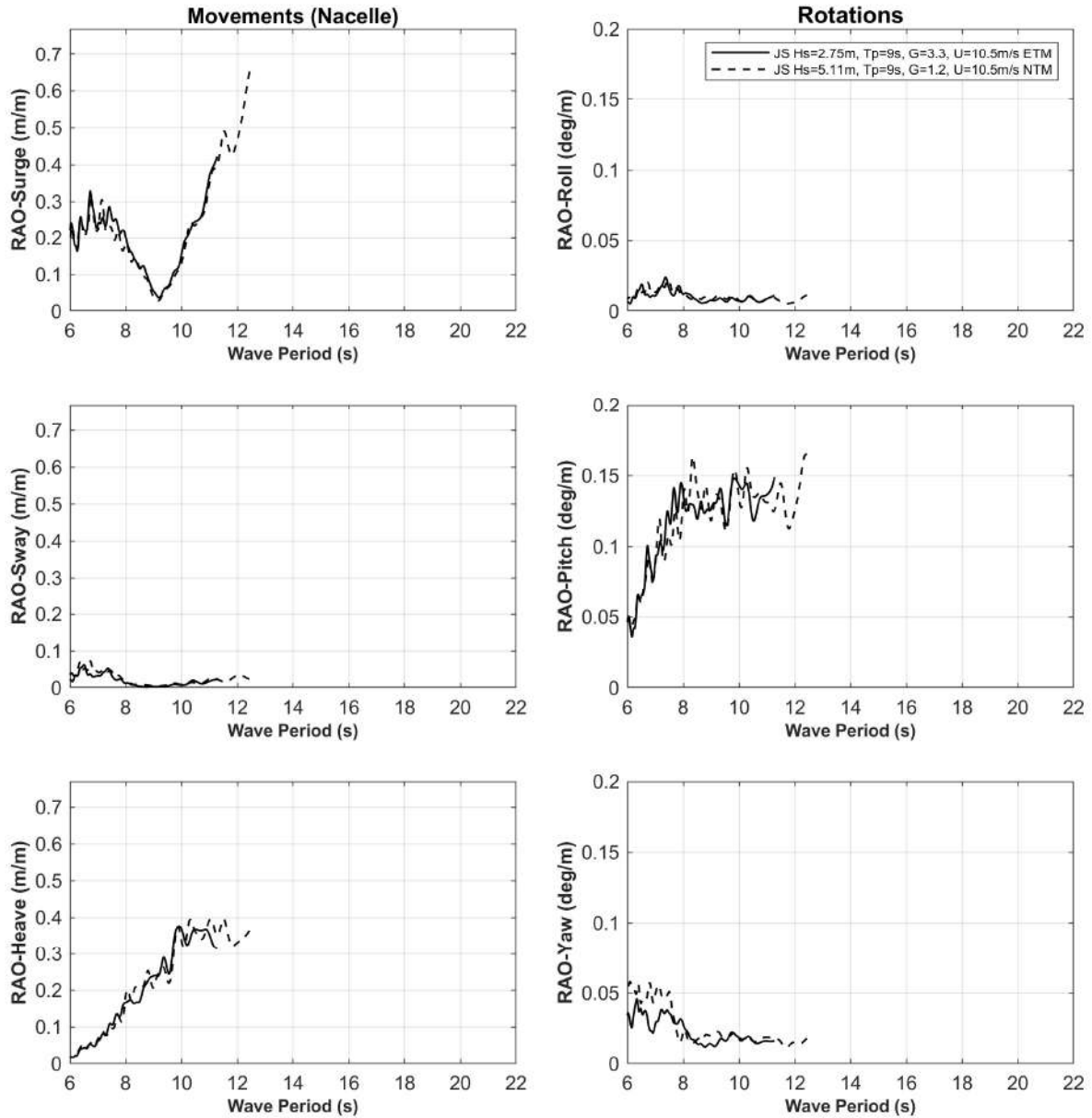


Figure 6-62. Configuration AF3: Combined Irregular Wave and Wind. RAO of motions (Nacelle)

ACTIVEFLOAT Configuration AF3: Irregular Wave and Wind - MSL

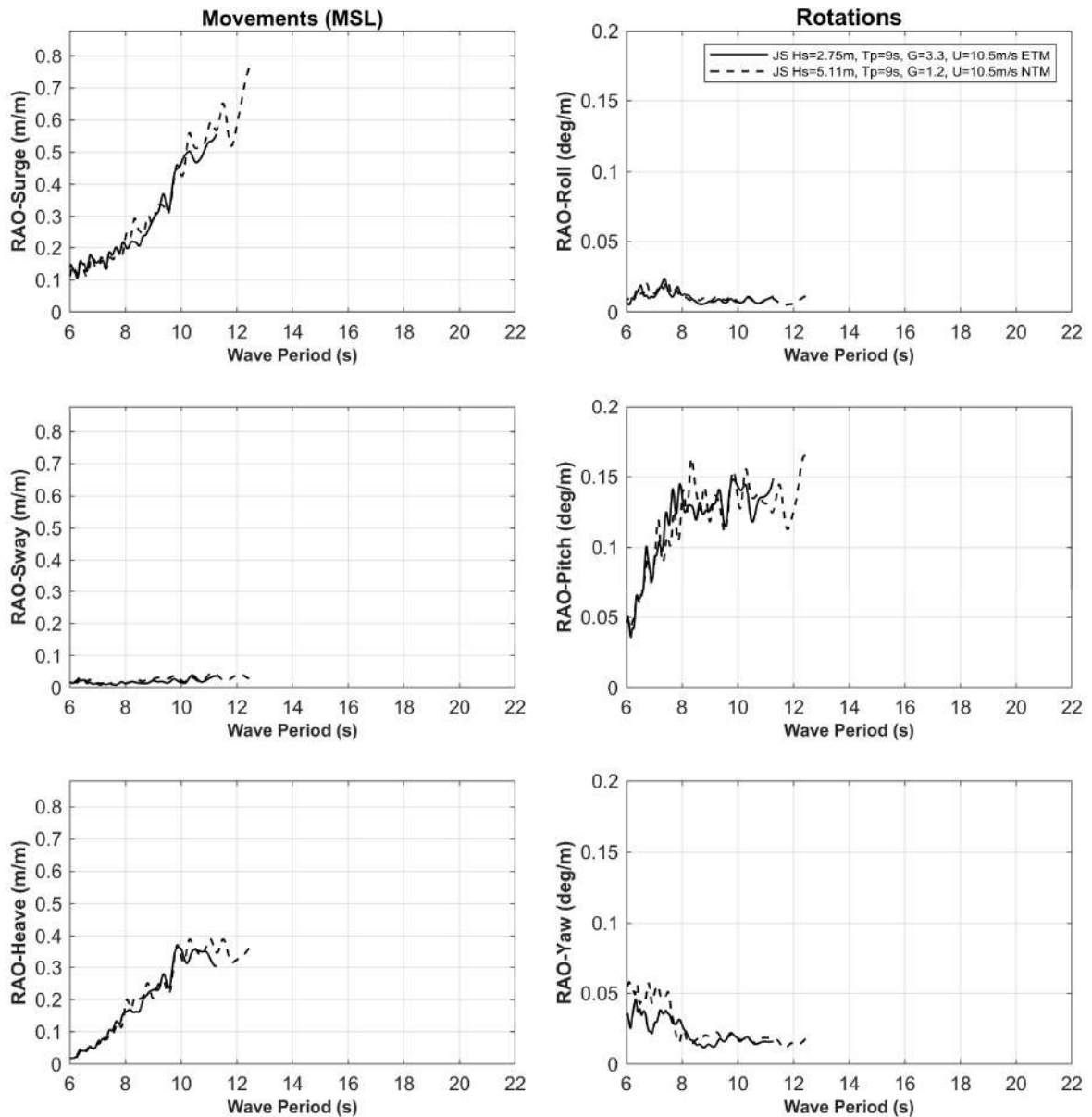


Figure 6-63. Configuration AF3: Combined Irregular Wave and Wind. RAO of motions (MSL)

Table 6-150 contains the information related to the tensions obtained during the execution of the tests. The maximum tension in the main line 1 equal to 449 tonnes is reached in the case of $H_s = 2.75\text{ m}$, $T_p = 9\text{ s}$, $\gamma = 3.3$ and $s = 6$ with rated wind with Extreme Turbulence Model.

Configuration AF3 - Irregular Wave + Wind at 0 deg										
#	Test/Laboratory Code	Mooring Lines - Load [tonnes]								
		LC1			LC2			LC3		
		mean	max	min	mean	max	min	mean	max	min
112	'FIH18-00014_AF3_JS_H2p75_T9_G3p3_ABS_WDT10p5_TCETM_00'	230.32	444.82	109.82	34.44	46.00	30.15	35.47	47.03	29.77
113	'FIH18-00014_AF3_JS_H5p11_T9_G1p2_ABS_WDT10p5_TCNTM_00'	267.51	428.87	149.15	33.16	38.98	29.76	33.36	40.79	29.21
114	'FIH18-00014_AF3_JS_H2p75_T9_G3p3_S6_ABS_WDT10p5_TCETM_00'	228.45	449.31	111.15	34.47	46.68	29.83	35.60	47.04	29.27
115	'FIH18-00014_AF3_JS_H2p75_T9_G3p3_S12_ABS_WDT10p5_TCETM_00'	227.92	439.37	104.56	34.48	47.74	30.11	35.43	47.47	29.53

Table 6-150. Configuration AF3: Combined Irregular Wave and Wind. Mooring system results

The accelerations at the nacelle are shown in Table 6-151.

Configuration AF3 - Irregular Wave + Wind at 0 deg									
#	Test/Laboratory Code	Accelerations - Nacelle [m/s ²]							
		Acc. X		Acc. Y		Acc. Z			
		max	min	max	min	max	min		
112	'FIH18-00014_AF3_JS_H2p75_T9_G3p3_ABS_WDT10p5_TCETM_00'	0.97	-0.62	0.13	-0.08	0.20	-0.27		
113	'FIH18-00014_AF3_JS_H5p11_T9_G1p2_ABS_WDT10p5_TCNTM_00'	0.78	-0.80	0.17	-0.16	0.33	-0.46		
114	'FIH18-00014_AF3_JS_H2p75_T9_G3p3_S6_ABS_WDT10p5_TCETM_00'	0.89	-0.63	0.25	-0.22	0.22	-0.31		
115	'FIH18-00014_AF3_JS_H2p75_T9_G3p3_S12_ABS_WDT10p5_TCETM_00'	1.10	-0.59	0.21	-0.22	0.15	-0.29		

Table 6-151. Configuration AF3: Combined Irregular Wave and Wind. Accelerations results in the Nacelle Position

Configuration AF3: Current at 0°

Table 6-152 provides the current characteristics reproduced during these tests, the average velocity value measured by the ADV placed at 60% of the basin depth from free surface.

Configuration AF3 – Current at 0 deg				
#	Test/Laboratory Code	h [m]	Current [m/s]	M. Current [m/s]
116	'FIH18-00014_AF3_SN0p168_26Hz_00'	120	1.06	1.05

Table 6-152. Configuration AF3: Current. Incident Analysis

The data provided in the following Table 6-153 and Table 6-154 report information about the initial position for each degree of freedom, as well as the mooring loads recorded. The tension in mooring line 1 is higher than the tensions in mooring lines 2 and 3.

Configuration AF3 – Current at 0 deg													
#	Equilibrium Condition	Motions - CoG: Initial Position						Motions - Nacelle: Initial Position			Motions - MSL: Initial Position		
	Test/Laboratory Code	X [m]	Y [m]	Z [m]	roll [deg]	pitch [deg]	yaw [deg]	X [m]	Y [m]	Z [m]	X [m]	Y [m]	Z [m]
116	'FIH18-00014_AF3_SN0p168_26Hz_00'	5.76	0.43	0.60	0.27	-7.94	-0.17	-14.41	-0.19	-0.80	4.24	0.38	0.49

Table 6-153. Configuration AF3: Current. Motions initial positions

Configuration AF3 – Current at 0 deg				
#	Equilibrium Condition	Mooring Lines - Pretension [tonnes]		
	Test/Laboratory Code	LC1	LC2	LC3
116	'FIH18-00014_AF3_SN0p168_26Hz_00'	88.52	54.44	55.30

Table 6-154. Configuration AF3: Current. Mooring system pretensions

Table 6-155, Table 6-156, Table 6-157 and Table 6-158 show mean, maximum and minimum values of motions related to the CoG, Nacelle and MSL positions. Surge values are higher when acting current. Considering the initial position, the current causes a maximum yaw over 15 degrees.

Configuration AF3 – Current at 0 deg										
#	Test/Laboratory Code	Motions - CoG: Position								
		X [m]			Y [m]			Z [m]		
		mean	max	min	mean	max	min	mean	max	min
116	'FIH18-00014_AF3_SN0p168_26Hz_00'	19.77	22.55	16.90	1.68	8.05	-10.03	0.47	0.57	0.38

Table 6-155. Configuration AF3: Current. Displacements results in the CoG Position

Configuration AF3 – Current at 0 deg										
#	Test/Laboratory Code	Motions - CoG: Position								
		roll [deg]			pitch [deg]			yaw [deg]		
		mean	max	min	mean	max	min	mean	max	min
116	'FIH18-00014_AF3_SN0p168_26Hz_00'	0.30	0.63	-0.09	-8.18	-7.81	-8.58	1.15	15.49	-13.11

Table 6-156. Configuration AF3: Current. Rotations results in the CoG Position

Configuration AF3 – Current at 0 deg										
#	Test/Laboratory Code	Motions - Nacelle: Position								
		X [m]			Y [m]			Z [m]		
		mean	max	min	mean	max	min	mean	max	min
116	'FIH18-00014_AF3_SN0p168_26Hz_00'	-0.90	2.25	-3.78	0.49	9.94	-11.11	-1.02	-0.87	-1.19

Table 6-157. Configuration AF3: Current. Motions results in the Nacelle Position

Configuration AF3 – Current at 0 deg										
#	Test/Laboratory Code	Motions - MSL: Position								
		X [m]			Y [m]			Z [m]		
		mean	max	min	mean	max	min	mean	max	min
116	'FIH18-00014_AF3_SN0p168_26Hz_00'	18.22	21.01	15.35	1.59	7.93	-10.11	0.36	0.45	0.26

Table 6-158. Configuration AF3: Current. Motions results in the MSL Position

Table 6-159 indicates the tensions obtained during the tests execution. In agreement with static offset tests in surge (Figure 6-3), mooring tensions are higher on windward lines and lower on leeward lines when acting current. The mean and maximum loads in the mooring line 1 are 161 tonnes and 195 tonnes, respectively.

Configuration AF3 – Current at 0 deg										
#	Test/Laboratory Code	Mooring Lines - Load [tonnes]								
		LC1			LC2			LC3		
		mean	max	min	mean	max	min	mean	max	min
116	'FIH18-00014_AF3_SN0p168_26Hz_00'	161.04	194.93	134.46	44.60	54.17	34.56	41.72	62.55	35.27

Table 6-159. Configuration AF3: Current. Mooring system results

Table 6-160 shows the accelerations at the nacelle with wind.

Configuration AF3 – Current at 0 deg							
#	Test/Laboratory Code	Accelerations - Nacelle [m/s ²]					
		Acc. X		Acc. Y		Acc. Z	
		max	min	max	min	max	min
116	'FIH18-00014_AF3_SN0p168_26Hz_00'	0.05	-0.04	0.03	-0.04	0.01	-0.01

Table 6-160. Configuration AF3: Current. Accelerations results in the Nacelle Position

Configuration AF3: Combined Irregular Wave and Current and Wind at 0°

Table 6-161 summarizes the main characteristics of the incident sea state and rotor thrust force measured during the combined irregular wave and current and wind tests.

Configuration AF3 - Irregular Wave + Current + Wind at 0 deg												
#	Test/Laboratory Code	h [m]	Hs [m]	Tp [s]	Spectrum	Gamma	Current [m/s]	Wind [m/s]	Thrust [tonnes]	Hinc [m]	Measured Current [m/s]	Measured Thrust [tonnes]
117	'FIH18-00014_AF3_JS_H2p75_T9_G1_SN0p168_WDT10p5_TCETM_26Hz_00'	120	2.75	9	'JS'	1.0	1.06	10.5	173.99	2.76	1.10	166.21
118	'FIH18-00014_AF3_JS_H5p11_T9_G1p2_SN0p168_WDT10p5_TCNTM_26Hz_00'	120	5.11	9	'JS'	1.2	1.06	10.5	193.63	5.28	1.03	184.70

Table 6-161. Configuration AF3: Combined Irregular Wave and Current and Wind. Incident Analysis

The data provided in the following two tables (see Table 6-162 and Table 6-163) report information about the initial position for each degree of freedom and mooring loads on the ACTIVEFLOAT floating wind turbine. The

Pitch is around -7.8 degrees to reach 0 degrees when the thrust associated to constant rated wind is acting on. The tension in mooring line 1 is higher than the tensions in mooring lines 2 and 3.

Configuration AF3 - Irregular Wave + Current + Wind at 0 deg													
#	Equilibrium Condition	Motions - CoG: Initial Position						Motions - Nacelle: Initial Position			Motions - MSL: Initial Position		
	Test/Laboratory Code	X [m]	Y [m]	Z [m]	roll [deg]	pitch [deg]	yaw [deg]	X [m]	Y [m]	Z [m]	X [m]	Y [m]	Z [m]
117	'FIH18-00014_AF3_JS_H2p75_T9_G1_SNOp168_WDT10p5_TCETM_26Hz_00'	6.74	0.75	0.56	0.29	-7.84	-0.06	-13.18	0.03	-0.80	5.24	0.70	0.46
118	'FIH18-00014_AF3_JS_H5p11_T9_G1p2_SNOp168_WDT10p5_TCNTM_26Hz_00'	5.73	0.61	0.56	0.29	-7.84	-0.41	-14.18	0.02	-0.80	4.23	0.56	0.46

Table 6-162. Configuration AF3: Combined Irregular Wave and Current and Wind. Motions initial positions

Configuration AF3 - Irregular Wave + Current + Wind at 0 deg					
#	Equilibrium Condition	Mooring Lines - Pretension [tonnes]			
	Test/Laboratory Code	LC1	LC2	LC3	
117	'FIH18-00014_AF3_JS_H2p75_T9_G1_SNOp168_WDT10p5_TCETM_26Hz_00'	87.31	53.01	54.51	
118	'FIH18-00014_AF3_JS_H5p11_T9_G1p2_SNOp168_WDT10p5_TCNTM_26Hz_00'	87.53	53.78	54.62	

Table 6-163. Configuration AF3: Combined Irregular Wave and Current and Wind. Mooring system pretensions

Table 6-164, Table 6-165, Table 6-166 and Table 6-167 report the mean, minimum and maximum values of the platform motions for each degree of freedom recorded during the tests. Considering the initial position, all cases of combined irregular wave and current and wind result in a mean excursion over 15 m and a maximum excursion over 30 m in surge.

Configuration AF3 - Irregular Wave + Current + Wind at 0 deg										
#	Test/Laboratory Code	Motions - CoG: Position								
		X [m]			Y [m]			Z [m]		
		mean	max	min	mean	max	min	mean	max	min
117	'FIH18-00014_AF3_JS_H2p75_T9_G1_SNOp168_WDT10p5_TCETM_26Hz_00'	36.28	43.35	29.34	1.98	18.78	-16.31	0.28	0.87	-0.31
118	'FIH18-00014_AF3_JS_H5p11_T9_G1p2_SNOp168_WDT10p5_TCNTM_26Hz_00'	39.55	47.19	33.48	3.38	22.19	-14.44	0.26	1.84	-1.23

Table 6-164. Configuration AF3: Combined Irregular Wave and Current and Wind. Displacements results in the CoG Position

Configuration AF3 - Irregular Wave + Current + Wind at 0 deg										
#	Test/Laboratory Code	Motions - CoG: Position								
		roll [deg]			pitch [deg]			yaw [deg]		
		mean	max	min	mean	max	min	mean	max	min
117	'FIH18-00014_AF3_JS_H2p75_T9_G1_SNOp168_WDT10p5_TCETM_26Hz_00'	0.53	0.99	-0.18	-2.12	2.78	-8.03	1.44	12.53	-9.76
118	'FIH18-00014_AF3_JS_H5p11_T9_G1p2_SNOp168_WDT10p5_TCNTM_26Hz_00'	0.54	1.28	-0.20	-1.45	2.06	-5.43	1.22	9.87	-6.70

Table 6-165. Configuration AF3: Combined Irregular Wave and Current and Wind. Rotations results in the CoG Position

Configuration AF3 - Irregular Wave + Current + Wind at 0 deg										
#	Test/Laboratory Code	Motions - Nacelle: Position								
		X [m]			Y [m]			Z [m]		
		mean	max	min	mean	max	min	mean	max	min
117	'FIH18-00014_AF3_JS_H2p75_T9_G1_SNOp168_WDT10p5_TCETM_26Hz_00'	30.93	46.82	16.39	0.49	16.95	-17.73	0.13	0.79	-1.09
118	'FIH18-00014_AF3_JS_H5p11_T9_G1p2_SNOp168_WDT10p5_TCNTM_26Hz_00'	35.89	46.28	24.10	1.93	20.29	-15.39	0.18	1.84	-1.36

Table 6-166. Configuration AF3: Combined Irregular Wave and Current and Wind. Motions results in the Nacelle Position

Configuration AF3 - Irregular Wave + Current + Wind at 0 deg										
#	Test/Laboratory Code	Motions - MSL: Position								
		X [m]			Y [m]			Z [m]		
		mean	max	min	mean	max	min	mean	max	min
117	'FIH18-00014_AF3_JS_H2p75_T9_G1_SNOp168_WDT10p5_TCETM_26Hz_00'	35.88	43.11	28.37	1.87	18.64	-16.41	0.27	0.86	-0.33
118	'FIH18-00014_AF3_JS_H5p11_T9_G1p2_SNOp168_WDT10p5_TCNTM_26Hz_00'	39.27	46.94	33.25	3.27	21.97	-14.49	0.25	1.84	-1.24

Table 6-167. Configuration AF3: Combined Irregular Wave and Current and Wind. Motions results in the MSL Position

The spectral RAOs obtained through the coupled tests with irregular wave are shown in Figure 6-64, Figure 6-65 and Figure 6-66.

ACTIVEFLOAT Configuration AF3: Irregular Wave and Current and Wind - CoG

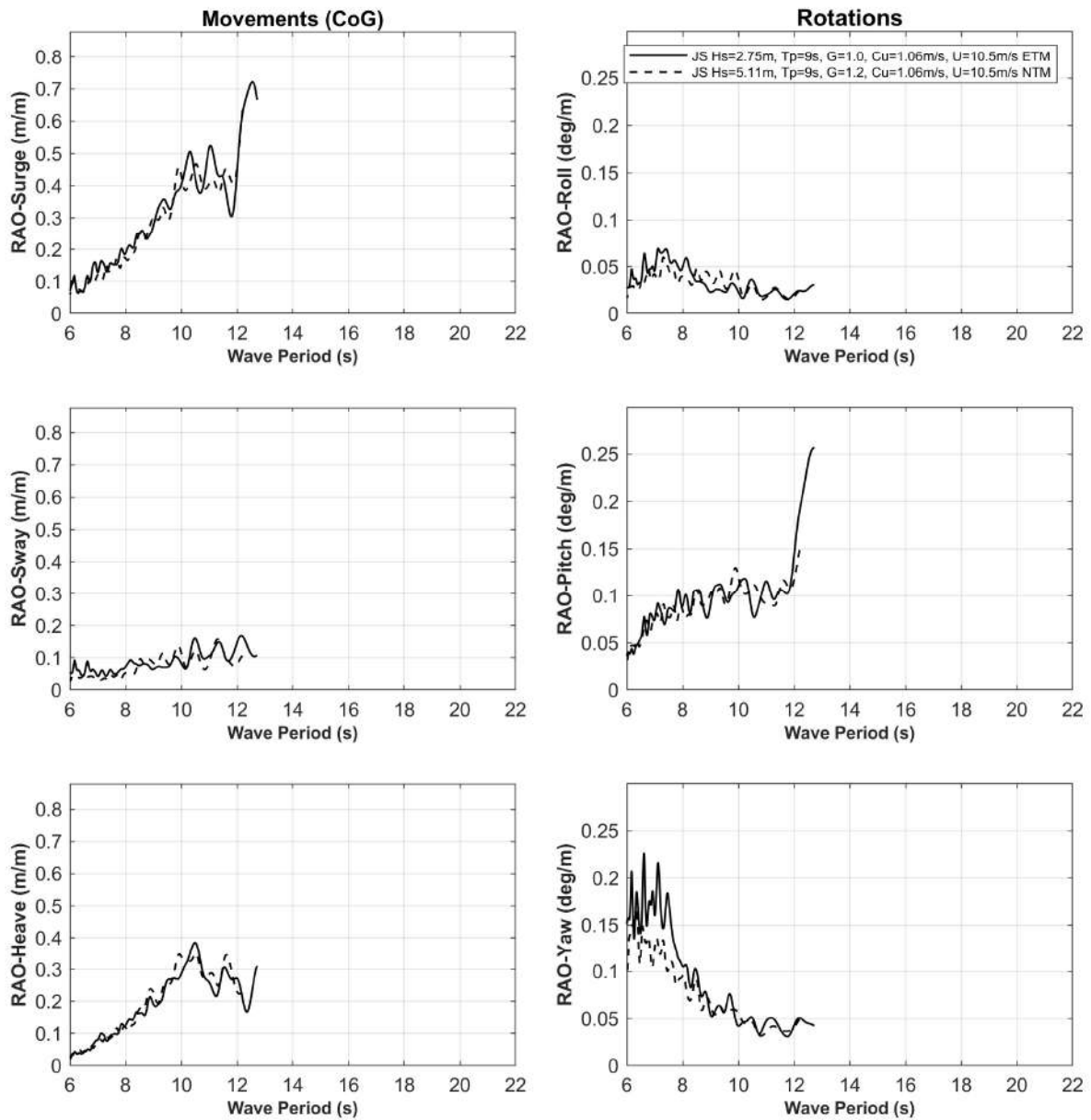


Figure 6-64. Configuration AF3: Combined Irregular and Current Wave and Wind. RAO of motions (CoG)

ACTIVEFLOAT Configuration AF3: Irregular Wave and Current and Wind - Nacelle

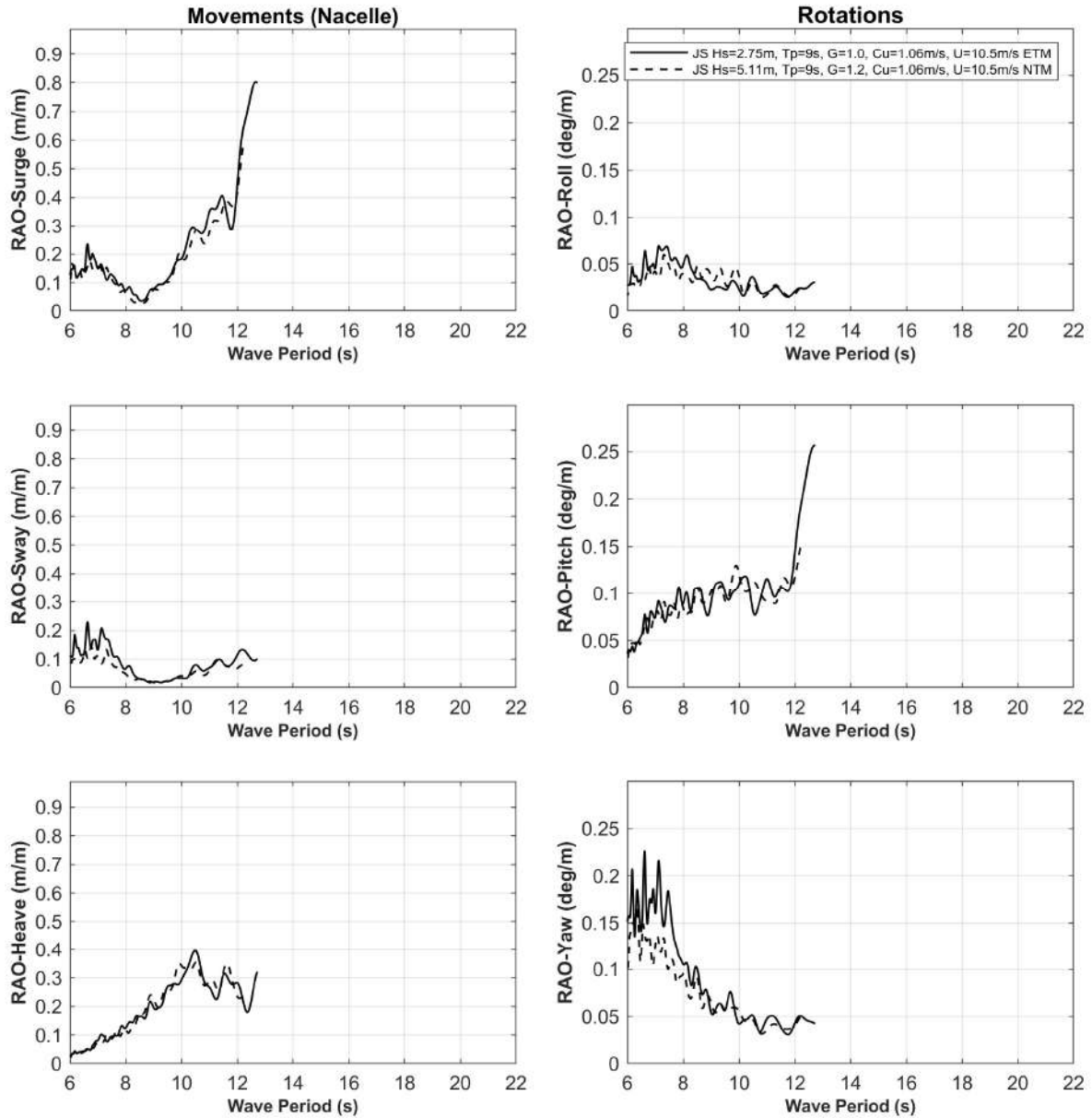


Figure 6-65. Configuration AF3: Combined Irregular Wave and Current and Wind. RAO of motions (Nacelle)

ACTIVEFLOAT Configuration AF3: Irregular Wave and Current and Wind - MSL

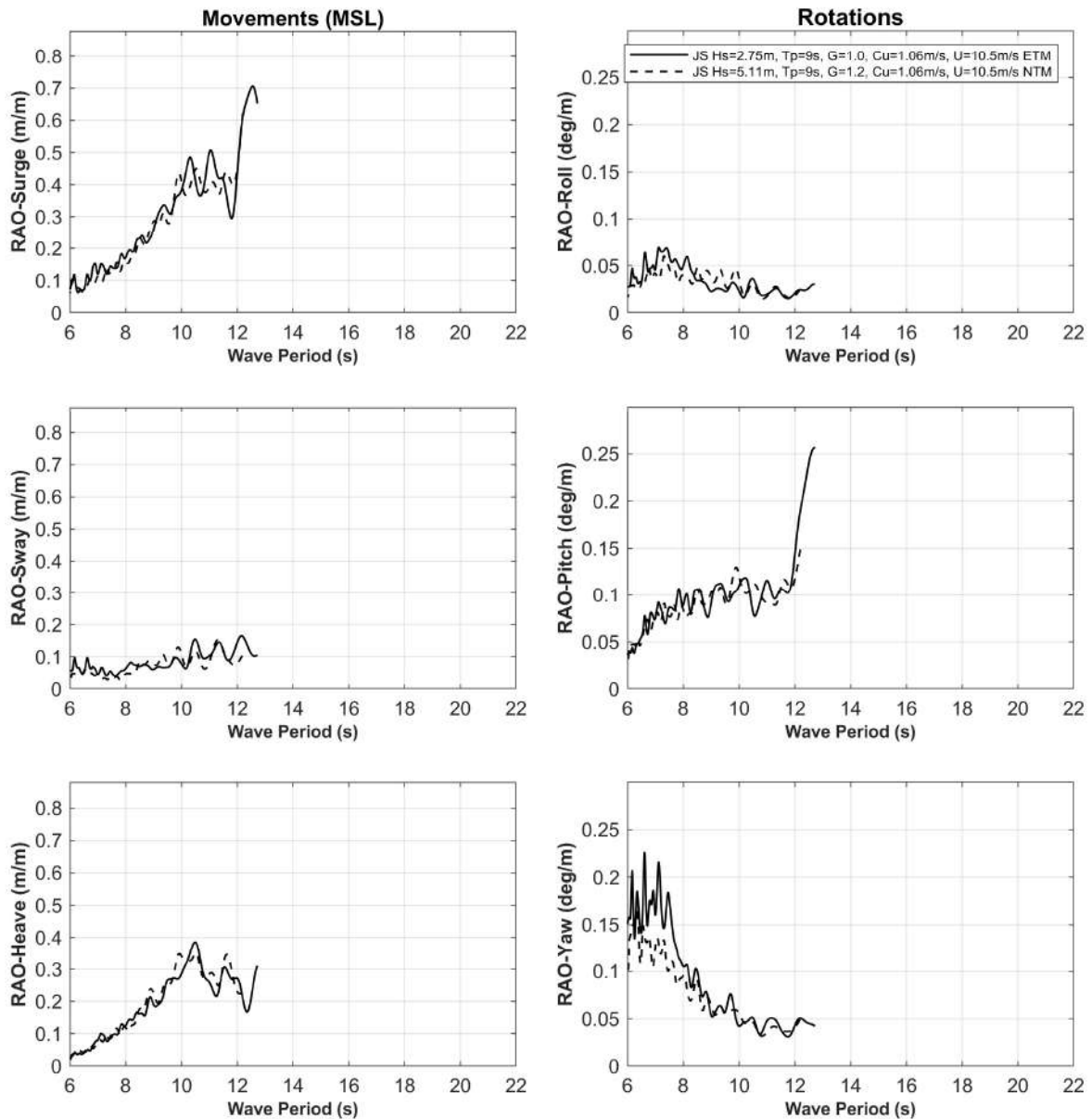


Figure 6-66. Configuration AF3: Combined Irregular Wave and Current and Wind. RAO of motions (MSL)

Table 6-168 contains the information related to the tensions obtained during the execution of the tests. The maximum tension in the main line 1 equal to 541 tonnes is reached in the case of $H_s = 5.11\text{ m}$, $T_p = 9\text{ s}$, $\gamma = 1.2$ with current and rated wind with Normal Turbulence Model.

Configuration AF3 - Irregular Wave + Current + Wind at 0 deg										
#	Test/Laboratory Code	Mooring Lines - Load [tonnes]								
		LC1			LC2			LC3		
		mean	max	min	mean	max	min	mean	max	min
117	'FIH18-00014_AF3_JS_H2p75_T9_G1_SN0p168_WDT10p5_TCETM_26Hz_00'	298.99	455.87	196.68	34.80	57.10	25.48	33.59	51.34	24.90
118	'FIH18-00014_AF3_JS_H5p11_T9_G1p2_SN0p168_WDT10p5_TCNTM_26Hz_00'	349.89	540.59	246.26	34.45	59.67	24.83	32.06	46.27	23.03

Table 6-168. Configuration AF3: Combined Irregular Wave and Current and Wind. Mooring system results

The accelerations at the nacelle are shown in Table 6-169.

Configuration AF3 - Irregular Wave + Current + Wind at 0 deg							
#	Test/Laboratory Code	Accelerations - Nacelle [m/s ²]					
		Acc. X		Acc. Y		Acc. Z	
		max	min	max	min	max	min
117	'FIH18-00014_AF3_JS_H2p75_T9_G1_SNOp168_WDT10p5_TCETM_26Hz_00'	0.89	-0.62	0.39	-0.30	0.22	-0.25
118	'FIH18-00014_AF3_JS_H5p11_T9_G1p2_SNOp168_WDT10p5_TCNTM_26Hz_00'	0.93	-0.77	0.50	-0.41	0.45	-0.58

Table 6-169. Configuration AF3: Combined Irregular Wave and Current and Wind. Accelerations results in the Nacelle Position

6.2.4 Installation Tests

Configuration AF0: Irregular Wave during Installation

Table 6-170 summarizes the main statistics of the incident sea states considered.

Configuration AF0 - Irregular Wave during Installation									
#	Test/Laboratory Code	h [m]	Hs [m]	Tp [s]	Spectrum	Gamma	Spread	Hinc [m]	Tinc [s]
119	'FIH18-00014_AF0_JS_H2p75_T9_G1_ABS_00'	120	2.75	9	JS	1.0	-	2.74	8.93
120	'FIH18-00014_AF0_JS_H2p75_T11_G1_ABS_00'	120	2.75	11	JS	1.0	-	2.77	11.02
121	'FIH18-00014_AF0_JS_H2p75_T14_G1_ABS_00'	120	2.75	14	JS	1.0	-	2.80	14.00

Table 6-170. Configuration AF0: Irregular Wave during Installation. Incident Analysis

The initial position as well as the soft-mooring line pretensions are summarized on the next two tables (see Table 6-171 and Table 6-172). The static position of the CoG of ACTIVEFLOAT with no ballast has a Z around -0.25 m because of the actual higher draft than 12 m. The tensions in all the soft-mooring lines are equal.

Configuration AF0 - Irregular Wave during Installation													
#	Equilibrium Condition	Motions - CoG: Initial Position						Motions - Nacelle: Initial Position			Motions - MSL: Initial Position		
	Test/Laboratory Code	X [m]	Y [m]	Z [m]	roll [deg]	pitch [deg]	yaw [deg]	X [m]	Y [m]	Z [m]	X [m]	Y [m]	Z [m]
119	'FIH18-00014_AF0_JS_H2p75_T9_G1_ABS_00'	-0.39	-1.35	-0.27	0.49	-0.20	1.48	-0.84	-2.56	-0.27	-0.37	-1.25	-0.27
120	'FIH18-00014_AF0_JS_H2p75_T11_G1_ABS_00'	0.31	-1.45	-0.26	0.50	-0.19	1.34	-0.12	-2.70	-0.26	0.33	-1.35	-0.25
121	'FIH18-00014_AF0_JS_H2p75_T14_G1_ABS_00'	-0.27	-1.89	-0.21	0.49	-0.21	1.53	-0.75	-3.10	-0.22	-0.25	-1.79	-0.21

Table 6-171. Configuration AF0: Irregular Wave during Installation. Motions initial positions

Configuration AF0 - Irregular Wave during Installation					
#	Equilibrium Condition	Mooring Lines - Pretension [tonnes]			
	Test/Laboratory Code	LC1	LC2	LC3	LC4
119	'FIH18-00014_AF0_JS_H2p75_T9_G1_ABS_00'	54.53	54.62	53.36	54.19
120	'FIH18-00014_AF0_JS_H2p75_T11_G1_ABS_00'	56.30	54.94	55.17	54.87
121	'FIH18-00014_AF0_JS_H2p75_T14_G1_ABS_00'	54.84	54.38	53.81	54.23

Table 6-172. Configuration AF0: Irregular Wave during Installation. Mooring system pretensions

Figure 6-67 shows this initial position of the platform in the wave basin for Installation tests.



Figure 6-67. Initial position for Installation tests

Table 6-173, Table 6-174, Table 6-175 and Table 6-176 show mean, maximum and minimum values of motions related to the CoG, Nacelle and MSL positions.

Configuration AF0 - Irregular Wave during Installation										
#	Test/Laboratory Code	Motions - CoG: Position								
		X [m]			Y [m]			Z [m]		
		mean	max	min	mean	max	min	mean	max	min
119	'FIH18-00014_AF0_JS_H2p75_T9_G1_ABS_00'	1.86	5.01	-0.70	-1.33	-0.54	-1.92	-0.37	0.58	-1.61
120	'FIH18-00014_AF0_JS_H2p75_T11_G1_ABS_00'	1.67	6.68	-2.57	-1.37	-0.65	-2.22	-0.36	1.10	-2.12
121	'FIH18-00014_AF0_JS_H2p75_T14_G1_ABS_00'	0.80	4.05	-1.97	-1.31	-0.57	-1.94	-0.27	1.76	-2.48

Table 6-173. Configuration AF0: Irregular Wave during Installation. Displacements results in the CoG Position

Configuration AF0 - Irregular Wave during Installation										
#	Test/Laboratory Code	Motions - CoG: Position								
		roll [deg]			pitch [deg]			yaw [deg]		
		mean	max	min	mean	max	min	mean	max	min
119	'FIH18-00014_AF0_JS_H2p75_T9_G1_ABS_00'	0.40	0.67	0.07	-0.46	1.09	-2.73	1.39	2.11	0.58
120	'FIH18-00014_AF0_JS_H2p75_T11_G1_ABS_00'	0.39	0.70	0.09	-0.60	0.91	-2.96	1.40	2.18	0.64
121	'FIH18-00014_AF0_JS_H2p75_T14_G1_ABS_00'	0.40	0.69	0.11	-0.61	1.09	-2.88	1.49	2.08	0.93

Table 6-174. Configuration AF0: Irregular Wave during Installation. Rotations results in the CoG Position

Configuration AF0 - Irregular Wave during Installation										
#	Test/Laboratory Code	Motions - Nacelle: Position								
		X [m]			Y [m]			Z [m]		
		mean	max	min	mean	max	min	mean	max	min
119	'FIH18-00014_AF0_JS_H2p75_T9_G1_ABS_00'	0.76	7.16	-3.93	-2.33	-1.23	-3.29	-0.38	0.55	-1.65
120	'FIH18-00014_AF0_JS_H2p75_T11_G1_ABS_00'	0.24	8.54	-5.51	-2.36	-1.36	-3.57	-0.37	1.04	-2.26
121	'FIH18-00014_AF0_JS_H2p75_T14_G1_ABS_00'	-0.66	5.27	-5.34	-2.33	-1.39	-3.29	-0.28	1.75	-2.52

Table 6-175. Configuration AF0: Irregular Wave during Installation. Motions results in the Nacelle Position

Configuration AF0 - Irregular Wave during Installation										
#	Test/Laboratory Code	Motions - MSL: Position								
		X [m]			Y [m]			Z [m]		
		mean	max	min	mean	max	min	mean	max	min
119	'FIH18-00014_AF0_JS_H2p75_T9_G1_ABS_00'	1.92	5.09	-0.70	-1.25	-0.47	-1.83	-0.37	0.58	-1.60
120	'FIH18-00014_AF0_JS_H2p75_T11_G1_ABS_00'	1.76	6.81	-2.48	-1.29	-0.58	-2.13	-0.36	1.11	-2.11
121	'FIH18-00014_AF0_JS_H2p75_T14_G1_ABS_00'	0.89	4.17	-1.90	-1.23	-0.48	-1.87	-0.26	1.76	-2.47

Table 6-176. Configuration AF0: Irregular Wave during Installation. Motions results in the MSL Position

The spectral RAOs shown in Figure 6-68, Figure 6-69 and Figure 6-70 are obtained through the irregular wave tests, using the equation presented in previous section 4.8.4 Statistical analysis.

ACTIVEFLOAT Configuration AF0 during Installation: Irregular Wave - CoG

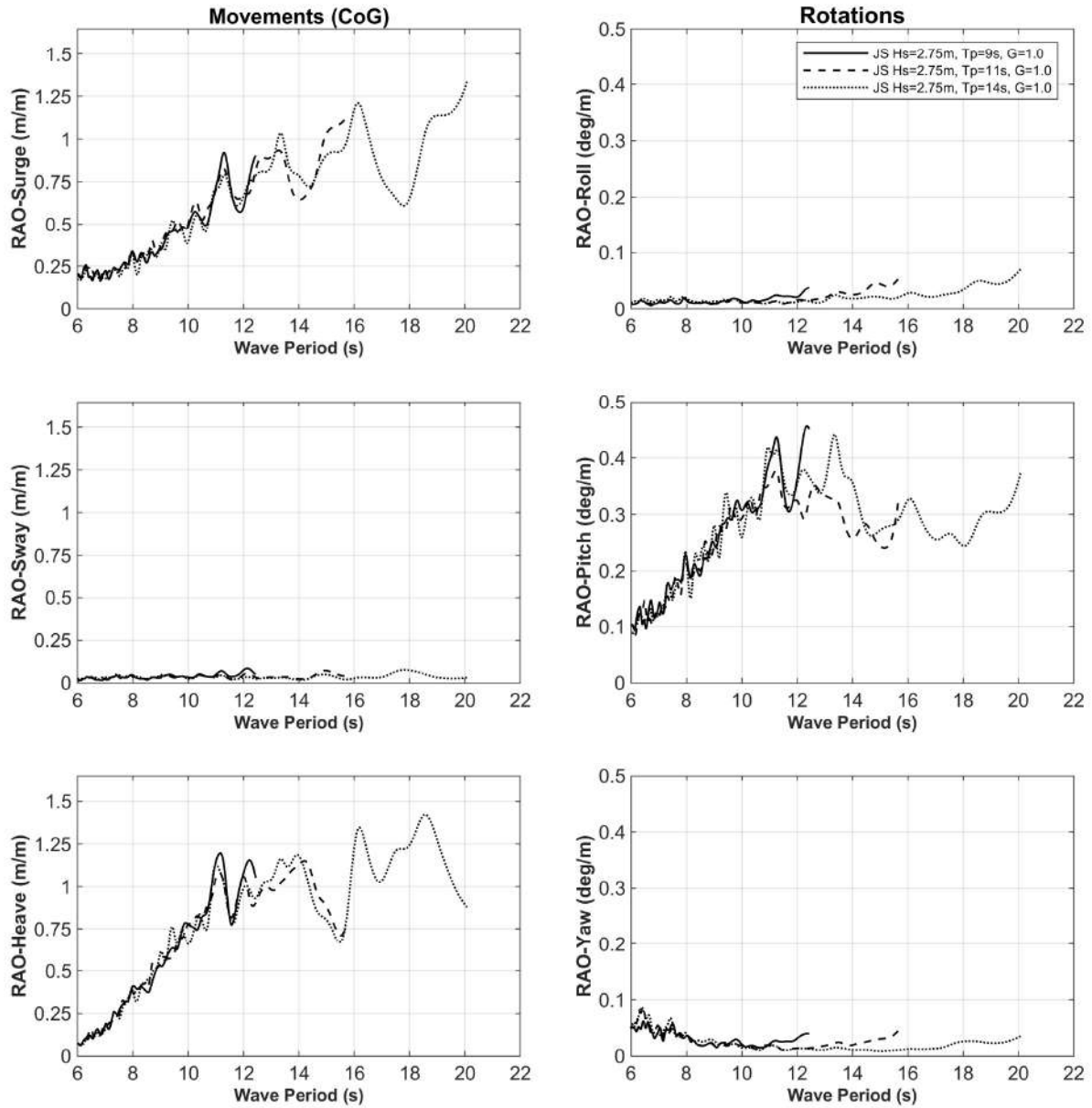


Figure 6-68. Configuration AF0: Irregular Wave during Installation. RAO of motions (CoG)

ACTIVEFLOAT Configuration AF0 during Installation: Irregular Wave - Nacelle

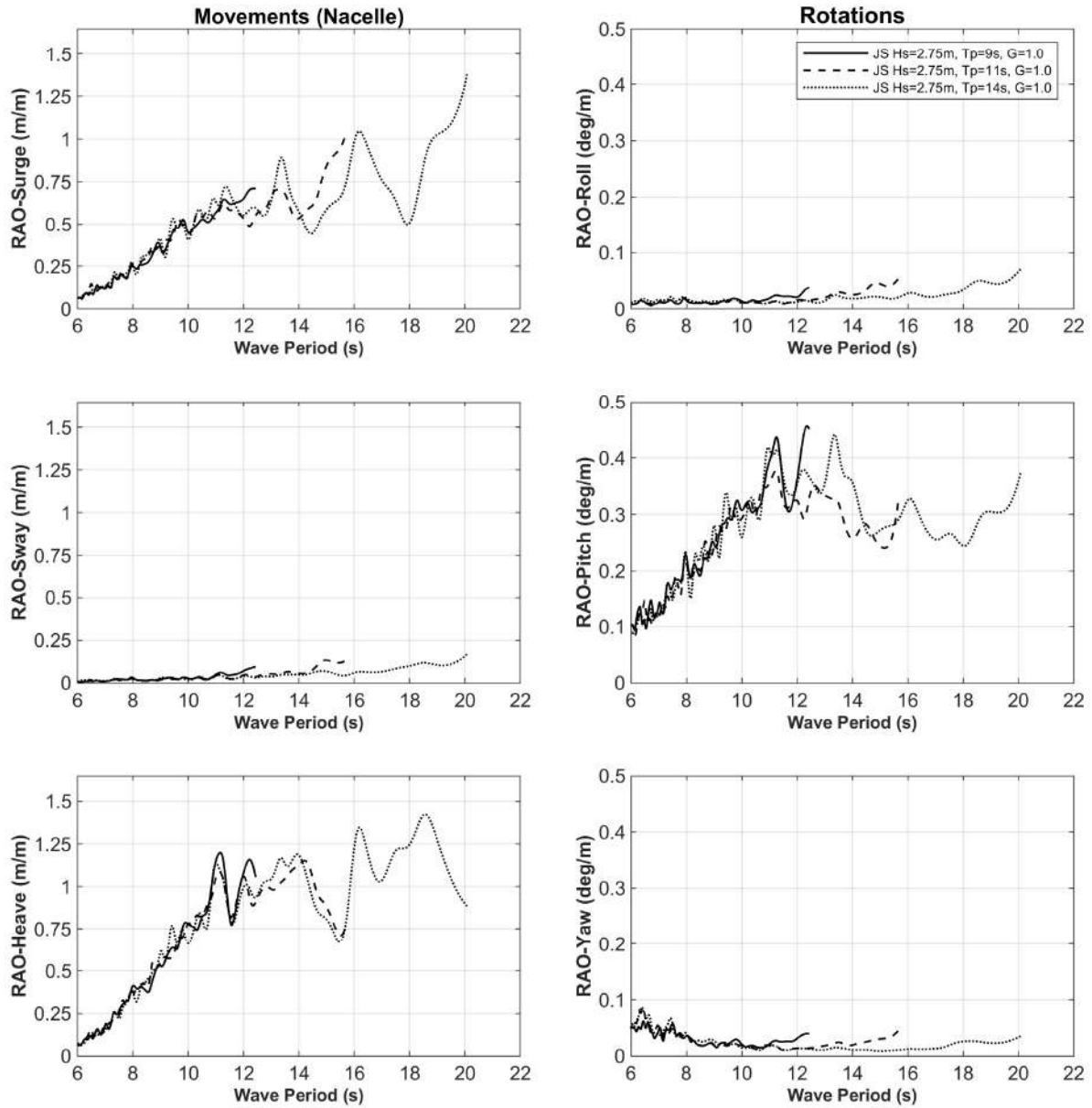


Figure 6-69. Configuration AF0: Irregular Wave during Installation. RAO of motions (Nacelle)

ACTIVEFLOAT Configuration AF0 during Installation: Irregular Wave - MSL

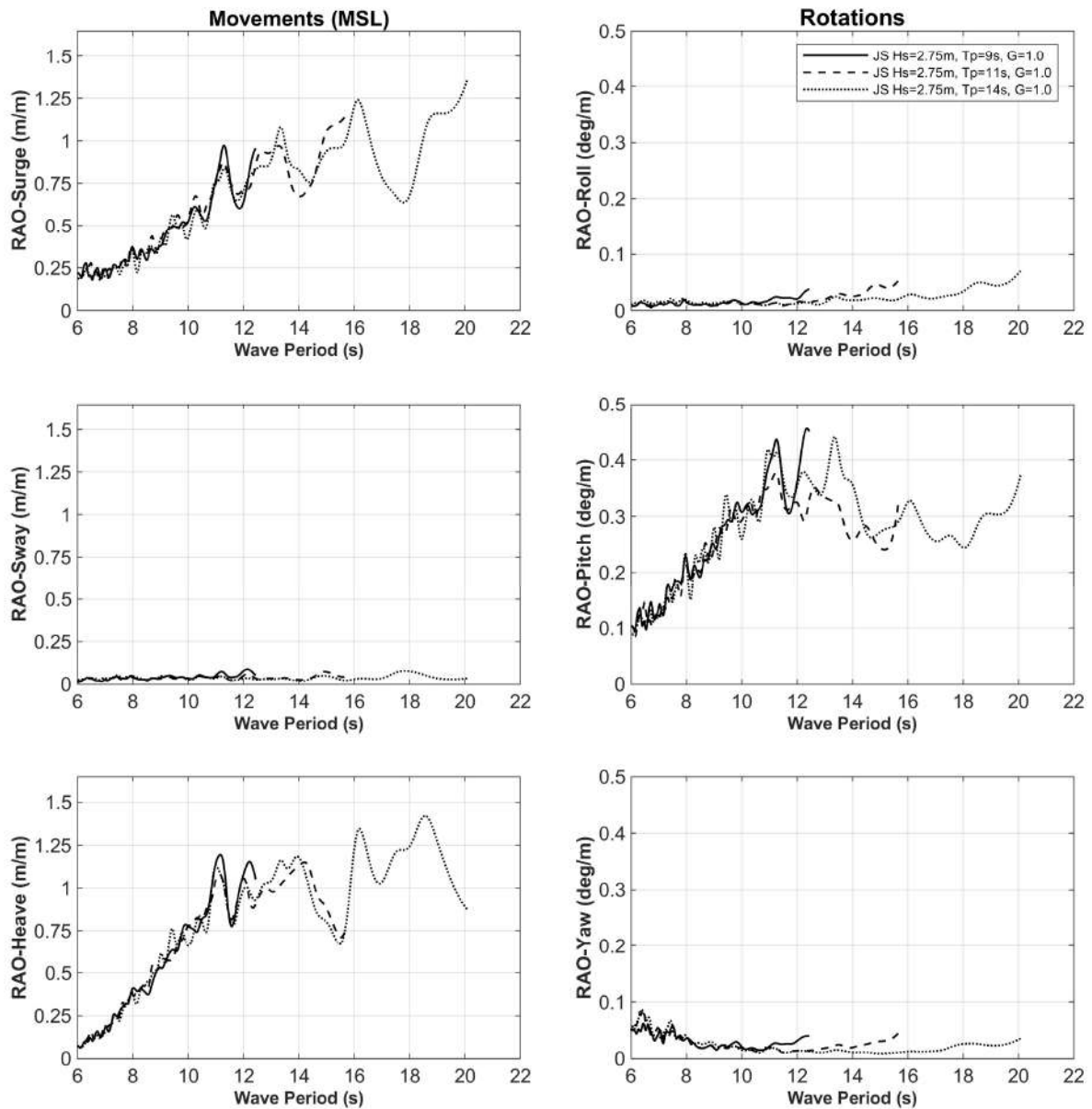


Figure 6-70. Configuration AF0: Irregular Wave during Installation. RAO of motions (MSL)

Table 6-177 indicates the tensions obtained during the tests carried out.

Configuration AF0 - Irregular Wave during Installation													
#	Test/Laboratory Code	Mooring Lines - Load [tonnes]											
		LC1			LC2			LC3			LC4		
		mean	max	min	mean	max	min	mean	max	min	mean	max	min
119	'FIH18-00014_AF0_JS_H2p75_T9_G1_ABS_00'	57.77	72.06	48.88	57.57	67.59	49.73	51.73	62.10	43.40	52.11	64.02	42.30
120	'FIH18-00014_AF0_JS_H2p75_T11_G1_ABS_00'	57.67	73.04	47.52	57.48	69.43	48.96	51.97	60.47	41.62	52.44	64.69	41.68
121	'FIH18-00014_AF0_JS_H2p75_T14_G1_ABS_00'	56.62	71.52	48.29	56.52	66.25	48.53	53.04	60.92	44.88	53.35	64.53	43.01

Table 6-177. Configuration AF0: Irregular Wave during Installation. Mooring system results

Table 6-111 shows the accelerations at the nacelle.

Configuration AF0 - Irregular Wave during Installation							
#	Test/Laboratory Code	Accelerations - Nacelle [m/s ²]					
		Acc. X		Acc. Y		Acc. Z	
		max	min	max	min	max	min
119	'FIH18-00014_AF0_JS_H2p75_T9_G1_ABS_00'	0.39	-0.44	0.05	-0.06	0.45	-0.39
120	'FIH18-00014_AF0_JS_H2p75_T11_G1_ABS_00'	0.47	-0.48	0.05	-0.06	0.54	-0.54
121	'FIH18-00014_AF0_JS_H2p75_T14_G1_ABS_00'	0.44	-0.49	0.05	-0.06	0.57	-0.52

Table 6-178. Configuration AF0: Irregular Wave during Installation. Accelerations results in the Nacelle Position

Configuration AF0: White Noise during Installation

Spectral RAOs are also obtained through a white noise test whose wave spectrum characteristics are presented in Table 6-179. During this test, the platform is hit by irregular waves defined by a limited white noise spectrum between the periods of 7.5 and 22 seconds.

Configuration AF0 – White Noise during Installation						
#	Test/Laboratory Code	h [m]	Hs [m]	T1 [s]	T2 [s]	Hinc [m]
122	'FIH18-00014_AF0_TH_H2p75_T11p19_DF0p088_ABS_00'	120	2.75	7.5	22	2.68

Table 6-179. Configuration AF0 during Installation: White Noise

The spectral RAOs obtained through the white noise test are shown in Figure 6-71, Figure 6-72 and Figure 6-73. These RAOs are in good agreement with the ones obtained through the irregular wave tests (Figure 6-68, Figure 6-69 and Figure 6-70).

ACTIVEFLOAT Configuration AF0 during Installation: White Noise - CoG

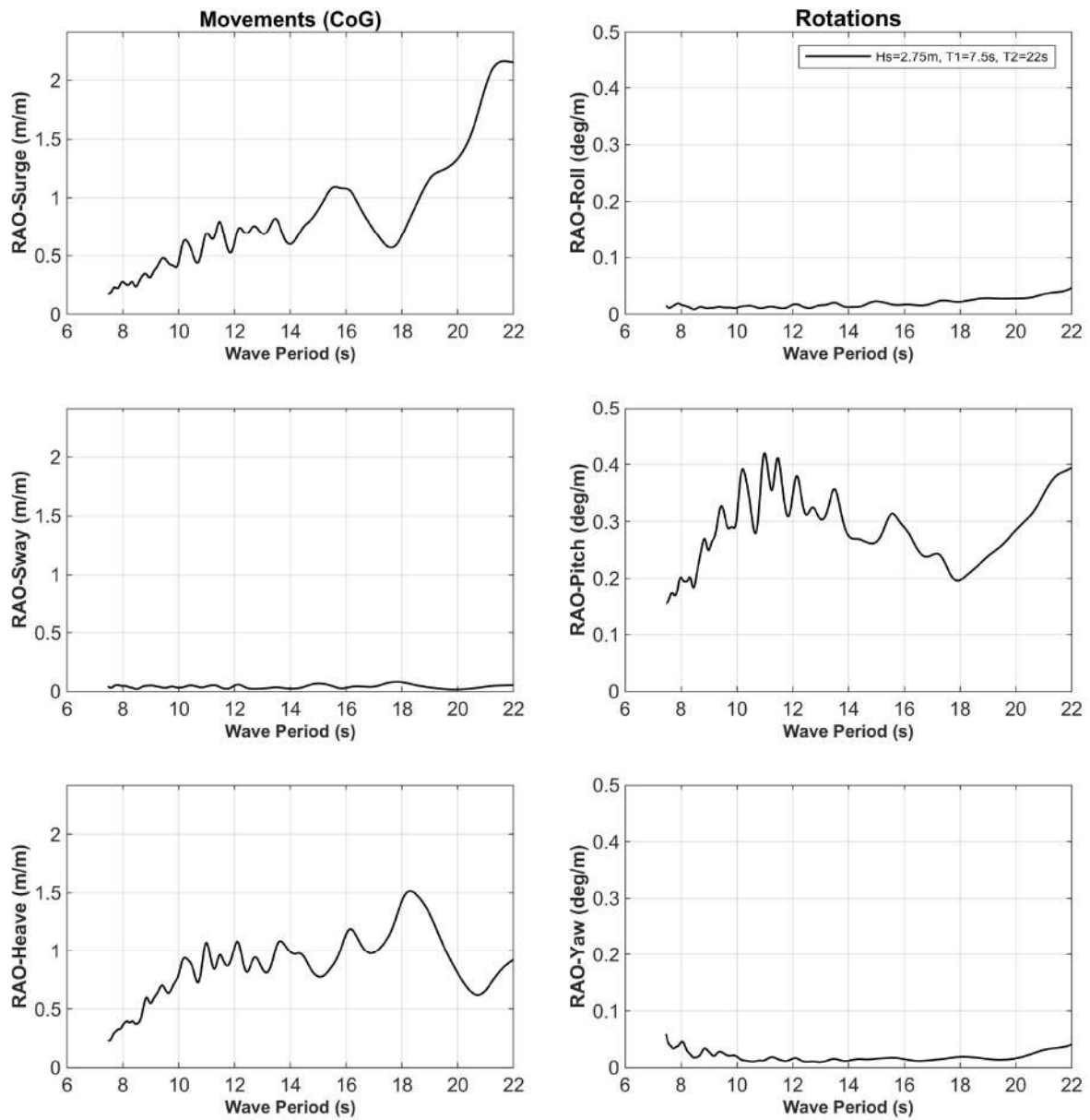


Figure 6-71. Configuration AF0 during Installation: White Noise. RAO of motions (CoG)

ACTIVEFLOAT Configuration AF0 during Installation: White Noise - Nacelle

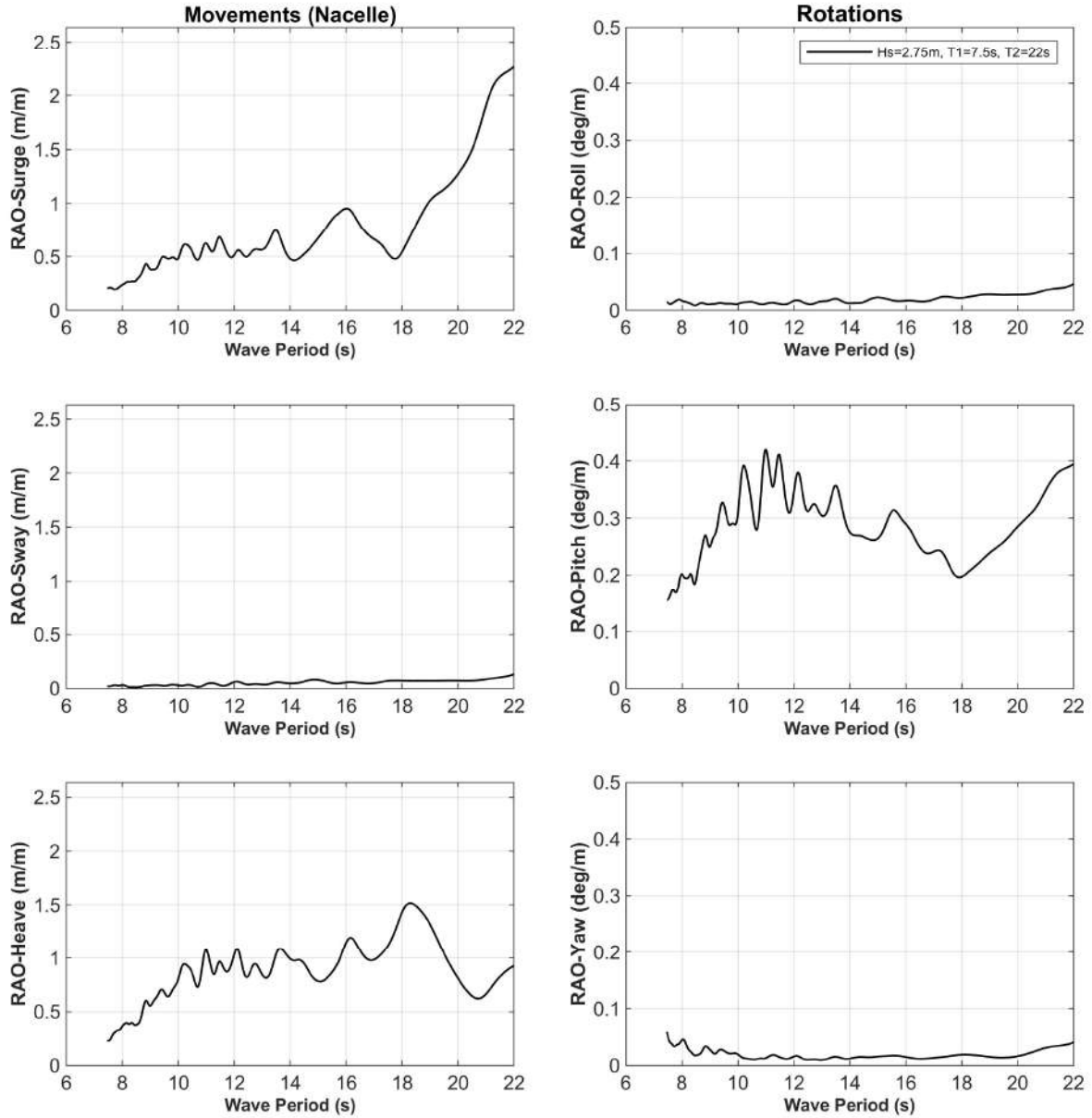


Figure 6-72. Configuration AF0 during Installation. RAO of motions (Nacelle)

ACTIVEFLOAT Configuration AF0 during Installation: White Noise - MSL

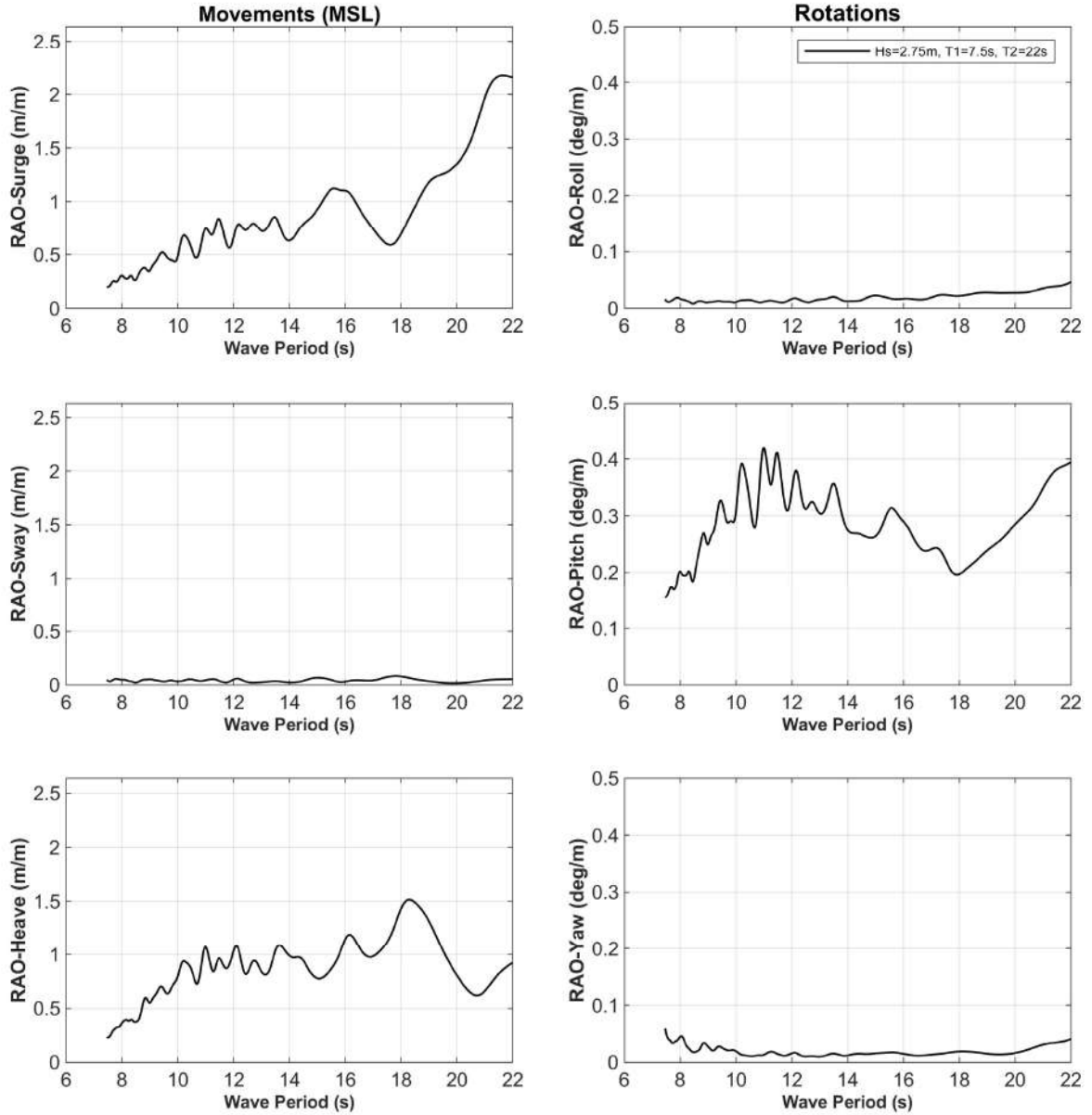


Figure 6-73. Configuration AF0 during Installation. RAO of motions (MSL)

7 CONCLUSIONS

A set of physical experiments have been carried out to evaluate the seakeeping of novel concrete-based WINDCRETE and ACTIVEFLOAT floating concepts under different environmental conditions, including waves and current and wind actions, as well as installation conditions. The tests campaign was conducted at the CCOB (Cantabria Coastal and Ocean Basin), part of MARHIS (Maritime Aggregated Research Hydraulic Infrastructures) a Unique Scientific and Technical Infrastructures (ICTS – Instalación Científico-Técnico Singular) from the Spanish Ministry of Science and Innovation, managed by IHCantabria.

Considering the dimensions of the basin as well as the wave generator capabilities, it was concluded that 1:55 for WINDCRETE and 1:40 for ACTIVEFLOAT were the most suitable test scales to carry out the physical experiments. Thus, the physical experiments for WINDCRETE and ACTIVEFLOAT platforms were conducted for water depths of 165 and 120 meters, respectively (3 m at model scale).

During the physical experiments the main properties of the models were scaled following the Froude scaling laws of similitude, trying to minimise scale effects that may perturb the model scale tests results. The mock-ups were designed to be able to reproduce the external geometry of the platform, as well as its mass properties (center of gravity and inertia moments). The mock-ups were made of steel, except for the ABS hemisphere in WINDCRETE and the aluminium tower in ACTIVEFLOAT. The wind loads were generated using the multi-fan system designed by IHCantabria, it reproduced the IEA-15MW. The mooring system was designed based on tested commercial wires, chains and springs able to reproduce the weight and the axial stiffness of the system. Moreover, a shielded silicone cable for WINDCRETE and rope string for ACTIVEFLOAT were used to simulate bending stiffness of the dynamic power export cable based on a bending stiffness portfolio previously generated in Deliverable D5.2 [1].

An extensive tests programme was designed to evaluate the dynamic performance of the floating wind concepts. The physical experiments were divided into five groups of tests depending on their nature, namely: (1) Dry Characterization Tests, (2) Installation Tests, (3) Wet Characterization Tests, (3) Wave Tests, (4) Wind Tests, (5) Current Tests, (6) Coupled Tests: Wave + Current + Wind Tests. Finally, a total of 122 tests were conducted. All the tests have been carried out according to DNV recommendations.

Thanks to these preliminary set of experiments the following list of objectives have been tackled:

- To validate the procedure and forces to be sustained during the installation of the floating concepts.
- To study the global dynamics of the platforms including natural periods and hydrodynamic damping of the system.
- To analyse the dynamic response of the floaters, including motions at CoG, Nacelle and MSL, and accelerations at Nacelle.
- To understand and deep into the mooring dynamics, including line tensions.
- To visualize the power cable dynamics, including clash events.
- To generate of a sizeable benchmarking database for numerical models calibration and validation.

The excursion and acceleration limits for each platform are shown in Table 7-1, obtained from [9] and actualized based on [16].

Limit for	Windcrete	Activefloat
OPERATION		
Yaw (10 min. max)	<15°	
Yaw (10 min. std)	<3°	
Pitch (max.)	[-10.0°, +10.0°]	
Pitch (10 min. average)	[-5.0°, +5.0°]	
Roll (max.)	[-5.0°, +5.0°]	
Pitch (10 min. std)	<1°	
Roll (10 min. std)	<1°	
IDLING CONDITION		
Pitch (10 min. average)	[-5°, +5°]	
Pitch (10 min. max)	[-15°, +15°]	
EMERGENCY STOP		
Max. pitch	[-15°, +15°]	

EXCURSION RESTRICTIONS	
Horizontal offset (alarm limit) (mean during operation)	15 m
Horizontal offset (WTG shutdown). Maximum during parked conditions	30 m

ACCELERATIONS LIMITS	
Operation (acc. XY / acc. Z)	2.94 m/s ² (0.3 g)
Survival (acc. XY / acc. Z)	4.41 m/s ² (0.45g)

Table 7-1. Excursion and acceleration limits [16]

On the other hand, Table 7-2 presents the minimum breaking load (MBL) and the design tension for mooring systems of both floaters at Gran Canaria.

	Type	d [m]	Grade	MBL [kN]	Td = 0.95MBL [kN]	Td = 0.95MBL [tonnes]
WindCrete	Upwind	0.111	R4	11856	11264	1148.2
	Downwind	0.100	R3S	8964	8516	868.1
	Delta lines	0.111	R3	9650	9167	934.5
ActiveFloat	Upwind	0.120	R3	11047	10494	1069.7
	Downwind	0.070	R3	4196	3986	406.3

Table 7-2. Design tension for mooring lines at Gran Canaria [7]

Next, a set more detailed conclusions are given based on the results recorded and the limits previously presented:

- **WINDCRETE Movements**

- Considering the initial position, the constant rated wind without or with regular wave with low periods ≤ 11 s cause a mean pitch below 4.5 degrees.
- Taking into account the initial position, the rated wind with both Extreme Turbulence Model and Normal Turbulence Model as well as the below rated wind with Normal Turbulence Model without or with irregular wave or current result in a maximum pitch below 6.75 degrees.
- There is no maximum acceleration at the Nacelle over 2.94 m/s² in surge in all the analysed cases. In Combined Irregular Wave and Current and Wind cases, the maximum acceleration in

surge equal to 1.74 m/s^2 is reached in the case of $H_s = 5.11 \text{ m}$, $T_p = 9 \text{ s}$, $\gamma = 1.2$ with current and rated wind with Normal Turbulence Model

- **WINDCRETE Mooring system**

- In Wind cases, the higher mean load in the main line 1 equal to 471 tonnes is obtained with the constant rated wind since it is directly related to the thrust value. The maximum tension in the main line 1 equal to 641 tonnes is reached in the case of rated wind with Extreme Turbulence Model.
- In Combined Regular Wave and Constant Wind cases, the maximum tension in the main line 1 equal to 557 tonnes is reached in the case of $H = 2.75 \text{ m}$ and $T = 20 \text{ s}$ with constant rated wind.
- In Combined Irregular Wave and Wind cases, the maximum tension in the main line 1 equal to 663 tonnes is reached in the case of $H_s = 2.75 \text{ m}$, $T_p = 9 \text{ s}$ and $\gamma = 3.3$ with rated wind with Extreme Turbulence Model.
- In Current tests, although the higher mean load equal to 432 tonnes is obtained in the main line 1, the maximum tensions over 683 tonnes take place in main lines 2 and 3.
- In Combined Irregular Wave and Current and Wind cases, the maximum tension in the main line 1 equal to 816 tonnes is reached in the case of $H_s = 5.11 \text{ m}$, $T_p = 9 \text{ s}$, $\gamma = 1.2$ with current and rated wind with Normal Turbulence Model.

- **ACTIVEFLOAT Movements**

- Considering the initial position, the mean drift of the regular wave with a height of 5.11 m and a period of 7.5 s results in a mean excursion over 15 m in surge.
- Taking into account the initial position, all wind cases without or with regular wave or irregular wave or current cause a mean excursion over 15 m and a maximum excursion over 30 m in surge.
- Considering the initial position, the current causes a maximum yaw over 15 degrees, quite different from results obtained in [7].
- There is no maximum acceleration at the Nacelle over 2.94 m/s^2 in surge in all the analysed cases. In Combined Irregular Wave and Current and Wind cases, the maximum acceleration in surge equal to 0.93 m/s^2 is reached in the case of $H_s = 5.11 \text{ m}$, $T_p = 9 \text{ s}$, $\gamma = 1.2$ with current and rated wind with Normal Turbulence Model.

- **ACTIVEFLOAT Mooring system**

- In Wind cases, the higher mean load in the main line 1 equal to 268 tonnes is obtained with the constant rated wind since it is directly related to the thrust value. The maximum tension in the main line 1 equal to 373 tonnes is reached in the case of rated wind with Extreme Turbulence Model.
- In Combined Regular Wave and Constant Wind cases, the maximum tension in the main line 1 equal to 308 tonnes is reached in the case of $H = 2.75 \text{ m}$ and $T = 7.5 \text{ s}$ with constant rated wind.
- In Combined Irregular Wave and Wind cases, the maximum tension in the main line 1 equal to 449 tonnes is reached in the case of $H_s = 2.75 \text{ m}$, $T_p = 9 \text{ s}$, $\gamma = 3.3$ and $s = 6$ with rated wind with Extreme Turbulence Model.
- In current tests, the mean and maximum loads in the mooring line 1 are 161 tonnes and 195 tonnes, respectively.
- In Combined Irregular Wave and Current and Wind cases, the maximum tension in the main line 1 equal to 541 tonnes is reached in the case of $H_s = 5.11 \text{ m}$, $T_p = 9 \text{ s}$, $\gamma = 1.2$ with current and rated wind with Normal Turbulence Model.

Comparing both platforms, WINDCRETE is prone to have larger mean pitch with constant rated wind without or with regular wave with low periods $\leq 11 \text{ s}$, and larger maximum pitch with operational conditions under turbulent rated or below rated wind than the ACTIVEFLOAT due to the absence of an active ballast system. The rotor of WINDCRETE suffers higher forces than that of ACTIVEFLOAT since in the extreme wind-current-sea state of $H_s = 5.11 \text{ m}$, $T_p = 9 \text{ s}$, $\gamma = 1.2$ with current and rated wind with Normal Turbulence Model, the maximum acceleration at the Nacelle reaches 1.74 m/s^2 in surge.

Moreover, the mooring system of WINDCRETE is more demanded than that of ACTIVEFLOAT, reaching the main line 1 a maximum tension equal to 816 tonnes in this extreme wind-current-sea state. However, the limit of ACTIVEFLOAT is reached for maximum yaw with current, for mean excursion with regular wave with a height of 5.11 m and a period of 7.5 s, as well as for mean and maximum excursion with constant rated wind without or with regular wave and with operational conditions under turbulent rated wind.

8 ANNEXES

ANNEX I: CHAIN LINES AND DYNAMIC CABLE COATING DEGRADATION IN MARINE ENVIRONMENT FOR 1 YEAR

ANNEX II: CHAIN LINES AND DYNAMIC CABLE COATING DEGRADATION IN MARINE ENVIRONMENT FOR 2 YEARS

9 REFERENCES

- [1] V. Arramounet, F. Castillo, S. Doole, C. Lourie, A. Hart, R. Guanche, M. Somoano, A. Rodriguez-Luis, D. Blanco, T. Battistella, J. Sarmiento, S. Fernandez-Ruano, A. Alvarez, M. Y. Mahfouz and Q. Pan, “COREWIND D5.2: Mooring and cable dynamic testing report,” 2021.
- [2] C. Barrera, R. Guanche and I. J. Losada, “Experimental modelling of mooring systems for floating marine energy concepts,” *Marine Structures*, vol. 63, p. 153–180, 2019.
- [3] M. Somoano, D. Blanco, A. Rodríguez-Luis and R. Guanche, “Experimental analysis of mooring and power cable dynamics when using elastic string models,” in *Proceedings of the International Conference on Offshore Mechanics and Arctic Engineering - OMAE*, 2022.
- [4] A. Facchinetti, S. Di Carlo, A. Fontanella, R. Guanche, T. Battistella, M. Somoano, J. Sarmiento and A. Rodriguez, “COREWIND D5.1: HIL 15MW development,” 2020.
- [5] M. Somoano, T. Battistella, S. Fernández-Ruano and R. Guanche, “Uncertainties assessment in real-time hybrid model for ocean basin testing of a floating offshore wind turbine,” 2021.
- [6] F. Vigarà, L. Cerdán, R. Durán, S. Muñoz, M. Lynch, S. Doole, C. Molins, P. Trubat and R. Guanche, “COREWIND D1.2: Design load basis,” 2019.
- [7] V. Arramounet, M. Chemineau, F. Castillo, P. Trubat, C. Molins, F. Vigarà, G. de Guglielmo and C. Cortes, “COREWIND D2.2: Design analysis and optimization of mooring and anchoring system for floating wind turbines (Innovations and breakthroughs),” 2022.
- [8] IEC 61400-3, Wind turbines — Part 3: design requirements for offshore wind turbines, Geneva (Switzerland), 2009, p. 132.
- [9] M. Y. Mahfouz, M. Salari, S. Hernández, F. Vigarà, C. Molins, P. Trubat, H. Bredmose and A. Pegalajar-Jurado, “COREWIND D1.3: Public design and FAST models of the two 15MW floater-turbine concepts,” 2020.
- [10] M. Ikhennicheu, M. Lynch, S. Doole, F. Borisade, F. Wendt, M. A. Schwarzkopf, D. Matha, R. Durán-Vicente, T. Habekost, L. Ramirez and S. Potestio, “COREWIND D3.1: Review of the state of the art of dynamic cable system design,” 2020b.
- [11] S. Doole, “COREWIND D3.2: Analysis and Optimisation of Dynamic Cabling Design for Floating Offshore Wind Farms,” 2022.
- [12] H. Bredmose, J. Rinker, W. Skrzypinski, F. Zahle, F. Meng, K. Dykes, E. Gaertner, G. Barter, P. Bortolotti, L. Sethuraman and M. Shields, “COREWIND D1.1: Definition of the 15MW Reference Wind Turbine,” 2019.
- [13] E. Gaertner, J. Rinker, L. Sethuraman, F. Zahle, B. Anderson, G. Barter, N. Abbas, F. Meng, P. Bortolotti, W. Skrzypinski, G. Scott, R. Feil, H. Bredmose, K. Dykes, M. Shields, C. Allen and A. Viselli, “IEA Wind TCP Task 37: Definition of the IEA Wind 15-Megawatt Offshore Reference Wind Turbine,” 2020.



- [14] T. Battistella, D. D. L. D. Paradinas, A. M. Urbán and R. G. Garcia, “High fidelity simulation of multi-MW rotor aerodynamics by using a multifan,” in *Proceedings of the International Conference on Offshore Mechanics and Arctic Engineering - OMAE*, 2018.
- [15] J. M. J. Journée and W. W. Massie, First ed., Delft University of Technology, 2001, p. 570.
- [16] H. Bredmose, “COREWIND: Updated motion limits as guidelines for floater design,” 2021.



D5.3: Integrated FOWT test report

FIHAC/CTC/VICINAY/INNOSEA/JDR

January 2023

A01

ANNEX I. Chain lines and dynamic cable coating degradation in marine environment for 1 year

Disclaimer:



This project has received funding from the European Union's Horizon 2020 Research and Innovation programme under grant agreement No 815083.

Project details:

Duration:
1 Sep 2019 - 28 Feb 2023
Grant agreement:
No: 815083

Table of contents

1	OBJECTIVE	3
2	METHODOLOGY	3
3	RESULTS	5
3.1	Photographic survey	7
3.2	Analysis in the FIHAC's laboratory	15
3.3	Analysis in the CTC's laboratory	16
3.3.1	Assessment of degree of blistering	18
3.3.2	Assessment of degree of rusting	21
3.3.3	Assessment of degree of cracking	24
3.3.4	Assessment of degree of flaking	27
3.3.5	Assessment of degree of chalking by tape method	30
4	REFERENCES	35

1 OBJECTIVE

The aim of this task is to test the behaviour of different cable coating and mooring chain materials exposed to biological and physicochemical elements of the marine environment.

2 METHODOLOGY

The material testing was carried out between November 17th 2020 and March 2nd 2022, under real marine conditions, in the Marine Corrosion Test Site El Bocal (MCTS El Bocal), located in the coastal area of Cantabria (North of Spain) (Figure 2-1). The test was carried out at three depth levels:

- The upper level: Located just below the splash zone.
- The middle level: Located at the intertidal zone.
- The lower level: Located at the submerged zone.

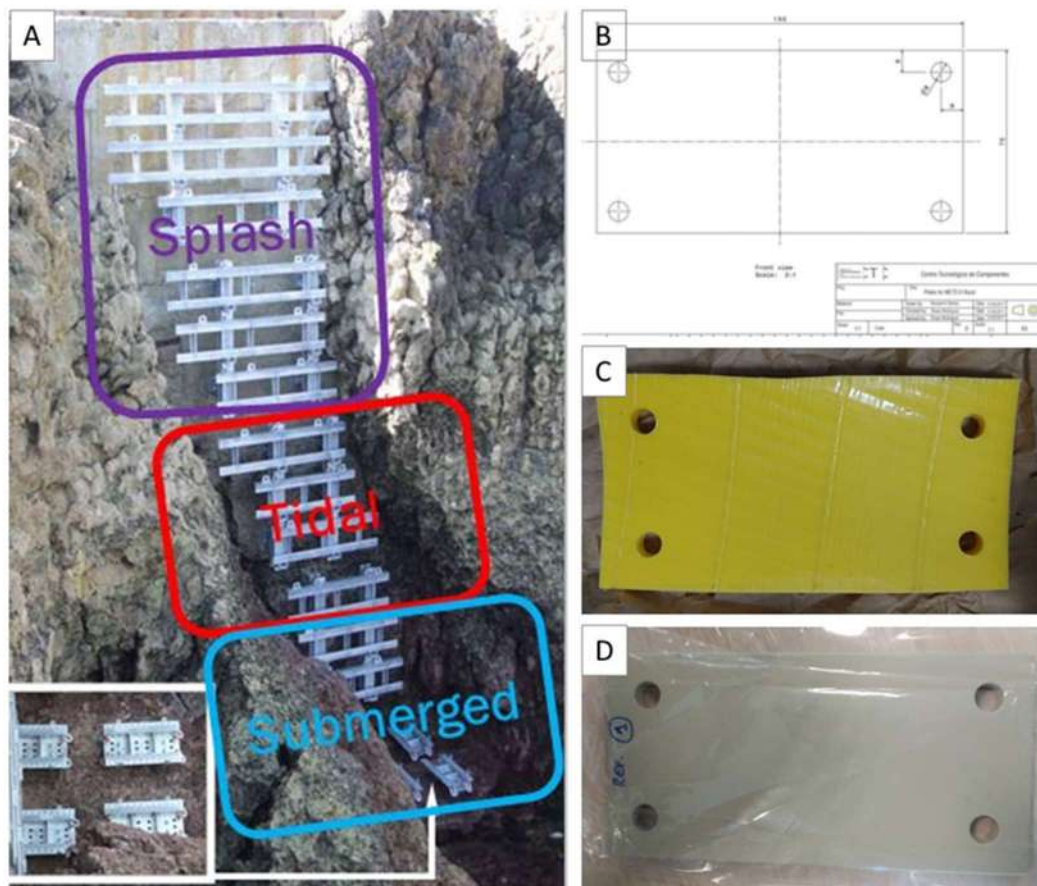


Figure 2-1. Installations of the Marine Corrosion Test Site El Bocal (A). Design of the material testing plates (B). Cable coating plastic testing plate (C). Cable mooring steel testing plate coated with an anticorrosive paint (D).

At each of these levels, several test plates, of 75x150mm and made up of different materials, were deployed to be exposed to the elements during 12 and 24 months (Figure 2-1). The installation of the plates was carried out on November 17th 2020.

Cable testing			
Material /Component	Depth	Number of plates	Timeframe
Cable coating	Sample just below the splash zone	1	12 months
Cable coating	Tidal area	1	12 months
Cable coating	Submerged	1	12 months
Cable coating	Sample just below the splash zone	1	24 months
Cable coating	Tidal area	1	24 months
Cable coating	Submerged	1	24 months
Mooring testing			
Material /Component	Depth	Number of plates	Timeframe
Mooring Chain	Tidal area	4	12 months
Mooring Chain	Submerged	4	12 months
Mooring Chain	Tidal area	4	24 months
Mooring Chain	Submerged	4	24 months

Table 2-1. Type and number of testing plates

The test plates used for the cable testing were made up of a plastic material, while the plates used for the mooring chain included:

- 4 replicated plates of bare steel.
- 4 replicates of steel coated with an unmodified reference hempadur 15570 paint (Type 0).
- 4 replicates of steel coated with a functionalized paint (HDK18+NP Cu) 23% SiO₂ + 6%CuO (Type 1).
- 4 replicates of steel coated with a functionalized paint (HDK18+NP Cu) 28% SiO₂ + 6%CuO (Type 2).

During the experiment, a photographic survey was carried out, taking photographs of the plates on a monthly basis, when possible.

After the first extraction, a replicate of each of the plates were carried out to the FIHAC's laboratory for their biotic assessment of the biofouling communities for both mooring chains and dynamic cable coating (Figure 2-2). Afterwards, a visual inspection of the corrosion applying the UNE-EN ISO 4628:2016 standard is conducted for the steel coating plates (assessment of degree of blistering, rusting, cracking, flaking and chalking).



Figure 2-2. Extraction of the structures in March 2022 (A), collection of the testing plates (B) and biological analysis of the plates in the laboratory (C).

3 RESULTS

The first extraction of the plates was carried out on March 2nd 2022, with a delay of 3.5 months from the estimated schedule. This delay was caused by adverse maritime conditions and Covid-19 incidences.

In addition, several incidences should be reported regarding the integrity of the structures and probes. By January 2022, 4 of the 10 probes of the submerged level were dropped from their base. Then, by February 2022, the whole submerged base, with the remaining testing probes, was ripped off the structure and lost during a storm event. Moreover, by February 2022, 2 of the 10 probes of the tidal level were dropped from their base and, by March 2022, one more was lost. Thus, at the extraction date, carried out on March 2nd 2022, only the following plates remained available:

- Splash zone:
 - 2 cable coating plates (one extracted in March 2022).
- Tidal zone:
 - 2 cable coating plates (one extracted in March 2022).
 - 2 bare steel plates (one extracted in March 2022).
 - 2 plates of steel coated with a functionalized paint (HDK18+NP Cu) 23% SiO₂ + 6%CuO. Type 1 (both extracted in March 2022).
 - 1 plate of steel coated with a functionalized paint (HDK18+NP Cu) 28% SiO₂ + 6%CuO. Type 2.

Due to a visual error, on March 2nd 2022, two Type 1 plates were extracted, instead of one Type 1 and one Type 2 plates. This mistake occurred because the apparent degree of corrosion and biofouling colonization of one of the Type 1 plates was higher than that of the other Type 1 plate, and conversely presented a similar state to that of the Type 2 plate at the time of extraction, as well as during the whole experiment.

The following Figure 3-1 shows the exposed plates, their exposure zones, and the specimens on which the visual inspection has been carried out.



Figure 3-1. Schematic of the installed plates

3.1 Photographic survey

Figure 3-2 to Figure 3-5 show the evolution of the plates between the installation in November 2020 and the extraction in March 2022.

As it can be seen in Figure 3-2, days after the installation, the uncoated steel plates showed early signs of oxidation and biological colonization by ephemeral pioneering species. Also, the Type 2 plates installed at the tidal zone showed slight signs of oxidation at the plates margins. The remaining mooring chain plates, as well as the cable coating plates, did not show apparent signs of deterioration, at none of the tidal levels.

By December 2020, the Type 2 plates installed at the tidal zone showed increasing signs of oxidation at the plates margins and one of the Type 1 plates, the one installed in the bottom, started showing a slight oxidative process. The uncoated steel plates showed advanced signs of oxidation and biological colonization by ephemeral pioneering species at both, tidal and submerged levels. Regarding cable coating plates, only one of the plates installed at the tidal level showed early signs of biological colonization by ephemeral pioneering species, probably filamentous brown algae from the genus *Ectocarpus*. The remaining plates did not show apparent signs of deterioration, at none of the tidal levels.

In January 2021, the Type 2 plates installed at the tidal zone showed increasing signs of oxidation at the plates margins, as well as early signs of biological colonization by ephemeral pioneering species. One of the Type 1 plates, the one installed in the bottom, shows an important coverage of a black biofilm. In addition, the plates painted with the Type 0 coating and installed in the tidal level, show the beginning of an oxidative process, which is specially advanced in the bottom plate. In the submerged level, only the bare steel plates show an important level of oxidation. The remaining plates at this level only show early signs of biological colonization by ephemeral pioneering species, probably filamentous brown algae from the genus *Ectocarpus*.

In February 2021, a generalized biological colonization by ephemeral pioneering species is observed at the plates of the tidal level. The oxidative process seems to be like that of January 2021. The splash level plates do not show any signs of biological colonization. At this month, it was not possible to obtain any photographs of the submerged level.

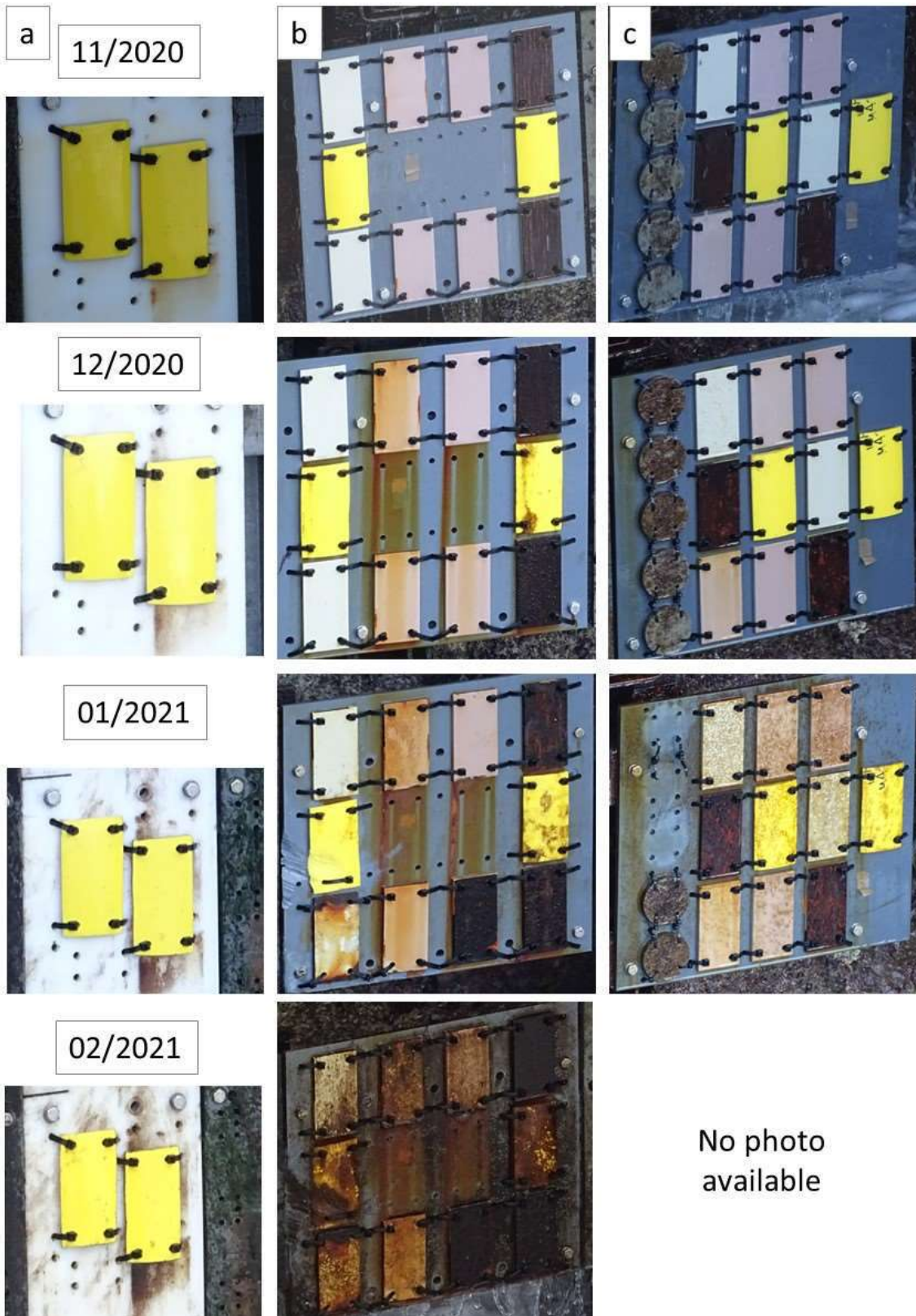


Figure 3-2. State of the plates between November 2020 and February 2021. Column a: Splash level; Column b: Tidal level; Column c: Submerged level.

Figure 3-3 shows that March 2021 continues with the generalized biological colonization by ephemeral pioneering species at all the plates of both the tidal and submerged levels. The splash level plates show early signs of biological colonization.

April 2021 is characterized by the beginning of the colonization by green filamentous algae of the genus *Ulva* in some of the plates of the tidal level (i.e., upper plates of the Types 0, 1 and 2, and bottom Type 2 plate). The submerged plates show an advanced colonization by ephemeral pioneering species and the splash level plates continue showing early signs of biological colonization.

May 2021 shows a similar pattern to that of April 2021. However, the presence of grazers of the genus *Patella* (limpets) seems to have reduced the number of ephemeral algae in some of the plates at the tidal level.

June 2021 is characterized by a notable decrease in the coverage of ephemeral algae in all the plates of the tidal level, probably associated to the grazing pressure of the limpets. The submerged level is characterized by the beginning of the colonization by green filamentous and foliose algae of the genus *Ulva* as well as the beginning of the colonization by red filamentous species.

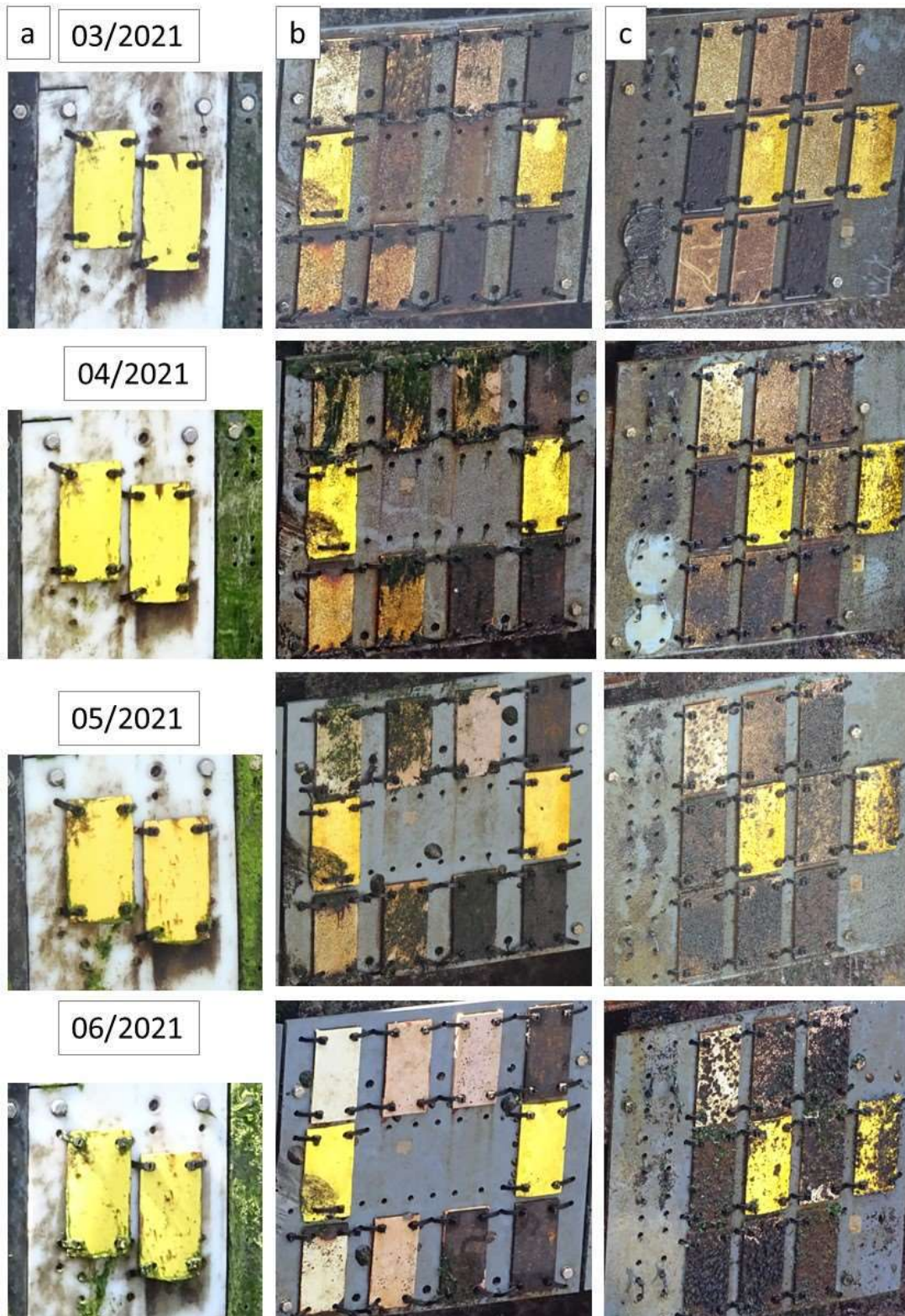


Figure 3-3. State of the plates between March 2021 and June 2021. Column a: Splash level; Column b: Tidal level; Column c: Submerged level.

As it can be seen in Figure 3-4, in July 2021, the splash and tidal levels show a similar pattern to that of June 2021 and there is no photo available of the submerged level.

August 2021 shows a similar pattern to those of June and July 2021. However, the green filamentous and foliose algae of the genus *Ulva* seem to have disappeared from the submerged plates. Instead, encrusting red algae of the genus *Lithophyllum* seem to be growing in some of the plates of the tidal (i.e., plates of the Types 1 and 2) and submerged (i.e. Type 0 and cable coating) levels. One of the Type 1 plates, the one at the top, shows an advanced level of corrosion since the last month. Finally, one of the splash level plates shows the presence of ephemeral brown filamentous pioneering species, probably of the genus *Ectocarpus*.

September and October 2021 show a similar pattern to that of August 2021 in all the plates and tidal levels. However, in October there is no photo available for the submerged level. Apparently, in October, one of the cable coating plates show the presence of cirripedians, probably of the genus *Chthamalus*, growing at the scrape probably produced by the impact of some floating object pushed by the waves.

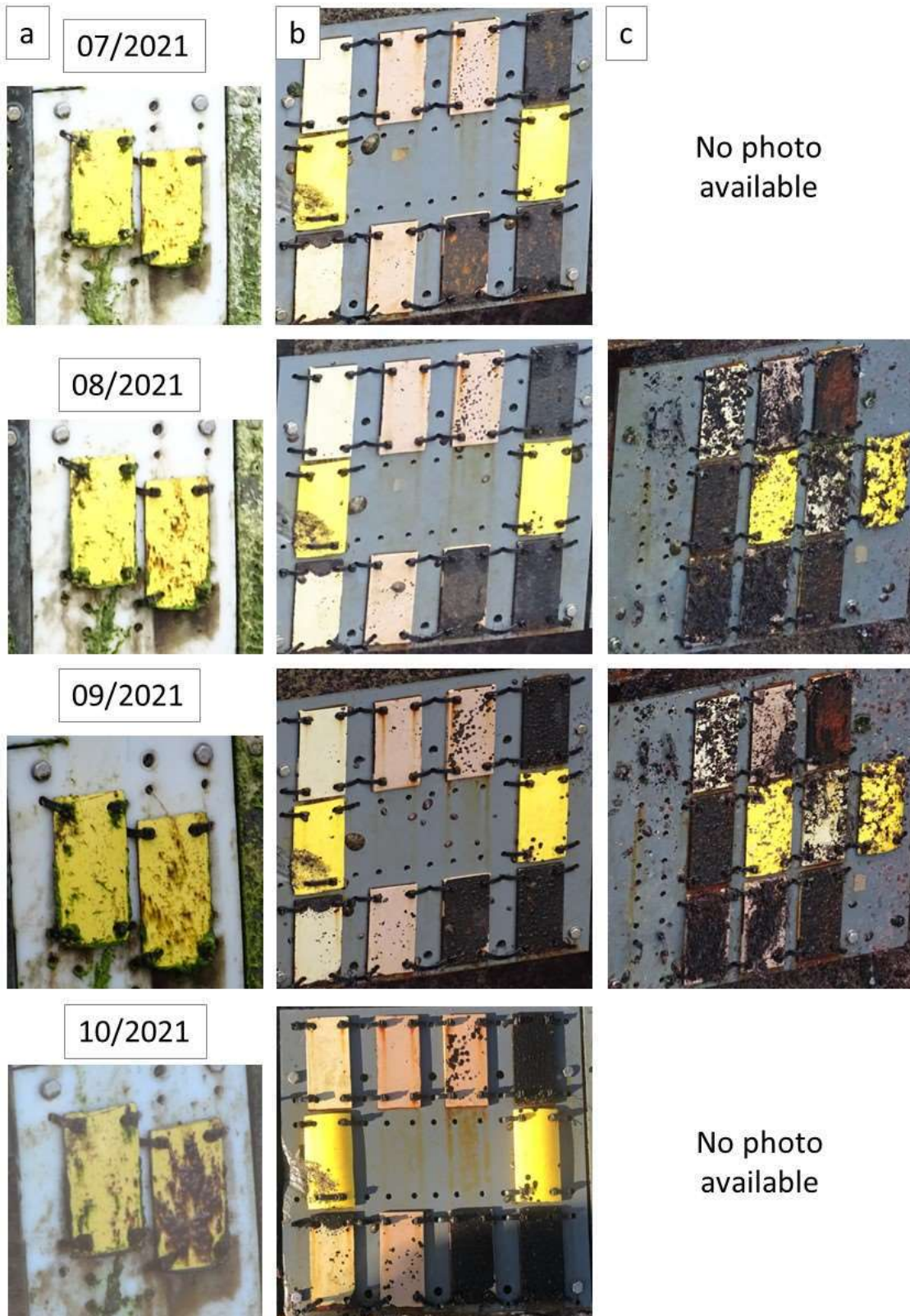


Figure 3-4. State of the plates between July 2021 and October 2021. Column a: Splash level; Column b: Tidal level; Column c: Submerged level.

As show in Figure 3-5, in January 2022 only one photo of the submerged level is available. Most of the ephemeral filamentous algae seem to have disappeared from the plates. Instead, encrusting red algae of the genus

Lithophyllum continue growing in the Type 0 and cable coating plates, and, to a lesser extent in the Type 1 and Type 2 plates. One of the Type 2 plates, the one at the bottom, shows an advanced level of corrosion and biological colonization by a dark biofilm. This phenomenon is not observed in the other Type 2 replicate, which continues unaltered, similarly as the remaining Type 1 plate. Both bare steel plates show an advanced level of corrosion and the presence of early populations of Spirorbidae polychaetes, which can be also found, in a smaller number, in the Type 1 and Type 2 plates.

In February 2022, the cable coating plates of the splash zone are mostly covered by ephemeral green and brown filamentous algae of the genus *Ulva* and *Ectocarpus*, respectively. The plates of the tidal zone are also covered by these opportunistic algae and, some of them (i.e., one of the cable coating plates, one of the bare steel plates and, to a lesser extent, one of the Type 1 plates) show some individuals of the foliose red macroalgae *Porphyra* sp. The remaining Type 0 plate seems to be relatively unaltered, with few signs of corrosion and a low level of biofouling. The structure of the submerged zone was lost during a storm, so, there is no information regarding the plates at this level.

In March 2022, the pattern is like that of February. One of the Type 2 and both of the Type 0 plates have been lost. The remaining plates are covered by ephemeral green and brown filamentous algae of the genus *Ulva* and *Ectocarpus*. Also, the plates mentioned before at the tidal level show growing populations of the foliose red macroalgae *Porphyra* sp. It is worth to mention that, regarding Type 1 and Type 2 plates, one of the Type 1 plates shows a higher level of corrosion and biological colonization, while the remaining Type 1 and Type 2 plates show similar and slightly lower levels of alteration. These phenomena contributed to the misleading of the plates to be removed, mistaking one of the Type 1 for the Type 2.

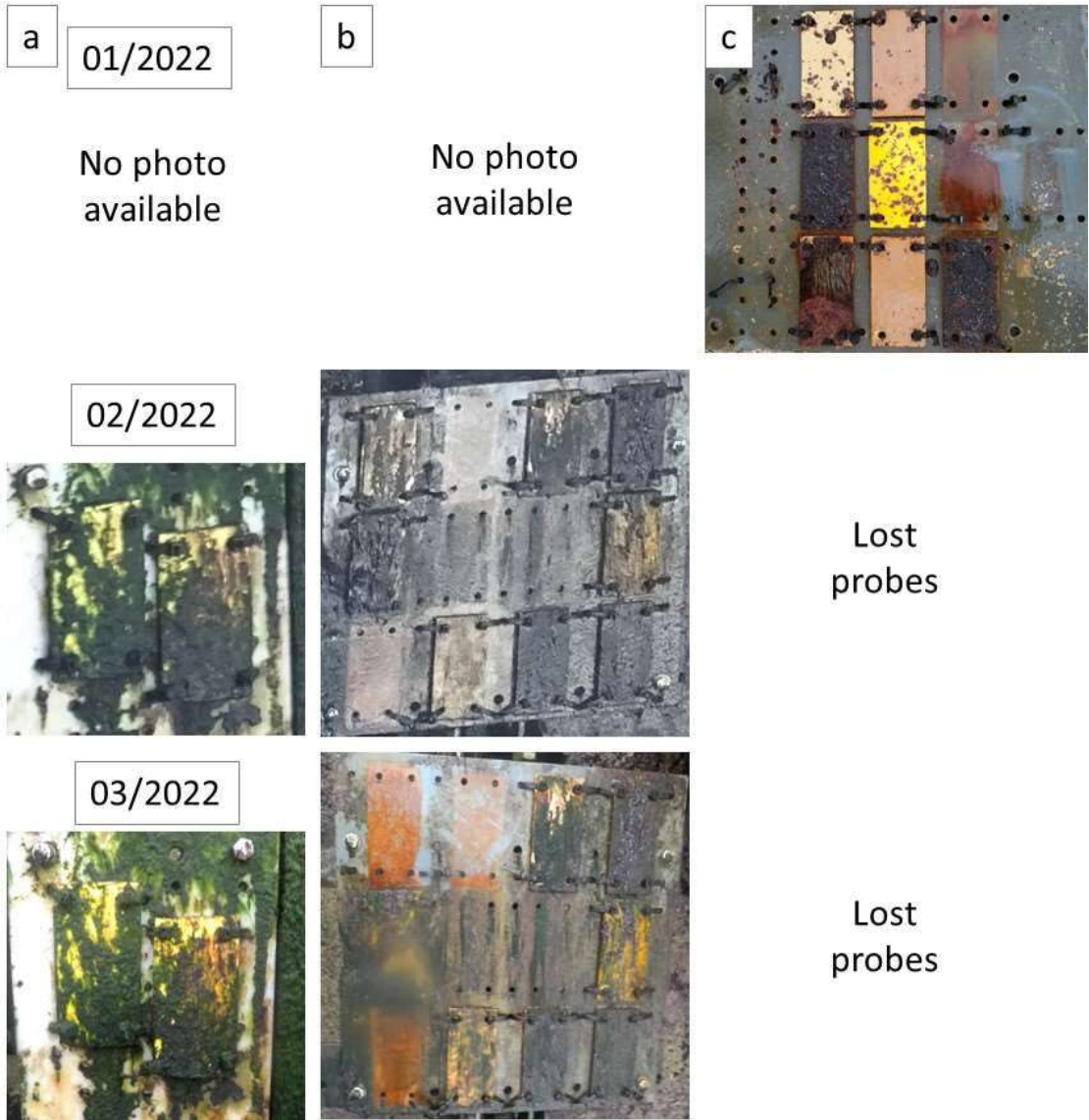


Figure 3-5. State of the plates between January 2021 and March 2022. Column a: Splash level; Column b: Tidal level; Column c: Submerged level.

3.2 Analysis in the FIHAC's laboratory

The state of the plates, once in the FIHAC's laboratory, are shown in Figure 3-6 and Figure 3-7, for the splash and tidal levels, respectively.



Figure 3-6. State of the cable coating plate extracted from the splash level.

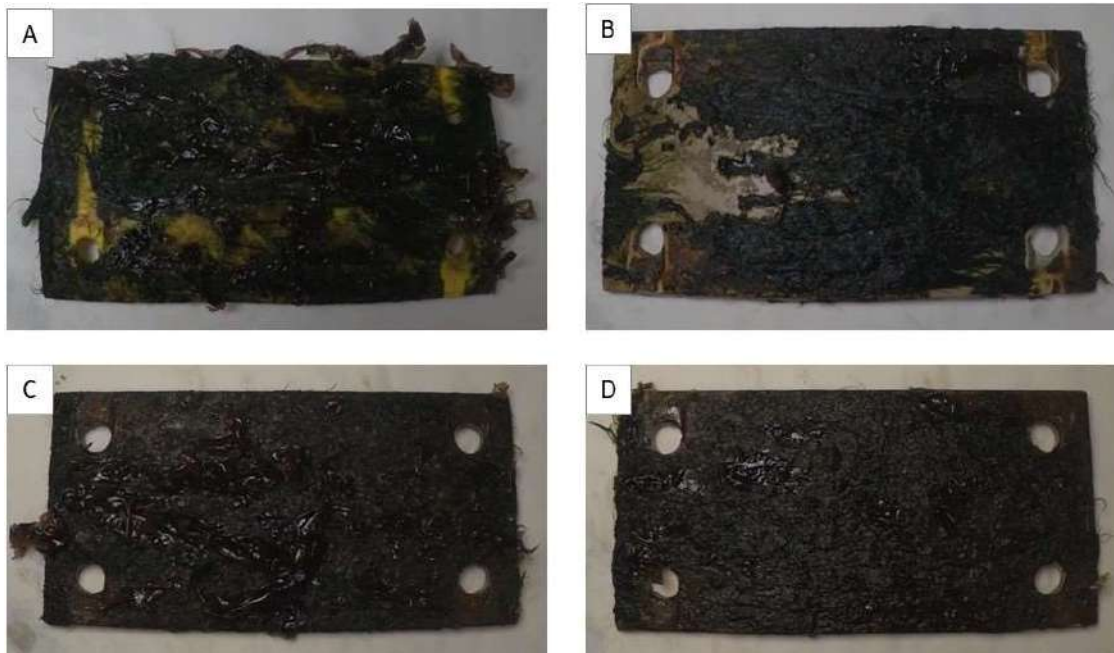


Figure 3-7. State of the different plates extracted from the tidal level. A: Cable coating, B: Type 1, C: Bare steel, D: Highly altered Type 1.

Table 3-1 shows the results of the biological analysis. The most abundant species colonizing the plates are the green filamentous opportunistic species *Ulva sp.* and the red foliose *Porphyra sp.* (this one only in the tidal level), with percentage coverages between 10%-70%.

Level	Splash	Tidal	Tidal	Tidal	Tidal
Plate Number	1CC	2CC	4	3	7
Plate Type	Cable coating	Cable coating	Bare steel	Type 1 R1	Type 1 R2
FLORA (% coverage)					
Ceramiales	10			2	
<i>Ectocarpus sp.</i>	40	20	5	5	5
<i>Lithophyllum sp.</i>		2	1	1	1
<i>Porphyra sp.</i>		60	50	10	20
<i>Scytosiphon sp.</i>			2		
<i>Taonia sp.</i>					1
<i>Ulva sp.</i>	40	30	40	60	70
FAUNA (% coverage)					
<i>Chthamalus sp.</i>		4	1		1
Spirorbidae		1	1		
FAUNA (Number)					
Chironomidae larvae	1				
COVERAGE (%)	90	112	98	78	97
RICHNESS (N)	4	6	7	5	6

Table 3-1. Results of the biological analysis of the plates extracted in March 2022.

In the splash level, also the brown filamentous *Ectocarpus sp.* is found with an elevated percentage coverage (40%), together with a small presence of red filamentous Ceramiales (10%) and one individual of a Chironimidae larvae. In the tidal level, the cable coating shows the higher abundance of biota, mostly due to the high coverage of *Porphyra sp.* (60%), *Ulva sp.* (30%) and *Ectocarpus sp.* (20%), but also due to the presence of the red encrusting *Lithophyllum sp.* (2%), as well as several individuals of *Chthamalus sp* cirripedians (4%) and Spirorbidae worms (1%).

The bare steel plate shows a similar composition of biota but with slightly lower coverage values. In addition, it shows the presence of some small filaments of the brown algae *Scytosiphon sp.* (2%), giving to this plate the highest species richness overall. Regarding Type 1 plates, the more altered one (Nº7 - R2) shows higher coverages of *Ulva sp.* (70%) and *Porphyra sp.* (20%), in addition to a small specimen of the brown algae *Taonia sp.* (1%) and some individuals of *Chthamalus sp.* (1%), while the less altered one (Nº3 - R1) shows the lowest values of species coverage and richness among all the plates.

3.3 Analysis in the CTC's laboratory

The state of the plates, once in the CTC's laboratory, are shown in Figure 3-8 to Figure 3-12, for the five selected specimens. In the left column are the exposed faces (face A) and in the right column, the unexposed faces (face B) glued to the panel at the Marine Corrosion Test Site El Bocal.

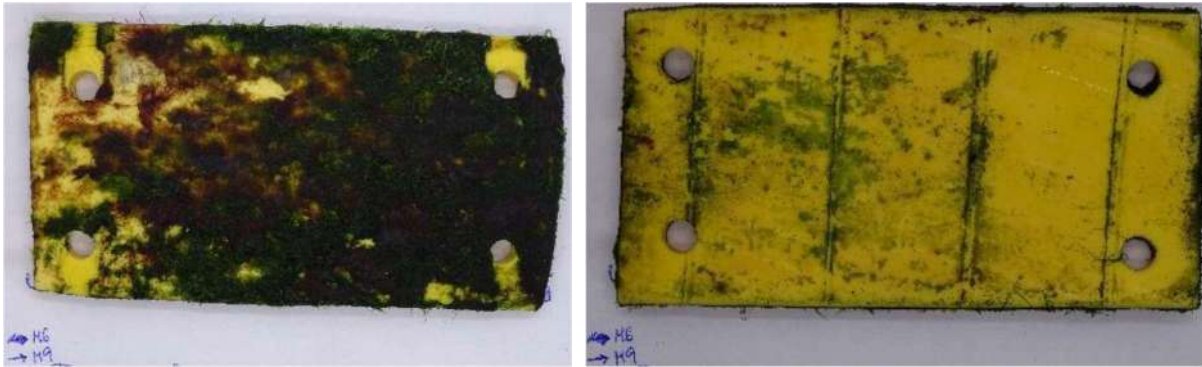


Figure 3-8. Plate # 1CC: Cable coating at Splash zone. Face A (left) and Face B (right)

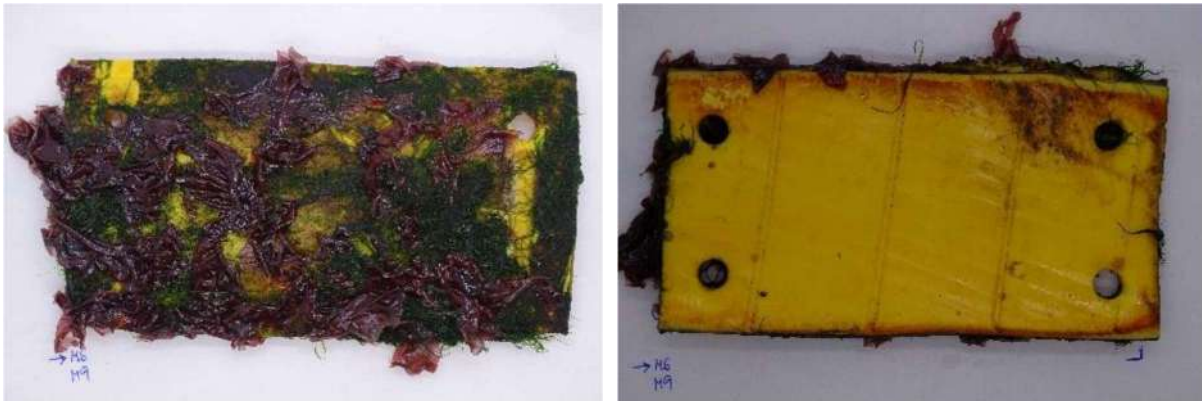


Figure 3-9. Plate # 2CC: Cable coating at Tidal area. Face A (left) and Face B (right)



Figure 3-10. Plate # 4: Bare steel at Tidal area. Face A (left) and Face B (right)

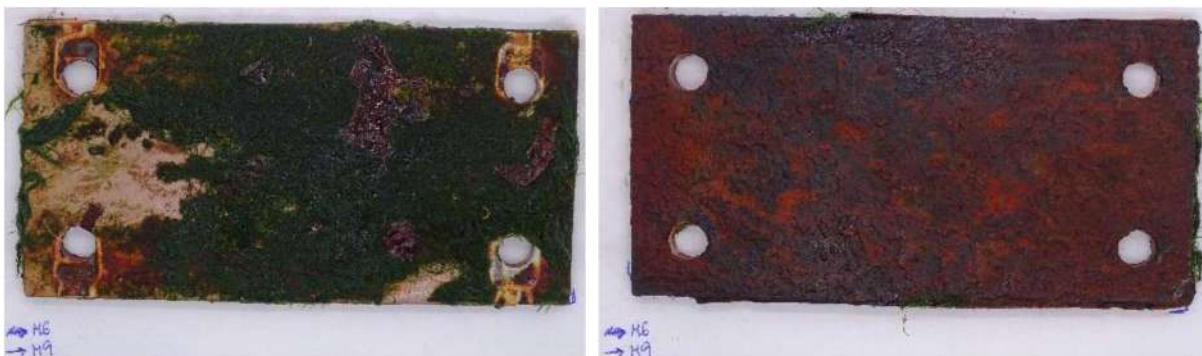


Figure 3-11. Plate # 3: Steel coated of Type 1 R1 at Tidal area. Face A (left) and Face B (right)

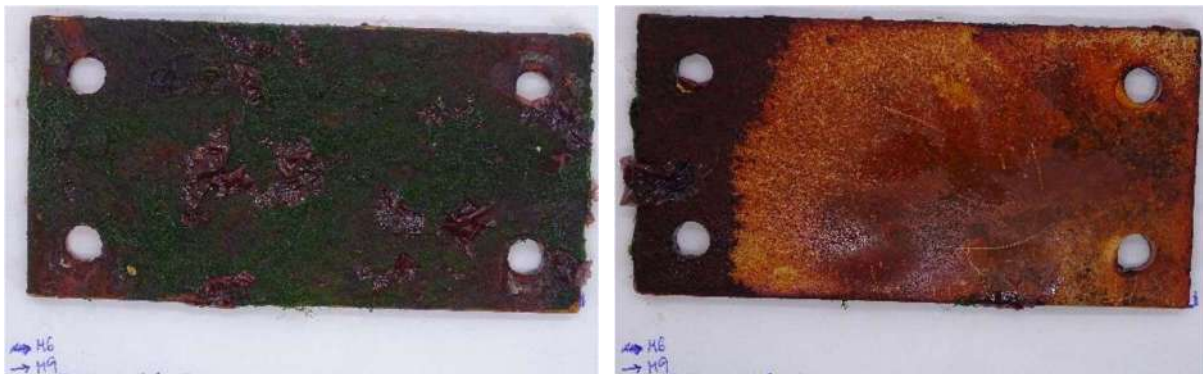


Figure 3-12. Plate # 7: Steel coated of Type 1 R2 at Tidal area. Face A (left) and Face B (right)

ISO 4628-1:2016 Standard (4628-1:2016 2016) defines the system used to designate the number and size of defects and the intensity of changes in appearance of paint coatings, and sets out the basic principles of the system. This system is intended, in particular, for defects caused by aging and weathering, as well as for uniform changes such as colour changes, such as yellowing. Below are the evaluations carried out according to ISO 4628-1:2016 Standard (4628-1:2016 2016):

- Assessment of degree of blistering (4628-2:2016 2016).
- Assessment of degree of rusting (4628-3:2016 2016).
- Assessment of degree of cracking (4628-4:2016 2016).
- Assessment of degree of flaking (4628-5:2016 2016).
- Assessment of degree of chalking by tape method (4628-6:2016 2016).

3.3.1 Assessment of degree of blistering

- **Object and field of application:**

ISO 4628-2:2016 Standard (4628-2:2016 2016) describes a method for assessing the degree of blistering of paint coatings by comparison with graphic standards. The graphic patterns provided show ampoules with sizes 2, 3, 4 and 5, and each size in quantities (densities) 2, 3, 4 and 5.

- **Assessment:**

The number and size of blisters in a paint coating are evaluated using the photographs provided in the standard. When the surface to be examined shows blisters of different sizes, refer to the size of the blisters that can be considered typical of the test area. The evaluation should be carried out under good lighting.

- **Expression of results:**

The grade is expressed for the amount (density) and for the size of the ampoules as shown in the standard, together with the approximate dimension of the test area, or its proportion with respect to the total area, expressed as a percentage. For example, if the coating is rated at blister density 2, size 2, that is, it should be recorded as: 'Blistering: blistering grade 2(S)'.

Below (Figure 3-13 to Figure 3-16) are the photographic patterns that have been used as a reference for the evaluation and expression of the results.

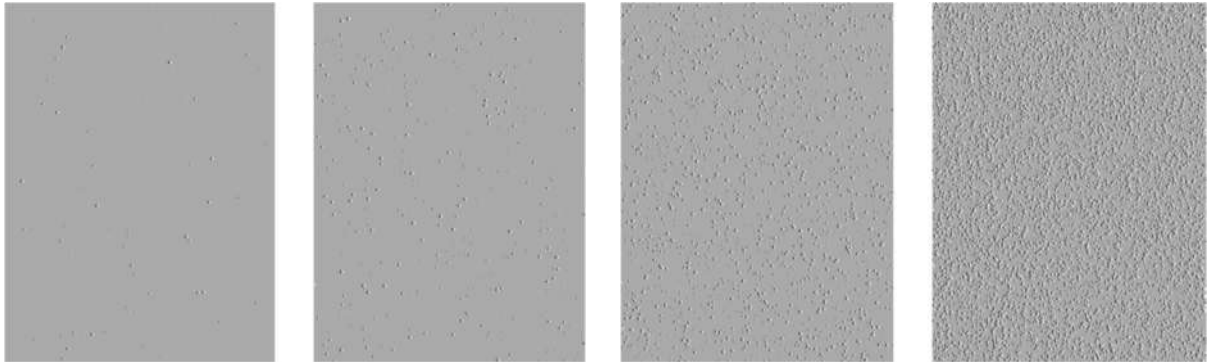


Figure 3-13. Size 2 ampoules. From left to right: Quantity (density) 2 – 2(S2), Quantity (density) 3 – 3(S2), Quantity (density) 4 – 4(S2) and Quantity (density) 5 – 5(S2)

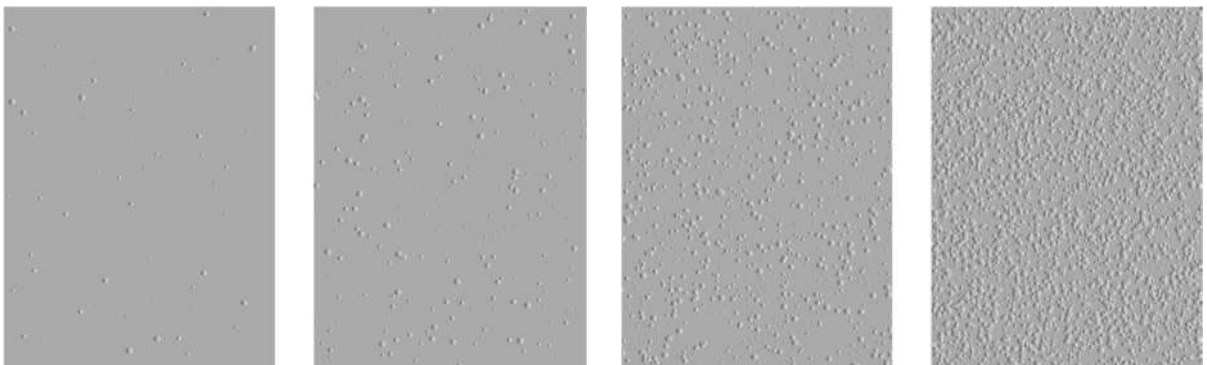


Figure 3-14. Size 3 ampoules. From left to right: Quantity (density) 2 – 2(S3), Quantity (density) 3 – 3(S3), Quantity (density) 4 – 4(S3) and Quantity (density) 5 – 5(S3)

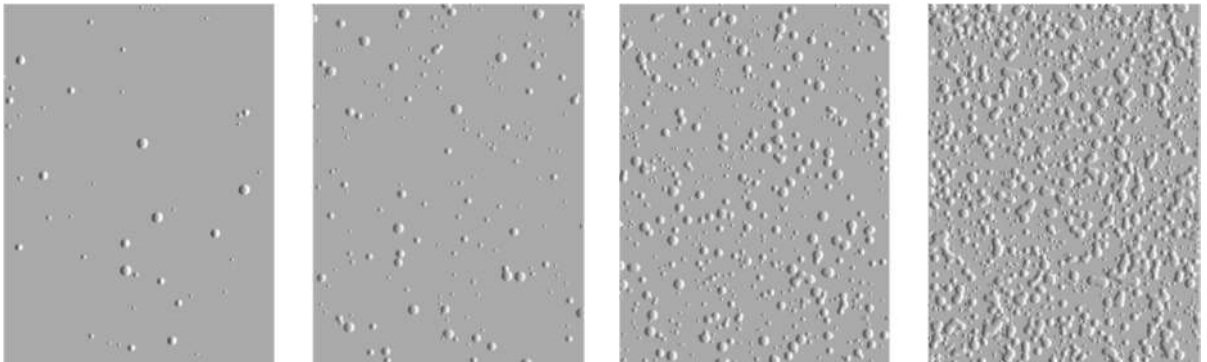


Figure 3-15. Size 4 ampoules. From left to right: Quantity (density) 2 – 2(S4), Quantity (density) 3 – 3(S4), Quantity (density) 4 – 4(S4) and Quantity (density) 5 – 5(S4)

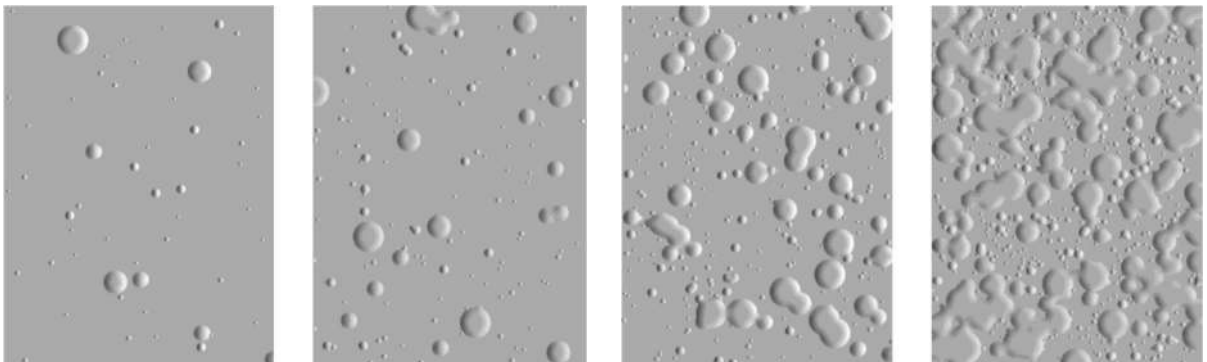


Figure 3-16. Size 5 ampoules. From left to right: Quantity (density) 2 – 2(S5), Quantity (density) 3 – 3(S5), Quantity (density) 4 – 4(S5) and Quantity (density) 5 – 5(S5)

- Results:**

Plate	Inspected face	Size	Quantity	Blistering	Observations
# 4	Face A	2	S5	2(S5)	Large and scattered
	Face B	2	S4	2(S4)	Medium and scattered
# 3	Face A	-	-	N/A	No blisters are seen, not even in x10 view
	Face B	3	S5	3(S5)	They look few but together and big
# 7	Face A	3	S5	3(S5)	Large blisters but slightly together
	Face B	3	S5	4(S5)	Large quantity and size

Table 3-2. Results of degree of blistering



Figure 3-17. Plate # 4: Face A (left), detail of Face A (centre) and Face B (right)



Figure 3-18. Plate # 3: Face A (left), Face B (centre) and detail of Face B (right)



Figure 3-19. Plate # 7: Face A (left), detail of Face A (centre) and Face B (right)

3.3.2 Assessment of degree of rusting

- **Object and field of application:**

ISO 4628-3:2016 Standard (4628-3:2016 2016) specifies a method for the evaluation of the degree of rusting of painted surfaces by comparison with graphic standards.

- **Assessment:**

The degree of rusting on a painted surface is evaluated by reference to the photographic patterns shown in the figures of the standard. Approximate amounts of rust (loose rust plus visible underlying rust) shown in these patterns are listed in Table 3-3. The procedure for the evaluation of the underlying rust, if required, should be agreed between the interested parties. When there are different degrees of oxidation in different parts of the area to be evaluated, these degrees must be indicated together with an indication of the area where they occur. The evaluation should be carried out under good lighting, as specified in ISO 13076:2019 Standard (13076:2019 2019). If the average size of the rust stains of the test piece to be evaluated differs considerably from those shown in the graphic patterns, an indication of the size shall be given by reference to the evaluation scheme in Table 3-3.

Degree of rusting	Rusty area %
Ri 0	0
Ri 1	0,05
Ri 2	0,5
Ri 3	1
Ri 4	8
Ri 5	40 to 50

Table 3-3. Degree of rusting and rusty area

- **Expression of results:**

The degree of rusting is expressed as the corresponding Ri of those represented in the figures of the standard. If applicable, the different degrees of rusting observed are indicated, along with the corresponding parts of the test area. If applicable, the degree of rusting Ri is recorded along with the degree, in numerical form, of the size of the rust marks. For example, if the rusty area corresponds to Figure 3-21 on the left-hand side, Ri 3, and the sizes of the individual rusty spots are 0.5 mm to 5 mm, the result is recorded as: 'Oxidation: degree of oxidation Ri 3 (S4)'.

Next, the photographic patterns that will be used for the evaluation and expression of the results are shown in Figure 3-20 to Figure 3-22.

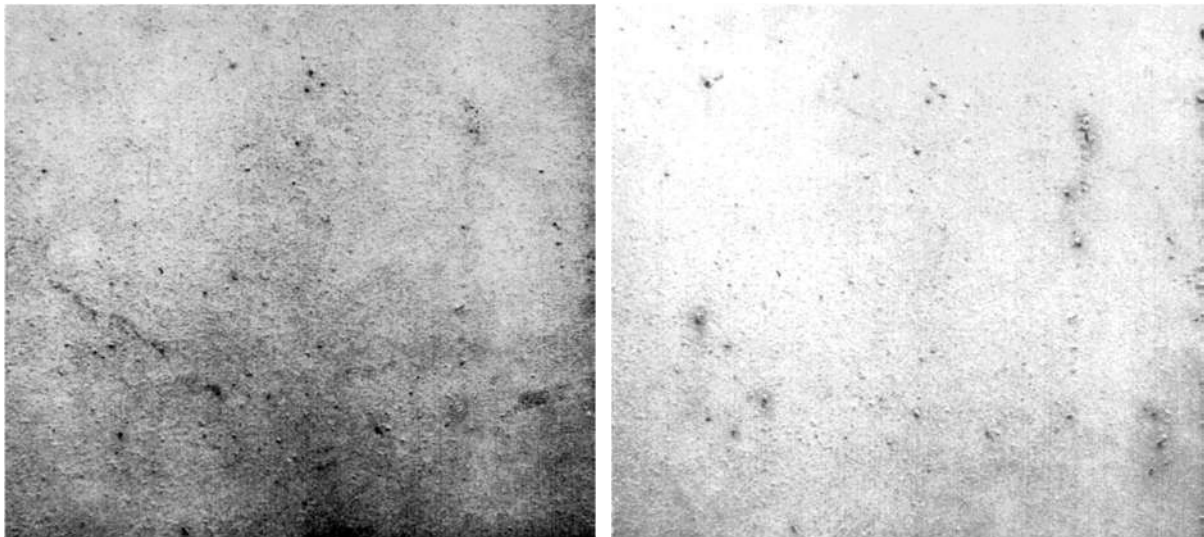


Figure 3-20. Degree of rusting: Ri 1 (left) and Ri 2 (right)

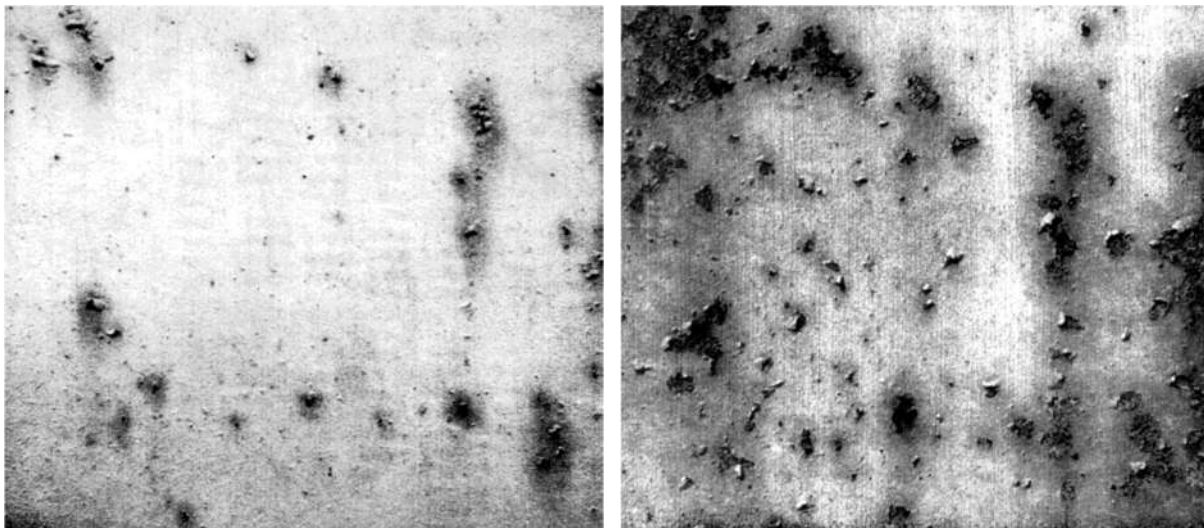


Figure 3-21. Degree of rusting: Ri 3 (left) and Ri 4 (right)

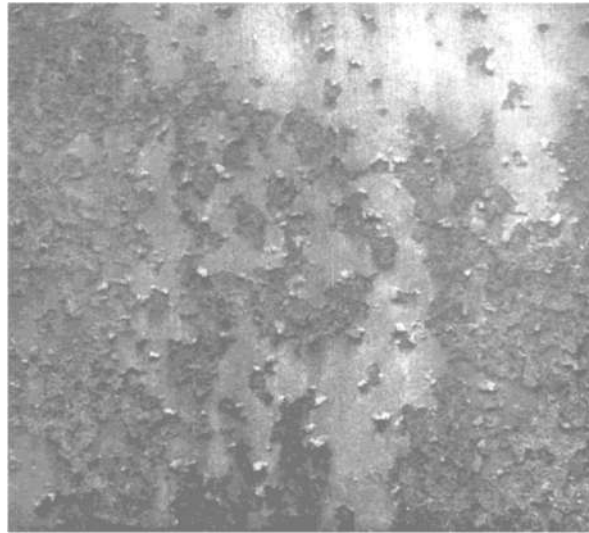


Figure 3-22. Degree of rusting: Ri 5

- Results:**

Plate	Inspected face	Degree of rusting	Rusty area (%)	Observations
# 4	Face A	Ri 4	8	It is observed in the part of the holes
	Face B	Ri 5	40-50	Delaminated rust flake. Part stayed in the plastic bag
# 3	Face A	Ri 3	1	Not much apparent corrosion, except in the holes
	Face B	Ri 5	40-50	More corrosion than on the Face B
# 7	Face A	Ri 4	8	Especially in the part of the holes
	Face B	Ri 3	1	In the lower part, 1/3 of the specimen, is in Ri 5

Table 3-4. Results of degree of rusting



Figure 3-23. Plate # 4: Face A (left), Face B (centre) and detail of Face B (right)



Figure 3-24. Plate # 3: Face A (left), detail of Face A (top centre), detail of Face B (bottom centre) and Face B (right)



Figure 3-25. Plate # 7: Face A (left), Face B (centre) and detail of Face B (right)

3.3.3 [Assessment of degree of cracking](#)

- **Object and field of application:**

ISO 4628-4:2016 Standard (4628-4:2016 2016) specifies a method for assessing the degree of cracking of painted surfaces by comparison with graphic standards.

- **Assessment:**

The number of cracks is evaluated by reference to the Table 3-5 shown in the standard and using the Figure 3-26 of the same as example, depending on the type of cracking.

Degree	Size of cracks
0	Not visible at 10x magnification
1	Visible only at magnifications up to 10x

2	Incipiently visible with normal corrected vision
3	Clearly visible with normal corrected vision
4	Large cracks, usually up to 1 mm wide
5	Very large cracks, usually more than 1 mm wide

Table 3-5. Size of cracks

When the test area shows cracks of different sizes, refer to the size of the cracks that are numerous enough to be considered typical of the test area. If possible, the depth of cracking is indicated by reference to the level of the paint system to which the cracks have penetrated. Three main types of crack failure must be distinguished:

- surface cracks that do not fully penetrate the finish coat (i.e., surface crazing);
- cracks that penetrate the finish layer, not substantially affecting the underlying layer(s);
- cracks that affect the entire paint system.

The evaluation should be carried out under good lighting, as specified in ISO 13076:2019 Standard (13076:2019 2019).

- Expression of results:**

The numerical value to designate the number and, if specified, the size of the cracks, together with the depth of the crack (a, b, or c), together with the approximate dimension of the affected area, or its proportion to the total area, expressed as percentage. For example, 'Cracking: degree of cracking 2(S3)b'.

Next, the photographic patterns that will be used for the evaluation and expression of the results are shown in Figure 3-26.

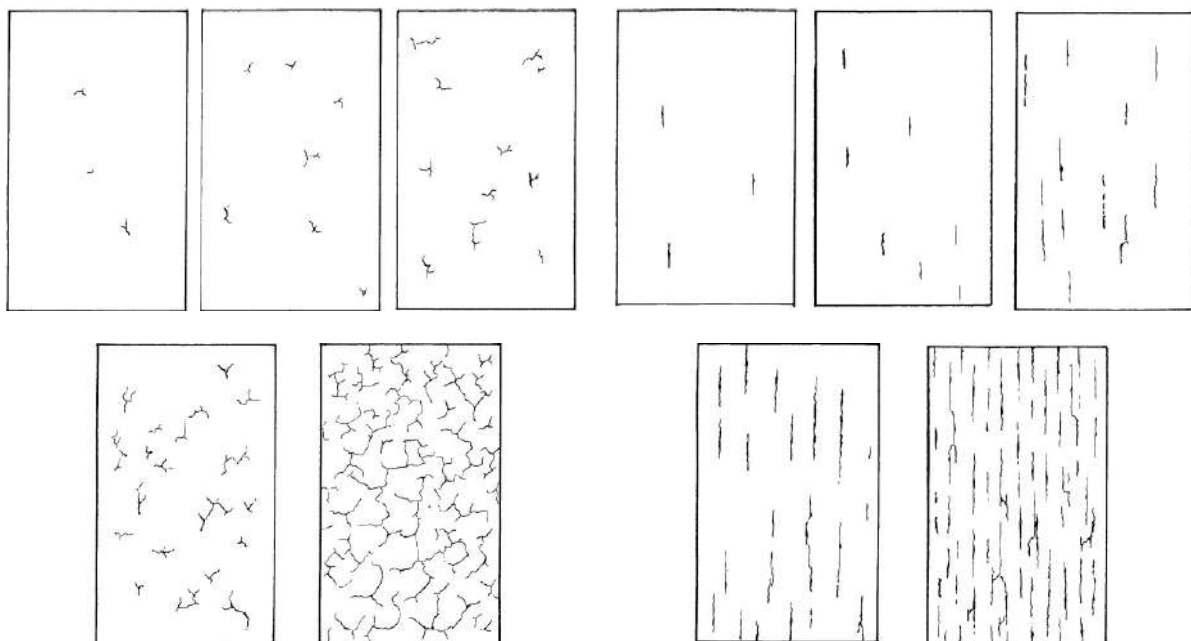


Figure 3-26. Top from left to right: Cracking with non-preferred direction quantity (density) 1, quantity (density) 2, quantity (density) 3; and Cracking with direction quantity (density) 1, quantity (density) 2, quantity (density) 3. Bottom from left to right: Cracking with non-preferred direction quantity (density) 4, quantity (density) 5; and Cracking with direction quantity (density) 4, quantity (density) 5.

- Results:**

Plate	Inspected face	Degree	Number of cracks	Degree	Size of cracks	Depth	Degree of cracking	Observations
# 4	Face A	1	Very few	2	Visible normal light	a	1(S2)a	Very few and small
	Face B	3	Moderate	3	Clearly visible	b	3(S3)b	Moderate amount of cracks
# 3	Face A	0	None	0	Not visible	-	-	No cracks visible
	Face B	1	Very few	2	Visible normal light	a	1(S2)a	Very few and small
# 7	Face A	0	None	0	Not visible	-	-	None
	Face B	3	Moderate	3	Clearly visible	a	3(S3)a	Moderate amount of cracks on Face B

Table 3-6. Results of degree of cracking



Figure 3-27. Plate # 4: detail of Face A (left), detail of Face A (centre) and Face B (right)



Figure 3-28. Plate # 3: Face A (left) and Face B (right)



Figure 3-29. Plate # 7: Face A (left) and Face B (right)

3.3.4 Assessment of degree of flaking

- **Object and field of application:**

ISO 4628-5:2016 Standard (4628-5:2016 2016) describes a method for the evaluation of the degree of flaking of paint coatings by comparison with graphic standards.

- **Assessment:**

The amount of flaking is evaluated by referring to the Table 3-7 and Table 3-8 shown in the standard and using the Figure 3-30 therein as example, depending on the type of flaking.

Degree	Flaking area %
0	0
1	0,1
2	0,3
3	1
4	3
5	15

Table 3-7. Evaluation scheme for the designation of the amount of flaking

Degree	Size of flakes (largest dimension)
0	Not visible at 10x magnification
1	Up to 1 mm
2	Up to 3 mm
3	Up to 10 mm
4	Up to 30 mm
5	Above 30 mm

Table 3-8. Evaluation scheme for the designation of the size of the area affected by desquamation

When the test area shows flakes of different sizes, refer to the size of the flakes that are largest and numerous enough to be typical of the test area. If possible, the depth of flaking is indicated by reference to the level of the paint system affected by the defect. Two main types of scaling faults should be distinguished:

- a) Layer(s) flaked from an underlying layer;
- b) flaking affecting the entire paint system, from the substrate.

The assessment should be carried out under good lighting, as specified in ISO 13076:2019 Standard (13076:2019 2019).

- **Expression of results:**

The numerical value of the quantity and size of the scales is expressed as shown in the Figure 3-30 of the standard, together with their depth (a or b), when possible, and with the approximate dimension of the affected test area, or its proportion with respect to the total area expressed as a percentage. For example, for quantity 3, size 2, with the entire paint system flaking from the substrate, record the result as follows: 'Flaking: degree of flaking 3(S2)b'. If necessary, the test result can be extended with words.

Next, the photographic patterns that will be used for the evaluation and expression of the results are shown in Figure 3-30.

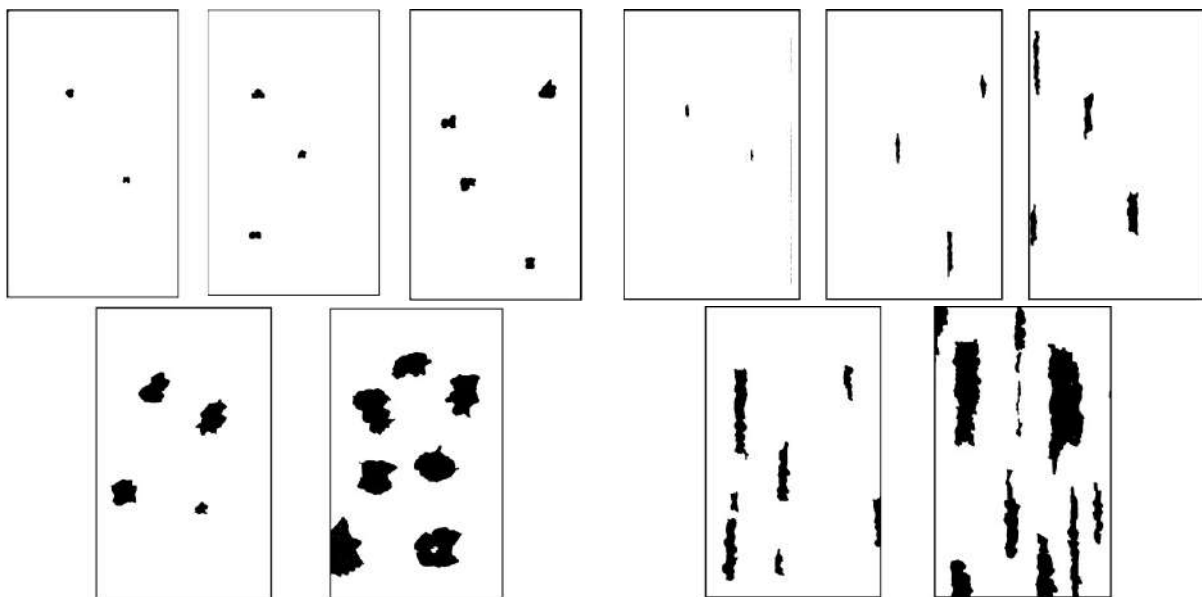


Figure 3-30. Top from left to right: Flaking with non-preferred direction quantity (density) 1, quantity (density) 2, quantity (density) 3; and Flaking with direction quantity (density) 1, quantity (density) 2, quantity (density) 3. Bottom from left to right: Flaking with non-preferred direction quantity (density) 4, quantity (density) 5; and Flaking with direction quantity (density) 4, quantity (density) 5.

- **Results:**

Plate	Inspected face	Degree	Flaking area	Degree	Size of flakes	Depth	Degree of flaking	Observations
# 4	Face A	2	0,30%	1	Up to 1 mm	a	2(S1)a	Very small and distant between them
	Face B	3	1%	1	Up to 1 mm	a	3(S1)a	Very small and distant between them
# 3	Face A	1	0,10%	1	Up to 1 mm	b	1(S1)b	Very small although somewhat deeper than the rest

	Face B	4	3%	3	Up to 10 mm	a	4(S3)a	Moderately large but shallow
# 7	Face A	3	1%	2	Up to 3 mm	a	3(S2)a	Quite corroded specimen but with little proportion of flaking
	Face B	3	1%	1	Up to 1 mm	a	3(S1)a	Quite corroded specimen but with little proportion of flaking

Table 3-9. Results of degree of flaking



Figure 3-31. Plate # 4: Face A (left) and Face B (right)



Figure 3-32. Plate # 3: detail of Face A (left), detail of Face A (centre) and Face B (right)



Figure 3-33. Plate # 7: Face A (left) and Face B (right)

3.3.5 [Assessment of degree of chalking by tape method](#)

- **Object and field of application:**

According to ISO 4628-6:2016 Standard (4628-6:2016 2016), with an adhesive tape, the chalking is removed from the coating under test. The chalking adhered to the tape is examined on a contrasting background (white or black, depending on whether a greater contrast is obtained) and the degree of chalking is evaluated with respect to a scale.

- **Assessment:**

The degree of chalking is evaluated by reference to the graphic patterns listed in the standard (Figure 3-34). The numerical values indicated correspond to those given in the standard.

- **Expression of results and method:**

Dry the surface at room temperature before carrying out the test. A strip of adhesive tape is placed over the dry coating and pressed down firmly with a fingertip. The length of the tape should be at least 40 mm. The tape is removed, perpendicular to the surface, and placed on a background of the appropriate color that provides the greatest contrast, with the adhesive in contact with the background. Light colored coatings are evaluated on a black background and dark colored coatings on a white background. Under appropriate light, the degree of chalking is immediately evaluated by comparing the amount of chalking material present on the tape with the reference graphic patterns shown in the standard (Figure 3-34). The degree will be lower the greater the amount of visible background. The illumination is recorded in the test report.

The tape is applied to an area of the specimen that has not been used for previous measurements to avoid false readings. The values obtained with coatings exposed to natural aging must be treated with care, since the dirt from the atmosphere deposited on the surface can lead to erroneous chalking values. After removing the chalking from the coating under test, the evaluation of each piece of adhesive tape should be made without delay, because the appearance of the chalking residue on the adhesive tape and the transmission of the tape

could vary with time. When testing low gloss paint coatings, a certain amount of chalking may be observed even with unaged specimens. A blank test with an unaged specimen is therefore recommended for these coatings.

Next, the photographic patterns that will be used for the evaluation and expression of the results are shown in Figure 3-34.

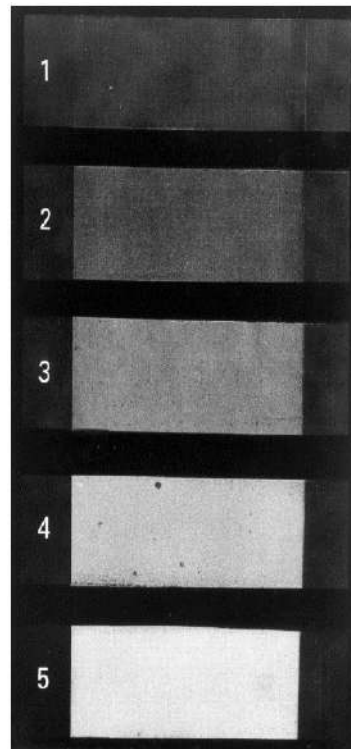


Figure 3-34. Photographic patterns

- **Results:**



Figure 3-35. Plates # 3 (left), # 4 (centre) and # 7 (right)

The upper Face A of the Plate # 4 has a degree of chalking = 2. The lower face of the Plate # 4 has a degree of chalking = 3.



Figure 3-36. Plate # 4: Face A (top left), Face B (top right) and Chalking adhered to the tapes (bottom)

The upper Face A of the Plate # 3 has a degree of chalking = 3. The lower face of the Plate # 3 has a degree of chalking = 4.

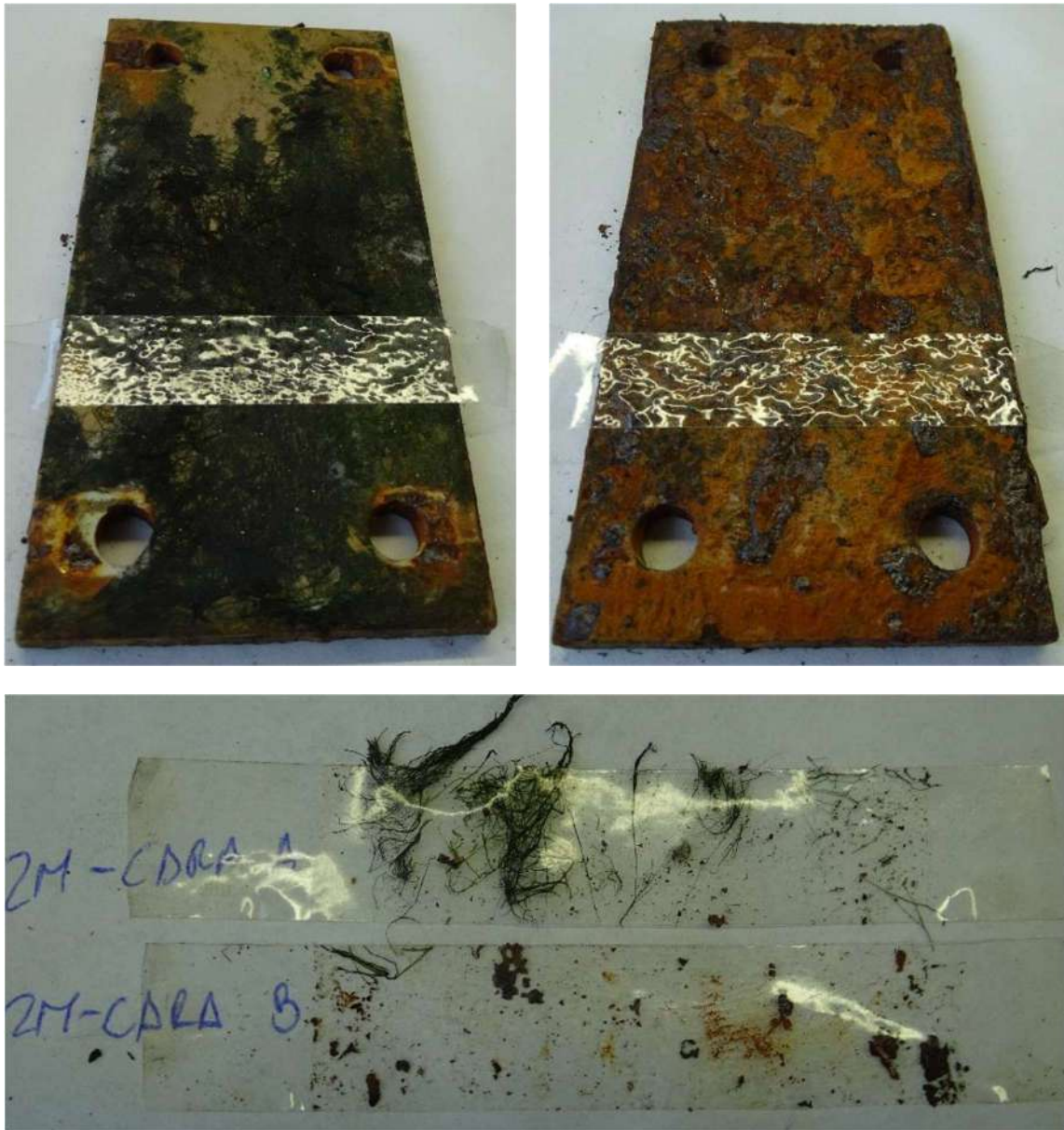


Figure 3-37. Plate # 3: Face A (top left), Face B (top right) and Chalking adhered to the tapes (bottom)

The upper Face A of the Plate # 7 has a degree of chalking = 4. The lower Face B of the Plate # 7 has a degree of chalking = 4. The latter test had to be carried out in the lower part of the Face B since it was the only area where we could find corrosion and make a good visual evaluation of it. Nothing was found in the rest of the unexposed Face B of the Plate # 7.

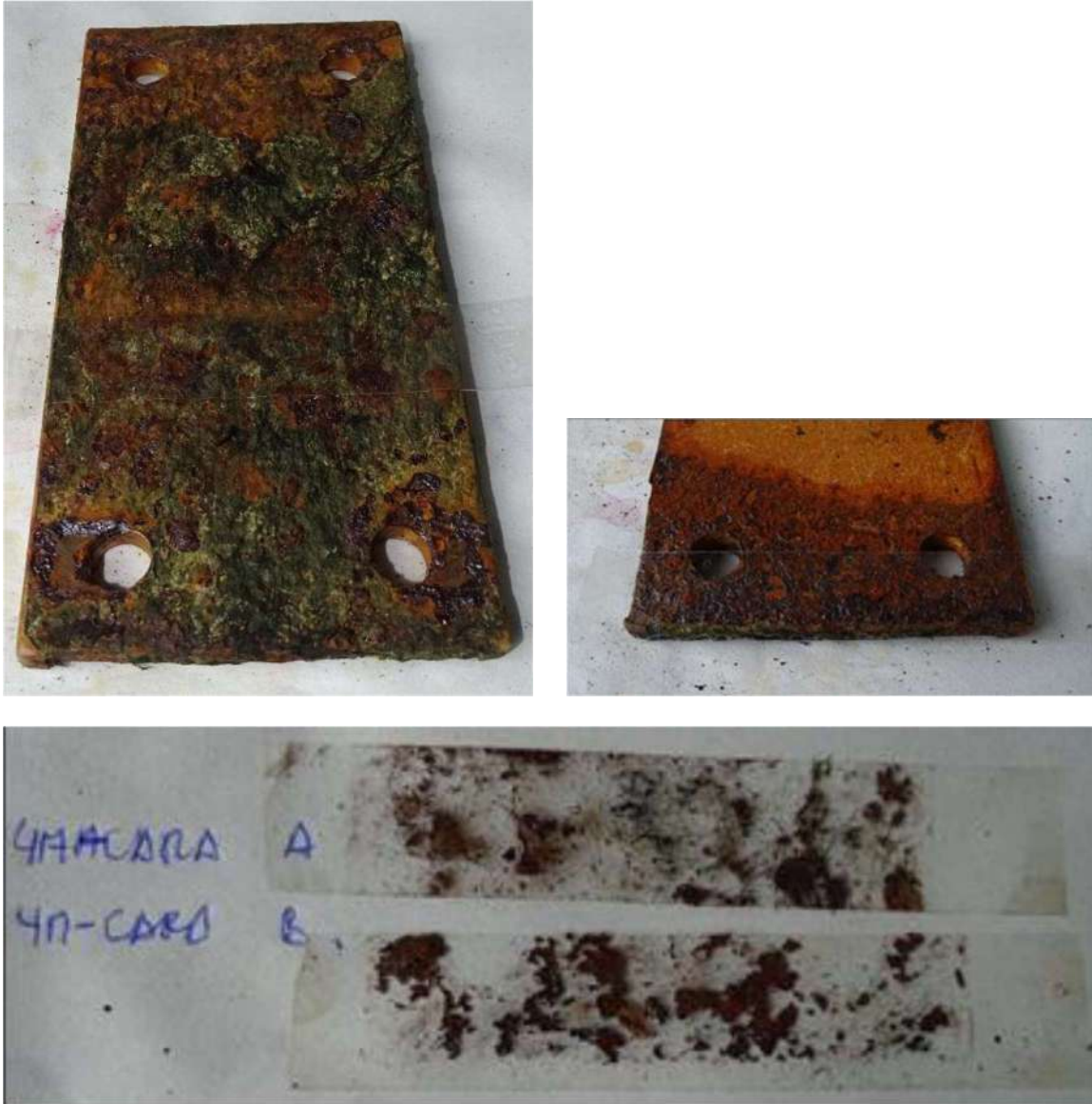


Figure 3-38. Plate # 7: Face A (top left), Face B (top right) and Chalking adhered to the tapes (bottom)

4 REFERENCES

13076:2019, UNE-ENISO 2019, *Paints and varnishes - Lighting and procedure for visual assessments of coatings.*

4628-1:2016, UNE-ENISO 2016, *Paints and varnishes - Evaluation of degradation of coatings - Designation of quantity and size of defects, and of intensity of uniform changes in appearance - Part 1: General introduction and designation system.*

4628-2:2016, UNE-ENISO 2016, *Paints and varnishes - Evaluation of degradation of coatings - Designation of quantity and size of defects, and of intensity of uniform changes in appearance - Part 2: Assessment of degree of blistering.*

4628-3:2016, UNE-ENISO 2016, *Paints and varnishes - Evaluation of degradation of coatings - Designation of quantity and size of defects, and of intensity of uniform changes in appearance - Part 3: Assessment of degree of rusting.*

4628-4:2016, UNE-ENISO 2016, *Paints and varnishes - Evaluation of degradation of coatings - Designation of quantity and size of defects, and of intensity of uniform changes in appearance - Part 4: Assessment of degree of cracking.*

4628-5:2016, UNE-ENISO 2016, *Paints and varnishes - Evaluation of degradation of coatings - Designation of quantity and size of defects, and of intensity of uniform changes in appearance - Part 5: Assessment of degree of flaking.*

4628-6:2016, UNE-ENISO 2016, *Paints and varnishes - Evaluation of degradation of coatings - Designation of quantity and size of defects, and of intensity of uniform changes in appearance - Part 6: Assessment of degree of chalking by tape method.*



D5.3: Integrated FOWT test report

FIHAC/CTC/VICINAY/INNOSEA/JDR

January 2023

A02

ANNEX II. Chain lines and dynamic cable coating degradation in marine environment for 2 years

Disclaimer:



This project has received funding from the European Union's Horizon 2020 Research and Innovation programme under grant agreement No 815083.

Project details:

Duration:
1 Sep 2019 - 28 Feb 2023
Grant agreement:
No: 815083

Table of contents

1	OBJECTIVE	3
2	METHODOLOGY	3
3	RESULTS	5
3.1	Photographic survey	7
3.2	Analysis in the FIHAC’s laboratory	18
3.3	Analysis in the CTC’s laboratory	20
3.3.1	Assessment of degree of blistering	21
3.3.2	Assessment of degree of rusting	24
3.3.3	Assessment of degree of cracking	27
3.3.4	Assessment of degree of flaking	29
3.3.5	Assessment of degree of chalking by tape method	32
4	REFERENCES	36

1 OBJECTIVE

The aim of this task is to test the behaviour of different cable coating and mooring chain materials exposed to biological and physicochemical elements of the marine environment.

2 METHODOLOGY

The material testing was carried out between November 17th 2020 and November 25th 2022, with an intermediate partial extraction in March 2nd 2022. The test was carried out under real marine conditions, in the Marine Corrosion Test Site El Bocal (MCTS El Bocal), located in the coastal area of Cantabria (North of Spain) (Figure 2-1). The test was carried out at three depth levels:

- The upper level: Located just below the splash zone.
- The middle level: Located at the intertidal zone.
- The lower level: Located at the submerged zone.

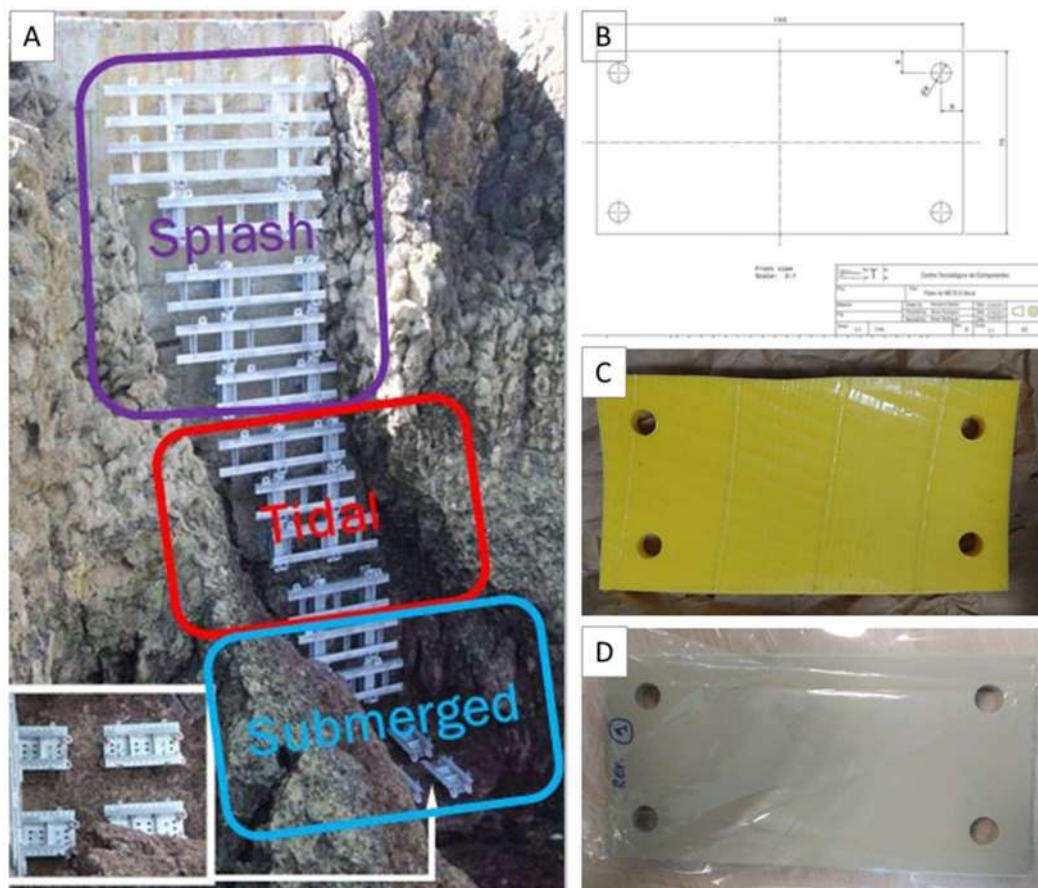


Figure 2-1. Installations of the Marine Corrosion Test Site El Bocal (A). Design of the material testing plates (B). Cable coating plastic testing plate (C). Cable mooring steel testing plate coated with an anticorrosive paint (D).

At each of these levels, several test plates, of 75*150mm and made up of different materials, were deployed to be exposed to the elements during 12 and 24 months (Table 2-1). The installation of the plates was carried out on November 17th 2020, but, due to adverse maritime conditions and Covid-19 incidences, the first extraction was carried out in March 2022 (at 16 months of experiment). The final extraction was carried out in November 2022 (at 24 months, as planned).

Cable testing			
Material /Component	Depth	Number of plates	Timeframe
Cable coating	Sample just below the splash zone	1	12 months
Cable coating	Tidal area	1	12 months
Cable coating	Submerged	1	12 months
Cable coating	Sample just below the splash zone	1	24 months
Cable coating	Tidal area	1	24 months
Cable coating	Submerged	1	24 months
Mooring testing			
Material /Component	Depth	Number of plates	Timeframe
Mooring Chain	Tidal area	4	12 months
Mooring Chain	Submerged	4	12 months
Mooring Chain	Tidal area	4	24 months
Mooring Chain	Submerged	4	24 months

Table 2-1. Type and number of testing plates

The test plates used for the cable testing were made up of a plastic material, while the plates used for the mooring chain included:

- 4 replicated plates of bare steel.
- 4 replicates of steel coated with an unmodified reference hempadur 15570 paint (Type 0).
- 4 replicates of steel coated with a functionalized paint (HDK18+NP Cu) 23% SiO₂ + 6%CuO (Type 1).
- 4 replicates of steel coated with a functionalized paint (HDK18+NP Cu) 28% SiO₂ + 6%CuO (Type 2).

During the experiment, a photographic survey was carried out, taking photographs of the plates on a monthly basis, when possible.

After each extraction, one replicate of each of the plates were carried out to the laboratory for their analysis, which included a biotic assessment of the biofouling communities (Figure 2-2). Afterwards, a visual inspection of the corrosion applying the UNE-EN ISO 4628:2016 standard is conducted for the steel coating plates (assessment of degree of blistering, rusting, cracking, flaking and chalking).

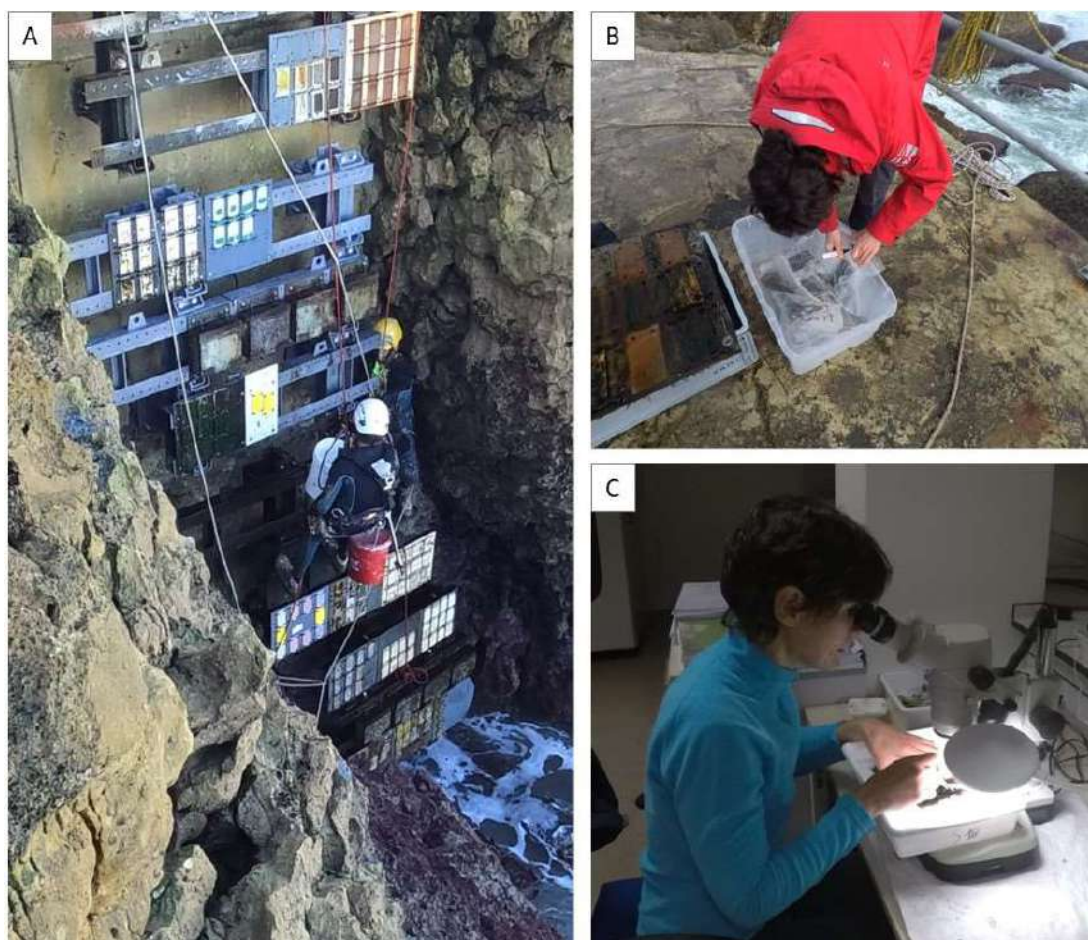


Figure 2-2. Extraction of the structures in March 2022 (A), collection of the testing plates (B) and biological analysis of the plates in the laboratory (C).

3 RESULTS

The analysis of the plates was carried out during two consecutive survey periods:

- First period: From November 2020 to March 2022 (16 months).
- Second period: From March 2022 to November 2022 (+8 months, total 24 months).

The results obtained in each of the periods are described below.

The first extraction of the plates was carried out on March 2nd 2022, with a delay of 3.5 months from the estimated schedule. This delay was caused by adverse maritime conditions and Covid-19 incidences.

In addition, several incidences should be reported regarding the integrity of the structures and probes. By January 2022, 4 of the 10 probes of the submerged level were dropped from their base. Then, by February 2022, the whole submerged base, with the remaining testing probes, was ripped off the structure and lost during a storm event. Moreover, by February 2022, 2 of the 10 probes of the tidal level were dropped from their base and, by March 2022, one more was lost. Thus, at the extraction date, carried out on March 2nd 2022, only the following plates remained available:

- Splash zone:
 - 2 cable coating plates (one extracted in March 2022).

- Tidal zone:
 - 2 cable coating plates (one extracted in March 2022).
 - 2 bare steel plates (one extracted in March 2022).
 - 2 plates of steel coated with a functionalized paint (HDK18+NP Cu) 23% SiO₂ + 6%CuO. Type 1 (both extracted in March 2022).
 - 1 plate of steel coated with a functionalized paint (HDK18+NP Cu) 28% SiO₂ + 6%CuO. Type 2.

Due to a visual error, on March 2nd 2022, two Type 1 plates were extracted, instead of one Type 1 and one Type 2 plates. This mistake occurred because the apparent degree of corrosion and biofouling colonization of one of the Type 1 plates was higher than that of the other Type 1 plate, and conversely presented a similar state to that of the Type 2 plate at the time of extraction, as well as during the whole experiment.

The second extraction of the plates was carried out on November 25th 2022, in accordance to the schedule established.

After the incidents that occurred during the first assessment period (loss of submerged base and several testing plates), no more mishaps have occurred in this second period. Thus, at the extraction date, the following plates remained available and were definitively extracted:

- Splash zone:
 - 1 cable coating plate (extracted).
- Tidal zone:
 - 1 cable coating plate (extracted).
 - 1 bare steel plate (extracted).
 - 1 plate of steel coated with a functionalized paint (HDK18+NP Cu) 28% SiO₂ + 6%CuO. Type 2 (extracted).

The following Figure 3-1 shows the exposed plates, their exposure zones, and the specimens on which the visual inspection has been carried out.

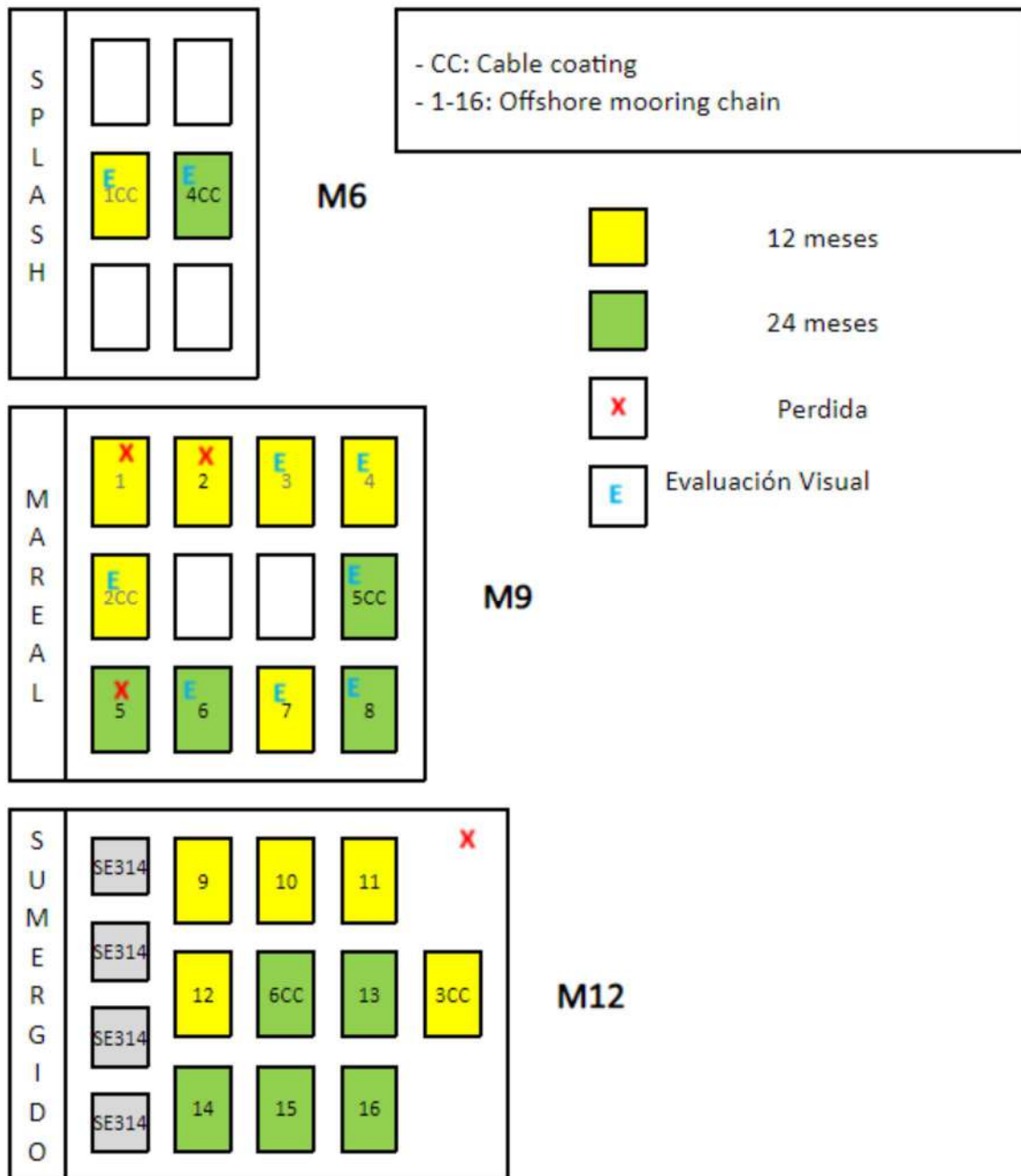


Figure 3-1. Schematic of the installed plates

3.1 Photographic survey

Figure 3-2 to Figure 3-5 show the evolution of the plates between the installation in November 2020 and the extraction in March 2022.

As it can be seen in Figure 3-2, days after the installation, the uncoated steel plates showed early signs of oxidation and biological colonization by ephemeral pioneering species. Also, the Type 2 plates installed at the tidal zone showed slight signs of oxidation at the plates margins. The remaining mooring chain plates, as well as the cable coating plates, did not show apparent signs of deterioration, at none of the tidal levels.

By December 2020, the Type 2 plates installed at the tidal zone showed increasing signs of oxidation at the plates margins and one of the Type 1 plates, the one installed in the bottom, started showing a slight oxidative process. The uncoated steel plates showed advanced signs of oxidation and biological colonization by ephemeral pioneering species at both, tidal and submerged levels. Regarding cable coating plates, only one of the plates installed at the tidal level showed early signs of biological colonization by ephemeral pioneering species, probably filamentous brown algae from the genus *Ectocarpus*. The remaining plates did not show apparent signs of deterioration, at none of the tidal levels.

In January 2021, the Type 2 plates installed at the tidal zone showed increasing signs of oxidation at the plates margins, as well as early signs of biological colonization by ephemeral pioneering species. One of the Type 1 plates, the one installed in the bottom, shows an important coverage of a black biofilm. In addition, the plates painted with the Type 0 coating and installed in the tidal level, show the beginning of an oxidative process, which is specially advanced in the bottom plate. In the submerged level, only the bare steel plates show an important level of oxidation. The remaining plates at this level only show early signs of biological colonization by ephemeral pioneering species, probably filamentous brown algae from the genus *Ectocarpus*.

In February 2021, a generalized biological colonization by ephemeral pioneering species is observed at the plates of the tidal level. The oxidative process seems to be like that of January 2021. The splash level plates do not show any signs of biological colonization. At this month, it was not possible to obtain any photographs of the submerged level.

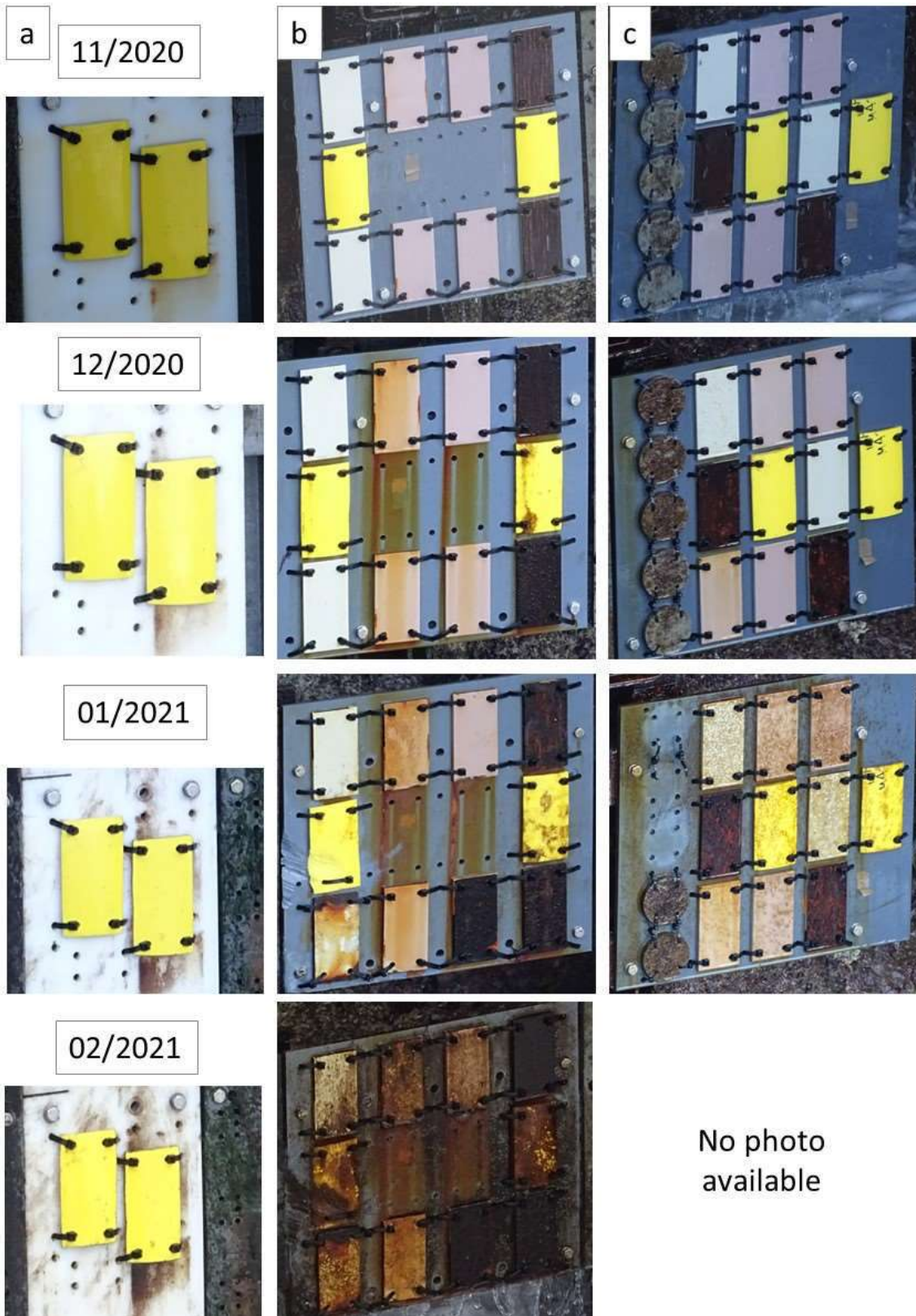


Figure 3-2. State of the plates between November 2020 and February 2021. Column a: Splash level; Column b: Tidal level; Column c: Submerged level.

Figure 3-3 shows that March 2021 continues with the generalized biological colonization by ephemeral pioneering species at all the plates of both the tidal and submerged levels. The splash level plates show early signs of biological colonization.

April 2021 is characterized by the beginning of the colonization by green filamentous algae of the genus *Ulva* in some of the plates of the tidal level (i.e., upper plates of the Types 0, 1 and 2, and bottom Type 2 plate). The submerged plates show an advanced colonization by ephemeral pioneering species and the splash level plates continue showing early signs of biological colonization.

May 2021 shows a similar pattern to that of April 2021. However, the presence of grazers of the genus *Patella* (limpets) seems to have reduced the number of ephemeral algae in some of the plates at the tidal level.

June 2021 is characterized by a notable decrease in the coverage of ephemeral algae in all the plates of the tidal level, probably associated to the grazing pressure of the limpets. The submerged level is characterized by the beginning of the colonization by green filamentous and foliose algae of the genus *Ulva* as well as the beginning of the colonization by red filamentous species.

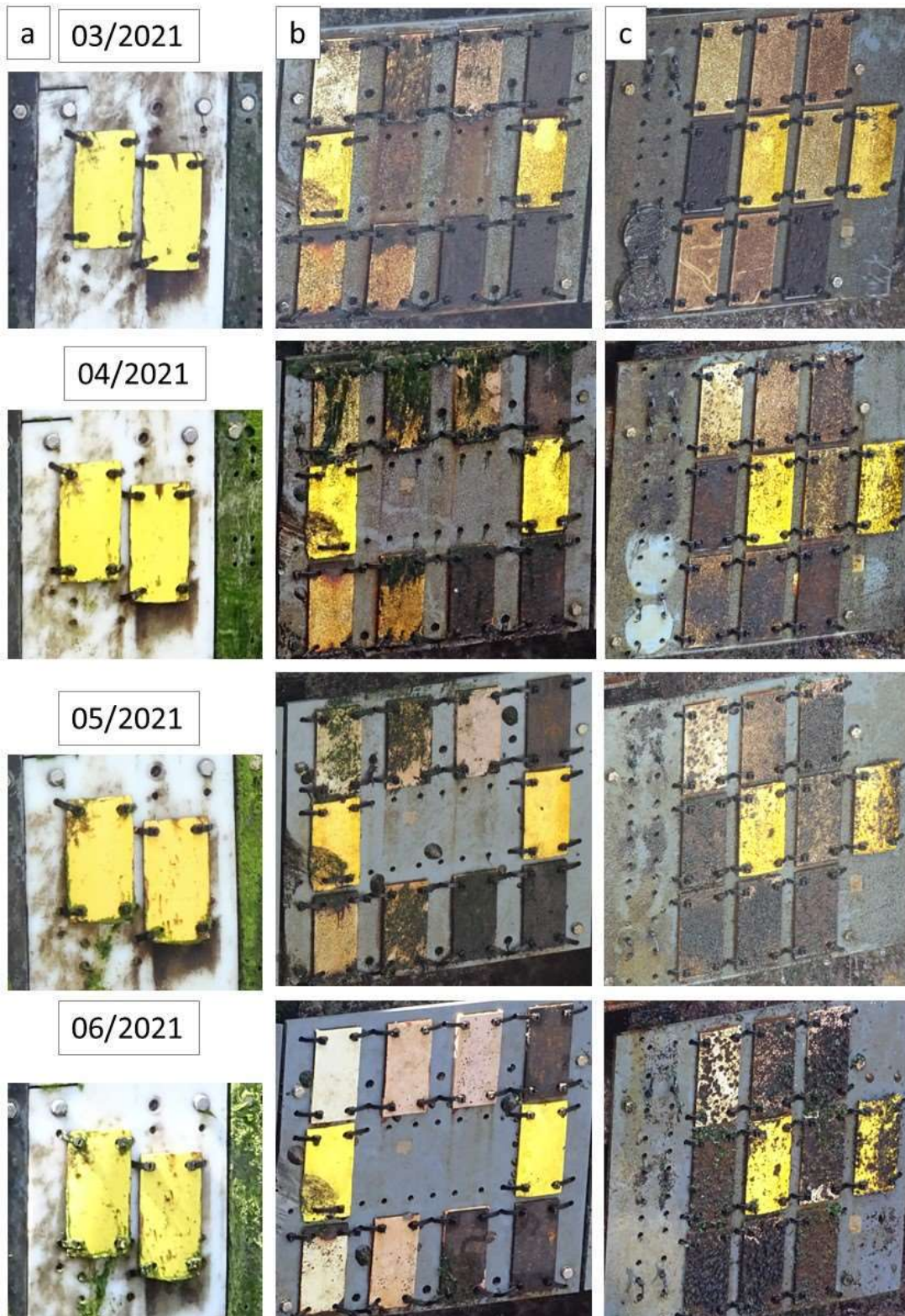


Figure 3-3. State of the plates between March 2021 and June 2021. Column a: Splash level; Column b: Tidal level; Column c: Submerged level.

As it can be seen in Figure 3-4, in July 2021, the splash and tidal levels show a similar pattern to that of June 2021 and there is no photo available of the submerged level.

August 2021 shows a similar pattern to those of June and July 2021. However, the green filamentous and foliose algae of the genus *Ulva* seem to have disappeared from the submerged plates. Instead, encrusting red algae of the genus *Lithophyllum* seem to be growing in some of the plates of the tidal (i.e., plates of the Types 1 and 2) and submerged (i.e. Type 0 and cable coating) levels. One of the Type 1 plates, the one at the top, shows an advanced level of corrosion since the last month. Finally, one of the splash level plates shows the presence of ephemeral brown filamentous pioneering species, probably of the genus *Ectocarpus*.

September and October 2021 show a similar pattern to that of August 2021 in all the plates and tidal levels. However, in October there is no photo available for the submerged level. Apparently, in October, one of the cable coating plates show the presence of cirripedians, probably of the genus *Chthamalus*, growing at the scrape probably produced by the impact of some floating object pushed by the waves.

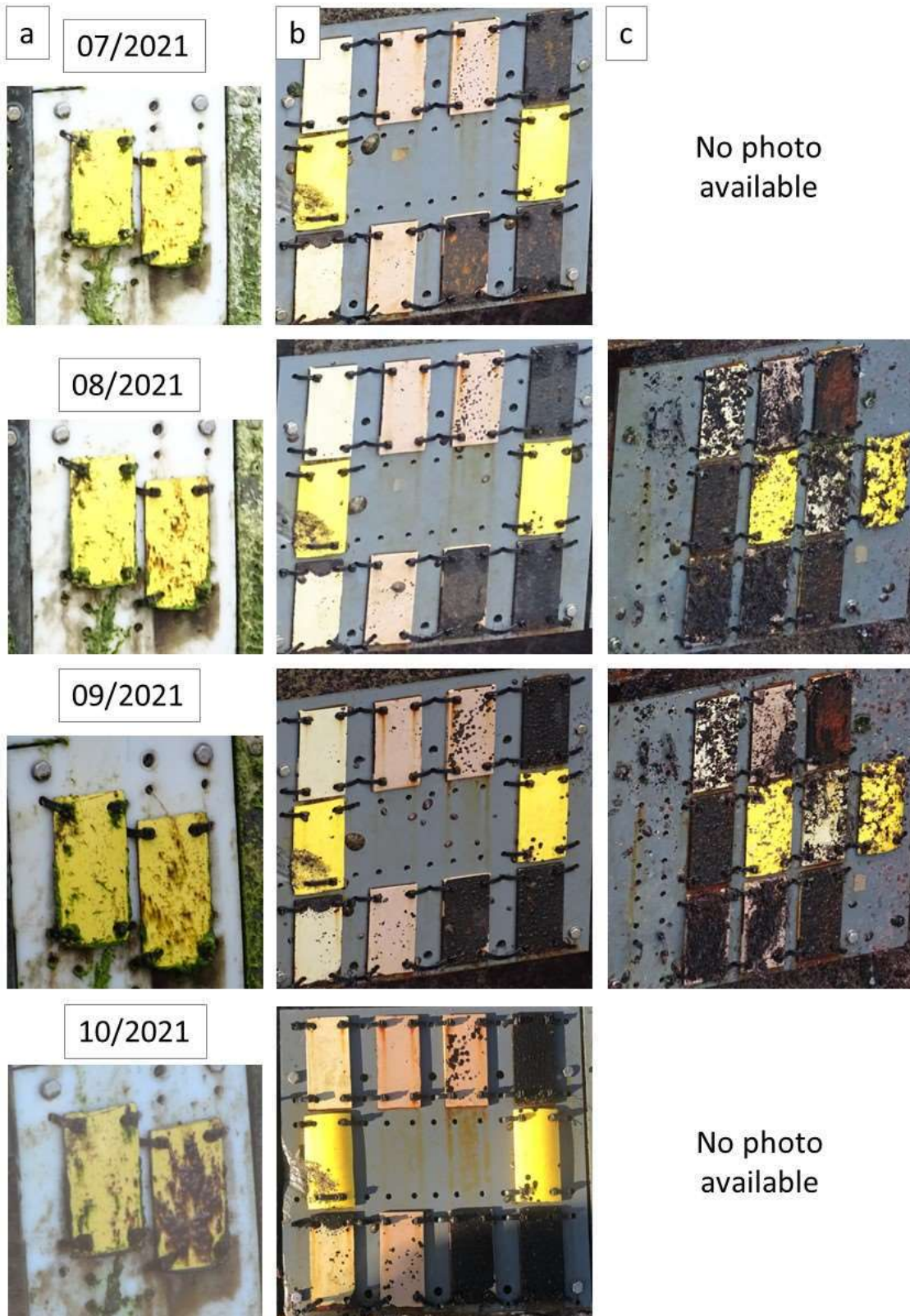


Figure 3-4. State of the plates between July 2021 and October 2021. Column a: Splash level; Column b: Tidal level; Column c: Submerged level.

As shown in Figure 3-5, in January 2022 only one photo of the submerged level is available. Most of the ephemeral filamentous algae seem to have disappeared from the plates. Instead, encrusting red algae of the genus *Lithophyllum* continue growing in the Type 0 and cable coating plates, and, to a lesser extent in the Type 1 and Type 2 plates. One of the Type 2 plates, the one at the bottom, shows an advanced level of corrosion and biological colonization by a dark biofilm. This phenomenon is not observed in the other Type 2 replicate, which continues unaltered, similarly as the remaining Type 1 plate. Both bare steel plates show an advanced level of corrosion and the presence of early populations of *Spirorbidae* polychaetes, which can be also found, in a smaller number, in the Type 1 and Type 2 plates.

In February 2022, the cable coating plates of the splash zone are mostly covered by ephemeral green and brown filamentous algae of the genus *Ulva* and *Ectocarpus*, respectively. The plates of the tidal zone are also covered by these opportunistic algae and, some of them (i.e., one of the cable coating plates, one of the bare steel plates and, to a lesser extent, one of the Type 1 plates) show some individuals of the foliose red macroalgae *Porphyra* sp. The remaining Type 0 plate seems to be relatively unaltered, with few signs of corrosion and a low level of biofouling. The structure of the submerged zone was lost during a storm, so, there is no information regarding the plates at this level.

In March 2022, the pattern is like that of February. One of the Type 2 and both of the Type 0 plates have been lost. The remaining plates are covered by ephemeral green and brown filamentous algae of the genus *Ulva* and *Ectocarpus*. Also, the plates mentioned before at the tidal level show growing populations of the foliose red macroalgae *Porphyra* sp. It is worth to mention that, regarding Type 1 and Type 2 plates, one of the Type 1 plates shows a higher level of corrosion and biological colonization, while the remaining Type 1 and Type 2 plates show similar and slightly lower levels of alteration. These phenomena contributed to the misleading of the plates to be removed, mistaking one of the Type 1 for the Type 2.



Figure 3-5. State of the plates between January 2021 and March 2022. Column a: Splash level; Column b: Tidal level; Column c: Submerged level.

As it can be seen in Figure 3-6, some days after the first extraction the remained plates were mostly covered by green filamentous algae of the genus *Ulva*. Also, some filaments of the ephemeral brown algae *Ectocarpus sp.* could be observed, especially at the splash level plate.

By May 2022 and June 2022 the situation was very similar, although with a decreasing coverage of algae at the splash level in June 2022.

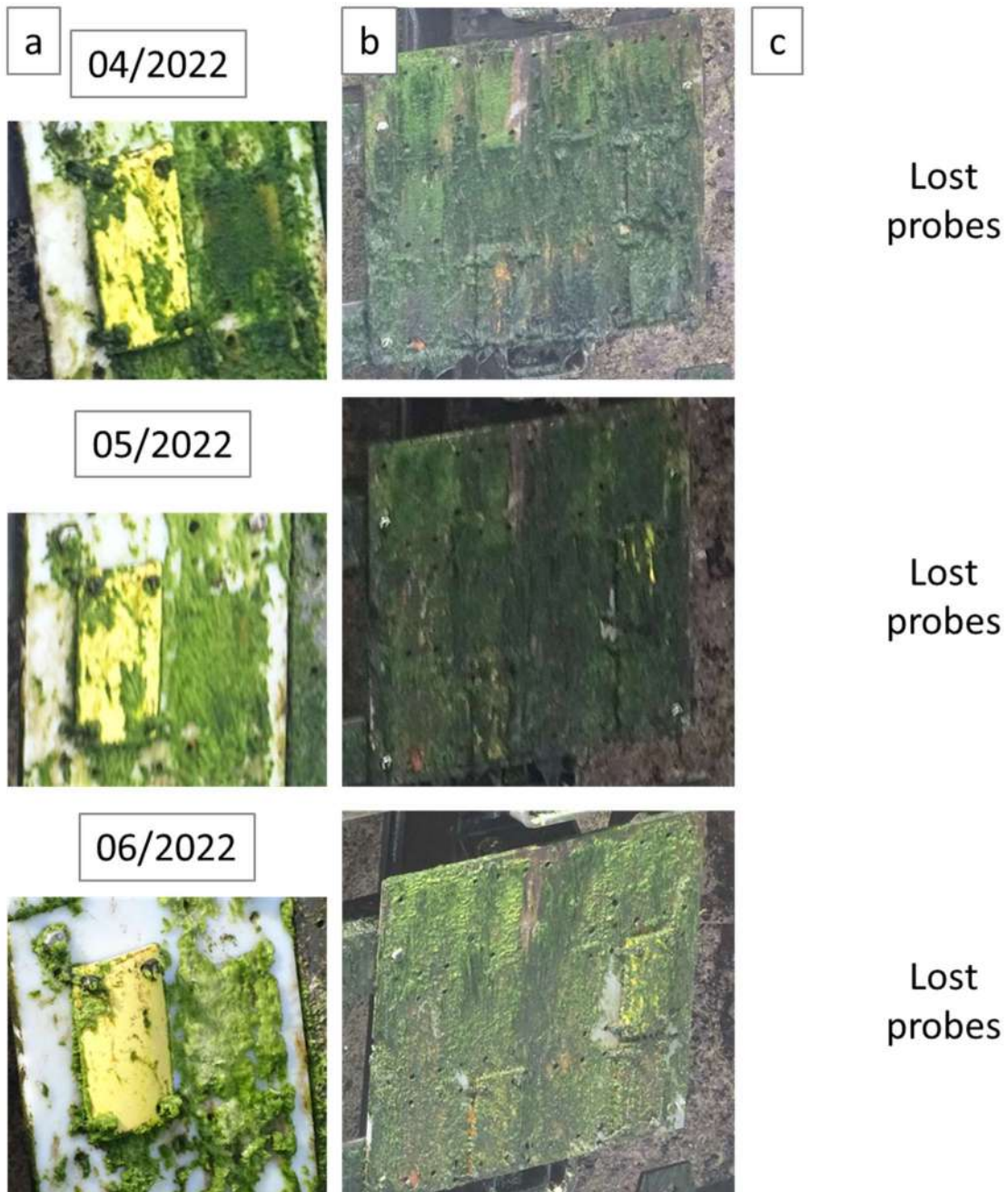


Figure 3-6. State of the plates between April 2022 and June 2022. Column a: Splash level; Column b: Tidal level; Column c: Submerged level.

In July and August 2022 the situation is quite similar, with the green filamentous algae of the genus *Ulva* covering most of the plates of the tidal level and decreasing in coverage at the splash level (Figure 3-7). However, during these two months, the biomass of the algae showed a notable decrease, especially at the tidal level. Here, the presence of several individuals of *Patella sp.* limpets can be clearly observed in the base where the plates are allocated. Thus, the decreasing biomass of the algae at the base and plates could be attributed to the grazing activity of the limpets.

In September 2022 this effect is more pronounced, with a notable decrease of the algae coverage in the base and plates of the tidal level and with the presence of various limpets in the area (Figure 3-7). Apparently, the cable coating plate at this level shows small patches of the encrusting red algae *Hildenbrandia sp.* In the splash zone, the cable coating plate shows a slight increase of some ephemeral brown algae of the genus *Ectocarpus*.

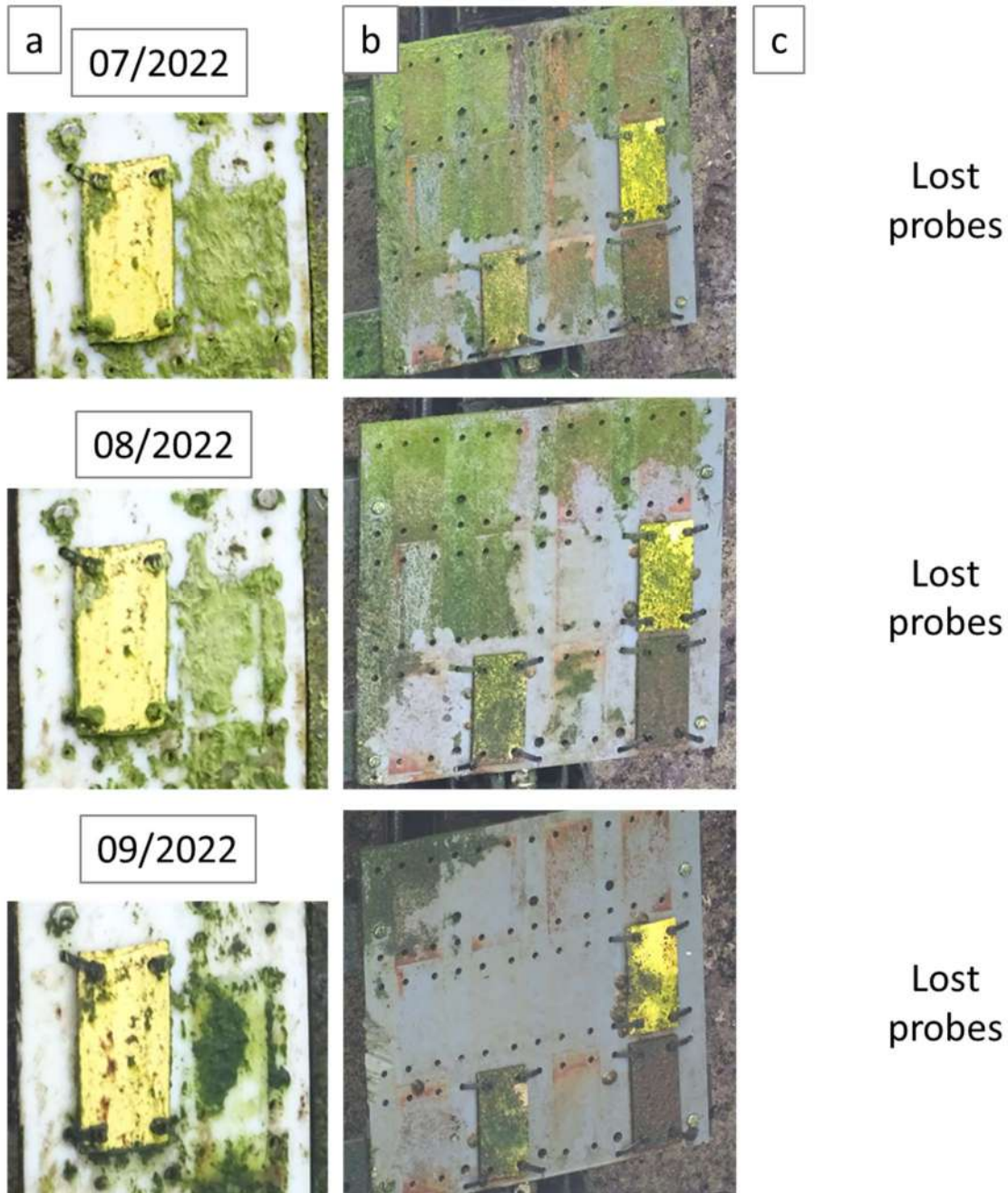


Figure 3-7. State of the plates between July 2022 and September 2022. Column a: Splash level; Column b: Tidal level; Column c: Submerged level.

During October 2022 and November 2022 most of the algae from the base and the plates of the tidal level have disappeared, supposedly due to the grazing activity of the limpets, which can still be observed in the area (Figure 3-8). On the contrary, the splash zone shows an increasing coverage of *Ectocarpus sp.* and *Ulva sp.* algae. At the extraction date, the situation is quite similar, although with a slight decrease of algae cover at the splash zone.

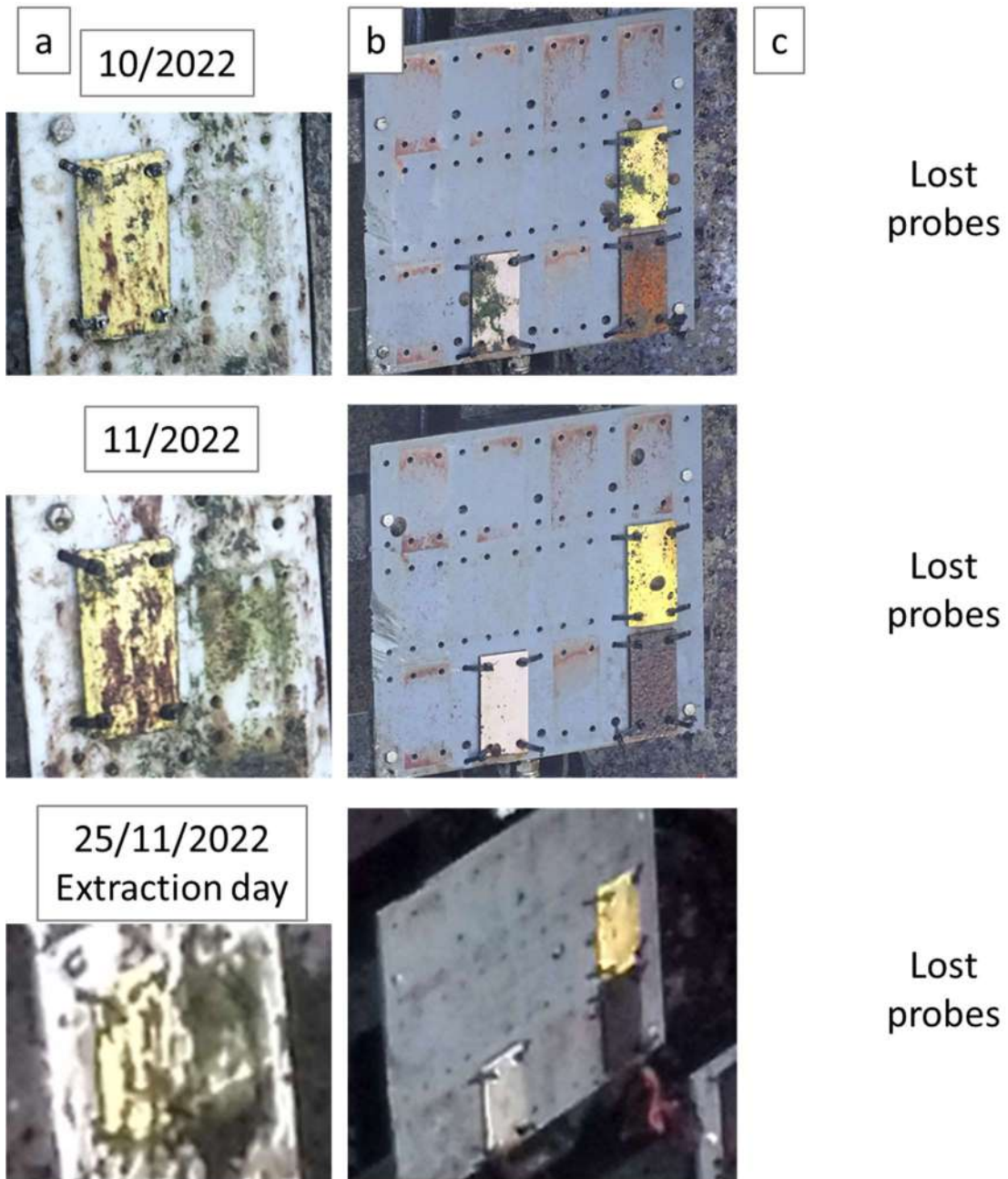


Figure 3-8. State of the plates between October 2022 and the day of extraction on November 25th 2022. Column a: Splash level; Column b: Tidal level; Column c: Submerged level.

3.2 Analysis in the FIHAC's laboratory

The state of the plates, once in the laboratory, is shown in Figure 3-9 for the splash and tidal levels.

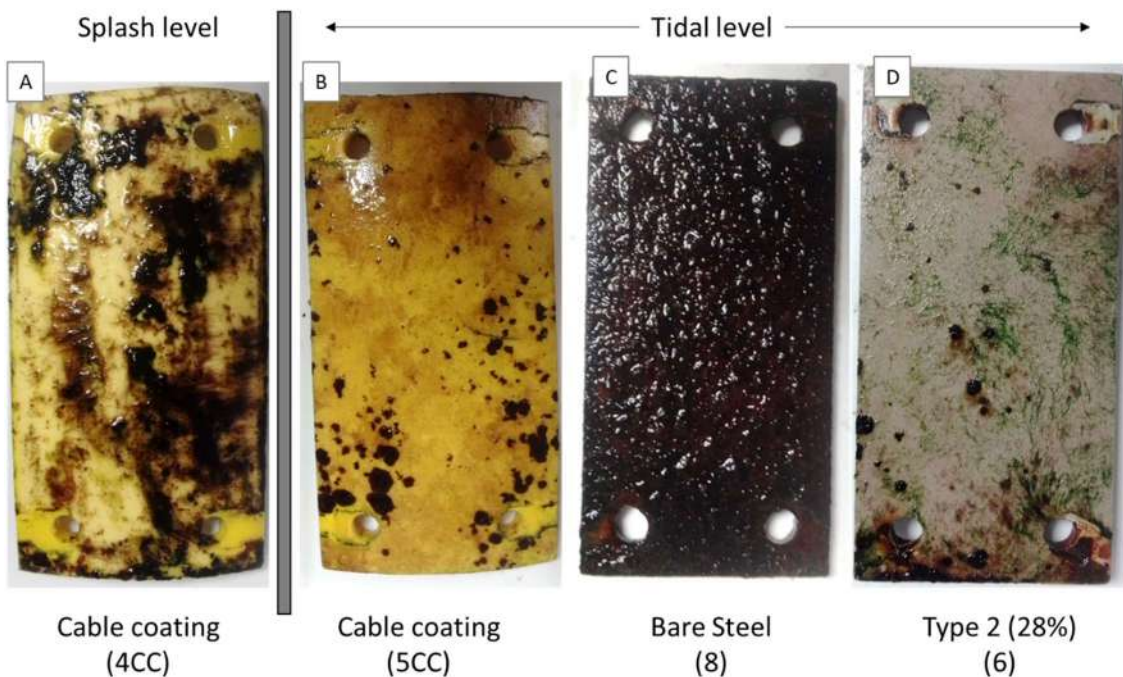


Figure 3-9. State of the different plates extracted from the splash and tidal levels. A: Cable coating (splash), B: Cable coating (tidal), C: Bare steel, D: Type 2 paint (28%).

As it can be seen in Table 3-1, showing the results of the biological analysis, the most abundant species colonizing the plates are the green filamentous opportunistic species *Ulva sp.* and the brown filamentous *Ectocarpus sp.* Also, a notable presence of the red encrusting *Hildenbradia sp.* is observed, but this one only in the cable coating and in the painted plate of the tidal level. The cable coating plate of the splash zone shows the higher coverage of macroalgae, with a 50% coverage of *Ectocarpus sp.* and a 25% of *Ulva sp.* However, no fauna biota is observed in this plate. On the other hand, at the tidal level, the bare steel plate shows the lower coverage of macroalgae (4% of the same ephemeral filamentous species), but it has a notable presence of *Chthamalus sp.* cirripedians (27 individuals) and a Chironimidae larvae. Also, the cable coating at this level, has a low coverage of macroalgae but has the presence of an *Hyale sp.* amphipod and two individuals of *Chthamalus sp.* cirripedians. Finally, the painted plate shows a moderate presence of ephemeral filamentous algae (30% of *Ulva sp.* and 5% of *Ectocarpus sp.*) as well as small patches of the red encrusting *Hildenbradia sp.* (5%) and 11 individuals of *Chthamalus sp.* cirripedians.

Level	Splash	Tidal	Tidal	Tidal
Plate Number	4CC	5CC	8	6
Plate Type	Cable coating	Cable coating	Bare steel	Type 2 (28%)
FLORA (% coverage)				
Ulva sp.	25	2	2	30
Ectocarpus sp.	50	2	2	5
Hildenbrandia sp.		8		5
FAUNA (Number)				
Chthamalus sp.		2	27	11
Hyle sp.		1		
Chironomidae larvae			1	
COVERAGE (%)	75	12	4	40
RICHNESS (N)	2	5	4	4

Table 3-1. Results of the biological analysis of the plates extracted in November 2022.

Surprisingly, the coverage and richness values obtained in this second extraction are lower than those observed after the first extraction. These phenomena can be attributed to the elevated grazing activity observed during the last months, especially at the tidal level, as described in the previous section.

In view of this, it could be said that, if the plates were left installed for a few more months, it is more than likely that they would be colonized again by various species of flora and fauna, as has happened with the succession of species described throughout the assessment period. Furthermore, once an initial biogenic matrix has been established, it is likely that, in the coming months, the plates would be colonized by more perennial and durable species, instead of the ephemeral species observed to the moment.

3.3 Analysis in the CTC’s laboratory

The state of the plates, once in the CTC’s laboratory, are shown in Figure 3-10 to Figure 3-13, for the four selected specimens. In the left column are the exposed faces (face A) and in the right column, the unexposed faces (face B) glued to the panel at the Marine Corrosion Test Site El Bocal.



Figure 3-10. Plate # 4CC: Cable coating at Splash zone. Face A (left) and Face B (right)



Figure 3-11. Plate # 5CC: Cable coating at Tidal area. Face A (left) and Face B (right)



Figure 3-12. Plate # 8: Bare steel at Tidal area. Face A (left) and Face B (right)



Figure 3-13. Plate # 6: Steel coated of Type 2 at Tidal area. Face A (left) and Face B (right)

ISO 4628-1:2016 Standard (4628-1:2016 2016) defines the system used to designate the number and size of defects and the intensity of changes in appearance of paint coatings, and sets out the basic principles of the system. This system is intended, in particular, for defects caused by aging and weathering, as well as for uniform changes such as colour changes, such as yellowing. Below are the evaluations carried out according to ISO 4628-1:2016 Standard (4628-1:2016 2016):

- Assessment of degree of blistering (4628-2:2016 2016).
- Assessment of degree of rusting (4628-3:2016 2016).
- Assessment of degree of cracking (4628-4:2016 2016).
- Assessment of degree of flaking (4628-5:2016 2016).
- Assessment of degree of chalking by tape method (4628-6:2016 2016).

3.3.1 [Assessment of degree of blistering](#)

- **Object and field of application:**

ISO 4628-2:2016 Standard (4628-2:2016 2016) describes a method for assessing the degree of blistering of paint coatings by comparison with graphic standards. The graphic patterns provided show ampoules with sizes 2, 3, 4 and 5, and each size in quantities (densities) 2, 3, 4 and 5.

- **Assessment:**

The number and size of blisters in a paint coating are evaluated using the photographs provided in the standard. When the surface to be examined shows blisters of different sizes, refer to the size of the blisters that can be considered typical of the test area. The evaluation should be carried out under good lighting.

- **Expression of results:**

The grade is expressed for the amount (density) and for the size of the ampoules as shown in the standard, together with the approximate dimension of the test area, or its proportion with respect to the total area, expressed as a percentage. For example, if the coating is rated at blister density 2, size 2, that is, it should be recorded as: 'Blistering: blistering grade 2(S)'.

Below (Figure 3-14 to Figure 3-17) are the photographic patterns that have been used as a reference for the evaluation and expression of the results.

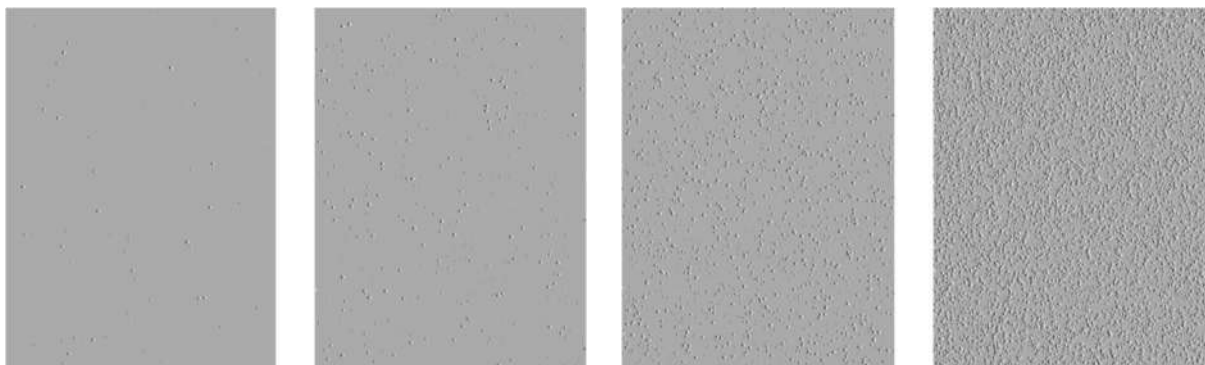


Figure 3-14. Size 2 ampoules. From left to right: Quantity (density) 2 – 2(S2), Quantity (density) 3 – 3(S2), Quantity (density) 4 – 4(S2) and Quantity (density) 5 – 5(S2)

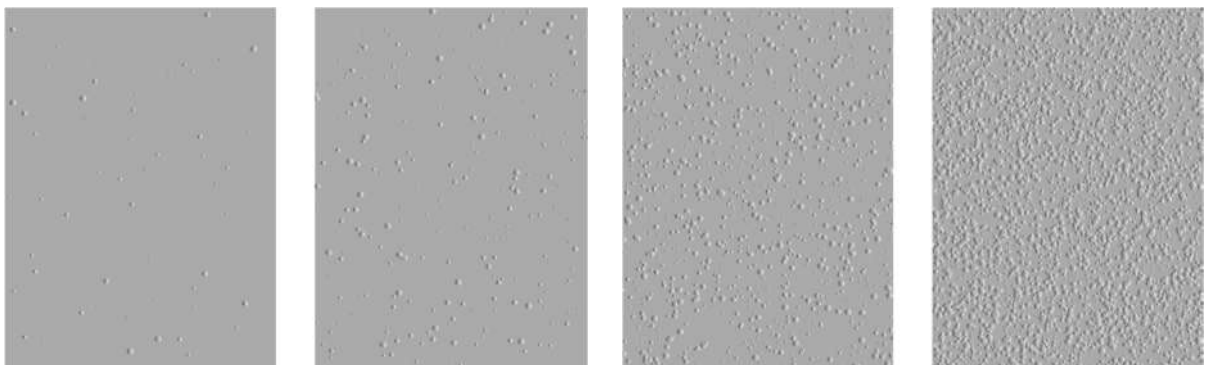


Figure 3-15. Size 3 ampoules. From left to right: Quantity (density) 2 – 2(S3), Quantity (density) 3 – 3(S3), Quantity (density) 4 – 4(S3) and Quantity (density) 5 – 5(S3)

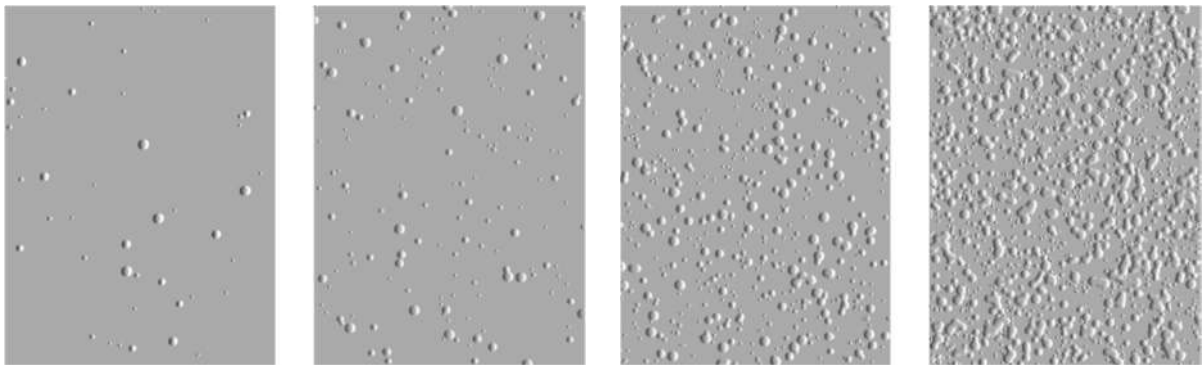


Figure 3-16. Size 4 ampoules. From left to right: Quantity (density) 2 – 2(S4), Quantity (density) 3 – 3(S4), Quantity (density) 4 – 4(S4) and Quantity (density) 5 – 5(S4)

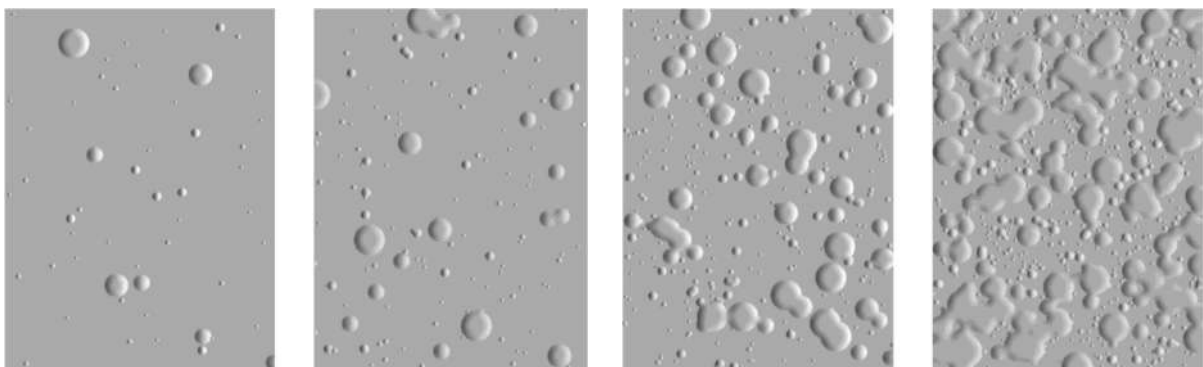


Figure 3-17. Size 5 ampoules. From left to right: Quantity (density) 2 – 2(S5), Quantity (density) 3 – 3(S5), Quantity (density) 4 – 4(S5) and Quantity (density) 5 – 5(S5)

- Results:**

Plate	Inspected face	Quantity	Size	Blistering	Observations
# 8	Face A	5	S5	5 (S5)	Large blisters and all together over the surface
	Face B	4	S5	4 (S5)	Same characteristics as on the previous face but in less quantity
# 6	Face A	-	-	-	No blisters are seen, not even in x10 view
	Face B	3	S5	3 (S5)	Large blisters but slightly close together

Table 3-2. Results of degree of blistering



Figure 3-18. Plate # 8: From left to right, Face A, detail of Face A, Face B and detail of Face B (right)



Figure 3-19. Plate # 6: Face A (left) and Face B (right)

3.3.2 [Assessment of degree of rusting](#)

- **Object and field of application:**

ISO 4628-3:2016 Standard (4628-3:2016 2016) specifies a method for the evaluation of the degree of rusting of painted surfaces by comparison with graphic standards.

- **Assessment:**

The degree of rusting on a painted surface is evaluated by reference to the photographic patterns shown in the figures of the standard. Approximate amounts of rust (loose rust plus visible underlying rust) shown in these patterns are listed in Table 3-3. The procedure for the evaluation of the underlying rust, if required, should be

agreed between the interested parties. When there are different degrees of oxidation in different parts of the area to be evaluated, these degrees must be indicated together with an indication of the area where they occur. The evaluation should be carried out under good lighting, as specified in ISO 13076:2019 Standard (13076:2019 2019). If the average size of the rust stains of the test piece to be evaluated differs considerably from those shown in the graphic patterns, an indication of the size shall be given by reference to the evaluation scheme in Table 3-3.

Degree of rusting	Rusty area %
Ri 0	0
Ri 1	0,05
Ri 2	0,5
Ri 3	1
Ri 4	8
Ri 5	40 to 50

Table 3-3. Degree of rusting and rusty area

- **Expression of results:**

The degree of rusting is expressed as the corresponding Ri of those represented in the figures of the standard. If applicable, the different degrees of rusting observed are indicated, along with the corresponding parts of the test area. If applicable, the degree of rusting Ri is recorded along with the degree, in numerical form, of the size of the rust marks. For example, if the rusty area corresponds to Figure 3-21 on the left-hand side, Ri 3, and the sizes of the individual rusty spots are 0.5 mm to 5 mm, the result is recorded as: 'Oxidation: degree of oxidation Ri 3 (S4)'.

Next, the photographic patterns that will be used for the evaluation and expression of the results are shown in Figure 3-20 to Figure 3-22.

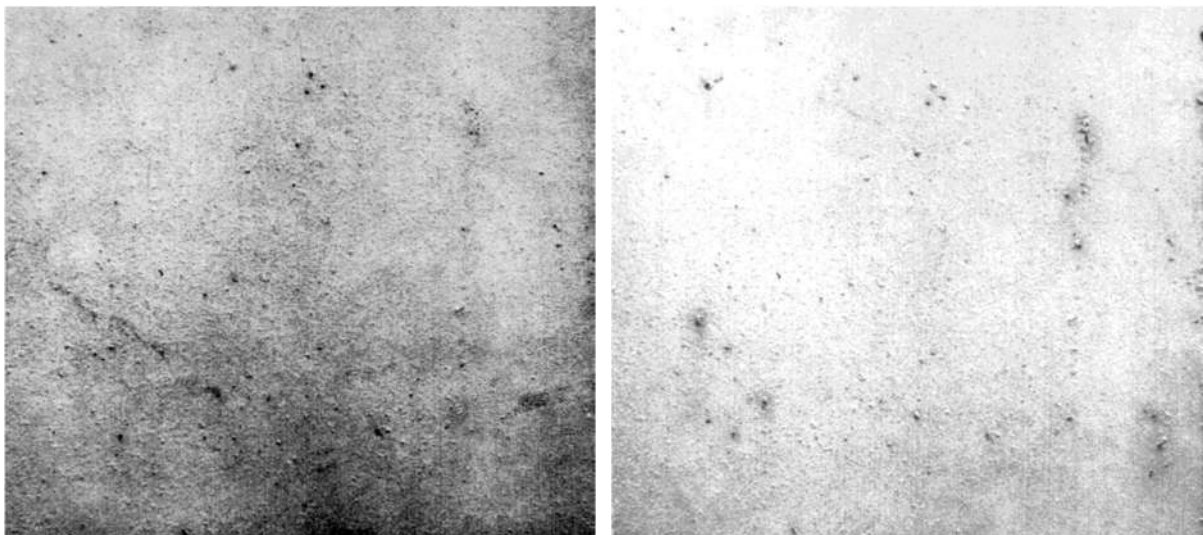


Figure 3-20. Degree of rusting: Ri 1 (left) and Ri 2 (right)

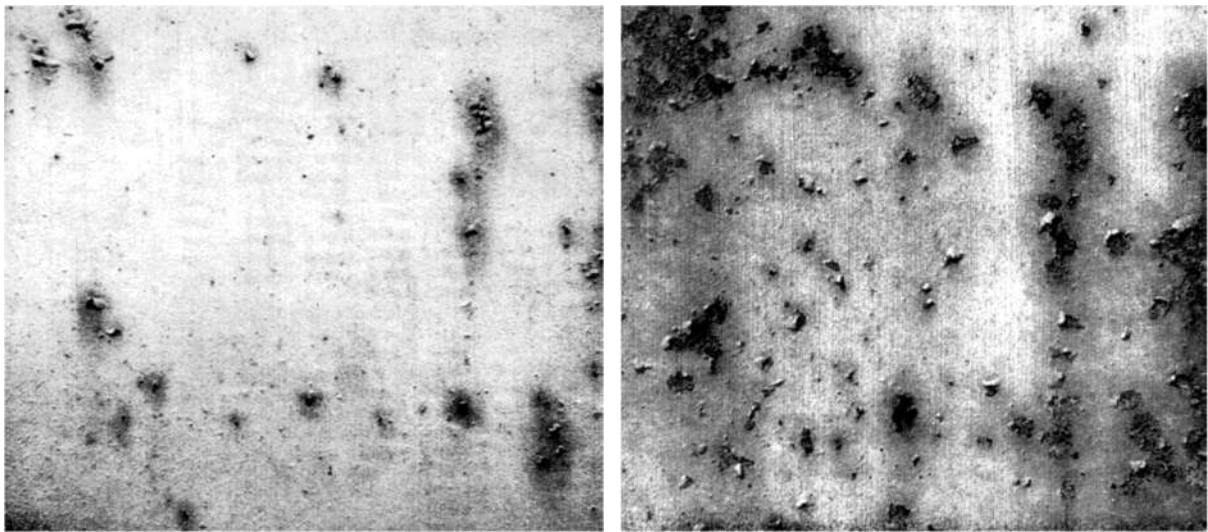


Figure 3-21. Degree of rusting: Ri 3 (left) and Ri 4 (right)

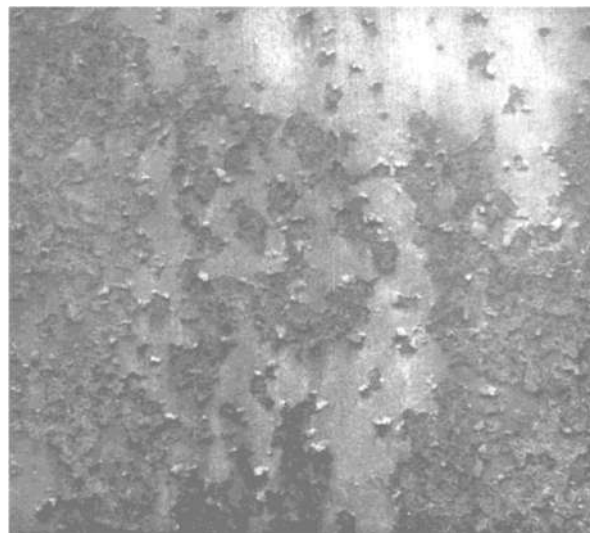


Figure 3-22. Degree of rusting: Ri 5

- Results:**

Plate	Inspected face	Degree of rusting	Rusty area (%)	Observations
# 8	Face A	Ri 5	40-50	Face where more corrosion can be seen
	Face B	Ri 4	8	Delaminate rust flakes. Some remained in the plastic bag.
# 6	Face A		1	Not much apparent corrosion, except at the tie-down holes.
	Face B	Ri 5	40-50	More corrosion than on the Face A

Table 3-4. Results of degree of rusting



Figure 3-23. Plate # 8: Face A (left), Face B (centre) and detail of Face B (right)



Figure 3-24. Plate # 6: Face A (left), detail of Face A (centre) and Face B (right)

3.3.3 [Assessment of degree of cracking](#)

- **Object and field of application:**

ISO 4628-4:2016 Standard (4628-4:2016 2016) specifies a method for assessing the degree of cracking of painted surfaces by comparison with graphic standards.

- **Assessment:**

The number of cracks is evaluated by reference to the Table 3-5 shown in the standard and using the Figure 3-25 of the same as example, depending on the type of cracking.

Degree	Size of cracks
0	Not visible at 10x magnification
1	Visible only at magnifications up to 10x
2	Incipiently visible with normal corrected vision
3	Clearly visible with normal corrected vision
4	Large cracks, usually up to 1 mm wide
5	Very large cracks, usually more than 1 mm wide

Table 3-5. Size of cracks

When the test area shows cracks of different sizes, refer to the size of the cracks that are numerous enough to be considered typical of the test area. If possible, the depth of cracking is indicated by reference to the level of the paint system to which the cracks have penetrated. Three main types of crack failure must be distinguished:

- a) surface cracks that do not fully penetrate the finish coat (i.e., surface crazing);
- b) cracks that penetrate the finish layer, not substantially affecting the underlying layer(s);
- c) cracks that affect the entire paint system.

The evaluation should be carried out under good lighting, as specified in ISO 13076:2019 Standard (13076:2019 2019).

- **Expression of results:**

The numerical value to designate the number and, if specified, the size of the cracks, together with the depth of the crack (a, b, or c), together with the approximate dimension of the affected area, or its proportion to the total area, expressed as percentage. For example, 'Cracking: degree of cracking 2(S3)b'.

Next, the photographic patterns that will be used for the evaluation and expression of the results are shown in Figure 3-25.

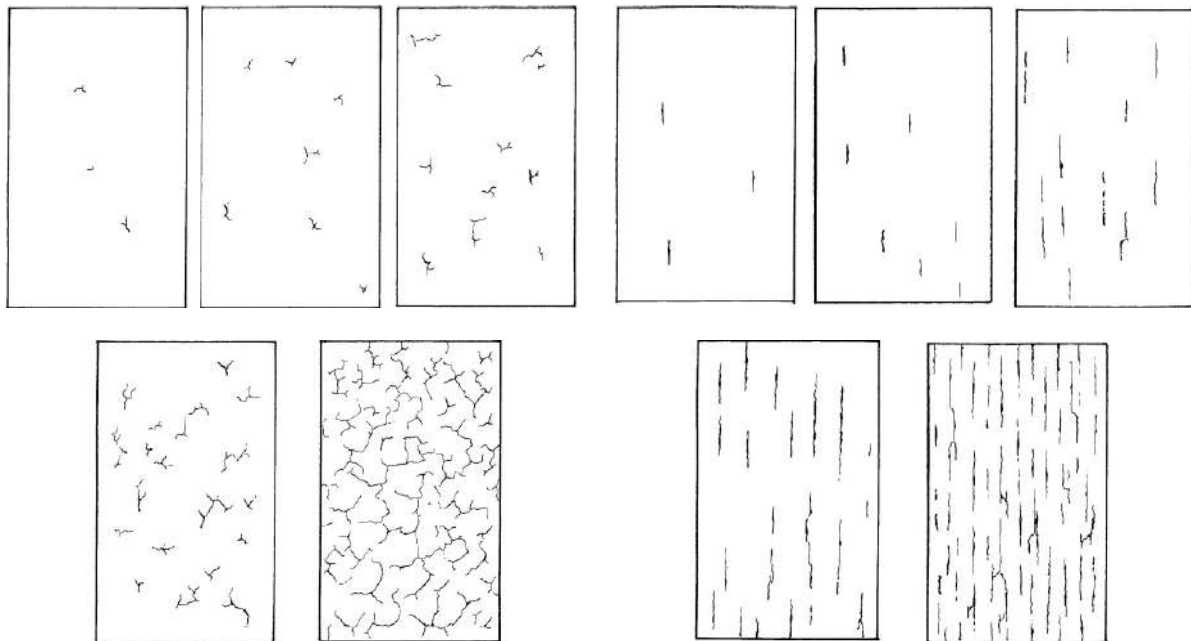


Figure 3-25. Top from left to right: Cracking with non-preferred direction quantity (density) 1, quantity (density) 2, quantity (density) 3; and Cracking with direction quantity (density) 1, quantity (density) 2, quantity (density) 3. Bottom from left to right: Cracking with non-preferred direction quantity (density) 4, quantity (density) 5; and Cracking with direction quantity (density) 4, quantity (density) 5.

- **Results:**

Plate	Inspected face	Degree	Number of cracks	Degree	Size of cracks	Depth	Degree of cracking	Observations
# 8	Face A	1	Very few	2	Visible normal light	a	1(S2)a	Very few and small
	Face B	3	Moderate	3	Clearly visible	b	3(S3)b	Moderate amount of cracks
	Face A	0	None	0	Not visible	-	-	No cracks visible

# 6	Face B	1	Very few	2	Visible normal light	a	1(S2)a	Very few and small
-----	--------	---	----------	---	----------------------	---	--------	--------------------

Table 3-6. Results of degree of cracking



Figure 3-26. Plate # 8: Face A (left) and Face B (right)



Figure 3-27. Plate # 6: Face A (left), detail of Face A (centre) and Face B (right)

3.3.4 Assessment of degree of flaking

- Object and field of application:**

ISO 4628-5:2016 Standard (4628-5:2016 2016) describes a method for the evaluation of the degree of flaking of paint coatings by comparison with graphic standards.

- Assessment:**

The amount of flaking is evaluated by referring to the Table 3-7 and Table 3-8 shown in the standard and using the Figure 3-28 therein as example, depending on the type of flaking.

Degree	Flaking area %
0	0

1	0,1
2	0,3
3	1
4	3
5	15

Table 3-7. Evaluation scheme for the designation of the amount of flaking

Degree	Size of flakes (largest dimension)
0	Not visible at 10x magnification
1	Up to 1 mm
2	Up to 3 mm
3	Up to 10 mm
4	Up to 30 mm
5	Above 30 mm

Table 3-8. Evaluation scheme for the designation of the size of the area affected by desquamation

When the test area shows flakes of different sizes, refer to the size of the flakes that are largest and numerous enough to be typical of the test area. If possible, the depth of flaking is indicated by reference to the level of the paint system affected by the defect. Two main types of scaling faults should be distinguished:

- a) Layer(s) flaked from an underlying layer;
- b) flaking affecting the entire paint system, from the substrate.

The assessment should be carried out under good lighting, as specified in ISO 13076:2019 Standard (13076:2019 2019).

- **Expression of results:**

The numerical value of the quantity and size of the scales is expressed as shown in the Figure 3-28 of the standard, together with their depth (a or b), when possible, and with the approximate dimension of the affected test area, or its proportion with respect to the total area expressed as a percentage. For example, for quantity 3, size 2, with the entire paint system flaking from the substrate, record the result as follows: 'Flaking: degree of flaking 3(S2)b'. If necessary, the test result can be extended with words.

Next, the photographic patterns that will be used for the evaluation and expression of the results are shown in Figure 3-28.

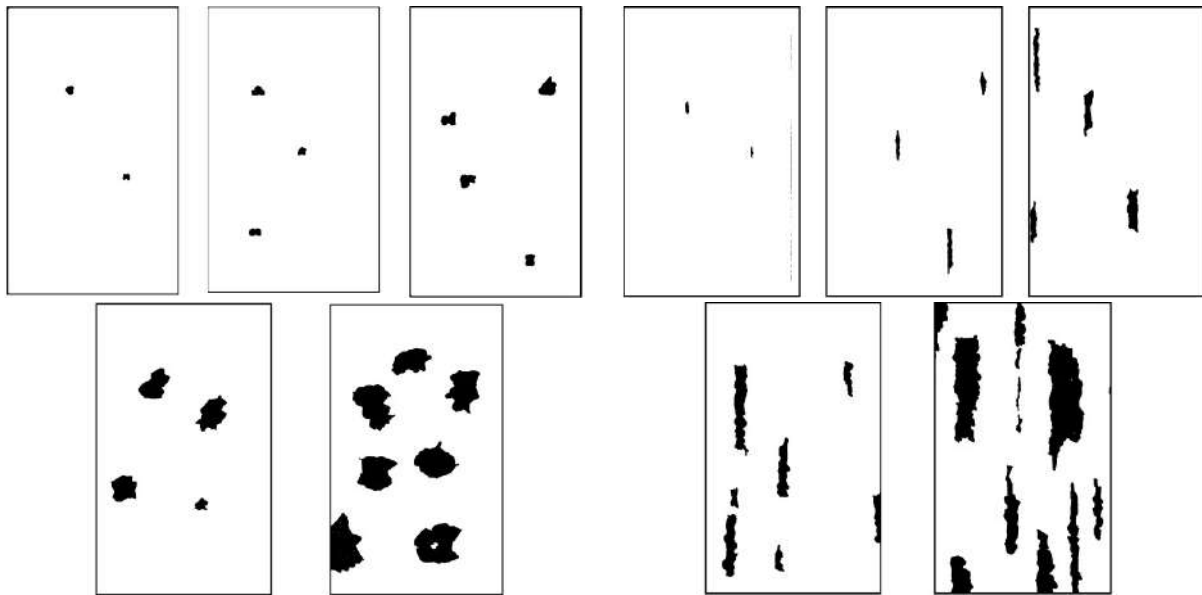


Figure 3-28. Top from left to right: Flaking with non-preferred direction quantity (density) 1, quantity (density) 2, quantity (density) 3; and Flaking with direction quantity (density) 1, quantity (density) 2, quantity (density) 3. Bottom from left to right: Flaking with non-preferred direction quantity (density) 4, quantity (density) 5; and Flaking with direction quantity (density) 4, quantity (density) 5.

- Results:**

Plate	Inspected face	Degree	Flaking area	Degree	Size of flakes	Depth	Degree of flaking	Observations
# 8	Face A	5	15%	2	Up to 3 mm	b	5 (S2) b	Abundant desquamation over the entire surface, reaching even to the first layers of depth
	Face B	2	0,30%	1	Up to 1 mm	a	2 (S1) a	Not as abundant as in Fase A but visible
# 6	Face A	2	0%	2	Up to 3 mm	a	2 (S2) a	Little flaking on the surface, visible in the area where the flanges are attached
	Face B	3	1%	2	Up to 3 mm	a	3 (S2) a	Greater desquamation than in Fase A, more corroded area

Table 3-9. Results of degree of flaking



Figure 3-29. Plate # 8: Face A (left), detail of Face A (centre) and Face B (right)



Figure 3-30. Plate # 6: Face A (left), Face B (centre) and detail of Face B (right)

3.3.5 Assessment of degree of chalking by tape method

- **Object and field of application:**

According to ISO 4628-6:2016 Standard (4628-6:2016 2016), with an adhesive tape, the chalking is removed from the coating under test. The chalking adhered to the tape is examined on a contrasting background (white or black, depending on whether a greater contrast is obtained) and the degree of chalking is evaluated with respect to a scale.

- **Assessment:**

The degree of chalking is evaluated by reference to the graphic patterns listed in the standard (Figure 3-31). The numerical values indicated correspond to those given in the standard.

- **Expression of results and method:**

Dry the surface at room temperature before carrying out the test. A strip of adhesive tape is placed over the dry coating and pressed down firmly with a fingertip. The length of the tape should be at least 40 mm. The tape is removed, perpendicular to the surface, and placed on a background of the appropriate color that provides the greatest contrast, with the adhesive in contact with the background. Light colored coatings are evaluated on a black background and dark colored coatings on a white background. Under appropriate light, the degree of chalking is immediately evaluated by comparing the amount of chalking material present on the tape with the reference graphic patterns shown in the standard (Figure 3-31). The degree will be lower the greater the amount of visible background. The illumination is recorded in the test report.

The tape is applied to an area of the specimen that has not been used for previous measurements to avoid false readings. The values obtained with coatings exposed to natural aging must be treated with care, since the dirt from the atmosphere deposited on the surface can lead to erroneous chalking values. After removing the chalking from the coating under test, the evaluation of each piece of adhesive tape should be made without delay, because the appearance of the chalking residue on the adhesive tape and the transmission of the tape could vary with time. When testing low gloss paint coatings, a certain amount of chalking may be observed even with unaged specimens. A blank test with an unaged specimen is therefore recommended for these coatings.

Next, the photographic patterns that will be used for the evaluation and expression of the results are shown in Figure 3-31.

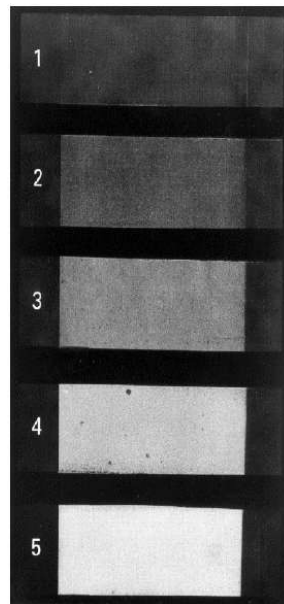


Figure 3-31. Photographic patterns

- **Results:**

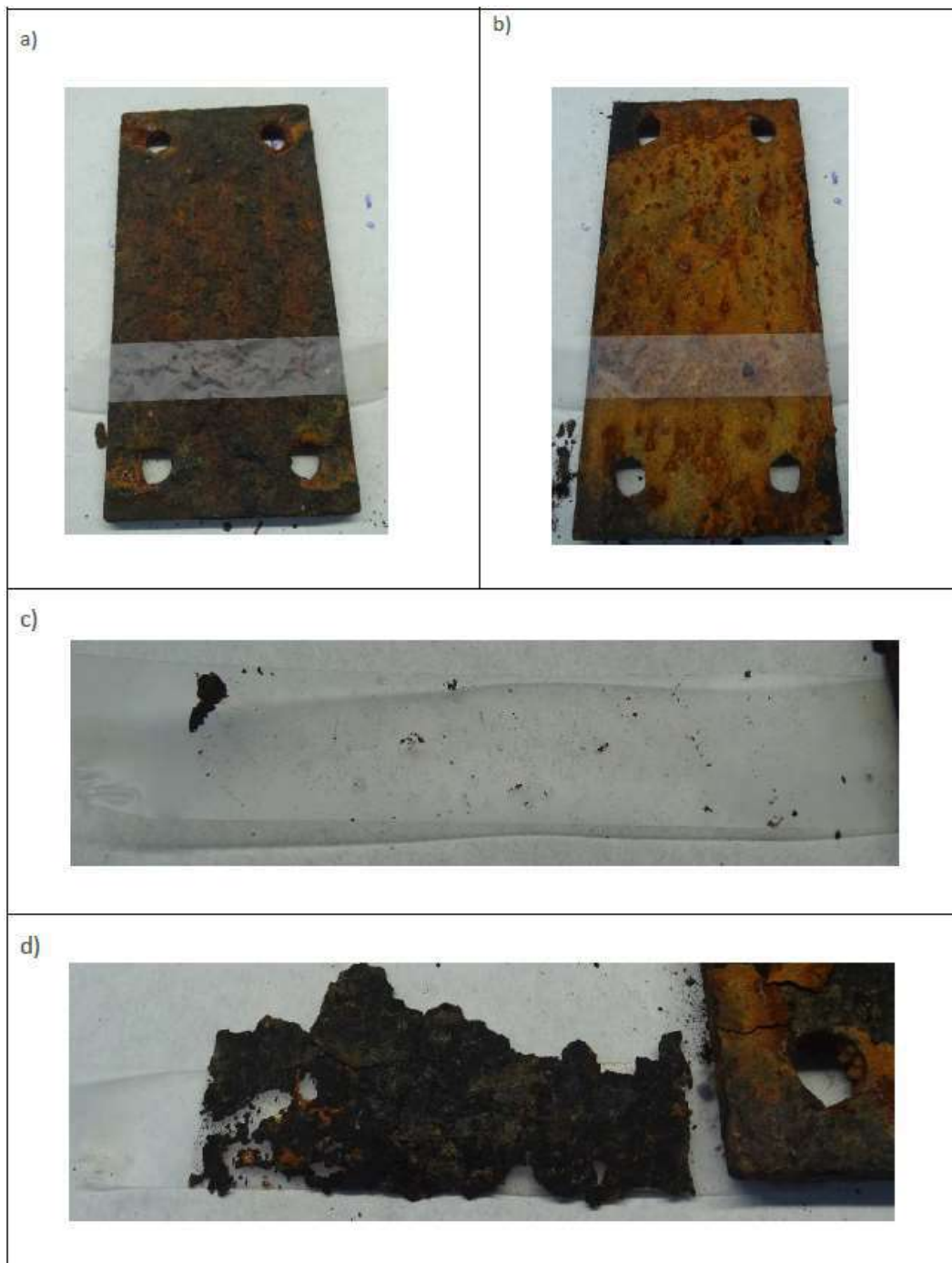


Figure 3-32. Plate # 8: Face A (top left), Face B (top right), Chalking adhered to the tape in Face A (centre) and Chalking adhered to the tape in Face B (bottom)

The upper Face A of the Plate # 8 has a degree of chalking = 2. The lower face of the Plate # 8 has a degree of chalking = 1.

When the adhesive tape was lifted, the entire oxide layer of the sample was detached, which would occur in the rest of the specimen. Thus, the test was not repeated.



Figure 3-33. Plate # 6: Face A (top left), Face B (top right), Chalking adhered to the tape in Face A (centre) and Chalking adhered to the tape in Face B (bottom)

The upper Face A of the Plate # 6 has a degree of chalking = 3. The lower face of the Plate # 3 has a degree of chalking = 2.

4 REFERENCES

13076:2019, UNE-ENISO 2019, *Paints and varnishes - Lighting and procedure for visual assessments of coatings.*

4628-1:2016, UNE-ENISO 2016, *Paints and varnishes - Evaluation of degradation of coatings - Designation of quantity and size of defects, and of intensity of uniform changes in appearance - Part 1: General introduction and designation system.*

4628-2:2016, UNE-ENISO 2016, *Paints and varnishes - Evaluation of degradation of coatings - Designation of quantity and size of defects, and of intensity of uniform changes in appearance - Part 2: Assessment of degree of blistering.*

4628-3:2016, UNE-ENISO 2016, *Paints and varnishes - Evaluation of degradation of coatings - Designation of quantity and size of defects, and of intensity of uniform changes in appearance - Part 3: Assessment of degree of rusting.*

4628-4:2016, UNE-ENISO 2016, *Paints and varnishes - Evaluation of degradation of coatings - Designation of quantity and size of defects, and of intensity of uniform changes in appearance - Part 4: Assessment of degree of cracking.*

4628-5:2016, UNE-ENISO 2016, *Paints and varnishes - Evaluation of degradation of coatings - Designation of quantity and size of defects, and of intensity of uniform changes in appearance - Part 5: Assessment of degree of flaking.*

4628-6:2016, UNE-ENISO 2016, *Paints and varnishes - Evaluation of degradation of coatings - Designation of quantity and size of defects, and of intensity of uniform changes in appearance - Part 6: Assessment of degree of chalking by tape method.*